

Topics in Current Chemistry 320

Markus R. Heinrich  
Andreas Gansäuer *Editors*

# Radicals in Synthesis III

 Springer

**320**

## **Topics in Current Chemistry**

**Editorial Board:**

**K.N. Houk • C.A. Hunter • M.J. Krische • J.-M. Lehn**

**S.V. Ley • M. Olivucci • J. Thiem • M. Venturi • P. Vogel**

**C.-H. Wong • H. Wong • H. Yamamoto**

# Topics in Current Chemistry

## Recently Published and Forthcoming Volumes

### **Radicals in Synthesis III**

Volume Editors: Markus R. Heinrich,  
Andreas Gansäuer  
Vol. 320, 2012

### **Chemistry of Nanocontainers**

Volume Editors: Markus Albrecht,  
F. Ekkehardt Hahn  
Vol. 319, 2012

### **Liquid Crystals: Materials Design and Self-Assembly**

Volume Editor: Carsten Tschierske  
Vol. 318, 2012

### **Fragment-Based Drug Discovery and X-Ray Crystallography**

Volume Editors: Thomas G. Davies,  
Marko Hyvönen  
Vol. 317, 2012

### **Novel Sampling Approaches in Higher Dimensional NMR**

Volume Editors: Martin Billeter,  
Vladislav Orekhov  
Vol. 316, 2012

### **Advanced X-Ray Crystallography**

Volume Editor: Kari Rissanen  
Vol. 315, 2012

### **Pyrethroids: From Chrysanthemum to Modern Industrial Insecticide**

Volume Editors: Noritada Matsuo, Tatsuya Mori  
Vol. 314, 2012

### **Unimolecular and Supramolecular Electronics II**

Volume Editor: Robert M. Metzger  
Vol. 313, 2012

### **Unimolecular and Supramolecular Electronics I**

Volume Editor: Robert M. Metzger  
Vol. 312, 2012

### **Bismuth-Mediated Organic Reactions**

Volume Editor: Thierry Ollevier  
Vol. 311, 2012

### **Peptide-Based Materials**

Volume Editor: Timothy Deming  
Vol. 310, 2012

### **Alkaloid Synthesis**

Volume Editor: Hans-Joachim Knölker  
Vol. 309, 2012

### **Fluorous Chemistry**

Volume Editor: István T. Horváth  
Vol. 308, 2012

### **Multiscale Molecular Methods in Applied Chemistry**

Volume Editors: Barbara Kirchner,  
Jadran Vrabec  
Vol. 307, 2012

### **Solid State NMR**

Volume Editor: Jerry C. C. Chan  
Vol. 306, 2012

### **Prion Proteins**

Volume Editor: Jörg Tatzelt  
Vol. 305, 2011

### **Microfluidics: Technologies and Applications**

Volume Editor: Bingcheng Lin  
Vol. 304, 2011

### **Photocatalysis**

Volume Editor: Carlo Alberto Bignozzi  
Vol. 303, 2011

### **Computational Mechanisms of Au and Pt Catalyzed Reactions**

Volume Editors: Elena Soriano,  
José Marco-Contelles  
Vol. 302, 2011

# Radicals in Synthesis III

Volume Editors: Markus R. Heinrich · Andreas Gansäuer

With Contributions by

G.K. Friestad · A. Gansäuer · M.R. Heinrich · I. Huth · U. Jahn ·  
A. Kirste · S. Mentizi · J.E. Oltra · M. Otte · N.M. Padial · G. Pratsch ·  
A. Rosales · I. Sancho-Sanz · L. Shi · S.R. Waldvogel

 Springer

*Editors*

Prof. Dr. Markus R. Heinrich  
Pharmazeutische Chemie  
Department für Chemie und Pharmazie der  
Friedrich-Alexander-Universität  
Erlangen-Nürnberg  
Erlangen  
Germany

Prof. Dr. Andreas Gansäuer  
Kekulé Institut für Organische Chemie und  
Biochemie der Universität Bonn  
Bonn  
Germany

ISSN 0340-1022

e-ISSN 1436-5049

ISBN 978-3-642-28122-8

e-ISBN 978-3-642-28123-5

DOI 10.1007/978-3-642-28123-5

Springer Heidelberg Dordrecht London New York

Library of Congress Control Number: 2012932054

© Springer-Verlag Berlin Heidelberg 2012

This work is subject to copyright. All rights are reserved, whether the whole or part of the material is concerned, specifically the rights of translation, reprinting, reuse of illustrations, recitation, broadcasting, reproduction on microfilm or in any other way, and storage in data banks. Duplication of this publication or parts thereof is permitted only under the provisions of the German Copyright Law of September 9, 1965, in its current version, and permission for use must always be obtained from Springer. Violations are liable to prosecution under the German Copyright Law.

The use of general descriptive names, registered names, trademarks, etc. in this publication does not imply, even in the absence of a specific statement, that such names are exempt from the relevant protective laws and regulations and therefore free for general use.

Printed on acid-free paper

Springer is part of Springer Science+Business Media ([www.springer.com](http://www.springer.com))

---

## Volume Editors

Prof. Dr. Markus R. Heinrich

Pharmazeutische Chemie  
Department für Chemie und Pharmazie der  
Friedrich-Alexander-Universität  
Erlangen-Nürnberg  
Erlangen  
Germany

Prof. Dr. Andreas Gansäuer

Kekulé Institut für Organische Chemie und  
Biochemie der Universität Bonn  
Bonn  
Germany

## Editorial Board

Prof. Dr. Kendall N. Houk

University of California  
Department of Chemistry and Biochemistry  
405 Hilgard Avenue  
Los Angeles, CA 90024-1589, USA  
*houk@chem.ucla.edu*

Prof. Dr. Steven V. Ley

University Chemical Laboratory  
Lensfield Road  
Cambridge CB2 1EW  
Great Britain  
*Svl1000@cus.cam.ac.uk*

Prof. Dr. Christopher A. Hunter

Department of Chemistry  
University of Sheffield  
Sheffield S3 7HF, United Kingdom  
*c.hunter@sheffield.ac.uk*

Prof. Dr. Massimo Olivucci

Università di Siena  
Dipartimento di Chimica  
Via A De Gasperi 2  
53100 Siena, Italy  
*olivucci@unisi.it*

Prof. Michael J. Krische

University of Texas at Austin  
Chemistry & Biochemistry Department  
1 University Station A5300  
Austin TX, 78712-0165, USA  
*mkrische@mail.utexas.edu*

Prof. Dr. Joachim Thiem

Institut für Organische Chemie  
Universität Hamburg  
Martin-Luther-King-Platz 6  
20146 Hamburg, Germany  
*thiem@chemie.uni-hamburg.de*

Prof. Dr. Jean-Marie Lehn

ISIS  
8, allée Gaspard Monge  
BP 70028  
67083 Strasbourg Cedex, France  
*lehn@isis.u-strasbg.fr*

Prof. Dr. Margherita Venturi

Dipartimento di Chimica  
Università di Bologna  
via Selmi 2  
40126 Bologna, Italy  
*margherita.venturi@unibo.it*

**Prof. Dr. Pierre Vogel**

Laboratory of Glycochemistry  
and Asymmetric Synthesis  
EPFL – Ecole polytechnique fédérale  
de Lausanne  
EPFL SB ISIC LGSA  
BCH 5307 (Bat.BCH)  
1015 Lausanne, Switzerland  
*pierre.vogel@epfl.ch*

**Prof. Dr. Chi-Huey Wong**

Professor of Chemistry, Scripps Research  
Institute  
President of Academia Sinica  
Academia Sinica  
128 Academia Road  
Section 2, Nankang  
Taipei 115  
Taiwan  
*chwong@gate.sinica.edu.tw*

**Prof. Dr. Henry Wong**

The Chinese University of Hong Kong  
University Science Centre  
Department of Chemistry  
Shatin, New Territories  
*hncwong@cuhk.edu.hk*

**Prof. Dr. Hisashi Yamamoto**

Arthur Holly Compton Distinguished  
Professor  
Department of Chemistry  
The University of Chicago  
5735 South Ellis Avenue  
Chicago, IL 60637  
773-702-5059  
USA  
*yamamoto@uchicago.edu*

# Topics in Current Chemistry Also Available Electronically

*Topics in Current Chemistry* is included in Springer's eBook package *Chemistry and Materials Science*. If a library does not opt for the whole package the book series may be bought on a subscription basis. Also, all back volumes are available electronically.

For all customers with a print standing order we offer free access to the electronic volumes of the series published in the current year.

If you do not have access, you can still view the table of contents of each volume and the abstract of each article by going to the SpringerLink homepage, clicking on "Chemistry and Materials Science," under Subject Collection, then "Book Series," under Content Type and finally by selecting *Topics in Current Chemistry*.

You will find information about the

- Editorial Board
- Aims and Scope
- Instructions for Authors
- Sample Contribution

at [springer.com](http://springer.com) using the search function by typing in *Topics in Current Chemistry*.

*Color figures* are published in full color in the electronic version on SpringerLink.

## Aims and Scope

The series *Topics in Current Chemistry* presents critical reviews of the present and future trends in modern chemical research. The scope includes all areas of chemical science, including the interfaces with related disciplines such as biology, medicine, and materials science.

The objective of each thematic volume is to give the non-specialist reader, whether at the university or in industry, a comprehensive overview of an area where new insights of interest to a larger scientific audience are emerging.



Thus each review within the volume critically surveys one aspect of that topic and places it within the context of the volume as a whole. The most significant developments of the last 5–10 years are presented, using selected examples to illustrate the principles discussed. A description of the laboratory procedures involved is often useful to the reader. The coverage is not exhaustive in data, but rather conceptual, concentrating on the methodological thinking that will allow the non-specialist reader to understand the information presented.

Discussion of possible future research directions in the area is welcome.

Review articles for the individual volumes are invited by the volume editors.

In references *Topics in Current Chemistry* is abbreviated *Top Curr Chem* and is cited as a journal.

Impact Factor 2010: 2.067; Section “Chemistry, Multidisciplinary”: Rank 44 of 144

# Preface

Radical chemistry, as any sub-discipline of synthetic chemistry, has to meet ever more complex demands, such as sustainability and selectivity, in order to be applied to the multifaceted challenges of today. In this volume of *Topics in Current Chemistry*, recent exciting developments that address these highly pertinent issues have been summarized by leading scientists of the field.

One of the economically and ecologically most attractive ways to generate radicals is electrochemistry. New materials, such as the BDD electrodes described here, will expand the relevance of this already important area. Arylation reactions are extremely important in synthesis in academic and industrial laboratories. The chemistry of aryl radicals highlighted here summarizes modern developments that are highly attractive for carrying out such transformations. The control of stereo-selectivity is of prime significance for any type of reactions. Radical addition to chiral hydrazones provides a convenient means for achieving this goal as also summarized here. The reductive termination of radicals by hydrogen atom donors has always been a critical aspect of radical chemistry with respect to environmental issues and novel exciting developments addressing this key issue are discussed. Finally, the use of radicals as key intermediates in catalysis has blossomed in recent years. This highly important field has been reviewed comprehensively for the first time in this issue. Special emphasis has been laid on all aspects of selectivity.

We hope that the exciting topics presented in this volume, ranging from the generation of radicals to applications in catalysis, will be able to convince scientists at all levels to consider using radical methods in their daily work and will provide further impetus for the development of novel methods of radical chemistry.

Erlangen and Bonn  
December 2011

Markus R. Heinrich  
Andreas Gansäuer



# Contents

<b>Boron-Doped Diamond Electrodes for Electroorganic Chemistry</b> .....	1
Siegfried R. Waldvogel, Stamo Mentizi, and Axel Kirste	
<b>Modern Developments in Aryl Radical Chemistry</b> .....	33
Gerald Pratsch and Markus R. Heinrich	
<b>Radical Additions to Chiral Hydrazones: Stereoselectivity and Functional Group Compatibility</b> .....	61
Gregory K. Friestad	
<b>Hydrogen Atom Donors: Recent Developments</b> .....	93
Andreas Gansäuer, Lei Shi, Matthias Otte, Inga Huth, Antonio Rosales, Iris Sancho-Sanz, Natalia M. Padial, and J. Enrique Oltra	
<b>Radicals in Transition Metal Catalyzed Reactions? Transition Metal Catalyzed Radical Reactions? A Fruitful Interplay Anyway</b>	
<b>Part 1. Radical Catalysis by Group 4 to Group 7 Elements</b> .....	121
Ullrich Jahn	
<b>Radicals in Transition Metal Catalyzed Reactions? Transition Metal Catalyzed Radical Reactions? – A Fruitful Interplay Anyway</b>	
<b>Part 2. Radical Catalysis by Group 8 and 9 Elements</b> .....	191
Ullrich Jahn	
<b>Radicals in Transition Metal Catalyzed Reactions? Transition Metal Catalyzed Radical Reactions?: A Fruitful Interplay Anyway</b>	
<b>Part 3: Catalysis by Group 10 and 11 Elements and Bimetallic Catalysis</b> .....	323
Ullrich Jahn	
<b>Index</b> .....	453



# Boron-Doped Diamond Electrodes for Electroorganic Chemistry

Siegfried R. Waldvogel, Stamo Mentizi, and Axel Kirste

**Abstract** Boron-doped diamond (BDD) electrodes provide an unusually wide electrochemical window in protic media, since there exist large offset potentials for the evolution of molecular hydrogen and oxygen, respectively. At the anode, alcohols are specifically converted to alkoxy radicals. These can be used for chemical synthesis. When the enormous reactivity of such intermediate spin centers is not controlled, mineralization or electrochemical incineration dominates. Efficient strategies include either high substrate concentrations or fluorinated alcohols which seem to stabilize the spin centers in the course of reaction.

**Keywords** Anode · Boron-doped diamond · Cathode · Electrochemistry · Electro-synthesis

## Contents

1	Introduction .....	2
2	Unique Properties of BDD Electrodes .....	4
3	Cathodic Conversion .....	7
3.1	Reductive Carboxylation .....	7
3.2	Reduction of Oximes .....	8
4	Anodic Transformations .....	9
4.1	Alkoxylation .....	10
4.2	Fluorination .....	12
4.3	Cyanation .....	13
4.4	Cleavage of C–C-Bonds .....	14
4.5	Oxidation of Activated Carbon Atoms .....	15
4.6	Anodic Phenol Coupling Reaction .....	16

---

S.R. Waldvogel (✉) and S. Mentizi

Institut für Organische Chemie, Johannes Gutenberg-Universität Mainz, Duesbergweg 10-14,  
55128 Mainz, Germany  
e-mail: waldvogel@uni-mainz.de

A. Kirste

Kekulé-Institut für Organische Chemie und Biochemie, Rheinische Friedrich-Wilhelms  
Universität Bonn, Gerhard-Domagk-Str. 1, 53121 Bonn, Germany

5	Anodic Stability of BDD Materials .....	23
6	Electrolysis Cells for the Use of BDD Electrodes .....	24
7	Outlook .....	26
	References .....	26

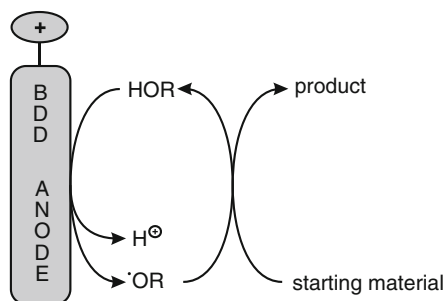
## Abbreviations

AA	Arene–arene homo-coupling product
BDD	Boron-doped diamond
CE	Current efficiency
DMF	<i>N,N</i> -Dimethylformamide
EPDM	Ethylene propylene diene monomer (M-class rubber)
GC	Glassy carbon
HFIP	1,1,1,3,3,3-Hexafluoroisopropanol
MHA	Methionine hydroxy analogue
PA	Phenol–arene cross-coupling product

## 1 Introduction

In electrochemical transformations only electrons serve as reagents. Consequently, almost no reagent waste is produced. Due to the outstanding atom economy and often pronounced energy efficiency, such electrochemical processes are mostly considered as green chemistry [1]. Approximately 7% of the total industrial electricity consumption is employed for electrochemical transformations and processes [2]. Therefore, electrosynthesis is of outstanding technical significance. In addition, electric current will be the prime energy of the future since bulk renewable energy resources will consist of photovoltaics, wind energy, water power, etc. Alternatively, other nations will rely heavily on nuclear power which also provides electric current as prime energy. However, novel electrosynthetic transformations will be the basis for technical innovations and future applications. In electrochemical transformations the coupled nature of anodic and cathodic processes links two contradictory transformations. But both reactions can be employed for synthetic purposes [3]. In most cases a divided electrolysis cell is used, which separates anolyte and cathodic compartment [4, 5]. In a few cases the transformation on the anode and cathode can be simultaneously exploited for preparative purposes. Such so-called 200%-cells fulfill all aspects of sustainable electrochemical processes and represent the state-of-the-art [6–8]. The technical realization is the “paired electrolysis” which has been carried out by BASF SE in Germany [9]. Alternative strategies for selective electrochemical transformations exploit mediators; these are electrochemically regenerated reagents.

In particular, the specific reactivity of a given reagent can be employed when using it catalytically. There are several advantages. Beside the electrochemically fueled transformation, these mediators can reach hidden places like active sites of enzymes [10–14] or solid supports [15, 16]. The use of electrochemically generated spin centers in biochemical and organic processes is rather limited because suitable techniques and in particular appropriate electrode materials are still challenging. Since aqueous media are commonly used in inorganic technical processes, the electrolysis of water is the significant side-reaction. Electrode materials with high offset potentials for molecular hydrogen and oxygen in cathodic and anodic processes, respectively, can eliminate this undesired drain of electric energy. The investigation and use of BDD as novel and innovative electrode material is a new and emerging area of chemical research. In particular, the nondestructive conversion of organic compounds on BDD anodes has started and experienced significant attention. Recently, BDD electrodes became available in a variety of sizes, on different support materials and with an enhanced stability in organic media. The BDD layer is formed on support materials by chemical vapor deposition. Therefore, even sophisticated and large electrode geometries up to 1 m<sup>2</sup> surface are accessible. High hopes are placed in this new BDD technology, since tremendous ameliorations in academic and industrial aspects seem to be possible. This is mainly due to the large potential window for boron-doped diamond in aqueous solutions. In particular, anodic processes allow the formation of OH radicals at potentials well below the onset of oxygen evolution. Boron-doped diamond electrodes can thus be used for new oxidation reactions which otherwise are not possible in water [17]. In methanol containing solutions, methoxyl radicals were also discussed as reactive intermediates [18]. The formation of OH spin centers has been demonstrated using spin traps [19]. The largest field of application for BDD anodes exploits the destructive performance including disinfection, detoxification, and wastewater treatment: At intermediate potentials a direct, simple electron transfer occurs, whereas the formation of hydroxyl radicals at highly positive potentials leads to a complete incineration (e.g., of 2-naphthol, 4-chlorophenol, and other compounds) via complex oxidation sequences [20, 21]. Partial oxidation, e.g., of phenol to benzoquinone, is also observed [22]. The destructive use of BDD electrodes represents cutting-edge-technology and has been summarized in several monographs [23, 24]. The likely degradation of organic compounds turns here into potential disadvantages which have to be controlled. In Fig. 1 a simplified



**Fig. 1** Simplified mode of action for BDD electrodes in protic media



mode of action for the BDD anodes is depicted. In electroorganic synthesis the oxyl species induces the reaction sequence which has to be terminated by another spin center. Therefore, current density will represent an important parameter to manipulate the chemical fate of the substrate.

The constructive and desired pathway towards the product competes with the electrochemical incineration. At high current densities the mineralization dominates. Therefore, lower current densities will be beneficial for a synthetic and nondestructive transformation. The compartment of electrochemical transformation caused by hydroxyl or methoxyl radicals can be estimated in the range of a few micrometers close to the BDD anode. Mass transport has to be efficient since the migration of products out of the electrochemical scene into bulk is crucial for avoiding the overoxidation. Control of both competing and critical processes will either cause failure (mineralization) or provide the opportunity for selective electroorganic synthesis (Fig. 2).

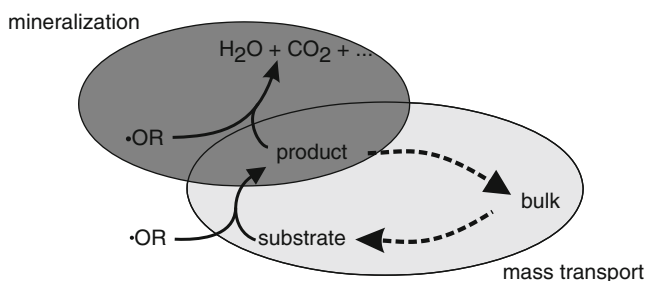


Fig. 2 Competing reaction pathways caused by BDD anodes

## 2 Unique Properties of BDD Electrodes

Boron-doped diamond is a narrow gap semiconductor which can be deposited on a variety of substrates including niobium, silicon, titanium, steel, etc. The carbon source for the diamond is methane which is decomposed in the plasma. Since methane is considered to be a renewable, BDD is also regarded to be a sustainable material. The boron content can be adjusted within the range of 200–5,000 ppm. The coating is usually 10–50  $\mu\text{m}$  thick. Consequently, the contribution to the overall cell resistance is observable but in most cases negligible. The diamond coating is chemically and electrochemically highly resistant. Therefore, this material should be ideal for oxidation processes. The most striking properties of boron-doped diamond are the unusual large offset potentials in aqueous media for both anodes and cathodes for the evolution of hydrogen and oxygen, respectively. The overpotential for the discharging of protons in a neutral aqueous electrolyte is stated to

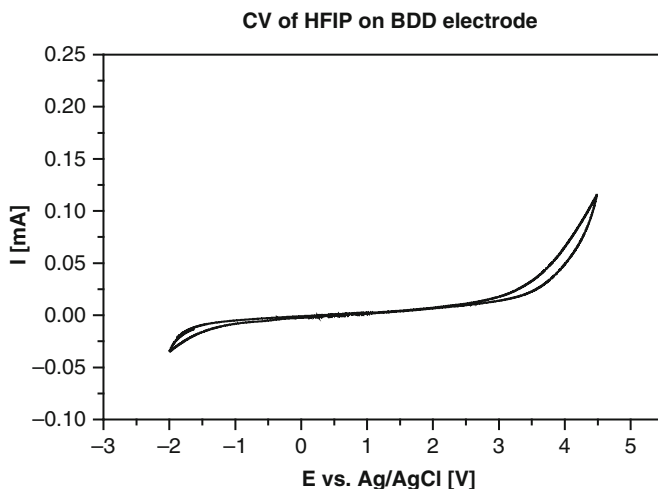
**Table 1** Offset potentials ( $\eta$ ) for the evolution of hydrogen or oxygen, respectively, at different electrode materials (aqueous media)

Electrode material	$\eta$ for H <sub>2</sub> evolution (V)	$\eta$ for O <sub>2</sub> evolution (V)
BDD	-1.10 [15]	2.30 [14]
Hg	-1.21 [16]	–
Pb	-1.26 [16]	1.02 [16]
Graphite	-0.99 [16]	1.12 [16]
Ag	-0.76 [16]	0.94 [16]
Au	-0.32 [16]	1.53 [16]
Pt (solid)	-0.40 [16]	1.50 [16]
Pd	–	1.12 [16]

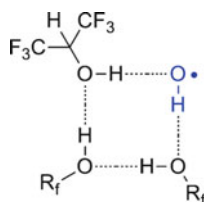
be  $-1.1$  V. This is a similar value found with mercury or lead as cathode (Table 1) [23]. Because of the toxicity of mercury and mercury compounds eventually appearing in the course of the reaction, there are severe environmental concerns connected with the application of mercury as cathode in process chemistry. Consequently, boron-doped diamond may find future applications in electrochemically fueled reductions wherein aqueous media cannot be circumvented, e.g., enzyme catalysis or post-modification of proteins. In addition, on the anodic side an offset potential for the generation of molecular oxygen from neutral aqueous media of about 2.3 V can be determined. This overpotential is significantly larger than common noble metal electrodes could provide [24–26]. The limited resources of platinum and other noble metals led to increasing cost for these electrode materials. Replacement by BDD would be another sustainable innovation. In particular, if noble metals like platinum are used as cathodes, contamination with other metals occurs, diminishing the desired electrochemical characteristics of platinum.

These offset potentials in neutral aqueous media for the evolution of hydrogen and oxygen open up an electrochemical window which should facilitate a variety of chemical transformations. Recently we found, when employing fluorinated alcohols instead of water, this window is drastically opened up: As anticipated the anodic region is expanded to 3.2 V since these alcohols are quite stable towards oxidation. More surprisingly, the overpotential for the reductive region gained almost  $-2$  V and represents the largest offset potential for the evolution of hydrogen (Fig. 3). Currently, the 1,1,1,3,3,3-hexafluoroisopropanol–BDD system represents the protic electrolyte with the largest electrochemical window of about 5 V. In the displayed example, methyltriethylammonium methylsulfate served as supporting electrolyte [27, 28]. The limitation in the anodic part might be caused by this supporting electrolyte which is very common in the chemical industry. The depicted foot potential shows slight conversions which can be attributed to impurities in the 1,1,1,3,3,3-hexafluoroisopropanol (HFIP). The employed quality was approximately 99% (Fig. 3).

In such expanded windows, solvents like water have an effect. It seems that hydroxyl groups preferably react with the BDD surface and form oxyl spin centers. As long as such intermediates are preferentially formed, a simplified mode of action



**Fig. 3** Very large electrochemical window for the system BDD/1,1,1,3,3,3-hexafluoroisopropanol (HFIP) with 0.1 M  $\text{Et}_3\text{NCH}_3$   $\text{O}_3\text{SOCH}_3$



**Fig. 4** Potential hydrogen bonding motif for stabilizing OH radicals

for BDD anodes can be anticipated (Fig. 1). The high reactivity of hydroxyl spin centers is outstanding and their estimated oxidation potential is right between fluorine and ozone [29, 30]. Control of these intermediates requires innovative strategies in order to accumulate the desired product. The use of the above-mentioned fluorinated alcohols seems to produce solvent clusters which stabilize the hydroxyl spin centers in a supramolecular network of hydrogen bonding (Fig. 4). This would enhance the lifetime of the intermediates significantly and suppress the mineralization process. The postulated structure is supported by X-ray analysis of the HFIP and hydrogen bonding network found by Berkessel et al. [31, 32]. In the solid state of HFIP a helical arrangement is formed since the fourth HFIP molecule does not have enough space in a tetramer. With a hydroxyl radical, the hydrogen bonding motive displayed in Fig. 4 should be possible. Currently, studies in our laboratory are being performed to verify this hypothesis [33].

For anodic processes BDD electrodes offer another very promising feature. Because of the highly reactive nature of the intermediates formed on the diamond surface, no electrode fouling by coating of byproducts or carbonization is found. Eventually formed deposits on the diamond layer will be mineralized to small

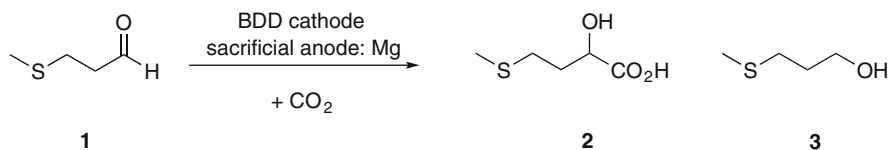
molecules and will be easily removed from the electrolyte and the electrolysis cell. Since no deactivation of the anode surface is anticipated and a significantly reduced effort for maintenance of electrodes is expected, a technical interest in these electrodes exists. Commonly used graphite electrode stacks have to be disassembled and mechanically cleaned to restore a suitable anode surface. Therefore, such self-maintaining electrodes based on BDD material could lead to a small but significant cost advantage for chemical processes.

### 3 Cathodic Conversion

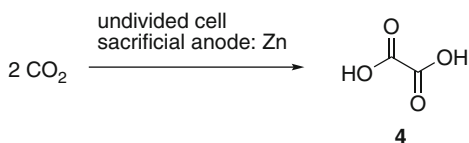
Compared to typical reducing agents like hydrides and molecular hydrogen, electric current is by far the least expensive reduction equivalent. While many anodic conversions are well studied, electrochemical reduction is less so. The key reason is based on the very few electrode materials which can be successfully applied. In general, protic media allow only cathode materials with high overpotentials for the evolution of hydrogen. Consequently, late transition metals such as lead, mercury, and cadmium most often show the best results. The high toxicity of these electrode materials and eventually formed organometallic species thereof result in a reluctant use of such reductions. Therefore, an environmentally benign replacement for these toxic heavy metals could have significant academic as well as technical impact. Because of the cathodic polarization of the BDD electrodes, the electrodes are protected. In general, no problems in stability or corrosion of BDD will occur.

#### 3.1 Reductive Carboxylation

For the carbon dioxide balance, and due to ecological considerations, the electrochemical fixation of this particular C1 building block into chemicals seems to be very attractive. Furthermore, carbon dioxide is a good electron acceptor which can be subjected to cathodic conversions [34]. 2-Hydroxy-4-methylsulfanylbutyric acid (**2**) is often named as methionine hydroxy analog (MHA). This intermediate represents an important technical product used on a large scale for animal feeding. **2** exhibits an enhanced bioavailability compared to the essential amino acid methionine. Consequently, **2** is made on a scale of several thousand tons by treatment of methylsulfanylpropionaldehyde (**1**) with cyanhydric acid to form the corresponding cyanohydrins. Subsequent hydrolysis of the nitrile provides **2**. An electrochemical approach to **2** performs a reductive carboxylation of **1** with magnesium as sacrificial anode. The transformation requires a CO<sub>2</sub> atmosphere and magnesium for both electrodes. Electrolysis in a DMF/NBu<sub>4</sub><sup>+</sup>BF<sub>4</sub><sup>-</sup> electrolyte resulted in, upon application of 5 F/mol, a conversion of 90% with a selectivity of 75% for **2** [35, 36]. The conversion can also be performed on BDD electrodes. If a divided cell is employed, much less magnesium electrode material is sacrificed. The direct reduction of



**Scheme 1** Carboxylation to methionine analogue



**Scheme 2** Cathodic reduction of carbon dioxide

aldehyde **1** to alcohol **3** is unfortunately a significant side reaction (Scheme 1). The yield for **2** in this process is lower than on magnesium electrodes (conversion 66%, current efficiency 22%, divided flow cell, Nafion membrane, BDD on silicon support, 20–25 °C, 0.6 A/dm<sup>2</sup>) [37]. However, this is an impressive example of the versatility of BDD electrodes in preparative electroorganic synthesis (Scheme 2).

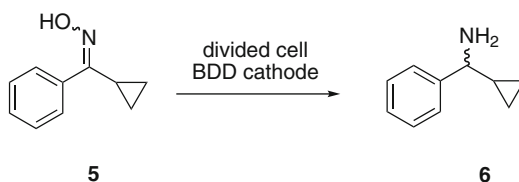
The good electron acceptor property of carbon dioxide can be used for the hydrodimerization to oxalic acid **4**. Electrolysis is performed in an undivided cell using zinc as sacrificial electrode material. The reported electrolysis data are 6 mA/cm<sup>2</sup> with 12 mM NBU<sub>4</sub><sup>+</sup>BF<sub>4</sub><sup>-</sup> in DMF. The current efficiency for the formation of oxalic acid is stated to be 60%. Unfortunately, no further details are currently available about this particular process (Lehmann and Dunach, 2009, personal communication).

### 3.2 Reduction of Oximes

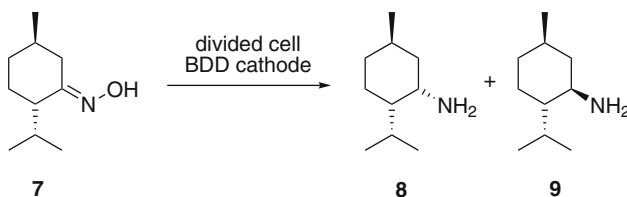
The preparation of amines starting from the corresponding oximes is a very common and versatile method since the full carbon skeleton is provided. Commonly, the reduction is performed in a Bouveault–Blanc-type reaction by treatment with alkali metals in the presence of a proton source, e.g., alcohols [38]. By conducting this transformation electrochemically generated reagent waste is avoided. Reductions at a mercury pool were mainly successful [39]. The high of BDD for the H<sub>2</sub> evolution by electrolysis of protic electrolytes should be beneficial for cathodic transformations [40]. The electrochemical and chemoselective reduction of cyclopropylphenylketone oxime (**5**) to rac- $\alpha$ -cyclopropylbenzylamine (**6**) was done with 96% yield on a BDD cathode. As electrolyte, a MeOH/NaOMe mixture in a divided cell was used. Similar results can be obtained using lead cathodes (1% NaOMe in anhydrous MeOH, 40 °C, 3.4 A/dm<sup>2</sup>) [41]. The electrochemical reduction is superior to a catalytic hydrogenation of oxime **5**. The product of the

conventional reduction by hydrogenation on noble metal catalyst is attended by significant amounts of ring-opened compounds, making purification by distillation almost impossible (Scheme 3).

**Scheme 3** Successful oxime reduction



Stimulated by this work, the electro reduction was tested on the sterically more congested menthoneoxime (**7**). Substrate **7** – which is derived from optically pure L-menthone – could provide, upon reduction, both epimeric products, (+)-neomenthylamine (**8**) and (–)-menthylamine (**9**), respectively. For both diastereomers there exist unique applications [38, 42–53]. The preparation was formerly conducted by treatment with 30 equiv. of sodium metal leading to safety concerns for a scale-up [54]. However, detailed investigations with BDD cathodes indicated that **7** is not a useful substrate. Almost no conversion is observed and only traces of both epimeric amines could be detected. However, the cathodic treatment of **7** using lead results in almost quantitative reduction and a splendid current efficiency (6 F/mol, 66%) [55] (Scheme 4).



**Scheme 4** Reduction of a nonsuitable substrate for BDD

Most probably, the successful conversion of substrates on BDD cathodes requires access to the diamond surface without spatial restrictions. Consequently, more sterically demanding substrates are not suitable.

## 4 Anodic Transformations

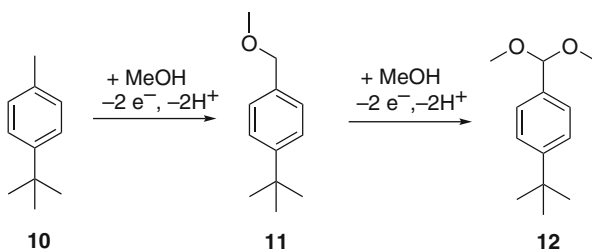
The wide electrochemical window in aqueous and protic media is the most intriguing feature of polycrystalline BDD material. Additionally, the specific formation of oxyl radicals is singular. In aqueous or alcoholic solutions such very reactive spin centers can be created in high concentration [56]. This opens unique reaction pathways which have previously been considered as inaccessible by

electrochemical means. Therefore, anodic transformations are most obvious on BDD electrodes. The generated hydroxyl or alkoxy species may act either as radicals being implemented into the product or serve as strong oxidants which transform the substrate. In the latter reaction sequence the oxyl spin centers play the role of a mediator.

## 4.1 Alkoxylation

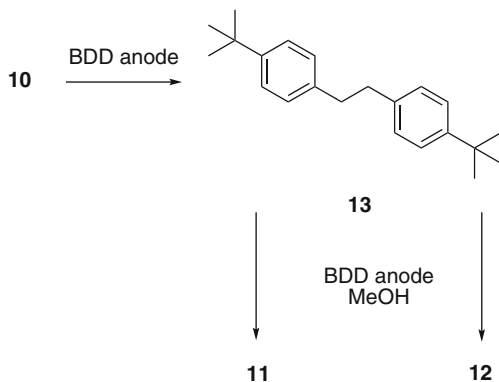
Since the extreme oxidizing power of the oxyl spin centers is successfully employed in waste water treatment, an application of these intermediates seems to be self-contradictory in terms of synthetic use. However, alkoxylation of hydrocarbons is a very important technical field since it allows the installation of functionalities without using the detour via halogenations. The selective introduction of functional groups on a completely nonactivated hydrocarbon has not yet been realized by BDD technology. In contrast, the direct anodic methoxylations of activated carbons exhibiting benzylic or allylic moieties can be performed at BDD anodes. The results obtained with BDD electrodes are quite similar to those when graphite serves as anode [57]. The anodic synthesis of benzaldehyde dimethyl ketals is industrially relevant and performed on the scale of several thousand tons. A detailed study of the anodic methoxylation of 4-*tert*-butyltoluene (**10**) at BDD was performed [58]. Usually, the first methoxylation product **11** and the twofold functionalized derivative **12** are found upon electrochemical treatment (Scheme 5).

If BDD is applied as anode material an accumulation of the dibenzyl derivative **13** is observed. It is noteworthy that this intermediate is not detected when graphite electrodes are used. This difference can be attributed to a mechanism based on the non-catalytic character of BDD electrodes and to the presence of active functionalities on graphite electrodes [59]. The occurrence of **13** might also be the consequence of hydrogen atom abstraction by intermediate methoxyl radicals. However, in the course of the electrolysis, **13** is then further converted into the desired products **11** and **12** by cleavage of the central C–C-bond. The cleavage of C–C-bonds in stilbenes or dibenzyl derivatives is found at graphite electrodes only at high current densities of approx. 10 A/dm<sup>2</sup>. The different reactivity is further confirmed by CV studies which reveal that BDD electrodes exhibit a 400 mV larger

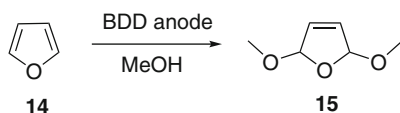


**Scheme 5** Anodic methoxylation of 4-*tert*-butyltoluene

**Scheme 6** Potential pathway of BDD mediated methoxylation reaction of 4-*tert*-butyltoluene



**Scheme 7** Methoxylation of furan



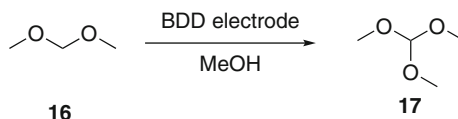
electrochemical window in methanol compared to graphite. This should promote a series of alkoxylation reactions which are not selective at conventional electrode materials (Scheme 6).

The direct electrochemical methoxylation of furan derivatives represents another technically relevant alkoxylation process. Anodic treatment of furan (**14**) in an undivided cell provides 2,5-dimethoxy-2,5-dihydrofuran (**15**). This particular product represents a twofold protected 1,4-dialdehyde and is commonly used as a C4 building block for the synthesis of N-heterocycles in life and material science. The industrial electroorganic processes employ graphite electrodes and sodium bromide which acts both as supporting electrolyte and mediator [60]. The same electrolysis of **14** can be carried out on BDD electrodes, but no mediator is required! The conversion is performed with 8% furan in MeOH, 3%  $\text{Bu}_4\text{N}^+\text{BF}_4^-$ , at 15 °C and 10 A/dm<sup>2</sup>. When 1.5 F/mol were applied, **15** is obtained in 75% yield with more or less quantitative current efficiency. Treatment with 2.3 F/mol is rendered by 84% chemical yield for **15** and a current efficiency of 84% [61, 62]. In contrast to the mediated process, furan is anodically oxidized in the initial step and subsequently methanol enters the scene (Scheme 7).

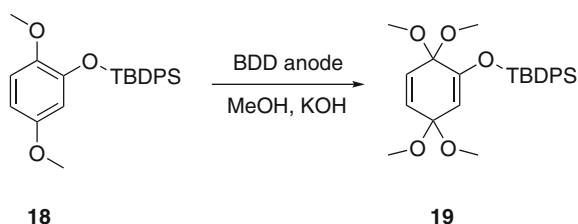
Trimethylorthoformate **17** is a highly activated C1 building block and a formic acid equivalent which is commonly applied in organic condensation reactions. **17** can be produced on an industrial scale by two major routes. The first starts with chloroform and sodium methanolate, but produces 3 equiv. of sodium chloride as waste. The second route is based on the acidic methanolysis of cyanhydric acid, which also produces stoichiometric amounts of ammonium chloride. Despite the reduced salt waste, the use and handling of cyanhydric acid mean high safety costs. Therefore, anodic methoxylation of formaldehyde dimethylacetal (**16**) to



**Scheme 8** Electroorganic synthesis of trimethylorthoformate



**Scheme 9** Electroorganic formation of benzoquinone ketal

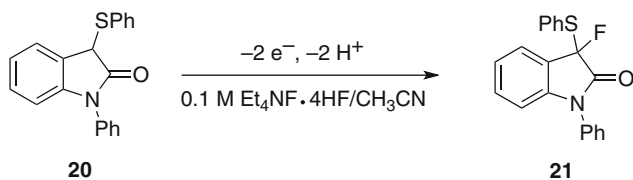


trimethylorthoformate (**17**) is an interesting alternative. The electrolysis can be performed on BDD electrodes in undivided cells. Product **17** is obtained in 75% selectivity with a partial conversion of 27% **16**. The consumed charge amounts to 0.4 F/mol, leading to a current efficiency of 41%. The electrolysis is carried out under ambient conditions in an undivided cell equipped with BDD anode and steel cathode (9 A/dm<sup>2</sup>). The electrolyte is based on 24% MeOH, 70% **16**, and LiN(SO<sub>2</sub>CF<sub>3</sub>)<sub>2</sub>/NaOCH<sub>3</sub> [63]. Most remarkably, the transformation cannot be performed on graphite electrodes. The clear advantages for the electrochemical synthesis of **17** on BDD electrodes are based on the attractive starting materials, reduced costs since no generation of waste salts are involved, and the safer operating requirements (Scheme 8).

Anodic treatment of 1,2- or 1,4-dihydroxy-substituted benzenes to form the corresponding quinones or masked congeners is well known, since they represent valuable synthetic intermediates [64]. Benzoquinone ketals of electron rich arenes like **18** can be challenging since the oxidative aryl–aryl coupling reaction usually competes. When using BDD anodes the benzoquinone ketal **19** is obtained in an almost quantitative manner, demonstrating the superior properties of this electrode material. Despite the basic conditions, no deblocking of the silyl-protected phenol moiety is observed [65] (Scheme 9).

## 4.2 Fluorination

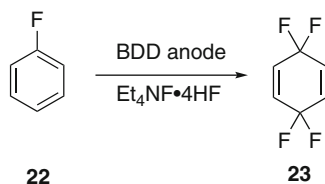
The electrochemical and chemical stability of diamond makes it an ideal electrode material for electrochemical fluorination reactions. The installation of fluorine  $\alpha$  to heteroatom-substituted positions can be anodically performed by hydrogen fluoride/triethylamine mixtures. The Fuchigami group studied several electrode materials for the fluorination of oxindole **20**. In this transformation to **21** only a



Anode	Yield 21 [%]
BDD	66
Pt	67
GC	31

**Scheme 10** Anodic fluorination using  $\text{Et}_4\text{NF} \cdot 4\text{HF/CH}_3\text{CN}$

**Scheme 11** Fluorination of fluorobenzene on BDD

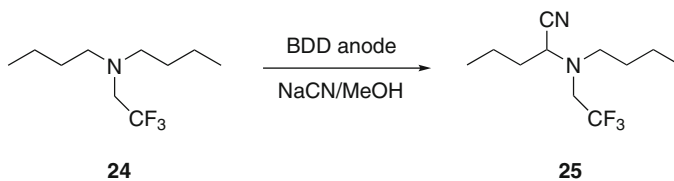


slightly superior behavior was found for BDD. The yields are comparable to platinum as anodic material. Glassy carbon turned out to be less efficient (Fuchigami, 2009 personal communication) (Scheme 10).

The anodic fluorination of 1,4-difluorobenzene (**22**) using BDD electrodes was reported more than a decade ago and represents the first synthetic use of BDD anodes.  $\text{NEt}_4\text{F} \cdot 4\text{HF}$  was employed as electrolyte. The electrochemical conversion was monitored by gas chromatography and the identity of the product **23** found by comparison with authentic material. The electrolysis was conducted at constant voltage conditions with 2.75 V (vs  $\text{Ag/Ag}^+$ ) at the BDD anode. Further preparative details for the formation of 3,3,6,6-tetrafluoro-1,4-cyclohexadiene (**23**) were not provided [66] (Scheme 11).

### 4.3 Cyanation

The anodic cyanation reaction allows the direct installation of cyanide without leaving groups. The cyanide acts in the electrochemical conversion similar to fluoride. After oxidation of the organic substrate the nucleophilic cyanide enters the reaction scene forming a less electron rich product which is deactivated for further anodic conversions. Therefore, the electrochemical cyanation reaction has some significance for aromatic substrates [67] (Scheme 12).

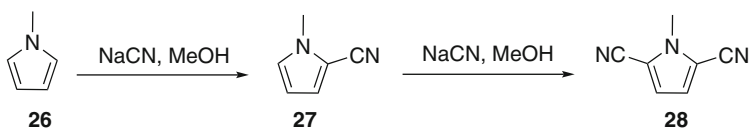


Electrode	Current efficiency [%]
BDD	77
Pt	75
GC	0

**Scheme 12** Anodic cyanation reaction

### 4.3.1 Cyanation of Tertiary Amines

The electrochemical cyanation reaction at BDD electrodes was investigated by the Fuchigami group using aliphatic and heteroaromatic amines as substrates. Anodic treatment of *N,N*-dibutyl-*N*-(2,2,2-trifluoroethyl)amine (**24**) installed a cyano moiety on a non-fluorinated alkyl portion forming the amino nitrile **25**. Best yields were found for BDD or platinum as anode materials, wherein BDD is only slightly superior [68]. The cyanation reaction of *N*-methylpyrrole (**26**) was performed under the same conditions, leading to the mono (**27**) and dicyanated products (**28**). Platinum as well as BDD anodes gave both compounds in excellent to total current efficiency. In contrast, glassy carbon gave rather poor results [68]. In conclusion, the BDD electrodes are very useful in the cyanation reaction and behave very much like platinum anodes. Since the performance is best in several examples, BDD might be the anode material of choice (Scheme 13).

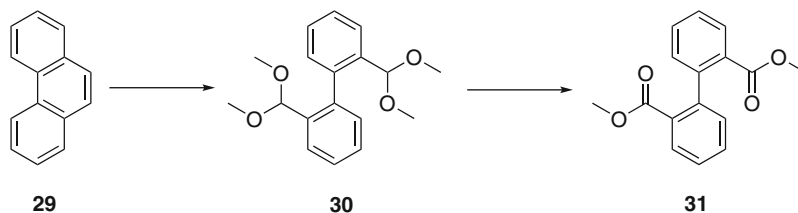


**Scheme 13** Anodic cyanation reaction of pyrrole

## 4.4 Cleavage of C–C-Bonds

Exposed multiple bonds of angular arenes are specifically prone to oxidation. The synthetic value of such double bonds arises from their high reactivity towards simple electrophiles, enophiles, and radicals. Heavy metal catalysis, periodate oxidation, and ozonolysis are the standard tools for oxidative bond cleavage in these substrates. For economic and ecological reasons, technically applicable alternatives are of great interest. Phenanthrene (**29**) represents a typical substrate

with such an exposed and activated multiple bond. Electrogenerated oxyl species on BDD selectively attack the double bond in positions 9 and 10 of **29**. Remarkably, aliphatic olefins proved to be stable towards electrochemical oxidation on BDD anodes in aqueous media [69]. Phenanthrene was successfully electrolyzed using acidic methanolic electrolytes [41]. The electrolysis was performed with 2% **29** and 0.5%  $\text{H}_2\text{SO}_4$  in methanol with a current density of  $3.4 \text{ A/dm}^2$  at  $54 \text{ }^\circ\text{C}$  and an applied charge of  $10 \text{ F/mol } \mathbf{29}$  ( $4 \text{ F/mol}$  would be required for the generation of **30**). Applying these conditions gave **30** and **31** in 15% and 39% yield, respectively. In spite of the C–C-bond cleavage of the dibenzyl derivative **13** described before, in this case the diester **31** represents the major product and not the fully masked dialdehyde **30** (Scheme 14).

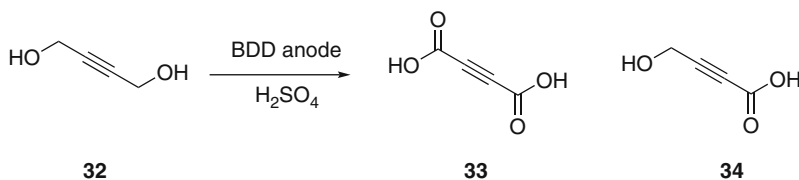


**Scheme 14** Degradation of phenanthrene

#### 4.5 Oxidation of Activated Carbon Atoms

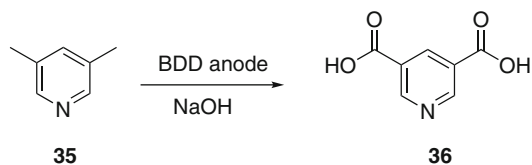
A variety of organic transformations in aqueous media using BDD anodes have been studied. The pronounced stability of the BDD material in the presence of water makes it obvious that it should be used in oxidation processes. However, the yields are usually low and therefore less attractive for synthetic purposes. The BASF company investigated the anodic oxidation of butyn-1,4-diol **32**. The anodic treatment in an electrolyte of dilute sulfuric acid gave small amounts of the monoacid **33** and the acetylene dicarboxylic acid **34**. The moderate product efficiency might be attributed to electrochemical incineration processes (Scheme 15).

Anodic treatment of 3,5-lutidine (**35**) on BDD electrodes also turned out to be challenging. Only traces of the desired pyridine-3,5-dicarboxylic acid (**36**) could be detected. As electrolyte a dilute NaOH solution was employed. The mineralization and decomposition seem to be the dominant reaction pathways (Scheme 16).



**Scheme 15** Oxidation of 1,4-butynediol in aqueous electrolyte

**Scheme 16** Unsuccessful synthesis of pyridine-3,5-dicarboxylic acid

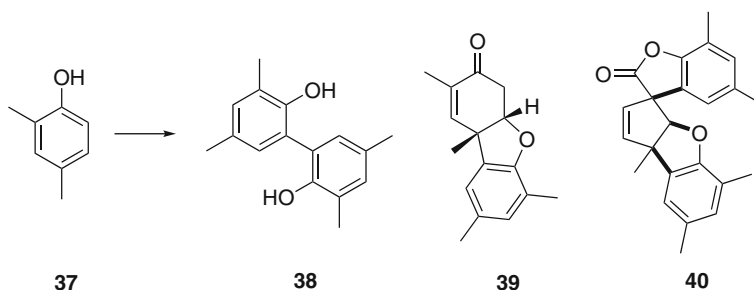


## 4.6 Anodic Phenol Coupling Reaction

In natural products biphenols represent very common motifs [70]. Such entities are widely used in technical applications [71, 72]. For the oxidative coupling process of electron rich arenes, several methodologies have been elaborated. In particular, the selective *ortho*-coupling process of phenols has been addressed by a variety of catalytic and stoichiometric approaches. In these methods sterically hindered *tert*-butylated phenols as well as naphthols turned out to be the superior substrates [73] whereas simple phenols and derivatives thereof with methyl substituents show a pronounced tendency to side-reactions. Most oxidative aryl–aryl coupling reactions do not rely on leaving functionalities in the substrates. Commonly, only hydrogen atoms are sacrificed in course of the reaction. Consequently, such transformations are of high atom economy and therefore of particular interest. Application of BDD electrodes in the anodic coupling of phenolic substrates was not very promising from the very beginning since several previous studies have underlined the mineralization of phenols, naphthols, and chlorinated derivatives [74]. Moreover, in the presence of water or aqueous media a sequence of degradation products is observed, which is consistent with the simplified mechanistic described above. Thus, control of the intermediate oxyl species represents the key for using BDD as a synthetic tool and avoiding the competitive mineralization process.

### 4.6.1 Anodic Homo-Coupling of Phenolic Substrates

Some simple biphenols equipped with methyl groups, e.g., 3,3',5,5'-tetramethyl-2,2'-biphenol **38**, have attracted attention as important components of highly potent ligand systems [75–86]. Remarkably, the sustainable synthesis of such biphenols is rather challenging despite their simple scaffolds. In particular, methyl-substituted phenols are prone to side reactions. This is especially the case when 2,4-dimethylphenol (**37**) is oxidatively treated. Upon anodic conversion **37** is preferably transformed into polycyclic architectures [87]. Direct electrolysis in basic media provided only traces of the desired biphenol **38** and the dominating components of the product mixture consisted of Pummerer's ketone **39** and the consecutive pentacyclic spiro derivative **40** [88]. For an efficient electrochemical access to 3,3',5,5'-tetramethyl-2,2'-biphenol (**38**) we developed a boron-based template strategy [89, 90]. This methods requires a multi-step protocol but can be conducted on a multi-kilogram scale (Scheme 17).



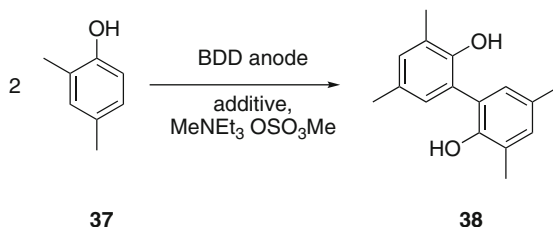
Anode	Solvent	Product ratio 38:39:40
Pt	MeOH, Ba(OH) <sub>2</sub> ·8H <sub>2</sub> O	1:11:6
BDD	neat + 11 % H <sub>2</sub> O Et <sub>3</sub> NCH <sub>3</sub> O <sub>3</sub> SOCH <sub>3</sub>	18:1:0

**Scheme 17** Product distribution for the anodic coupling of 2,4-dimethylphenol

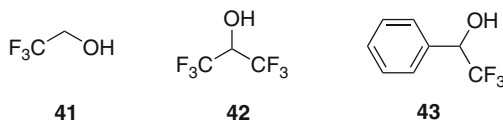
The direct conversion of almost neat phenol **37** on BDD electrodes has been elaborated. The electrolysis in solvent-containing electrolytes ended up mainly in mineralization processes. The first strategy for control of these intermediates involves the use of statistics: Since the oxidized intermediates seem not to meet a suitable reaction partner before other oxyl species could attack, the concentration of the substrate has to be increased. When the electrolysis was carried out in almost neat phenol as electrolyte, the over oxidation could be circumvented. The desired biphenol **38** was obtained in a chemoselectivity of about 90–95%. The chemical incineration is dramatically reduced if the electrolysis is performed to a partial conversion of about 30%. The resulting product is then very clean and the starting material **37** is efficiently recycled. Somehow this protocol was restricted to 2,4-dimethylphenol (**37**). When other phenols were subjected to this method, either no detectable products were found or the electrolysis resulted in a tarry residue. The latter was especially found with very electron rich phenols like sesamol [91]. Consideration of the free path length of the oxyl radicals involved reveal that it might be only in the range of some nanometers (the range can be assumed when free hydroxyl radicals are anticipated and the simulation is based on diffusion controlled recombination of these radicals). The exchange from the bulk to the vicinity of BDD electrode seems to be essential. The success in the conversion of **37** to **38** can be attributed to the low viscosity of the starting material (Scheme 18).

In former investigations the use of organic solvent was inferior because of the preferential anodic degradation [91]. Therefore, more redox-stable additives, e.g., fluorinated alcohols, were envisioned. Screening of appropriate solvents for the conversion of **37** to **38** excluded simple acids and *tert*-butanol as potential additives [27]. Primary alcohols with fluorous moieties in  $\beta$  position like **41** can be employed.

**Scheme 18** Phenol coupling on BDD anodes using additives



**Scheme 19** Some tested additives



**Table 2** Anodic treatment of **37** with different additives

Additive	$T$ ( $^{\circ}\text{C}$ )	$j$ ( $\text{mA}/\text{cm}^2$ )	<b>38</b> (%) <sup>a</sup>	CE (%) <sup>b</sup>
<b>41</b>	45	4.7	26	26
<b>42</b>	45	4.7	47	47
<b>43</b>	70	4.7	43	43

Reaction conditions: 2.44 g**37**, 30 mL additive, 0.68 g supporting electrolyte, BDD anode, nickel cathode,  $Q = 1.0$  F per mol**37**

<sup>a</sup>Determined from crude product by GC using an internal standard

<sup>b</sup>Current efficiency

Best results were obtained when HFIP (**42**) was added. Furthermore, this conversion is very clean and 2,4-dimethylphenol (**37**) is transformed to **38** in 47% yield. Application of abundant electric current renders a lower yield and product quality of **38**. A trifluoromethyl group of the additive can be substituted by a phenyl moiety in order to stabilize the oxyl spin center. Therefore, alcohol **43** provides results similar to the additive HFIP. In conclusion, the chemical yield reached about 50%, a maximum when a current of 1–1.3 F was applied per mole **37** and represents a reasonable compromise between yield and current efficiency [27] (Scheme 19) (Table 2).

The elaborated conditions for the anodic coupling for **37** were applied to a variety of substrates in order to determine the scope. The first requirement for conversion of substrates is the solubility in the electrolyte. Sterically demanding phenol **44** could be converted in moderate yield (Table 3). Better yields were obtained with 2-naphthol (**45**) providing binol as sole product. Most remarkably, sesamol (**46**) was anodically coupled in very good yield. Moreover, halogenated phenolic substrates **47–50** were selectively coupled to the corresponding biphenols. The low yield is based on the electron-withdrawing nature of the substituents. **47** represents the first direct example of oxidative coupling of such a fluorinated substrate. Although the biphenols are obtained in moderate yield, the protocol is easy to perform and practical. When only 1 F per mol phenol/substrate electric current is applied a clean reaction mixture is obtained consisting of products, starting material, and electrolyte [27] (Scheme 20).

**Table 3** Electrochemical synthesis of biphenols

Substrate	$j$ (mA/cm <sup>2</sup> )	Yield (product) (%) <sup>a</sup>	CE (%) <sup>b</sup>
<b>44</b> <sup>c</sup>	4.7	22	22
<b>45</b> <sup>d</sup>	4.7	41	41
<b>46</b> <sup>e</sup>	2.8	74	74
<b>47</b>	4.7	13	13
<b>48</b>	4.7	30	30
<b>49</b> <sup>f</sup>	4.7	24	12
<b>50</b>	4.7	30	30

Reaction conditions: 0.02 mol phenol, 0.1 M supporting electrolyte in 30 mL HFIP (**37**), BDD anode, nickel cathode,  $Q = 1.0$  F per mol phenol

<sup>a</sup>Isolated biphenol

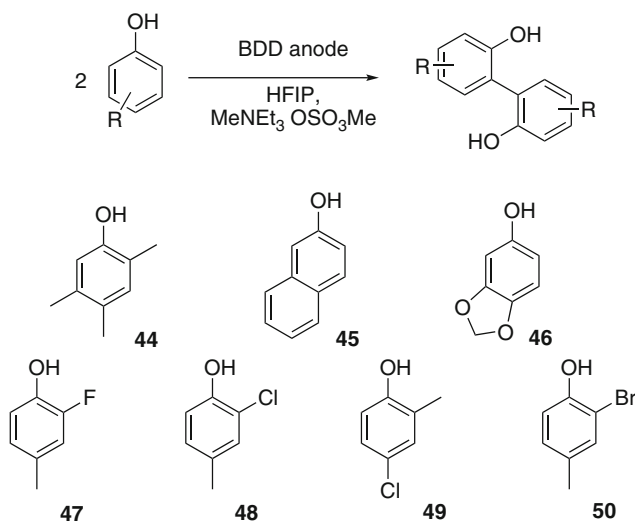
<sup>b</sup>Current efficiency

<sup>c</sup>0.01 mol phenol

<sup>d</sup>0.005 mol phenol

<sup>e</sup>0.012 mol phenol

<sup>f</sup>0.04 mol phenol,  $Q = 2.0$  F per mol phenol

**Scheme 20** Selection of some electrolyzed phenolic substrates

#### 4.6.2 Phenol–Arene Cross-Coupling and Nonsymmetrical Coupling Products

The cross-coupling reaction currently provides the best and most versatile access to nonsymmetric biaryls [92–97]. Several transformations belong to the standard repertoire of organic synthesis and require mostly leaving functionalities on both reaction partners. Additionally, toxic transition metal catalysts based, e.g., on



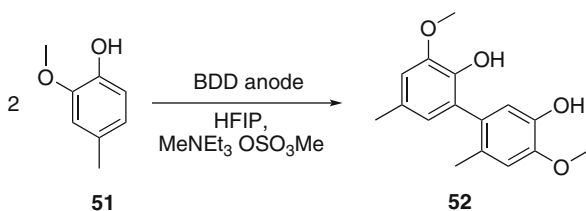
palladium are necessary for the arylation reaction [98–101]. The most common transformations exploit arylboronic acids, arylstannanes, benzoic acid derivatives, arylzinc, or arylmagnesium reagents producing waste by the used leaving functionalities [102–107]. The direct oxidative cross-coupling of arenes is a modern concept which only sacrifices hydrogen atoms and is therefore very attractive in terms of atom economy. Such an approach requires a particular reactivity of one reaction partner towards an employed oxidant which commences the reaction sequence. The oxidized intermediate will attack the other reaction partner and the transformation can be accomplished. This concept was shown by Kita et al. using stoichiometric amounts of phenyliodine(III)-bis(trifluoroacetate) [108]. Unfortunately, the anodic treatment of arenes usually ends up with the formation of the homo-coupling product because the oxidation potential is the key property for the reactivity. In a very few examples the reactive radical cation can be trapped by an abundant reaction partner which is not affected by the electrode in the applied potential range [109] (Table 4).

Anodic treatment of 4-methyl guaiacol (**51**) by the elaborated protocol using HFIP at BDD anodes yields exclusively the *ortho-meta* coupled product **52**. Based on the previous results a selective *ortho* coupling to symmetric products was anticipated.

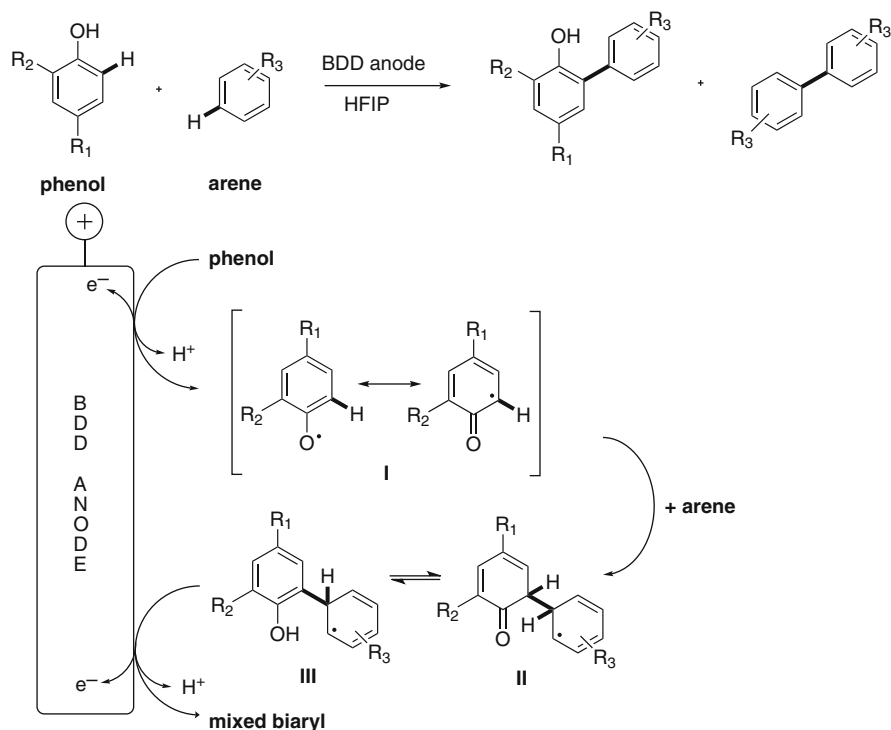
The current density has a dramatic influence on the yield of **52** and reveals that more than one electrode reaction is involved in the sequence. When the current density is in the range of 2.8–4.7 mA/cm<sup>2</sup>, **52** is directly obtained in about 30% yield. The rationale for the formation of **52** starts with the direct or indirect generation of phenoxyl radicals at the BDD anode. Since the used conditions will provide concentrations of oxyl spin centers, which exclude a recombination, the transformation has to follow a different mechanistic course. The anodic treatment will cause an Umpolung effect because the electron rich phenol is oxidized [110–113]. Such phenoxyl species are still electrophilic despite the liberation of a proton [114–119]. The electrophilic attack occurs at the most electron rich position of the reaction partner which provides the observed connectivity in **52** (Scheme 21).

**Table 4** Influence of the current density

$j$ (mA/cm <sup>2</sup> )	Current (F/mol)	Yield (%)	CE (%)
2.8	1.0	27	27
4.7	1.0	33	33
9.5	1.0	14	14



**Scheme 21** Unusual dehydrodimer of 4-methyl guaiacol (**51**)



**Scheme 22** Potential rationale for the anodic cross-coupling process

Although the role of HFIP is currently not clear, the transformation requires this or a similar additive. However, it is known that **34** enhances the stability of radical intermediates by several magnitudes [120, 121]. Inspired by the formation of **52** and the potential rationale, a novel concept for the first phenol–arene cross-coupling reaction was elaborated (Scheme 22). The transformation starts with the electro-generation of the phenoxyl species **I** which represents a reactive intermediate. Excess of arene will trap this species, providing the intermediate **II**. This radical or its tautomeric species **III** will experience directly or indirectly the final oxidation, furnishing the cross-coupling product. Several different electron rich arenes were subjected to the cross-coupling with the 4-methyl guaiacol as phenolic reactions partner. Remarkably, no dehydrodimer **52** was detected. The electrolysis with 1,2,4-trimethoxybenzene yields, besides the desired cross-coupling product (PA), some concomitant oxidative homo-coupling product of the arene (AA). Because of the electron rich nature of this particular arene, the side-reaction cannot be suppressed (Table 5). When the amount of electric current is doubled and the current density lowered, the yield as well as the selectivity for the cross-coupling product **53** is tremendously increased. Employing 1,3,5-trimethoxy benzene affords the mixed biaryl **54** in good selectivity, wherein the current density has little influence

**Table 5** Electrolysis conditions: BDD anode, nickel cathode, 30 mL HFIP, 50 °C, P:A = 1:10

Coupling product	$j$ (mA/cm <sup>2</sup> )	Current (F/mol A)	PA: AA <sup>a</sup> (GC)	Yield of PA (%)	CE (%)
<b>53</b>	4.7	1.0	1:1	17	34
	4.7	2.0	1.5:1	39	39
	2.8	2.0	5:1	47	47
<b>54</b>	2.8	3.0	1.5:1	34	22
	4.7	1.0	11:1	12	23
	4.7	2.0	7:1	16	16
<b>55</b>	4.7	1.0	>50:1	18	37
	4.7	2.0	15:1	14	15
	2.8	2.0	>50:1	8	8
<b>56</b>	4.7	1.0	>50:1	11	23
	4.7	2.0	13:1	18	15
<b>57</b>	4.7	2.0	9:1	30	30
	2.8	2.0	23:1	25	25
<b>58</b>	4.7	1.0	>50:1	10	19
	4.7	2.0	>50:1	18	15
<b>59</b>	4.7	2.0	12:1	33	33
<b>60</b>	4.7	1.0	2.5:1	11	22

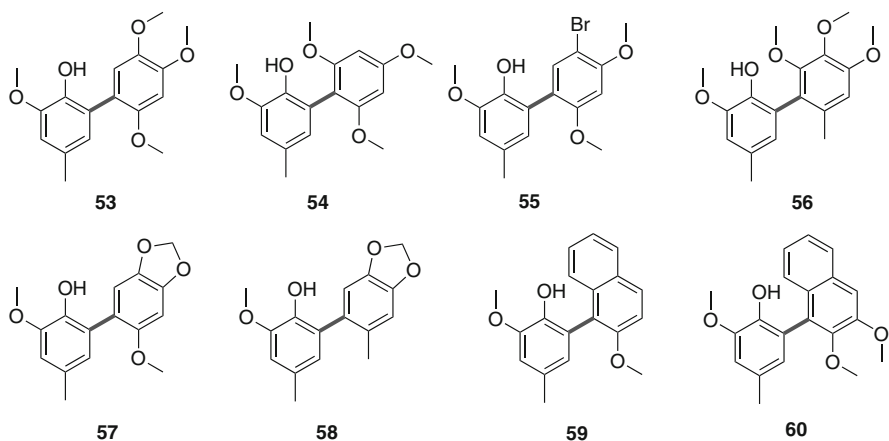
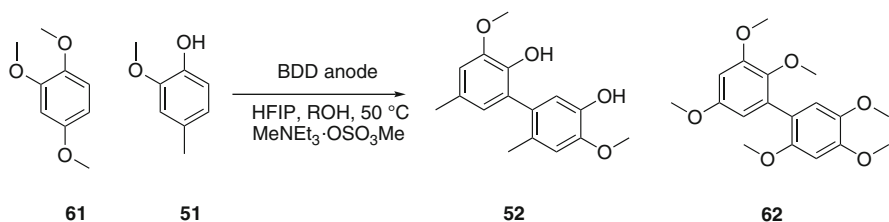
<sup>a</sup>PA: cross-coupling product; AA: homo-coupling product of the arene component

(Table 5). The anodic cross-coupling reaction in the undivided cell is compatible with bromo substrates as product **55** reveals.

The observed chemoselectivity is unique. Anodic treatment on BDD of 3,4,5-trimethoxy toluene results in the exclusive formation of the mixed biaryl **56**. This method can be further performed with benzo[1,3]dioxole-containing arenes as reaction partners, giving biaryls **57** and **58** in acceptable yields. Furthermore, naphthalene moieties can be directly located onto 4-methyl guaiacol as the products **59** and **60** reveal. This novel cross-coupling can be expanded to other phenolic reaction partners as well [28]. The displayed selection of mixed biaryls **53–60** is accessible in a single step. In the workup protocol, HFIP is almost quantitatively recovered since it represents the most volatile component in the electrolyte. In addition, nonconverted starting materials can be recycled by short path distillation with approximately 80% efficiency (Scheme 23).

The efficiency of the mixed electrolysis between phenol and arene components can be substantially ameliorated and is the subject of current research. The application of very pure HFIP in this electrolysis led to loss of selectivity and dramatically inferior yield. Therefore, an optimized protocol was developed which requires a specific amount of water or methanol as mediator in the electrolyte. This allows the formation of the biaryl **53** in exclusive selectivity and in almost 70% isolated yield.

These results illustrate several important points. The mediating oxyl species are crucial for the transformation and seem to be stabilized by the fluorinated media. A supramolecular hydrogen bonding network can be anticipated as outlined in Scheme 24. Furthermore, BDD electrodes can not only be used for destructive

**Scheme 23** Selection of anodic cross-coupling products

Ration of 61:51	HFIP + ROH	Yield	Ration of 52:62
1:5	Pure HFIP	21 %	1:3
1:5	9 Vol% H <sub>2</sub> O	67 %	85:1
1:5	18 Vol% MeOH	69 %	90:1
1:3	18 Vol% MeOH	69 %	>90:1

**Scheme 24** Optimized protocol

purposes. The cross-coupling electrolysis underlines the potential of this research area which is just emerging. Exploitation of the intermediate oxyl spin centers by the development of suitable additives will be the key to make this methodology attractive to several other anodic cross-coupling reactions.

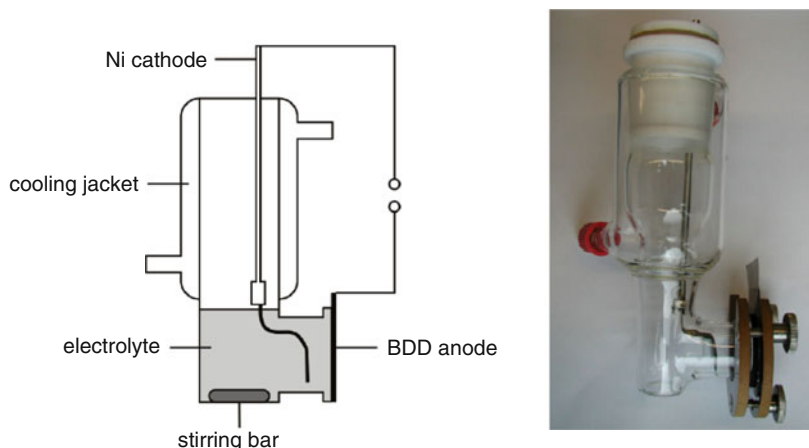
## 5 Anodic Stability of BDD Materials

Diamond coatings – and in particular semiconducting variations like boron-doped diamond – are currently available on different support materials from various suppliers. The most prominent supports utilize silicon, titanium, or niobium.

Originally, the conductive diamond surfaces were developed for electrolysis in aqueous media, e.g., waste water treatment or ozone production. Under these conditions the coating and support stay intact even when the electrochemically very stable diamond layer may be perforated. If a pinhole is formed and the support comes in contact with the aqueous electrolyte, insoluble oxides of the support material will be formed by the anodic reaction of water. In particular, when silicon is used as support material, the silicon dioxide formed will lead to an insulating protection. Such mechanisms efficiently deactivate any pinholes eventually appearing and further corrosion is avoided. This passivation pathway of pinholes no longer applies if the electrolysis is performed in alcohols, e.g., methanol or phenol, because no protective oxide layer could be formed. In these organic media, well soluble silicon species will be generated anodically. Upon formation they can diffuse into the bulk and further anodic dissolution of the support is allowed. The BDD layer will still remain intact, whereas the support is continuously eroded. Finally, the diamond surface will collapse mechanically and open up the door for a quick and dramatic corrosion. The microscopic event turns into a macroscopic visible perforation. The disintegration of the electrode will then occur within minutes. This effect is not limited to silicon. Titanium as well as niobium also shows quick degradation under anodic treatment in organic media. Therefore, good quality diamond coatings are required when performing electrochemistry in organic media. Currently, 20  $\mu\text{m}$  thick diamond layers as a result of multiple diamond coatings are available and should work for these electrochemical transformations. However, development of boron-doped diamond coatings on anodically inert support materials is currently under way. Such electrodes will alleviate current concerns about the employment of BDD electrodes and will provide appropriate BDD electrode material for a wide range of applications. More innovative supports might be based on conductive ceramics or carbon materials, e.g., glassy carbon. Self-healing support materials could be an alternative strategy, providing reasonable stable BDD electrodes.

## 6 Electrolysis Cells for the Use of BDD Electrodes

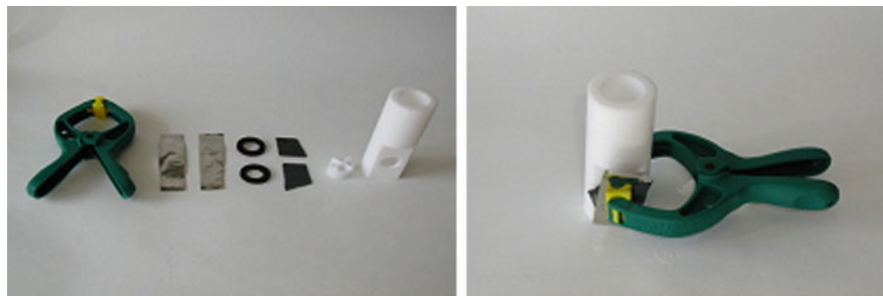
Since boron-doped diamond electrodes are commercially available, most of these suppliers offer a wide variety of electrolysis cells. Modular electrochemical cells equipped with BDD electrodes have been reported in detail [122]. However, most of these cells were designed for waste water treatment and were not suitable for electrosynthesis in organic media. Electrolysis cells for synthetic purposes designed for a small volume made of organic-compatible materials are required. Additionally, any contact of the support with the organic electrolyte has to be strictly eliminated in order to avoid the corrosion. Most BDD electrodes are on a silicon support which causes eventual loss of the BDD electrode by the brittle nature of crystalline silicon. Consequently, the material used for sealing has to be inert but soft enough to avoid friction of the silicon support. The available BDD



**Fig. 5** Preparative electrolysis cell (40–120 mL) for organic transformations on BDD electrodes

electrodes usually exhibit a planar geometry, with BDD coating on one side. For experiments with electrolyte volumes in the range 40–120 mL, an electrolysis cell equipped with flange fittings has been developed (Fig. 5). The cell depicted is undivided and the BDD electrode is employed as anode. A net of nickel serves as cathode. The BDD electrode surface is approx. 5 cm<sup>2</sup>. The flange arrangement is fixed by a standard flange clamp [91]. Such an assembly allows the use of common BDD electrodes, which are easily contacted by a metal foil on the back. If the applied voltage on such an electrolysis cell is significantly too high, the oxide layer on the support, e.g., silicon, causes the electric resistance. Treatment of the support face with sandpaper will solve this problem. A significant challenge was the sealing between BDD electrode and the flange of glass. Best results were obtained by a sealing made of EPDM, a highly resistant terpolymer. EPDM foils are freely available since they are widely used for garden ponds and chemical sealings. Thermal stability was found up to 120 °C. A swelling is observed with hot phenols. Hot organic and aggressive media as well as highly anodic potentials do not seem to affect the sealing over a long process time. The displayed cell geometry offers the possibility of heating the electrolyte. Usually a sand bath or silicon oil heating was employed. The cooling jacket in the upper part keeps more volatile components in the electrolysis compartment [91].

One way to control the reactivity of the intermediates appearing is the electrolysis performance at high concentrations of substrate up to 90% of the electrolyte composition. Additionally, a good mass transport from the anode into bulk is important to avoid electrochemical incineration. For such preparative work a conceptually novel architecture is required. The two major issues are an electrolysis cell on the micro scale and avoiding nonemployed volumes by efficient stirring of the electrolyte. A micro electrolysis cell with volumes of 0.7–4 mL has been designed (Fig. 6). All components are made of Teflon™ or coated by this inert material. A cylindrical



**Fig. 6** Micro electrolysis cell; assembled and disassembled

Teflon™ tube which is closed on one side was routed off in a parallel fashion. Onto these planes the sealing and electrode materials are placed. A clamp will tighten the operating cell by gentle pressing.

## 7 Outlook

The nondestructive and synthetic application of boron-doped diamond electrodes in preparative organic chemistry has only just commenced. Therefore, only a small portion of the synthetic options has been explored. The unique electrochemical characteristics of the semiconducting diamond surface will allow manifold applications and realization of novel electrosynthetic concepts. Because BDD will tolerate extremely strong oxidizing species, the fluorination and even fluorine generation of BDD seems to be an interesting subject. The key issue for anodic transformations will be the efficient control of the reactive intermediates generated on BDD. Possible strategies for diminishing mineralization encounter ultrastable electrolytes. Alternatively, the exchange between electrode surface and bulk should be enhanced for diluting the reactive intermediates. Such approaches may include electrolysis in micro reactors or combination with ultrasonic methods.

**Acknowledgment** The authors are very grateful for the support by the SFB 813 Chemistry at Spin Centers (DFG).

## References

1. Steckhan E, Arns T, Heineman WR, Hilt G, Hoormann D, Jorissen J, Kroner L, Lewall B, Pütter H (2001) Environmental protection and economization of resources by electroorganic and electroenzymatic syntheses. *Chemosphere* 43:63–73
2. Weissermel K, Arpe H, Lindley CR (eds) (1997) *Industrial organic chemistry*, 3rd completely revised edition. VCH, Weinheim
3. Fry AJ (1989) *Synthetic organic electrochemistry*, 2nd edn. Wiley, New York

- Schäfer HJ (2004) In: Schäfer HJ, Bard AJ, Stratmann M (eds) *Organic electrochemistry*. Wiley-VCH, Weinheim, pp 125–170
- Schäfer HJ (2001) In: Lund H, Hammerich O (eds) *Organic electrochemistry*, 4th edition, revised and expanded. Marcel Dekker, New York, pp 207–222
- Hilt G (2003) Convergent paired electrolysis for the three-component synthesis of protected homoallylic alcohols. *Angew Chem Int Ed* 42:1720–1721
- Ishifune M, Yamashita H, Matsuda M, Ishida H, Yamashita N, Kera Y, Kashimura S, Masuda H, Murase H (2001) Electro reduction of aliphatic esters using new paired electrolysis systems. *Electrochim Acta* 46:3259–3264
- Chen YL, Chou TC (1996) Paired electrooxidation part 3. Production of n-butyric acid from n-butanol. *J Appl Electrochem* 26:543–545
- Pütter H (2001) In: Lund H, Hammerich O (eds) *Organic electrochemistry*, 4th ed., revised and expanded. Marcel Dekker, New York, p 1259
- Hildebrand F, Kohlmann C, Franz A, Lütz S (2008) Synthesis, characterization and application of new rhodium complexes for indirect electrochemical cofactor regeneration. *Adv Synth Catal* 350:909–918
- Kohlmann C, Maerkle W, Lütz S (2008) Electroenzymatic synthesis. *J Mol Catal B Enzym* 51:57–72
- Maerkle W, Lütz S (2008) Electroenzymatic strategies for deracemization, stereoinversion and asymmetric synthesis of amino acids. *Electrochim Acta* 53:3175–3180
- Hildebrand F, Lütz S (2007) Electroenzymatic synthesis of chiral alcohols in an aqueous – organic two-phase system. *Tetrahedron Asymmetry* 18:1187–1193
- Rao N, Lütz S, Seelbach K, Liese A (2006) In: Liese A (ed) *Industrial biotransformations*, 2nd completely revised and extended edition. Wiley-VCH, Weinheim, pp 115–145
- Nad S, Breinbauer R (2004) Electroorganic synthesis on the solid phase using polymer beads as supports. *Angew Chem Int Ed* 43:2297–2299
- Nad S, Breinbauer R (2005) Electroorganic synthesis of 2,5-dialkoxydihydrofurans and pyridazines on solid phase using polymer beads as supports. *Synthesis* 3654–3665
- Iniesta J, Michaud PA, Panizza M, Comninellis C (2001) Electrochemical oxidation of 3-methylpyridine at a boron-doped diamond electrode: application to electroorganic synthesis and wastewater treatment. *Electrochem Commun* 3:346–351
- Zollinger D, Griesbach U, Putter H, Comninellis C (2004) Methoxylation of p-tert-butyltoluene on boron-doped diamond electrodes. *Electrochem Commun* 6:600–604
- Marselli B, Garcia-Gomez J, Michaud PA, Rodrigo MA, Comninellis C (2003) Electrogeneration of hydroxyl radicals on boron-doped diamond electrodes. *J Electrochem Soc* 150: D79–D83
- Rodrigo MA, Michaud PA, Duo I, Panizza M, Cerisola G, Comninellis C (2001) Oxidation of 4-chlorophenol at boron-doped diamond electrode for wastewater treatment. *J Electrochem Soc* 148:D60–D64
- Panizza M, Michaud PA, Cerisola G, Comninellis C (2001) Anodic oxidation of 2-naphthol at boron-doped diamond electrodes. *J Electroanal Chem* 507:206–214
- Iniesta J, Michaud PA, Panizza M, Cerisola G, Aldaz A, Comninellis C (2001) Electrochemical oxidation of phenol at boron-doped diamond electrode. *Electrochim Acta* 46:3573–3578
- Comninellis C, Chen G (eds) (2010) *Electrochemistry for the environment*. Springer, New York, NY
- Fujishima A, Einaga Y (eds) (2005) *Diamond electrochemistry*. BKC; Elsevier, Amsterdam
- Hickling A (1940) Hydrogen overvoltage at high current densities. I. Influence of electrode material, current density and time in aqueous solution. *Trans Faraday Soc* 36:1226
- Hickling A, Hill S (1947) Oxygen overvoltage. 1. The influence of electrode material, current density, and time in aqueous solution. *Discuss Faraday Soc* 1:236–246
- Kirste A, Nieger M, Malkowsky IM, Stecker F, Fischer A, Waldvogel SR (2009) ortho-Selective phenol-coupling reaction by anodic treatment on boron-doped diamond electrode using fluorinated alcohols. *Chem-Eur J* 15:2273–2277



28. Kirste A, Schnakenburg G, Stecker F, Fischer A, Waldvogel SR (2010) Anodic phenol-arene cross-coupling reaction on boron-doped diamond electrodes. *Angew Chem Int Ed* 49:971–975
29. Koppenol WH, Liebman JF (1984) The oxidizing nature of the hydroxyl radical – a comparison with the ferryl ion (FeO<sub>2</sub><sup>+</sup>). *J Phys Chem* 88:99–101
30. Honda K, Yamaguchi Y, Yamanaka Y, Yoshimatsu M, Fukuda Y, Fujishima A (2005) Hydroxyl radical-related electrogenerated chemiluminescence reaction for a ruthenium tris (2, 2')bipyridyl/co-reactants system at boron-doped diamond electrodes. *Electrochim Acta* 51:588–597
31. Berkessel A, Adrio JA (2006) Dramatic acceleration of olefin epoxidation in fluorinated alcohols: activation of hydrogen peroxide by multiple H-bond networks. *J Am Chem Soc* 128:13412–13420
32. Berkessel A, Adrio JA, Hüttenhain D, Neudörfl JM (2006) Unveiling the “booster effect” of fluorinated alcohol solvents: aggregation-induced conformational changes and cooperatively enhanced H-bonding. *J Am Chem Soc* 128:8421–8426
33. Kirste A (2010) PhD thesis, University of Bonn
34. Yoshida J, Kataoka K, Horcajada R, Nagaki A (2008) Modern strategies in electroorganic synthesis. *Chem Rev* 108:2265–2299
35. Lehmann T, Schneider R, Weckbecker C, Dunach E, Olivero S (2002) PCT Int Appl WO 02/16671
36. Lehmann T, Schneider R, Reufer C, Sanzenbacher R (2001) GDCh-Monographie 251–258
37. Bilz J, Hateley M, Lehmann T, Reufer C, Sanzenbacher R, Weckbecker C (2006) *Eur Pat Appl EP* 1 63 1702
38. Looft J, Vössing T, Ley J, Backes M, Blings M (2008) *Eur Pat Appl EP* 1989944 A1
39. Tafel J, Pfeffermann E (1902) Elektrolytische Reduktion von Oximen und Phenylhydrazonen in schwefelsaurer Lösung. *Ber Dtsch Chem Ges* 35:1510–1518
40. Martin HB, Argoitia A, Landau U, Anderson AB, Angus JC (1996) Hydrogen and oxygen evolution on boron-doped diamond electrodes. *J Electrochem Soc* 143:L133–L136
41. Griesbach U, Zollinger D, Pütter H, Comminellis C (2005) Evaluation of boron doped diamond electrodes for organic electrosynthesis on a preparative scale. *J Appl Electrochem* 35:1265–1270
42. Schopohl MC, Siering C, Kataeva O, Waldvogel SR (2003) Reversible enantiofacial differentiation of a single heterocyclic substrate by supramolecular receptors. *Angew Chem Int Ed* 42:2620–2623
43. Siering C, Grimme S, Waldvogel SR (2005) Direct assignment of enantiofacial discrimination on single heterocyclic substrates by self-induced CD. *Chem-Eur J* 11:1877–1888
44. Schopohl MC, Faust A, Mirk D, Fröhlich R, Kataeva O, Waldvogel SR (2005) Synthesis of rigid receptors based on triphenylene ketals. *Eur J Org Chem* 14:2987–2999
45. Bomkamp M, Siering C, Landrock K, Stephan H, Fröhlich R, Waldvogel SR (2007) Extraction of radio-labelled xanthine derivatives by artificial receptors: deep insight into the association behaviour. *Chem Eur J* 13:3724–3732
46. Schade W, Bohling C, Hohmann K, Bauer C, Orghici R, Waldvogel SR, Scheel D (2007) Photonic sensors for security applications. *Photonic International* 32–34
47. Schade W, Bohling C, Hohmann K, Bauer C, Orghici R, Waldvogel SR, Scheel D (2006) Photonische Sensoren für die Sicherheitstechnik. *Photonic* 70–73
48. Orghici R, Willer U, Gierszewska M, Waldvogel SR, Schade W (2008) Fiber optic evanescent field sensor for detection of explosives and CO<sub>2</sub> dissolved in water. *Appl Phys B* 90:355–360
49. Börner S, Orghici R, Waldvogel SR, Willer U, Schade W (2009) Evanescent field sensors and the implementation of waveguiding nanostructures. *Appl Opt* 48:B183–B189
50. Schwartz U, Grosser R, Piejko KE, Bömer B, Arlt D (1987) *Ger Offen DE* 3532356 A1
51. Grose-Bley M, Bömer B, Grosser R, Arlt D, Lange W (1992) *Ger Offen DE* 4120695
52. Bömer B, Grosser R, Lange W, Zweering U, Koehler B, Sirges W, Grosse-Bley M (1997) *Ger Offen DE* 19546136 A1

53. Lange W, Grosser R, Köhler B, Michel S, Bömer B, Zweering U (1998) Ger Offen DE 19714343 A1
54. Schopohl MC, Bergander K, Kataeva O, Fröhlich R, Waldvogel SR (2003) Synthesis and characterization of enantiomerically pure menthylamines and their isocyanates. *Synthesis* 2689–2694
55. Griesbach U, Waldvogel SR, Kulisch J, Malkowsky IM (2008) PCT Int Appl WO 2008 003620 A2
56. Wilson NR, Clewes SL, Newton ME, Unwin PR, Macpherson JV (2006) Impact of grain-dependent boron uptake on the electrochemical and electrical properties of polycrystalline boron doped diamond electrodes. *J Phys Chem B* 110:5639–5646
57. Pütter H, Weiper-Idelmann A, Merk C, Fryda M, Klages C-P, Hampel A (2000) Eur Pat Appl EP 1 036 861 B1
58. Bosma C, Gouws S, Loyson P, Zeelie B (1999) Anodic oxidation of 4-t-butyltoluene to 4-t-butylbenzaldehyde dimethyl acetal: optimisation and scale-up. *S Afr J Chem* 52:133–144
59. Zollinger D, Griesbach U, Pütter H, Comninellis C (2004) Electrochemical cleavage of 1, 2-diphenylethanes at boron-doped diamond electrodes. *Electrochem Commun* 6:605–608
60. Degner D (1988) Organic electrosynthesis in industry. *Top Curr Chem* 148:1–95
61. Reufer C, Möbus K, Lehmann T, Weckbecker C (2004) PCT Int Appl WO 2004 087999 A2
62. Reufer C, Lehmann T, Sanzenbacher R, Weckbecker C (2004) PCT Int Appl WO 2004 085710 A2
63. Fardel R, Griesbach U, Pütter H, Comninellis C (2006) Electrosynthesis of trimethylorthoformate on BDD electrodes. *J Appl Electrochem* 36:249–253
64. Quideau S (2002) In: Astruc D (ed) *Modern arene chemistry. Concepts, synthesis, and applications.* Wiley-VCH, Weinheim, pp 539–572
65. Saitoh T, Suzuki E, Takasugi A, Obata R, Ishikawa Y, Umezawa K, Nishiyama S (2010) 217th ECS Meeting abstract 809, Vancouver
66. Okino F, Shibata H, Kawasaki S, Touhara H, Momota K, Nishitani-Gamo M, Sakaguchi I, Ando T (1999) Electrochemical fluorination of 1, 4-difluorobenzene using boron-doped diamond thin-film electrodes. *Electrochem Solid-State Lett* 2:382–384
67. Yoshida K (1979) Regiocontrolled anodic cyanation of nitrogen heterocycles. Pyrroles and indoles. *J Am Chem Soc* 101:2116–2121
68. Fuchigami T (2003) 203rd ECS Meeting abstract 2604, Paris
69. Bäumer US, Schäfer HJ (2005) Cleavage of alkenes by anodic oxidation. *J Appl Electrochem* 35:1283–1292
70. Bringmann G, Günther C, Ochse M, Schupp OTS (2001) In: Herz W, Falk H, Kirby GW, Moore RE (eds) *Progress in the chemistry of organic natural products.* Springer, Wien
71. Knowles WS (2003) Asymmetric hydrogenations (Nobel lecture 2001). *Adv Synth Catal* 345:3–13
72. Noyori R (2003) Asymmetric catalysis: science and opportunities (Nobel lecture 2001). *Adv Synth Catal* 345:15–32
73. Lessene G, Feldman KS (2002) In: Astruc D (ed) *Modern arene chemistry. Concepts, synthesis, and applications.* Wiley-VCH, Weinheim, pp 479–538
74. Boye B, Michaud PA, Marselli B, Dieng MM, Brillas E, Comninellis C (2002) Anodic oxidation of 4-chlorophenoxyacetic acid on synthetic boron-doped diamond electrodes. *New Diamond Front Carbon Technol* 12:63–72
75. Hawner C, Li K, Cirrie V, Alexakis A (2008) Copper-catalyzed asymmetric conjugate addition of aryl aluminum reagents to trisubstituted enones: construction of aryl-substituted quaternary centers. *Angew Chem Int Ed* 47:8211–8214
76. Palais L, Mikhel IS, Bournaud C, Micouin L, Falcicola CA, Vuagnoux-d'Augustin M, Rosset S, Bernardinelli G, Alexakis A (2007) SimplePhos monodentate ligands: synthesis and application in copper-catalyzed reactions. *Angew Chem Int Ed* 46:7462–7465

77. Vuagnoux-d'Augustin M, Kehrli S, Alexakis A (2007) Enantioselective copper-catalyzed conjugate addition to 2- or 3-substituted cyclopent-2-en-1-ones: construction of stereogenic quaternary carbon centers. *Synlett* 2057–2060
78. Li K, Alexakis A (2007) Copper-catalyzed enantioselective intramolecular conjugate addition/trapping reactions: synthesis of cyclic compounds with multichiral centers. *Chem-Eur J* 13:3765–3771
79. Raluy E, Dieguez M, Pamies O (2007) Sugar-based diphosphoramidite as a promising new class of ligands in Pd-catalyzed asymmetric allylic alkylation reactions. *J Org Chem* 72:2842–2850
80. Mata Y, Pamies O, Dieguez M (2007) Screening of a modular sugar-based phosphite-oxazoline ligand library in asymmetric Pd-catalyzed Heck reactions. *Chem-Eur J* 13:3296–3304
81. Li K, Alexakis A (2006) Asymmetric conjugate addition to alpha-halo enones: dramatic effect of styrene on the enantioselectivity. *Angew Chem Int Ed* 45:7600–7603
82. Garner JM, Lenges CP, McKinley RJ (2008) PCT Int Appl WO 2008 008927
83. Bartsch M, Baumann R, Haderlein G, Aechtner T, Scheidel J, Luyken H, Pfab P, Siegel W, Weiskopf V (2006) PCT Int Appl WO 2006 040023
84. Bartsch M, Baumann R, Haderlein G, Flores MA, Jungkamp T, Luyken H, Scheidel J, Siegel W (2005) PCT Int Appl WO 2005 042547
85. Bartsch M, Baumann R, Haderlein G, Flores MA, Jungkamp T, Luyken H, Scheidel J, Siegel W, Molnar F (2004) PCT Int Appl WO 2004 087314
86. Bartsch M, Baumann R, Kunsmann-Keitel DP, Haderlein G, Jungkamp T, Altmayer M, Siegel W, Molnar F (2003) PCT Int Appl WO 2003 033142
87. Malkowsky IM, Rommel CE, Wedeking K, Fröhlich R, Bergander K, Nieger M, Quaiser C, Griesbach U, Pütter H, Waldvogel SR (2006) Facile and highly diastereoselective formation of a novel pentacyclic scaffold by direct anodic oxidation of 2,4-dimethylphenol. *Eur J Org Chem* 241–245
88. Barjau J, Koenigs P, Kataeva O, Waldvogel SR (2008) Reinvestigation of highly diastereoselective pentacyclic spiro lactone formation by direct anodic oxidation of 2,4-dimethylphenol. *Synlett* 2309–2312
89. Malkowsky IM, Rommel CE, Fröhlich R, Griesbach U, Pütter H, Waldvogel SR (2006) Novel template-directed anodic phenol-coupling reaction. *Chem Eur J* 12:7482–7488
90. Malkowsky IM, Fröhlich R, Griesbach U, Pütter H, Waldvogel SR (2006) Facile and reliable synthesis of tetraphenoxyborates and their properties. *Eur J Inorg Chem* 1690–1697
91. Malkowsky IM, Griesbach U, Pütter H, Waldvogel SR (2006) Unexpected highly chemoselective anodic ortho-coupling reaction of 2,4-dimethylphenol on boron-doped diamond electrodes. *Eur J Org Chem* 4569–4572
92. de Meijere A, Diederich F (eds) (2004) *Metal-catalyzed cross-coupling reactions*. Wiley-VCH, Weinheim
93. Chen X, Engle KM, Wang D, Yu J (2009) Palladium(II)-catalyzed C-H activation/C-C cross-coupling reactions: versatility and practicality. *Angew Chem Int Ed* 48:5094–5115
94. Cepanec I (2004) *Synthesis of biaryls*, 1st edn. Elsevier, Amsterdam
95. Beller M, Bolm C (eds) (2004) *Transition metals for organic synthesis. Building blocks and fine chemicals*, 2nd rev. and enl. ed. Wiley-VCH, Weinheim
96. Hassan J, Sevignon M, Gozzi C, Schulz E, Lemaire M (2002) Aryl-aryl bond formation one century after the discovery of the Ullmann reaction. *Chem Rev* 102:1359–1469
97. Zapf A, Beller M (2002) Fine chemical synthesis with homogeneous palladium catalysts: examples, status and trends. *Top Catal* 19:101–109
98. Ackermann L (ed) (2009) *Modern arylation methods*. Wiley-VCH, Weinheim
99. Ackermann L (2008) In: Chatani N (ed) *Directed metallation*. Springer, Berlin
100. Seregin IV, Gevorgyan V (2007) Direct transition metal-catalyzed functionalization of heteroaromatic compounds. *Chem Soc Rev* 36:1173–1193

101. Dyker G (ed) (2005) Handbook of C-H transformations. Applications in organic synthesis. Wiley-VCH, Weinheim
102. Miyaura N, Suzuki A (1995) Palladium-catalyzed cross-coupling reactions of organoboron compounds. *Chem Rev* 95:2457–2483
103. Molander GA, Ellis N (2007) Organotrifluoroborates: protected boronic acids that expand the versatility of the Suzuki coupling reaction. *Acc Chem Res* 40:275–286
104. Farina V, Krishnamurthy V, Scott WJ (1997) The Stille reaction. *Org React* 50:1–652
105. Gooßen LJ, Rodriguez N, Gooßen K (2008) Carboxylic acids as substrates in homogeneous catalysis. *Angew Chem Int Ed* 47:3100–3120
106. Negishi EI (1982) Palladium-catalyzed or nickel-catalyzed cross-coupling – a new selective method for carbon-carbon bond formation. *Acc Chem Res* 15:340–348
107. Knochel P (2005) Handbook of functionalized organometallics. Applications in synthesis, 1. Aufl. Wiley-VCH, Weinheim
108. Dohi T, Ito M, Morimoto K, Wata M, Kita Y (2008) Oxidative cross-coupling of arenes induced by single-electron transfer leading to biaryls by use of organoiodine(III) oxidants. *Angew Chem Int Ed* 47:1301–1304
109. Yamamura S, Nishiyama S (2002) Anodic oxidation of phenols towards the synthesis of bioactive natural products. *Synlett* 533–543
110. Schäfer HJ (1981) Anodic and cathodic CC-bond formation. *Angew Chem Int Ed* 20:911–934
111. Little RD, Moeller KD (2002) Organic electrosynthesis as a tool for synthesis. *Electrochem Soc Interface* 11:36–42
112. Moeller KD (1997) Intramolecular carbon-carbon bond forming reactions at the anode. *Top Curr Chem* 185:49–86
113. Moeller KD (2000) Synthetic applications of anodic electrochemistry. *Tetrahedron* 56:9527–9554
114. Heinrich MR (2009) Intermolecular olefin functionalisation involving aryl radicals generated from arenediazonium salts. *Chem-Eur J* 15:821–833
115. Wetzel A, Ehrhardt V, Heinrich MR (2008) Synthesis of amino- and hydroxybiphenyls by radical chain reaction of arenediazonium salts. *Angew Chem Int Ed* 47:9130–9133
116. Blank O, Wetzel A, Ullrich D, Heinrich MR (2008) Radical carbodiazonylation – a convenient and effective method to achieve carboamination of non-activated olefins. *Eur J Org Chem* 3179–3189
117. Albarran G, Schuler RH (2005) Concerted effects of substituents in the reaction of center dot OH radicals with aromatics: the cresols. *J Phys Chem A* 109:9363–9370
118. Iida T, Ohshita J, Ohta N, Komaguchi K, Itagaki Y, Shiotani M, Kunai A (2003) Spin-spin interaction between phenoxy radicals through sigma-pi system. *J Organomet Chem* 688:192–199
119. Hristea EN, Covaci-Cimpeanu IC, Ionita G, Ionita P, Draghici C, Caproiu MT, Hillebrand M, Constantinescu T, Balaban AT (2009) Reactions of 2,2-diphenyl-1-picrylhydrazyl (DPPH) with two syringic phenols or one aroxide derivative. *Eur J Org Chem* 626–634
120. Ebersson L, Hartshorn MP, Persson O (1995) 1,1,1,3,3,3-Hexafluoropropan-2-ol as a solvent for the generation of highly persistent radical cations. *J Chem Soc Perkin Trans II* 1735–1744
121. Ebersson L, Hartshorn MP, Persson O (1995) Detection and reaction of radical cations generated by photolysis of aromatic compounds with tetranitromethane in 1, 1, 1, 3, 3, 3-hexafluoro-2-propanol at room temperature. *Angew Chem Int Ed* 34:2268–2269
122. Haenni W, Perret A, Rychen P (2002) PCT Int Appl WO 2002 061181

# Modern Developments in Aryl Radical Chemistry

Gerald Pratsch and Markus R. Heinrich

**Abstract** This review summarizes recent advances in the field of aryl radical chemistry. In particular, modern developments of the well-known Meerwein, Pschorr, and Gomberg–Bachmann reactions are presented along with new applications in natural product syntheses. Among the methods for the generation of aryl radicals, tin hydrides play a predominant role, but more and more attractive and promising alternatives are beginning to emerge.

**Keywords** Aryl radicals · Natural products · Radical addition · Radical cyclization

## Contents

1	Introduction	34
2	Intramolecular Meerwein Reactions: Meerwein Cyclizations	35
2.1	Cyclization to Carbon–Carbon Double and Triple Bonds	35
2.2	Cyclization to Carbon–Heteroatom Double Bonds	38
2.3	Applications in Natural Product Synthesis	39
3	Intermolecular Meerwein Arylations	43
3.1	Carbohalogenation Reactions	43
3.2	Carboamination Reactions	44
3.3	Carboxygenation Reactions	45
3.4	Carbothiolation Reactions	45
4	Pschorr Reactions	46
4.1	Cyclizations to Substituted Benzenes	46
4.2	Cyclizations Featuring <i>Ips</i> o Substitution	48
4.3	Cyclizations to Heteroaromatics	50
4.4	Application in Natural Product Synthesis	50
5	Gomberg–Bachmann Reactions	51
5.1	Biphenyls: New Aryl Radical Sources	51

---

G. Pratsch and M.R. Heinrich (✉)

Pharmazeutische Chemie, Department für Chemie und Pharmazie der, Friedrich-Alexander-Universität Erlangen-Nürnberg, Schuhstraße 19, 91052 Erlangen, Germany  
e-mail: Markus.Heinrich@medchem.uni-erlangen.de

5.2 Biphenyls: New Substrates .....	53
5.3 Heteroaromatics .....	55
6 Radical–Organometallic Hybrids .....	55
References .....	56

## Abbreviations

AIBN	Azo-bis(isobutyronitrile)
PTGB	Phase-transfer Gomberg–Bachmann
TEMPO	2,2,6,6-Tetramethylpiperidine-1-oxyl (radical)

## 1 Introduction

With his report on the formation of iodobenzene from phenyl diazonium salts and iodide in 1866, Peter Griess became one of the earliest pioneers in the field of aryl radical chemistry [1]. The official birthday of radical chemistry itself, which is assigned to Moses Gomberg's description of a trivalent carbon atom in triphenylmethane, at that time still lay 36 years in the future [2]. Today, almost 150 years later, aryl radical chemistry is well known among chemists due to four prominent name reactions. As a result of their early discovery, all of them have seen a long history of development, amendment, and improvement. Sandmeyer's [3] conversion of aryl diazonium salts to halobenzenes in 1884 was followed by the Pschorr [4] cyclization in 1896 and biaryl syntheses by Gomberg and Bachmann [5] in 1924. As the last of the four reactions, the Meerwein arylation appeared in the literature in the year 1939 [6]. Although the number of substrates which were found to be suitable for being attacked by an aryl radical increased constantly, aryl diazonium salts [7] remained for a long period of time the most commonly used source of aryl radicals [8–11]. A boost of versatility came when the wide-ranging applicability of stannanes for radical reactions started to show in the late 1960s [12]. In the presence of organotin compounds, aryl radicals now also became available from bromo- and iodoarenes. Given the number of recent reports and publications, samarium- and tin-mediated reactions have probably taken over the lead as sources of aryl radicals. The classical diazonium salts today take second place with respect to frequency of use. In addition, a number of innovative and promising methods for the generation of aryl radicals have been invented.

In this chapter, we would like to focus on recent developments in the field of aryl radical chemistry, especially on new variants and applications of the Meerwein, Pschorr, and Gomberg–Bachmann reactions. These are presented in combination with a closer look at new aryl radical sources and new substrates. Moreover, the interface between aryl radical and organometallic chemistry has emerged as a field with new opportunities. Due to the large number of publications in this field and the

limited space available, we would like to apologize for all those developments that could not be mentioned and recommend excellent reviews that have recently appeared [13–15].

## 2 Intramolecular Meerwein Reactions: Meerwein Cyclizations

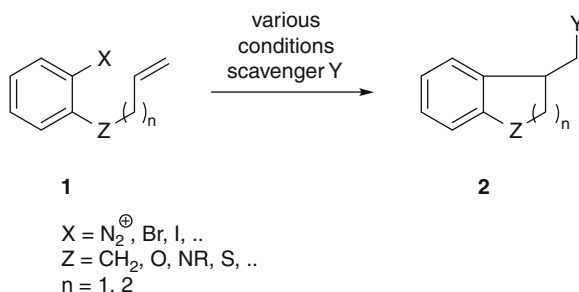
### 2.1 Cyclization to Carbon–Carbon Double and Triple Bonds

For intramolecular Meerwein reactions, compounds of type **1** can serve as attractive test systems for new initiators, reaction conditions, and trapping reagents, which are finally responsible for the substituent Y in the cyclized product **2** (Scheme 1) [16, 17].

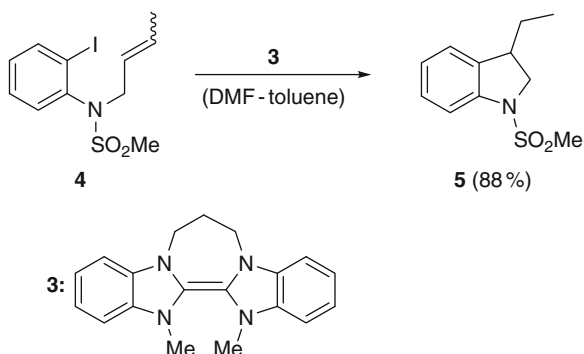
With diazonium salts as starting materials **1** ( $X = N_2^+$ ), pioneering experiments have been performed using sodium iodide [18, 19], copper salts [20], tin hydrides [21, 22], thioacetate [23], and organic reductants [24–26]. Bromides **1** ( $X = Br$ ) have been cyclized in the presence of tin hydrides [27], titanium complexes [28], and, very recently, triethylborane [29]. Not surprisingly, a large number of dihydrobenzofuran syntheses are based on iodinated allylphenyl ethers **1** ( $X = I$ ,  $Z = O$ ) as starting materials. The first initiators used therefore range from irradiation [30], distannanes [31], samarium diiodide [32–34], to cobalt complexes [35].

In recent years, strong organic electron donors have been further improved as powerful replacements for the so far widely used metals [36, 37]. Tetraazaalkenes, such as **3**, have been shown to cyclize iodide **4** to dihydroindole **5** in high yield (Scheme 2) [38].

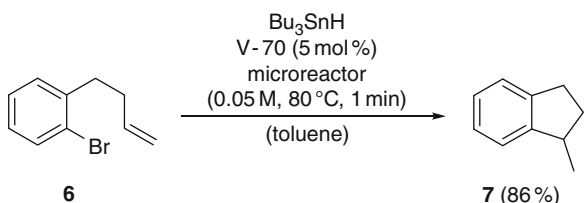
As in other fields of organic chemistry, the use of microreactors represents a new method to accelerate reactions significantly. Within a larger study on tin hydride and tris(trimethylsilyl)silane-mediated reactions, the continuous flow system has also been applied to conduct an intramolecular Meerwein reaction. The cyclization of bromide **6** to indane **7** was completed in less than 1 min (Scheme 3) [39].



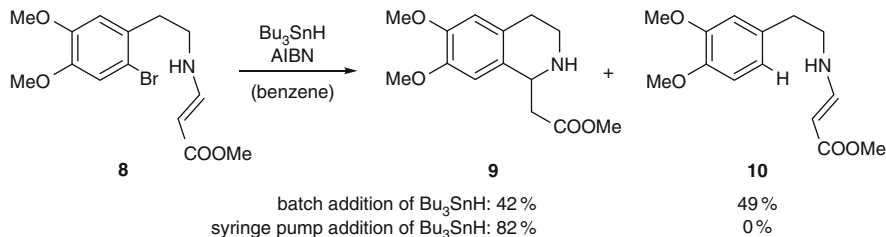
**Scheme 1** Intramolecular aryl radical addition to alkenes



**Scheme 2** Strong organic reductants as initiators [38]



**Scheme 3** Cyclization in a microreactor [39]



**Scheme 4** Cyclization onto vinylogous amides [45]

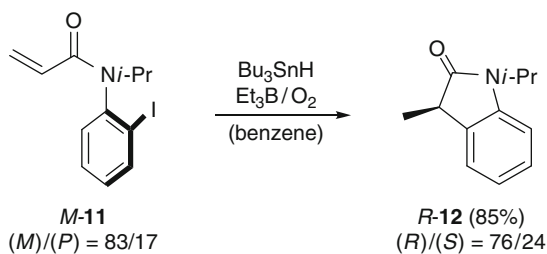
Concerning the substrates suitable for intramolecular Meerwein reactions, several studies on ring strain [40], regioselectivity [41], undesired hydrogen transfer [42], and unusual cyclization modes [43, 44] have been reported. Due to the partial delocalization of their double bond, vinylogous amides are known as poorer substrates for radical addition or cyclization reactions than comparable enamides [45]. A first example, in which bromide **8** was successfully cyclized to give tetrahydroisoquinoline **9**, is shown in Scheme 4. The efficacy of the aryl radical addition to the olefinic push-pull system of **8** is strongly dependent on the low concentration of tributyltin hydride since reduction of the aryl radical to **10** occurs as a competing process. High yields were obtained using a syringe pump.



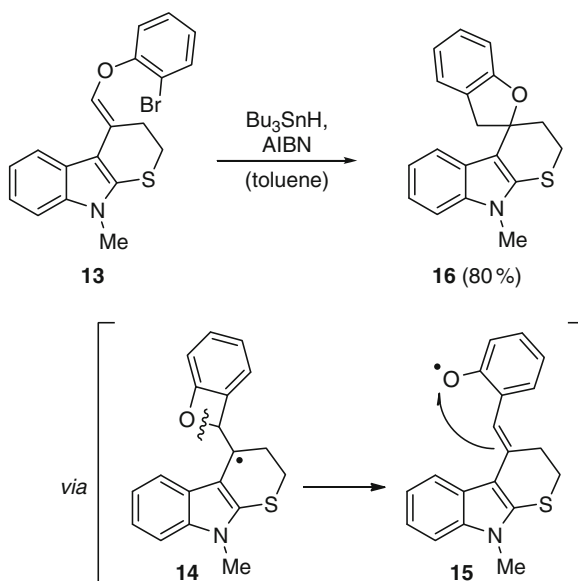
Transfer of axial chirality to centrochirality by a 5-*exo* type aryl radical cyclization onto acrylamides has been reported by Curran (Scheme 5) [46, 47]. Among the examples reported, indolone **12** was obtained from acrylanilide **11** with a high degree of chirality transfer.

An unusual 4-*exo*-trig cyclization accompanied by a later rearrangement was observed with aryl enoether **13** (Scheme 6) [48]. The benzoxetane **14**, which is formed in the initial cyclization step, undergoes ring-opening to form the phenoxy radical **15**. 5-*Endo* cyclization of **15** and reduction of the resulting benzylic radical leads to the spirocycle **16**. Diverse polycyclic products have also recently been obtained by intramolecular aryl radical cyclizations to tetrahydropyridines [49].

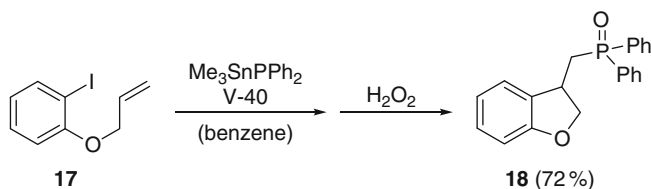
Various radical scavengers have been employed for the trapping of the alkyl radicals arising from the cyclization step. In two new studies, subsequent radical additions to phosphorus have been achieved. Suitable reagents for this purpose



**Scheme 5** Chirality transfer in cyclizations to acrylamides [46, 47]



**Scheme 6** Synthesis of spirocycles by cyclization and rearrangement [48]



**Scheme 7** Cyclization and radical addition to phosphorus [51]

are chlorodiphenylphosphine ( $\text{ClPPh}_2$ ), which is in situ converted to the active radical scavenger tetraphenylbiphosphine ( $\text{Ph}_2\text{P-PPh}_2$ ) [50], as well as stannylated or silylated diphenylphosphanes (Scheme 7) [51]. In this reaction, the alkyl diphenylphosphanes obtained from the cyclization of **17** were oxidized to phosphine oxides **18** for reasons of stability.

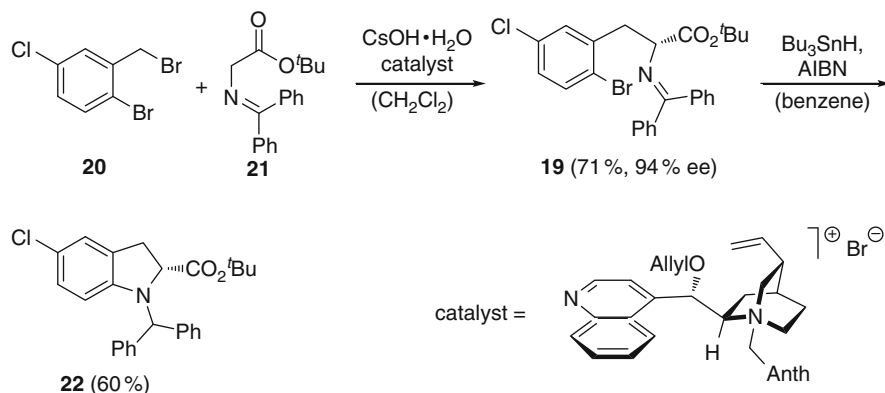
## 2.2 Cyclization to Carbon–Heteroatom Double Bonds

Early examples of intramolecular aryl radical addition reactions to heteroatom containing multiple bonds included cyclizations on  $\text{N}=\text{N}$  and  $\text{C}=\text{S}$  moieties [52, 53]. Recently, cyclizations to imines have been used as part of a new enantioselective approach to indolines (Scheme 8). In the first step of the sequence, the required ketimines **19** were obtained by phase-transfer catalyzed alkylation of 2-bromobenzyl bromides **20** with glycynyl imines **21** in the presence of a cinchonidinium salt [54]. Due to the favorable substitution pattern on the imine moiety of **19**, the tributyltin hydride mediated radical cyclization to **22** occurred exclusively in the 5-*exo* mode. The indoline synthesis can therefore also be classified as a radical amination.

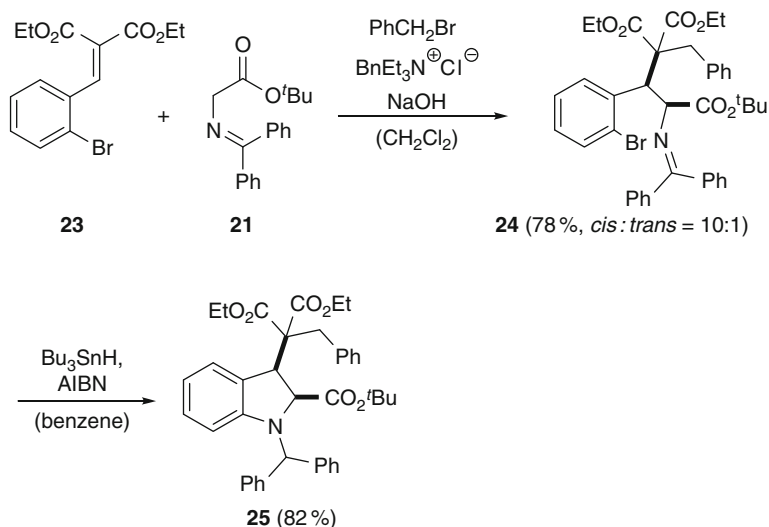
A similar 5-*exo* aryl radical cyclization onto nitrogen atoms has been observed with imidate esters [55]. In contrast, structurally comparable but sterically less hindered imines preferentially undergo 6-*endo* cyclizations to give tetrahydroisoquinolines [56, 57]. As a valuable extension, the indoline synthesis has been further developed towards a multicomponent reaction (Scheme 9) [58]. Michael addition of glycynyl imine **21–23** in the presence of the alkylating agent benzyl bromide gave **24** with a strong predominance of the *cis* isomer. Indoline **25** was then formed by intramolecular aryl radical addition.

Cyclizations to sulfones which lead to a homolytic substitution at sulfur have been employed for the preparation of cyclic sulfinamides [59].

In some recently reported cyclization reactions, the radical undergoing the cyclization step is not an aryl radical itself, but it is generated by either aryl radical-induced fragmentation [60–62] or hydrogen abstraction [63–65]. By cyclizations on heteroatoms, benzoselenophenes and benzotellurophenes are also available [66–68].



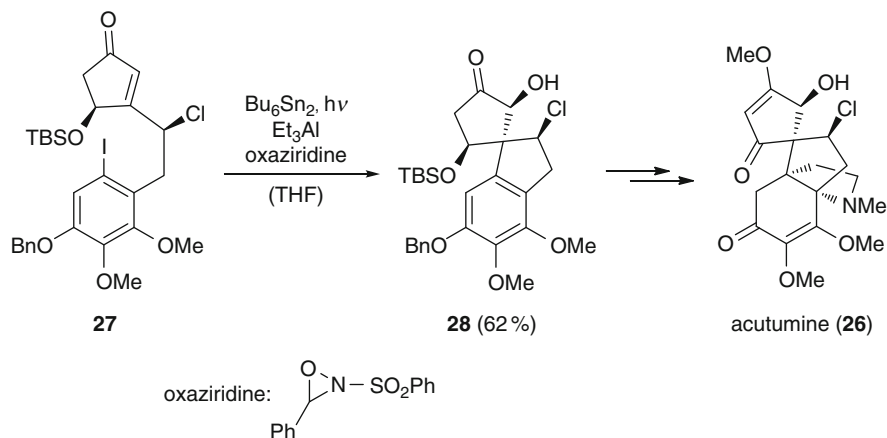
**Scheme 8** Indoline synthesis via aryl radical cyclization on imines [54]



**Scheme 9** Indoline synthesis as a multicomponent reaction including a radical cyclization step [58]

### 2.3 Applications in Natural Product Synthesis

Natural products have always been attractive targets for the application of newly developed synthetic strategies. In this field, only a few examples have been reported, in which intramolecular aryl radical addition reactions occur to non-activated carbon–carbon double bonds [69]. One of the early examples is the first total synthesis of (–)- $\gamma$ -lycorane [70]. More recently, formal total syntheses of aspidospermidine [71] and vindoline [72] have been accomplished by an aryl radical



**Scheme 10** Radical cyclization as key step in the total synthesis of acutumine (**26**) [75]

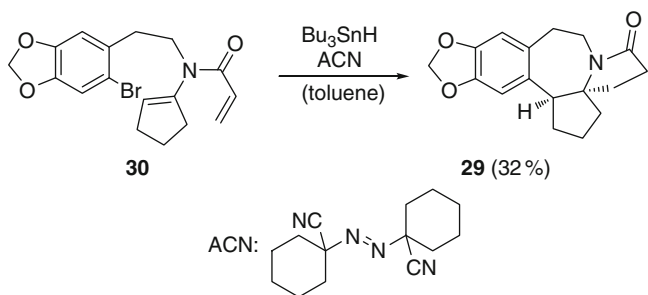
cyclization onto a non-activated internal alkene. Cyclizations to cyclobutenes provided fast access to the BCD ring system of penitremis [73].

In all the following examples, the targeted double bonds were activated by suitable substituents to increase the efficacy of the desired cyclization mode. For the total synthesis of acutumine (**26**), an activated  $\alpha,\beta$ -unsaturated ketone **27** was chosen as precursor (Scheme 10) [74, 75]. Aryl radical additions to this type of alkenes are known to proceed about ten times faster than to comparable allylic alcohols. In a radical-polar crossover reaction, the spirocyclic product **28** was obtained in the presence of triethylaluminum as promoter and an oxaziridine as hydroxylating agent. The fact that even the efficient hydrogen donor tetrahydrofuran could be used as solvent nicely demonstrates the high efficacy of the cyclization step.

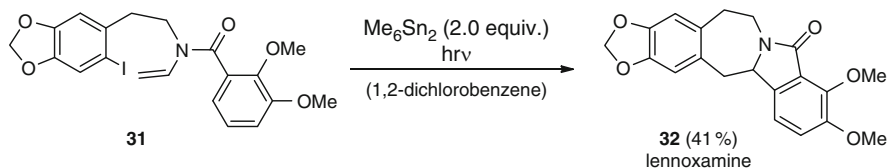
The group of activated olefins, which has so far probably received most attention in radical cyclizations, are enamides. Syntheses of various natural products, especially alkaloids, have been successfully completed using this strategy. Cyclizations onto enamides of the 6-*endo* type led to erysotrine [76] and lycorine alkaloids [77–79]. The skeleton of hydroapoerysopinines [80] was successfully constructed by a 7-*endo* cyclization. Two new examples of radical tandem reactions, which commence with a 7-*endo* type cyclization, have appeared in recent literature. Construction of the cephalotaxine core structure **29** was achieved from enamide **30** in only one step (Scheme 11) [81].

Similarly, enamide **31** was shown to be a direct precursor of lennoxamine (**32**) (Scheme 12) [82].

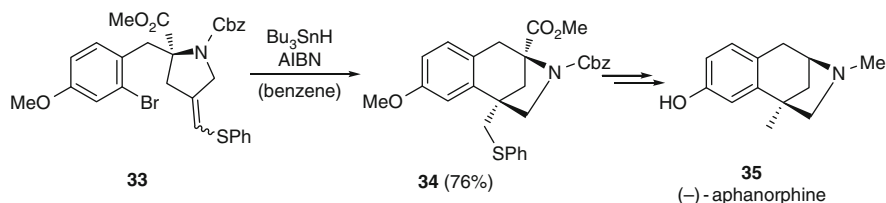
In addition to the well exploited radical additions to enamides, thiovinyl ethers have been shown to be suitable intramolecular acceptors for aryl radicals. By placing a thiophenyl substituent on terminal alkene of **33**, the cyclization to **34** occurred exclusively in the 6-*exo* mode and was not complicated by internal hydrogen abstraction from the allylic positions of the alkene (Scheme 13) [83, 84].



**Scheme 11** Synthesis of the cephalotaxine core structure **29** [81]



**Scheme 12** Synthesis of lennoxamine (**32**) [82]

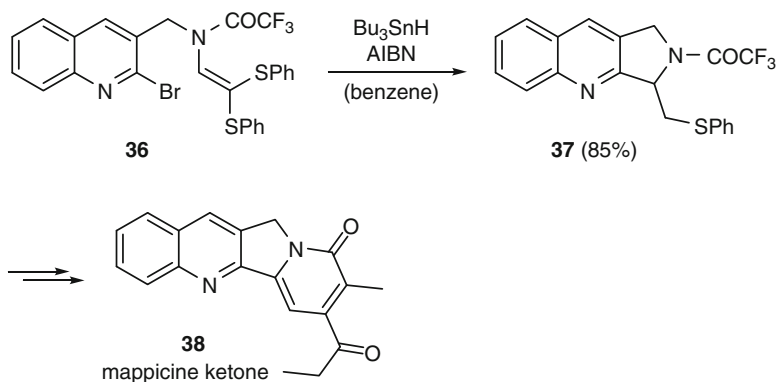


**Scheme 13** Key step in the total synthesis of (-)-aphanorphine (**35**) [83]

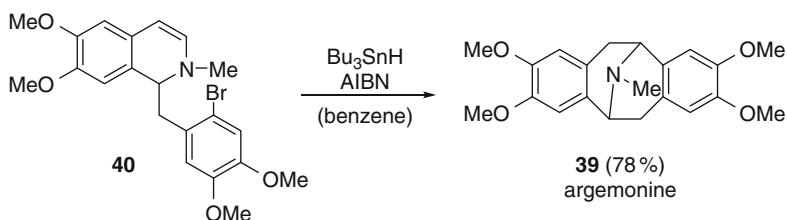
The significant gain in selectivity is ascribed to the increased sulfur-induced stabilization of the alkyl radical resulting from the cyclization step.

A second example for a sulfur-directed cyclization, in which even two thiophenyl groups were present as substituents on the target alkene **36**, is shown in Scheme 14 [85]. This substitution pattern is capable of reversing the usual regioselectivity observed for aryl radical additions to enamides. In the presence of a fivefold excess of tributyltin hydride, one sulfur group is removed immediately after the cyclization step. The resulting tricyclic thioether **37** was further converted to mappicine ketone **38**.

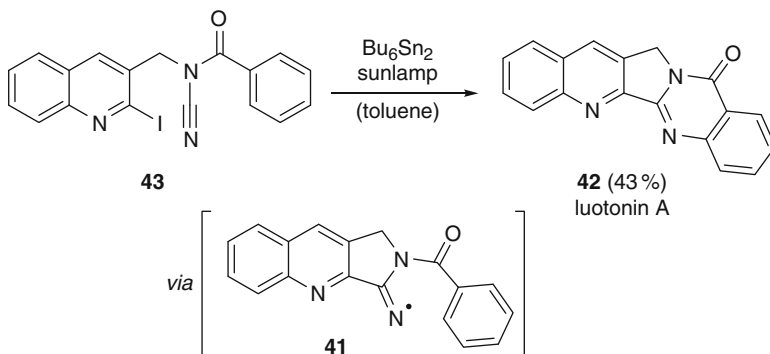
Reversed regioselectivity in aryl radical additions to enamides and enamines can also be observed with aryl substituents on the alkene [86]. This cyclization type has been successfully applied in the synthesis of protoberberines and the pavine alkaloids. Argemonine (**39**) was obtained from a 6-exo cyclization of **40** passing through a well-stabilized benzylic radical (Scheme 15).



**Scheme 14** Radical cyclization as key step towards mappicine ketone **38** [85]



**Scheme 15** Cyclization to argemonine (**39**) [86]

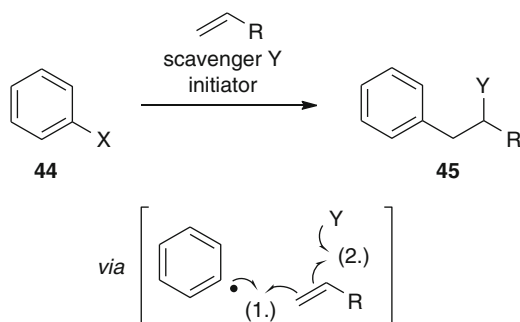


**Scheme 16** Tandem radical cyclization to luotonin A (**42**) [88]

As an extension of the known radical additions to isonitriles [87], aryl radical cyclizations to *N*-acyl cyanamides provide new access to pyrrolo-quinazolines (Scheme 16) [88]. In a tandem process, the iminyl radical **41** resulting from the 5-*exo* cyclization onto the nitrile was used for a second cyclization step. In this way, the alkaloid luotonin A (**42**) was synthesized from cyanamide **43** in a single reaction.

### 3 Intermolecular Meerwein Arylations

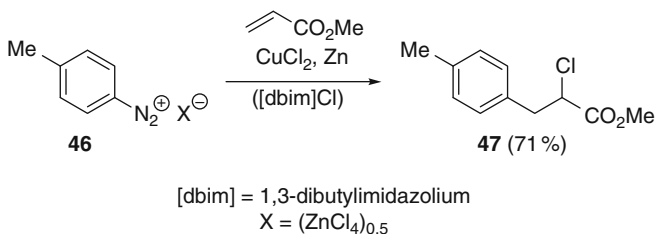
In comparison to the cyclization reactions shown above, intermolecular Meerwein arylations are often more difficult to conduct. Since the aryl radical addition to the alkene is no longer favored by the close proximity of the reacting centers, the probability for a direct recombination of the aryl radical with scavengers Y is significantly increased (Scheme 17). To maintain the desired reaction course from **44** to **45** including steps (1) and (2) [89, 90], Meerwein arylations have for a long time mostly been conducted with activated alkenes, such as acrylates ( $R = \text{COOR}'$ ), vinylketones ( $R = \text{COR}'$ ), styrenes ( $R = \text{Ph}$ ), or conjugated dienes [91, 92]. These types of alkenes are known for fast addition of aryl radicals.



**Scheme 17** Intermolecular Meerwein arylations [91, 92]

#### 3.1 Carbohalogenation Reactions

An improvement of the previously reported Meerwein protocols was achieved by employing ionic liquids as chloride sources (Scheme 18) [93]. Although this new version of the Meerwein reaction is still limited to activated alkenes such as acrylates, electron-donating as well as electron-withdrawing groups on the diazonium salt are tolerated. In earlier Meerwein arylations, a change in the substitution



**Scheme 18** Meerwein arylation in ionic liquids [92, 93]

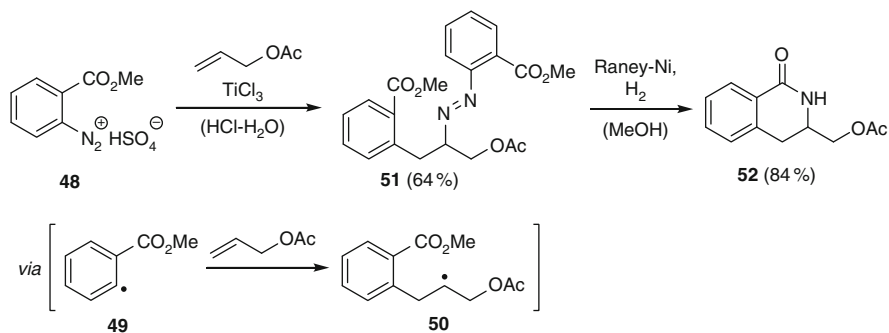
pattern of the diazonium salt often also required an adjustment of the reaction conditions. With diazonium tetrachlorozincate **46** as starting material the chlorinated 3-aryl propanoate **47** was obtained.

Further new applications of the Meerwein arylation include the synthesis of benzothiophenes [94] and benzylmethyl ketones [95].

### 3.2 Carboamination Reactions

The ability of diazonium salts to act as radical scavengers for nucleophilic alkyl radicals was first discovered in mechanistic studies on the Meerwein arylation [96]. Shortly after, this concept was applied for the functionalization of a limited group of activated alkenes [97–99]. The much greater synthetic potential of this functionalization type, which arises from the successful use of non-activated alkenes as substrates, has recently been investigated. In a typical reaction, as illustrated in Scheme 19, the diazonium salt **48** acts as source for aryl radicals **49** and as radical scavenger [100].

In contrast to classical Meerwein arylation, non-activated alkenes are well suited for this reaction type for two reasons. First, due to the relatively slow formation of azo compounds by addition of aryl radical **49** to **48**, this undesired pathway cannot compete successfully with the attack of **49** on the alkene to give radical adduct **50**. Second, a nucleophilic alkyl radical **50** arises from the addition step, which is effectively trapped by electrophilic salt **48** to give azo compound **51**. As a result of several improvements, the methodology is now applicable for a wide range of polar to non-polar alkenes with almost no restrictions on the substitution pattern of the diazonium salt [101, 102]. Moderate diastereoselectivities have been obtained in first attempts with chiral auxiliaries [103]. The azo compounds accessible, such as **51**, can be converted to carboamination products **52** by hydrogenation and to various other heterocycles.

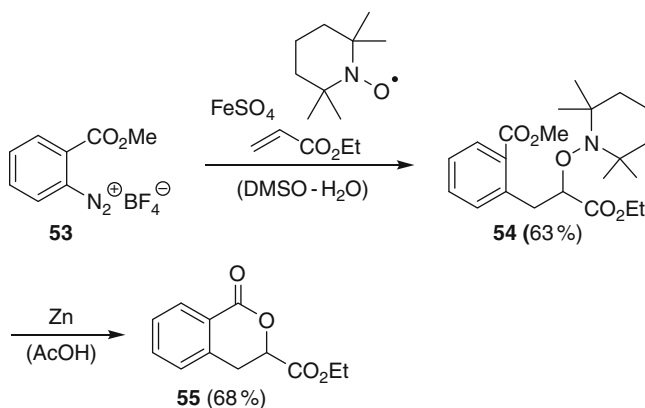


**Scheme 19** Carboamination of non-activated alkenes [100]



### 3.3 Carboxylation Reactions

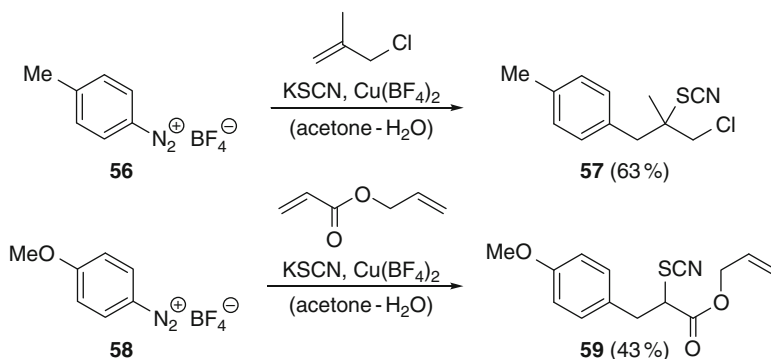
The first carboxylation reactions in which aryl radicals were involved have been reported for 1,3-dienes [104, 105]. With photochemically generated aryl radicals and in presence of the aminooxyl radical TEMPO as radical scavenger, carboxylations could at first only be extended to activated alkenes [106]. A significant improvement came with the use of aqueous dimethyl sulfoxide as solvent. By this modification, the reactivity of the scavenger TEMPO is lowered considerably so that practically no direct recombination of aryl radicals and TEMPO is observed [107]. As a consequence, activated as well as non-activated alkenes can be converted to carboxylation products without adjustments (Scheme 20) [108]. Carboxylations using TEMPO are therefore among some of the most general Meerwein type reactions reported so far. In the example shown, aryl radicals were generated from the diazonium tetrafluoroborate **53** by the reductant iron(II)-sulfate. Addition to the ethyl acrylate and trapping by TEMPO gave **54**, which could be further converted to lactone **55**.



Scheme 20 Carboxylation of alkenes [92, 108]

### 3.4 Carbothiolation Reactions

A number of sulfur-centered radical scavengers have been employed for Meerwein type carbothiolation reactions [109, 110]. The most prominent of those are certainly xanthates [111–113] and thiocyanates, among which the latter have received special attention recently. As shown in Scheme 21, thiocyanates are well-suited for the functionalization of activated and non-activated alkenes [114, 115]. Remarkably, the reaction of **56** with 2-methylallyl chloride to give **57** is not significantly impeded by the possible  $\beta$ -fragmentation of a chlorine radical, which would lead to allylation products [116]. With an activated and a non-activated alkene present in a substrate



**Scheme 21** Carbothiolation of non-activated and activated alkenes with thiocyanates [92, 114, 115]

such as allyl acrylate, the carbothiolation with diazonium salt **58** and potassium thiocyanate occurred preferentially at the activated double bond and gave **59**.

Meerwein type arylations involving radical additions to carbon–heteroatom multiple bonds such as in isothiocyanates have been further extended to tandem reactions leading to heterocycles [117, 118].

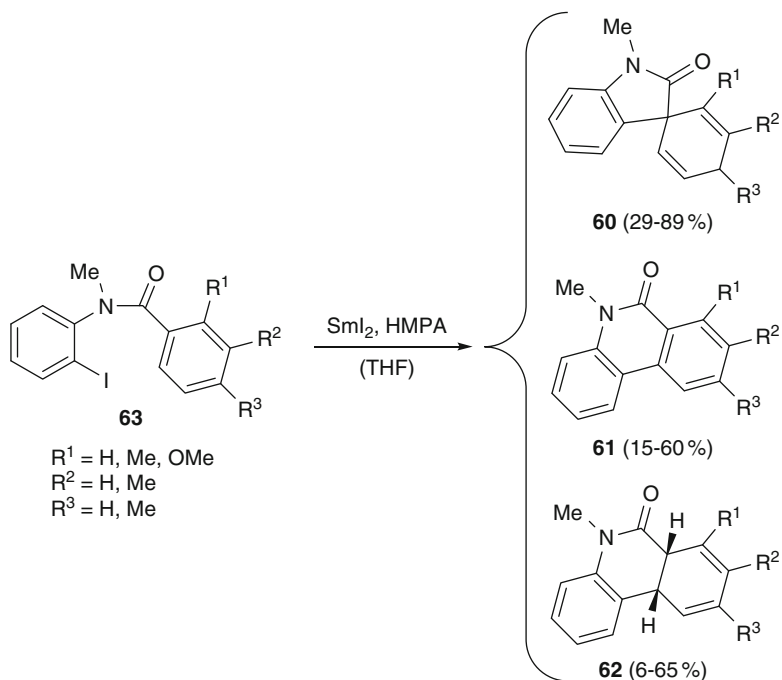
## 4 Pschorr Reactions

### 4.1 Cyclizations to Substituted Benzenes

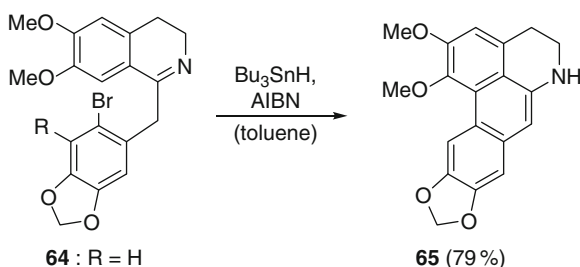
As shown in other sections of this chapter, overall attention has shifted from diazonium salts as aryl radical sources to bromo- or iodobenzenes. One of the few recent attempts to improve the classical Pschorr cyclization using diazonium ions as starting materials led to the discovery of new catalysts [119]. Results from a first samarium-mediated Pschorr type show the variety of products that can be expected from intramolecular biaryl syntheses under reductive conditions (Scheme 22). Depending on the substitution pattern of the target aromatic core and the reaction conditions, either the spirocycle **60**, the biphenyl **61**, or the dearomatized biphenyl **62** were formed as major product from **63** [120].

Many reports on tributyltin hydride-mediated intramolecular aryl–aryl coupling reactions have appeared in the literature in the 1990s [27, 121]. One of the latest articles, in which many references on previous work have been included, focuses on the preparation of aporphines (Scheme 23) [122]. Due to steric repulsion, an undesired 5-*endo* cyclization of the aryl radical on the imine nitrogen atom occurs only when more bulky substituents R are present in the benzyldihydroisoquinoline **64**. With R = H, the cyclization to **65** proceeds in high yields.

A comparable cyclization under  $S_{RN}1$  conditions [123, 124] has been reported by Cuni and Rossi [125]. Alternatively, electrochemical generation of aryl radicals



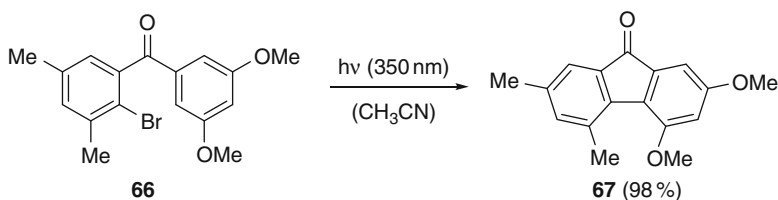
**Scheme 22** Samarium-mediated Pschorr cyclization [120]



**Scheme 23** Tin-mediated Pschorr type cyclization [122]

can be employed [126]. This methodology has recently been used for an intramolecular cyclization to give helicenes [127, 128].

Among the initiation methods available, photochemistry has already been used successfully for Pschorr reactions [122]. A new study, from which one example is shown in Scheme 24, revealed a dramatic influence of the substituents on the 2-bromobenzophenone **66**. Methoxy groups in the radical ring led to a highly electrophilic  $\sigma$ -aryl radical which proved unreactive for hydrogen abstraction and cyclization. Substituents in the non-radical ring that stabilize the cyclohexadienyl

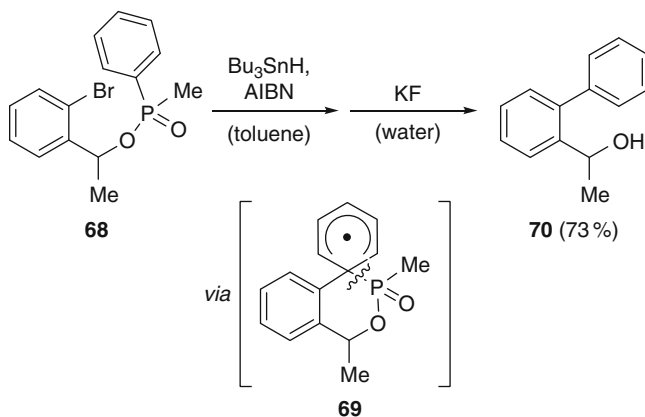


**Scheme 24** Photochemically induced cyclization to fluorenones [129]

intermediate, such as methoxy groups, promote the cyclization to furnish fluorenones **67** in excellent yields [129].

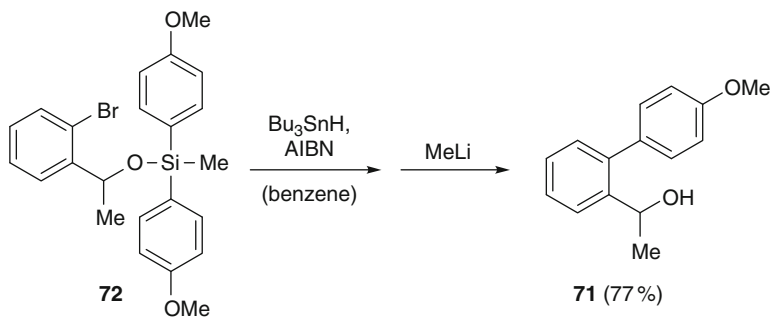
## 4.2 Cyclizations Featuring *Ips*o Substitution

Due to the relatively slow addition of aryl radicals to substituted benzenes [7], intermolecular Gomberg–Bachmann type arylations often require favorable reaction conditions in which the substrate arene is used as solvent to be efficient. To achieve good control and selectivity in the addition step, radical biphenyl synthesis can alternatively be conducted in an intramolecular fashion by taking advantage of a removable tether. In the first examples, sulfonamides, sulfonates [130], and azetidinones [131] were employed as linkers between the two aryl moieties. Recently, phosphinates [132] and siloxanes [133] have been used for this purpose (Scheme 25).

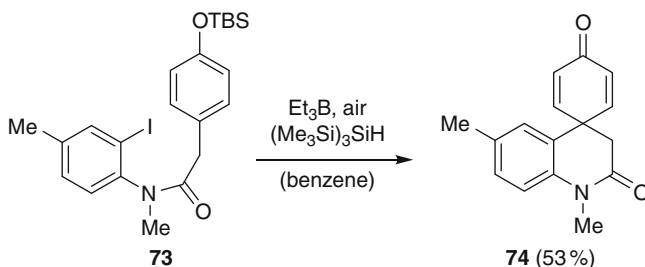


**Scheme 25** Biphenyl synthesis via *ipso* cyclization of phosphinates [132]

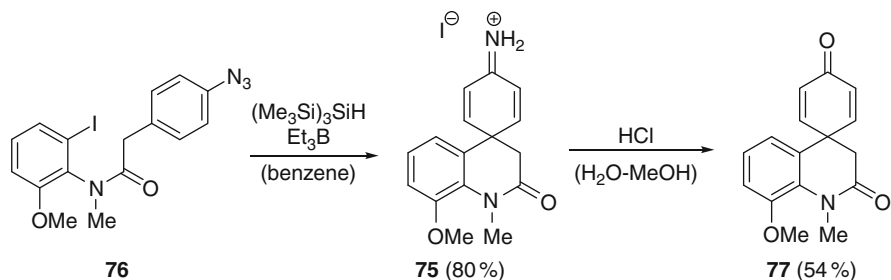
In this variant, the *ipso* substitution of **68** led to the cyclohexadienyl radical **69** which underwent C–P bond cleavage and expulsion of the tether to give biphenyl **70**. A comparable mechanism is operative for the aryl transfer from silicon to carbon in which a comparable biphenyl **71** (c.f. **70**) was synthesized from siloxane **72** (Scheme 26) [65, 133].



**Scheme 26** Biphenyl synthesis via *ipso* cyclization of siloxanes [133]



**Scheme 27** *Ipso* cyclization to phenylsilylethers [135]



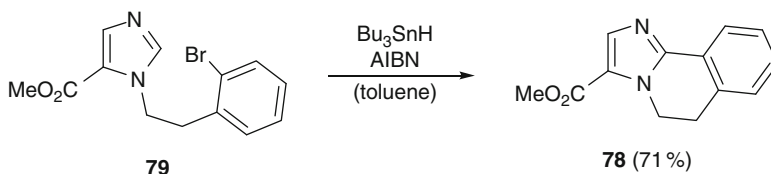
**Scheme 28** *Ipso* cyclization to phenylazides [136]

Spirocycles can be obtained from intramolecular radical biaryl coupling reactions when suitable substituents are present for an alternative stabilization of the cyclohexadienyl intermediate (c.f. **69**, Scheme 25). Otherwise, rearomatization can occur by cleavage of one substituent from the quaternary center of the spirocycle, such as the C–P bond in **69**. First examples for an alternative reaction course have been reported in studies on the photochemically induced cyclization of iodoarenes [134]. Recently, *tert*-butyldimethylsilyl ethers [135] and azides [136] were identified as well-suited substituents to lead the *ipso* substitution into the pathway towards spirocycles (Scheme 27).

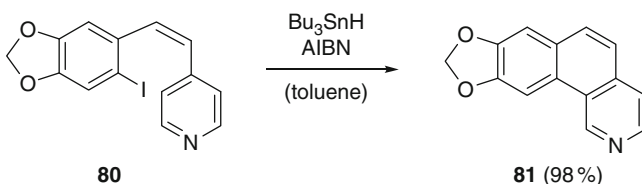
While the cyclization of the *tert*-butyldimethylsilyl ether **73** furnished the spirocyclohexadienone **74** directly as reaction product, the iminium hydroiodide **75** was isolated as intermediate from the reaction of azide **76** (Scheme 28) [136]. Subsequent aqueous hydrolysis of **75** under acidic conditions led to the spirocyclohexadienone **77**.

### 4.3 Cyclizations to Heteroaromatics

Although the addition of aryl radicals is more efficient to many heterocycles than to most substituted benzenes, the formation of the desired heterobiaryls can significantly be hindered in the rearomatization step [137–140]. Two examples from recent studies on Pschorr-type cyclizations on nitrogen-containing heterocycles are shown in Schemes 29 and 30 [141–143].



**Scheme 29** Cyclization to imidazoles [141]

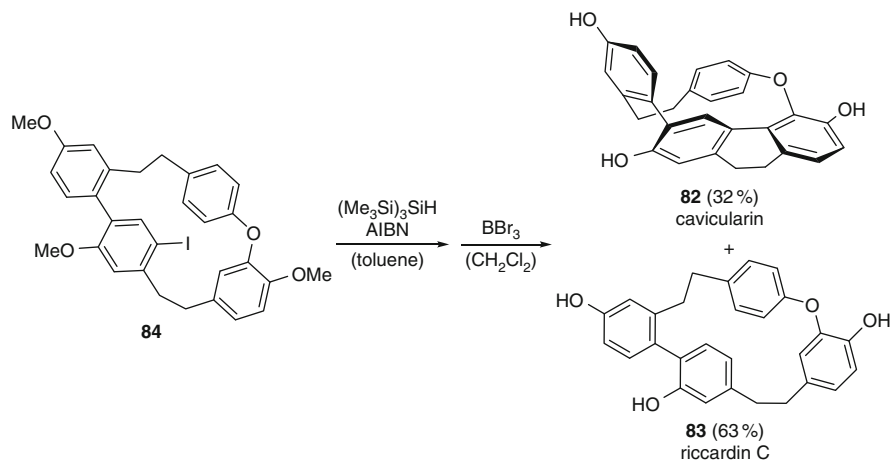


**Scheme 30** Cyclization to pyridine [142]

The imidazolyl-annulated dihydroisoquinoline **78** was accessible from the cyclization of imidazole **79**. The outcome of intramolecular substitutions on pyridines turned out to be strongly dependent on the linker between the aromatic cores (Scheme 30). With a *cis*-configured alkene in place, as in **80**, the expected benzoisoquinoline **81** was isolated in excellent yield. The *trans*-configured alkene and the saturated C<sub>2</sub>-alkane were shown to be less suitable tethers due to the formation of side products.

### 4.4 Application in Natural Product Synthesis

Beautiful examples of applications of Pschorr type cyclizations are the total syntheses of cavicularin (**82**) and riccardin C (**83**) (Scheme 31) [144]. Cavicularin (**82**)



**Scheme 31** Key cyclization in the total synthesis of cavicularin (**82**) [144]

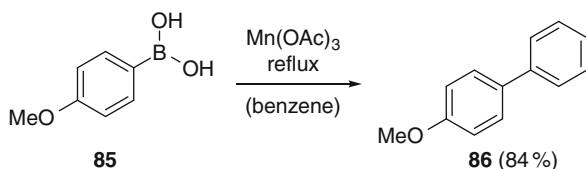
was obtained from precursor **84** by transannular ring-contraction along with riccardin C (**83**) although the cavicularin macrocycle is highly strained. Due to this strain in the cavicularin core the only *para*-substituted phenyl ring in the cycle is forced to adopt a boatlike configuration and its substituents are twisted out of the plane by ca.  $15^\circ$  in the solid state.

## 5 Gomberg–Bachmann Reactions

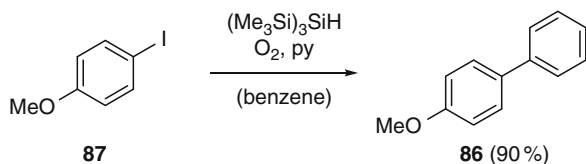
### 5.1 Biphenyls: New Aryl Radical Sources

The development of phase-transfer Gomberg–Bachmann (PTGB) reactions more than 30 years ago turned out to be a major advance in radical biaryl synthesis [145]. To this day these protocols represent benchmarks, since good to high yields can be obtained with a large variety of substrates under non-demanding conditions. Remaining drawbacks, however, are the need for a large excess of aromatic substrates in relation to the diazonium salts as well as moderate to low regioselectivities.

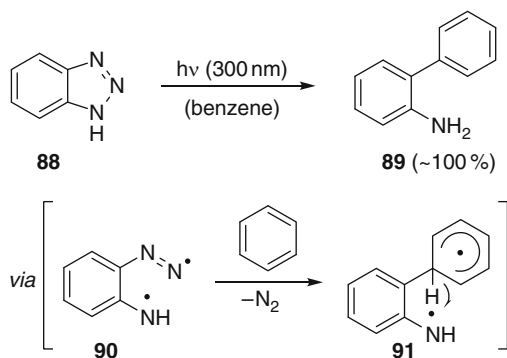
Besides aryl diazonium salts, a number of new aryl radical sources have appeared in recent years. Aryl boronic acids were used as aryl radical precursors in the presence of the strong oxidant manganese(III) acetate [146]. Earlier, the same group had reported on radical biaryl syntheses using manganese(III) acetate in combination with aryl hydrazines [147]. In a comparative arylation study on the use of aryl boronic acids, hydrazines, and aryl diazonium salts (PTGB protocol) for couplings with benzene, furan, or thiophene, the best yields were obtained when boronic acids were employed as radical sources. As shown in Scheme 32, boronic acid **85** was converted in high yield to biphenyl **86**.



**Scheme 32** Boronic acid as aryl radical precursors under strongly oxidizing conditions [146]



**Scheme 33** Biphenyl synthesis in the presence of oxygen [148]

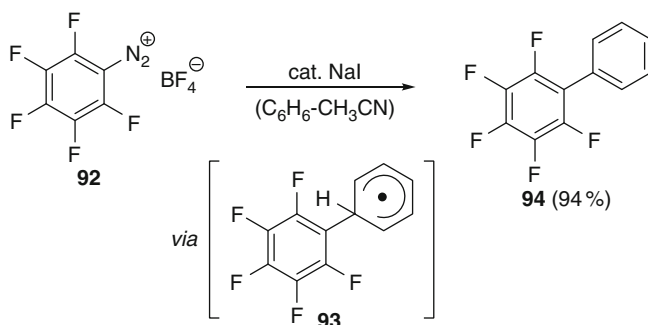


**Scheme 34** Benzotriazole (**88**) as source for aryl radicals [150]

Alternatively, aryl radicals can readily be generated from bromo- or iodobenzenes with  $\text{Bu}_3\text{SnH}$  or  $(\text{TMS})_3\text{SiH}$  and a radical initiator. Most of these reactions have so far been conducted in an intramolecular fashion (see Sect. 4). In a study on the intermolecular Gomberg–Bachmann type version, Curran et al. discovered that the reoxidation of the cyclohexadienyl adducts occurring as intermediates can be significantly facilitated by dioxygen (Scheme 33) [148]. In these reactions, aryl radicals were generated from iodobenzenes, such as **87**, using  $(\text{TMS})_3\text{SiH}$  [149]. In this way, better yields of biphenyls, such as **86**, were achieved than with  $\text{Bu}_3\text{SnH}$  as initiator.

Benzotriazoles, when irradiated at a wavelength of 300 nm, have turned out to be convenient sources for the previously unknown 2-amino-substituted aryl radical (Scheme 34) [150]. From a solution of benzotriazole **88** in benzene, 2-aminobiphenyl **89** was isolated in quantitative yield. This elegant approach





**Scheme 35** Radical arylations with pentafluorophenyl diazonium salts **92** [151]

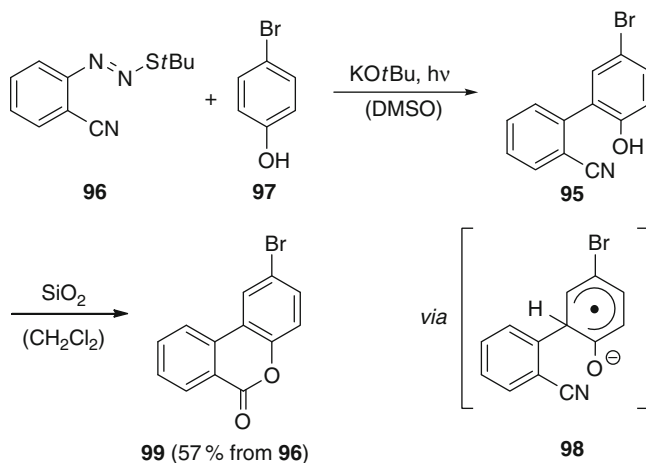
could become especially valuable since the alternative access to 2-aminobiphenyls via radical arylation of anilines or anilinium salts has so far not been put into practice with satisfactory regioselectivities and yields. The proposed reaction mechanism involves the radical intermediates **90** and **91**.

Electron-deficient aryl diazonium salts such as the pentafluoro derivative can offer the attractive option to conduct radical arylations as chain reactions with an  $S_{RN}1$  mechanism (Scheme 35) [151]. In these special cases, only catalytic amounts of an initiating reductant, such as sodium iodide, are required. In the propagation step, the diazonium salt **92** acts as oxidant for the cyclohexadienyl intermediate **93**. Rearomatization of **93** to **94** as well as the generation of a new pentafluorophenyl radical are achieved through this step.

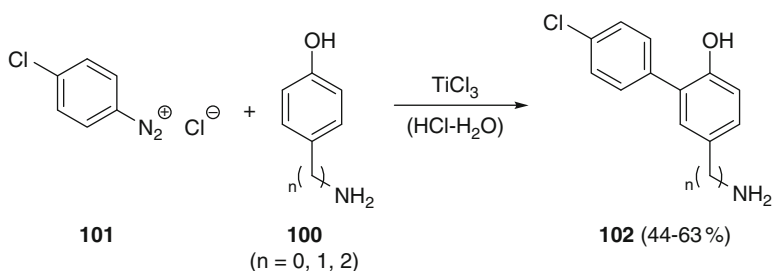
## 5.2 Biphenyls: New Substrates

From a general point of view, electron-rich benzenes such as anilines or phenols should be well-suited substrates for radical arylations due to the electrophilic character ascribed to the group of aryl radicals. Moreover, amino and hydroxy groups can have a remarkably high stabilizing effect on the cyclohexadienyl intermediates arising from the addition of the aryl radical to the phenol or aniline. Among the radical sources available, the use of aryl diazonium salts is strongly limited by competing azo coupling reactions and triazene formation.  $\text{Bu}_3\text{SnH}$ - and  $(\text{TMS})_3\text{SiH}$ -mediated arylations of anilines and phenols, for which side-reactions are not that obvious, have not yet been studied in detail.

A practical access to 2-biphenyl alcohols **95** has been discovered by Petrillo (Scheme 36) [152]. Azo sulfides **96**, which are employed as masked diazonium salts, do not undergo azo coupling reactions. In combination with 4-substituted phenolates **97**, photochemically initiated arylations can even be conducted as chain processes according to the  $S_{RN}1$  mechanism. Given their high reductive potential, the cyclohexadienyl intermediates **98** are able to rearomatize by a single electron



**Scheme 36** Radical arylation of phenolates [152]



**Scheme 37** Radical arylation of phenols [153, 154]

transfer to an unreacted azo sulfide **96**, which in turn fragments to form a new aryl radical. Cyclization of **95** under mildly acidic conditions gave dibenzopyranone **99**.

Radical arylations of phenols differ in some respects from those of phenolates (Scheme 37). First, the decreased nucleophilicity of the phenol, such as **100**, allows the use of “unmasked” aryl diazonium chlorides **101** as radical sources. Given that an efficient reductant is present in the reaction mixture and that the diazonium salt is added slowly, biphenyl alcohols **102** can be prepared in moderate to good yields [153, 154]. In this way, the concentration of the salt **101** is kept low at any time and homocoupling reactions (addition of the aryl radical to diazonium ions) as well as azo coupling to the phenol **100** can be successfully overcome.

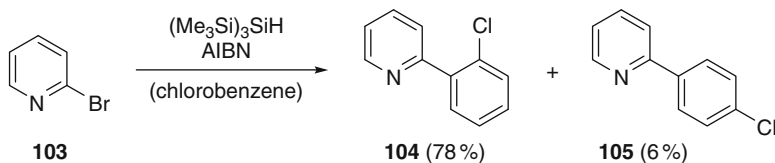
Since phenols can act as hydrogen donors, the use of polar solvents stabilizing the phenolic hydrogen by hydrogen bonding is beneficial. Other than with phenolates, efficient chain reactions have so far only been observed with reactive phenols such as 1,4-hydroquinone. In all other cases, catalytic amounts of the reductant proved insufficient to achieve clean conversions. As with 4-substituted phenolates, comparably good regioselectivities can be achieved with 4-substituted phenols.

Due to their high solubility in acidic aqueous solutions, 4-aminophenols, tyramines, and tyrosine derivatives are well-suited substrates for this type of arylation reactions [154].

### 5.3 Heteroaromatics

With many heterocycles as substrates, radical substitutions can be successfully carried out under the conditions of phase-transfer Gomberg–Bachmann reactions [145]. Again, as above, mainly aryl and heteroaryl halides have recently been used as precursors for heterobiaryl compounds. A study including the arylation of a large number of heterocycles in the presence of tributyltin hydride and catalytic benzeneselenol led to the results that mostly biaryl products are obtained from nitrogen-containing heterocycles, whereas furan and thiophene gave partially dearomatized compounds [155].

An example from a recent report on arylations with aryl and heteroaryl radicals is depicted in Scheme 38. Within this series of experiments, in which the substrate was used as solvent, remarkable regioselectivities were observed for some examples. The arylation of chlorobenzene with a 2-pyridinyl radical derived from bromide **103** gave a ratio of *ortho:para* arylation products **104** and **105** of 13:1 [156, 157].

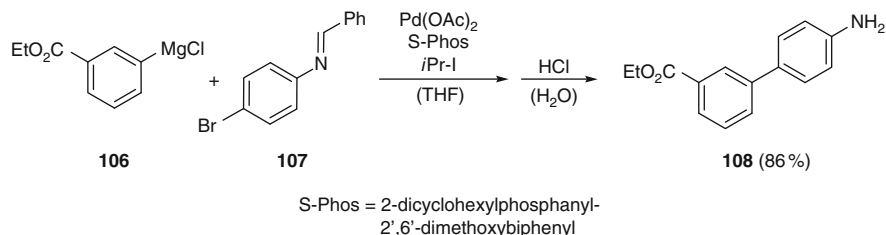


**Scheme 38** Arylation of chlorobenzene with 2-pyridinyl radicals [156]

## 6 Radical–Organometallic Hybrids

A first study on the combination of transition metal catalysis with radical chemistry was published in 2002 by Ryu [158]. Under CO pressure (40 atm), and in the presence of a palladium catalyst, cyclopentanones were formed from 4-pentenyl iodide in a photochemically initiated reaction.

This concept has now been extended to arylations. First evidence for a catalytic cycle involving a radical chain process in Kumada cross-coupling reactions of aryl Grignard reagents with aryl bromides was provided by Knochel and Manolikakes (Scheme 39) [159]. A remarkable difference was observed when the Grignard reagent was not classically prepared by oxidative addition of magnesium to iodobenzenes but instead by iodine–magnesium exchange with an *i*-PrMgCl/LiCl complex. As a result of the presence of *i*-PrI along with the Grignard reagent in



**Scheme 39** A radical chain process as part of a Kumada coupling [159]

the reaction mixture, the coupling of reactants such as **106** and **107** to give **108** occurred at room temperature and was completed in a few minutes. The mechanism proposed on experimental observations includes a catalytic Pd(I)/Pd(III) system.

Further reactions [160], in which radical and organometallic chemistry have been successfully combined, are the regioselective dehydrohalogenation by Oshima [161] and the catalytic reductive ring opening of epoxides by Gansäuer [162].

## References

- Griess P (1866) *Justus Liebig Ann* 137:39
- Gomberg M (1900) *J Am Chem Soc* 22:757
- Sandmeyer T (1884) *Chem Ber* 17:1633
- Pschorr R (1896) *Chem Ber* 29:496
- Gomberg M, Bachmann WE (1924) *J Am Chem Soc* 46:2339
- Meerwein H, Büchner E, Emster Kv (1939) *J Prakt Chem* 152:237
- Galli C (1988) *Chem Rev* 88:765
- Walters WA (1967) *The chemistry of free radicals*. Wiley, Boca Raton
- Zollinger H (1973) *Acc Chem Res* 6:335
- Cohen T, Lewarchik RJ, Tarino JZ (1974) *J Am Chem Soc* 96:7753
- Cohen T, Dietz AG, Miser JR (1977) *J Org Chem* 42:2053
- Kerk GM vd (1957) *J Appl Chem* 356
- Studer A, Bossart M (2001) In: Renaud P, Sibi M (eds) *Radicals in organic synthesis*, 2nd edn. Wiley-VCH, Weinheim
- Bowman WR, Storey JMD (2007) *Chem Soc Rev* 36:1803
- Vaillard SE, Schulte B, Studer A (2009) In: Ackermann L (ed) *Modern arylation methods*. Wiley-VCH, Weinheim
- Majumdar KC, Basu PK, Mukhopadhyay PP (2005) *Tetrahedron* 61:10603
- Majumdar KC, Basu PK, Chattopadhyay SK (2007) *Tetrahedron* 63:793
- Beckwith ALJ, Meijs GF (1987) *J Org Chem* 52:1922
- Bhandal H, Patel VF, Pattenden G, Russell JJ (1990) *J Chem Soc Perkin Trans 1* 10:2691
- Meijs GF, Beckwith ALJ (1986) *J Am Chem Soc* 108:5890
- Beckwith ALJ, Gara WB (1975) *J Chem Soc Perkin Trans 2* 795
- Beckwith ALJ, Meijs GF (1981) *J Chem Soc Chem Commun* 3:136
- Petrillo G, Novi M, Garbarino G, Filiberti M (1988) *Tetrahedron Lett* 29:4185
- Fletcher RJ, Lampard C, Murphy JA, Lewis N (1995) *J Chem Soc Perkin Trans 1* 6:623
- Koizumi T, Bashir N, Murphy JA (1997) *Tetrahedron Lett* 38:7635
- Koizumi T, Bashir N, Kennedy AR, Murphy JA (1999) *J Chem Soc Perkin Trans 1* 24:3637

27. Togo H, Kikuchi O (1988) *Tetrahedron Lett* 29:4133
28. Liu Y, Schwartz J (1995) *Tetrahedron* 51:4471
29. Perchyonok VT, Tuck KL, Langford SJ, Hearn MW (2008) *Tetrahedron Lett* 49:4777
30. Abeywickrema AN, Beckwith ALJ (1986) *Tetrahedron Lett* 27:109
31. Boivin J, Camara J, Zard SZ (1992) *J Am Chem Soc* 114:7909
32. Totleben MJ, Curran DP, Wipf P (1992) *J Org Chem* 57:1740
33. Curran DP, Totleben MJ (1992) *J Am Chem Soc* 114:6050
34. Molander GA, Harring LS (1990) *J Org Chem* 55:6171
35. Patel VF, Pattenden G (1987) *Tetrahedron Lett* 28:1451
36. Martin GC, Murphy JA, Smith CR (2000) *Tetrahedron Lett* 41:1833
37. Mahesh M, Murphy JA, LeStrat F, Wessel HP (2009) *Beilstein J Org Chem* 5(1)
38. Murphy JA, Khan TA, Zhou S, Thomson DW, Mahesh M (2005) *Angew Chem Int Ed* 44:1356
39. Fukuyama T, Kobayashi M, Rahman MT, Kamata N, Ryu I (2008) *Org Lett* 10:533
40. Alabugin IV, Manoharan M (2005) *J Am Chem Soc* 127:12583
41. Ishibashi H, Kobayashi T, Nakashima S, Tamura O (2000) *J Org Chem* 65:9022
42. Curran D, Fairweather M (2003) *J Org Chem* 68:2972
43. Kamimura A, Ishihara Y, So M, Hayashi T (2009) *Tetrahedron Lett* 50:1727
44. De la Fuente MC, Dominguez D (2007) *J Org Chem* 72:8804
45. Navarro-Vázquez A, García A, Dominguez D (2002) *J Org Chem* 67:3213
46. Petit M, Lapierre AJB, Curran DP (2005) *J Am Chem Soc* 127:14994
47. Petit M, Geib SJ, Curran DP (2004) *Tetrahedron* 60:7543
48. Majumdar KC, Alam S (2006) *Org Lett* 8:4059
49. Dandapani S, Duduta M, Panek JS, Porco JA Jr (2007) *Org Lett* 9:3849
50. Sato A, Yorimitsu H, Oshima K (2006) *J Am Chem Soc* 128:4240
51. Vaillard SE, Mueck-Lichtenfeld C, Grimme S, Studer A (2007) *Angew Chem Int Ed* 46:6533
52. Beckwith ALJ, Wang S, Warkentin J (1987) *J Am Chem Soc* 109:5289
53. Beak P, Park YS, Reif LA, Liu C (1994) *J Org Chem* 59:7410
54. Viswanathan R, Prabhakaran EN, Plotkin MA, Johnston JN (2003) *J Am Chem Soc* 125:163
55. McClure CK, Kiessling AJ, Link JS (1998) *Tetrahedron* 54:7121
56. Tomaszewski MJ, Warkentin J (1992) *Tetrahedron Lett* 33:2123
57. Johnston JN, Plotkin MA, Viswanathan R, Prabhakaran EN (2001) *Org Lett* 3:109
58. Viswanathan R, Smith CR, Prabhakaran EN, Johnston JN (2008) *J Org Chem* 73:3040
59. Coulomb J, Certal V, Fentserbank L, Lacôte E, Malacria M (2006) *Angew Chem Int Ed* 45:633
60. Benati L, Leardini R, Minozzi M, Nanni D, Spagnolo P, Strazzari S, Zanardi G (2002) *Org Lett* 4:3079
61. Oii T, Furuya M, Sakai D, Maruoka K (2001) *Adv Synth Catal* 343:166
62. Carta P, Puljic N, Robert C, Dhimane AL, Fensterbank L, Lacôte E, Malacria M (2007) *Org Lett* 9:1061
63. Hilton ST, Ho TCT, Pljevaljcic G, Schulte M, Jones K (2001) *Chem Commun* 2:209
64. Rey V, Pierini AB, Penéroy AB (2009) *J Org Chem* 74:1223
65. Amrein S, Bossart M, Vasella T, Studer A (2000) *J Org Chem* 65:4281
66. Schiesser CH, Sutej K (1992) *Tetrahedron Lett* 33:5137
67. Engman L, Laws MJ, Malmström J, Schiesser CH, Zugaro LM (1999) *J Org Chem* 64:6764
68. Laws MJ, Schiesser CH (1997) *Tetrahedron Lett* 38:8429
69. Bowman WR, Fletcher AJ, Potts GBS (2002) *J Chem Soc Perkin Trans 1* 2747
70. Ikeda M, Ohtani S, Sato T, Ishibashi H (1998) *Synthesis* 12:1803
71. Patro B, Murphy JA (2000) *Org Lett* 2:3599
72. Zhou SZ, Bommeziijn S, Murphy JA (2002) *Org Lett* 4:443
73. Rivkin A, Nagashina T, Curran DP (2003) *Org Lett* 5:419
74. Li F, Castle SL (2007) *Org Lett* 9:4033

75. Li F, Tartakoff SS, Castle SL (2009) *J Org Chem* 74:9082
76. Rigby JH, Qabar M (1991) *J Am Chem Soc* 113:8976
77. Rigby JH, Mateo ME (1996) *Tetrahedron* 52:10569
78. Schultz AG, Holoboski MA, Smyth MS (1993) *J Am Chem Soc* 115:7904
79. Schultz AG, Holoboski MA, Smyth MS (1996) *J Am Chem Soc* 118:6210
80. Rigby JH, Qabar MN (1993) *J Org Chem* 58:4473
81. Taniguchi T, Ishita A, Uchiyama M, Tamura O, Muraoka O, Tanabe G, Ishibashi H (2005) *J Org Chem* 70:1922
82. Taniguchi T, Iwasaki K, Uchiyama M, Tamura O, Ishibashi H (2005) *Org Lett* 7:4389
83. Tamura O, Yanagimachi T, Kobayashi T, Ishibashi H (2001) *Org Lett* 3:2427
84. Tamura O, Yanagimachi T, Ishibashi H (2003) *Tetrahedron Asymmetry* 14:3033
85. Kato I, Higashimoto M, Tamura O, Ishibashi H (2003) *J Org Chem* 68:7983
86. Orito K, Satoh Y, Nishizawa H, Harada R, Tokuda M (2000) *Org Lett* 2:2535
87. Nanni D (2001) In: Renaud P, Sibi MP (eds) *Radicals in organic synthesis*, 2nd edn. Wiley-VCH, Weinheim
88. Servais A, Azzouz M, Lopes D, Courillon C, Malacria M (2007) *Angew Chem Int Ed* 46:576
89. Kochi JK (1955) *J Am Chem Soc* 77:5090
90. Kochi JK (1955) *J Am Chem Soc* 77:5274
91. Rondestvedt CS (1976) *Org React* 24:225
92. Heinrich MR (2009), Intermolecular Olefin Functionalisation Involving Aryl Radicals Generated from Arenediazonium Salts, *Chem Eur J* 15:820, Copyright Wiley-VCH Verlag GmbH & Co. KGaA. Schemes 11, 13 and 16 reproduced with permission
93. Mastroilli P, Nobile CF, Taccardi N (2006) *Tetrahedron Lett* 47:4759
94. Obushak ND, Matiichuk VS, Matyak RL (2003) *Heterocycl Compd* 39:878
95. Molinaro C, Mowat J, Gosselin F, O'Shea PD, Marcoux JF, Angelaud R, Davies IW (2007) *J Org Chem* 72:1856
96. Adel IA, Salami BA, Levisalles J, Rudler H (1976) *Bull Soc Chim Fr* 934
97. Citterio A, Minisci F, Albinati A, Bruckner S (1980) *Tetrahedron Lett* 21:2909
98. Citterio A, Ramperti M, Vismara E (1981) *J Heterocycl Chem* 18:763
99. Citterio A, Minisci F, Vismara E (1982) *J Org Chem* 47:81
100. Heinrich MR, Blank O, Wölfel S (2006) *Org Lett* 8:3323
101. Heinrich MR, Blank O, Wetzel A (2007) *J Org Chem* 72:476
102. Blank O, Wetzel A, Ullrich D, Heinrich MR (2008) *Eur J Org Chem* 18:3179
103. Heinrich MR, Blank O, Wetzel A (2006) *Synlett* 19:3352
104. Ganushchak NI, Grishchuk BD, Dombrovskii AV (1973) *J Org Chem USSR* 9:1030
105. Grishchuk BD, Gorbovoi PM, Ganushchak NI, Dombrovskii AV (1994) *Russ Chem Rev* 63:257
106. Heinrich MR, Kirschstein M (2006) *Tetrahedron Lett* 47:2115
107. Beckwith ALJ, Bowry VW, Ingold KU (1992) *J Am Chem Soc* 114:4983
108. Heinrich MR, Wetzel A, Kirschstein M (2007) *Org Lett* 9:3833
109. Grishchuk BD, Gorbovoi PM, Kudrik EY, Ganushchak NI, Kaspruk BI (1997) *Russ J Gen Chem* 67:362
110. Grishchuk BD, Kudrik EY, Gorbovoi PM, Ganushchak NI, Avrashkova TV (1997) *Russ J Gen Chem* 67:1556
111. Gorbovoi PM, Kudrik EY, Grishchuk BD (1998) *Russ J Gen Chem* 68:1132
112. Grishchuk BD, Kudrik EY, Gorbovoi PM, Ganushchak NI (1996) *Russ J Gen Chem* 66:1482
113. Tournier L, Zard SZ (2005) *Tetrahedron Lett* 46:971
114. Gorbovoi PM, Tulaidan GN, Grishchuk BD (2008) *Russ J Gen Chem* 78:133
115. Grishchuk BD, Baranovskii VS, Simchak RV, Tulaidan GN, Gorbovoi PM (2006) *Russ J Gen Chem* 76:936
116. Heinrich MR, Blank O, Ullrich D, Kirschstein M (2007) *J Org Chem* 72:9609
117. Benati L, Leardini R, Minozzi M, Nanni D, Spagnolo P, Zanardi G (2000) *J Org Chem* 65:8669

118. Benati L, Calestani G, Leardini R, Minozzi M, Nanni D, Spagnolo P, Strazzari S, Zanardi G (2003) *J Org Chem* 68:3454
119. Wassmundt FW, Kiesman WF (1995) *J Org Chem* 60:196
120. Ohno H, Iwasaki H, Eguchi T, Tanaka T (2004) *Chem Commun* 19:2228
121. Narasimhan NS, Aidhen IS (1988) *Tetrahedron Lett* 29:2987
122. Orito K, Uchiito S, Satoh Y, Tatsuzawa T, Harada R, Tokuda M (2000) *Org Lett* 2:307 and references cited therein
123. Rossi RA (2005) *Synthetic organic photochemistry*, 2nd edn. Marcel Dekker, New York
124. Rossi RA, Pierini AB, Peñeñory AB (2003) *Chem Rev* 103:71
125. Barolo SM, Teng X, Cuny GD, Rossi RA (2006) *J Org Chem* 71:8493
126. Donnelly S, Grimshaw J, Trocha-Grimshaw J (1994) *J Chem Soc Chem Commun* 18:2171 and references cited therein
127. Harrowven DC, Nunn MIT, Fenwick DR (2002) *Tetrahedron Lett* 43:7345
128. Harrowven DC, Guy IL, Nanson L (2006) *Angew Chem Int Ed* 45:2242
129. Moorthy JN, Samanta S (2007) *J Org Chem* 72:9786
130. Da Mata MLEN, Motherwell WB, Ujjainwalla F (1997) *Tetrahedron Lett* 38:137
131. Alcaide B, Rodriguez-Vicente A (1998) *Tetrahedron Lett* 39:6589
132. Clive DLJ, Kang S (2000) *Tetrahedron Lett* 41:1315
133. Studer A, Bossart M, Vasella T (2000) *Org Lett* 2:985
134. Hey DH, Jones GH, Perkins MJ (1971) *J Chem Soc C* 116
135. De Turiso FGL, Curran DP (2005) *Org Lett* 7:151
136. Lanza T, Leardini R, Minozzi M, Nanni D, Spagnolo P, Zanardi G (2008) *Angew Chem Int Ed* 47:9439
137. Ho TCT, Jones K (1997) *Tetrahedron* 53:8287
138. Harrowven DC, Sutton BJ, Coulton S (2002) *Tetrahedron* 58:3387
139. Flanagan SR, Harrowven DC, Bradley M (2003) *Tetrahedron Lett* 44:1795
140. Ganguly AK, Wang CH, Chan TM, Ing YH, Buevich AV (2004) *Tetrahedron Lett* 45:883
141. Allin SM, Bowman WR, Elsegood MRJ, McKee V, Karim R, Rahman SS (2005) *Tetrahedron* 61:2689
142. Harrowven DC, Sutton BJ, Coulton S (2003) *Org Biomol Chem* 1:4047
143. Escolano C, Jones K (2002) *Tetrahedron* 58:1453
144. Harrowven DC, Woodcock T, Howes PD (2005) *Angew Chem Int Ed* 44:3899
145. Beadle JR, Korzeniowski SH, Rosenberg DE, Garcia-Slanga BJ, Gokel GW (1984) *J Org Chem* 49:1594
146. Demir AS, Reis Ö, Emrullahoglu M (2003) *J Org Chem* 68:578
147. Demir AS, Reis Ö, Özgül-Karaaslan (2001) *J Chem Soc Perkin Trans 1* 3042
148. Curran DP, Keller AI (2006) *J Am Chem Soc* 128:13706
149. Chatgililoglu C (2008) *Chem Eur J* 14:2310
150. Androsov DA, Neckers DC (2007) *J Org Chem* 72:1148
151. Kosynkin D, Bockman TM, Kochi JK (1997) *J Am Chem Soc* 119:4846
152. Petrillo G, Novi M, Dell'Erba C, Tavan C (1991) *Tetrahedron* 47:9297
153. Wetzel A, Ehrhardt V, Heinrich MR (2008) *Angew Chem* 120:9270; (2008) *Angew Chem Int Ed* 47:9130
154. Wetzel A, Pratsch G, Kolb R, Heinrich MR (2010) *Chem Eur J* 16:2547
155. Crich D, Patel M (2006) *Tetrahedron* 62:7824
156. Martinez-Barrasa V, De Viedma AG, Burgos C, Alvarez-Builla J (2000) *Org Lett* 2:3933
157. Núñez A, Sánchez A, Burgos C, Alvarez-Builla J (2004) *Tetrahedron* 60:6217
158. Ryu I, Kreimerman S, Araki F, Nishitani S, Oderaotoshi Y, Minakata S, Komatsu M (2002) *J Am Chem Soc* 124:3812
159. Manolikakes G, Knochel P (2009) *Angew Chem Int Ed* 48:205
160. Ford L, Jahn U (2009) *Angew Chem Int Ed* 48:6386
161. Kobayashi T, Ohmiya H, Yorimitsu H, Oshima KJ (2008) *J Am Chem Soc* 130:11276
162. Gansäuer A, Fan CA, Piestert FJ (2008) *J Am Chem Soc* 130:6916

# Radical Additions to Chiral Hydrazones: Stereoselectivity and Functional Group Compatibility

Gregory K. Friestad

**Abstract** Free radical additions to imino compounds offer increased synthetic accessibility of chiral amines, but lack of general methods for stereocontrol has hindered their development. This review focuses on two asymmetric amine synthesis strategies designed to address this problem, with emphasis on addition of functionalized radicals which may facilitate applications to synthesis of complex targets. First, chiral *N*-acylhydrazones are acceptors for intermolecular radical additions of a wide range of primary, secondary, and tertiary alkyl halides to the C=N bond, with radicals generated under manganese-, tin-, or boron-mediated conditions. A variety of aldehydes and ketones serve as viable precursors for the chiral hydrazones, and the highly stereoselective reactions tolerate electrophilic functionality in both coupling components. Second, radical precursors may be linked to chiral  $\alpha$ -hydroxyhydrazones via a silicon tether to the hydroxyl group; conformational constraints impart stereocontrol during 5-*exo* radical cyclization under stannyl- or thiy- mediated conditions. The silicon tether may later be removed to reveal the formal adducts of hydroxymethyl, vinyl, acetyl, and 2-oxoethyl radicals to the C=N bond. Methodology development and applications to biologically important targets are discussed.

**Keywords** Asymmetric synthesis · Chiral amines · Hydrazones · Radical reactions

## Contents

1	Background and Introduction .....	62
2	Intermolecular Radical Addition to Chiral <i>N</i> -Acylhydrazones .....	63
2.1	Design of Chiral <i>N</i> -Acylhydrazones .....	63
2.2	Preparation and Initial Reactivity Studies of Chiral <i>N</i> -Acylhydrazones .....	64
2.3	Manganese-Mediated Radical Addition .....	70
2.4	Hybrid Radical-Ionic Annulation .....	70

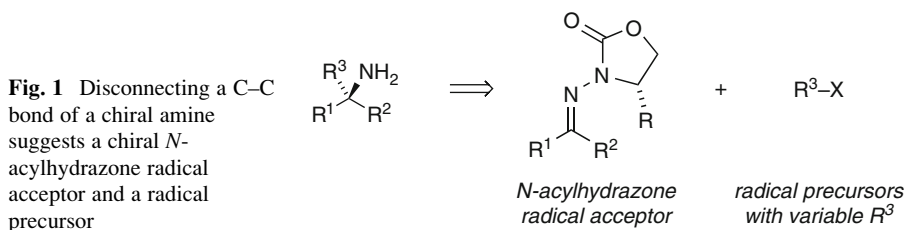


2.5	Applications in Amino Acid Synthesis .....	74
2.6	Stereoconvergence for Synthetic Design Flexibility .....	78
3	Silicon-Tethered Addition of Functionalized Radicals .....	79
3.1	Development of Additions to $\alpha$ -Hydroxyhydrazones .....	79
3.2	Reactivity and Stereocontrol in 6- <i>Exo</i> Cyclizations .....	82
3.3	Application to Aminosugar Synthesis .....	84
4	Summary .....	87
	References .....	87

## 1 Background and Introduction

Free radical additions (general reviews of radical reactions and their stereocontrol [1–7]) to imino compounds (reviews of radical additions to imines and related acceptors [8, 9]) provide an entry to chiral  $\alpha$ -branched amine functionality present in a wide range of bioactive synthetic targets. A variety of methods for direct asymmetric amine synthesis by addition to the C=N bond of carbonyl imino derivatives (Fig. 1) has been introduced (recent reviews [10–19]). Typically, new methods in this area strive for complete control of the configuration while forging a carbon–carbon bond under mild conditions; nucleophilic additions of carbanion-type reagents to C=N bonds according to Fig. 1 may be compromised by functional group incompatibilities or competing *aza*-enolization due to the basicity of many organometallic reagents (for examples of *aza*-enolization of imino compounds by organometallic reagents see [20–23]). Milder Strecker and Mannich addition reactions allow for a wider range of functionality in the imino acceptor, but are quite limited with respect to the incoming nucleophile [1–7]. Radical additions are a valuable alternative to these important methods, expanding the scope of the retrosynthetic disconnection of Fig. 1.

Organometallic nucleophiles and free radicals offer complementary functional group compatibility, such that a proper selection of the reactive intermediate could allow for the presence of a desired spectator functional group needed for later elaboration to synthetic targets of interest. Seeking to demonstrate this potential for improved versatility, we initiated a program to develop a variety of radical addition reactions of imino compounds [24]. In the process, we introduced new modes of



stereocontrol for radical additions to hydrazones, and this review will describe the design and experimental evaluation of these strategies.

## 2 Intermolecular Radical Addition to Chiral *N*-Acyldiazones

### 2.1 Design of Chiral *N*-Acyldiazones

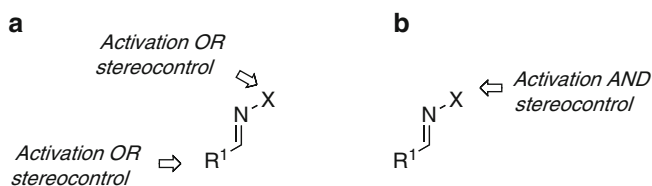
The C=N bond of simple imines possesses modest reactivity toward intermolecular radical additions, so such acceptors have rarely been exploited. To enhance their reactivity toward nucleophilic radicals, electron-withdrawing groups at the imine carbon have been effective, as demonstrated by Bertrand in radical additions to  $\alpha$ -iminoesters prepared from chiral amines [25]. Also, more reactive oxime ethers have been exploited extensively for radical addition, mainly through the longstanding efforts of Naito [26]. In most cases, stereocontrol has been imparted through the substituents on the imino carbon; chiral O-substituents on oximes for stereocontrol were ineffective, presumably due to poor rotamer control [27, 28].

On the other hand, we viewed hydrazones as promising radical acceptors for asymmetric transformations. Linking an amino or amido substituent to the C=N nitrogen atom could enhance reactivity in a fashion similar to oxime ethers, yet the nitrogen would offer an additional valence not available in the oxime ethers. Properly chosen substituents at this extra linkage point could enable better rotamer control than available in oxime ethers, and could accomplish both activation and stereocontrol through one removable N-substituent on the imine, independent of limitations posed by many of the structural features of the target itself. Confining the control elements of the reaction to one removable N-substituent would potentially broaden the scope of the reaction. Moreover, aldehyde hydrazones generally adopt C=N E-geometry, which avoids the problematic E/Z mixtures frequently encountered in oxime ethers.

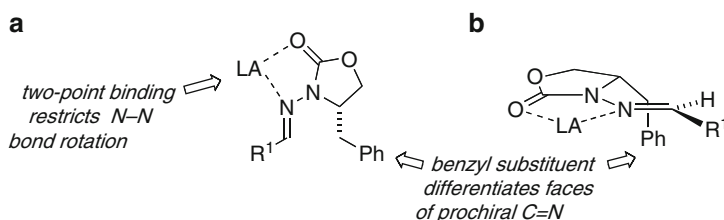
It is worth mentioning that chiral *N,N*-dialkylhydrazones (SAMP, RAMP) had been introduced by Enders for asymmetric  $\alpha$ -alkylation of carbonyl compounds [29], and addition of organometallic reagents to the C=N bond had also been demonstrated ([30]; selected organometallic additions to other chiral hydrazones [31–34]). However, the SAMP and RAMP hydrazones require a multistep preparation, and lacked a carbonyl function for two-point binding, which we regarded as a key design element (see below).

Based on all these considerations, we chose to develop a new type of chiral hydrazone, tailored for use in free radical addition reactions, which would incorporate Lewis acid activation [35–37] and restriction of rotamer populations as key design elements [1–7] (Fig. 2).

An early transition state is commonly assumed for exothermic radical addition reactions, and this enables approximation of the transition state geometry based on the ground-state structure. From this assumption, we hypothesized that a substituent above or below the plane of the C=N bond in the ground state hydrazone structure



**Fig. 2** (a) Earlier efforts to design asymmetric additions to imino compounds required two separate modifications to substituents of the C=N bond to accomplish both activation and stereocontrol. (b) With chiral *N*-acylhydrazone acceptors, the carbon branch ( $R^1$ ) of the imine may be varied freely, enabling improved versatility



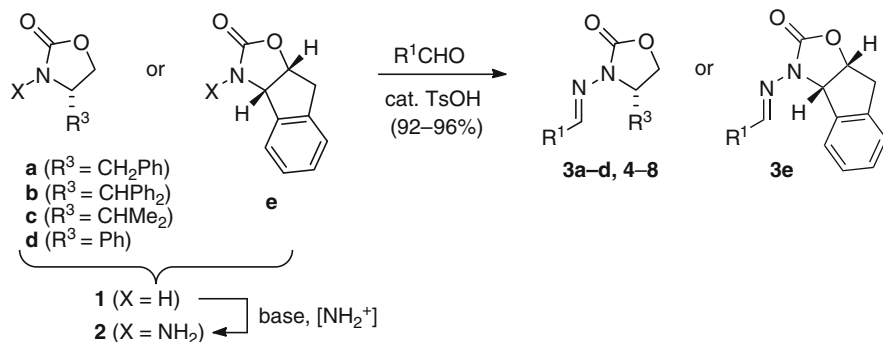
**Fig. 3** (a) Lewis acid chelation induces rigidity and electron-deficiency into the *N*-acylhydrazone radical acceptor (LA = Lewis acid). (b) Benzyl substituent of 4-benzyl-2-oxazolidinone provides facial differentiation of the C=N bond

would also provide steric blocking of one of the enantiotopic approach trajectories in the transition state, and would allow for effective stereocontrol.

Next, design elements were incorporated to address the restriction of rotamer populations and provide a Lewis basic site for Lewis acid activation [35–37]. An *N*-heterocyclic acylhydrazone (Fig. 3) constrains the C–N  $\sigma$  bonds within a ring and includes a carbonyl group for two-point binding of a Lewis acid in a rigid chelate structure. The Lewis acid would also lower the LUMO energy of the C=N  $\pi$  bond, increasing its reactivity toward nucleophilic alkyl radicals, ensuring selective reactivity via the chelated structure, and suppressing the non-selective background reaction. Following the hypothesized radical addition, purification of the adduct to diastereomeric homogeneity and reductive cleavage of the N–N bond [38, 39] would provide an enantiomerically pure amine and release the N-linked auxiliary for reuse. For the first test of our design, *N*-acylhydrazones (i.e., hydrazides) derived from *N*-aminooxazolidinones [40] were chosen to satisfy all the design criteria.

## 2.2 Preparation and Initial Reactivity Studies of Chiral *N*-Acylhydrazones

Although *N*-amino derivatives of oxazolidinones were sporadically reported in the literature [41–43], no applications in asymmetric synthesis were known prior to our



**Scheme 1** Preparation of chiral *N*-acylhydrazones

work. Therefore we began with a study of electrophilic amination of commercial oxazolidinones. In a series of trials, deprotonation of oxazolidinone **1a** (Scheme 1) and introduction of various  $\text{NH}_2^+$  equivalents afforded *N*-aminooxazolidinone **2a** in good yield.

One of the amination reagents initially employed, *O*-(mesitylenesulfonyl)hydroxylamine ( $\text{MtsONH}_2$ ), was effective, but its use is discouraged due to a tendency toward potentially hazardous exothermic decomposition. Preferred reagents are *O*-(*p*-nitrobenzoyl)hydroxylamine ( $\text{NbzONH}_2$ ), *O*-(diphenylphosphinyl)hydroxylamine ( $\text{Ph}_2\text{P}(=\text{O})\text{ONH}_2$ ), and  $\text{NH}_2\text{Cl}$  [44, 45]. Our optimized procedure for *N*-amination with  $\text{NbzONH}_2$  entailed deprotonation with  $\text{NaH}$  (or  $\text{KH}$ ) in hot dioxane, followed by introduction of  $\text{NbzONH}_2$  as a solid at ambient temperature [46]. With  $\text{NH}_2\text{Cl}$  the same procedure may be followed, but the stoichiometry of base and chloramine should be carefully controlled to nearly 1 equiv in order to obtain reproducible yields in the amination. The convenience and low cost of  $\text{NH}_2\text{Cl}$  is attractive, but its preparation and use as a dilute solution could be cumbersome for scale-up. Preparation of  $\text{NbzONH}_2$  is more expensive, but on the other hand this reagent allows operation at higher concentrations during the amination step.

With the *N*-amination chemistry established, condensation with aldehydes was examined. Initial efforts at this reaction proceeded reliably to afford a wide range of chiral hydrazones **3-8** in good overall yields (Table 1), with or without isolation of the intermediate *N*-aminooxazolidinone [47, 48]. Small amounts of **1a** which may remain after amination do not interfere with the condensation of **2a** with aldehydes, so it is generally convenient to use unpurified **2a** directly in the condensation step. Using the same two-step sequence, chiral *N*-acylhydrazones bearing different substituents on the oxazolidinone unit were prepared (Scheme 1). Moreover, the preparation of benzaldehyde hydrazone **7** (80% on the mmol scale) was validated on the multigram scale using crystallization to recover pure product from the crude mixture; **7** (9.4 g) was obtained in 74% yield from **1a** in this manner. The carbonyl component of these *N*-acylhydrazones may be exchanged with other carbonyl compounds [46]. Thus one can prepare in bulk a crystalline, indefinitely stable

**Table 1** Preparation of *N*-acylhydrazones from commercially available chiral oxazolidinones

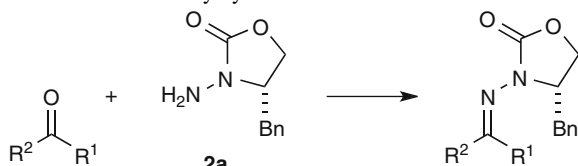
Entry	Oxazolidinone	R <sup>1</sup>	Method <sup>a</sup>	Product <sup>b</sup>
1	<b>1a</b>	Et	A	<b>3a</b> , 81%
2	<b>1a</b>	<i>i</i> -Pr	A	<b>4</b> , 70%
3	<b>1a</b>	<i>t</i> -Bu	A	<b>5</b> , 72%
4	<b>1a</b>	<i>c</i> -C <sub>6</sub> H <sub>11</sub>	A	<b>6</b> , 65%
5	<b>1a</b>	Ph	A	<b>7</b> , 67%
6	<b>1a</b>	Ph	B <sup>c</sup>	<b>7</b> , 80% (74%) <sup>d</sup>
7	<b>1a</b>	CO <sub>2</sub> Me	A	<b>8a</b> , 71%
8	<b>1b</b>	Et	B	<b>3b</b> , 75%
9	<b>1c</b>	Et	B	<b>3c</b> , 49%
10	<b>1d</b>	Et	B <sup>c</sup>	<b>3d</b> , 65%
11	<b>1e</b>	Et	B	<b>3e</b> , 87%

<sup>a</sup>Method A: i. *n*-BuLi, THF, -78 °C, 40 min; ii. MtsONH<sub>2</sub>, -78 °C → rt; iii. R<sup>1</sup>CHO, rt. Method B: (1) i. KH, dioxane, 60 °C, 1 h; ii. NBzONH<sub>2</sub>, rt. (2) R<sup>1</sup>CHO, cat. *p*-TsOH, toluene, rt

<sup>b</sup>Isolated yield except where noted

<sup>c</sup>NaH was used in place of KH

<sup>d</sup>Yield on 10 g scale, employing crystallization

**Table 2** Chiral *N*-acylhydrazones from ketones**9–11**

Entry	R <sup>1</sup>	R <sup>2</sup>	Hydrazone (yield %)	<i>E/Z</i> Ratio
1	Et	<i>i</i> -Pr	<b>9a</b> (84)	77:23
2	Et	<i>c</i> -C <sub>5</sub> H <sub>9</sub>	<b>9b</b> (49)	79:21
3	Et	<i>c</i> -C <sub>6</sub> H <sub>11</sub>	<b>9c</b> (64)	85:15
4	Et	<i>t</i> -Bu	<b>9d</b> (67)	>98:2
5	Ph	<i>i</i> -Pr	<b>10a</b> (55)	19:81
6	Ph	<i>c</i> -C <sub>5</sub> H <sub>9</sub>	<b>10b</b> (59)	26:74
7	Ph	<i>c</i> -C <sub>6</sub> H <sub>11</sub>	<b>10c</b> (55)	13:87
8	Ph	<i>t</i> -Bu	<b>10d</b> (73)	<2:98
9	Me	CO <sub>2</sub> Me	<b>11</b> (75)	92:8

hydrazone such as **7** for long-term storage, then convert portions of it to a variety of other hydrazones as desired.

Ketone-derived chiral *N*-acylhydrazones may also be prepared by direct condensation with *N*-aminooxazolidinone **2a** (Table 2) [45, 49]. Mixtures of *E/Z* isomers were usually obtained, although ketone *N*-acylhydrazones **9d** and **10d**, with highly branched tertiary butyl (*t*-Bu) substituents, were formed as single isomers. Pyruvate-derived hydrazone (*E*)-**11** was formed with high selectivity, and the major isomer was readily separated from its minor (*Z*)-isomer by flash chromatography [45]. Others have recently used these amination and condensation

procedures to prepare very similar chiral *N*-acylhydrazones from ketones with excellent results [50].

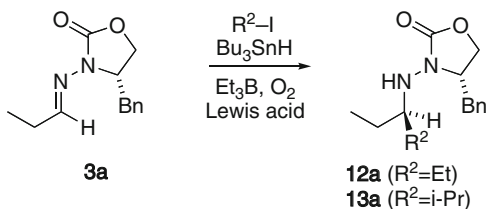
### 2.2.1 Additions of Secondary and Tertiary Radicals

The first test of the chiral *N*-acylhydrazones was in tin-mediated radical addition [47, 48]. Addition of isopropyl iodide to propionaldehyde hydrazone **3a** was chosen for initial screening (Scheme 2). Using the tin hydride method with triethylborane initiation [51, 52] ( $\text{Bu}_3\text{SnH}$ ,  $\text{Et}_3\text{B}/\text{O}_2$ ), with  $\text{InCl}_3$  and  $\text{ZnCl}_2$  as Lewis acid additives, desired adduct **13a** was obtained with high diastereoselectivity. In contrast, **13a** was produced with poor selectivity (diastereomer ratio, dr 2:1) in the absence of Lewis acid.

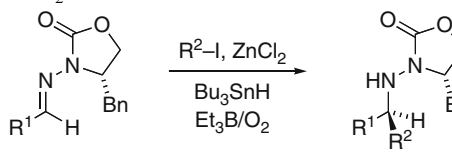
Additions of various organic iodides to propionaldehyde *N*-acylhydrazone **3a** were examined in order to evaluate the scope of the reaction with respect to the radical component. In the presence of  $\text{ZnCl}_2$ , radical additions proved successful with secondary and tertiary iodides in moderate yields (Table 3, entries 1–4), while primary and allylic radicals were ineffective under these conditions (entries 5 and 6). Ethyl radicals generated from triethylborane can compete for the radical acceptor and, as a result, the separable ethyl radical adduct **12a** (Scheme 2) was observed (<10% yield) in all cases.

Variations to the radical acceptor component were also examined with a series of aldehyde hydrazones (Table 3, entries 7–15) [48]. Branching at a saturated  $\alpha$ -carbon diminished the yields (entries 7–10), but the aromatic hydrazone **7** allowed successful radical addition (entries 11–14). The reactions were generally quite clean with the exception of **8a**, which decomposed under these conditions (entry 15). It should be noted that low yields were accompanied by unreacted hydrazones; 80–90% mass balance was generally observed.

Diastereoselectivity in radical additions to hydrazones **3** and **7** proved to be quite promising, with diastereomer ratios ranging from 93:7 to 99:1 (Table 3) [47]. In search of optimal stereocontrol, substituents on the oxazolidinone moiety were varied. Thus, isopropyl radical additions to several *N*-acylhydrazones **3a–3e** were compared for stereoselectivity (Scheme 3). High diastereoselectivities were observed in all adducts **13a–13e**, although a rigorous measurement was not obtained on **13c**. All of the auxiliaries impart stereocontrol suitable for practical synthetic application [48].



**Scheme 2** Preliminary test of radical additions to chiral *N*-acylhydrazones

**Table 3** Scope of tin-mediated radical addition to chiral *N*-acylhydrazone **3a** in the presence of ZnCl<sub>2</sub>


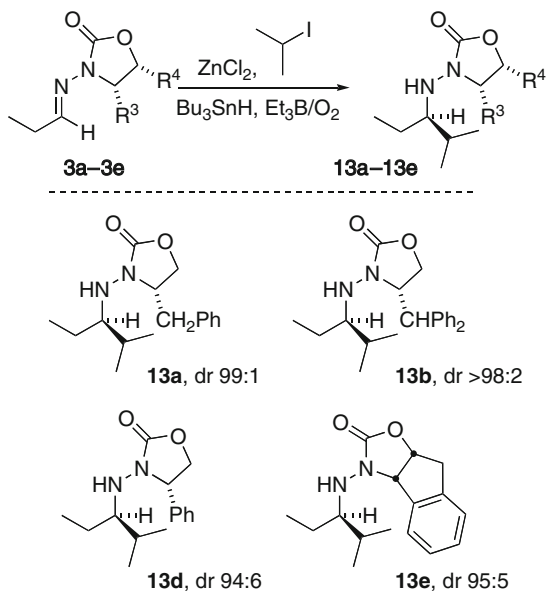
Entry	R <sup>1</sup>	R <sup>2</sup>	Recovery <sup>a</sup> (%)	Yield <sup>b</sup> (%) ( <i>dr</i> )
1	Et ( <b>3a</b> )	<i>i</i> -Pr	29	60 (99:1)
2	Et ( <b>3a</b> )	<i>c</i> -C <sub>5</sub> H <sub>9</sub>	– <sup>c</sup>	59 (96:4)
3	Et ( <b>3a</b> )	<i>c</i> -C <sub>6</sub> H <sub>11</sub>	60	28 (97:5)
4	Et ( <b>3a</b> )	<i>t</i> -Bu	14	54 (95:5)
5	Et ( <b>3a</b> )	<i>i</i> -Bu	50	6
6	Et ( <b>3a</b> )	Allyl	73	7
7	<i>i</i> -Pr ( <b>4</b> )	Et	88	6
8	<i>i</i> -Pr ( <b>4</b> )	<i>c</i> -C <sub>6</sub> H <sub>11</sub>	77	9
9 <sup>b</sup>	<i>c</i> -C <sub>6</sub> H <sub>11</sub> ( <b>6</b> )	Et	61	15
10	<i>c</i> -C <sub>6</sub> H <sub>11</sub> ( <b>6</b> )	<i>i</i> -Pr	79	9
11	Ph ( <b>7</b> )	<i>i</i> -Pr	33	42 (99:1)
12	Ph ( <b>7</b> )	<i>c</i> -C <sub>5</sub> H <sub>9</sub>	23	59 (96:4)
13	Ph ( <b>7</b> )	<i>c</i> -C <sub>6</sub> H <sub>11</sub>	64	30 (99:1)
14	Ph ( <b>7</b> )	<i>t</i> -Bu	– <sup>c</sup>	83 (93:7)
15	CO <sub>2</sub> Me ( <b>8a</b> )	<i>i</i> -Pr	0	0

Reaction conditions: Bu<sub>3</sub>SnH (5 equiv) and O<sub>2</sub> (7 mL/mmol) by syringe pump, *i*-PrI (10 equiv), Et<sub>3</sub>B (10 equiv), and Lewis acid (2 equiv), 2:1 CH<sub>2</sub>Cl<sub>2</sub>/ether, –78 °C → rt

<sup>a</sup>Recovered hydrazone, %

<sup>b</sup>Isolated yield, %

<sup>c</sup>Not determined

**Scheme 3** Role of oxazolidinone substituents on diastereoselectivity in isopropyl radical addition

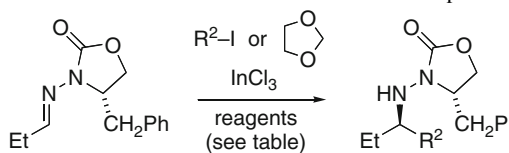
## 2.2.2 Triethylborane-Mediated Radical Additions Without Tin

Triethylborane and diethylzinc may serve both as initiator and chain transfer agents in radical additions to C=N bonds [25, 26]. This raised the question of whether similar additions to chiral *N*-acylhydrazones may occur in the absence of tin hydride. Accordingly, we attempted tin-free additions of various halides to the propionaldehyde hydrazone **3a** in the presence of triethylborane, using InCl<sub>3</sub> as the Lewis acid [48]. These reactions were indeed successful with secondary iodides (Table 4, entries 2–4). Chloriodomethane also gave successful addition of the chloromethyl group, giving a product bearing functionality suitable for subsequent manipulations.

Tin-free photolytic conditions for addition of formyl radical equivalents to **3a** have been reported by Alonso [53]. Photolysis of 1,3-dioxolane solutions of **3a** in the presence of 1 equiv of benzophenone led to formation of the 1,3-dioxolan-2-yl radical from solvent, followed by intermolecular radical addition in 87% yield (entry 6). A one-pot variant without isolation of **3a** increased the yield and selectivity (entry 7). These conditions gave good yields across a range of chiral *N*-acylhydrazones (not shown), but synthetically useful levels were restricted to aliphatic aldehyde precursors.

A limitation of the aforementioned methods is that they are unsuitable for the use of primary alkyl iodides. Under Et<sub>3</sub>B/O<sub>2</sub> initiation conditions, the desired radical is intended to be generated by iodine atom transfer to ethyl radicals, which is not favorable in the case of primary iodides. Thus ethyl radical addition competes with the desired radical when using triethylborane initiation along with primary iodides. In addition, generating radicals by hydrogen atom transfer from ethers or acetals has limited applicability. Because of the expanded synthetic potential of primary alkyl iodides as

**Table 4** Tin-free radical additions to **3a** in the presence of InCl<sub>3</sub>



Entry	R <sup>2</sup>	Method	Yield <sup>a</sup> (%)
1	Et	A	33
2	<i>i</i> -Pr	A	75 <sup>b</sup>
3	<i>c</i> -C <sub>5</sub> H <sub>9</sub>	A	47
4	<i>c</i> -C <sub>6</sub> H <sub>11</sub>	A	56
5	ClCH <sub>2</sub>	A	33
6	1,3-dioxolan-2-yl	B	87 <sup>c</sup>
7	1,3-dioxolan-2-yl	C	96 <sup>d</sup>

Reaction conditions: A: As in Table 3, minus Bu<sub>3</sub>SnH. B: 1,3-dioxolane, Ph<sub>2</sub>CO, InCl<sub>3</sub>, hv, -78 °C. C: Same as B, except one-pot; *N*-acylhydrazone prepared and used in situ

<sup>a</sup>Isolated yield

<sup>b</sup>*dr* >95:5 (<sup>1</sup>H NMR)

<sup>c</sup>*dr* 91:9 (Alonso [53])

<sup>d</sup>*dr* 98:2 (Alonso [53])



radical precursors, great importance is attached to finding alternatives to triethylborane which can accomplish iodine atom transfers of broader utility for radical additions.

### 2.3 Manganese-Mediated Radical Addition

Our attention was drawn to photolytic radical generation with hexamethylditin because it showed promise in Kim's prior work with C=N radical acceptors, which included additions of primary radicals [54–60]. Adapting Kim's photolysis conditions, with hexamethylditin in the presence of InCl<sub>3</sub>, ethyl and isopropyl additions to hydrazone **3a** occurred in reasonable yield [48]. Unfortunately, a carbonyl exchange side reaction [46] with acetone (used as a sensitizer under Kim's conditions) interfered with further development of this reaction.

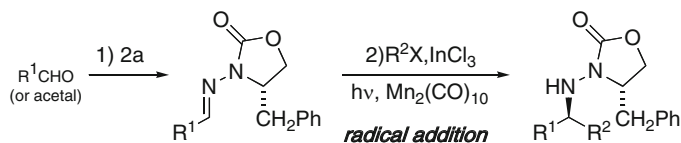
We noted, however, that manganese carbonyl [61–63] [Mn<sub>2</sub>(CO)<sub>10</sub>] ( $\lambda_{\text{max}}$  340 nm,  $\sigma_{\text{Mn-Mn}} \rightarrow \sigma^*_{\text{Mn-Mn}}$ ) may be photolyzed without any sensitizer, leading to homolytic metal–metal bond cleavage. This produces two •Mn(CO)<sub>5</sub> radicals, which are well known to abstract halogen atoms from alkyl halides [64]. Despite its longtime familiarity in organometallic chemistry, the first studies of the synthetic scope of this reactivity mode appeared in a series of papers by Parsons (for seminal examples see [65–68]).

Armed with a strong set of precedents, we applied this photolysis to the reaction of ethyl iodide with *N*-acylhydrazone **3a** (Table 5) [69, 70]. Irradiation (300 nm) with Mn<sub>2</sub>(CO)<sub>10</sub> using InCl<sub>3</sub> as a Lewis acid furnished the ethyl adduct in 85% yield, a dramatic improvement over experiments using triethylborane or hexamethylditin. Control experiments revealed a requirement for both irradiation and Mn<sub>2</sub>(CO)<sub>10</sub>; on the other hand, the reaction proceeded without InCl<sub>3</sub>, though sluggishly (21% yield, 2 days).

A variety of other halides, including methyl iodide and dihaloalkanes, were also effective (Table 5). An exception was a low-yielding addition of 2-chloroethyl iodide, which presumably was compromised by fragmentation of the 2-chloroethyl radical. Similar versatility was displayed with respect to the hydrazone component; ethyl radical addition to *N*-acylhydrazones **14–22** occurred in good yields. These adducts are epimeric to those derived from hydrazone **3a** with respect to the new stereogenic center, as a result of simply changing the roles of the aldehyde and iodide precursors. From the strategy standpoint, this combination of stereocontrol flexibility and functional group compatibility is advantageous for total synthesis applications.

### 2.4 Hybrid Radical–Ionic Annulation

Applying radical addition reactions in the presence of electrophilic spectator functionalities was attractive, as such demonstrations of compatibility would illustrate

**Table 5** Mn-mediated radical additions to *N*-acylhydrazones

Aldehyde (or acetal)	Hydrazone <sup>a</sup>	Halide R <sup>2</sup> X	Yield (%), config <sup>b</sup>	<i>dr</i>
CH <sub>3</sub> CH <sub>2</sub> CHO	<b>3a</b> , 81%	CH <sub>3</sub> CH <sub>2</sub> I	85	–
		CH <sub>3</sub> I	48 <sup>c,d</sup> , <i>S</i>	95:5 <sup>e</sup>
			66, <i>R</i>	94:6 <sup>e</sup>
			78, <i>R</i>	95:5 <sup>e</sup>
			79, <i>R</i>	96:4 <sup>e</sup>
			54 <sup>c</sup> , <i>R</i>	95:5 <sup>f</sup>
			75, <i>R</i>	95:5 <sup>f</sup>
		ClCH <sub>2</sub> I	63, <i>R</i>	93:7 <sup>e</sup>
		Cl	52, <i>R</i>	96:4 <sup>f</sup>
		Cl	55, <i>R</i>	96:4 <sup>e</sup>
		Cl <sub>2</sub> CHBr	38 <sup>c,d</sup> , <i>R</i>	98:2 <sup>f</sup>
CH <sub>3</sub> CHO	<b>14</b> , 66%	CH <sub>3</sub> CH <sub>2</sub> I	66, <i>R</i>	95:5 <sup>e</sup>
	<b>15</b> , 87%		63, <i>S</i>	95:5 <sup>e</sup>
	<b>16</b> , 89%		72, <i>S</i>	97:3 <sup>e</sup>
Cl	<b>17</b> , 88%		77, <i>S</i>	97:3 <sup>e</sup>
	<b>18</b> , 85%		65, <i>S</i>	95:5 <sup>f</sup>
ClCH <sub>2</sub> CH(OMe) <sub>2</sub>	<b>19</b> , 85%		57, <i>S</i>	93:7 <sup>e</sup>
Cl	<b>20</b> , 95%		60, <i>S</i>	93:7 <sup>f</sup>
Cl	<b>21</b> , 89%		62, <i>S</i>	97:3 <sup>e</sup>
Cl <sub>2</sub> CHCH(OEt) <sub>2</sub>	<b>22</b> , 54%		34 <sup>c</sup> , <i>S</i>	89:11 <sup>f</sup>

Reaction conditions: (1) Aldehyde or acetal (5–10 equiv), **2a**, *p*-toluenesulfonic acid, CH<sub>2</sub>Cl<sub>2</sub>, rt. (2) Hydrazone in deoxygenated CH<sub>2</sub>Cl<sub>2</sub> (0.1 M), InCl<sub>3</sub> (2.2 equiv), Mn<sub>2</sub>(CO)<sub>10</sub> (1–2 equiv), R<sup>2</sup>X (10 equiv), hv (300 nm, pyrex), 1–2 d, ca. 35 °C

<sup>a</sup>Isolated yield

<sup>b</sup>Isolated yields of purified diastereomer mixtures. *R* or *S* denotes the configuration of the new stereogenic center. Addition of methyl iodide gives opposite configurations due to the lower priority of the methyl ligand

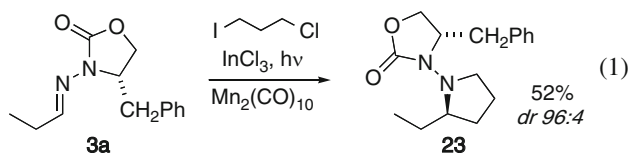
<sup>c</sup>20 equiv of R<sup>2</sup>X was used

<sup>d</sup>1,8-Diazabicyclo[5.4.0]undec-7-ene (DBU) was used in removal of Mn byproducts

<sup>e</sup>Ratio by HPLC (Chiralcel OD, 2-PrOH/hexane)

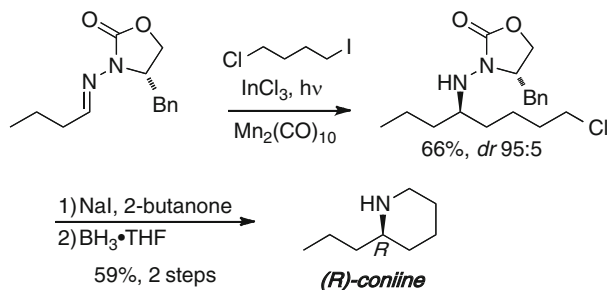
<sup>f</sup>Ratio by <sup>1</sup>H NMR

the complementarity of radical conditions and strongly nucleophilic conditions. In this regard, it should be noted that dihaloalkanes had been used as radical precursors (Table 5), preserving halide functionality in most cases. However, in one case, addition of 3-chloro-1-iodopropane (1), characterization of the adduct indicated there was no chlorine present; this reaction had afforded pyrrolidine **23** [69, 70]. This outcome may be explained by sequential radical addition and S<sub>N</sub>2-type cyclization in situ. Support for such a process was also found upon addition of ethyl iodide to the 3-chlorobutyraldehyde hydrazone **20** (Table 5), which gave the epimeric pyrrolidine (*epi*-**23**). These radical–polar crossover reactions (for selected recent examples of radical–polar crossover reactions see [71–80]), which may also be termed hybrid radical–ionic annulations, offer a novel way to achieve 1,2-bis-functionalization of the C=N bond.

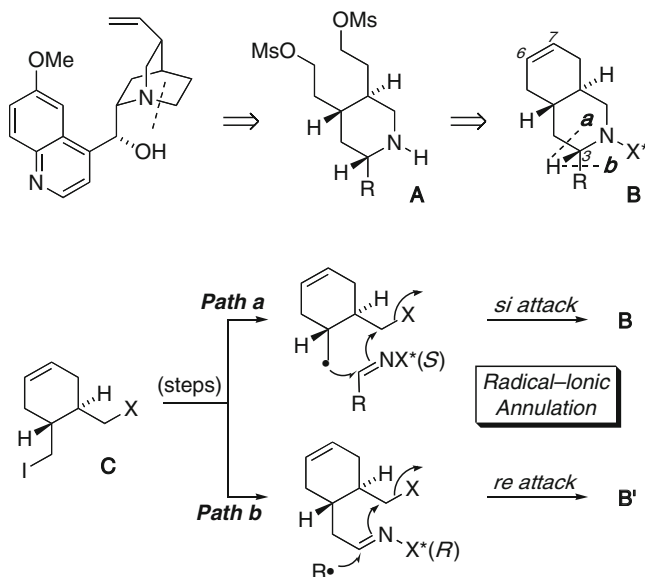


The simple piperidine alkaloid coniine (for selected asymmetric syntheses of coniine see [22, 81–85]) offered a preliminary test case for hybrid radical–ionic annulation in alkaloid synthesis. From butyraldehyde hydrazone and 4-chloro-iodobutane (Scheme 4), manganese-mediated photolysis afforded the acyclic adduct in 66% yield (dr 95:5); the cyclization did not occur in situ [69, 70]. Nevertheless, Finkelstein conditions afforded the piperidine, and reductive removal of the auxiliary afforded coniine in 34% overall yield for four steps. This reaction sequence enables a direct comparison between radical- and carbanion-based syntheses using the same retrosynthetic disconnection: an alternative carbanion approach required nine to ten steps [81, 85]. The potential for improved efficiency through novel radical addition strategies becomes quite evident in such comparisons where multifunctional precursors are employed.

Our approach to the antimalarial alkaloid quinine focuses on strategic application of the manganese-mediated hybrid radical–ionic annulation. Retrosynthetically, this is illustrated (Scheme 5) by disconnection of either of two C–C bonds



**Scheme 4** Hybrid radical-ionic annulation route to (*R*)-coniine

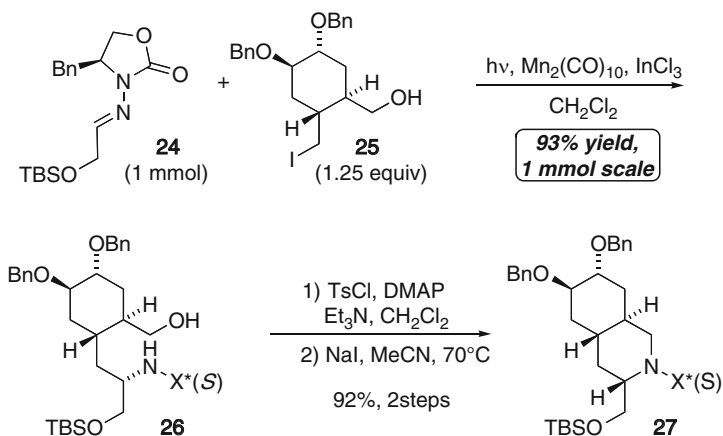


**Scheme 5** Radical addition strategy for quinine synthesis

in structure **B**, involving either *Path a* or *Path b*. With enantiomeric chiral auxiliaries, these paths converge to the same structure upon auxiliary removal from structures **B** (S auxiliary) and **B'** (R auxiliary). Thus the radical-ionic annulation strategy suggested retrosynthetic disconnection to a pseudo-C<sub>2</sub>-symmetric precursor **C**, which facilitated efficient access to coupling components.

The flexibility of the manganese-mediated radical coupling enabled the two alternative pathways to be examined experimentally; the iodide and hydrazone functionality of the two components could be interchanged such that both could serve as either radical precursor or radical acceptor. Unfortunately, experimental evaluation revealed that both options suffered from interference by the alkene functionality present in precursors of type **C** [86]. As the strategy called for the alkene to be cleaved eventually by ozonolysis or the like, it was decided to oxidize it partially at an earlier stage, while preserving the ability to take advantage of the C<sub>2</sub>-symmetric aspects of the strategy. Thus the alkene was oxidized to a *trans*-1,2-diol bearing benzyl ether protecting groups, then processed in standard fashion to iodide **25** (Scheme 6).

In the key manganese-mediated radical addition to couple **24** with **25**, stoichiometry was a concern, as large excesses of radical precursor commonly required for many intermolecular radical additions would be prohibitive for an iodide such as **25**, prepared through several synthetic steps. Fortunately, the manganese-mediated coupling of **24** and **25** with only 1.25-fold excess of **25** proceeded in 93% yield in 1 mmol scale, giving **26** as a single diastereomer. Although completion of the hybrid radical-ionic annulation in situ during the manganese-mediated coupling



**Scheme 6** Key carbon-carbon bond construction en route to quinine

has not yet been achieved, a stepwise process provided decahydroisoquinoline **27** in a quite satisfactory overall yield (85% for three steps) [86]. Recently, the conversion of adduct **26** to quincorine has been achieved [174], completing a formal synthesis of quinine and validating the application of Mn-mediated radical addition to alkaloid synthesis. The low stoichiometric requirement in the coupling of the multifunctional iodide **25** to an imino compound is attractive and should enable broader applications of this manganese-mediated coupling process in complex target synthesis.

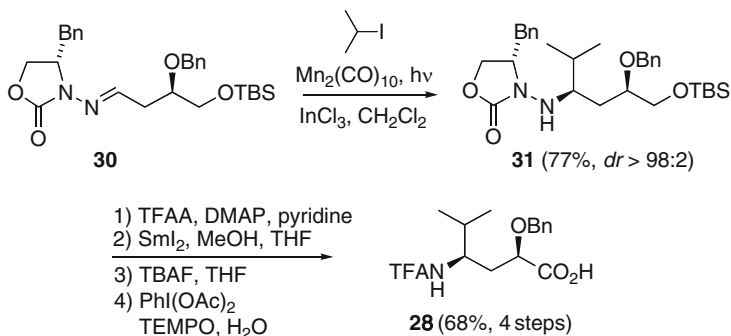
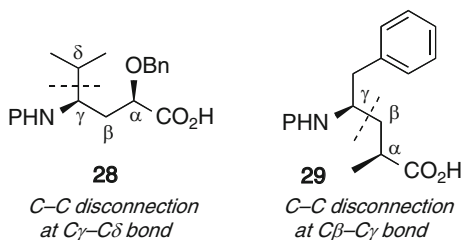
## 2.5 Applications in Amino Acid Synthesis

### 2.5.1 Synthesis of $\gamma$ -Amino Acids

Although  $\alpha$ - and  $\beta$ -amino acids have drawn more attention in synthetic chemistry,  $\gamma$ -amino acids such as **28** and **29** (Fig. 4) are also important targets from the perspective of bioorganic and medicinal chemistry (reviews [87, 88]; examples [89–102]). Disconnections of C–C bonds as shown calls for iodides and hydrazones bearing oxygen-containing functional groups, an important challenge to the synthetic versatility of the manganese-mediated coupling reactions. With this in mind, we employed manganese-mediated radical addition for a novel synthesis of  $\gamma$ -amino acids **28** and **29** [103].

Because disconnection of  $\alpha$ -alkoxy- $\gamma$ -amino acid **28** calls for  $\beta$ -alkoxyhydrazone **30**, the potential for  $\beta$ -elimination of the alkoxy group from the hydrazone precursor **30** (Scheme 7) makes non-basic conditions critical. In fact, treatment of **30** with TBAF in THF led to just such a  $\beta$ -elimination (Marié, University of Iowa, unpublished). However, the manganese-mediated radical addition of isopropyl iodide proceeded in 77% yield, without any evidence of  $\beta$ -elimination, to afford **31** as a single diastereomer. Reductive removal of the chiral auxiliary and oxidation to the carboxylic acid gave **28** in good overall yield [103].

**Fig. 5** Representative  $\gamma$ -amino acids found as substructures in the tubulysins [101, 102] with strategic bond disconnections at the  $\gamma$ - $\delta$  and  $\beta$ - $\gamma$  carbons (P = protecting group)

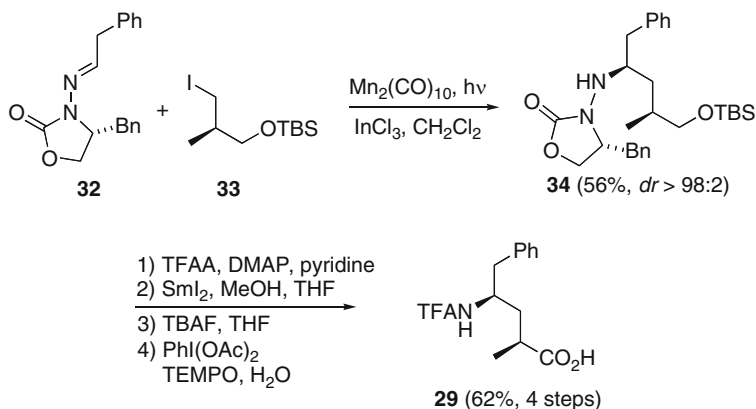


**Scheme 7** Synthesis of tubovaline

Phenylacetaldehyde *N*-acylhydrazone **32** served as the radical acceptor for assembly of  $\gamma$ -amino acid **29** (Scheme 8), employing difunctional iodide **33** in the manganese-mediated radical addition (56% yield, single diastereomer) [103]. As with **31** (shown above), this radical adduct **34** was converted through the same four-step sequence to  $\gamma$ -amino acid **29**.

Although the aforementioned routes provided the desired  $\gamma$ -amino acids, it was desirable to develop a synthesis which incorporates the carboxylic acid oxidation state *prior to coupling*. We hypothesized that manganese-mediated radical addition would accomplish this objective, and therefore initiated a study of manganese-mediated coupling of alkyl iodides with  $\gamma$ -hydrazoneesters [104]. We had already shown that the manganese-mediated radical addition conditions offer excellent chemoselectivity, but it remained to be seen whether the stereocontrol model would be disrupted; would an additional Lewis basic ester function in the hydrazone interfere with the role of In(III) in two-point binding and rotamer control?

Prototypical radical additions were examined under manganese-mediated photolysis conditions with InCl<sub>3</sub> as the Lewis acid, coupling isopropyl iodide with a variety of  $\gamma$ -hydrazoneesters **35a–35d** (Table 6) bearing varied substitution at the position  $\alpha$  to the ester. The  $\alpha$ -methyl,  $\alpha,\alpha$ -dimethyl, and  $\alpha$ -benzyloxy substituents appeared to have little effect on reaction efficiency and selectivity, as all provided the isopropyl adducts with consistently high diastereoselectivities and excellent yields (91–98%). Surprisingly, the selectivity was only slightly



**Scheme 8** Synthesis of tubophenylalanine

diminished in the absence of  $\text{InCl}_3$  (entries 5 and 6); the yield in the absence of Lewis acid activation was modest but synthetically useful.

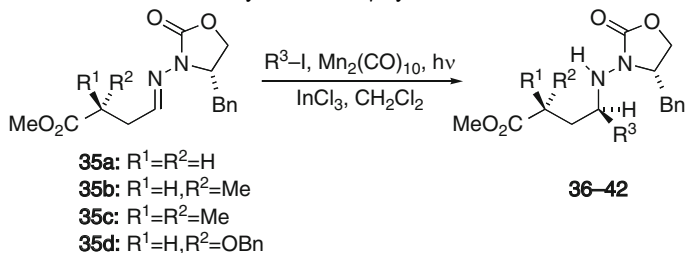
For the  $\gamma$ -hydrazoneesters, NMR experiments substantiated the chelation model. A mixture of **35a** with  $\text{InCl}_3$  in  $\text{CD}_2\text{Cl}_2$  exhibited the  $\text{H}-\text{C}=\text{N}$  absorbance of the  $\gamma$ -hydrazoneester at 7.74 ppm, 0.30 ppm upfield from **35a** alone, consistent with precedent regarding Lewis acid coordination to imino compounds [105]. Also, the carbons of the oxazolidinone  $\text{C}=\text{O}$  and the hydrazone  $\text{C}=\text{N}$  were shifted downfield by 8 and 5 ppm on mixing with  $\text{InCl}_3$ . In contrast, the  $\text{C}=\text{O}$  carbon of the ester showed minimal change (<1 ppm). This suggests that the  $\text{InCl}_3$  is chelated by the imino nitrogen and the oxazolidinone carbonyl in the usual way, without significant interference by the ester function.

A range of iodides were next examined in reactions with and without  $\text{InCl}_3$ , starting with a comparison of secondary and primary iodides (Table 6). When secondary iodides were subjected to coupling with  $\gamma$ -hydrazoneester **35a** the yields were excellent (entries 1 and 5), while primary iodides gave the desired adducts in moderate yields (33–66%, entries 6–10). All of these reactions occurred with excellent diastereoselectivities, and it was worth noting that both silyl ether and alcohol functionality were compatible with the coupling.

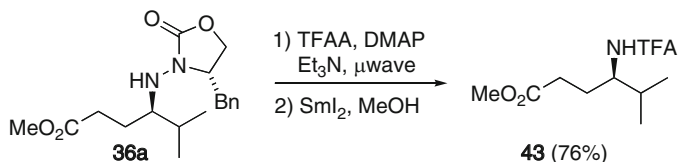
To document the synthetic applicability of these reactions, N–N bond cleavage was needed. After trifluoroacetylation of **36a** (Scheme 9) under microwave irradiation [106–108], exposure to  $\text{SmI}_2$  smoothly furnished known  $\gamma$ -aminoester **43** and offered proof of absolute configuration (allylation of the  $\alpha$ -carbon of **15** established correlation with a known derivative [109]).

## 2.5.2 Synthesis of $\alpha,\alpha$ -Disubstituted $\alpha$ -Amino Acids

Although radical additions to aldimine-type acceptors have now become well-established, intermolecular additions to ketimine radical acceptors are rare by

**Table 6** Additions of alkyl iodides to  $\gamma$ -hydrazonoesters

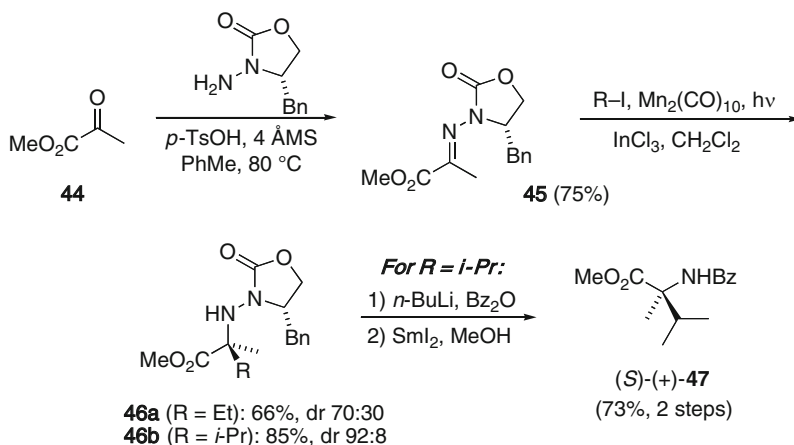
Entry	Hydrazone	Iodide $R^3I$	Product, yield (%)	<i>dr</i>
1	<b>35a</b>	<i>i</i> -PrI	<b>36a</b> , >99	94:6
2	<b>35b</b>		<b>36b</b> , 98	95:5
3	<b>35c</b>		<b>36c</b> , 96	99:1
4	<b>35d</b>		<b>36d</b> , 96	90:10
5	<b>35a</b>		<b>37</b> , 82	–
6			<b>38</b> , 66	94:6
7		TBSO	<b>39</b> , 37	96:4
8		HO	<b>40</b> , 61	97:3
9		HO	<b>41</b> , 33	96:4
10		Cl	<b>42</b> , 45	85:15

**Scheme 9** Nitrogen-nitrogen bond cleavage of gamma hydrazinoester **36a**

comparison [110, 111]. We envisioned that the versatility of the manganese-mediated radical additions might offer potential access to a diverse range of *tert*-alkyl amines which are difficult to prepare by other means [112]. In planning a study of such reactions we were cognizant of the importance of ensuring the reaction takes place exclusively through a single  $C=N$   $\pi$ -bond geometry. Aldehyde *N*-acylhydrazone derivatives are exclusively obtained in *E* geometry, making this issue of little relevance, but ketone hydrazones are generally formed as mixtures of *E* and *Z* isomers. Therefore we sought a ketone hydrazone which could be obtained predominantly as one isomer.

The *N*-amino-2-oxazolidinone **2a** was condensed with methyl pyruvate (**44**) to give hydrazone **45** (Scheme 10) as an *E/Z* mixture (*dr* 92:8), from which the minor (*Z*)-isomer was removed via flash chromatography to give pure (*E*)-**45** in 75%





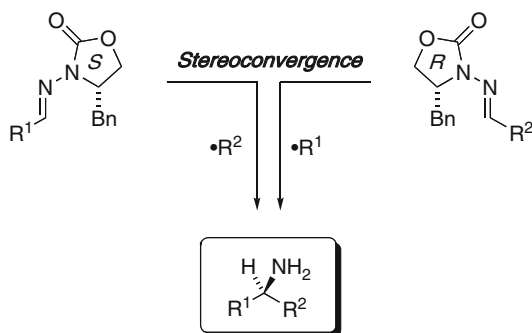
**Scheme 10** Radical additions to ketimine **45**

yield. Addition of ethyl iodide under manganese-mediated photolysis conditions in the presence of  $\text{InCl}_3$  gave a moderate yield of **46a** (66% yield, dr 70:30), while the corresponding isopropyl adduct **46b** was very effectively produced (85% yield, dr 92:8). The N–N bond was cleaved upon conversion of isopropyl adduct **46b** to the benzamide derivative and treatment with  $\text{SmI}_2/\text{MeOH}$  (Scheme 10) to afford known benzamide (*S*)-(+)-**47** [113] and confirm the assigned configuration.

In the additions to **45** it was noted, through variations of the stoichiometric loading of Lewis acid, that amounts of  $\text{InCl}_3$  less than 2 equiv resulted in lower diastereoselectivity. From this it may be inferred that the Lewis acid, aside from its usual chelation by the *N*-acylhydrazone, may interact with another Lewis basic site (e.g., the ester).

## 2.6 Stereoconvergence for Synthetic Design Flexibility

Considering the examples discussed above, it is clear that the manganese-mediated radical additions offer broad functional group compatibility in both the radical precursor and aldehyde hydrazone acceptor. And, the epimeric configuration can be selected by either (1) employing the enantiomeric auxiliary or (2) interchanging the roles of  $\text{R}^1$  and  $\text{R}^2$  in the alkyl halide and aldehyde precursors of Scheme 1 (for other applications of this strategy see [29, 114]). Thus, stereoconvergent construction of alternative C–C bonds at the chiral amine stereocenter (Scheme 11) can be readily conceived so that the roles of these precursors can be chosen on the basis of synthetic strategy rather than on the basis of functional group limitations of the methodology. Such strategic flexibility contributes to the synthetic potential of these radical addition reactions.

**Scheme 11** Stereoconvergent synthesis via radical addition

### 3 Silicon-Tethered Addition of Functionalized Radicals

#### 3.1 Development of Additions to $\alpha$ -Hydroxyhydrazones

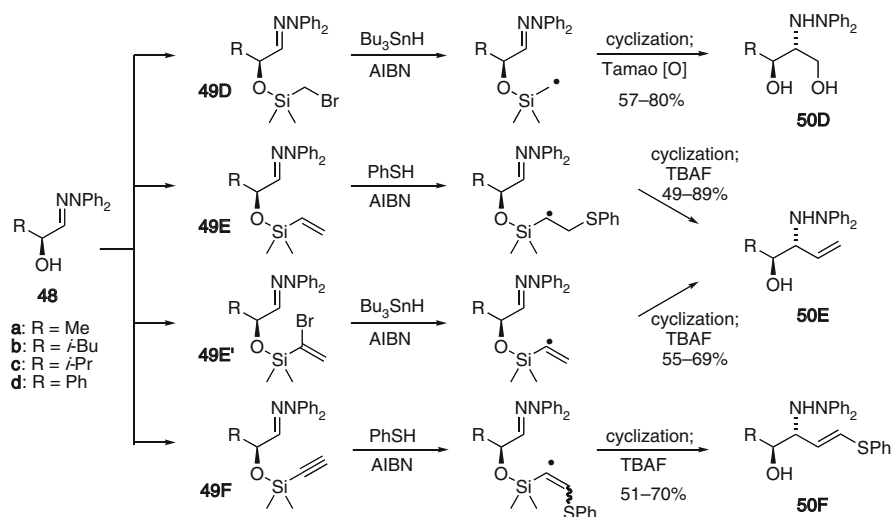
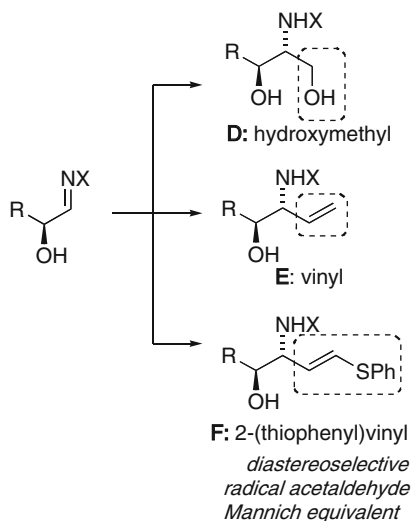
Despite the development of various intermolecular radical addition methods, those studies have rarely accommodated additional functionality, our discovery of the manganese-mediated photolysis conditions notwithstanding. Prior to that discovery, we began to elaborate an alternative strategy which employs temporary tethers ([115, 116]; reviews of silicon-tethered reactions [117–120]) (silyl ether or acetal linkages) linking radical and acceptor. In this scenario the C–C bond is constructed via cyclization, in which internal conformational constraints can control diastereoselectivity. The tether itself would be converted to useful functionality upon cleavage, and once the tether is cleaved the net result may be considered as “formal acyclic stereocontrol.”

According to this concept, several functionalized C1 and C2 units have been installed (Scheme 12). The relevant methods we have developed include Si-tethered additions of hydroxymethyl [121] (**D**), vinyl [122–124] (**E**), and 2-(thiophenyl)vinyl [125] (**F**) groups. The latter are radical equivalents of an acetaldehyde Mannich reaction (for other radical equivalents to Mannich-type reactions see [126–128]) and well-suited to syntheses of 3-aminosugars containing the  $\beta$ -aminoaldehyde functional group array. In general, the hydroxyalkyl amine structures produced in all of these methods are of interest for their relevance to biologically active sphingolipids (for a review see [129]), hydroxylated nitrogen heterocycles (“azasugars”) (reviews [130–132]), and aminosugars [133].

The methodology was developed using a series of  $\alpha$ -hydroxyhydrazones **48a–d** (Scheme 13) prepared from the corresponding  $\alpha$ -hydroxyesters by standard transformations. These were converted to a series of 16 silyl ethers (**49Da–d**, **49Ea–d**, **49E’a–d**, **49Fa–d**) by reaction with the appropriate chlorosilanes.

Tin-mediated cyclizations were then carried out on halides **49D** and **49E**’ ( $\text{Bu}_3\text{SnH}$ , AIBN, heat), followed by Tamao oxidation (for **49D**; KF,  $\text{KHCO}_3$ ,  $\text{H}_2\text{O}_2$ ) or fluoride-induced desilylation (for **49E**’; TBAF) [121, 124]. Here,

**Scheme 12** Addition of functionalized radical synthons



**Scheme 13** Silicon-tethered radical addition approach to chiral amines

abstraction of halogen from the halide precursor by  $\text{Bu}_3\text{Sn}^\bullet$  led to the intermediate carbon-centered radical for C–C bond construction.

As an alternative to tin-mediated conditions, thiyl radicals are an attractive alternative; they generate carbon-centered radicals upon reversible addition to a multiple bond. This was found to be effective for cyclizations of **49E** and **49F** (Scheme 13). Treatment with AIBN and PhSH, followed by fluoride-induced desilylation, afforded vinyl and 2-(thiophenyl)vinyl adducts **50E** and **50F**, respectively [122, 123, 125]. Interestingly, during fluoride-induced (TBAF) desilylation of the intermediate formed

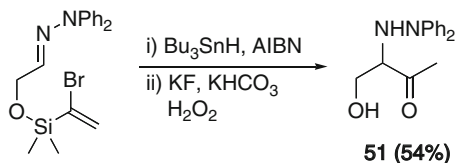
upon addition–cyclization of **49E**, the vinyl group was regenerated by elimination of benzenethiolate. No such elimination occurred in the adduct from **49F**.

With the exception of the cyclization of (bromovinyl)silyl ether in the mandelate series (**49E'd**), which gave a complex mixture, good yields were consistently obtained for all of the two step sequences shown in Scheme 13 (49–89%, 15 examples).

The diastereomeric ratios of all these adducts are compiled in Table 7, and illustrate the impact of radical reactivity on stereocontrol. Vinylic radical intermediates formed from **49E'** and **49F** cyclize with consistently lower selectivity than the corresponding alkyl radicals formed from **49D** and **49E**, which may reflect a shift to an earlier transition state, which could reasonably be expected for the more reactive vinylic radicals.

The regular variation of the product distribution in concert with the A-value of the  $\alpha$ -substituent in the  $\alpha$ -hydroxyhydrazone is consistent with a diastereocontrol model involving a chair-like transition state wherein allylic strain is minimized in the preferred chair-equatorial conformation (Scheme 14). Minor isomers would arise through chair-axial and/or boat-equatorial transition states. Less reactive alkyl radicals would have a later (“tighter”) transition state in which the forming C–C bond is shorter, and consequently they would be subject to greater impact from allylic strain, strengthening the diastereocontrol. Thus the highest selectivities are observed for cyclizations of the secondary alkyl radical formed from **49E**.

In the case of vinyl radical cyclizations of **49E'**, the intermediate silacycle could be oxidized under Tamao conditions to afford ketone **51** (2) [124]. The consequence is an umpolung installation of an acetyl group, with the vinyl radical serving as an acyl anion equivalent, further expanding the synthetic potential of the Si-tethered radical additions.



**Table 7** Correlation of substituent A-values with diastereoselectivity in hydroxymethyl, vinyl, and 2-(thiophenyl)vinyl addition

Entry	R	A-value (kcal/mol) <sup>a</sup>	dr, <b>50D</b> <sup>b</sup>	dr, <b>50E</b> <sup>c</sup>	dr, <b>50E</b> <sup>d</sup>	dr, <b>50F</b> <sup>e</sup>
1	Me	1.6	79:21	90:10	66:34	78:22
2	<i>i</i> -Bu	1.8 (est.)	85:15	94:6	78:22	86:14
3	<i>i</i> -Pr	2.2	96:4	98:2	96:4	96:4
4	Ph	2.9	>98:2 <sup>f</sup>	>98:2 <sup>f</sup>	–	>98:2 <sup>f</sup>

<sup>a</sup>Free energy differences between equatorial and axial chair conformers of the monosubstituted cyclohexane

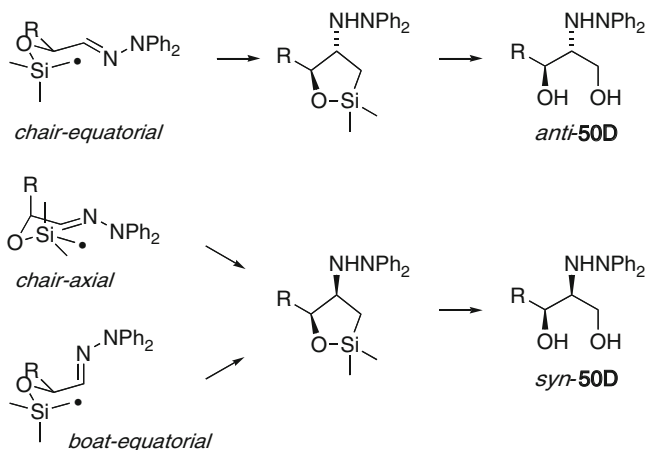
<sup>b</sup>Hydroxymethyl addition via **49D**

<sup>c</sup>Vinyl addition via thiol addition to **49E**

<sup>d</sup>Vinyl addition via Br-abstraction from **49E'**

<sup>e</sup>2-(Thiophenyl)vinyl addition via **49F**

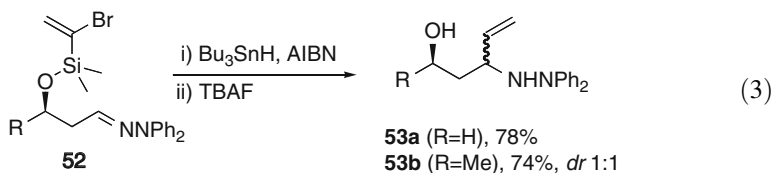
<sup>f</sup>Minor isomer not detected



**Scheme 14** Stereocontrol in 5-*exo* silicon-tethered radical addition

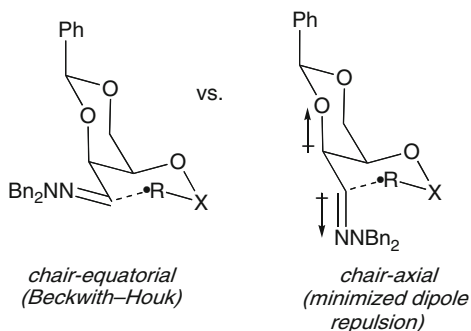
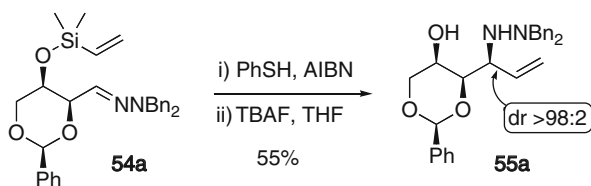
### 3.2 Reactivity and Stereocontrol in 6-*Exo* Cyclizations

Attempts to achieve 6-*exo* cyclizations via the Si-tether strategy encountered some difficulty. Success could not be achieved via vinylsilyl ethers derived from  $\beta$ -hydroxyhydrazones (i.e., homologs of **49E**), presumably due to the reduced rate of cyclization in combination with the reversibility of thiyl addition. Although more reactive vinyl radicals generated from vinyl bromide **52** (a homolog of **49E'**) did provide reasonable yields of adducts **53a** and **53b** (3) [124], the absence of stereocontrol detracts from the utility of these reactions.

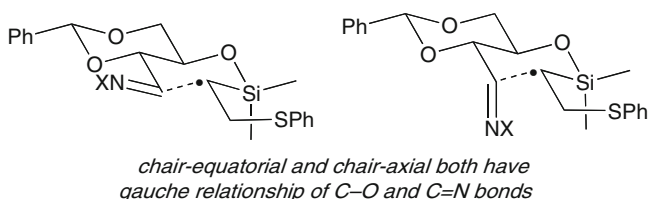
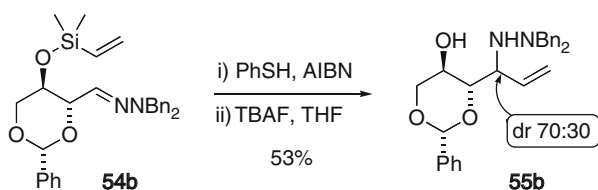


In contrast, when 6-*exo* cyclizations are effected in the presence of an  $\alpha$ -alkoxy or  $\alpha$ -silyloxy substituent, the stereocontrol can be excellent, as has been observed in a Si-tethered cyclization of **54a** (Scheme 15) where a single diastereomeric product was obtained [134]. In this case, additional conformational constraints aided the cyclization, as became evident upon finding that the product configuration was inconsistent with the standard Beckwith–Houk chair-equatorial transition state model. For **54a** there are two chairlike conformations (chair-equatorial and chair-axial) conceivably leading to cyclization; the latter has the C–O and C=N bonds in an *anti* relationship to minimize dipole repulsion (Scheme 15). The

## Unexpected Selectivity



## Control Experiment



**Scheme 15** Dipole repulsion models for stereocontrol by alpha-alkoxy substituents

chair-axial structure predicts the correct product configuration, contradicting the standard Beckwith-Houk model.

To confirm the existence of the dipole repulsion effect, a related substrate **54b** was conceived, differing only in the configuration at the  $\alpha$ -carbon. The expected chair-axial and chair-equatorial transition states for cyclization of **54b** each have their C-O and C=N bonds in a gauche relationship; the dipole repulsion model therefore predicts minimal differentiation. In this control experiment, cyclization of

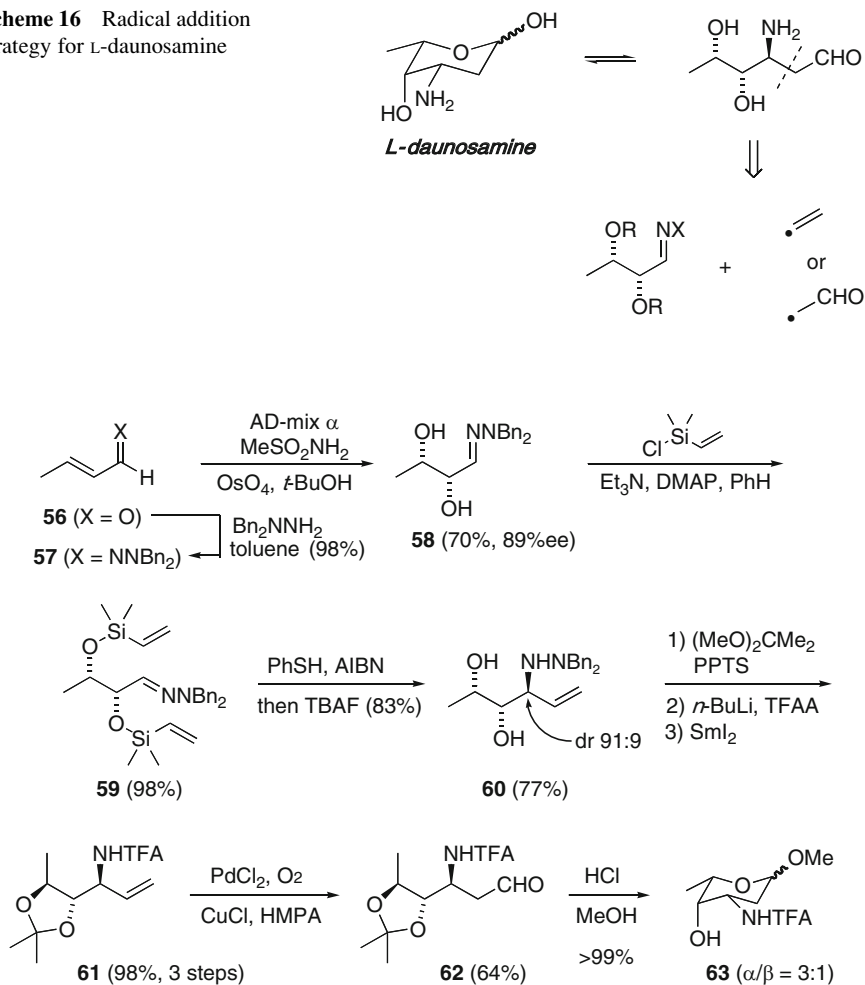
**54b** to afford **55b** exhibited poor differentiation (dr 70:30), as noted above for other 6-*exo* cyclizations, providing confirmation of the importance of dipole repulsion. The dipole repulsion modification to the Beckwith–Houk model has also been examined in Ueno–Stork haloacetal radical cyclizations [135, 136] and cyclizations of propargylic ethers [134].

The studies outlined in this section indicate that 5-*exo* cyclizations which employ the Si-tethered radical precursor attached at the  $\alpha$ -hydroxy group of hydrazones can afford reliable stereoselective installation of several one- and two-carbon fragments bearing functionality useful for further elaboration. The configuration of the  $\alpha$ -hydroxy group controls the outcome in a predictable manner for 5-*exo* cyclizations, which may be rationalized using the simple Beckwith–Houk chair-equatorial transition state model. Although stereocontrol in 6-*exo* cyclizations is not as reliable in this methodology, in certain cases the  $\alpha$ -C–O bond may assist in stereocontrol through dipole repulsion effects. It remains to test the application of these Si-tethered cyclizations to target-directed synthesis.

### 3.3 Application to Aminosugar Synthesis

Daunosamine is a biologically important target which showcases the problem of generating aminosugars from achiral non-carbohydrate precursors. In fact, the vast majority of syntheses of daunosamine involve functional group interconversions from other carbohydrates (for some representative daunosamine syntheses see [137–144]). A potentially efficient alternative strategy for accessing L-daunosamine derivatives involves addition of an acetaldehyde equivalent to a 2,3-dihydroxyimine acceptor (Scheme 16) [135, 136]. Among numerous prior approaches to daunosamine are nitrene cycloadditions [145, 146] and Mannich-type reactions [147–151], which accomplish this same bond construction using negatively charged or polarized acetaldehyde *enolate* equivalents. We sought to develop a complementary alternative which would involve a non-polar *radical* equivalent of the acetaldehyde Mannich reaction. For this purpose, either vinyl or 2-oxoethyl radical addition would be required, and neither of these had been achieved with imino acceptors in an intermolecular fashion. Intramolecular tethering would therefore be a key enabling tactic.

The synthesis of L-daunosamine began with the condensation of *trans*-crotonaldehyde (**56**) with dibenzylhydrazine (Scheme 17). Sharpless asymmetric dihydroxylation of the resulting (*E*)- $\alpha,\beta$ -unsaturated hydrazone **57** afforded the *syn*-diol **58** (70% yield, 89% ee by HPLC), and silylation with chlorodimethylvinylsilane then provided the radical cyclization precursor **59** in 98% yield. In the key step, exposure to thiyl radicals generated from PhSH and AIBN led to radical cyclization of dibenzylhydrazone **59**. The unstable cyclic intermediate was then directly treated with fluoride to afford vinyl adduct **60** in 77% yield (dr 91:9,  $^1\text{H}$  NMR). In control experiments with corresponding monosilyl derivatives, the  $\beta$ -O-silyl

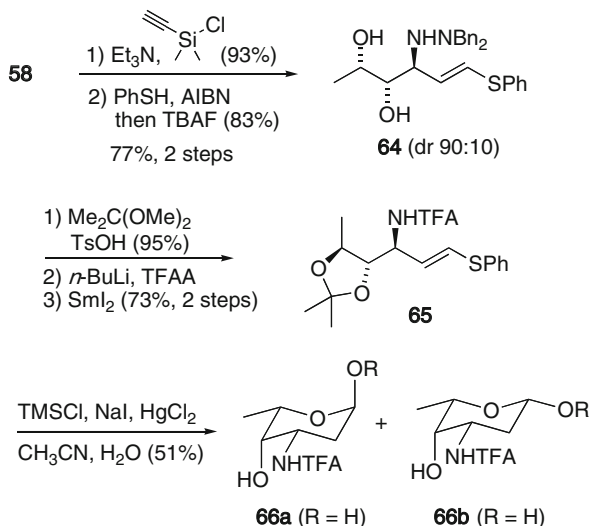
**Scheme 16** Radical addition strategy for L-daunosamine**Scheme 17** Synthesis of L-daunosamine

derivative did not cyclize, suggesting that the vinyl group is preferentially transferred from the  $\alpha$ -O-silyl group via 5-*exo* radical cyclization. After N–N bond cleavage [152] to allylic trifluoroacetamide **61**, an aldehyde-selective Wacker oxidation [153–157] furnished aldehyde **62** in moderate yield, with small amounts of the methyl ketone. Then, with the correct oxidation state established, exposure of **62** to methanolic HCl resulted in removal of the acetonide protecting group and cyclization to **63** [158–160], the methyl pyranoside form of the TFA-protected L-daunosamine, in quantitative yield.

Considering the moderate yield in the Wacker oxidation, our attention turned to a radical addition of a two-carbon fragment already in a higher oxidation state. With this in mind, we tested the hypothesis that daunosamine might be obtained



**Scheme 18** Second synthesis of L-daunosamine



by an analogous sequence replacing the vinyl group with an ethynyl group as a silicon-tethered radical precursor [125, 135, 136]. We had already shown that thiyl addition to ethynylsilyl groups could lead to vinyl sulfides (Scheme 13). Considering the abundant methods for conversion of vinyl sulfides to carbonyl compounds [for representative methods see ( $\text{HClO}_4$  [161];  $\text{HgCl}_2$  [162];  $\text{TiCl}_4$  [163];  $\text{HCl}$  then  $\text{HgCl}_2$  [164];  $\text{CF}_3\text{CO}_2\text{H}$  [165];  $\text{HCl}$  [166];  $\text{Fe}(\text{NO}_3)_3$ -clay (“clayfen”) [167]), an ethynyl group addition would serve as an equivalent to the acetaldehyde Mannich reaction, and as a potentially useful complement to our vinyl addition methodology.

Silylation of **58** with chlorodimethylethynylsilane [168, 169] afforded the corresponding bis-silyl ether in 93% yield (Scheme 18), which in turn was submitted to thiyl addition-cyclization. Without isolation, the crude product was subjected to TBAF in THF to afford **64** in 83% yield.

Protection of **64** as an acetonide (Scheme 18) followed by TFA-assisted N–N bond cleavage [152] furnished the corresponding amide **65** in 73% yield. Finally, Grieco’s vinyl sulfide hydrolysis conditions [164] entailing in situ generation of hydrogen iodide in moist acetonitrile in the presence of mercuric chloride<sup>1</sup> furnished 51% of anomeric mixture **66a** and **66b**. Recrystallization afforded known **66a** (mp 146–148 °C, literature value 146–147 °C;  $[\alpha]_D^{30} -120$ , literature value  $[\alpha]_D^{20} -127$ ) [170], confirming the stereochemical course of the tandem thiyl radical additions–cyclizations. The radical Mannich strategy avoids a late-stage oxidation step and affords *N*-trifluoroacetyl-L-daunosamine in 17% overall yield from crotonaldehyde.

<sup>1</sup>An alternative 2-step procedure involving prior removal of the acetonide [(1) 0.1 M methanolic  $\text{HCl}$ ; (2)  $\text{HgCl}_2$  aq  $\text{CH}_3\text{CN}$ ] afforded the same mixture in 23% yield.

In combination with the range of standard transformations of alcohols, alkenes, and vinylsulfides, these silicon-tethered additions of functionalized radicals offer a versatile and stereoselective approach to amino alcohol synthesis. Whereas vinyl and 2-oxoethyl radicals have not yet been demonstrated as competent participants in the various intermolecular additions reported in the literature, the temporary tether approach allows such functionalized fragments to be installed in an efficient and stereoselective manner. Synthesis of the aminosugar daunosamine from achiral precursors shows how this concept, employing hydrazone radical acceptors, can be merged with asymmetric catalysis to achieve practical synthetic advances.

## 4 Summary

With the advent of methods applicable to multifunctional compounds, radical addition to imino compounds has emerged as a general approach with broad versatility that complements non-radical methodology. Our work has discovered and elaborated two such methods: First, highly stereoselective intermolecular additions of alkyl iodides to chiral hydrazones in the presence of  $\text{Mn}_2(\text{CO})_{10}$  accommodate a broad range of functionality, including esters and unprotected hydroxyl groups which may not be compatible with carbanion chemistry. Second, the use of a silicon tether to link radical precursors to hydroxyl groups at the  $\alpha$ -carbon of hydrazones enables predictable stereocontrol via cyclization. Removal of the temporary tether reveals adducts of hydroxymethyl, vinyl, 2-oxoethyl, and acetyl groups. The viability of these two general strategies for stereocontrol has now been established in applications to target-directed synthesis.

A frontier which remains to be developed is catalytic asymmetric induction in radical addition to  $\text{C}=\text{N}$  bonds, although there are promising results which suggest asymmetric catalysis of broad scope may be on the horizon (for the first examples of asymmetric induction with catalyst turnover [171–173]). Hopefully this review will inspire new explorations in this direction.

**Acknowledgment** Generous support for our programs in radical addition methods and applications to natural products by NSF (CHE-0096803 and CHE-0749850) and NIH (R01-GM67187) are deeply appreciated. Research Corporation, Petroleum Research Fund, and Vermont EPSCoR have also provided funding for parts of this work. Many devoted students and postdoctoral associates are responsible for developing our program in chiral amine synthesis, and their efforts are gratefully acknowledged. This chapter was prepared during an appointment as an Obermann Scholar in the Obermann Center for Advanced Studies (University of Iowa) which is acknowledged with appreciation.

## References

1. Rowlands GJ (2009) *Tetrahedron* 65:8603–8655
2. Renaud P, Sibi M (eds) (2001) *Radicals in organic synthesis*. Wiley-VCH, New York

3. Giese B, Kopping B, Gobel T, Dickhaut J, Thoma G, Kulicke KJ, Trach F (1996) *Org React* 48:301–856
4. Curran DP, Porter NA, Giese B (1995) *Stereochemistry of radical reactions: concepts guidelines and synthetic applications*. VCH, New York
5. Jasperse CP, Curran DP, Fevig TL (1991) *Chem Rev* 91:1237–1286
6. Giese B (1986) *Radicals in organic synthesis: formation of carbon-carbon bonds*. Pergamon Press, New York
7. Hart DJ (1984) *Science* 223:883–887
8. Friestad GK (2001) *Tetrahedron* 57:5461–5496
9. Fallis AG, Brinza IM (1997) *Tetrahedron* 53:17543–17594
10. Friestad GK (2009) Addition of carbanions to azomethines. In: Enders D, Shaumann E (eds) *Science of synthesis vol 40a: compounds with one saturated carbon-heteroatom bond: amines and ammonium salts*. Thieme, Stuttgart
11. Yamada K-I, Tomioka K (2008) *Chem Rev* 108:2874–2886
12. Friestad GK, Mathies AK (2007) *Tetrahedron* 63:2541–2569
13. Ding H, Friestad GK (2005) *Synthesis* 2815–2829
14. Alvaro G, Savoia D (2002) *Synlett* 651–673
15. Kobayashi S, Ishitani H (1999) *Chem Rev* 99:1069–1094
16. Bloch R (1998) *Chem Rev* 98:1407–1438
17. Davis FA, Zhou P, Chen B-C (1998) *Chem Soc Rev* 27:13–18
18. Enders D, Reinhold U (1997) *Tetrahedron Asymmetry* 8:1895–1946
19. Denmark SE, Nicaise OJ-C (1996) *J Chem Soc Chem Commun* 999–1004
20. Stork G, Dowd SR (1963) *J Am Chem Soc* 85:2178–2180
21. Wittig G, Frommheld HD, Suchanek P (1963) *Angew Chem Int Ed Engl* 2:683
22. Guerrier L, Royer J, Grierson DS, Husson H-P (1983) *J Am Chem Soc* 105:7754–7755
23. Enders D, Diez E, Fernandez R, Martin-Zamora E, Munoz JM, Pappalardo RR, Lassaletta JM (1999) *J Org Chem* 64:6329–6336
24. Friestad GK (2005) *Eur J Org Chem* 3157–3172
25. Bertrand M, Feray L, Gastaldi S (2002) *C R Acad Sci Paris Chimie* 5:623–638, review
26. Miyabe H, Ueda M, Naito T (2004) *Synlett* 1140–1157
27. Booth SE, Jenkins PR, Swain CJ, Sweeney JB (1994) *J Chem Soc Perkin Trans 1* 3499–3508
28. Booth SE, Jenkins PR, Swain CJ (1998) *J Braz Chem Soc* 9:389–395 (Chemical Abstracts 130:38274)
29. Enders D (1984) In: Morrison JD (ed) *Asymmetric synthesis*. Academic Press, New York, review
30. Enders D, Schubert H, Nubling C (1986) *Angew Chem Int Ed Engl* 25:1109–1110
31. Takahashi H, Tomita K, Otomasu H (1979) *J Chem Soc Chem Commun* 668–669
32. Takahashi H, Suzuki Y (1983) *Chem Pharm Bull* 31:4295–4299
33. Denmark SE, Weber T, Piotrowski DW (1987) *J Am Chem Soc* 109:2224–2225
34. Breuil-Desvergnès V, Compain P, Vatière J-M, Goré J (1999) *Tetrahedron Lett* 40:5009–5012
35. Russell GA, Yao C-F, Rajaratnam R, Kim BH (1991) *J Am Chem Soc* 113:373–375
36. Renaud P, Gerster M (1998) *Angew Chem Int Ed* 37:2563–2579
37. Guerin B, Ogilvie WW, Guindon Y (2001) In: Renaud P, Sibi M (eds) *Radicals in organic synthesis*. Wiley-VCH, New York
38. Burk MJ, Feaster JE (1992) *J Am Chem Soc* 114:6266–6267
39. Sturino CF, Fallis AG (1994) *J Am Chem Soc* 116:7447–7448
40. Evans DA, Kim AS (1995) In: Paquette LA (ed) *Encyclopedia of reagents for organic synthesis*, vol 1. Wiley, New York
41. Kim M, White JD (1977) *J Am Chem Soc* 99:1172–1180
42. Ciufolini MA, Shimizu T, Swaminathan S, Xi N (1997) *Tetrahedron Lett* 38:4947–4950
43. Evans DA, Johnson DS (1999) *Org Lett* 1:595–598

44. Hynes J Jr, Doubleday WW, Dyckman AJ, Godfrey JD Jr, Grosso JA, Kiau S, Leftheris K (2004) *J Org Chem* 69:1368–1371
45. Friestad GK, Ji A (2008) *Org Lett* 10:2311–2313
46. Shen Y, Friestad GK (2002) *J Org Chem* 67:6236–6239
47. Friestad GK, Qin J (2000) *J Am Chem Soc* 122:8329–8330
48. Friestad GK, Draghici C, Soukri M, Qin J (2005) *J Org Chem* 70:6330–6338
49. Qin J, Friestad GK (2003) *Tetrahedron* 59:6393–6402
50. Lim D, Coltart DM (2008) *Angew Chem Int Ed* 47:5207–5210
51. Nozaki K, Oshima K, Utimoto K (1991) *Bull Chem Soc Jpn* 64:403–409
52. Brown HC, Midland MM (1972) *Angew Chem Int Ed Engl* 11:692–700
53. Fernandez M, Alonso R (2003) *Org Lett* 5:2461–2464
54. Kim S, Lee IY, Yoon J-Y, Oh DH (1996) *J Am Chem Soc* 118:5138–5139
55. Kim S, Yoon J-Y (1997) *J Am Chem Soc* 119:5982–5983
56. Ryu I, Kuriyama H, Minakata S, Komatsu M, Yoon J-Y, Kim S (1999) *J Am Chem Soc* 121:12190–12191
57. Jeon G-H, Yoon J-Y, Kim S, Kim SS (2000) *Synlett* 128–130
58. Kim S, Kim N, Yoon J-Y, Oh DH (2000) *Synlett* 1148–1150
59. Kim S, Song H-J, Choi T-L, Yoon J-Y (2001) *Angew Chem Int Ed* 40:2524–2526
60. Kim S, Kavali R (2002) *Tetrahedron Lett* 43:7189–7191
61. Pauson PL (1995) In: Paquette LA (ed) *Encyclopedia of reagents for organic synthesis*, vol 2. Wiley, New York
62. Meyer TJ, Caspar JV (1985) *Chem Rev* 85:187
63. Gilbert BC, Parsons AF (2002) *J Chem Soc Perkin Trans* 2:367–387
64. Herrick RS, Herrinton TR, Walker HW, Brown TL (1985) *Organometallics* 4:42–45
65. Giese B, Thoma G (1991) *Helv Chim Acta* 74:1135–1142
66. Gilbert BC, Kalz W, Lindsay CI, McGrail PT, Parsons AF, Whittaker DTE (1999) *Tetrahedron Lett* 40:6095–6098
67. Gilbert BC, Lindsay CI, McGrail PT, Parsons AF, Whittaker DTE (1999) *Synth Commun* 29:2711–2718
68. Gilbert BC, Kalz W, Lindsay CI, McGrail PT, Parsons AF, Whittaker DTE (2000) *J Chem Soc Perkin Trans* 1 1187–1194
69. Friestad GK, Qin J (2001) *J Am Chem Soc* 123:9922–9923
70. Friestad GK, Qin J, Suh Y, Marié J-C (2006) *J Org Chem* 71:7016–7027
71. Callaghan O, Lampard C, Kennedy AR, Murphy JA (1999) *J Chem Soc Perkin Trans* 1 995–1001
72. Jahn U, Muller M, Aussieker S (2000) *J Am Chem Soc* 122:5212–5213
73. Harrowven DC, Lucas MC, Howes PD (2001) *Tetrahedron* 57:791–804
74. Rivkin A, Nagashima T, Curran DP (2003) *Org Lett* 5:419–422
75. Denes F, Chemla F, Normant JF (2003) *Angew Chem Int Ed* 42:4043–4046
76. Bazin S, Feray L, Vanthuynne N, Bertrand MP (2005) *Tetrahedron* 61:4261–4274
77. Ueda M, Miyabe H, Sugino H, Miyata O, Naito T (2005) *Angew Chem Int Ed* 44:6190–6193
78. Denes F, Cutri S, Perez-Luna A, Chemla F (2006) *Chem Eur J* 12:6506–6513
79. Maruyama T, Mizuno Y, Shimizu I, Suga S (2007) *J Am Chem Soc* 129:1902–1903
80. Miyata O, Takahashi S, Tamura A, Ueda M, Naito T (2008) *Tetrahedron* 64:1270–1284
81. Enders D, Tiebes J (1993) *Liebigs Ann Chem* 173–177
82. Yamazaki N, Kibayashi C (1997) *Tetrahedron Lett* 38:4623–4626
83. Reding MT, Buchwald SL (1998) *J Org Chem* 63:6344–6347
84. Wilkinson TJ, Stehle NW, Beak P (2000) *Org Lett* 2:155–158
85. Kim YH, Choi JY (1996) *Tetrahedron Lett* 37:5543–5546
86. Korapala CS, Qin J, Friestad GK (2007) *Org Lett* 9:4243–4246
87. Ordonez M, Cativiela C (2007) *Tetrahedron Asymmetry* 18:3–99
88. Trabocchi A, Guarna F, Guarna A (2005) *Curr Org Chem* 9:1127–1153
89. Matthew S, Schupp PJ, Leusch H (2008) *J Nat Prod* 71:1113–1116

90. Kunze B, Bohlendorf B, Reichenbach H, Hofle G (2008) *J Antibiot* 61:18–26
91. Oh D-C, Strangman WK, Kauffman CA, Jensen PR, Fenical W (2007) *Org Lett* 9:1525–1528
92. Milanowski DJ, Gustafson KR, Rashid MA, Pannell LK, McMahon JB, Boyd MR (2004) *J Org Chem* 69:3036–3042
93. Williams PG, Luesch H, Yoshida WY, Moore RE, Paul VJ (2003) *J Nat Prod* 66:595–598
94. Horgen FD, Kazmierski EB, Westenburg HE, Yoshida WY, Scheuer PJ (2002) *J Nat Prod* 65:487–491
95. Dado GP, Gellman SH (1994) *J Am Chem Soc* 116:1054–1062
96. Hanessian S, Luo X, Schaum R, Michnick S (1998) *J Am Chem Soc* 120:8569–8570
97. Sanjayan GJ, Stewart A, Hachisu S, Gonzalez R, Watterson MP, Fleet GWJ (2003) *Tetrahedron Lett* 44:5847–5851
98. Seebach D, Schaeffer L, Brenner M, Hoyer D (2003) *Angew Chem Int Ed* 42:776–778
99. Farrera-Sinfreu J, Zaccaro L, Vidal D, Salvatella X, Giralt E, Pons M, Albericio F, Royo M (2004) *J Am Chem Soc* 126:6048–6057
100. Vasudev PG, Ananda K, Chatterjee S, Aravinda S, Shamala N, Balam P (2007) *J Am Chem Soc* 129:4039–4048
101. Sasse F, Steinmetz H, Heil J, Höfle G, Reichenbach H (2000) *J Antibiot* 53:879–885
102. Höfle G, Glaser N, Leibold T, Karama U, Sasse F, Steinmetz H (2003) *Pure Appl Chem* 75:167–178
103. Friestad GK, Deveau AM, Marié J-C (2004) *Org Lett* 6:3249–3252
104. Friestad GK, Banerjee K (2009) *Org Lett* 11:1095–1098
105. Lin CH (1993) *Synth React Inorg Met-Org Chem* 23:1097–1106
106. Salazar J, Lopez SE, Rebollo O (2003) *J Fluorine Chem* 124:111–113
107. Iranpoor N, Zeynizadeh B (1999) *J Chem Res (S)* 124–125
108. Prashad M, Hu B, Har D, Repic O, Blacklock TJ (2000) *Tetrahedron Lett* 41:9957–9961
109. Schaum R (1998) Ph.D Thesis, Université de Montreal, Montreal, Canada
110. Torrente S, Alonso R (2001) *Org Lett* 3:1985–1987
111. Miyabe H, Yamaoka Y, Takemoto Y (2005) *J Org Chem* 70:3324–3327
112. Ramon DJ, Yus M (2004) *Curr Org Chem* 8:149–183, review
113. Obrecht D, Bohdal U, Broger C, Bur D, Lehmann C, Ruffieux R, Schönholzer P, Spiegler C, Müller K (1995) *Helv Chim Acta* 78:563–580
114. Husson H-P, Royer J (1999) *Chem Soc Rev* 28:383–394
115. Nishiyama H, Kitajima T, Matsumoto M, Itoh K (1984) *J Org Chem* 49:2298–2300
116. Stork G, Kahn M (1985) *J Am Chem Soc* 107:500–501
117. Gauthier DR Jr, Zandi KS, Shea KJ (1998) *Tetrahedron* 54:2289–2338
118. Fensterbank L, Malacria M, Sieburth SM (1997) *Synthesis* 813–854
119. Fleming I, Barbero A, Walter D (1997) *Chem Rev* 97:2063–2192
120. Bols M, Skrydstrup T (1995) *Chem Rev* 95:1253–1277
121. Friestad GK (1999) *Org Lett* 1:1499–1501
122. Friestad GK, Massari SE (2000) *Org Lett* 2:4237–4240
123. Friestad GK, Massari SE (2004) *J Org Chem* 69:863–875
124. Friestad GK, Jiang T, Mathies AK (2007) *Tetrahedron* 63:3964–3972
125. Friestad GK, Jiang T, Fioroni GM (2003) *Tetrahedron: Asymmetry* 14:2853–2856
126. Miyabe H, Fujii K, Goto T, Naito T (2000) *Org Lett* 2:4071–4074
127. Inokuchi T, Kawafuchi H (2001) *Synlett* 421–423
128. Clerici A, Cannella R, Pastori N, Panzeri W, Porta O (2006) *Tetrahedron* 62:5986–5994
129. Kolter T, Sandhoff K (1999) *Angew Chem Int Ed* 38:1532–1568
130. Heightman TD, Vasella AT (1999) *Angew Chem Int Ed* 38:750–770
131. Chapleur Y (ed) (1998) *Carbohydrate mimics*. Wiley-VCH, Weinheim
132. Nash RJ, Watson AA, Asano N (1996) In: Pelletier SW (ed) *Alkaloids: chemical and biological perspectives*. Tarrytown New York, Pergamon
133. Hauser FM, Ellenberger SR (1986) *Chem Rev* 86:35–67, review

134. Friestad GK, Mathies AK (2007) *Tetrahedron* 63:9373–9381 (Corrigendum: Friestad GK, Mathies AK (2007) *Tetrahedron* 63:13039)
135. Friestad GK, Jiang T, Fioroni GM (2008) *Tetrahedron* 64:11549–11557
136. Friestad GK, Fioroni GM (2005) *Org Lett* 7:2393–2396
137. Doi T, Shibata K, Kinbara A, Takahashi T (2007) *Chem Lett* 36:1372–1373
138. Mendlik MT, Tao P, Hadad CM, Coleman RS, Lowary TL (2006) *J Org Chem* 71:8059–8070
139. Parker KA, Chang W (2005) *Org Lett* 7:1785–1788
140. Trost BM, Jiang CH, Hammer K (2005) *Synthesis* 3335–3345
141. Ginesta X, Pasto M, Pericas MA, Riera A (2003) *Org Lett* 5:3001–3004
142. Cutchins WW, McDonald FE (2002) *Org Lett* 4:749–752
143. Davies SG, Smyth GD, Chippindale AM (1999) *J Chem Soc Perkin Trans 1* 3089–3104
144. Sibi M, Lu J, Edwards J (1997) *J Org Chem* 62:5864–5872
145. DeShong P, Dicken CM, Leginus JM, Whittle RR (1984) *J Am Chem Soc* 106:5598–5602
146. Xu Z, Johannes CW, La DS, Hofilena GE, Hoveyda AH (1997) *Tetrahedron* 53:16377–16390
147. Mukaiyama T, Goto Y, Shoda S (1983) *Chem Lett* 671–674
148. Fuganti C, Grasselli P, Pedrocchi-Fantoni G (1983) *J Org Chem* 48:910–912
149. Kita Y, Itoh F, Tamura O, Ke YY, Miki T, Tamura Y (1989) *Chem Pharm Bull* 37:1446–1451
150. Hatanaka M, Ueda I (1991) *Chem Lett* 61–64
151. Po S-Y, Uang B-J (1994) *Tetrahedron: Asymmetry* 5:1869–1872
152. Ding H, Friestad GK (2004) *Org Lett* 6:637–640
153. Feringa BL (1986) *J Chem Soc Chem Commun* 909–910
154. Kang S-K, Jung K-Y, Chung J-U, Namkoong E-Y, Kim T-H (1995) *J Org Chem* 60:4678–4679
155. Stragies R, Blechert S (2000) *J Am Chem Soc* 122:9584–9591
156. Hosokawa T, Aoki S, Takano M, Nakahira T, Yoshida Y, Murahashi S-I (1991) *J Chem Soc Chem Commun* 1559–1560
157. Lai J, Shi X, Dai L (1992) *J Org Chem* 57:3485–3487
158. Abbaci B, Florent J-C, Monneret C (1989) *Bull Soc Chim Fr* 667–672
159. Shelton CJ, Harding MM (1995) *J Chem Res (S)* 158
160. Shelton CJ, Harding MM (1995) *J Chem Res (M)* 1201–1219
161. Autrey RL, Scullard PW (1968) *J Am Chem Soc* 90:4924–4929
162. Corey EJ, Shulman JI (1970) *J Org Chem* 35:777–780
163. Mukaiyama T, Kamio K, Kobayashi S, Takei M (1972) *Bull Chem Soc Jpn* 45:3723
164. Mura AJ Jr, Majetich G, Grieco PA, Cohen T (1975) *Tetrahedron Lett* 16:4437–4440
165. Grayson JI, Warren S (1977) *J Chem Soc Perkin Trans 1* 2263–2272
166. Pearson WH, Bergmeier SC, Williams JP (1992) *J Org Chem* 57:3977–3987
167. Almqvist F, Ekman N, Frejd T (1996) *J Org Chem* 61:3794–3798
168. Barton TJ, Lin J, Ijadi-Maghsoodi S, Power MD, Zhang X, Ma Z, Shimizu H, Gordon MS (1995) *J Am Chem Soc* 117:11695–11703
169. Matsumoto H, Kato T, Matsubara I, Hoshino Y, Nagai Y (1979) *Chem Lett* 1287–1290
170. Kimura Y, Matsumoto T, Suzuki M, Terashima S (1986) *Bull Chem Soc Jpn* 59:663–664
171. Friestad GK, Shen Y, Ruggles EL (2003) *Angew Chem Int Ed* 42:5061–5063
172. Jang DO, Kim SY (2008) *J Am Chem Soc* 130:16152–16153
173. Lee S, Kim S (2009) *Tetrahedron Lett* 50:3345–3348
174. Friestad GK, Ji A, Korapala CS, Qin J (2011) *Org Biomol Chem* 4039–4043

# Hydrogen Atom Donors: Recent Developments

Andreas Gansäuer, Lei Shi, Matthias Otte, Inga Huth, Antonio Rosales,  
Iris Sancho-Sanz, Natalia M. Padial, and J. Enrique Oltra

**Abstract** This review highlights recent developments in the field of hydrogen atom transfer (HAT) reagents that circumvent the disadvantages of classical group 14 reagents, such as  $\text{Bu}_3\text{SnH}$ . Special emphasis is laid on the lowering of bond dissociation energies (BDEs) of molecules that could, as yet, not be used as HAT reagents and on the use of organometallic HAT reagents.

**Keywords** Bond dissociation energies · Catalysis · Chain reactions · Hydrogen atom transfer · Metal-hydrogen bonds · Radicals

## Contents

1	Introduction .....	94
2	Complexes of Borane and N-Heterocyclic Carbenes as HAT Reagents .....	95
3	Organometallic Complexes as HAT Reagents .....	97
3.1	Organometallic Complexes as HAT Reagents in Radical Chain Reactions .....	97
3.2	Organometallic HAT Reagents in Catalytic and Stoichiometric Metal Mediated Reactions .....	103
4	Generation of HAT Reagents from Water and Alcohols Through Coordination .....	108
4.1	Activation of Water by Ti(III) .....	108
4.2	Activation of Water by Boron .....	115
4.3	Activation of Alcohols by Boron? .....	116
5	Conclusion .....	117
	References .....	118

---

A. Gansäuer (✉), L. Shi, M. Otte, and I. Huth  
Kekulé Institut für Organische Chemie und Biochemie der Universität Bonn, Gerhard-  
Domagk-Str. 1, 53121 Bonn, Germany  
e-mail: andreas.gansaeuer@uni-bonn.de

A. Rosales, I. Sancho-Sanz, N.M. Padial, and J. Enrique Oltra (✉)  
Department of Organic Chemistry, Faculty of Sciences, University of Granada, 18071 Granada,  
Spain  
e-mail: joltra@ugr.es

## Abbreviations

AIBN	Azobisisobutyronitrile
BDE	Bond dissociation energy
CHAT	Catalytic hydrogen atom transfer
CHD	Cyclohexadiene
dppe	1,2-Bis(diphenylphosphino)ethane
dppf	1,1'-Bis(diphenylphosphino)ferrocene
dppm	Bis(diphenylphosphino)methane
HAT	Hydrogen atom transfer
NHC	N-Heterocyclic carbene
TMP	2,2,6,6-Tetramethylpiperidine

## 1 Introduction

The reduction of radicals to the corresponding hydrocarbons through hydrogen atom transfer (HAT) is one of the most important radical reactions. This is highlighted by the use of HATs as essential parts of reductive radical chain reactions. To date, trialkylstannanes are the most popular reagents for carrying out this particular transformation due to their low Sn–H bond dissociation energies (BDE) and the accordingly fast HAT from tin to carbon-centered radicals [1–4]. However, rather serious drawbacks exist. The toxicity of these reagents and the necessity of a sometimes difficult removal of side-products preclude their use in pharmaceutical applications, especially on a large scale [5]. Moreover, the high efficiency of the HAT from tin-based reagents can also result in chemical disadvantages. If the desired radical chain reaction contains propagation steps that are noticeably slower than HAT from trialkylstannanes, the intermediate radicals will be prematurely reduced.

In the field of metal-mediated and metal-catalyzed reactions, similar issues can be critical. Radical reduction by a HAT must be slow enough to allow any desired reaction to occur, but the HAT must also be fast enough to prevent any undesired trapping of the radicals by metal centers with unpaired electrons.

Over the past few years significant progress has been made in replacing trialkylstannanes as radical generating reagents and hydrogen atom donors. Some aspects, such as the use of silanes and related compounds, and of cyclohexadienes have been reviewed recently and will not be covered here [1–5].

Instead, it is the goal of this chapter to highlight some conceptually novel developments in the field of HAT reactions. We will concentrate on complexes of borane with N-heterocyclic carbenes (NHCs), on organometallic hydrogen atom donors in stoichiometric and catalytic reactions, and on the activation of water and alcohols for HAT.



## 2 Complexes of Borane and N-Heterocyclic Carbenes as HAT Reagents

One of the novel exiting developments in the field of tin-free radical chain reactions is the development of complexes of borane with NHCs as HAT reagents [6]. Borane ( $\text{BH}_3$ ) itself has a BDE of  $106.6 \text{ kcal mol}^{-1}$  which is much too high for its use in organic radical chain reactions. The group of Roberts and others have demonstrated that complexes of boranes with amines and phosphines have a reduced BDE and that they can be used in radical chain reactions [7]. However, the reduction is only moderate and too low to make these complexes generally applicable.

Computational studies by Rablen have suggested that ligands with  $\pi$ -donor abilities are much more efficient in the reduction of the B-H BDE [8]. On the basis of this finding, it has recently been demonstrated that complexes of NHCs and borane (NHC boranes) constitute a very interesting new class of radical hydrogen atom donors. Two of the first examples, **1** and **2**, together with their calculated BDEs, are shown in Scheme 1.

These NHC boranes can be employed as reducing agents for xanthates either with AIBN (Scheme 2) or  $\text{Et}_3\text{B}/\text{O}_2$  as initiating system. The reaction is thought to proceed via a “normal” radical chain process. Chain initiation with  $\text{Et}_3\text{B}/\text{O}_2$  resulted in higher yields of the desired product than the use of AIBN. Moreover, the amount of  $\text{Et}_3\text{B}$  could be reduced to 0.2 equiv. without significant reduction of the isolated yields.

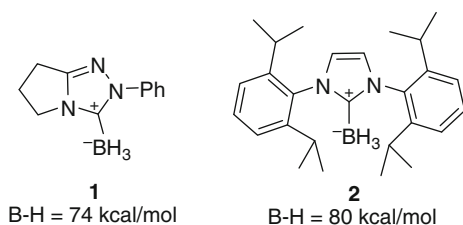
The intermediacy of free radicals is further supported by the observation of 5-*exo* cyclizations and the ring opening of cyclopropyl carbonyl radicals.

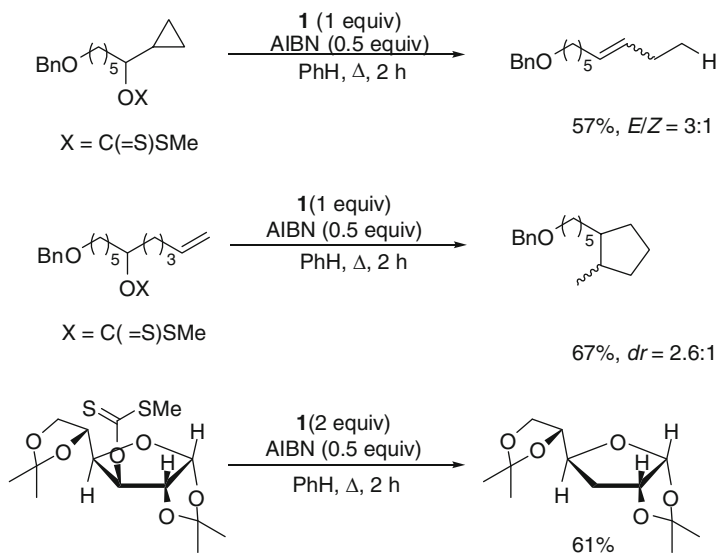
A highly attractive feature of the NHC boranes is their straightforward synthesis and the availability of large numbers of NHCs. Thus, many NHC boranes have already been investigated in the short time since their discovery. It turned out that the performance of the reaction noticeably depends on the substitution pattern of the NHC. Gratifyingly, the “minimalist” low-weight NHC carbenes **3** and **4** are more efficient reagents than the initially developed **1** and **2** as shown in Scheme 3 [9].

Their reactions are faster and they do not have to be employed in overstoichiometric amounts to achieve complete conversion of the starting materials.

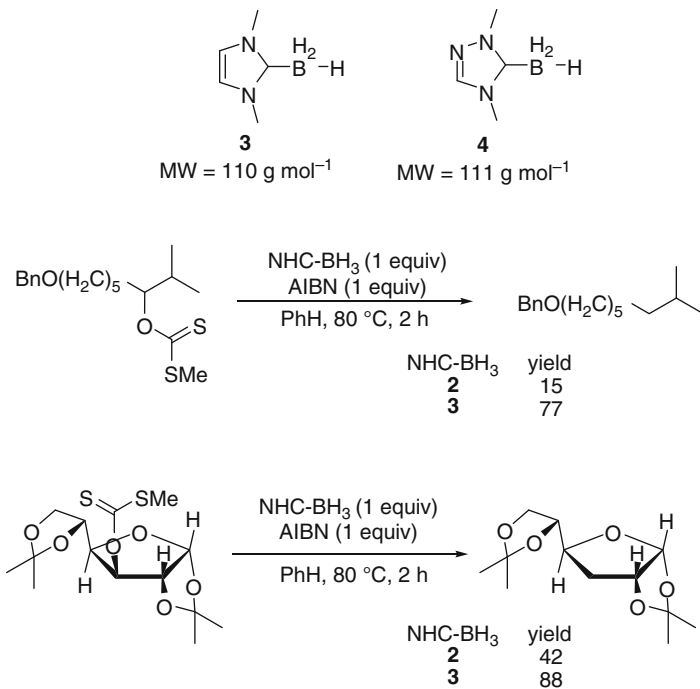
The reactions of NHC boranes have also been studied mechanistically in some detail [10]. It has been possible to isolate and characterize fully the (methylthio-carbonylthio)boranes arising from the reduction of xanthates.

**Scheme 1** First NHC boranes, their BDEs, and mechanism of the deoxygenation of xanthates





**Scheme 2** Performance of NHC boranes in deoxygenation reactions



**Scheme 3** Second generation “minimalist” NHC boranes and their reactions

The rate constant of HAT from **1** has been determined as  $(3.4 \pm 1.0) \times 10^4 \text{ M}^{-1} \text{ s}^{-1}$  at 28 °C by using a cyclobutyl carbinyl radical as clock. Also, the log A term of the Arrhenius equation is “normal” for a second-order HAT and thus the entropic demand of the NHC boranes is similar to that of group 14 metal hydrides. From the rate constant a BDE of about 88 kcal mol<sup>-1</sup> for **2** was estimated by applying an Evans-Polanyi relationship. This value is somewhat higher than the calculated value of 80 kcal mol<sup>-1</sup>.

For about 20 NHC boranes the HAT rate constants were estimated by competition experiments and found to be in the range of  $10^4 - 8 \times 10^4 \text{ M}^{-1} \text{ s}^{-1}$ . They are thus lower than for Bu<sub>3</sub>SnH ( $3 \times 10^6 \text{ M}^{-1} \text{ s}^{-1}$ ), (Me<sub>3</sub>Si)<sub>3</sub>SiH ( $4 \times 10^5 \text{ M}^{-1} \text{ s}^{-1}$ ), and Bu<sub>3</sub>GeH ( $10^5 \text{ M}^{-1} \text{ s}^{-1}$ ) but still above the threshold for successful radical chain reactions [11].

The EPR spectra of the NHC boryl radicals that were generated through HAT to the *tert*-butoxyl radical clearly show the delocalized π-type nature of these intermediates postulated to be essential by calculations [10, 12]. It was also demonstrated that the decay of the EPR signals could be fitted to a second-order decay having  $2k_t = 9 \times 10^6 \text{ M}^{-1} \text{ s}^{-1}$ . In agreement with this kinetic analysis, the NHC boryl radicals ultimately dimerize to give bis-NHC diborane derivatives. With the aid of EPR spectroscopy it was also established that the NHC boryl radicals readily abstract bromine atoms from primary, secondary, and tertiary alkyl bromides. However, chlorine atom abstraction is much slower and useful only for benzyl chloride.

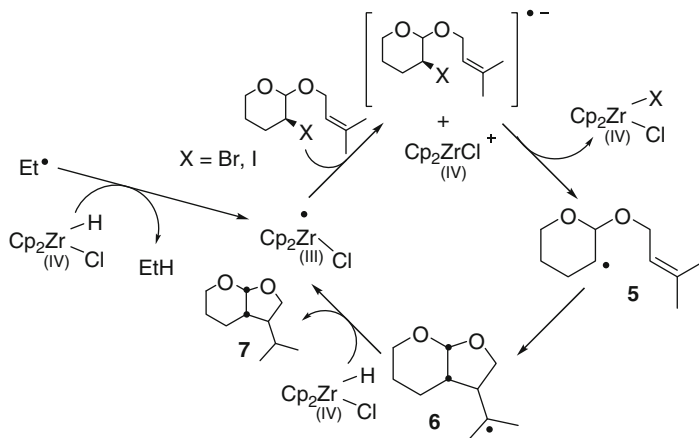
Very recently, the NHC boranes have been used as initiators for the photopolymerization of acrylates [13].

In conclusion, within a very short period of time NHC boranes have been developed into an attractive novel class of modular HAT reagents for conducting radical chain reactions through an impressive interplay of synthetic and mechanistic studies. The reagents should be especially attractive for reactions featuring slow propagation steps.

### 3 Organometallic Complexes as HAT Reagents

#### 3.1 Organometallic Complexes as HAT Reagents in Radical Chain Reactions

In principle, organometallic complexes are also highly interesting candidates for efficient HAT reagents. This is because M–H bonds are usually much weaker than C–H bonds [14–16]. Also, it has been established for a number of cases that HAT from organometallic complexes can be very fast. Still, the rates of the processes can be modulated by the introduction of steric bulk around the metal center. Moreover, low valent hydrido metal complexes can also act as chain carrying reagents because



**Scheme 4** Ueno-Stork cyclizations mediated by  $\text{Cp}_2\text{Zr}(\text{H})\text{Cl}$

the M–Hal bonds can be substantially stronger than C–Hal bonds. Thus, radical generation from organic halides is often possible.

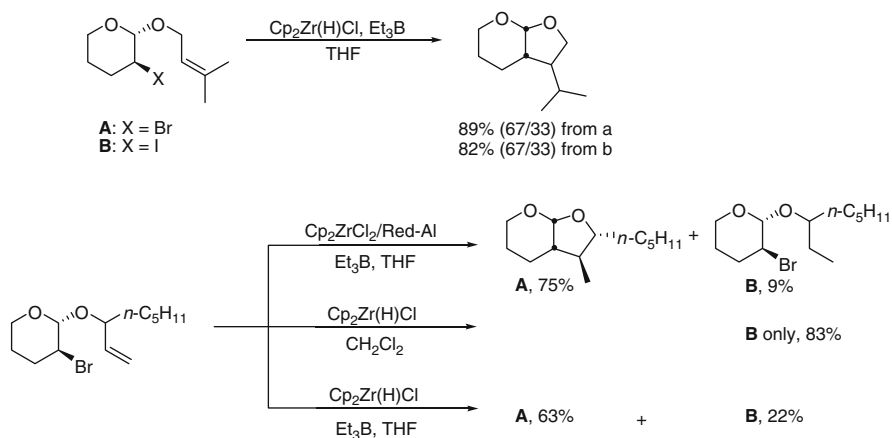
Oshima has demonstrated that the Schwartz reagent  $\text{Cp}_2\text{Zr}(\text{H})\text{Cl}$  can act as an excellent replacement for  $\text{Bu}_3\text{SnH}$  for Ueno-Stork cyclizations (Scheme 4) [17].

With an ethyl radical that is generated from the initiator  $\text{BET}_3$ ,  $\text{Cp}_2\text{Zr}(\text{H})\text{Cl}$  reacts via HAT to generate  $\text{Cp}_2\text{ZrCl}$ . This species constitutes a strong reductant and abstracts bromine or iodine from the organic substrate to generate free radical **5**. After cyclization, **6** is formed. HAT from  $\text{Cp}_2\text{Zr}(\text{H})\text{Cl}$  generates the desired product **7** and  $\text{Cp}_2\text{ZrCl}$  is regenerated. The overall reactions proceed efficiently with yields over 80%. Substrates containing chlorides are not sufficiently reactive, though. The process can also be used for other 5-*exo* cyclizations or the direct reduction of bromides and iodides.

A highly attractive feature of the process is that it can be conducted with catalytic amounts of the organometallic reagent. This is achieved by addition of Red-Al [ $\text{NaAlH}_2(\text{OCH}_2\text{CH}_2\text{OCH}_3)_2$ ] as terminal reductant that is able to convert  $\text{Cp}_2\text{ZrCl}_2$  and its mixed halide derivatives into the Schwartz reagent in situ. A minor drawback compared to the stoichiometric process is that Red-Al is reactive towards carbonyl groups. Thus, the functional group tolerance of the catalytic reaction is somewhat reduced. Examples are shown in Scheme 5.

Finally, it should be noted that enantiomerically pure derivatives of the Schwartz reagent are very appealing candidates for reagent controlled enantioselective and diastereoselective radical reductions. This is because a plethora of enantiomerically pure zirconocenes are available from other applications in enantioselective catalysis.

While this methodology is very useful, it is even more desirable to use milder and more readily available terminal reductants in these chain processes. Of special importance in this respect are  $\text{H}_2$ ,  $\text{H}_2\text{O}$ , and simple alcohols as the ultimate hydrogen atom donors. We will start the discussion with the use of  $\text{H}_2$ , while the use of  $\text{H}_2\text{O}$  and alcohols will be treated separately at the end of this chapter.



**Scheme 5** Radical reactions catalyzed by  $\text{Cp}_2\text{Zr}(\text{H})\text{Cl}$

In order to be able to use  $\text{H}_2$  as the terminal reductant, a reagent must be available that activates  $\text{H}_2$  to generate the desired HAT reagent. Many metal complexes are capable of doing so, of course, as hydrogen activation is essential for the extremely important field of hydrogenation methodology.

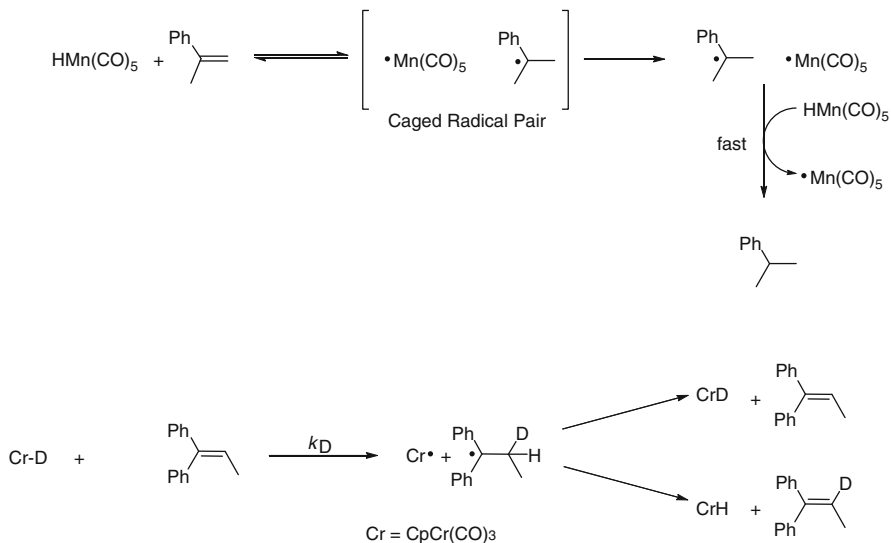
Before discussing catalytic hydrogen mediated radical reactions, processes based on preformed organometallic reagents will be discussed, because in this manner the elementary steps can be highlighted in a more accessible manner.

It has been demonstrated for some time that a number of metal monohydrides in stoichiometric amounts can reduce activated alkenes such as acrylates, styrenes, 1,3-dienes, and allenes by two consecutive HAT steps as shown in Scheme 6 [18–26].

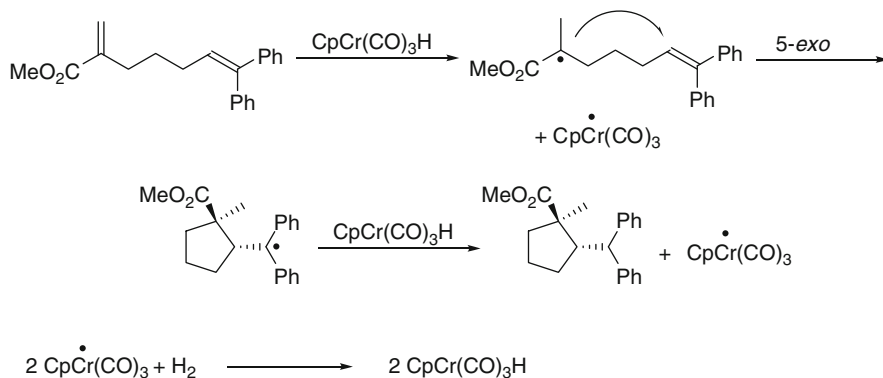
While these reactions are of limited use in the synthesis of complex molecules, they are very interesting from a mechanistic point of view. It has been firmly established that benzylic or allylic radicals and metal centered radicals are formed as intermediates through hydrogen atom transfer from the M–H bond to the C–C double bond. Interestingly, the addition of the hydrogen atom is reversible as demonstrated by isotope scrambling with deuterated olefins. If the radicals possess multiple sites for hydrogen atom abstraction, olefin isomerization can ultimately occur. HAT to unactivated olefins was not observed.

The radicals formed through HAT are then reduced by a second equivalent of the organometallic reagent to the corresponding hydrocarbon resulting in an overall “radical hydrogenation” of the olefin. In the cases investigated, the metal centered radicals dimerized and no attempts were made to regenerate the monohydrides by activation of  $\text{H}_2$ .

Polymerization reactions of suitably substituted acrylates can be initiated by radical generation through HAT [27]. It should be noted that hydrogen atom abstraction from the growing chain leads to interruption of chain growth. In such cases the organometallic complex possessing the pivotal M–H bond is reformed and



**Scheme 6** Radical hydrogenations of activated olefins



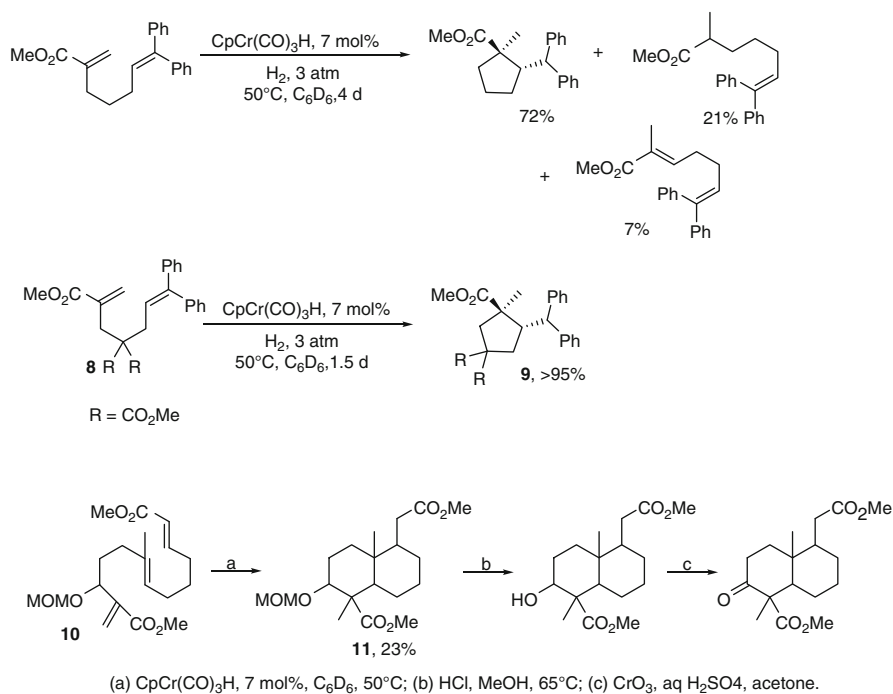
**Scheme 7** CpCr(CO)<sub>3</sub> catalyzed, H<sub>2</sub> mediated radical cyclization

a novel chain can be initiated. Thus, complexes such as CpCr(CO)<sub>3</sub>H or HMn(CO)<sub>5</sub> can act as chain-transfer catalysts in the polymerization of olefins.

Thus, radical generation, the formation of C–C bonds, and radical reductions are possible in reactions with alkenes and organometallic complexes with M–H bonds.

Norton has recently combined these key-steps with the activation of H<sub>2</sub> by CpCr(CO)<sub>3</sub> to very elegant tin-free and catalytic radical cyclization mediated by H<sub>2</sub> that is highlighted in Scheme 7 [28, 29].

The Cp(CO)<sub>3</sub>Cr radical serves a threefold purpose in this process. First, it activates H<sub>2</sub> to give the pivotal Cp(CO)<sub>3</sub>CrH. Second, Cp(CO)<sub>3</sub>CrH adds a hydrogen atom to the acrylates. Third, after the radical formed through a 5-*exo* cyclization, it is



**Scheme 8** Examples of the catalytic radical cyclizations

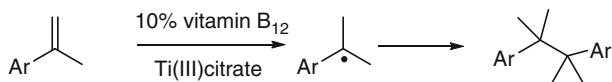
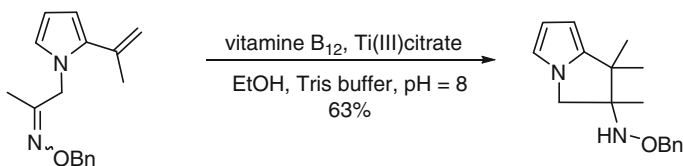
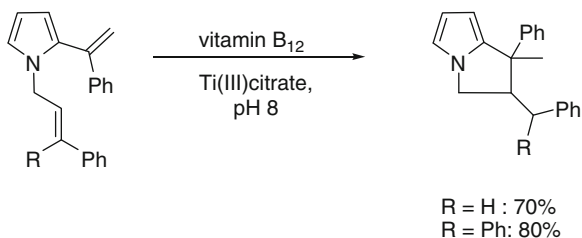
reduced by a HAT from  $\text{Cp}(\text{CO})_3\text{CrH}$  and the  $\text{H}_2$ -activating  $\text{CpCr}(\text{CO})_3$  is regenerated. These conditions have been applied to a number of other substrates as summarized in Scheme 8.

The substrate scope reveals the critical aspects of the process. The cyclization must be faster than the competing radical reduction through HAT. Thus, the olefin that serves as radical acceptor should be activated in order to achieve high yields. However, the HAT for radical generation must be chemoselective and thus the olefin that serves as radical acceptor should be at least trisubstituted to disfavor HAT kinetically to this functional group.

The introduction of the two ester groups in **8** results in an acceleration of the cyclization and hence in an almost quantitative yield of **9**. Unfortunately, alkyl substituted olefins as in **10** do not appear to be efficient radical acceptors in 6-*exo* cyclizations because the isolated yield of the desired product **11** is not high.

Despite these slight shortcomings, the development of the catalytic conditions constitutes a major conceptual advance in the field of radical cyclizations.

It should be noted that a related reaction has been developed by the Norton group, with  $\text{HV}(\text{CO})_4\text{dppe}$ , a compound with an unusually weak M–H bond (about  $57 \text{ kcal mol}^{-1}$ ), serving as a stoichiometric HAT reagent. The organometallic complex cannot be employed catalytically because  $\text{V}(\text{CO})_4\text{dppe}$  that is formed after HAT is unable to activate  $\text{H}_2$  [29, 30].

**Scheme 9** Vitamin B<sub>12</sub> catalyzed radical cyclizations

Ar	yield
Ph	85
4-Cl-C <sub>6</sub> H <sub>4</sub>	80
4-F-C <sub>6</sub> H <sub>4</sub>	70

**Scheme 10** Unusual radical cyclizations and dimerizations of styrenes catalyzed by vitamin B<sub>12</sub>

Another system for cyclizations based on HAT has been described by the group of van der Donk. It relies on vitamin B<sub>12</sub> as the HAT-catalyst precursor [31]. The buffered Ti(III) citrate solution generates the active species containing the pivotal Co–H bond of vitamin B<sub>12</sub>. Examples of cyclization reactions are shown in Scheme 9.

The reaction is broader in scope than the H<sub>2</sub> mediated cyclizations.

The Co-derived system constitutes a distinctly less efficient HAT reagent than CpCr(CO)<sub>3</sub>H and can also be used in kinetically less favored radical addition reactions, such as additions to oximes, and even dimerizations of benzylic radicals as shown in Scheme 10 [31, 32].

The mechanism of this unusual transformation has been studied very carefully and compelling evidence for the intermediacy of radicals has been presented. One of the arguments is the low diastereoselectivity of the dimerizations that is typical for a radical process. Moreover, it has been demonstrated that the persistent radical effect is “overcome” by reduction of the Co(II) metalloradicals to the catalytically



active Co(I) species by Ti(III)citrate. It remains to be seen whether further applications of this very efficient system for radical generation will be reported in the future.

### 3.2 Organometallic HAT Reagents in Catalytic and Stoichiometric Metal Mediated Reactions

Radical chain reactions are established as very powerful tools in the synthesis of complex molecules. The complementary approach to radical chemistry that relies on radical generation through electron transfer is also attractive, especially when radical generation is decoupled from the ensuing radical transformations and the final radical reduction. This is especially so for catalytic reactions.

Two major potential advantages of this approach are the possibility to use hydrogen atom donors that are not suitable for propagating a radical chain and a high functional group tolerance.

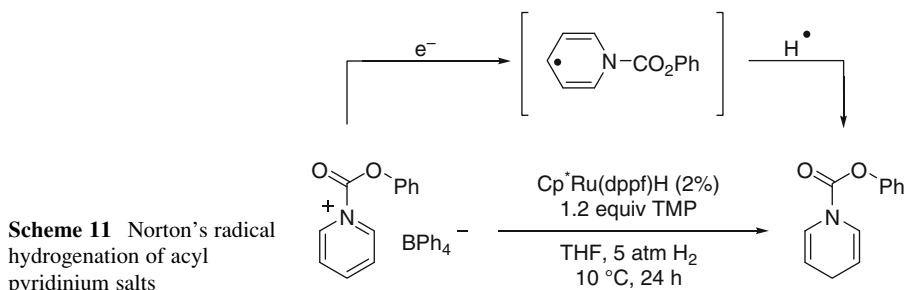
The Norton group has reported two examples of this type of transformation. In the first, a 1,4-reduction of pyridinium ions by Ru(II) hydrido complexes takes place in two steps, an SET followed by a HAT, as shown in Scheme 11 [33].

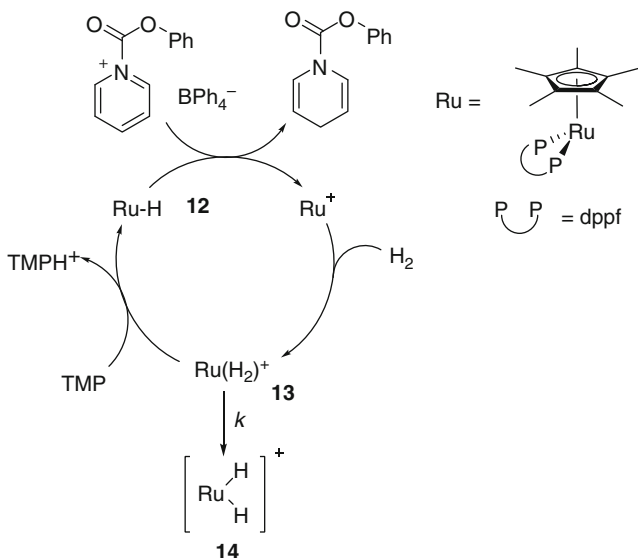
The presence of the Ru(III)-complex  $[\text{Ru}-\text{H}]^+$  that is formed from **12** through electron transfer to the acyl pyridinium has been demonstrated by EPR spectroscopy. The reaction can be rendered catalytic in Ru by the addition of a base (Scheme 12).

In this manner, the cationic dihydrogen complex **13** can be deprotonated to the catalytically active Ru(II) hydrido complexes. The undesired isomerization of **13** to the dihydride complex **14** can be avoided by lowering the reaction temperature and changing the solvent to THF.

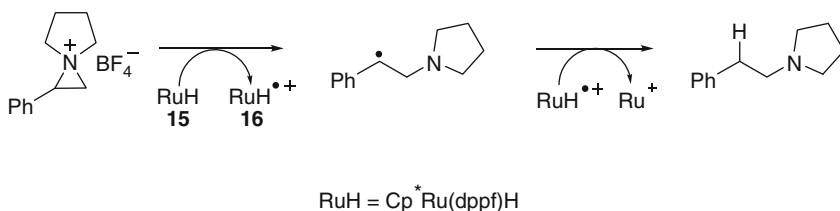
In a second example, the Norton group has presented evidence that the reduction of phenyl substituted aziridinium cations to the corresponding amines by  $\text{Cp}^*\text{Ru}(\text{dppf})\text{H}$  proceeds via a similar mechanism [34] that is shown in Scheme 13.

A key issue of this reaction is that aziridinium cations are electrochemically much more readily reduced (by 0.6–0.9 V) than their alkyl substituted analogs.





**Scheme 12** Mechanism of the catalytic radical hydrogenation of acyl pyridinium salts

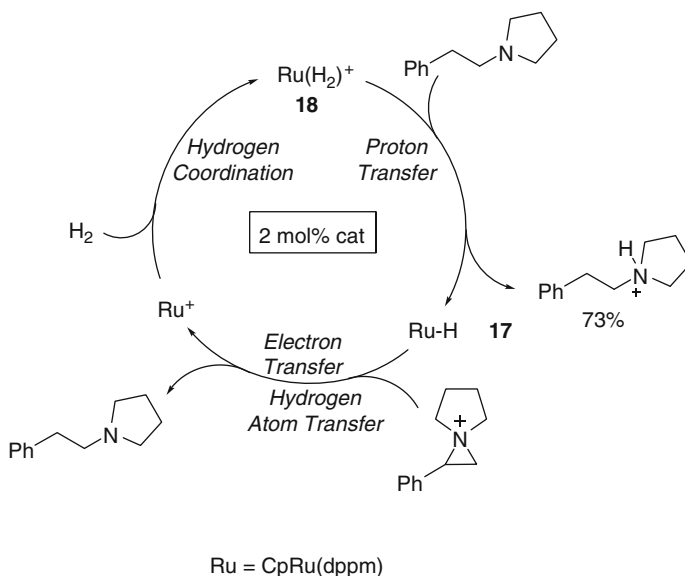


**Scheme 13** Hydrogenation of aziridinium cations via Ru-mediated HAT

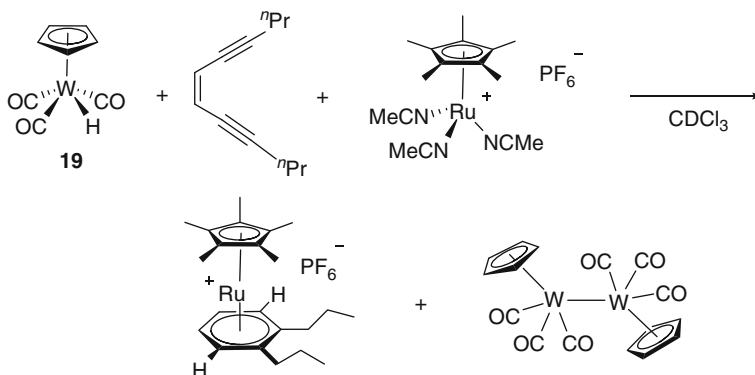
Moreover, the alternative pathway of an  $\text{S}_{\text{N}}1$ -type ring opening does not seem to operate as the necessary generation of the benzylic cation is too slow to be in agreement with the measured rate constants. Another strong piece of argument in favor of the ET mechanism is the significant line broadening of the Ru–H, the Cp\*, and the ferrocenyl signals in the  $^1\text{H}$ -NMR spectra that can be attributed to a self-exchange process of the catalyst **15** and its oxidized form **16**. The reaction can also be conducted with catalytic amounts of the Ru-complex as shown in Scheme 14.

The amine product plays a critical role, as it deprotonates the  $\text{H}_2$  complex **18** to regenerate the catalytically active **17**. This also prevents side reactions based on nucleophilic ring opening of the aziridinium cations by the amine products. Alkyl substituted aziridinium cations react via a classical  $\text{S}_{\text{N}}2$ -mechanism.

The common feature of the radical hydrogenations and  $\text{H}_2$ -mediated cyclizations is that the metal complexes serve as both radical generating and reducing reagents. A complementary approach uses different reagents for both purposes. In this manner,



**Scheme 14** Hydrogenation of aziridinium cations via Ru-catalyzed HAT



**Scheme 15** Bergman cycloaromatization terminated by HAT from CpW(CO)<sub>3</sub>H

the particular features of two reagents, such as chemo- and stereoselectivity, can be combined. This is especially attractive for catalytic processes.

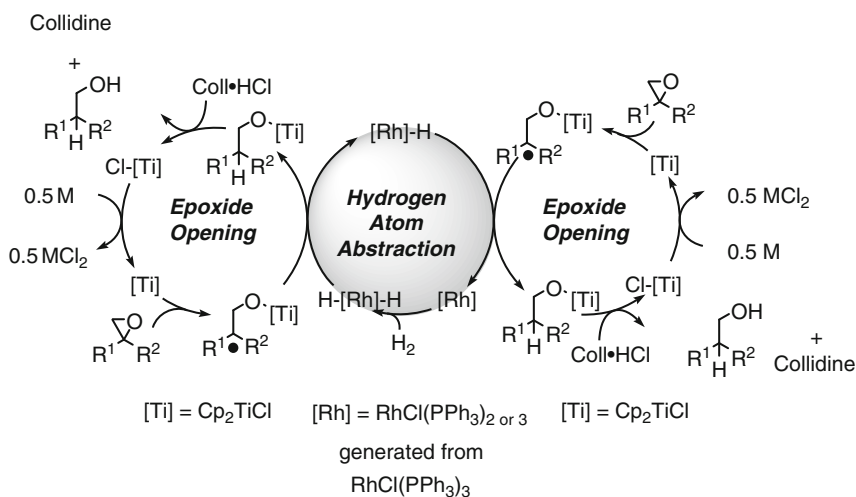
A stoichiometric example of the combination of two reagents has recently been reported by O'Connor in the context of the Bergman cycloaromatization. The generation of the aromatic diradical can be induced by [Cp\*Ru(CH<sub>3</sub>CN)<sub>3</sub>]PF<sub>6</sub>. Radical reduction occurs through HAT from CpW(CO)<sub>3</sub>H to provide a cationic Ru-arene complex as shown in Scheme 15 [35].

It has been pointed out that the relatively high strength of the W–H bond is critical for the success of the cycloaromatization. The use of  $\text{CpCr}(\text{CO})_3\text{H}$ , with a BDE of  $10 \text{ kcal mol}^{-1}$  less than **19**, does not result in the desired transformation, even though it is a better reducing agent for the diradical. This failure is due to a HAT of  $\text{CpCr}(\text{CO})_3\text{H}$  to the endiynes substrate that leads to extensive decomposition of the substrate. This very nicely highlights the importance of properly adjusting the reactivity of the reagents involved.

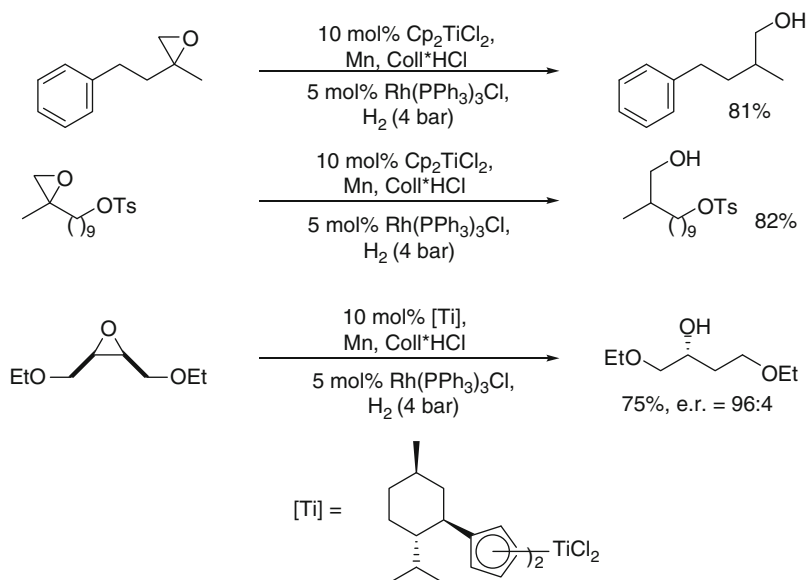
The coupling of independent catalytic cycles for both radical generation and reduction has been realized by the combination of the titanocene catalyzed reductive epoxide opening [36–40] via electron transfer and the catalytic reduction of radicals after  $\text{H}_2$  activation by Wilkinson's complex  $[\text{Rh}(\text{PPh}_3)_3\text{Cl}]$  as shown in Scheme 16 [41–43].

Two key issues are essential for the success of the catalytic HAT (CHAT) reaction. First, the two catalytic systems must be compatible. Because early and late transition metals usually bind ligands with opposing donor properties, they should remain mutually unaffected. Also, the Wilkinson catalyst should be stable under the slightly acidic conditions of the titanocene regeneration system (Zn, 2,4,6-collidine hydrochloride). Since it has been reported that  $\text{Rh}(\text{PPh}_3)_3\text{Cl}$  is even stable towards  $\text{BF}_3 \cdot \text{Et}_2\text{O}$ , this was expected to be the case [44].

Second, it is essential that both  $\text{H}_2\text{Rh}(\text{PPh}_3)_3\text{Cl}$  and  $\text{H}_2\text{Rh}(\text{PPh}_3)_2\text{Cl}$  formed after the oxidative addition to  $\text{H}_2$  react faster with the  $\beta$ -titanoxy radicals than  $\text{Cp}_2\text{TiCl}$ . Since the ring opening via ET is the rate determining step, this is critical. It is known that HAT from Rh-hydrides proceeds with rate constants as high as  $10^9 \text{ M}^{-1} \text{ s}^{-1}$  and thus it seemed possible that the HAT may be faster than the reactions with titanocenes [45, 46]. Some of the results obtained with this system



**Scheme 16** Coupled cycles for Rh-catalyzed HAT to  $\beta$ -titanoxy radicals



**Scheme 17** Examples of catalytic HAT for the reduction of epoxides

are summarized in Scheme 17. The reaction is compatible with Kagan's complex [47, 48] in enantioselective and regiodivergent radical generations [49–54].

In general, the isolated yields are good and in the same range as those obtained with 5 equiv. of 1,4-CHD as hydrogen atom donor [55]. Thus, the concept of coupling catalytic cycles for enforcing a catalytic HAT (CHAT) has been successfully realized. In this manner, the use of expensive and toxic stoichiometric reagents can, in principle, be avoided.  $\text{CpCr}(\text{CO})_3\text{H}$  and Pd/C were also investigated for the CHAT. Both reagents gave substantially lower and varying yields of the desired products. It seems that the problem with these reagents is that they cannot activate  $\text{H}_2$  swiftly enough to compete efficiently with radical trapping by the titanocenes.

The major problem with using Wilkinson's catalyst is that it also constitutes an excellent hydrogenation catalyst [56]. Thus, alkynes and terminal alkenes are not tolerated under the conditions of the coupled catalytic cycles. This implies that radical cyclizations terminated by a CHAT cannot be carried out under these conditions.

Therefore, CHAT reagents that activate  $\text{H}_2$  efficiently without being hydrogenation catalysts were investigated. It turned out that Vaska's complex  $\text{Ir}(\text{CO})\text{Cl}(\text{PPh}_3)_2$  [57, 58] also gives satisfactory, albeit slightly lower, yields of the desired product as shown [42]. Since  $\text{H}_2\text{Ir}(\text{CO})\text{Cl}(\text{PPh}_3)_2$  does not possess a vacant coordination site, it is known not to be an active hydrogenation catalyst. Vaska's complex can also efficiently terminate radical cyclizations via CHAT [43]. Especially difficult but potentially rewarding reactions in this context are cyclizations leading to small rings and tandem cyclizations [59–69].

## 4 Generation of HAT Reagents from Water and Alcohols Through Coordination

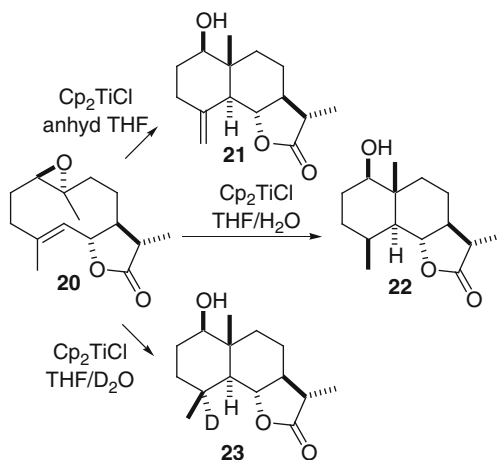
### 4.1 Activation of Water by Ti(III)

Since the discovery of free radicals, it has been believed that they are inert against water [70]. This lack of reactivity has been attributed to the strength of the H–OH bond ( $\text{BDE} = 117.6 \text{ kcal mol}^{-1}$ ) which in theory prevents any potential H-atom transfer from water to free radicals [71].

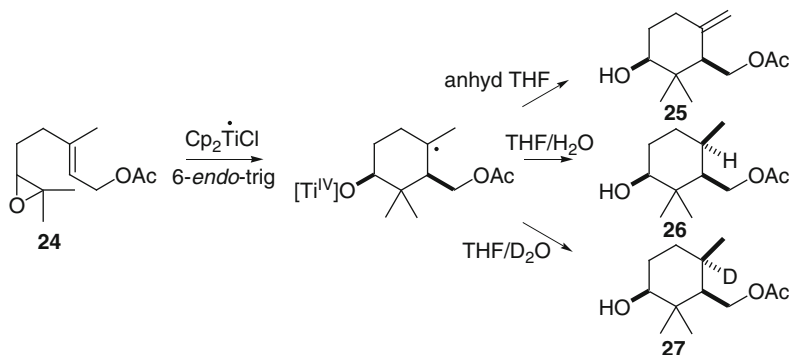
In 2002, however, it was observed that water did substantially affect radical cyclizations mediated by Ti(III) complexes. Thus, for example, when epoxide **20** was treated with  $\text{Cp}_2\text{TiCl}$  in dry THF, the exocyclic alkene **21** was obtained. When the same epoxide was treated with  $\text{Cp}_2\text{TiCl}$  in the presence of water, however, the corresponding reduction product **22** was formed. Moreover, with deuterium oxide instead of water, the deuterium labeled isotopomer **23** (Scheme 18) was isolated [72].

These and other preliminary results prompted Oltra and Rosales to publish the following comment: *Our results demonstrate that in Ti(III)-mediated free-radical chemistry water can act in a reductive way, working as a hydrogen atom donor. Therefore, we believe that the generally accepted passivity of water in free-radical chemistry should be carefully revised, especially in the presence of Ti(III) and other metal-centered free radicals* [72].

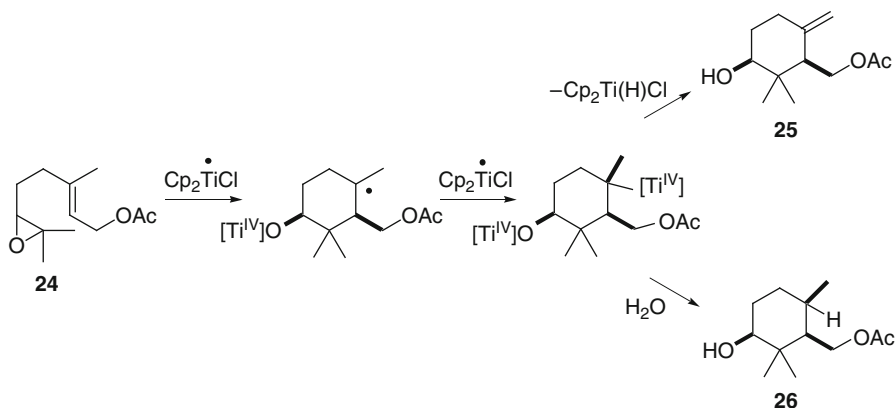
Subsequently, similar results were obtained with **24**. When treated with  $\text{Cp}_2\text{TiCl}$  in dry THF, **24** yielded the exocyclic alkene **25**. In contrast, in the presence of water, the corresponding reduction product **26**, and with  $\text{D}_2\text{O}$ , the deuterium labeled **27**, were isolated (Scheme 19) [73, 74].



**Scheme 18** Dependence of the transannular cyclization of **20** on the presence of additives



**Scheme 19** Dependence of the cyclization of epoxygeranyl acetate on the presence of additives

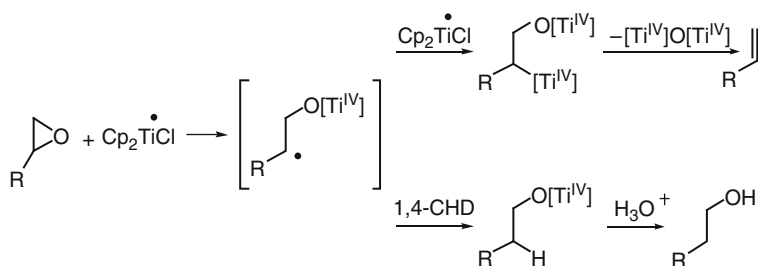


**Scheme 20** Fate of the organometallic intermediate potentially formed during the cyclization of 24

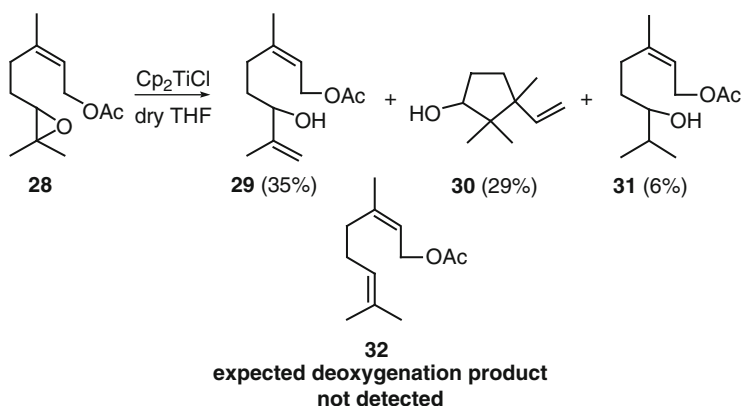
Nevertheless, the possibility of a more conventional mechanism involving the formation and subsequent hydrolysis of an organometallic alkyl-Ti(IV) intermediate (Scheme 20) was initially also considered.

However, since then, compelling evidence has been accumulated that this pathway is not relevant.

Under the deoxygenation conditions for epoxides introduced by Nugent and RajanBabu, the more stable  $\beta$ -titanoxy radical, which is generated through reductive epoxide opening, can be trapped by a second equivalent of  $\text{Cp}_2\text{TiCl}$  to produce an organometallic alkyl-titanium(IV) intermediate, which, after  $\beta$ -elimination, gives an alkene, the pivotal deoxygenation product. Nevertheless, in the presence of a hydrogen-atom donor such as 1,4-CHD, the  $\beta$ -titanoxy radical is reduced to give the less substituted alcohol (Scheme 21) [75].



**Scheme 21**  $\text{Cp}_2\text{TiCl}$  mediated deoxygenation and reduction of monosubstituted epoxides



**Scheme 22**  $\text{Cp}_2\text{TiCl}$  mediated opening of epoxyneryl acetate without water

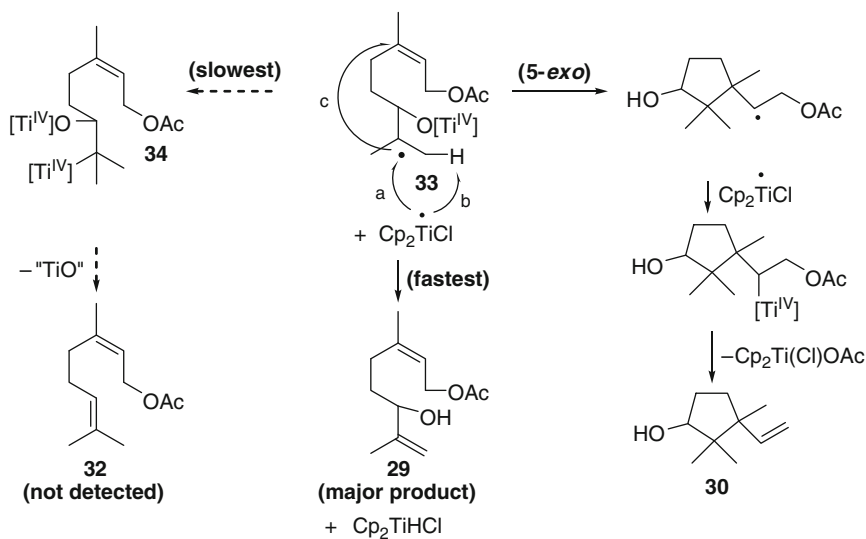
When **28** was subjected to  $\text{Cp}_2\text{TiCl}$  in dry THF, the allylic alcohol **29**, together with the cyclization product **30** and a minor quantity of the reduction product **31**, was isolated. The expected deoxygenation product **32** was not formed at all (Scheme 22) [73, 74].

The formation of the major product suggested that a mixed disproportionation reaction between the radical intermediate **33** and a second equivalent of  $\text{Cp}_2\text{TiCl}$  had taken place [76]. This process was slightly faster than the cyclization reaction leading to **30** and much faster than the potential radical trapping by the second titanium species, which would have led to the elusive deoxygenation product **32** (Scheme 23).

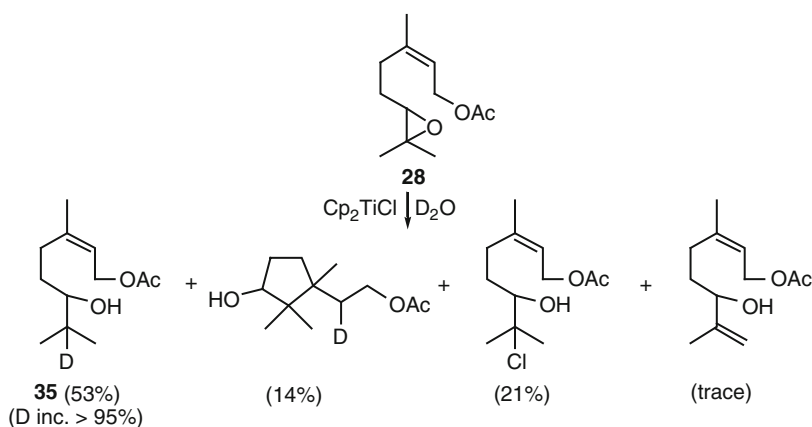
Subsequently, **28** was treated with  $\text{Cp}_2\text{TiCl}$  in the presence of  $\text{D}_2\text{O}$ . Under these conditions, the deuterium-labeled alcohol **35** became the main product, at the expense of allylic alcohol **29** (Scheme 24) [73, 74].

Thus, deuterium transfer from  $\text{D}_2\text{O}$  was faster than the mixed disproportionation leading to the allylic alcohol **29**, which in turn had proved to be much faster than the potential radical trapping leading to the organometallic intermediate **34**. This strongly suggests that deuterium incorporation in **35** cannot occur via hydrolysis of **34** [73, 74].





**Scheme 23** Potential pathways in the  $\text{Cp}_2\text{TiCl}$  mediated cyclization of epoxyneryl acetate



**Scheme 24**  $\text{Cp}_2\text{TiCl}$  mediated opening of epoxyneryl acetate in the presence of  $\text{D}_2\text{O}$

Ultra and Cuerva explored the fate of primary radicals in the presence of water next. However, since the titanium-promoted opening of epoxides generally gives the higher substituted radicals, the generation of primary radicals directly from epoxides seemed impossible. Nevertheless, primary radicals can be readily generated via cyclization to suitably substituted olefins. To this end, the transannular cyclization of caryophyllene oxide (**36**) that generates a *neopentyl*-type primary radical was employed. After treatment of **36** with  $\text{Cp}_2\text{TiCl}$  a mixture of stereoisomers **37** and **38** was formed via reduction of the intermediate primary radicals (Scheme 25) [73, 74].

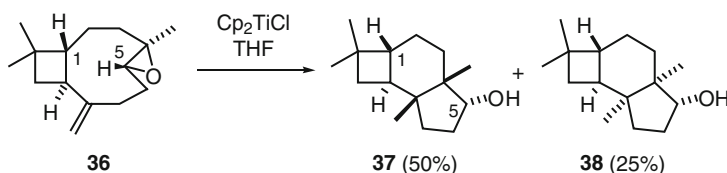
Subsequently, the following experiments were carried out to find out whether this radical reduction occurred through hydrolysis of an organometallic intermediate or from a hydrogen-atom transfer process.

First, **36** was treated with  $\text{Cp}_2\text{TiCl}$  in the presence of 1,4-CHD. After consumption of **36** (1 h),  $\text{D}_2\text{O}$  was added. From this reaction a mixture of **37** and **39** was obtained (Scheme 26).

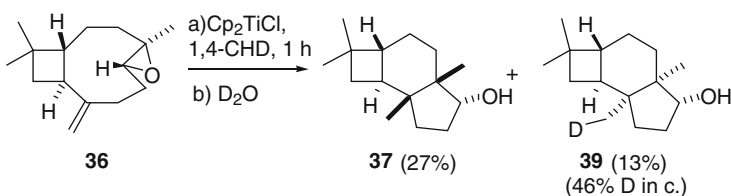
The lack of deuterium labeling in **37** indicated that the reduction of the primary radical took place by hydrogen-atom transfer from 1,4-CHD and not by hydrolysis of a potential organometallic intermediate. Then **36** was treated with  $\text{Cp}_2\text{TiCl}$  in the presence of 1,4-CHD and  $\text{D}_2\text{O}$ . A mixture of the “normal” products **37** and **38** as well as the deuterium-labeled **39** and **40** could be isolated (Scheme 27).

The 57% of deuterium incorporation in **40** demonstrates that deuterium transfer from  $\text{D}_2\text{O}$  was slightly faster than the hydrogen transfer from 1,4-CHD, which had been shown to be much faster than the radical trapping by a second equivalent of  $\text{Cp}_2\text{TiCl}$ . As before, deuterium incorporation in **40** can therefore not occur via protonation of an organometallic intermediate, such as **41** (Scheme 28).

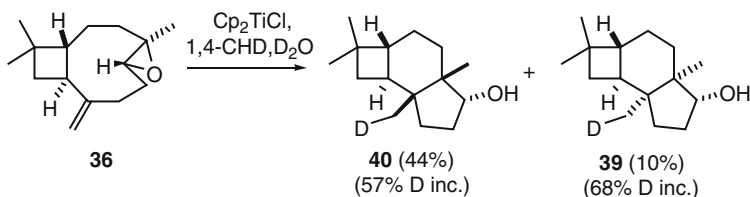
Finally, a kinetic isotope effect of 3.0 was determined for these HATs. This value is similar to that reported for a HAT from *tert*-butyl thiol to primary radicals [77].



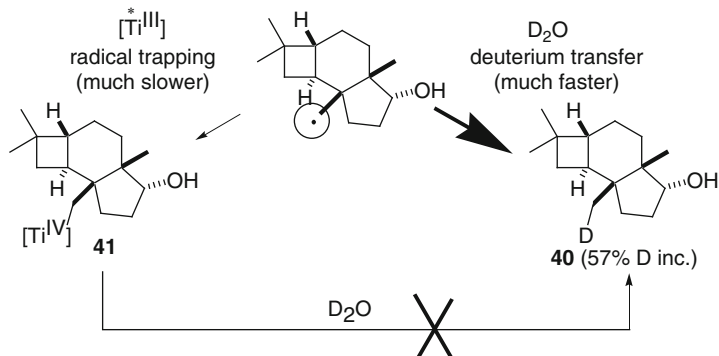
**Scheme 25** Titanocene mediated cyclization of caryophyllene oxide



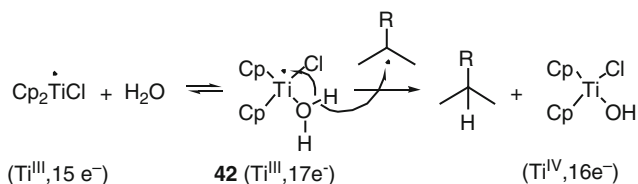
**Scheme 26** Deuteration studies in the cyclization of caryophyllene oxide



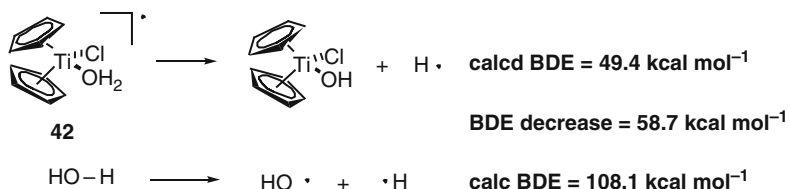
**Scheme 27** Deuteration studies in the cyclization of caryophyllene oxide



**Scheme 28** Deuteration studies in the cyclization of caryophyllene oxide



**Scheme 29** HAT from water to free radicals mediated by **42**



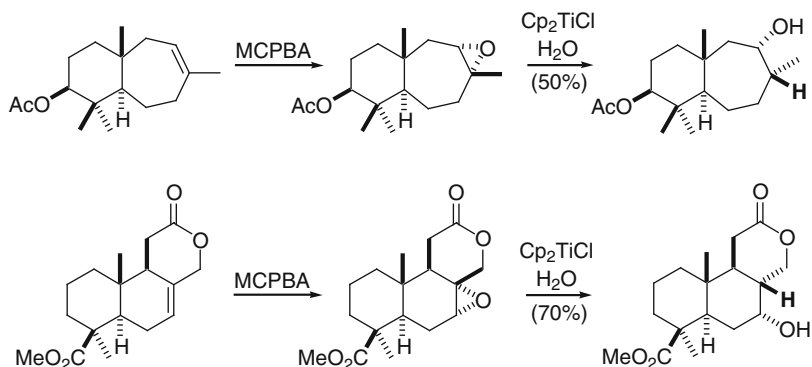
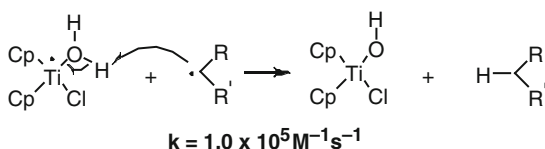
**Scheme 30** BDE of water coordinated to  $Cp_2TiCl$

To explain the unprecedented HATs from water it was proposed that the co-ordination of water to Ti(III) might weaken the strength of the O–H bond. In this manner a single-electron transfer from titanium to oxygen might facilitate the HAT from the titanocene aqua-complex **42** to the free radicals (Scheme 29).

Theoretical calculations supported this hypothesis, indicating a bond-dissociation energy (BDE) for the titanocene aqua-complex **42** of only  $49.4 \text{ kcal mol}^{-1}$ , which represents a decrease of almost  $60 \text{ kcal mol}^{-1}$  compared to the calculated BDE of  $H_2O$  (Scheme 30) [73, 74].

In 2008, Jin and Newcomb confirmed the findings on the activation of water as hydrogen atom donor by  $Cp_2TiCl$  and, by using radical clocks, determined the rate constant for the H-atom transfer from the Ti(III) aqua-complex to secondary radicals (Scheme 31) [78].

**Scheme 31** Rate constant of the reduction of secondary radicals by  $\text{Cp}_2\text{TiCl}/\text{H}_2\text{O}$



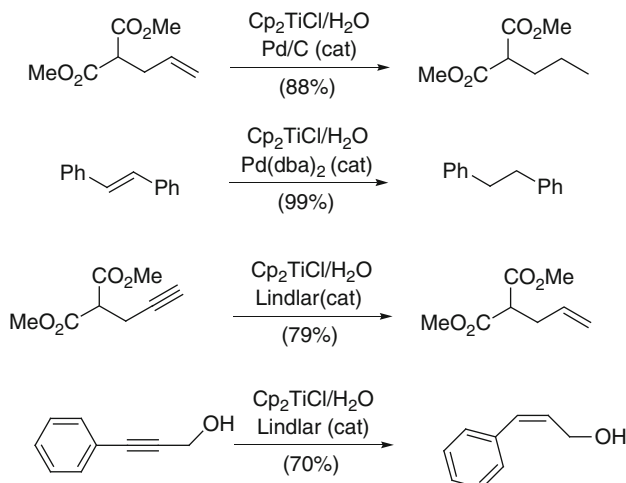
**Scheme 32** *Anti*-selective reduction of epoxides by  $\text{Cp}_2\text{TiCl}/\text{H}_2\text{O}$

Apart from these mechanistic considerations, the  $\text{Cp}_2\text{TiCl}/\text{H}_2\text{O}$  couple has emerged as an excellent reagent for the reductive opening of epoxides, avoiding the use of conventional hydrogen-atom donors such as 1,4-CHD, *tert*-butyl thiol, or  $\text{Bu}_3\text{SnH}$ , which are toxic, expensive, and/or foul-smelling.

The epoxidation-epoxide opening sequence with this reagent provides a convenient access to the products of an *anti*-Markovnikov addition of water to olefins. Interestingly, the  $\text{Cp}_2\text{TiCl}/\text{H}_2\text{O}$  couple combination shows *anti* stereoselectivity in the reduction step [73, 74], which is complementary to the hydroboration-oxidation method (Scheme 32).

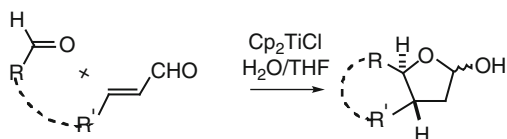
The reductive epoxide opening can also be carried out using substoichiometric quantities of  $\text{Cp}_2\text{TiCl}$  in the presence of collidine hydrochloride. Moreover, with  $\text{D}_2\text{O}$  deuterium-labeled alcohols can easily be obtained using relatively cheap  $\text{D}_2\text{O}$  as deuterium source [79].

The  $\text{Cp}_2\text{TiCl}/\text{H}_2\text{O}$  combination can also be used for the chemoselective reduction of aromatic ketones. The reaction discriminates between ketones and alkenes, between ketones and esters and, remarkably, between conjugated and non-conjugated ketones [80]. There is strong evidence that this reduction proceeds via ketyl-type radicals, which are finally reduced by H-atom transfer from **42** [81]. Under dry conditions, titanium-promoted ketyl radicals from aromatic ketones can be used for intermolecular and intramolecular cross-coupling of ketones [82]. Thus, depending on whether water is added or not, complementary and versatile synthetic procedure protocols are available.



**Scheme 33** Hydrogenation of olefins and alkynes mediated by  $\text{Cp}_2\text{TiCl}/\text{H}_2\text{O}$

**Scheme 34** Radical additions of aldehydes to conjugated alkenals mediated by  $\text{Cp}_2\text{TiCl}/\text{H}_2\text{O}$



Furthermore, in the presence of Pd or Rh catalysts, the  $\text{Cp}_2\text{TiCl}/\text{H}_2\text{O}$  couple can also be used for the hydrogenation of alkenes and alkynes by hydrogen transfer from water (Scheme 33) [83].

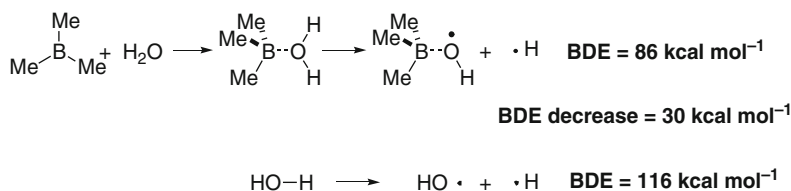
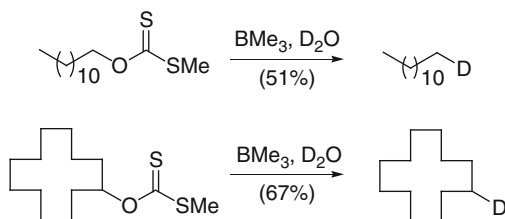
If  $\text{D}_2\text{O}$  is used instead of water, this method provides a straightforward access to doubly labeled products. The reaction mechanism seems to proceed via hydrogen transfer from **42** to the late-transition metal complex. This results in the formation of a hydrido metal complex that hydrogenates the alkene or alkyne substrate. Theoretical calculations strongly support this mechanistic proposal by suggesting an activation energy of only  $17.3 \text{ kcal mol}^{-1}$  for the HAT [83].

The  $\text{Cp}_2\text{TiCl}/\text{H}_2\text{O}$  couple can also be used to achieve inter- and intramolecular Michael-type additions of aldehydes to conjugated alkenals (Scheme 34) [84].

## 4.2 Activation of Water by Boron

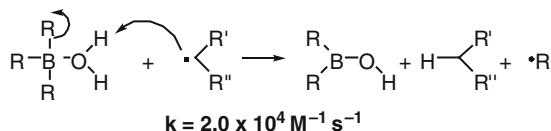
In 2005, Wood and co-workers reported a conceptionally new version of the Barton-McCombie reaction by using water as hydrogen-atom source for the reduction of free radicals in the presence of trialkylboranes (Scheme 35) [85].

**Scheme 35** Barton-McCombie reaction in the presence of trialkylboranes and water



**Scheme 36** BDE of water coordinated to trimethylborane

**Scheme 37** Rate constant of the reduction of secondary radicals by trialkylborane coordinated water



The authors proposed that the HAT from water was mediated by a boron aqua complex in which the strength of the O–H bond was weakened by 30 kcal mol<sup>-1</sup> with respect to non-coordinated water (Scheme 36).

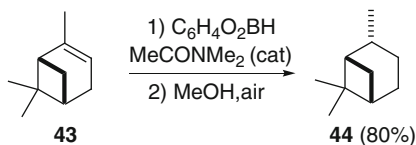
In 2007 the scope of the trialkylborane/water system was extended to the dehalogenation of alkyl iodides and the chemoselective deoxygenation of secondary alcohols in the presence of alkyl and aryl halides [86]. The rate constants for the hydrogen-atom transfer from this reagent to secondary radicals (Scheme 37) are substantially lower than those of the Ti(III) aqua-complex [78, 87].

### 4.3 Activation of Alcohols by Boron?

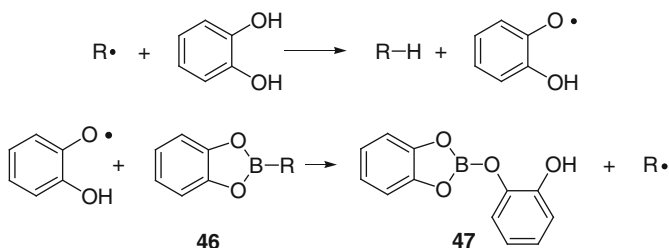
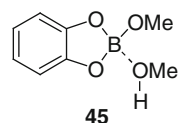
In 2005, Renaud and co-workers reported a novel procedure for the formal hydrogenation of alkenes via hydroboration with an excess of catecholborane, followed by treatment of the intermediate boronic acid esters with methanol in the presence of air as a radical initiator [88]. A typical example, the reduction of **43** to **44**, is shown in Scheme 38. Similar results were obtained for a wide range of primary, secondary, and tertiary alkylcatecholboranes.

Kinetic and mechanistic investigations on this reaction were subsequently carried out by Jin and Newcomb [78, 89].

**Scheme 38** “Radical hydrogenation” of olefins with catecholborane and methanol



**Scheme 39** Postulated activation of  $\text{MeOH}$  by coordination with boron



**Scheme 40** Mechanism of the radical reduction of boronates with free catechol

In the original paper, Renaud and co-workers hypothesized that complex **45**, resulting from the complexation of methoxycatecholborane, generated in situ from the excess of catecholborane and methanol, was the main source of H atoms. The authors proposed that the O–H bond of methanol was activated by complexation with the boron Lewis acid (Scheme 39).

More recently, experiments from the same group indicated that boronate complex **45** cannot be the source of hydrogen atoms [90]. Instead, it was suggested that “free” catechol was the actual source of hydrogen atoms.

Radical reduction is followed by a rapid reaction of the 2-hydroxyphenoxyl radical with the boronate **46**. In this manner, chain propagation is ensured by the regeneration of the initial alkyl radical and the formation of Meulenhoff’s free acid **47** (Scheme 40).

## 5 Conclusion

Over the last few years, significant progress has been made in the development of novel hydrogen atom donor reagents that are attractive surrogates for the classical group 14 reagents. The issue of toxicity is addressed by using readily available, non-venomous terminal reductants, such as borane, water, methanol, or hydrogen.

Borane, methanol, and water, which have B–H and O–H bonds too strong to allow participation in radical reactions, are activated towards HAT by complexation with NHCs, boranes, or titanocene(III) complexes. This novel concept has resulted in exciting applications in both radical chain reactions and transition metal mediated and catalyzed transformations.

The use of hydrogen as terminal reductant has been accomplished by its activation with transition metal complexes. The resulting weak M–H bonds can be used in both radical generation and reduction through HAT. In this manner, conceptually novel radical chain reactions, such as hydrogen mediated cyclizations, or metal catalyzed processes with coupled catalytic cycles for radical generation and reduction, have been realized. The latter transformations are especially attractive for enantioselective synthesis.

It is expected that the use of boranes, methanol, water, and hydrogen as terminal HAT reagents will lead to the invention of exciting novel reactions in the near future.

**Acknowledgements** We are grateful for continued financial support by the Deutsche Forschungsgemeinschaft, the Alexander von Humboldt-Stiftung, and the Fonds der Chemischen Industrie. We also thank the Spanish Ministry of Science and Innovation and the Regional Government of Andalusia for projects CTQ2008-06790/BQU and P07-FQM-03213 and aids to the PAI group FQM-339.

## References

1. Gilbert BC, Parsons AF (2002) *J Chem Soc Perkin Trans 2* 367
2. Studer A, Amrein S (2002) *Synthesis* 835
3. Walton JC, Studer A (2005) *Acc Chem Res* 38:794
4. Chatgililoglu C (2008) *Chem Eur J* 14:2310
5. Baguley PA, Walton JC (1998) *Angew Chem Int Ed* 37:3072
6. Ueng SH, Makhlof Brahmi M, Derat É, Fensterbank L, Lacôte E, Malacria M, Curran DP (2008) *J Am Chem Soc* 130:10082
7. Roberts BP (1999) *Chem Soc Rev* 28:25
8. Rablen PR, Hartwig JF (1996) *J Am Chem Soc* 118:4648
9. Ueng SH, Fensterbank L, Lacôte E, Malacria M, Curran DP (2010) *Org Lett* 12:3002
10. Ueng SH, Solovyev A, Yuan X, Geib SJ, Fensterbank L, Lacôte E, Malacria M, Newcomb M, Walton JC, Curran DP (2009) *J Am Chem Soc* 131:12256
11. Solovyev A, Ueng SH, Monot J, Fensterbank L, Malacria M, Lacôte E, Curran DP (2010) *Org Lett* 12:2998
12. Walton JC, Makhlof Brahmi M, Fensterbank L, Lacôte E, Malacria M, Chu Q, Ueng SH, Solovyev A, Curran DP (2010) *J Am Chem Soc* 132:2350
13. Tehfe MA, Makhlof Brahmi M, Fouassier JP, Curran DP, Malacria M, Fensterbank L, Lacôte E, Lalevée J (2010) *Macromolecules* 43:2261
14. Pearson RG (1985) *Chem Rev* 85:41
15. Simões JAM, Beauchamp JL (1990) *Chem Rev* 90:629
16. Eisenberg DC, Norton JR (1991) *Isr J Chem* 31:55
17. Fujita K, Nakamura T, Yorimitsu H, Oshima K (2001) *J Am Chem Soc* 123:3137
18. Roth JA, Orchin M (1979) *J Organomet Chem* 182:299



19. Sweany RL, Comberrel DS, Dombourian MF, Peters NA (1981) *J Organomet Chem* 216:57
20. Ungváry F, Markó L (1982) *Organometallics* 1:1120
21. Roth JA, Wiseman P, Ruzsala L (1983) *J Organomet Chem* 240:271
22. Connolly JW (1984) *Organometallics* 3:1333
23. Garst JF, Bockman TM, Batlaw R (1986) *J Am Chem Soc* 108:1689
24. Thomas MJ, Shackleton TA, Wright SC, Gillis DJ, Colpa JP, Baird MC (1986) *Chem Commun* 312
25. Wassink B, Thomas MJ, Wright SC, Gillis DJ, Baird MC (1987) *J Am Chem Soc* 109:1995
26. Choi J, Tang L, Norton JR (2007) *J Am Chem Soc* 129:234
27. Tang L, Papish ET, Abramo GP, Norton JR, Baik MH, Friesner RA, Rappé A (2003) *J Am Chem Soc* 125:10093
28. Smith DM, Pulling ME, Norton JR (2007) *J Am Chem Soc* 129:770
29. Hartung J, Pulling ME, Smith DM, Yand DX, Norton JR (2008) *Tetrahedron* 64:11822
30. Choi J, Pulling ME, Smith DM, Norton JR (2008) *J Am Chem Soc* 130:4250
31. McGinley CM, Relyea HA, van der Donk WA (2006) *Synlett* 211
32. Shey J, McGinley SJ, McCauley CM, Dearth A, Young B, van der Donk WA (2002) *J Org Chem* 67:837
33. Shaw AP, Ryland BL, Franklin MJ, Norton JR, Chen JYC, Hall ML (2008) *J Org Chem* 73:9668
34. Guan H, Saddoughi SA, Shaw AP, Norton JR (2005) *Organometallics* 24:6358
35. O'Connor JM, Friese SJ (2008) *Organometallics* 27:4280
36. RajanBabu TV, Nugent WA (1994) *J Am Chem Soc* 116:986
37. Gansäuer A, Bluhm H, Pierobon M (1998) *J Am Chem Soc* 120:12849
38. Barrero AF, Rosales A, Cuerva JM, Oltra JE (2003) *Org Lett* 5:1935
39. Cuerva JM, Justicia J, Oller-López JL, Oltra JE (2007) *Top Curr Chem* 264:63
40. Gansäuer A, Justicia J, Fan CA, Worgull D, Piestert F (2007) *Top Curr Chem* 279:25
41. Gansäuer A, Fan CA, Piestert F (2008) *J Am Chem Soc* 130:6916
42. Gansäuer A, Otte M, Piestert F, Fan CA (2009) *Tetrahedron* 65:4984
43. Gansäuer A, Otte M, Shi L (2011) *J Am Chem Soc* 133:417
44. Shi L, Tu YQ, Wang M, Fan CA, Zhao YM, Xia WJ (2005) *J Am Chem Soc* 127:10836
45. Bakac A, Thomas LM (1996) *Inorg Chem* 35:5880
46. Bakac A (1998) *Inorg Chem* 37:3548
47. Cesarotti E, Kagan HB, Goddard R, Krüger C (1978) *J Organomet Chem* 162:297
48. Gansäuer A, Bluhm H, Pierobon M, Keller M (2001) *Organometallics* 20:914
49. Gansäuer A, Bluhm H, Lauterbach T (2001) *Adv Synth Catal* 343:785
50. Gansäuer A, Bluhm H, Rinker B, Narayan S, Schick M, Lauterbach T, Pierobon M (2003) *Chem Eur J* 9:531
51. Gansäuer A, Barchuk A, Keller F, Schmitt M, Grimme S, Gerenkamp M, Mück-Lichtenfeld C, Daasbjerg K, Svith H (2007) *J Am Chem Soc* 129:1359
52. Gansäuer A, Fan CA, Keller F, Keil J (2007) *J Am Chem Soc* 129:3484
53. Gansäuer A, Fan CA, Keller F, Karbaum P (2007) *Chem Eur J* 13:8084
54. Gansäuer A, Shi L, Otte M (2010) *J Am Chem Soc* 132:11858
55. Gansäuer A, Barchuk A, Fielenbach D (2004) *Synthesis* 2567
56. Osborn JA, Jardine FH, Young JF, Wilkinson G (1965) *J Chem Soc A* 1711
57. Vaska L, Diluzio JW (1961) *J Am Chem Soc* 83:2784
58. Vaska L, Diluzio JW (1962) *J Am Chem Soc* 84:679
59. Gansäuer A, Pierobon M, Bluhm H (2002) *Angew Chem Int Ed* 41:3206
60. Gansäuer A, Rinker B, Pierobon M, Grimme S, Gerenkamp M, Mück-Lichtenfeld C (2003) *Angew Chem Int Ed* 42:3687
61. Justicia J, Rosales A, Buñuel E, Oller-López JL, Valdivia M, Haïdour A, Oltra JE, Barrero AF, Cárdenas DJ, Cuerva JM (2004) *Chem Eur J* 10:1778
62. Gansäuer A, Rinker B, Ndene-Schiffer N, Pierobon M, Grimme S, Gerenkamp M, Mück-Lichtenfeld C (2004) *Eur J Org Chem* 2337

63. Gansäuer A, Lauterbach T, Geich-Gimbel D (2004) *Chem Eur J* 10:4983
64. Friedrich J, Dolg M, Gansäuer A, Geich-Gimbel D, Lauterbach T (2005) *J Am Chem Soc* 127:7071
65. Gansäuer A, Franke D, Lauterbach T, Nieger M (2005) *J Am Chem Soc* 127:11622
66. Justicia J, Oller-Lopez JL, Campaña AG, Oltra JE, Cuerva JM, Buñuel E, Cárdenas DJ (2005) *J Am Chem Soc* 127:14911
67. Friedrich J, Walczak K, Dolg M, Piestert F, Lauterbach T, Worgull D, Gansäuer A (2008) *J Am Chem Soc* 130:1788
68. Gansäuer A, Fleckhaus A, Lafont MA, Okkel A, Kotsis K, Anoop A, Neese F (2009) *J Am Chem Soc* 131:16989
69. Gansäuer A, Worgull D, Knebel K, Huth I, Schnakenburg G (2009) *Angew Chem Int Ed* 48:8882
70. Curran DP, Porter NA, Giese B (1976) *Stereochemistry of radical reactions*. VCH, Weinheim, p 4
71. Ruscic B, Wagner AF, Harding LB, Asher RL, Felle D, Dixon DA, Peterson KA, Song Y, Qian X, Ng CY, Liu J, Chen W, Schwenke DW (2002) *J Phys Chem A* 106:2727
72. Barrero AF, Oltra JE, Cuerva JM, Rosales A (2002) *J Org Chem* 67:2566
73. Cuerva JM, Campaña AG, Justicia J, Rosales A, Oller-López JL, Robles R, Cárdenas DJ, Buñuel E, Oltra JE (2006) *Angew Chem Int Ed* 45:5522
74. Paradas M, Campaña AG, Jimenez T, Robles R, Oltra JE, Buñuel E, Justicia J, Cárdenas DJ, Cuerva JM (2010) *J Am Chem Soc* 132:12748
75. RajanBabu TV, Nugent WA, Beattie MS (1990) *J Am Chem Soc* 112:6408
76. Justicia J, Jiménez T, Morcillo SP, Cuerva JM, Oltra JE (2009) *Tetrahedron* 65:10837
77. Pryor WA, Kneipp KG (1971) *J Am Chem Soc* 93:5584
78. Jin J, Newcomb M (2008) *J Org Chem* 73:7901
79. Jiménez T, Campaña AG, Bazdi B, Paradas M, Arráez-Román D, Segura-Carretero A, Fernández-Gutiérrez A, Oltra JE, Robles R, Justicia J, Cuerva JM (2010) *Eur J Org Chem* 4288
80. Barrero AF, Rosales A, Cuerva JM, Gansäuer A, Oltra JE (2003) *Tetrahedron Letters* 44:1079
81. Paradas M, Campaña AG, Marcos ML, Justicia J, Haidour A, Robles R, Cárdenas DJ, Oltra JE, Cuerva JM (2010) *Dalton Trans* 39:8796–8800
82. Paradas M, Campaña AG, Estévez RE, Álvarez de Cienfuegos L, Jiménez T, Robles R, Cuerva JM, Oltra JE (2009) *J Org Chem* 74:3616
83. Campaña AG, Estévez RE, Fuentes N, Robles R, Cuerva JM, Buñuel E, Cárdenas DJ, Oltra JE (2007) *Org Lett* 9:2195
84. Estévez RE, Oller-López JL, Robles R, Melgarejo CR, Gansäuer A, Cuerva JM, Oltra JE (2006) *Org Lett* 8:5433
85. Spiegel DA, Wiberg KB, Schacherer LN, Medeiros MR, Wood JL (2005) *J Am Chem Soc* 127:12513
86. Medeiros MW, Schacherer LN, Spiegel DA, Wood JL (2007) *Org Lett* 9:4427
87. Jin J, Newcomb M (2007) *J Org Chem* 72:5098
88. Pozzi D, Scanlan E, Renaud P (2005) *J Am Chem Soc* 127:14204
89. Jin J, Newcomb M (2008) *J Org Chem* 73:4740
90. Povie G, Villa G, Ford L, Pozzi D, Schiesser CH, Renaud P (2010) *Chem Commun* 46:803

# Radicals in Transition Metal Catalyzed Reactions? Transition Metal Catalyzed Radical Reactions? A Fruitful Interplay Anyway

## Part 1. Radical Catalysis by Group 4 to Group 7 Elements

Ullrich Jahn

**Abstract** This review summarizes the current status of radical-based transition metal catalyzed reactions in organic chemistry. The underlying features of radical generation from transition metal complexes and radical reactivity in the framework of transition metal catalysis are discussed. The available arsenal to detect radicals in transition metal catalyzed transformations is presented. Available strategies to combine radical intermediates with transition metal catalysis are outlined. In the main part the currently known synthetic methodology of transition metal catalyzed reactions proceeding via radical intermediates is discussed. This part covers catalytic radical reactions involving group 4 to group 7 elements.

**Keywords** Addition • Catalysis • Cross-coupling • Cyclization • Electron transfer • Radicals • Transition metals

### Contents

1	Introduction .....	122
2	Basic Principles of Organotransition Metal Chemistry and Radical Reactivity .....	123
	2.1 Oxidative Radical Generation .....	124
	2.2 Reductive Radical Generation .....	125
	2.3 Paramagnetic Metal Complexes: Valence Tautomerism and Persistent Radical Effect .....	127
	2.4 The Radical Reaction Steps .....	127
	2.5 How to Detect Radical Intermediates in Transition Metal-Catalyzed Reactions .	129
	2.6 Why and How Transition Metal-Catalyzed and Radical Reactions Fit Together .	132

---

U. Jahn (✉)

Institute of Organic Chemistry and Biochemistry, Academy of Sciences of the Czech Republic,  
Flemingovo namesti 2, 16610 Prague 6, Czech Republic  
e-mail: [jahn@uochb.cas.cz](mailto:jahn@uochb.cas.cz)

2.7	Methods to Achieve Turnover of the Metal Complex in Chain and Non-Chain Radical Reactions .....	132
2.8	Scope and Limitations of the Review .....	135
3	Titanium-Catalyzed Radical Reactions .....	136
3.1	Low-Valent Titanium-Catalyzed Radical Reactions .....	136
3.2	Ti(II)-Ti(III)-Ti(IV) Catalysis: Radical Additions .....	136
3.3	Ti(III)-Ti(IV) Catalysis .....	143
4	Zirconium Catalysis .....	148
5	Vanadium-, Niobium-, and Tantalum-Catalyzed Radical Reactions .....	150
5.1	Low-Valent Vanadium-Catalyzed Reactions .....	150
5.2	V(III)-V(IV)-V(V) Catalysis: Kumada Coupling .....	151
5.3	V(IV)-V(V) Catalysis .....	152
6	Chromium-Catalyzed Radical Reactions .....	155
6.1	Cr(0)-Cr(I)-Catalyzed Radical Additions .....	155
6.2	Cr(I)-Cr(II)-Catalyzed Radical Cyclizations .....	156
6.3	Cr(II)-Cr(III)-Catalyzed Radical Cyclizations .....	157
7	Molybdenum-Catalyzed Radical Reactions .....	158
8	Tungsten-Catalyzed Radical Reactions .....	161
9	Manganese-Catalyzed Radical Reactions .....	164
9.1	Mn(-I)-Mn(0)-Mn(I) and Mn(0)-Mn(I) Catalysis .....	164
9.2	Mn(0)-Mn(I)-Mn(II) Catalysis .....	166
9.3	Mn(II)-Mn(III) Catalysis: Radical Additions .....	168
9.4	Mn(II)-Mn(III) Catalysis: Radical Cyclizations .....	172
9.5	Mn(II)-Mn(III)-(Mn(IV)) Catalysis: Hydrofunctionalization of Alkenes .....	174
10	Rhenium-Catalyzed Radical Reactions .....	178
11	Transition Metal-Catalyzed Radical Reactions According to Reaction Type .....	179
	References .....	183

## 1 Introduction

Unraveling the fundamental reactivity patterns of organotransition metal chemistry and radical chemistry is an ongoing process that has increased its pace steadily starting from the beginning of the twentieth century when both types of intermediates were discovered. Especially the 1960s and 1970s saw an explosive growth of the investigation of organometallic reaction behavior and the establishment of a consistent mechanistic picture of organotransition metal reactivity. From those fundamental studies a number of useful organic transformations emerged that today bear the names of their discoverers, such as the Mirozoki–Heck reaction, the Kumada–Corriu, Suzuki–Miyaura, Stille, and Negishi cross-coupling reactions to name just a few. Since then an explosive growth of transition metal-catalyzed transformations set in (selected books and reviews [1–18]).

At the same time radical chemistry experienced a similar development. Except for extensive application in polymer chemistry, radical reactions were not considered generally useful synthetically. However, in these years fundamental studies in physical organic chemistry led to the establishment of a consistent picture of radical reaction kinetics, which triggered an explosion of synthetic applications in the 1980s (selected books and reviews [19–30]). Thanks to the ground-breaking studies by Kochi and others, the importance of transition metal chemistry for

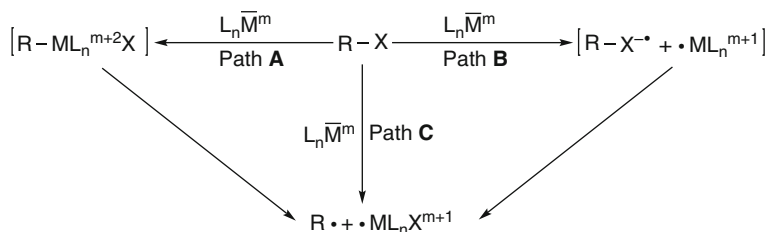
radical chemistry and vice versa was uncovered (selected reviews [31–36], For a summary of early transition metal-promoted radical processes see [37]). It was found that single electron transfer (SET) is an extremely important process in organotransition metal catalysis and in free radical chemistry; however, the close relationship of transition metal catalysis and radical chemistry was neglected later on and was only recently appreciated again.

## 2 Basic Principles of Organotransition Metal Chemistry and Radical Reactivity

Generally transition metal compounds may act differently according to their electronic properties with neutral or charged organic substrates (Fig. 1). One of the general reaction pathways is two-electron transfer (Path A). Overall the oxidation state of the metal changes by two and the result of this process is the formation of an organometallic species with a stable metal-carbon bond. This pathway is well documented in the literature and a large number of transition metal-catalyzed reactions occur by this process [38]. When the resulting metal-carbon bond is weak, homolysis may subsequently take place and release a radical.

A second basic interaction pathway between transition metal complexes and organic substrates is SET (Path B). The overall processes can involve one individual or several sequential SET steps. For the latter, timing and direction of SET steps determine the reaction outcome significantly. The catalyzed reaction can proceed either as redox-neutral processes, in which oxidative and reductive SET steps are involved in the catalytic cycle, or as overall oxidative or reductive catalytic reactions, where two oxidative or reductive SET steps occur consecutively in the catalytic cycle. The third pathway (Path C) consists of a direct atom or group abstraction by the metal complex, which is possible for a weak R–X bond.

The potential of a metal or complexes thereof for SET can be derived very roughly by assessing its first ionization potential or its electron affinity. In general 3d metals display a lower first ionization potential than 4d or 5d metals. Consequently, 3d metals are more active in donating single electrons to organic substrates than 4d or 5d metals. The same holds in general for low-valent metal complexes. Thus single electron donation competes successfully with two-electron oxidative addition in 3d metal complexes but less in 4d and 5d metal complexes. Therefore,



**Fig. 1** Metal-mediated activation of organic molecules

a multitude of reductive and electroneutral catalytic processes of 3d metal complexes involving SET are known, while two-electron pathways seem to be more common for 4d and 5d metal complexes. High-valent metal complexes, on the other hand, are better stabilized in higher oxidation states for 4d and 5d metal ions or complexes and are thus often better and more selective oxidants. Predictive trends are, however, more difficult, since the accessibility of higher oxidation states varies strongly in a group. It must be emphasized that ligands profoundly influence the character of active metal centers so that the rationalization and comparison of experimental results must be performed at this stage with great care.

## 2.1 Oxidative Radical Generation

High-valent oxo-complexes, isolated or in situ-generated, interact most often with electron-rich  $\pi$ -systems **1** or suitable C–H bonds with low bond dissociation energy (BDE) in substrates **3** (Fig. 2). These reactions may occur concerted via transition states **1A** or **3A** leading to epoxides **2** or alcohols **4**. On the other hand, a number of epoxidation reactions, such as the Jacobsen–Katsuki epoxidation, is known to proceed by a stepwise pathway via transition state **1B** to radical intermediate **1C** [39]. Similarly, hydrocarbon oxidation to **4** can proceed by a hydrogen abstraction/ $S_H2$

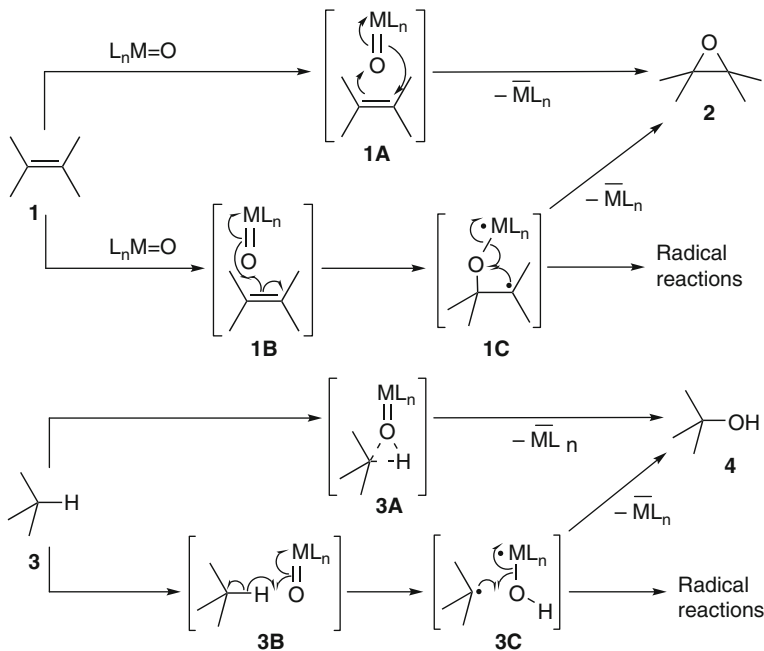
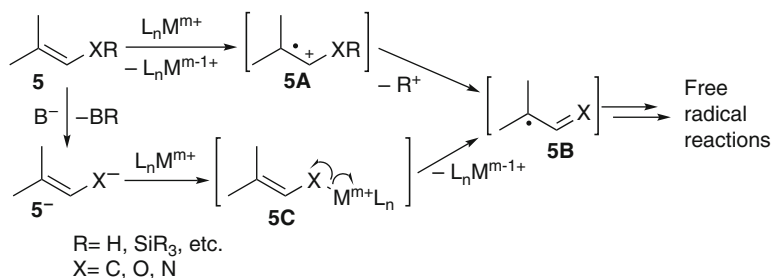


Fig. 2 Radical intermediates generated by metal oxo complexes



**Fig. 3** Oxidative radical generation by high-valent transition metal salts

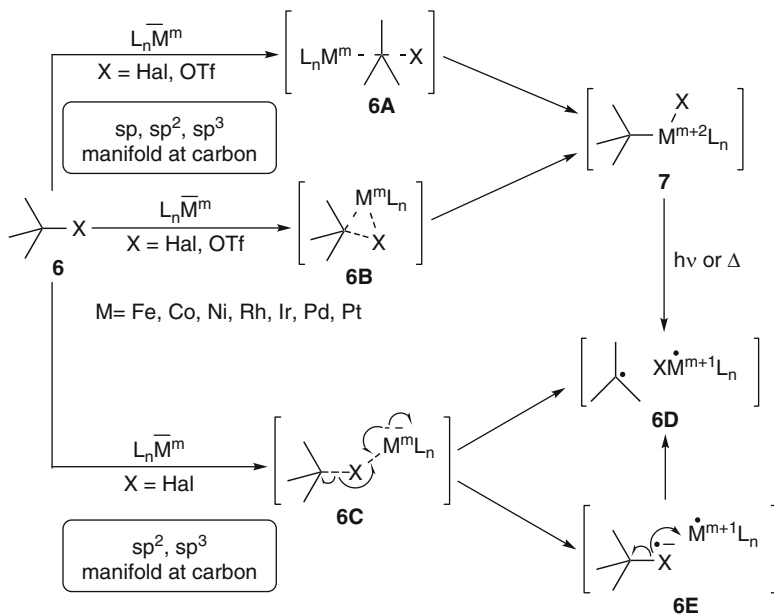
pathway via **3B** and **3C**. This mechanism is often discussed in enzyme-catalyzed oxidations, such as those induced by cytochrome P450 (selected reviews [40, 41]).

Other metal compounds of higher oxidation states, such as simple salts or complexes of manganese(III), iron(III), copper(II), or silver(I) act as SET oxidants for functional groups, electron-rich  $\pi$ -systems **5**, or anions **5<sup>-</sup>** derived thereof (Fig. 3). Initially radical cations **5A** and subsequently radicals **5B** are generated. Anionic species **5<sup>-</sup>** react mostly by transmetalation to transient metal enolate **5C** which homolyzes to radical **5B**. The reduced form of the oxidant often does not participate in the further course and free radical reactivity is observed. However, great care must be taken in assigning reactivity patterns, since especially 3d transition metal salts are not only potent oxidants but also good Lewis acids promoting two-electron processes.

## 2.2 Reductive Radical Generation

Transition metal compounds of low oxidation states can interact in several ways with organic substrates **6** triggering overall stoichiometric or catalytic reductive or electroneutral transformations dependent on the reduction capacity of the metal (Fig. 4). Low-valent metal complexes that are able to undergo two-electron oxidations react with halides or sulfonates **6** to organometallic intermediates **7**. Its formation can occur by an  $S_N2$  process (back side attack) at carbon via **6A** manifesting itself by inversion of configuration with chiral substrates ([42] and cited ref, [43, 44]). For the majority of substrates with  $sp$ - or  $sp^2$ -carbon–element bonds the formation of **7** proceeds through oxidative addition into the carbon–element bond via **6B** [38]. Retention of configuration is observed with chiral substrates. Some organometallic compounds **7** homolyze with ease to generate a radical pair **6D** initially, which can lead to freely diffusing radicals after cage escape.

Metal salts and complexes of Ti(II,III), Cr(0 to II), Mn(0 to II), Fe(–II to II), Co(0,I), Ni(0,I), Cu(I), Ru(II), Rh(I), Pd(0), Ag(0), or Pt(0) can donate a single electron to organic substrates. Thus, they are able to activate good electron acceptors, such as alkyl halides **6**, but also carbonyl compounds, epoxides, or



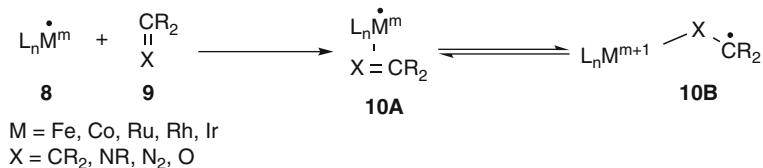
**Fig. 4** Interaction of low-valent metal complexes with organic substrates

peroxides (Fenton reaction) reductively. These radicals often do not couple particularly fast with the oxidized metal species and free radical reactions can be performed subsequently.

Especially for alkyl halides **6** the transfer of a single electron from the metal center is facile and occurs at the halide via transition state **6C**, which stabilizes either by direct abstraction of the halide to a carbon-metal complex radical pair **6D** or via a distinct radical anion-metal complex pair **6E**. This process was noted early but not exploited until recently (review [45]). Alkyl tosylates or triflates are not easily reduced by SET, and thus  $S_N2$  and/or oxidative addition pathways are common. The generation of  $\sigma$ -radicals from aryl and vinyl halides has been observed, but is rarer due to the energy requirement for their generation. Normally, two-electron oxidative addition prevails.

In reductive transition metal-catalyzed radical reactions, information about the actual oxidation state of the involved metal center in the studied reaction is of great importance. The transition metal catalyst added to the reaction mixture often serves only as a precatalyst. It is initially activated by transmetalation and/or ate complex formation by an organometallic reagent. Transmetalation is very often followed by reductive elimination from a diorganometal intermediate resulting in homocoupling products of the organometallic component. Thus, noticeable amounts of homocoupling products serve as an indication that the organometallic reagent reduces the precatalyst to a low-valent species. It may be considered as evidence for no change of the oxidation state of the catalyst, when homocoupling products are not





**Fig. 5** Generation of valence tautomeric ligand-centered radicals from paramagnetic transition metal complexes

detectable. A stoichiometric probe experiment is a valuable test. Ate complex formation can be detected similarly by simple stoichiometric experiments varying the concentration and detecting at what concentration of the organometallic reagent the desired reaction sets in.

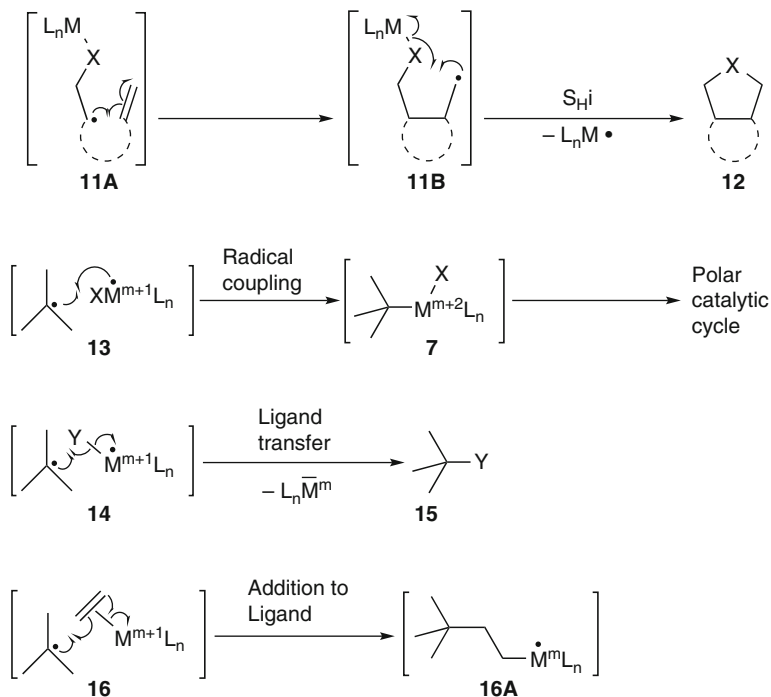
### 2.3 Paramagnetic Metal Complexes: Valence Tautomerism and Persistent Radical Effect

Paramagnetic metal complexes **8** can transfer electrons not only to substrates but also to their ligands **9** after coordination (Fig. 5). This generates valence tautomeric metal complex pairs **10A/10B**, in which the metal as well as the ligand can carry the spin (reviews [46–48]; see also [49–51]). These species are not resonance hybrids but equilibrium structures, since they differ in their  $\sigma$ -bond framework and thus their physical properties. This principle can also be used in catalysis. Such non-redox-innocent ligands **9** can be alkenes, imines, carbonyl groups, differently substituted arenes, or diazo compounds. The ligand-centered radical **10B** so generated can in turn initiate further radical reactions. This chemistry is so far not widely applied, but it offers an interesting potential for the design of new synthetic methodology.

Another basic feature of paramagnetic transition metal complexes is that the persistent radical effect operates with them (reviews [52, 53]). Since most organic radicals have a much shorter lifetime than paramagnetic transition metal complexes even in unusual oxidation states, even a small concentration difference between them will favor cross-coupling of the transient organic radical with the – in comparison to it, persistent – paramagnetic transition metal complex. Such a homolysis-cross-coupling equilibrium in organotransition metal compounds effectively extends the lifetime of radicals that may result from them in catalysis.

### 2.4 The Radical Reaction Steps

What follows after radical generation depends very much on the electronic properties of the metal complex mentioned above and the radicals. Moreover, it is important whether the generated radicals are directly bound to the metal center,



**Fig. 6** Radical reaction steps in the coordination sphere of a metal complex

remain in its vicinity, or are freely diffusing. All typical elementary radical steps, such as abstraction, coupling, substitution, addition, or rearrangement reactions [19–30], were observed when freely diffusing radicals were generated. In a number of transition metal-catalyzed radical reactions, radical generation goes along with covalent bond formation of the metal center to the organic substrate (Fig. 6). Thus, radical and metal fragment remain connected in a subsequent reaction, such as that shown for the transformation of **11A** to **12** via **11B**. The catalyst can be liberated by an  $S_{Hi}$  reaction in such a case.

Often the radicals remain in the vicinity of the cogenerated paramagnetic metal complex (**13**). Such a caged situation often leads to direct coupling of the radical with the metal generating a  $\sigma$ -bond organometallic complex **7** of the next higher oxidation state, resulting in a net two-electron oxidation of the metal center, giving the same result as an oxidative addition (see Fig. 4). Thus generated **7** continues in a conventional two-electron catalytic cycle. The relative rates of coupling of **13** to **7** vs radical-molecule reaction steps determine the product distribution strongly; fast enough radical processes will proceed prior to coupling. The kinetics of radical reactions with some coordinatively unsaturated transition metal complexes were determined (reviews [31, 54, 55]).

Radicals in the vicinity of the metal complex can not only couple to it but also attack its ligands [56]. Two pathways are possible. Oxidized transition metal

complexes **14** bearing simple donor ligands, such as halides, transfer the halide to the radical generating a neutral organic molecule **15** and a reduced transition metal complex. This process, called ligand transfer, is typical for metal complexes that have the most stable oxidation state separated by one, but for whom two sequential electron transfers do not lead to a favorable oxidation state (Fe(II/III), Cu(I/II), Ru(II/III) halide complexes). This has been known in organic chemistry since the discovery of the metal-catalyzed Kharasch addition ([57, 58], review [59]) (nowadays more generally called atom transfer radical addition – ATRA) [60, 61]. Applications of this reactivity principle are the even industrially important atom transfer radical polymerization (ATRP) [62–64] and the transition metal-catalyzed radical polymerization (selected books and reviews [62–67]).

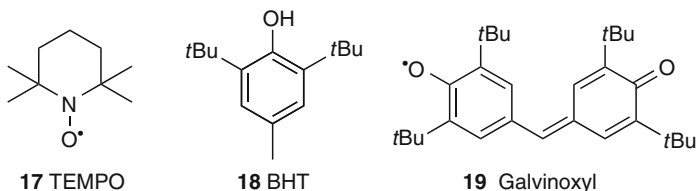
On the other hand, radicals may also attack  $\pi$ -bonded ligands of **16** by addition reactions leading to metal complex **16A**. Investigations of radical reactions with (allyl)palladium complexes showed that radicals couple faster to the metal center if it is coordinatively unsaturated than they add to the ligand [68–70]. Additions to alkene and arene ligands resulting in  $\pi$ - or  $\sigma$ -bound complexes may, however, be possible for coordinatively saturated complexes [68]. According to theoretical investigations, radical additions to bound alkenes [71] and CO [72] are feasible.

## 2.5 *How to Detect Radical Intermediates in Transition Metal-Catalyzed Reactions*

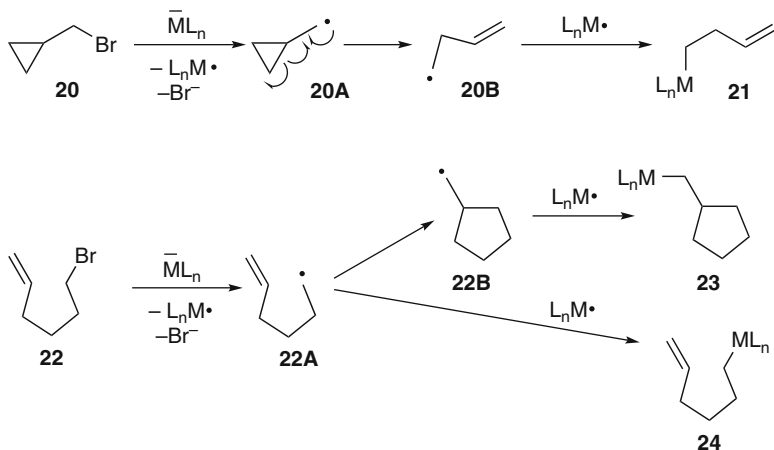
The mechanistic basis to radical reactivity of organotransition metal compounds is still not very well developed. Mechanisms very often remain speculative, since the information about involved intermediates is scarce. Mechanistic information can be gathered by using physical methods, such as ESR spectroscopy. Changes in the oxidation state of metal complexes indicating SET, paramagnetic metal centers or the radicals themselves, provided their lifetime allows it, can be detected (selected reviews [73–75]). CIDNP measurements can also provide valuable information, but were rarely used in the past [76–78].

Most common for the synthetic practitioner are inhibition studies or probe reactions making use of typical competitive radical reactions with known rate constants. Stereochemical probe studies pointing to the involvement of planar radical intermediates are also valuable. An approximate lifetime of radicals can in principal be estimated from such reactions.

Inhibition by radical traps, such as TEMPO **17**, was used to explain the involvement of radicals in the course of transition metal-catalyzed reactions (Fig. 7). Typical cross-coupling reactions, such as Heck or Suzuki–Miyaura reactions, proceeded even with nitroxyls as substrates, although the yields were sometimes low. Thus, nitroxyls do not necessarily interfere very much with the course of two-electron catalytic processes [79–81]. However, it must be critically mentioned that **17** and related nitroxides are both oxidants and reductants for metal species.



**Fig. 7** Typical radical inhibitors



**Fig. 8** Typical kinetic probe reactions indicating the occurrence of radical processes

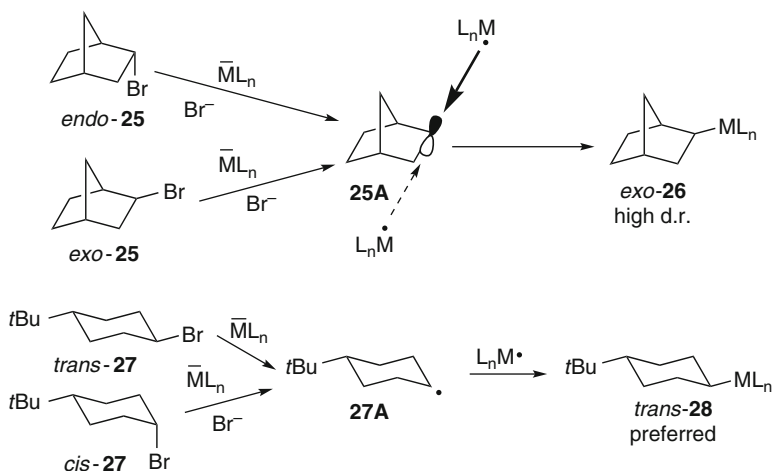
Thus, **17** may sometimes rather switch the oxidation state of the metal and change reactivity patterns. Both inhibition and activation [82] of reactions or even C–C bond cleavage [83] were observed; however, trapping of radicals does not necessarily occur. In fact, **17** was recently used to close the catalytic cycles of Rh- or Pd-catalyzed coupling reactions by reoxidation of the final low-valent rhodium or palladium complexes [84–87]. It was recently demonstrated that **17** abstracts hydrogen from palladium(II) hydride complexes, abolishing their reactivity by reduction and thus pretending inhibition. Isolated bulky alkyl or arylpalladium(II) complexes, however, remain intact in the presence of **17** under ordinary conditions [88]. Aryloxy-based inhibitors such as BHT **18** or galvinoxyl **19** can also be applied to obtain information about the involvement of radical intermediates in the studied reaction. Especially the former often display a strongly retarding effect, but undesired reactions with palladium complexes were also observed [88]. Nitroarenes also display strongly retarding effects [89, 90].

A significantly more important tool to decipher the reaction mechanism is probe reactions (Fig. 8). Most commonly used are cyclopropylcarbiny radical ring opening reactions and radical 5-*exo* cyclizations to intercept coupling reactions with metal centers. Cyclopropylmethyl bromide **20** is reduced by a metal complex and generates cyclopropylcarbiny radical **20A**. Unimolecular ring opening to

3-butenyl radical **20B** occurs with a rate constant of  $10^7$ – $10^9$  s<sup>-1</sup> [19, 23, 91]. Radical **20B** couples subsequently with the oxidized metal complex to a 3-butenylmetal complex **21**, which continues the catalytic cycle. If ambiguities remain more sensitive cyclopropanes can be applied [92]. The failure to detect ring-opened products was taken as evidence for a two-electron reaction mechanism [93–95]. Since some late transition metal complexes are known to insert directly into cyclopropanes according to a two-electron pathway, the regioselectivity of 2-arylcyclopropylmethyl bromide may be taken as a guideline [96]. Direct oxidative insertions proceed preferentially, if not exclusively, at the least hindered C–C bond (review [97], [98–100]), but the radical opens toward the most stable (=substituted) radical. Thus oxidative additions lead to branched dienes after  $\beta$ -hydride elimination, while radical opening forms the benzylic radical giving linear dienes.

5-Hexenyl bromide **22** can be activated similarly to 5-hexenyl radical **22A**, which cyclizes to cyclopentylmethyl radical **22B** with a rate constant of  $2.3 \times 10^5$  s<sup>-1</sup> [91]. For this slower reaction, a competition between direct trapping of **22A** to **24** and 5-*exo* cyclization to **22B** followed by coupling to **23** is often found. These unimolecular reaction steps are in comparison to bimolecular transition metal-centered transformations faster or at least as fast.

Another important factor to deduce the involvement of radicals in a transition metal-catalyzed process is the integrity of stereocenters. In oxidative addition or S<sub>N</sub>2-type processes the stereochemical information – retention or inversion, respectively – is preserved for optically active substrates like *sec*-butyl bromide (Sect. 2.2), while racemic products are observed when radical intermediates are generated. On the other hand, stereochemical convergence is observed for strongly biased diastereomeric substrates, such as *exo*- and *endo*-norbornyl substrates **25** (Fig. 9). The reactions occur almost exclusively at the *exo*-face of the norbornyl



**Fig. 9** Product convergence from diastereomeric substrates **25** or **27** due to radical intermediates

radical **25A** giving *exo*-**26**. 4-*tert*-Butylcyclohexyl halides **27** can also be used although the preference for the formation of *trans*-**28** is sometimes not as pronounced. The similarity of the stereochemical outcome of a transition metal-catalyzed and a traditional radical process often provides a hint to the involvement of the same intermediates in both processes.

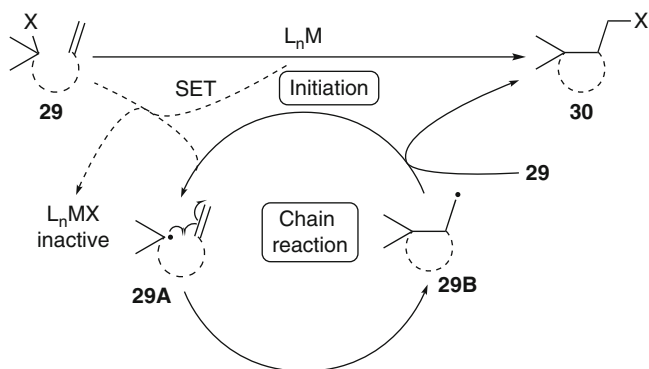
## 2.6 *Why and How Transition Metal-Catalyzed and Radical Reactions Fit Together*

Radical intermediates and transition metal-catalyzed reactions are in principle ideally suited to be linked together. A prerequisite to perform successful radical reactions is that the concentration of radicals has to be kept low to promote the desired reaction and to avoid competing homocoupling and disproportionation, which occur often diffusion-controlled. Including radical intermediates in the regime of a transition metal catalyzed process is thus ideal to keep their concentrations low, since their maximum concentration cannot exceed that of the metal catalyst. On the other hand, radicals are much more reactive than closed-shell organotransition metal intermediates. Thus, the involvement of radicals in transition metal catalysis often leads to a strong acceleration of the reactions compared to a process where only closed-shell intermediates are involved [101].

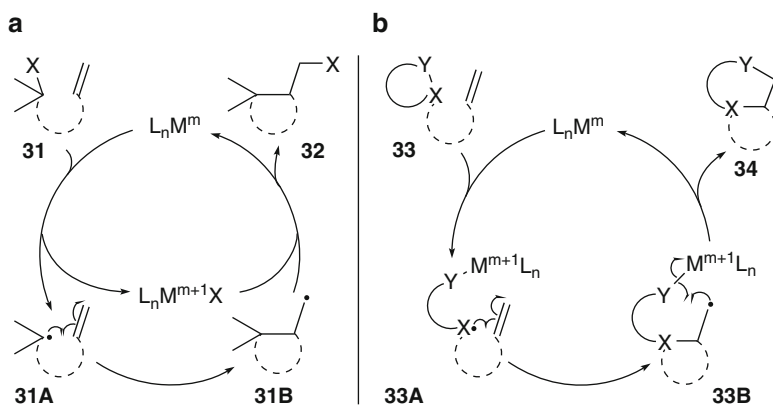
## 2.7 *Methods to Achieve Turnover of the Metal Complex in Chain and Non-Chain Radical Reactions*

To achieve low radical concentrations, most radical reactions are traditionally performed as chain reactions. Atom or group transfer reactions are one of the two basic chain modes. In this process the atom or group X is the chain carrier. A metal complex can promote such chain reactions in two ways. On one hand, the catalyst acts only to initiate the chain process by generating the initial radical **29A** from substrate **29** (Fig. 10). This intermediate undergoes the typical radical reactions, such as additions or cyclizations leading to radical **29B**, which stabilizes to product **30** by abstracting the group X from **29**. A typical example is the use of catalytic amounts of cobalt(II) salts in oxidative radical reactions catalyzed by *N*-hydroxyphthalimide (NHPI), which is the chain carrier [102].

In the other chain reaction mode the redox state of the transition metal changes reversibly by one in the course of the reaction (Fig. 11). Such redox chain reactions are mostly electroneutral and the SET active metal complex acts as the chain carrier. Two modes are generally observed, which are different according to the location of the radical and the release of the catalytically active species after the radical process. Catalysis may occur by SET to a suitable substrate **31**, from which



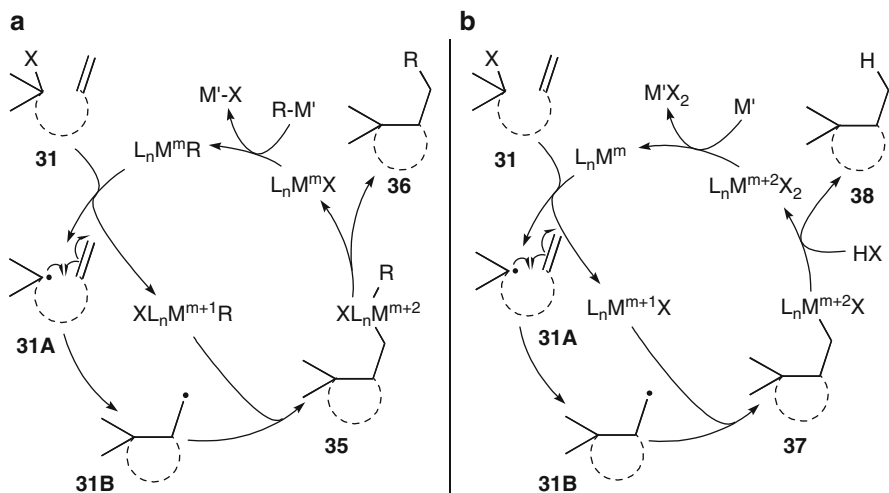
**Fig. 10** Transition metal catalysts as initiators in atom or group transfer reactions.



**Fig. 11** Transition metal catalyzed in radical reactions based on the involved electron transfer steps. **(a)** Redox chain reactions by metal-catalyzed single electron transfer. **(b)** Coordinative radical reactions by metal-catalyzed single electron transfer

a radical **31A** and an oxidized (or reduced – not shown) metal complex is released (Fig. 11a). A radical reaction ensues and the product radical **31B** stabilizes by ligand transfer from the oxidized (or reduced) metal species, regenerating the catalyst in another SET event.

On the other hand, it was shown more recently that radicals could be generated from suitable substrates **33** in the coordination sphere of a SET active metal complex. The metal changes its oxidation state in this process by one (Fig. 11b). In such a coordinative chain reaction, the coordinated radical **33A** is subject to the subsequent process. The product **34** is in this case released from radical **33B** by a homolytic substitution reaction ( $S_{Hi}$ ) with respect to the coordinated atom or group and by SET at the metal.



**Fig. 12** Non-chain transition metal-catalyzed radical reactions with internal or external catalyst regeneration (For **b** an analogous oxidative process is possible – not shown). **(a)** Metal-catalyzed non-chain radical reactions by single- and two-electron transfers. **(b)** Metal-catalyzed radical reactions using a sacrificial reducing agent

Many radical reactions are also conducted as non-chain reactions. Transition metal catalysis is very useful when the catalyst can be regenerated by a two-electron reduction (or oxidation – not shown) in the catalytic cycle (Fig. 12). The active catalyst can reform in one mode by self-regeneration (Fig. 12a). Here, the catalytic reaction is initiated by SET to **31** as before leading to radical **31A**. After the radical reaction the resulting organic radical **31B** stabilizes by coupling to the oxidized metal complex generating an organometallic species **35**. This complex releases the product **36** and regenerates the active catalyst by a two-electron transfer process, such as reductive elimination.  $\beta$ -Hydride elimination followed by reductive elimination is also often observed as a pathway to catalyst regeneration.

Metal salts or complexes able to mediate SET, but not easily amenable to catalyst regeneration by two-electron transfer by reductive or  $\beta$ -hydride elimination, are frequently applied as stoichiometric promoters of non-chain radical reactions. Typical reductive mediators are  $SmI_2$  or  $[Cp_2TiCl]_2$ . In such processes stable organometallic species result in the final step, which release the product by hydrolysis. Such stoichiometric reactions can be transformed to one being catalytic in the mediator by applying a cheap sacrificial redox reagent (Fig. 12b). Similar to the processes shown before, radical **31A** is generated reductively from substrate **31** by applying catalytic amounts of a transition metal complex  $ML_n$ . The oxidized form of the mediator couples in the further process with the final radical **31B**, resulting in organometallic species **37**. The product **38** has subsequently to be liberated by protonation or reaction with other electrophiles, which cofirms an oxidized metal complex. Reduction by a sacrificial reducing agent  $M'$  regenerates the catalyst and allows turnover.



For metal complexes, which promote only the initial SET process  $31 \rightarrow 31A$ , but do not couple efficiently subsequently, stabilization of the final radical often occurs by hydrogen transfer from the reaction medium. In such reactions the catalyst can be regenerated similarly. Using this principle, many transition metal complexes become efficient catalysts for radical reactions. Similar oxidative processes using a catalytic SET oxidant, such as Fe(III) or Mn(III) in combination with a cheap sacrificial oxidant, are also attractive, but less developed. Electrochemical catalyst regeneration may serve well for this purpose.

## 2.8 *Scope and Limitations of the Review*

In this review, reactions involving radical intermediates, which are catalyzed by transition metal complexes, are covered. C–C bond formation reactions are the focus, but reactions in which more than one carbon-heteroatom bond is formed or cleaved are also treated. Stoichiometric transformations are mentioned only as they contribute to enhance the mechanistic understanding. Early catalytic examples, where a mechanism was not discussed or discussed differently, but which fit to the reactivity patterns of the treated topic, are mentioned in the individual sections. Reductive or oxidative homocouplings, such as pinacol couplings or oxidative dimerizations, are only mentioned. Simple oxidations involving radicals, such as Kharasch–Sosnovsky reactions (allylic oxidations) (reviews [103–106]), epoxidations, such as the Jacobsen–Katsuki epoxidation, (reviews [39], [107–109]), as well as functional group interconversions or reduction reactions of functional groups or alkenes are not covered in this review. One-pot sequential processes, in which a radical reaction follows a transition metal-catalyzed reaction or vice versa and in which radical and transition metal intermediates are separated by a neutral organic (in principle isolable) species, are not included to avoid confusion. Reactions involving radicals, which are generated between two directly following sequential SET steps resulting in overall two-electron oxidations or reductions, or reactions, in which an abstraction reaction generates a radical, which is transformed immediately by SET oxidation to carbocations, iminium or oxycarbenium ions or by SET reduction to organometallics, are not covered, since the radical does not play a significant role in the reaction course. Such reactions include cross-dehydrogenative couplings pioneered by Li (reviews [110–113]) and some other recent examples [114–118]. Traditional radical reactions catalyzed by transition metal Lewis acids are not treated, since the metal does not participate actively in the reaction course except for modulating the electronic properties of the involved radicals by coordination, thus constraining the transition states with the aim of enforcing stereoselection ([24], selected recent reviews [119–122]).

The organization of the review follows the simple scheme that the metals in a group of the periodic table are treated together. A further classification is made by the oxidation states of the involved catalytic species starting with the lowest. The reactions are then further divided by the involved radical reaction types.

This principle links the typical organometallic oxidation state-based view of transition metal catalysis reactions best with the radical reaction manifold. At the end a table that links the typical radical reaction types to the different metals catalyzing them is provided. Throughout the review, series of stable organic compounds or transition metal complexes are numbered by arabic numerals and small letters, while reactive intermediates or transition states are designated by arabic numerals followed by capital letters.

### 3 Titanium-Catalyzed Radical Reactions

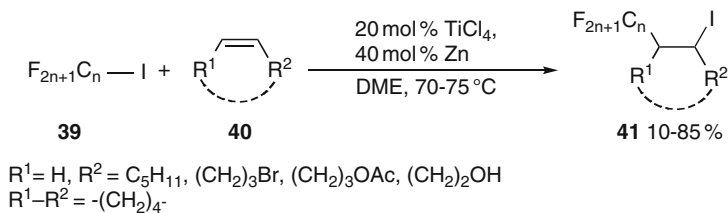
Titanium compounds are used very frequently in organic synthesis, however, often stoichiometrically [8].  $[\text{Cp}_2\text{TiCl}]_2$  is the most frequently applied titanium reagent to mediate radical reactions (reviews [123, 124]). Radicals are also often invoked in McMurry couplings mediated by low-valent titanium species (reviews [125–127]) and in the related pinacol coupling (reviews [128–130]).

#### 3.1 Low-Valent Titanium-Catalyzed Radical Reactions

Fürstner reported the first McMurry-type reactions working with 5–10 mol% of titanium trichloride and stoichiometric amounts of zinc powder in the presence of chlorotrimethylsilane. The amount of  $\text{TiCl}_3$  could be reduced to 2 mol% when  $(\text{ClMe}_2\text{SiCH}_2)_2$  was used as a reagent [125, 131]. At the same time, Burton and coworkers reported atom transfer radical additions of perfluoroalkyl iodides **39** to alkenes **40** catalyzed by 20 mol% of a low-valent titanium compound generated from  $\text{TiCl}_4$  and zinc powder affording **41** in 10–85% yield (Fig. 13). A tandem radical addition/5-*exo* cyclization/iodine transfer reaction with diallyl ether proceeded in 66% yield [132].

#### 3.2 Ti(II)-Ti(III)-Ti(IV) Catalysis: Radical Additions

Buchwald and coworkers studied  $\text{Cp}_2\text{Ti}$  complexes and developed a titanium(II)-catalyzed Pauson–Khand-type reaction (Fig. 14) [133]. When a number of *ortho*-allylacetophenones **42** was subjected to 5–20 mol% of  $\text{Cp}_2\text{Ti}(\text{PMe}_3)_2$  in the



**Fig. 13** Low-valent titanium-catalyzed atom transfer radical additions

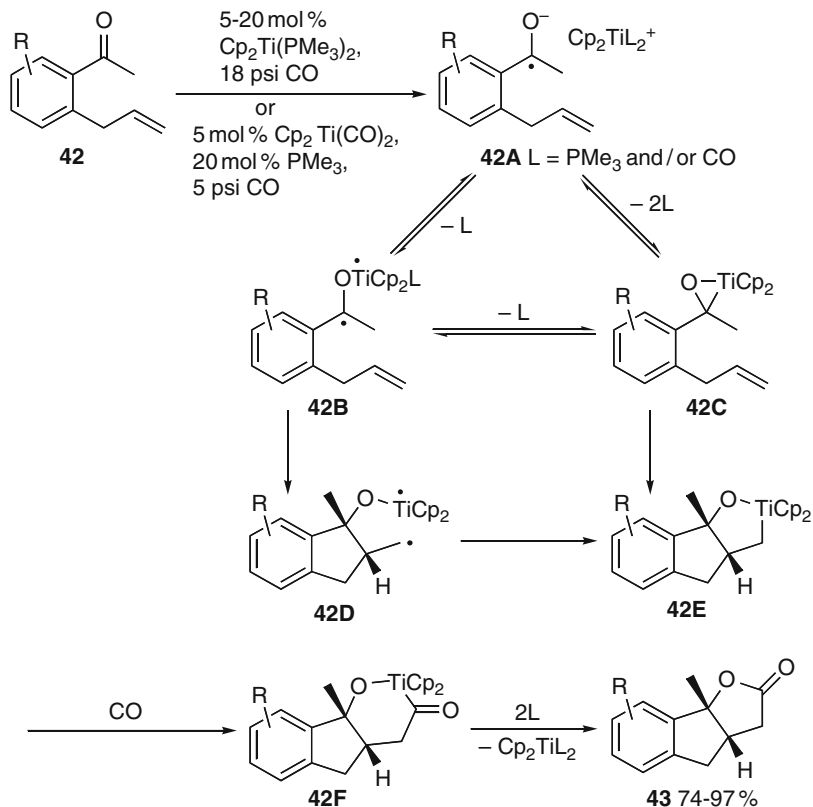
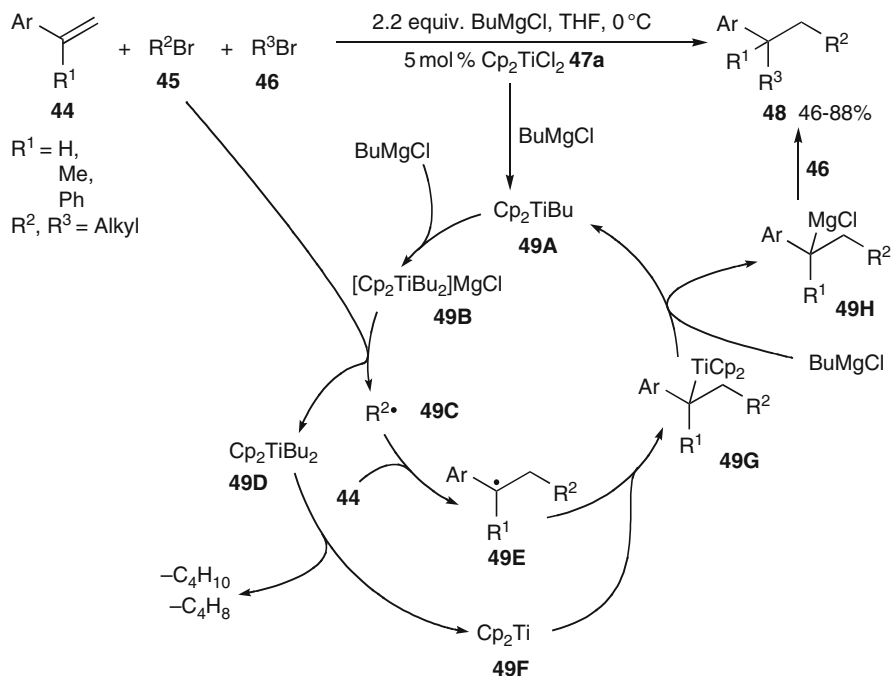


Fig. 14 Titanium-catalyzed Pauson–Khand-type reactions

presence of carbon monoxide annulated butyrolactones **43** were isolated in 74–97% yield. The involvement of radicals seems to be likely. The active catalyst is probably a titanium(II) complex with both CO and  $\text{PMe}_3$  ligands and reaction is thought to proceed by SET reduction of the carbonyl function to a ketyl radical anion- $\text{Cp}_2\text{Ti}(\text{III})$  complex **42B**. From this intermediate or the corresponding oxatitanacyclopentane **42C** a 5-*exo* cyclization and coupling proceeds to oxatitanacyclopentanes **42E**. CO insertion generates **42F**, from which reductive elimination provided products **43**. Aliphatic systems react in contrast most likely according to a two-electron mechanism.

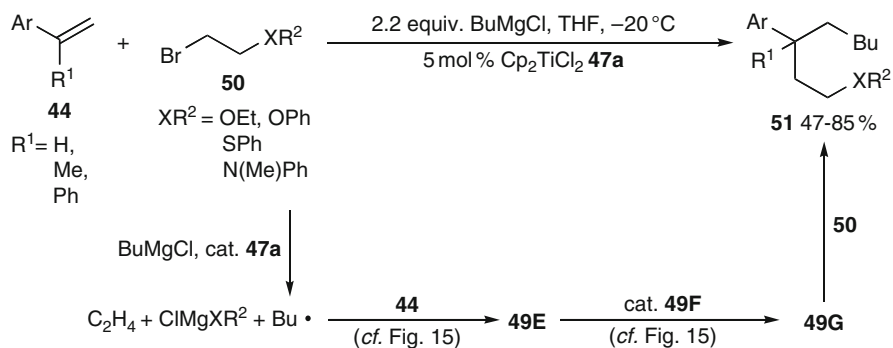
Shortly after, Terao and coworkers started a program to develop titanium catalyzed coupling reactions of Grignard reagents with olefins [134]. Initially an efficient dialkylation protocol of arylalkenes **44** with structurally different alkyl halides **45** and **46** was disclosed, which gave branched arylalkanes **48** catalyzed by 5 mol% of  $\text{Cp}_2\text{TiCl}_2$  **47a** in the presence of butylmagnesium chloride (Fig. 15) [135]. The SET active species was suggested later to be the Ti(III)-ate complex  $\text{Cp}_2\text{TiBu}_2^-$  **49B** formed from  $\text{Cp}_2\text{TiCl}_2$  and excess butyl Grignard reagent via



**Fig. 15** Titanium-catalyzed dialkylation of styrenes

$\text{Cp}_2\text{TiBu}$  **49A** [136]. Electron-rich **49B** reduces the alkyl bromide **45** in the first step of the reaction to an alkyl radical **49C**, which adds to the styrene **44**. The resulting benzylic radical **49E** couples in turn to coformed  $\text{Cp}_2\text{Ti(II)}$  **49F** resulting from fragmentation of unstable dibutyltitanocene(IV) **49D**. Thus generated benzylic Ti(III) species **49G** transmetalates with the butyl Grignard reagent being present in excess releasing butyltitanocene(III) **49A**, which reenters the catalytic cycle by addition of the Grignard reagent. The benzylic Grignard intermediate **49H** is alkylated by the second alkyl bromide **46**. Two different alkyl bromides can be applied. The more easily reducible **45** adds as the radical to **44**, while the less reducible alkyl bromide **46** alkylates the Grignard reagent. The involvement of radicals in the reaction course is supported by the use of the isomeric norbornyl bromides **25**, which affords the *exo*-alkylated product **26** (cf. Fig. 9). More rigorous support for the mechanism was provided by the reaction with cyclopropylmethyl bromide **20** (cf. Fig. 8), which occurred with ring opening in the first alkylation step, but without for the second alkylation step, indicating subsequent radical and polar alkylation steps, respectively. A double silylation under very similar conditions was also reported, but no mechanistic evidence was provided [137].

Similar conditions were also applied with the aim to couple styrenes **44** with 2-bromoalkyl ethers or 2-bromoalkyl amines **50** and Grignard reagents (Fig. 16) [138]. In contrast to alkyl halides bearing donor functionalities more remote from



**Fig. 16** Dialkylation of styrenes **44** by incorporation of the alkyl group of the Grignard reagent

the bromide, which reacted as other alkyl bromides **45** according to Fig. 15, substrates **50** provided products **51**, in which the alkyl group present in the Grignard reagent surprisingly added first to **44**, while the 2-functionalized alkyl halide alkylated the benzylic position. This allowed the preparation of unsymmetrically branched dialkylated arylalkanes **51** in 47–85% yield. The involvement of free radical intermediates is supported by the application of 1-(2-phenylcyclopropyl) styrene as a substrate, which gave exclusively the ring opened product in 71% yield (cf. Fig. 8). This excludes a polar carbomagnesation mechanism. Kinetic investigations showed that the product ratio was dependent on the styrene concentration – the higher the styrene concentration, the higher the amount of normal symmetric dialkylation product.

In separate experiments it was shown that titanium species are not involved in the generation of the alkyl radical derived from the Grignard reagent. It was, however, demonstrated that butylmagnesium chloride reacts with 2-alkoxyalkyl radicals by an alkyl exchange leading to a butyl radical and a 2-alkoxyalkyl Grignard reagent, which is subject to E1cB elimination furnishing an alkene. This was unequivocally proven by the reaction of 2-(bromomethyl)tetrahydrofuran with butyl magnesium chloride, which gave the ring opened 4-pentenol, which can only result from E1cB of the corresponding Grignard reagent, but not through a radical process. Therefore, the course of these alkylations can be best rationalized by an initial generation of a 2-functionalized alkyl radical by titanate(III) as shown in Fig. 15. The rate of addition of the resulting radical to styrene is considerably slower than its exchange with excess butyl Grignard reagent, potentially via coordinative interactions. Thus liberated butyl radical adds to **44** forming **49E** (cf. Fig. 15), while the functionalized Grignard reagent degrades quickly to ethylene and the corresponding magnesium alkoxide. Benzylic radical **49E** continues the catalytic cycle as described in Fig. 15.

A similar strategy was used to catalyze the carbosilylation of styrenes and dienes **52** (Fig. 17) [138]. The reaction proceeds similarly to the dialkylation presented in Fig. 15 with the difference that chlorosilanes **53** were applied instead of **46**. The resulting benzylic or allylic silanes **54** were isolated in 35–95% yield. The reaction



labile and undergoes  $\beta$ -hydride elimination with release of product **56**. The resulting titanium hydride complex **57E** is transformed to titanocene **49F** by reductive elimination. This adds to radical **43** and closes the catalytic cycle. The involvement of free radicals in the course of the reaction is supported by the reaction with 5-hexenyl bromide **22** leading to isolation of 22% of cyclic and 52% of linear products **23** and **24** (cf. Fig. 8). When the alkyl halide is secondary, small amounts of dimer were also formed. Dimers become, however, the exclusive products when *tert*-butyl bromide is applied, whose formation can be explained by homolysis of **57D** to relieve strain and subsequent dimerization. Similar dehydrogenative alkylations were also performed with 2-bromoalkyl ethers **50** (cf. Fig. 16). As shown above, products resulting from addition of the alkyl group present in the Grignard reagent were isolated in 59–75% yield [138].

Radical carbomagnesation reactions are also possible when less reactive alkyl halides were used (Fig. 19) [140]. Thus treating alkyl chlorides or less reactive alkyl bromides as well as aryl bromides or vinyl bromides **59** with arylalkenes, vinylsilanes or 1,3-dienes **58** and butylmagnesium chloride as the stoichiometric reducing agent in the presence of 5 mol%  $\text{Cp}_2\text{TiCl}_2$  afforded hydrocarbons **60** ( $\text{E}=\text{H}$ ) after hydrolysis in 48–94% yield. Trapping of the reaction mixture by other electrophiles, such as benzoyl chloride, benzyl bromide, or  $\text{TMSCl}$ , was also possible giving functionalized branched hydrocarbons in 40–93% yield. Allylic *ortho*-bromophenyl ethers or *ortho*-(3-butenyl)bromobenzene furnished cyclized products under similar conditions in 70–95% yield. Even radical cyclization/radical addition sequences of *ortho*-bromophenyl prenyl ethers **61** with styrenes **55** were developed. The reaction proceeds initially as shown before (cf. Fig. 15) by reductive generation of an aryl radical and cyclization to **61A**. Radical addition of **55**, coupling to alkyltitanocene(III), transmetalation with butylmagnesium chloride and silylation furnishes product **62** in 75% yield.

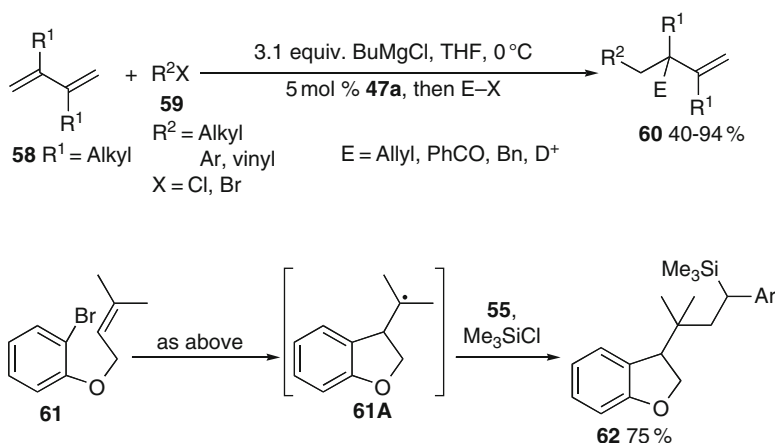
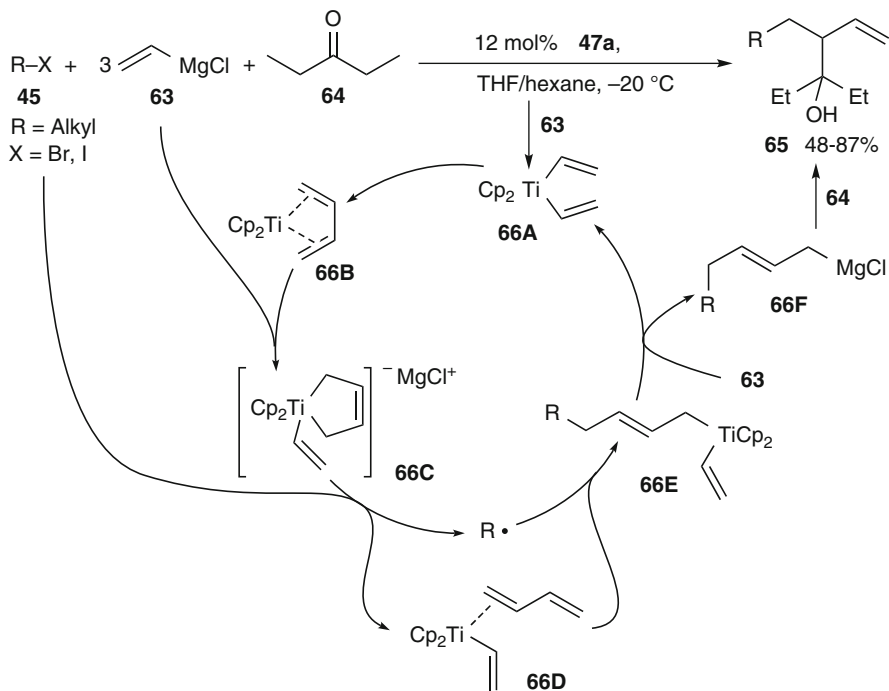


Fig. 19 Radical carbomagnesation reactions and cyclization/addition sequences



**Fig. 20** Titanium-catalyzed dimerization/radical addition/nucleophilic addition sequences

The same group demonstrated recently that vinyl Grignard reagents **63** undergo alkylative dimerization reactions catalyzed by 12 mol% of Cp<sub>2</sub>TiCl<sub>2</sub> leading to functionalized olefins **65** in 48–87% yield (Fig. 20) [141]. Tertiary alkyl bromides reacted fastest and in the highest yield followed by secondary and primary alkyl bromides. Alkyl chlorides or fluorides as well as 1- or 2-substituted vinyl Grignard reagents were not applicable under the reaction conditions. When cyclopropylmethyl bromide **20** was employed as the substrate, a ring-opened product was obtained exclusively (cf. Fig. 8). Competition experiments using an excess of butadiene over 2,3-dimethylbutadiene as a ligand demonstrated that the ratio of products does not correlate with the excess of free butadiene, suggesting that the radical adds selectively to the titanium-coordinated diene and not to free diene present in the reaction mixture. Thus, the reaction begins with the substitution of the chloride function in Cp<sub>2</sub>TiCl<sub>2</sub> by vinyl groups from the Grignard reagents leading to divinyltitanocene(IV) **66A**. An isomerization generates a (butadiene)titanocene(II) complex **66B**. After formation of titanate(IV) **66C** by addition of another molecule of Grignard reagent, SET reduction of the alkyl halide **45** occurs, which results in formation of an alkyl radical. This adds to the diene activated by coordination to titanium(III) in **66D** leading to allyltitanium(IV) species **66E**. Transmetalation by excess vinyl Grignard reagent liberates catalyst **66A** and gives allyl Grignard reagent **66F**, which reacts with ketone **64** to products **65**.



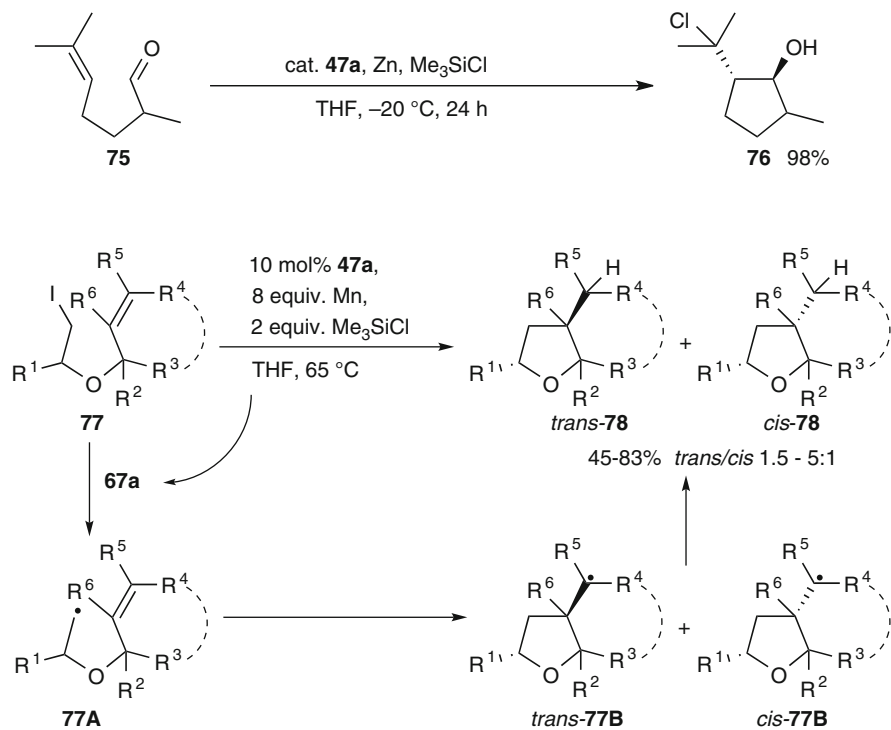


chloride dimer catalyst **67a** acts in two ways. It promotes the SET reduction of **69a** to allylic radical **71A** thus regenerating  $\text{Cp}_2\text{TiCl}_2$ . On the other hand it acts as a Lewis acid toward nonconjugated aldehydes or ketones **68** forming complex **71B**. A full electron transfer to the valence tautomeric titanium ketyl **71C**, however, apparently does not proceed. Both **71A** and **71B** couple subsequently furnishing homoallylic titanium alkoxides **71D**. Transmetalation of **71D** mediated by chlorosilane-collidine complex **72** regenerates the titanocene dichloride precatalyst and homoallyl silyl ether **73**, from which homoallylic alcohols **70** are isolated on work up in 56–99% yield. The assumption that a radical coupling, but not a two-electron nucleophilic addition mechanism operates is based on the fact that coupling of  $\alpha,\beta$ -unsaturated aldehydes with prenyl chloride **69b** afforded exclusively the  $\alpha$ -addition products. Known prenyltitanium(IV) compounds furnish in contrast the  $\gamma$ -addition products **74** preferentially. The radical coupling pathway is also supported by the fact that  $\alpha,\beta$ -unsaturated carbonyl compounds react faster than aldehydes. More easily reducible  $\alpha,\beta$ -unsaturated aldehydes are fully converted by **67a** to ketyl-type radicals **71E**, which couple faster with **71A**. Intramolecular Barbier reactions proceed smoothly in 57–80% yield and also point to a radical coupling mechanism. In contrast, a nucleophilic mechanism operates probably in Barbier reactions of ketones with prenyl chloride **69b**, since the experimental results are very similar to those of known polar nucleophilic addition reactions. Similar propargylation reactions were also conducted. Homopropargylic alcohols were isolated as the exclusive products. The authors proposed a polar course involving nucleophilic addition of an allenyltitanocene intermediate for these reactions [151].

### 3.3.2 Radical Cyclizations

Hirao and coworkers used catalytic amounts of titanocene dichloride and stoichiometric amounts of zinc and  $\text{TMSCl}$  to perform a reductive radical cyclization of 2,6-dimethyl-5-heptenal **75** (Fig. 22) [152]. 2-(2-Chloroisopropyl)cyclopentanol **76** was formed in 98% yield and with exclusive *trans*-cyclization diastereoselectivity. Later Mn and  $\text{TMSCl}$  were used to (re)generate catalyst **67a** in Ueno–Stork cyclizations of allylic iodoacetaldehyde acetals **77** or  $\beta$ -iodo ethers to tetrahydrofuran derivatives **78**. The products were obtained in 45–83% yields with preferred *trans*-diastereoselectivity of 1.5–4:1 [153]. The reaction proceeds by reductive generation of radical **77A** triggered by catalyst **67a**. A subsequent 5-*exo* cyclization affords the diastereomeric cyclic radicals **77B** via a preferred chair- and a minor competing boat transition state [20, 154, 155]. Radicals **77B** stabilize either by hydrogen abstraction from THF or by coupling with **67a** to give a Ti(IV) intermediate, which is subject to hydrolysis.

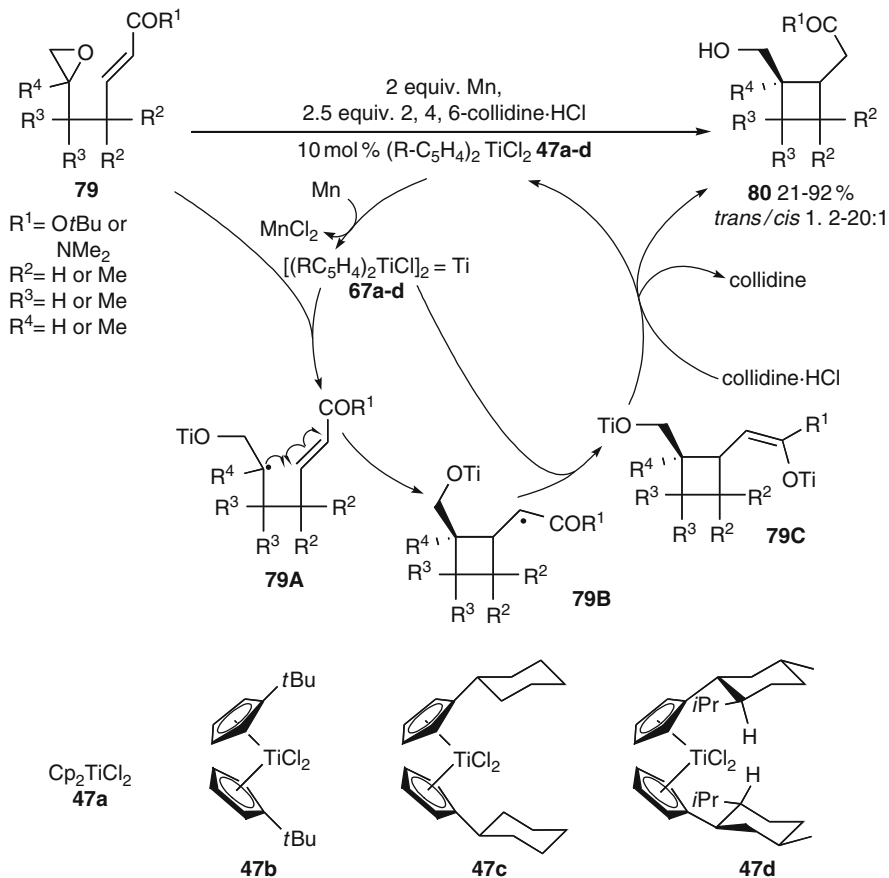
Gansäuer and coworkers studied very thoroughly titanocene chloride-catalyzed radical cyclizations using epoxides as starting materials [142–145]. More recently the applicability of 10 mol% of titanocene chloride complexes **47a–d** in radical 4-*exo* cyclizations of 6,7-epoxy-2-heptenoate derivatives **79** was demonstrated



**Fig. 22** Hirao's titanocene chloride-catalyzed radical cyclizations

(Fig. 23) [156]. The process starts with reductive generation of titanium(III) complexes **67a–d** using manganese metal. Reductive epoxide ring opening generates a  $\beta$ -titanoxyalkyl radical **79A**, which undergoes the desired 4-*exo* cyclization to the  $\alpha,\beta$ -unsaturated carbonyl unit. SET reduction of the resulting radical **79B** and hydrolysis of titanium enolate **79C** provided the cyclic products **80** in 21–92% yield with moderate to very good *trans*-diastereoselectivity. For the success of these cyclizations it was necessary to rely on the *gem*-dialkyl effect, electron-poor radical acceptors, and more sterically hindered titanium complexes **47b–d** to reduce the rate of potential premature reduction of radical **79A** to an organotitanium.

Radical 4-*exo* cyclizations can also be catalyzed without recourse to the Thorpe–Ingold effect by applying the concept of template catalysis (Fig. 24) [157]. Here, 20 mol% of a cationic titanocene(IV) precatalyst **82** is applied, which contains a coordinating neutral tether. After reductive opening of epoxide **81**, a cationic titanocene(III) complexed radical **83** is formed, in which both the epoxide and the  $\alpha,\beta$ -unsaturated carboxamide radical acceptor are coordinated. This provides the template to accelerate the slow 4-*exo* radical cyclization step considerably. Cyclobutanes **84** were isolated in 46–84% yield with mostly good *trans*-diastereoselectivity, which can be explained by favored transition state **83**.

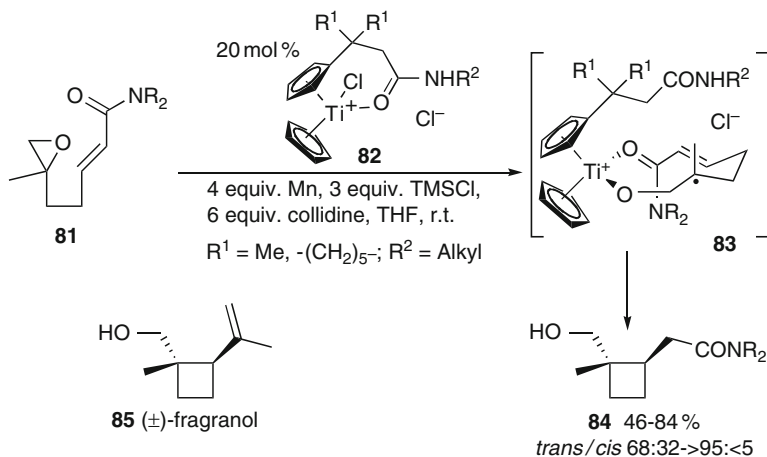


**Fig. 23** Titanocene chloride-catalyzed radical 4-*exo* cyclizations

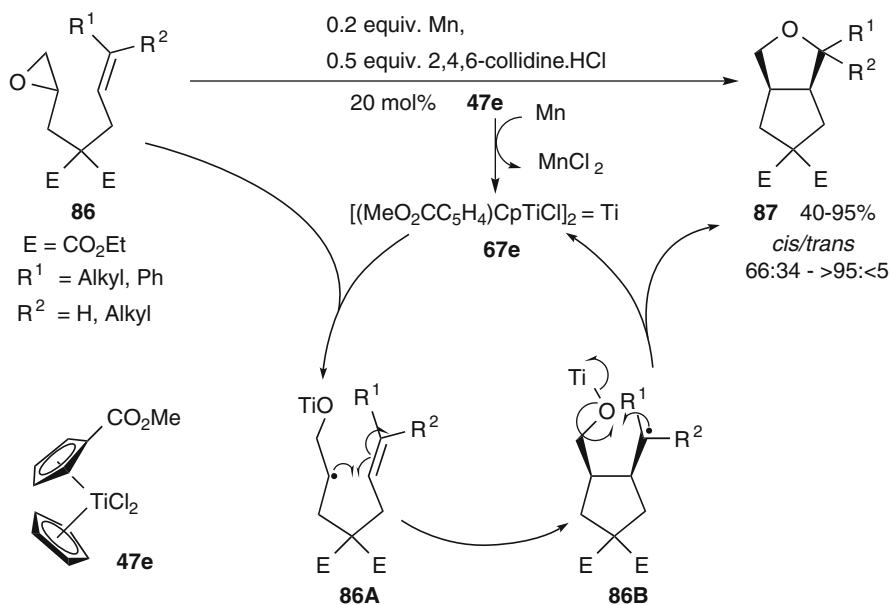
This method was successfully applied to the total synthesis of the monoterpene ( $\pm$ )-fragranol **85** [158].

Moreover, it was demonstrated that not only alkenes may serve as radical acceptors in radical cyclizations. Substrates with polar carbonyl and cyano groups afforded cyclic alcohols and ketones in 30–87% yield [146, 159].

Radical cyclizations catalyzed by **67a** require the regeneration of the titanocene catalysts by a stoichiometric reductant, such as manganese. When 10 mol% of substituted cyclopentadienyltitanium complex **47e** is applied instead truly catalytic cyclization sequences of epoxides **86** are possible (Fig. 25) [160]. Reductive radical generation from **86** promoted by titanocene chloride **67e** and subsequent 5-*exo* cyclization of radical **86A** generates a titanoxo cyclopentylalkyl radical **86B**. Since the electron-poor titanocene chloride **67e** reduces the tertiary radical **86B** only sluggishly, its extended lifetime allows for a 1,5- $\text{S}_{\text{H}}$  affording the bicyclic tetrahydrofuran ring system **87**. At the same time catalyst **67e** is liberated. The reaction

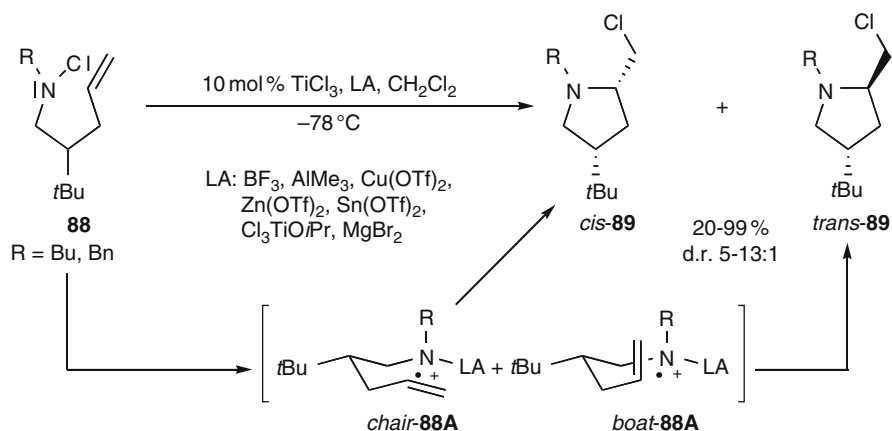


**Fig. 24** Template-catalysis in radical 4-*exo* cyclizations (only major *trans*-diastereomers shown)



**Fig. 25** Titanium-catalyzed radical cyclization with catalyst regeneration by homolytic substitution (only major diastereomer shown)

worked for a number of substrates in 40–95% yield and required only catalytic amounts of manganese to generate **67e** initially and 0.5 equiv. of collidinium chloride. 6-*exo* Cyclizations also proceeded in high yield. Simple titanocene



**Fig. 26** Titanium-initiated Hofmann-Löffler-Freytag reactions

chloride **67a** was used for comparison. The bicyclization also took place, but the yields were considerably lower.

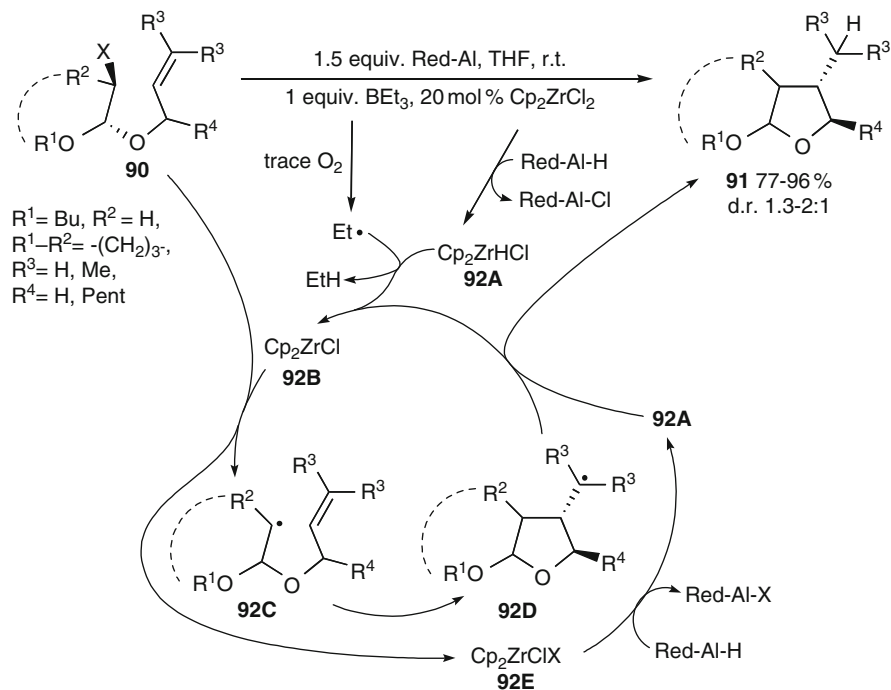
With chiral catalyst **47d** regioselective reductive ring opening reactions of racemic epoxides can be achieved. For alkynyl epoxy ethers it leads to effective asymmetric 5-*exo* cyclization of one radical, but reduction of the other [161, 162].

Hofmann-Löffler-Freytag-type reactions of *N*-chloro 4-pentenyl amines **88** catalyzed by 10 mol% of  $\text{TiCl}_3$  in the presence of several activating Lewis acids was reported recently by Somfai and colleagues (Fig. 26) [163, 164]. Lewis acid coordination accelerated chlorine abstraction by  $\text{TiCl}_3$ . The resulting coordinated cationic aminyl radical **88A** cyclizes and undergoes chlorine transfer from starting **88**. 2-(Chloromethyl)pyrrolidines **89** were formed in 20–99% yield. Thus,  $\text{TiCl}_3$  serves only as an initiator in these reactions (cf. Fig. 10). The *cis*-diastereoselectivity of the process was good to excellent for unsubstituted alkene acceptors and can be explained by a Beckwith-Houk transition state *chair-88A*. When di- or trisubstituted acceptors are used a lower *cis*-selectivity was observed.

## 4 Zirconium Catalysis

Although the ability of zirconium complexes to generate radicals selectively was noted early [165, 166], not many radical reactions mediated by zirconium complexes are known [167]. Oshima et al. reported the only examples of zirconium-catalyzed radical reactions.

A reductive radical cyclization methodology, which is catalyzed by zirconocene complexes, furnished butyrolactols **91** (Fig. 27) [168, 169]. When 2-allyloxy-3-halotetrahydropyrans or bromoacetaldehyde allyl acetals **90** were treated with 20–30 mol% of zirconocene dichloride, 1 equiv. of  $\text{BEt}_3$  and an excess Red-Al as the stoichiometric reductant, tetrahydrofurotetrahydropyrans or butyrolactols **91**



**Fig. 27** Zirconium-catalyzed reductive radical cyclizations of haloacetals **90** (major diastereomer shown)

were obtained in 77–96% yield. Based on stoichiometric experiments the following catalytic cycle was proposed to operate. Cp<sub>2</sub>ZrCl<sub>2</sub> is transformed to Schwartz's reagent **92A** by Red-Al. BEt<sub>3</sub> serves to generate ethyl radicals initially by reaction with trace amounts of oxygen. They serve to abstract the hydrogen atom from **92A** leading to the formation of the actual catalyst Cp<sub>2</sub>ZrCl(III) **92B**. This is a very effective SET reducing agent giving an alkyl radical **92C** and Cp<sub>2</sub>ZrClX **92E**. The latter is reduced by Red-Al to Schwartz's reagent **92A**, which serves as a hydrogen donor to reduce radicals **92D** formed by 5-*exo* cyclization of **92C**. The radical mechanism is supported by cyclizations using cyclopropane-substituted allyl ether functions (R<sup>3</sup>=cyclopropyl), which gave exclusively ring-opened products. The diastereoselectivity of the cyclizations is similar to those mediated by Bu<sub>3</sub>SnH.

In a later study it was demonstrated that alkyl halides add to 2-methylene-1,3-dithianes catalyzed by 20–30 mol% of Cp<sub>2</sub>ZrCl<sub>2</sub> mediated by butylmagnesium chloride [170].  $\alpha$ -Diketone tetrathioacetals were obtained in 21–71% yield. A tandem cyclization/dimerization reaction gave **95** in 67% yield (Fig. 28). The reaction is thought to proceed by initial generation of zirconocene(II) by excess Grignard reagent (cf. Fig. 15). It serves as the SET reducing agent for alkyl iodide **93**. The derived radical **93A** undergoes a 5-*exo* cyclization. The cyclized radical

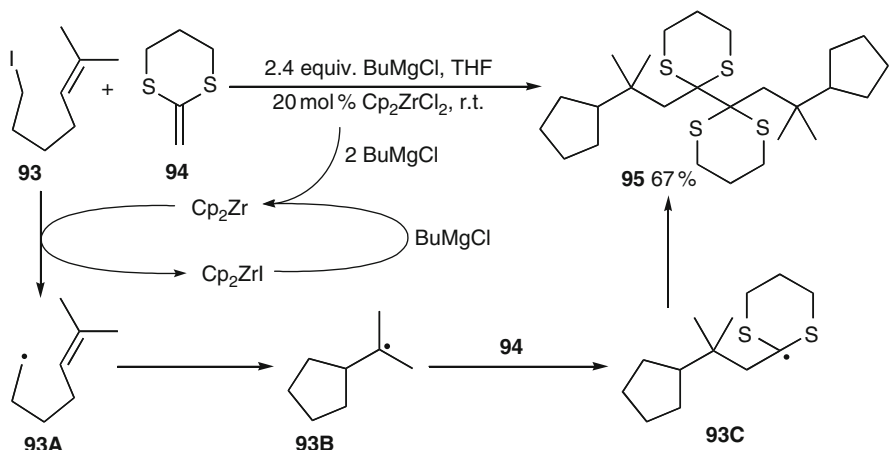


Fig. 28 Zr(II)-catalyzed radical cyclization/addition/dimerization sequence

**93B** adds to the ketene dithioacetal **94**. Since for the resulting stabilized dithioalkyl radical **93C** no further reaction is possible, dimerization to **95** proceeds.

## 5 Vanadium-, Niobium-, and Tantalum-Catalyzed Radical Reactions

Not many catalyzed processes involving free radicals are known with these metals. Some vanadium-catalyzed pinacol coupling reactions were developed (reviews [129, 171], [172, 173] and cited ref. [174]). Niobium and tantalum complexes were applied in pinacol coupling reactions [130]. Vanadium(IV) [175–179] and vanadium(V) ([129], reviews [180–186]) complexes are known to catalyze asymmetric oxidative dimerizations of phenols and naphthols in moderate to excellent yields applying oxygen as the terminal oxidant. Biaryls are accessible by intramolecular coupling of sodium tetraarylborates, catalyzed by EtOVOC<sub>2</sub> in the presence of air [187].

### 5.1 Low-Valent Vanadium-Catalyzed Reactions

Zhou and Hirao showed that a low-valent catalyst generated from Cp<sub>2</sub>VCl<sub>2</sub> or VCl<sub>2</sub> and zinc in the presence of chlorotrimethylsilane is active in tandem reductive dimerization/Thorpe-Ziegler-type cyclizations of arylidenemalononitriles **96** (Fig. 29) [188]. The low-valent catalyst transfers an electron to **96** and the thus generated radical anion **96A** adds to another molecule of **96**. The resulting dionic



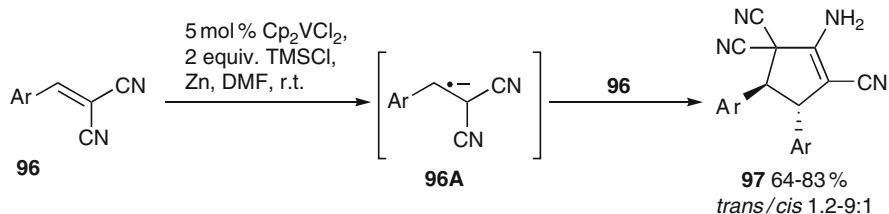


Fig. 29 Low-valent vanadocene-catalyzed reductive cyclization of arylidenemalononitriles

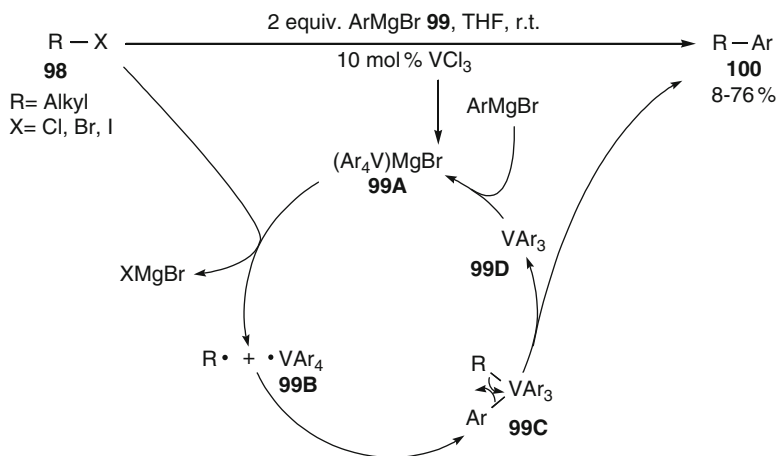


Fig. 30 Vanadium-catalyzed Kumada coupling reactions of alkyl halides

radical anion cyclizes to one of the nitrile functions. Final SET reduction gives the product. The catalyst is regenerated by reduction with zinc. The addition/cyclization sequence proceeds in good yields and with moderate to good *trans*-diastereoselectivity.

Similarly, a catalyst (10 mol%) generated in situ from  $\text{Cp}_2\text{VCl}_2$  and manganese/chlorotrimethylsilane promotes a radical 5-*exo* cyclization of  $\beta$ -iodo allylic ether **68** to tetrahydrofuran **69** in 62% yield (cf. Fig. 22) [153]. The reaction should proceed analogously to the corresponding  $\text{Cp}_2\text{TiCl}_2$ -catalyzed transformation.

## 5.2 V(III)-V(IV)-V(V) Catalysis: Kumada Coupling

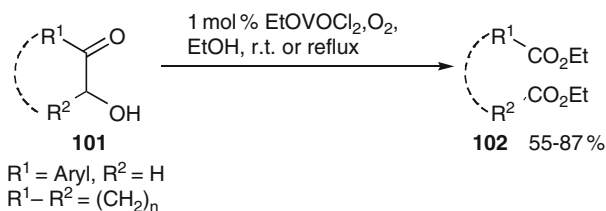
Kumada-type couplings of alkyl halides **98** with aryl Grignard reagents **99** yielding alkylarenes **100** recently received much attention (see Part 2, Sects. 2.1 and 5.1, Part 3, Sect. 2.1). A vanadium-based method was developed by Oshima and coworkers (Fig. 30) [189]. Primary and secondary alkyl bromides, iodides, and also chlorides were coupled to phenylmagnesium bromide catalyzed by 10 mol%

vanadium trichloride in 21–76% yield. A stoichiometric experiment revealed that the catalytically active species is most likely ate complex **99A**, since a strong acceleration of the reaction was observed only on the addition of the fourth equivalent of **99** based on  $\text{VCl}_3$ . Almost no biphenyl was formed during the reaction. This speaks against further reduction to a low-valent vanadium species. Thus generated vanadate species **99A** acts probably as a SET reducing agent toward **98** leading to an alkyl radical and  $\text{Ar}_4\text{V}$  **99B**. Both species couple to an alkyltetraarylvanadium(V) species **99C**, which is prone to reductive elimination to **100** and triarylvanadium **99D**. This adds another equivalent of the Grignard reagent to reenter the catalytic cycle. Several observations support the radical mechanism of this coupling, such as the stereoconvergent coupling of the individual *exo*- or *endo*-norbornyl bromides **25** or 4-*tert*-butylcyclohexyl bromides **27** to *exo*-phenyl-norbornane and *trans*-4-*tert*-butylcyclohexylbenzene, respectively (cf. Fig. 9). When 5-hexenyl bromide **22** was used as the substrate a radical 5-*exo* cyclization occurred prior to coupling (cf. Fig. 8).

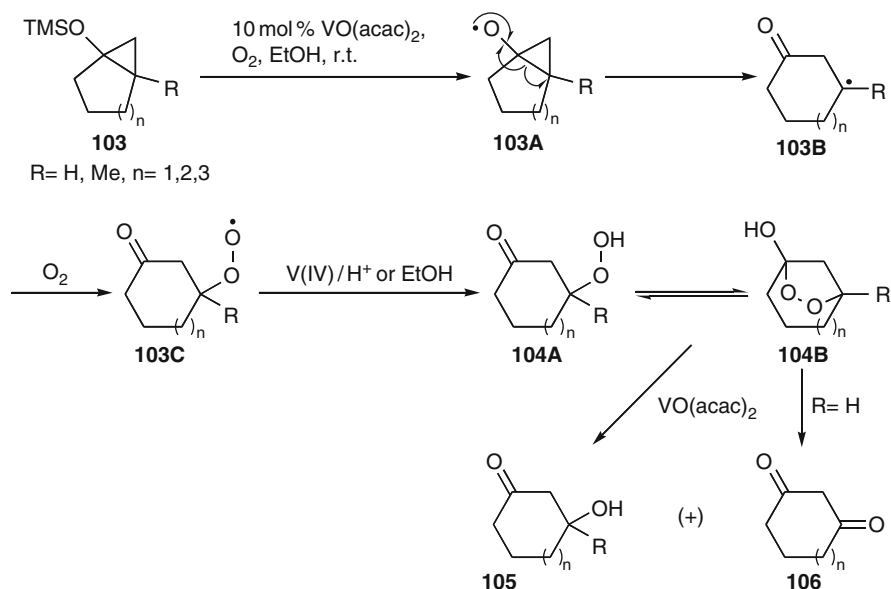
### 5.3 V(IV)-V(V) Catalysis

Aside from oxidative dimerizations [175–186] vanadium catalysts are able to induce C–C and C–O bond cleavages. Momose and coworkers developed a catalytic system to fragment  $\alpha$ -hydroxy ketones **101** to diesters or ketoesters **102** (Fig. 31) [190]. Using 1 mol% of  $\text{EtOVOCl}_2$  as a catalyst and oxygen as the terminal oxidant, 55–87% of **102** was obtained. The reaction mechanism is not known, but the reaction is inhibited by 2,6-di-*tert*-butylcresol (BHT) pointing to the involvement of a radical process.

Bridgehead bicyclic cyclopropanols or cyclopropyl silyl ethers **103** ( $\text{R}=\text{H}$ ) cleaved to ring-expanded mixtures of cyclic  $\beta$ -hydroxy ketones **105** and  $\beta$ -diketones **106** in good overall yields catalyzed by 10 mol% of  $\text{VO}(\text{acac})_2$  in the presence of oxygen (Fig. 32) [191, 192]. With 3-substituted substrates **103** ( $\text{R}=\text{Me}$ ), mixtures of bicyclic endoperoxide hemiketals **104B** and  $\beta$ -hydroxy ketones **105** arose. In separate experiments it was shown that **105** is not oxidized to **106** under the reaction conditions, and thus the products most likely form from



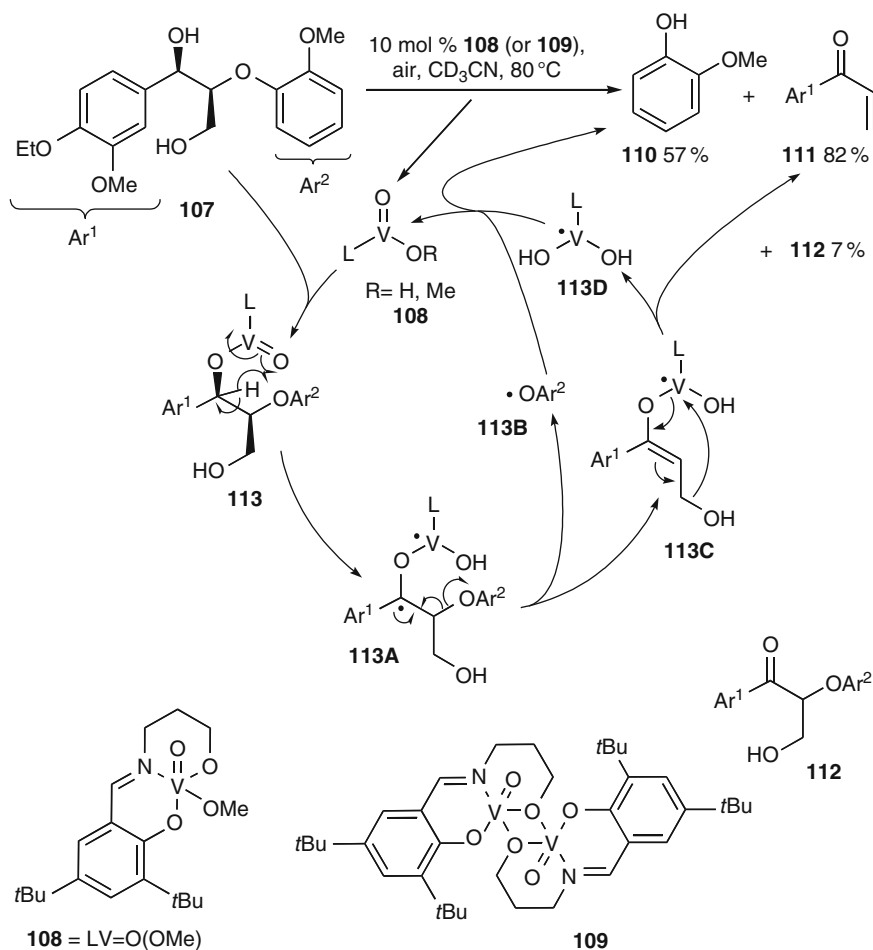
**Fig. 31** Oxidative cleavage of  $\alpha$ -hydroxy ketones catalyzed by  $\text{EtOVOCl}_2$



**Fig. 32** Vanadyl acetylacetonate-catalyzed oxidative ring expansion of bicyclic cyclopropanols **103**

a common peroxide intermediate **104**. The endoperoxide **104B** ( $\text{R}=\text{Me}$ ) was indeed converted to hydroxy ketone **105** in 78% yield under the reaction conditions. Based on these results, it was proposed that the V(IV) catalyst oxidizes the substrates **103** to alkoxyl radicals **103A**, which cleaves to  $\beta$ -keto radical **103B** as commonly observed in Booker–Milburn-type reactions [193, 194]. Coupling with oxygen provides the corresponding peroxy radical **103C**, which can be reduced to hydroperoxide **104A** by the vanadium(IV) species or hydrogen abstraction from the solvent. Reductive cleavage of the peroxide **104** ( $\text{R}=\text{H}$ ) results in **105**, while dehydration leads to **106**. Alternatively, dimerization of **103C** and tetroxide fragmentation (leading references [195, 196]) may also contribute to formation of the mixture of **105** and **106**. Substrates substituted in 3-position ( $\text{R}=\text{Me}$ ) can only undergo reductive peroxide cleavage to **105**.

Recently Toste and coworkers reported a V(V)-catalyzed aerobic C–O cleavage of 1-arylpropan-1,2,3-triol 2-ethers **107**, which are lignin model compounds (Fig. 33) [197]. The reaction proceeded at 80 °C in ethyl acetate or acetonitrile and afforded catechol derivative **110**,  $\alpha,\beta$ -unsaturated ketone **111**, and small amounts of ketone **112** using 10 mol% of vanadium(V) Schiff base complex **108**. The reaction is thought to proceed by transesterification of **107** with V(V)-catalyst **108** generating **113**. This intermediate is prone to abstraction of the benzylic hydrogen atom leading to radical **113A**.  $\beta$ -Fragmentation forms aryloxy radical **113B** and  $\beta$ -hydroxyvanadium(IV) enolate **113C**. The latter is susceptible to E1cB elimination giving **111**. Aryloxy radical **113B** can be reduced to phenol **110** by



**Fig. 33** V(V)-Catalyzed cleavage of lignin model compound **107**

the resulting vanadium(IV) species **113D**, thus regenerating the V(V)-catalyst **108**. The role of oxygen is not clear at present. It accelerates the reaction considerably and prevents formation of an insoluble precipitate of V(IV)-complex **109**, which forms in its absence. Complex **109** is a considerably less active catalyst in the absence of air but active in its presence.

Alkenes were cleaved to aldehydes by 5 mol% of a (salen)<sub>2</sub>VCl complex in the presence of air and thiophenols in 58–95% yield. Other V(III) and V(IV) catalysts are similarly effective. The reaction involves an initial thiyl radical addition to the olefin and trapping by oxygen. The resulting peroxy radical is in turn most likely transformed to an alkoxyl radical by the catalyst and undergoes β-fragmentation to form the most stable radical [198].

## 6 Chromium-Catalyzed Radical Reactions

Chromium-mediated reactions are frequently applied in organic chemistry. A number of oxidation reactions promoted by high-valent chromium compounds exist. The mechanistic spectrum of these reactions is very broad and cannot be discussed here. The most frequently applied low-valent chromium catalyst precursor is  $\text{CrCl}_2$  (reviews [199–202]) which is applied stoichiometrically or catalytically ([203, 204] and references cited therein) in Nozaki–Kishi–Hiyama reactions [205], Reformatsky reactions (review [206]), and reductive radical reactions. The kinetics for the addition of radicals to chromium(II) compounds were determined [54]. Chromium compounds were applied stoichiometrically in pinacol coupling reactions [128, 201, 202]. Catalytic pinacol coupling protocols applying 5 mol% of  $\text{CrCl}_3$  or 2–3 mol% of chromocene ( $\text{Cp}_2\text{Cr}$ ) [207] or 10 mol% of  $\text{CrCl}_2$  ([208] and references cited therein) and excess amounts of manganese and chlorosilanes were developed. The reaction also proceeds in water with zinc as terminal reductant [209]. An asymmetric version using binaphthyl ligands was reported [210]. Pinacol-type cross-couplings of  $\alpha,\beta$ -unsaturated aldehydes and aldehydes using  $\text{CrCl}_2$  were also disclosed; however, the reaction involves a twofold SET reduction followed by a nucleophilic addition of the resulting allylic chromium reagent to the aldehyde [211]. A catalytic reductive generation of allyl chromium(III) compounds by desulfonylation of allylsulfonyl chlorides was reported using 10 mol%  $\text{CrCl}_2$ , Mn, and  $\text{TMSCl}$  [212]. The photolytic radical generation from organochromium complexes was explored recently and may open new avenues for transition metal-catalyzed radical reactions, though synthetic applications are missing so far [213].

### 6.1 *Cr(0)-Cr(I)-Catalyzed Radical Additions*

Anionic chromium hydride complexes proved to be efficient hydrogen atom donors. Newcomb determined  $\text{PPN}^+ \text{HCr}(\text{CO})_5^-$  to be an efficient radical initiator and reducing agent for radicals and determined the kinetics of the hydrogen abstraction reaction [214]. In line with the observation that 3d metal complexes are much more prone to radical pathways than the corresponding 4d and 5d complexes, an increase of the extent of competing  $\text{S}_{\text{N}}2$ -pathways for the bromide abstraction was found for molybdenum and tungsten complexes compared to the chromium complex.

A few Cr(0) complexes were reported to catalyze the Kharasch addition of polyhalocarbons to olefins. (Naphthalene)chromium tricarbonyl exhibited low to moderate activity in additions of tetrachloromethane to olefins. The reactions were proposed to occur by a non-radical mechanism [215]. A later kinetic study showed that a radical mechanism operates (see Sect. 7) [216, 217]. Shvo et al. used 5 mol%  $\text{Cr}(\text{CO})_6$  in acetonitrile to add tetrachloromethane to 1-octene [218]. It was necessary to transform the precatalyst first to the active catalyst

(MeCN)<sub>3</sub>Cr(CO)<sub>3</sub>, which gave 40% of the product. Compared to the corresponding molybdenum complex it is much less active (see Sect. 7).

## 6.2 Cr(I)-Cr(II)-Catalyzed Radical Cyclizations

Based on a study of the kinetics of hydrogen transfer to several alkenes [219, 220], Norton and coworkers recently designed a Cr(II)-catalyzed reductive radical cyclization of 2-substituted acrylates **114** using CpCr(CO)<sub>3</sub>H **115** as the catalyst in the presence of dihydrogen (Fig. 34) [221]. Hydrogen atom addition to **114** from **115** generates  $\alpha$ -ester radical **114A** and the Cr(I) complex **114C**. The former cyclizes preferentially to the alkene unit. Since the resulting cyclized radical **114B** is more easily reduced than **114A**, cyclopentane derivatives **116** were isolated in good yield. However, some premature reduction of **114A** by **115** and  $\beta$ -hydrogen abstraction by **114C** giving esters **117** and **118** could not be avoided. Catalyst **115** is regenerated by reduction of **114C** with dihydrogen. A disadvantage is that the reaction times are rather long. Bicyclizations also occur, albeit in lower yield.  $\alpha,\beta$ -Unsaturated ketones cannot be used, since they are hydrogenated quantitatively under the reaction conditions [222].

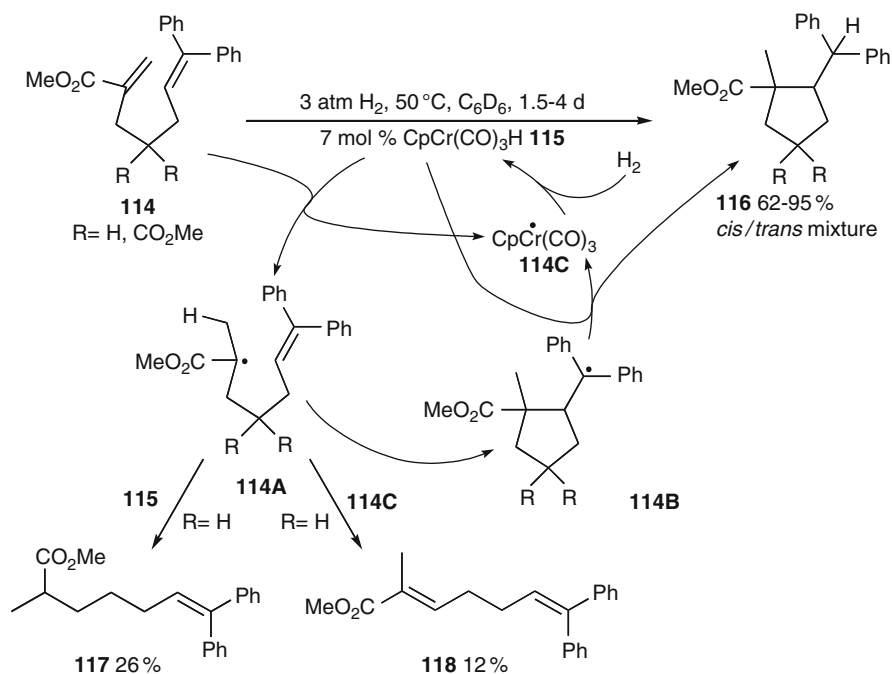


Fig. 34 Chromium-catalyzed reductive radical cyclizations

### 6.3 Cr(II)-Cr(III)-Catalyzed Radical Cyclizations

Two protocols for chromium(II)-catalyzed Ueno–Stork cyclizations of bromoacetaldehyde allyl acetals **90** were disclosed by Hackmann and Schäfer (Fig. 35) [223]. The active catalysts for both methods were generated from 15 or 30 mol%  $\text{Cr}_2(\text{OAc})_4$  **119a** and ethylenediamine **120** (or 2,2-dipyridylamine – not shown). The reactions can be performed either by using  $\text{LiAlH}_4$  (Conditions A) or cathodic reduction (Conditions B) for catalyst regeneration. Butyrolactols **91** were isolated in 71–93% yield for the former and 67–84% for the latter method. The lowest observed diastereoselectivity was 5:1, very often much better in the range of 15–30:1. When acyclic  $\alpha$ -bromoaldehyde allyl acetals ( $\text{R}^3=\text{R}^4=\text{H}$ ) were applied the simple diastereoselectivity of the cyclization was in contrast low with a slight preference for the relative *cis*-orientation of the substituents.

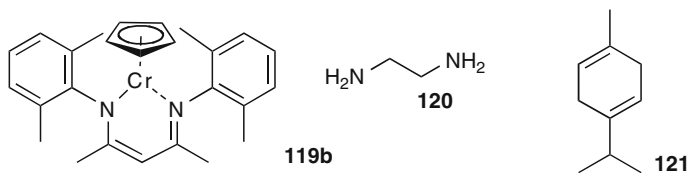
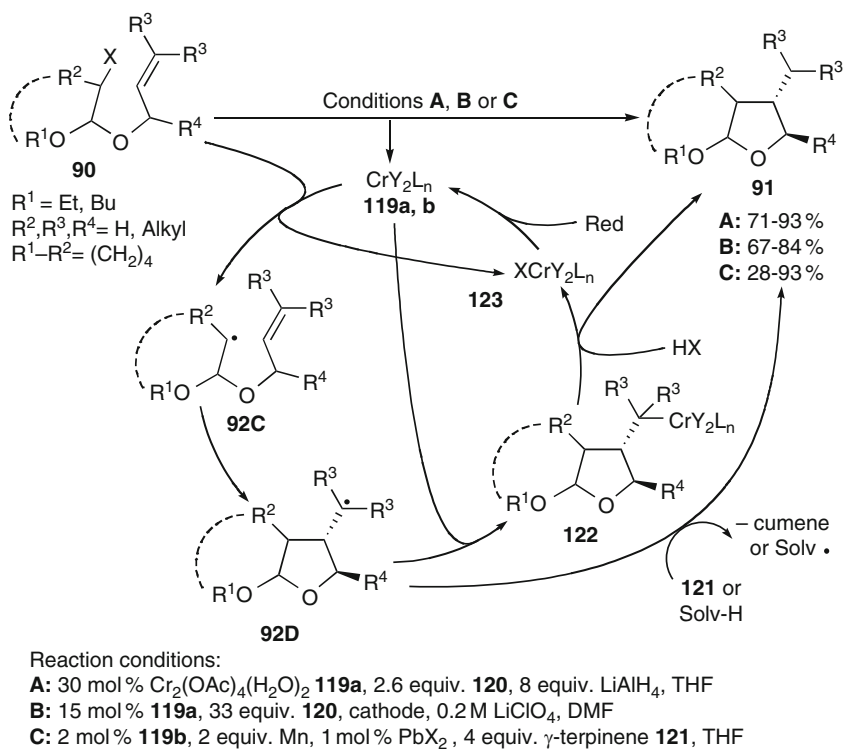


Fig. 35 Chromium(II)-catalyzed reductive radical cyclizations

Smith and colleagues recently published a similar chromium(II)-catalyzed Ueno–Stork cyclization [224]. The chromium(II) ketiminate complex **119b** (2 mol%) triggered 5-*exo* radical cyclization reactions of bromo allylacetals **90**. Manganese and a catalytic amount of  $\text{PbBr}_2$  were applied as the stoichiometric reducing agent (Conditions C). The corresponding chloro acetals also reacted, but required 20 mol% of catalyst **119b** and much longer reaction times. Substituted allylic acetals ( $\text{R}^3=\text{Alkyl}$ ) gave the cyclized products **91** in 28–93% yield. Substrate **90** ( $\text{R}^3=\text{H}$ ) cyclized very slowly under standard conditions and formed organochromium species. When this reaction was performed by irradiation with a fluorescent light bulb product **91** was isolated in 48% yield. The cyclization is probably modulated by the steric strain imposed by the substituents. More hindered organochromium(III) derivatives tend to homolyze more efficiently and more hindered radicals couple more slowly with the catalyst in equilibrium under irradiation. Therefore application of the external reducing agent  $\gamma$ -terpinene **121** was preferred to obtain **91** by hydrogen abstraction.

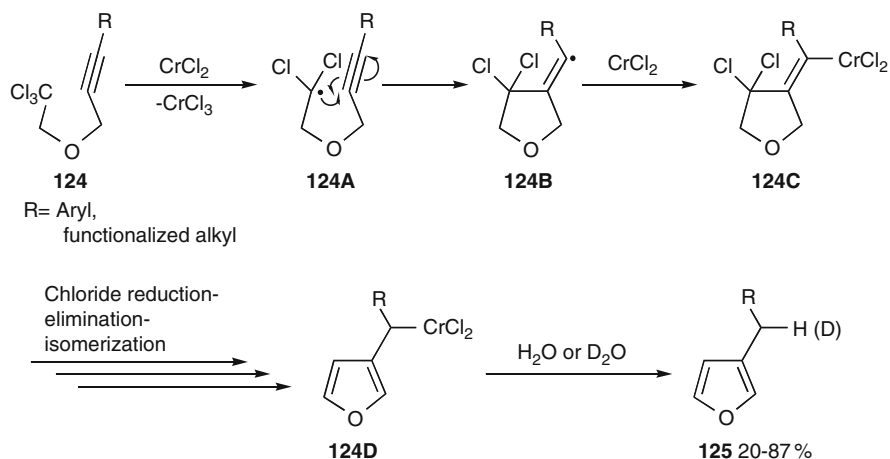
The reaction course can be rationalized as follows. The initial chromium(II) complexes **119** reduce the cyclization precursors **90** to the corresponding radical **92C**, which cyclizes according to a Beckwith–Houk transition state, in which the substituents are oriented equatorially (except for the diastereomeric acetal linkage). The reactivity of the cyclized radicals **92D** is apparently dependent on their degree of substitution. They may be converted to products **91** either by direct hydrogen abstraction from the medium or from added hydrogen donor  $\gamma$ -terpinene **121**. Reduction to an organochromium(III) complex **122** and subsequent hydrolysis represents an alternative pathway to provide **91**. Cogenerated Cr(III) complex **123** is reduced to the catalytically active Cr(II) catalyst by the added reducing agent.

Falck, Mioskowski, and coworkers realized a synthesis of 3-substituted furans **125** catalyzed by 15 mol% of  $\text{CrCl}_2$  using Fürstner's Mn/TMSCl system as a stoichiometric reducing system (Fig. 36) [225]. The reaction starts by reductive radical generation from propargylic 2,2,2-trichloroethyl ethers **124**. The resulting dichloromethyl radical **124A** cyclizes to the alkyne unit providing vinyl radical **124B**, which is reduced by  $\text{CrCl}_2$  to vinylchromium(III) intermediate **124C**. After a series of reductive dehalogenation, elimination, and tautomerization steps, aromatic furylalkylchromium intermediate **124D** is formed, which is hydrolyzed or quenched by deuterium oxide to the products **125**. The yields are mostly good to very good. Surprisingly, the reaction was much less efficient when a stoichiometric amount of  $\text{CrCl}_2$  was used, probably due to strongly competing two-fold SET reduction of the chloride functions and trapping of the resulting radicals to organochromium intermediates, which do not cyclize.

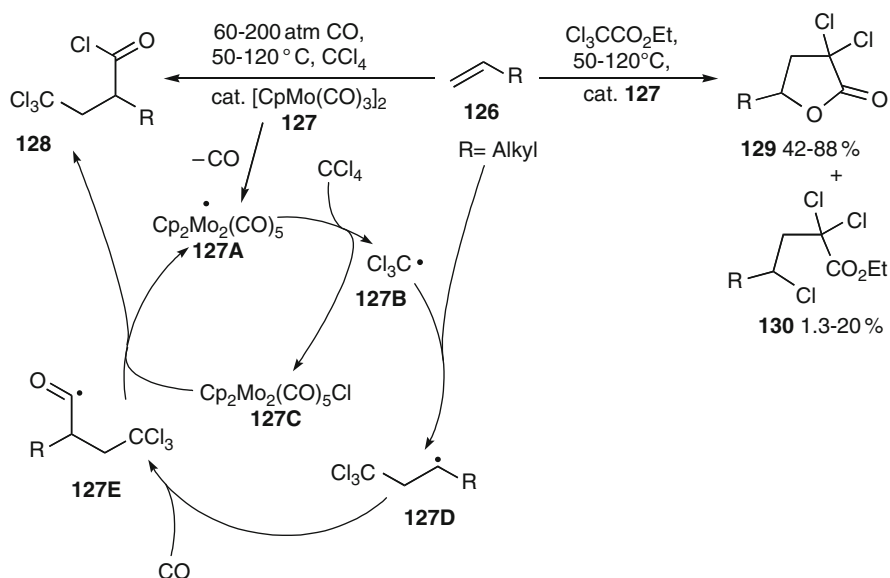
## 7 Molybdenum-Catalyzed Radical Reactions

$\text{CpMo}(\text{CO})_3\text{H}$  proved to be a very efficient hydrogen donor, rivaling thiophenols. The rate constant for radical reduction was determined to be in the range of  $10^7$ – $10^8 \text{ M}^{-1} \text{ s}^{-1}$  at 25 °C [226]. Several CpMo(III) complexes were used as





**Fig. 36** Chromium(II)-catalyzed cyclizations of propargylic 2,2,2-trichloroethyl ethers to 3-substituted furans



**Fig. 37** Atom transfer radical addition reactions catalyzed by molybdenum complexes

efficient catalysts in ATRP or stable free radical polymerizations (SFRP) [227, 228]. These complexes must await, however, a further investigation of their use in synthetic organic chemistry.

Susuki and Tsuji reported the first Kharasch addition/carbonylation reactions of olefins **126** with  $\text{CCl}_4$  and carbon monoxide catalyzed by  $[\text{CpMo}(\text{CO})_3]_2$  **127** and proposed a carbometalation mechanism (Fig. 37) [229]. A kinetic study disproved

the organometallic pathway later and clearly supports a radical mechanism [230]. It was shown that the Mo–Mo bond in **127** does not homolyze to a potential monomeric molybdenum-centered radical under the reaction conditions, but that CO dissociation to **127A** prevails. Related experiments with  $[\text{CpMo}(\text{CO})_2]_2$  showed that the reaction rate was similar. Crossover experiments using mixtures of different CpMo catalysts gave no scrambling of the recovered complexes supporting the dimer-based radical mechanism. Halogen abstraction from the halocarbon by catalyst **127A** starts the reaction. Addition of trichloromethyl radical **127B** generates alkyl radical **127D**, which adds to CO forming acyl radical **127E**. Ligand transfer from cogenerated molybdenum complex **127C** leads to product **128** and regenerates catalyst **127A**, which continues the catalytic cycle. The reaction requires a high CO pressure and the yields were moderate.

Mori and Tsuji extended the study toward trichloroacetate and found that lactone **129** formed as the major product in 42–88% yield, while the expected ATRA product **130** was produced in only 1.3–20% yield [231]. The adduct radical corresponding to **127D** probably undergoes a 5-*endo* radical cyclization to the carbonyl group in competition with ligand transfer, which seems to be slow. Subsequently, either  $\beta$ -fragmentation followed by ligand transfer to the resulting ethyl radical or SET oxidation of the cyclized electron-rich dialkoxyalkyl radical and subsequent cleavage of ethyl chloride may lead to **129**.

$\text{Mo}(\text{CO})_6$  was also used to catalyze Kharasch addition reactions of tetrachloromethane or trichloroacetates to terminal olefins in acetonitrile (Fig. 38) [218]. A precomplexation like for  $\text{Cr}(\text{CO})_6$  was not necessary. The ligand exchange

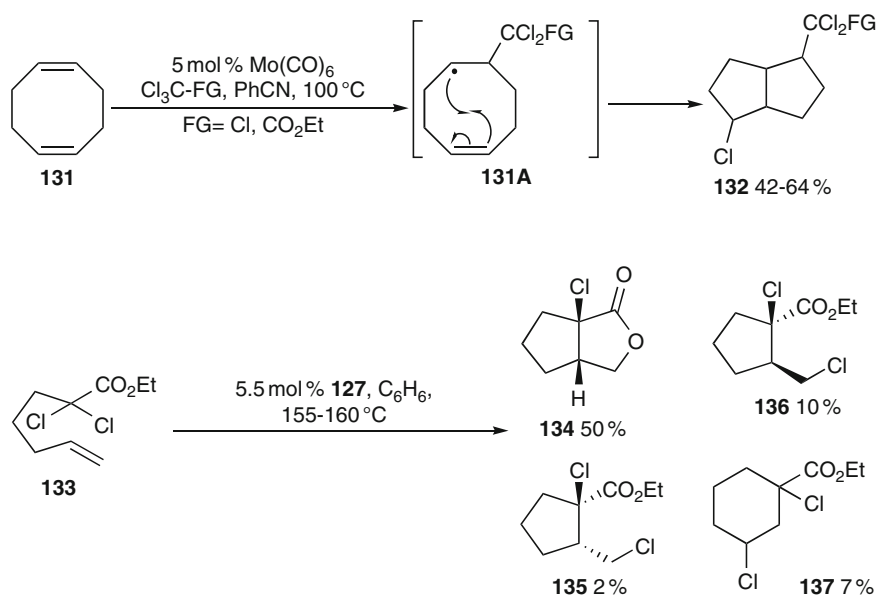


Fig. 38 Molybdenum-catalyzed atom transfer radical cyclization reactions

to the active  $(\text{MeCN})_3\text{Mo}(\text{CO})_3$  complex was fast. The products were isolated in 80–85% yield. The addition to cyclohexene gave the products only in low yield, but cyclooctene reacted in 62–88% yield. The authors proposed a two-electron mechanism for the transformation, based on the observation that hydroquinone or galvinoxyl did not inhibit the reaction. This is, however, not conclusive, since other oxidation states of molybdenum resulting from oxidation by the inhibitor may also catalyze the reactions with similar efficiency (see above). Moreover, with 1,5-cyclooctadiene **131** bicyclooctane **132** was isolated as a diastereomeric mixture as the sole product, whose formation in 42–64% yield is best accommodated by a tandem radical addition/radical 5-*exo* cyclization/ligand transfer sequence via **131A**, but not well by a two-electron polar reaction mechanism.

Weinreb demonstrated that **127** is an efficient catalyst in atom transfer radical cyclizations (ATRC) of 2,2-dichloro-6-heptenoate esters **133** (Fig. 38) [232–235]. It catalyzed the cyclizations at similar catalyst loadings and reaction times as  $\text{Ru}(\text{PPh}_3)_3\text{Cl}_2$  or  $\text{Fe}(\text{P}(\text{OEt})_3)_3\text{Cl}_2$  (see Part 2, Sects. 2.4 and 3.3.2), but is complementary in its reactivity. While iron or ruthenium catalysts gave chlorinated cyclopentanecarboxylates **135** and **136** preferentially, the molybdenum complex promoted a bicyclization leading to cyclopentane-fused butyrolactone **134** in 50% yield similar to Tsuji's result above. Monocyclic **135** and **136** were isolated only in 2% and 10% yield, respectively. Additionally, some 6-*endo* cyclization product **137** was also formed. This indicates that chlorine transfer from the more electropositive molybdenum complex is slower than from the iron- or ruthenium-based systems. Annulation reactions also proceeded in high yield, while 6-*exo* cyclization reactions were much less efficient. 2-Bromo- or 2-chloro-6-heptenoates were also applied under similar conditions, affording 58–63% yield of cyclized products [234]. The *cis/trans*-selectivity was not high for most acyclic substrates, but lactonization was facile again for most *cis*-derivatives. Annulation reactions also proceeded in 78% yield with moderate to excellent diastereoselectivity (see Part 2, Sects. 2.4 and 3.3.2).  $[\text{CpMo}(\text{CO})_2]$  triggered, in contrast to iron and ruthenium catalysts, 5-*exo* or 6-*exo* cyclizations of simple 1,1,1-trichloro-5-hexenes or 6-heptenes only in 11–21% yields (see Part 2, Sect. 2.4) [235].

A  $(\text{salan})\text{Mo}(\text{VI})$  oxo complex proved to be an efficient precatalyst for the pinacol coupling of aromatic aldehydes [236]. After reduction to the catalytically active  $(\text{salan})\text{Mo}(\text{IV})$  complex using stoichiometric amounts of Zn and  $\text{TMSCl}$ , pinacols were obtained with moderate to good *D,L*-selectivities and ee values.

## 8 Tungsten-Catalyzed Radical Reactions

A large body of work exists on radical reactions initiated by photocatalysis using tungsten polyoxometalate complexes [237]. Jaynes and Hill reported the first radical additions of hydrocarbons **138** to olefins **126** or acetylene (Fig. 39) [238]. The alkyl radicals were generated by hydrogen abstraction by photoexcited tetrakis-(tetrabutylammonium) decatungstate  $(\text{Bu}_4\text{N})_4\text{W}_{10}\text{O}_{32}$  catalyst **139** resulting from

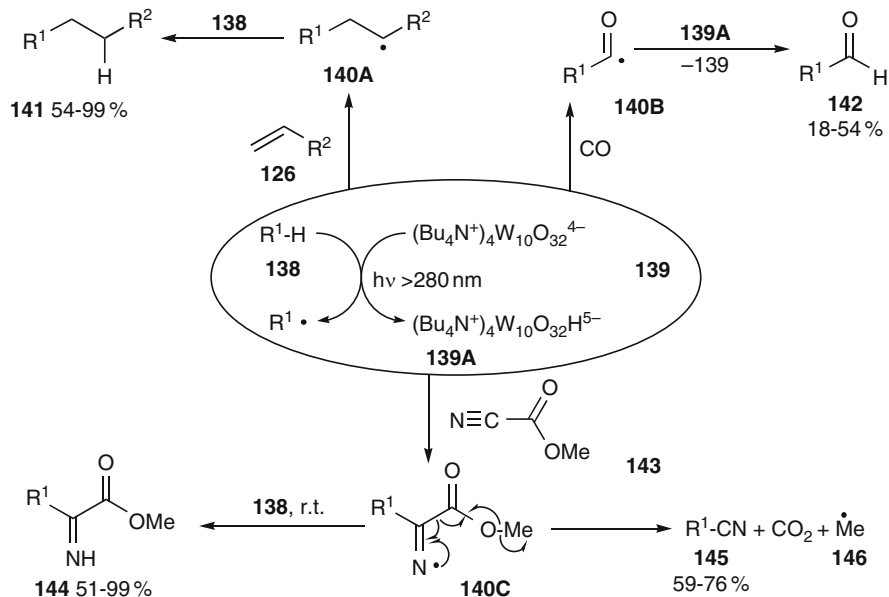
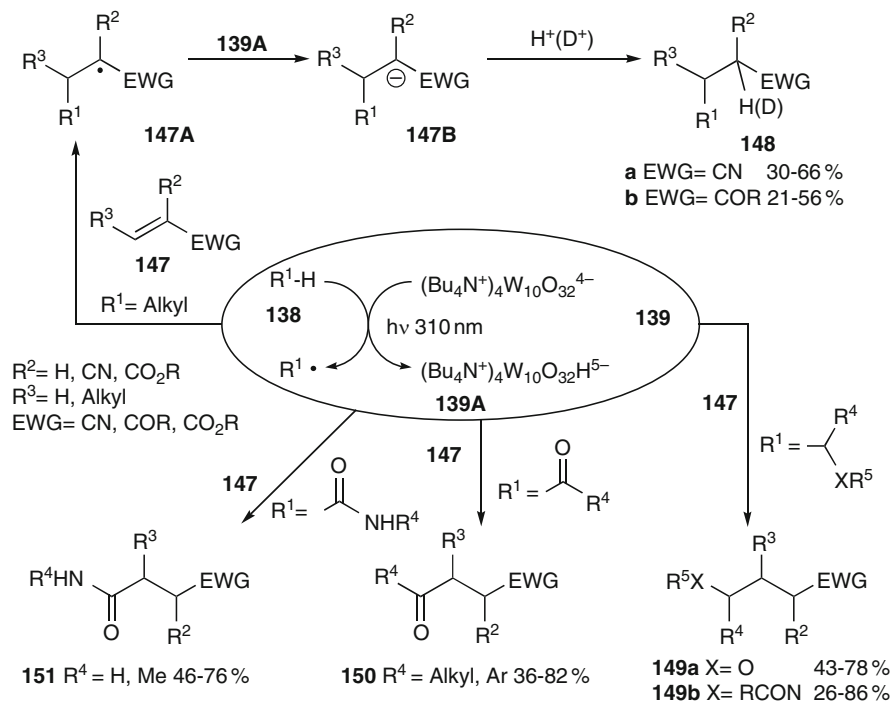


Fig. 39 Photocatalyzed radical reactions of hydrocarbons by tungstate complexes

irradiation with Pyrex-filtered light ( $\lambda > 280$  nm). The resulting alkyl radical **140A** forms product **141** by hydrogen abstraction from the substrate. The catalyst acts only as an initiator. A radical carbonylation under 1 atm of carbon monoxide providing aldehydes **142** succeeded under similar reaction conditions [239]. The reaction course for the carbonylation was proposed to be different from the radical addition, in that catalyst **139** is regenerated by hydrogen donation from reduced tungstate **139A** to acyl radical **140B**, which is thermodynamically more favorable than a chain process. For both processes a phosphotungstate catalyst  $(\text{Bu}_4\text{N})_3\text{PW}_{12}\text{O}_{32}$  is less efficient concerning yield and turnover.

The photocatalytic radical generation was also used in additions to methyl cyanofornate **143** [240]. The product distribution was dependent on the reaction temperature. At room temperature  $\alpha$ -imino esters **144** were formed in 51–99% yield, while at 90 °C nitriles **145** were isolated in 59–76% yield. At low temperature, the iminyl radical **140C** generated by the radical addition, abstracts a hydrogen atom from the substrate to continue a chain reaction, while its fragmentation to the nitrile prevails at high temperature, generating carbon dioxide and a methyl radical **146**, which acts as a chain carrier.

The concept of tungstate-catalyzed radical reactions was recently extended by Albini and coworkers to efficient radical addition reactions to electrophilic alkenes **147** (Fig. 40). Dondi et al. described the photocatalyzed addition of alkyl radicals generated by 310 nm irradiation of 2 mol% decatungstate **139** to  $\alpha,\beta$ -unsaturated nitriles [241] or  $\alpha,\beta$ -unsaturated ketones [242]. The yields of saturated nitriles **148a** were 30–66%, while those of saturated ketones **148b** amounted to 21–56% after



**Fig. 40** Photocatalyzed radical additions to electron-deficient olefins

16 h irradiation. Alkyl radical generation and radical addition to **147** occur similarly as above, the termination of the reactions proceeding by SET reduction of the resulting  $\alpha$ -cyano or  $\alpha$ -carbonyl radical **147A** by the reduced photocatalyst  $\text{HW}_{10}\text{O}_{32}^{5-}$ . Protonation of anionic species **147B** leads to the product **148** as confirmed by deuteration experiments using  $\text{D}_2\text{O}$ . The use of deuterated substrates **138** does not lead to deuterium incorporation in **148**. The intermediate radicals were trapped by the nitron spin trap PBN and detected by EPR spectroscopy. The regioselectivity of hydrogen abstraction from unsymmetric substrates **138** was probed [243]. Nucleophilic radicals, such as ketyl or  $\alpha$ -alkoxyalkyl radicals, were efficiently generated from alcohols or ethers and added to **147** providing  $\gamma$ -functionalized carbonyl compounds **149a** in 43–78% yield [244]. *N,N*-Dialkylamides underwent hydrogen abstraction at the nitrogen substituent to afford  $\gamma$ -amino carbonyl compounds **149b** in 26–86% yield [245]. Acyl radicals were similarly generated by hydrogen abstraction from aldehydes. They added under very mild conditions to **147** giving  $\gamma$ -oxo carbonyl compounds **150** in 36–82% yield [246, 247]. Carbamoyl radicals were formed from formamides and afforded substituted amides **151** in 46–76% yield [245]. Ordinary sunlight was used to trigger these radical addition reactions in 40–90% yield [248]. Acyl or ketyl radical additions to  $\text{C}_{60}$  were also successful [249, 250].

## 9 Manganese-Catalyzed Radical Reactions

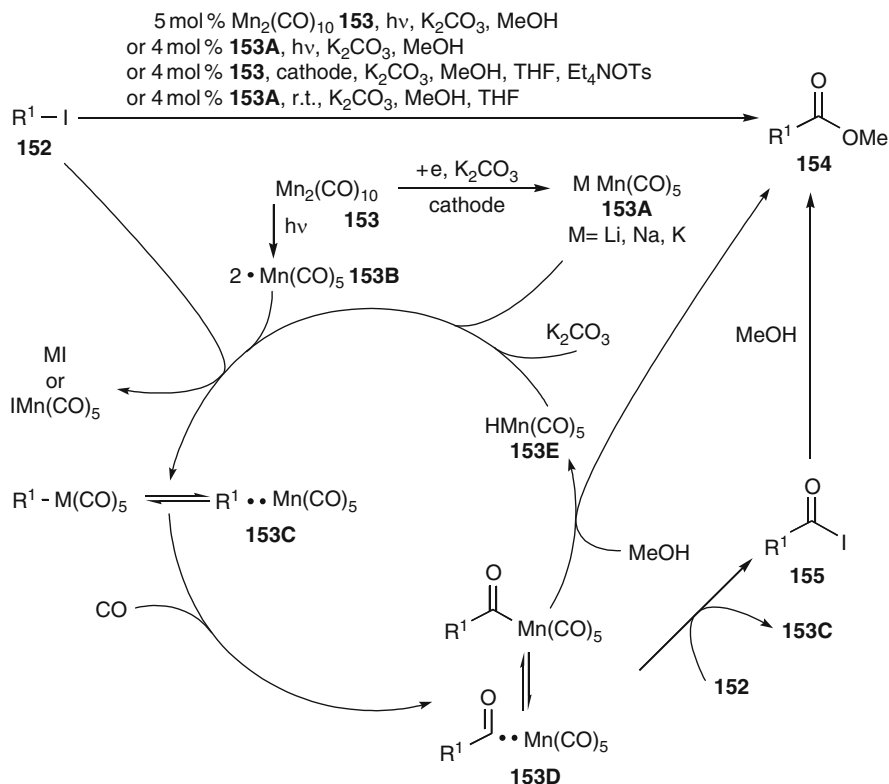
Organomanganese compounds are versatile reagents in organic chemistry [251]. In radical chemistry  $\text{Mn}(\text{OAc})_3$  is applied frequently as a stoichiometric oxidant to trigger radical additions and cyclizations ([22], recent reviews [252–255]). Manganese (salen) complexes gained considerable importance as precatalysts in the Jacobsen–Katsuki epoxidation, which involves a radical process [39, 107]. Groves recently reported an oxidative halogenation of hydrocarbons catalyzed by (tetraphenylporphyrin) $\text{MnCl}$  using bleach [256]. Catalytic oxidative dimerization reactions of alkynyl, aryl, and vinylstannanes using 10 mol%  $\text{MnCl}_2$  and stoichiometric amounts of iodine leading to diynes, dienes, or biaryls were developed [257].

### 9.1 $\text{Mn}(-\text{I})$ - $\text{Mn}(0)$ - $\text{Mn}(\text{I})$ and $\text{Mn}(0)$ - $\text{Mn}(\text{I})$ Catalysis

Kondo and coworkers studied the photochemically stimulated alkoxyacylation of alkyl iodides **152** by 1 atm of carbon monoxide catalyzed by a large number of metal carbonyl complexes [258, 259]. Among them 5 mol%  $\text{Mn}_2(\text{CO})_{10}$  **153** and manganates  $\text{MMn}(\text{CO})_5$  ( $\text{M}=\text{Na}, \text{K}, \text{Li}, \text{PPN}, \text{SnPh}_3$ ) **153A** were highly active giving 62–98% yield of esters **154** (Fig. 41). The reaction can be alternatively initiated by cathodic reduction, but only  $\text{Mn}_2(\text{CO})_{10}$  **153** was catalytically active in the presence of a base like  $\text{K}_2\text{CO}_3$ . Alkali manganates  $\text{MMn}(\text{CO})_5$  **153A**, but not **153**, catalyzed the thermal alkoxyacylation at room temperature in the absence of light. The latter reaction is completely inhibited by a radical scavenger like galvinoxyl. Ryu and coworkers reported similar photochemically initiated radical alkoxyacylation and aminocarbonylation reactions of **152** using 2.5–4 mol% of **153** as the catalyst providing esters **154** and amides in 48–91% yield [260].

Kinetic investigations point to a radical process. The initiating species after photochemical homolysis of **153** is probably  $\text{Mn}(\text{CO})_5$  **153B**, which abstracts iodine from substrate **152**. In the reductive and thermal variant the pentacarbonylmanganate anion **153A**, from which electron transfer to the iodide readily occurs, is catalytically active. Both radicals, **153C** and  $\text{Mn}(\text{CO})_5$  were detected by ESR spectroscopy. The radical seems, however, not to be free but caged. It adds to carbon monoxide forming acyl radical-manganese pentacarbonyl pair **153D**. It was proposed that ligand substitution by methanol leads to ester **154** and  $\text{HMn}(\text{CO})_5$  **153E**, which re-forms catalyst **153B** with base. It can, however, not be completely excluded that a radical chain process is involved, in which the acyl radical abstracts iodine from **152** giving acyl iodide **155**. This would undergo classical alcoholysis to **154**, since atom transfer radical carbonylations [261, 262] and also manganese-catalyzed atom transfer reactions (see below) are precedented.

Parsons and coworkers proved that photochemically induced atom transfer radical cyclization of *N*-allyl iodoacetamide **156** proceeded smoothly in the presence of 10 mol% of  $\text{Mn}_2(\text{CO})_{10}$  **153** at room temperature affording 4-iodomethylpyrrolidone



**Fig. 41** Manganese-catalyzed carbonylation under photochemical, reductive and thermal initiation

**157** in 78% yield (Fig. 42) [263, 264]. The reaction was independent of the amount of **153**. Product **157** was inert to **153** on photolysis. Moreover, it was shown that hexyl iodide was recovered in 77% yield after photolysis under similar conditions. The authors concluded that  $\text{IMn}(\text{CO})_5$  **156B** does not transfer the iodine atom to radical **156C** (dashed arrow). A direct atom transfer between **156** and **156C** operates.

Addition/cyclization sequences using diallyl ethers, diallylamines, and diallylmalonates **158** and bromotrichloromethane as the substrates provided cyclic products **159** in 60–99% yield in a 2.5–18:1 *cis/trans*-diastereomeric ratio (Fig. 43). Here, catalyst **153B** abstracts the bromine atom from  $\text{Cl}_3\text{CBr}$ . The generated trichloromethyl radical adds subsequently to **158** forming radical **158A**, which cyclizes to radical **158B**. The stabilization to product **159** can occur either by ligand transfer from coformed bromomanganese pentacarbonyl (dashed cycle) or by direct bromine transfer from  $\text{Cl}_3\text{CBr}$  (full cycle). The exact course of the atom transfer process has so far not been established. Therefore, the exact role of  $\text{Mn}(\text{CO})_5$  being either a chain carrier or only an initiator remains to be clarified. The reactions can also be performed in a biphasic medium to facilitate separation of manganese byproducts [265]. The methodology was later extended to tandem atom

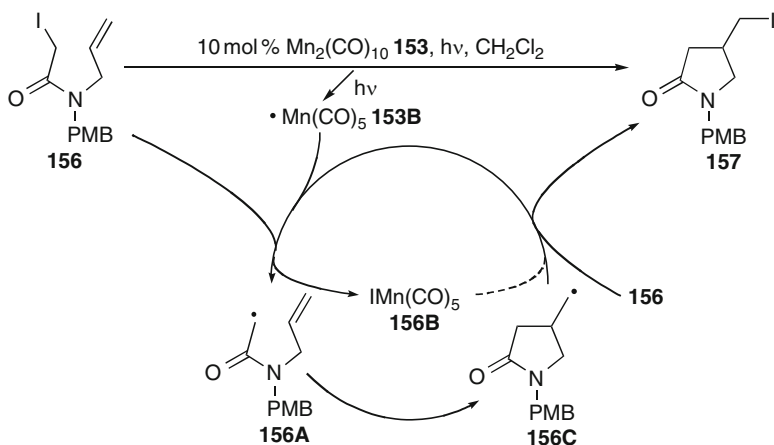


Fig. 42  $\text{Mn}_2(\text{CO})_{10}$ -catalyzed atom transfer radical cyclizations

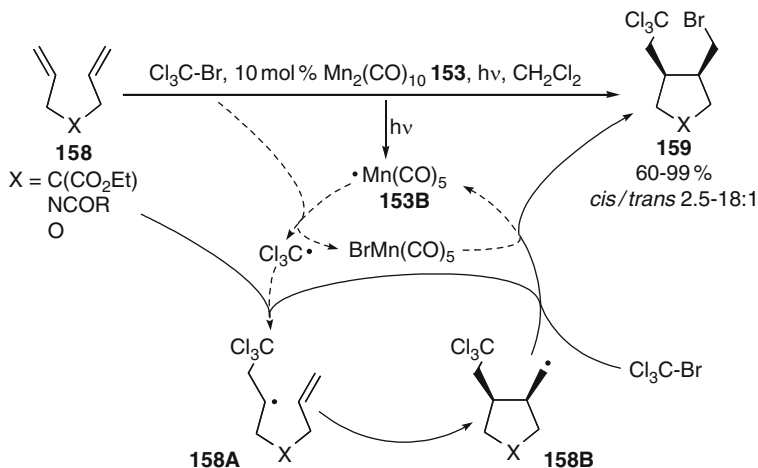


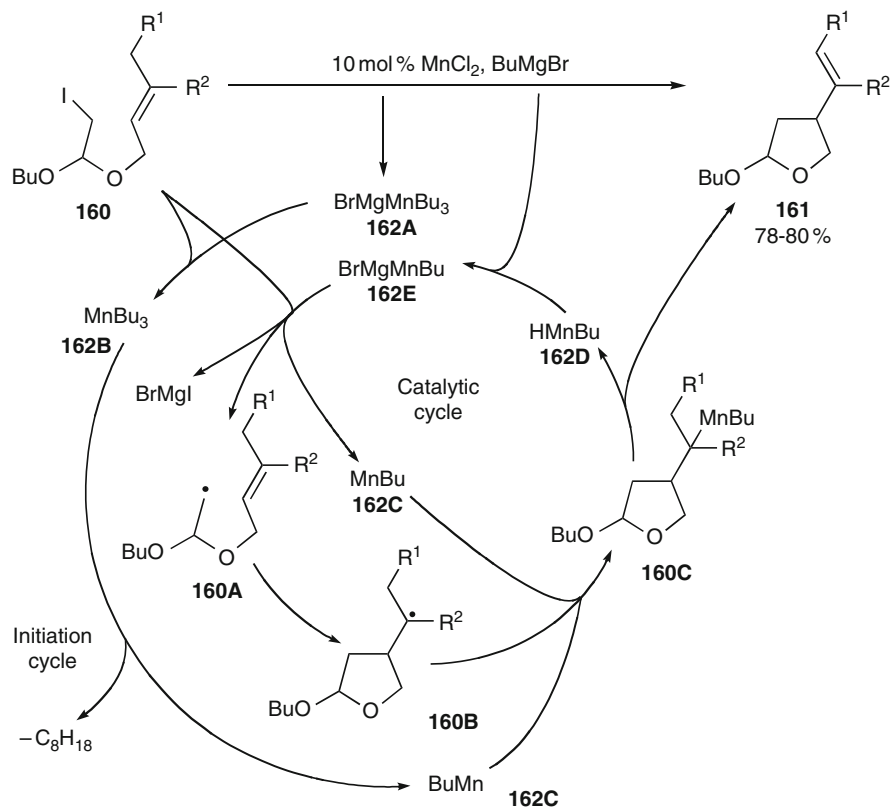
Fig. 43 Atom transfer radical addition/cyclizations initiated by  $\text{Mn}_2(\text{CO})_{10}$

transfer radical addition/5-*exo* cyclization sequences applying sulfonyl chlorides instead of  $\text{Cl}_3\text{CBr}$  as the reagents [266]. Kharasch additions to allylmalonate were also possible using 10 mol% of  $\text{Mn}_2(\text{CO})_{10}$ . The products can be cyclized in sequence with an intramolecular alkylation mediated by DBU giving cyclopropanes in 56–88% yield [266].

## 9.2 $\text{Mn}(0)$ - $\text{Mn}(I)$ - $\text{Mn}(II)$ Catalysis

Alkyl and aryl radical cyclizations were developed using catalytic amounts of  $\text{MnCl}_2$  and butylmagnesium bromide as a stoichiometric reductant (Fig. 44)





**Fig. 44** Manganate-catalyzed radical 5-*exo* cyclizations with  $\beta$ -hydride elimination

[267, 268]. Iodoacetaldehyde allyl acetals **160** gave alkenyl substituted butyrolactols **161** in 80 and 78% yield as a diastereomeric mixture. The reaction starts with initial generation of bromomagnesium tributylmanganate **162A** by reaction of  $\text{MnCl}_2$  with the butyl Grignard reagent. This electron-rich complex acts as a SET reductant to the alkyl iodide [269] giving rise to alkyl radical **160A**, which cyclizes to radical **160B**. The cogenerated tributylmanganese **162B** is prone to reductive elimination affording butylmanganese(I) **162C**, which is able to couple with radical **160B**. The resulting dialkylmanganese(II) **160C** stabilizes by  $\beta$ -hydride elimination to product **161** and manganese hydride complex **162D**. The latter may be transformed by excess Grignard reagent and reductive elimination of butane to the likely catalytically active manganese(0) species, the manganate complex **162E** (or the metal itself). This even more electron-rich intermediate continues the catalytic cycle by SET reduction of the substrate **160**.

*ortho*-Iodophenyl prenyl ether **163a** or *ortho*-iodo-*N,N*-diprenylaniline **163b** gave 3-isopropenyldihydrobenzofurans **164a** or 3-isopropenyldoline **164b** in 70 and 81% yield, respectively, when treated with 20 mol%  $\text{MnCl}_2$  and excess

butylmagnesium bromide (Fig. 45) [267]. This reaction requires oxygen to proceed catalytically. The mechanism and especially the role of oxygen is not entirely clear. Bromomagnesium tributylmanganate(II) **162A** was probably also initially generated and reduces the aryl iodide. Subsequently a radical 5-*exo* cyclization follows providing **163A** after coupling with a manganese species. The radical nature of the cyclization is supported by the complete ring opening of 3-cyclopropylallyl *ortho*-iodophenyl ether after cyclization.

### 9.3 Mn(II)-Mn(III) Catalysis: Radical Additions

#### 9.3.1 Mn(II) as an Initiator

Oshima et al. observed that lithium tributylmanganate **166** can be used as a radical initiator to catalyze the hydrogermylation of alkynes **167** or alkenes (Fig. 46) [270]. The catalyst was generated in situ from 10 mol% of  $\text{MnCl}_2$  and 3 equiv. of butyllithium. It reduces  $\text{Ph}_3\text{GeH}$  **165** to a triphenylgermyl radical, which adds to the substrate **167**. Hydrogen abstraction of **167A** from **165** leads to products **168**, which were isolated in 61–97% yield. In case of terminal vinylgermanes, products were isolated as 4–10:1 *Z/E*-mixtures. Internal alkynes gave only (*Z*)-vinylgermanes. The radical nature of the hydrogermylation is supported by the fact that classical radical conditions give the products with similar diastereomeric ratios and that

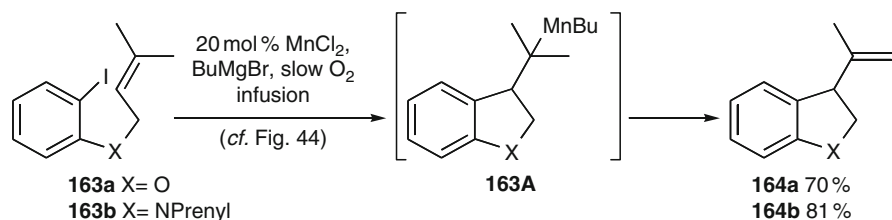


Fig. 45 Manganate-catalyzed aryl radical cyclization reactions

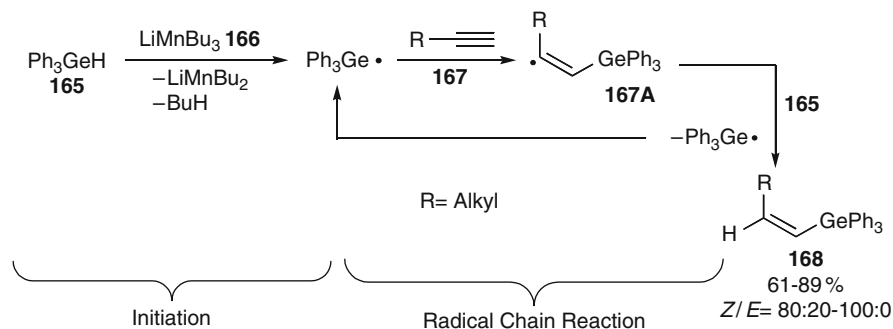


Fig. 46 Manganate(II)-initiated hydrogermylations of alkynes



adduct radical **172B** carries on with halogen abstraction from **172**. The yield of adducts **173** amounted to 40–98%. The method is also applicable to tandem addition/5-*exo* cyclization sequences similar to those in Figs. 38 and 43 furnishing cyclopentane derivatives in 60–83% yield. Similar ATRA of bromomalonate to alkenes are possible in 40–80% yield using catalytic oxidative malonyl radical generation from electrochemically formed  $\text{Mn}(\text{OAc})_3$  [273].

### 9.3.2 Mn(II)-Mn(III) Oxidative Catalysis

A wealth of  $\text{Mn}(\text{OAc})_3$ -mediated radical additions and cyclizations is documented in the literature [22, 252–255]. However, only very limited success was achieved rendering these useful transformations catalytic. Shundo and coworkers reported the radical addition of ethyl cyanoacetate **174** to alkenes **175** catalyzed by  $\text{Mn}(\text{OAc})_3$  formed under constant current conditions from 20 mol%  $\text{Mn}(\text{OAc})_2$  (Fig. 49) [274, 275]. The reaction proceeds by oxidative generation of radical **174A** catalyzed by Mn(III) and subsequent addition to **175**. The adduct radical **174B** stabilizes by reduction giving alkylcyanoacetates **176** in 50–64% yield. When 10 mol%  $\text{Cu}(\text{OAc})_2$  was added, radical **174B** couples to Cu(II) forming a Cu(III) species **174C**, which is subject to  $\beta$ -hydride elimination leading to allylic cyanoacetates **177** in 44–58% yield. Warsinsky and Steckhan subsequently disclosed similar  $\text{Mn}(\text{OAc})_3$ -catalyzed electrochemically mediated addition reactions of  $\alpha$ -nitroacetophenone or nitroacetamides to simple olefins applying 10 mol%  $\text{Mn}(\text{OAc})_2$ . The addition products were isolated in 37–54% yield [276]. Linker and colleagues used cheap potassium permanganate to mediate the

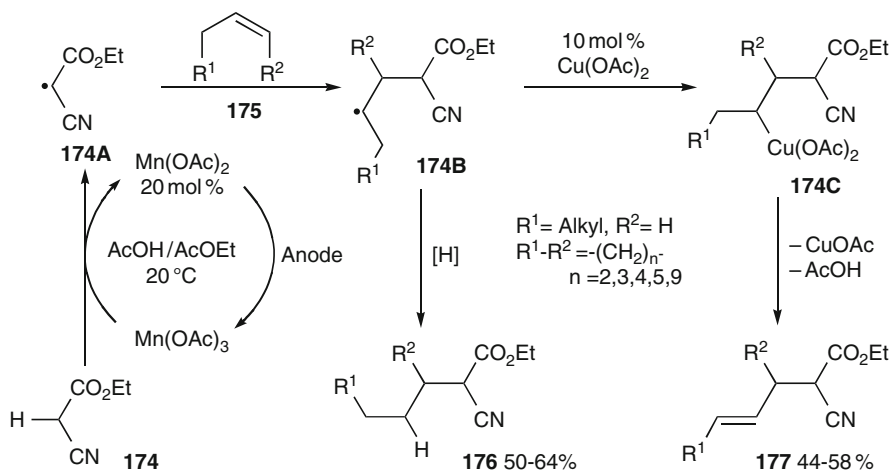
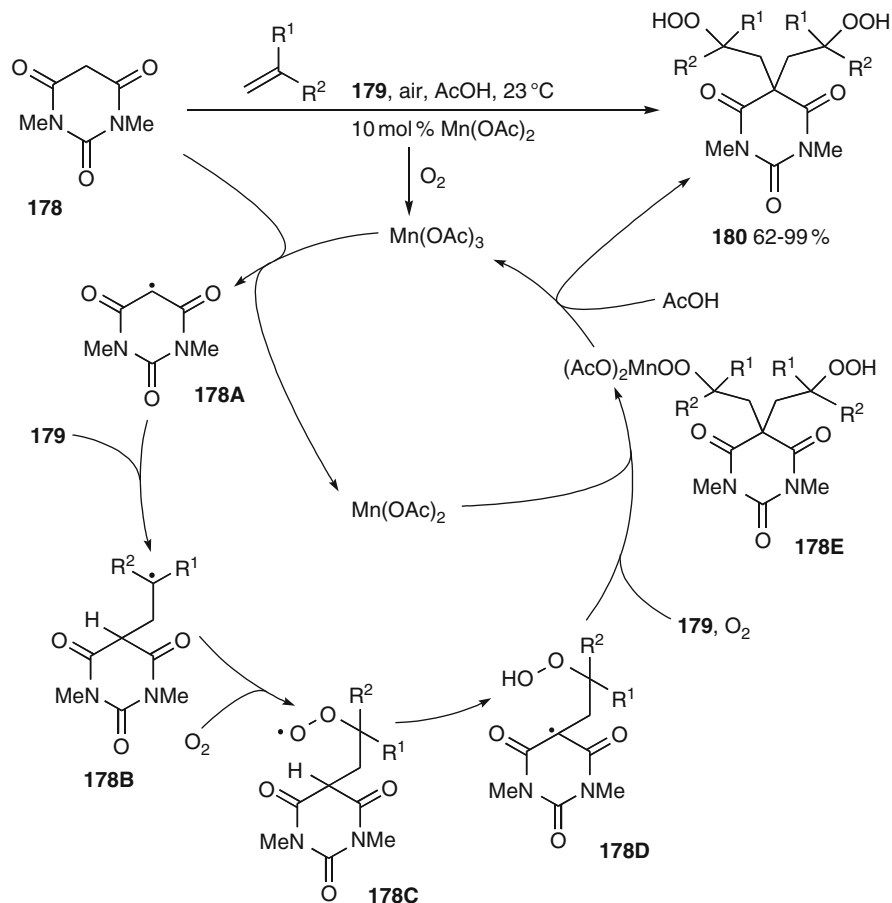


Fig. 49 Electrochemically mediated manganese-catalyzed radical additions



**Fig. 50** Manganese(III)-catalyzed radical addition/peroxidation reactions

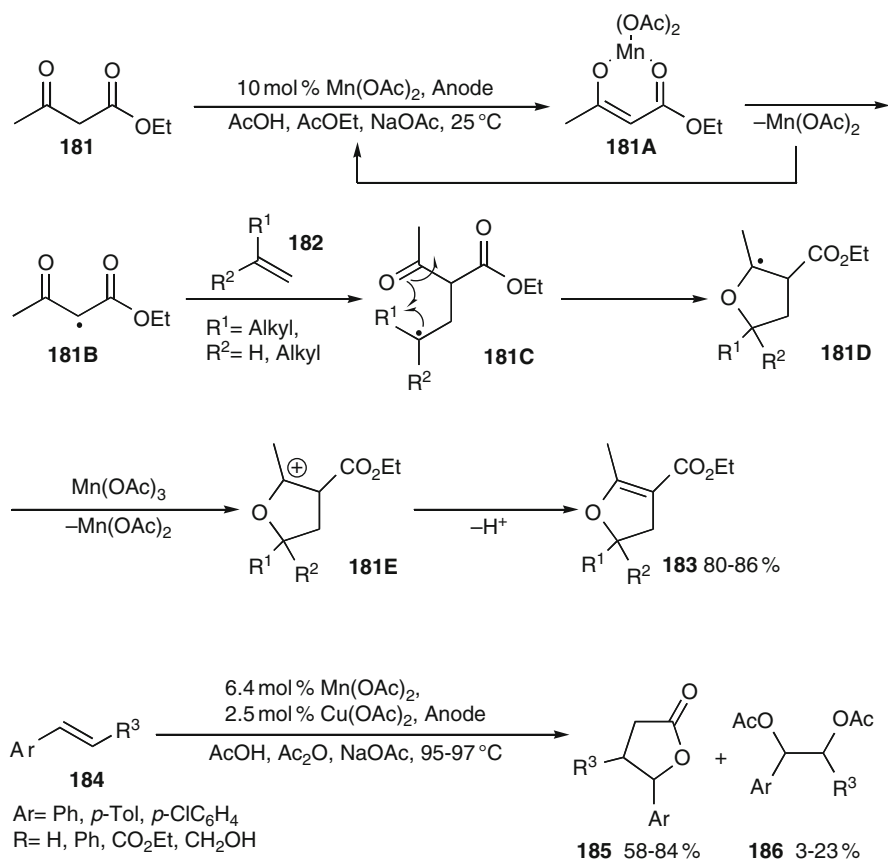
Mn(III)-catalyzed radical addition of dimethyl malonate to alkenes. Alkylmalonates were isolated in 32–41% yield [277].

Nishino et al. found that barbiturates **178** undergo a double radical addition/hydroperoxidation catalyzed by 10 mol% Mn(OAc)<sub>2</sub> in the presence of oxygen in 62–99% yield (Fig. 50) [278]. The active Mn(III) catalyst is generated by air oxidation. It oxidizes **178** to radical **178A**, which adds to olefin **179**. The resulting radical **178B** couples with oxygen to peroxy radical **178C**. This radical is activated for a 1,5-hydrogen transfer leading to radical **178D**. Another radical addition to **179** and coupling with oxygen furnishes a peroxy radical that is reduced by Mn(OAc)<sub>2</sub> to manganese peroxide **178E**. Ligand exchange by acetic acid liberates product **180** and regenerates the manganese(III) catalyst. Pyrazolidin-3,5-diones react similarly in 75–98% yield [279, 280]. Quinoline-2,4-diones can also be applied in these reactions [281].

### 9.4 Mn(II)-Mn(III) Catalysis: Radical Cyclizations

Electrochemically mediated, Mn(OAc)<sub>3</sub>-catalyzed radical addition/cyclization reactions were reported by Shundo and coworkers (Fig. 51) [275, 282]. Ethyl acetoacetate **181** added to olefins **182** using 10 mol% of Mn(OAc)<sub>2</sub> under constant current conditions. The β-keto ester initially forms a manganese(III) chelate **181A** according to the accepted mechanism for such reactions, which fragments homolytically to radical **181B** in an inner-sphere electron transfer process. Addition of this radical to **182** leads to radical **181C**. This radical underwent a 5-*endo* cyclization to the carbonyl group forming radical **181D**, which is easily oxidized to carbocation **181E**. Deprotonation furnishes dihydrofuran derivatives **183** in 80–86% yield.

Acetic acid can be used in carboxymethylation/lactonization reactions of arylalkenes **184** catalyzed by electrochemically generated Mn(OAc)<sub>3</sub> and Cu(OAc)<sub>2</sub>



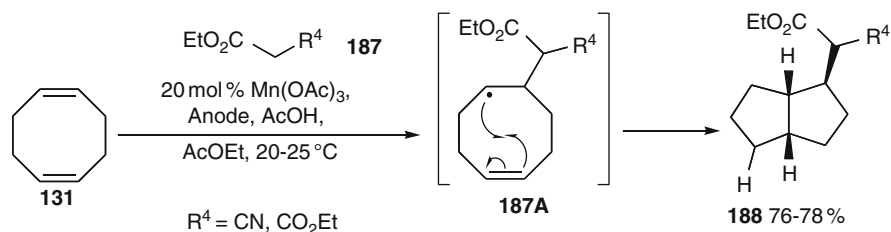
**Fig. 51** Oxidative radical addition/lactonization reactions catalyzed by Mn(OAc)<sub>3</sub>

in the presence of sodium acetate as the supporting electrolyte. The reaction gave 5-arylbutyrolactones **185** in 58–84% yield. The transformation proceeds via oxidative carboxymethyl radical generation from acetic acid induced by  $\text{Mn}(\text{OAc})_3$  and subsequent radical addition to **184**. The resulting benzylic radical is most likely oxidized by  $\text{Cu}(\text{OAc})_2$  to a benzylic carbocation, which is trapped by the carboxylate function affording **185**. Some direct SET oxidation of **184** and nucleophilic trapping by acetate leading to product **186** was also observed. When ammonium acetates were used as supporting electrolytes **186** became the major products. A Monsanto group reported a similar carboxymethylation of butadiene with acetic acid for the preparation of sorbic acid [283].

Diethyl malonate or ethyl cyanoacetate **187** afforded bicyclo[3.3.0]octane derivatives **188** in a tandem radical addition/transannular 5-*exo* cyclization sequence with cyclooctadiene **131** in 76 and 78% yield, respectively [275]. (4-Pentenyl)arenes were employed in a similar tandem radical addition/radical 6-*exo* cyclization process yielding tetraline derivatives in 37–79% yields. Linker used cheap potassium permanganate to mediate the Mn(III)-catalyzed radical addition/cyclization of dimethyl malonate to **131** in 58% yield [277]. Similar conditions were later used by Parsons and coworkers in a radical addition/cyclization of 4-hydroxy-2-quinolone to 3-methyl-1-buten-3-ol [284] (Fig. 52).

Nishino and coworkers reported a number of oxidative radical addition/cyclization sequences catalyzed by manganese triacetate. An early example was the reaction of ethyl acetoacetate **181** to 1,1-diphenylethylene **189** catalyzed by 10 mol%  $\text{Mn}(\text{OAc})_3$  in the presence of oxygen, which led to radical **189A** (Fig. 53; cf. Figs. 50 and 51). Coupling with reduced  $\text{Mn}(\text{OAc})_2$ , hydrolysis of manganese peroxide **189B**, and cyclization provided endoperoxide **190** in 65% yield as a single product [285]. *N*-Acyl-4-pyridone-3-carboxylates [286] or 2,4-piperidindiones [287] reacted analogously in 17–99% yield. Similar reaction conditions, but a higher catalyst loading of 40 mol%, was necessary to promote the synthesis of endoperoxy propellanes in 28–85% yield [288].

The oxidative radical ring opening of cyclopropanols **191** mediated by  $\text{Mn}(\text{pic})_3$  was developed by Narasaka and coworkers. Their efforts culminated recently in the development of a silver-catalyzed method (see Part 3, Sect. 6.2). Kulinkovich et al. based a manganese-catalyzed process on it. Manganese abietate **192** (1–1.5 mol%) was used as the catalyst and oxygen as the terminal oxidant (Fig. 54) [289].



**Fig. 52** Tandem oxidative radical addition/transannular radical cyclization reactions

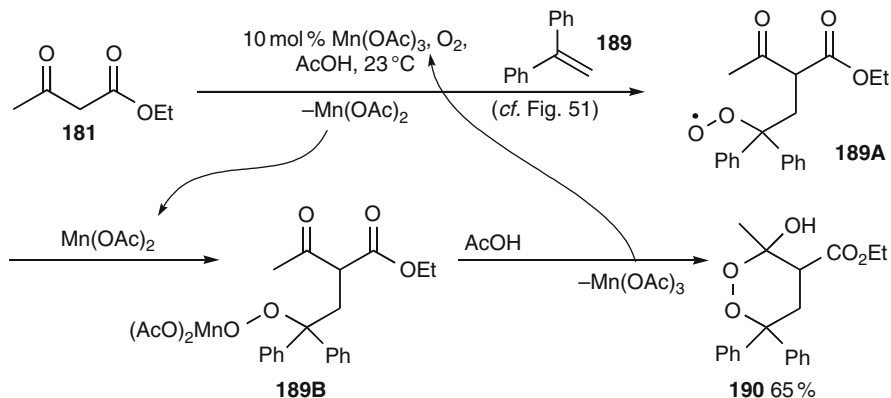


Fig. 53 Manganese-catalyzed radical addition/peroxidation reactions

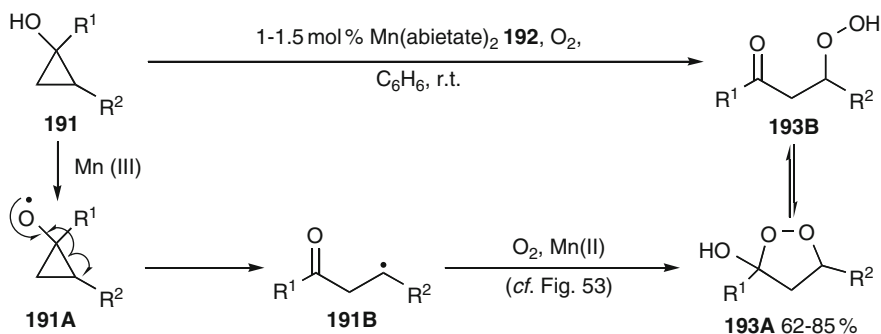


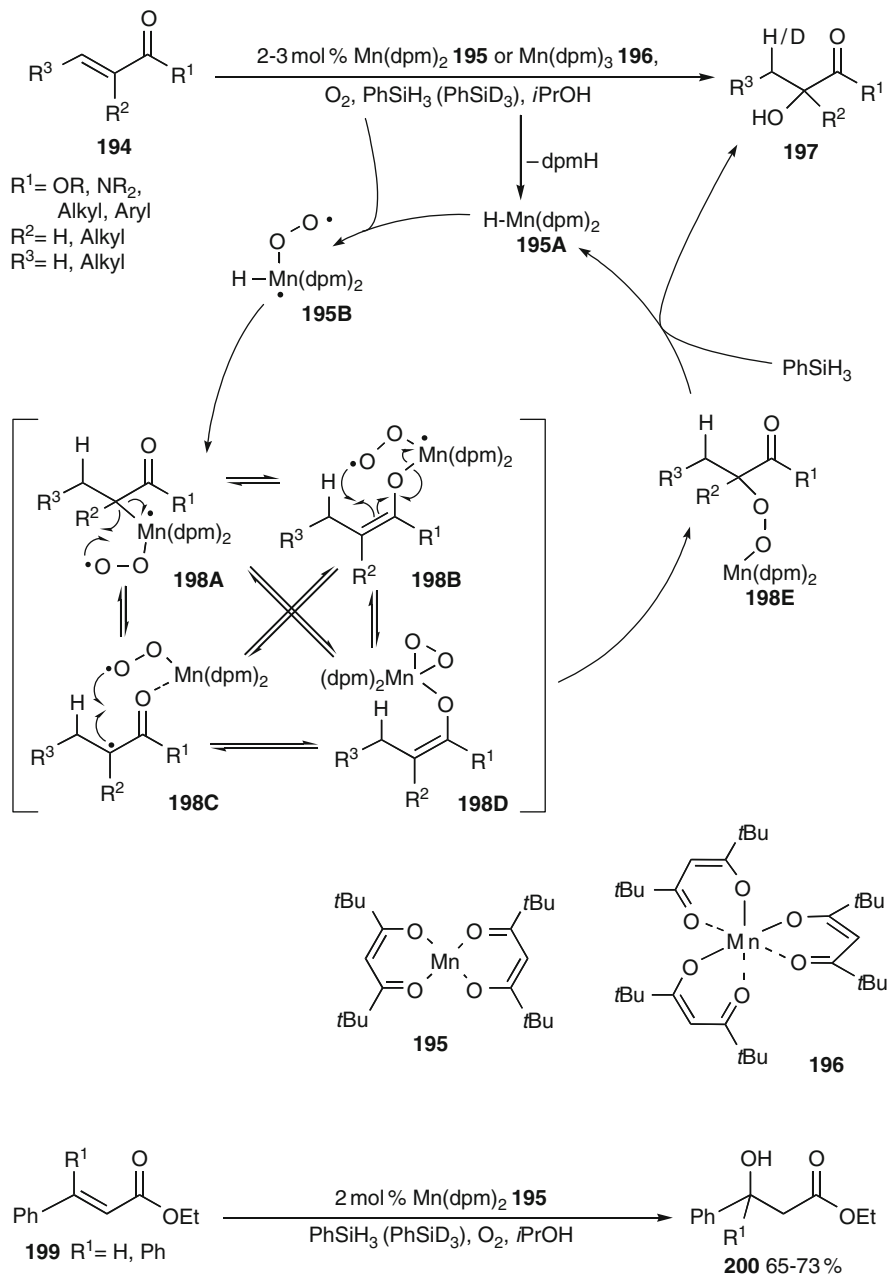
Fig. 54 Oxidative cyclopropanol cleavage catalyzed by Mn(III) abietate

A manganese(III) species is probably initially formed, which generates cyclopropyloxy radical **191A**. This undergoes an almost barrierless ring opening to  $\beta$ -keto radical **191B**, which is trapped by excess oxygen. SET reduction of the resulting peroxy radical by manganese(II) regenerates the catalyst and gives the final  $\beta$ -hydroperoxy ketones **193**. The products were isolated in 62–85% yield and consist of an equilibrium mixture of cyclic 1,2-dioxolane isomers **193A** and acyclic  $\beta$ -hydroperoxy ketone **193B**. Compounds **193** can easily be transformed to valuable epoxyketones by base treatment.

## 9.5 Mn(II)-Mn(III)-(Mn(IV)) Catalysis: Hydrofunctionalization of Alkenes

Mukaiyama and colleagues reported a manganese-catalyzed hydration of  $\alpha,\beta$ -unsaturated esters **194** ( $\text{R}^1=\text{OR}$ ) (Fig. 55) [290]. Using bis(divaloyl-methanato)-manganese(II) **195** as the catalyst in the presence of oxygen and





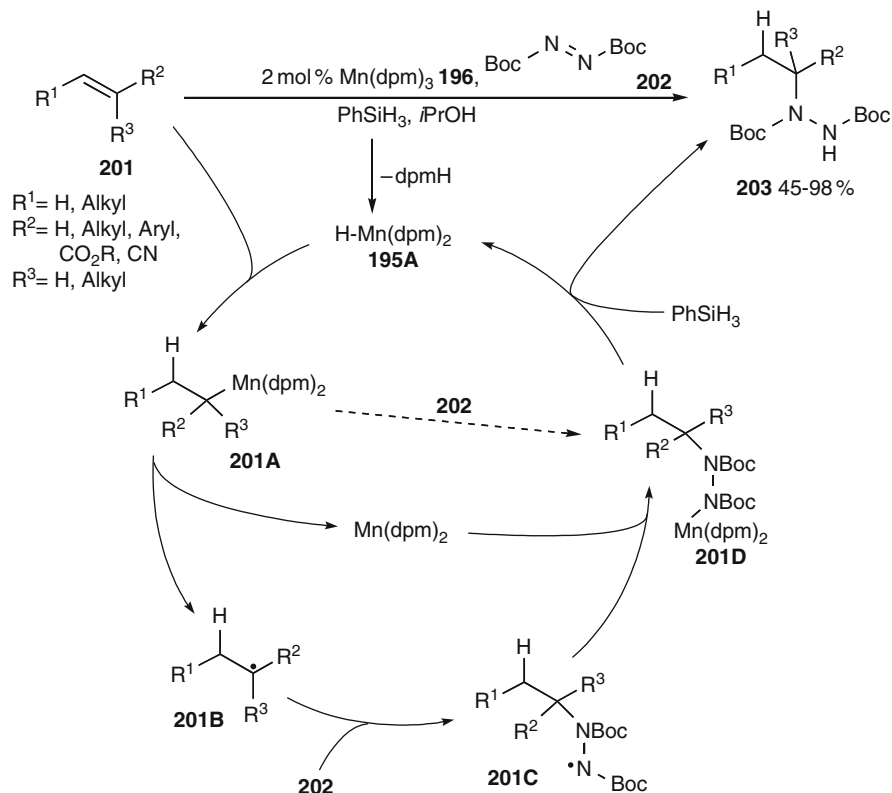
**Fig. 55** Mn(II)-Mn(III)-catalyzed hydration of  $\alpha,\beta$ -unsaturated carbonyl compounds

phenylsilane as the reducing agent  $\alpha$ -hydroxy esters **197** were obtained in 76–94% yield as single isomers. The regioselectivity of the hydration reverses to products **200**, however, when  $\beta$ -arylenoates **199** are used as substrates.

This method was applied by Magnus and coworkers in total syntheses of complex *Kopsia* alkaloids [291–294] and very recently by Carreira and colleagues in the total synthesis of Banyaside B [295]. Magnus and coworkers extended the method to  $\alpha,\beta$ -unsaturated ketones **194** ( $R^1$ =Alkyl, Aryl) and found that the reaction proceeds not only with  $Mn(dpm)_2$  **195**, but also with  $Mn(dpm)_3$  **196** in the presence of  $PhSiH_3/iPrOH/O_2$  under identical conditions.  $\alpha$ -Hydroxy ketones were isolated in 50–95% yield [296]. Control experiments showed that  $Mn(dpm)_3$  was converted to  $HMn(dpm)_2$  **195A** by the silane in the presence of *iPrOH*, but not in its absence. When this complex was exposed to oxygen a new complex, presumably manganese(IV) peroxy complex **195B** results as indicated by totally different UV/vis spectra. This complex undergoes hydromanganation leading to a manganese enolate **198**. This adduct can be assumed to be one of the enolate or diradical valence tautomeric structures **198A–D**. No matter what species dominates, the peroxy unit can be transferred to the  $\alpha$ -carbon by homolysis and recombination as in **198A**. It may react intramolecularly by coupling or addition as in **198B** or diradical **198C** or be transferred via nucleophilic attack at the peroxide as in **198D**. This coupling gives rise to manganese peroxide **198E**. The intermediacy of a carbon-centered radical was not proven rigorously, but seems more likely than a closed-shell pathway via **198D**. Especially the reversal of regioselectivity (**197** vs **200**) and the occurrence of the typical radical probe reactions in the related hydrohydrazination reaction (see below) are not easily accommodated by a closed-shell pathway. Reduction of **198E** by  $PhSiH_3$  provides hydroxy carbonyl compounds **197** either directly by reduction of the O–O bond of **198E** or by reduction of an intermediate hydroperoxide, which forms after hydrolytic cleavage of the manganese–oxygen bond in **198E**. Hydroperoxides were sometimes isolated as side products in the hydration of ketones. The active catalyst **195A** is regenerated by reaction with excess silane.  $\alpha,\beta$ -Unsaturated nitriles are also subject to hydration of the double bond providing a convenient access to cyanohydrins in 13–54% yield [297]. When  $\alpha,\beta,\gamma,\delta$ -unsaturated carbonyl compounds were used, the more electron-rich remote double bond is hydrated with good regioselectivity. In the absence of oxygen, only conjugate reduction of the enone function occurs [298].

This reaction can be also performed asymmetrically, when it is applied to  $\alpha,\beta$ -unsaturated amide derivatives bearing a chiral auxiliary [299]. Among several common auxiliaries, the *trans*-2,5-dinaphthylpyrrolidine unit proved to be optimal, giving  $\alpha$ -hydroxy amides in 62–87% yield and diastereomeric ratios ranging from 78:22 up to 97:3 for the compound with (*R*)-configuration.

Carreira and coworkers recently investigated hydrohydrazination reactions of olefins **201** with azodicarboxylate **202** (Fig. 56) [300, 301]. Similar to the hydration described above, 2 mol% of  $Mn(dpm)_3$  **196** as the catalyst and phenylsilane as the reducing agent proved to be optimal to obtain alkylhydrazines **203** in 45–98% yield. The manganese catalyst is considerably more reactive than cobalt catalysts applied in the same reaction (see Part 2, Sect. 5.7). Even tetrasubstituted alkenes underwent



**Fig. 56** Manganese(III)-catalyzed hydrohydrazination of olefins

the reaction in good yields. It is, however, sometimes less regioselective for the Markovnikov product. Attempts to conduct the hydrohydrazination asymmetrically using Evans' auxiliary failed, but a pantolactone ester gave moderate diastereoselectivity. The intermediacy of radicals is supported by the ring opening of vinylcyclopropane during the reaction and by the radical 5-*exo* cyclizations at the faster end of the kinetic scale, which proceeded in good yields (cf. Fig. 8). From a variation of the applied probes, a rate constant for the subsequent addition of the radical to the azodicarboxylate of ca.  $2.0\text{--}2.5 \times 10^8 \text{ mol}^{-1} \text{ s}^{-1}$  was derived. The reaction was assumed to proceed by initial hydromanganation of olefins **201** providing organomanganese species **201A**. Although a direct carbomanganation of the azodicarboxylate **202** cannot be excluded completely, the radical probe reactions suggest a homolysis to radical **201B**, which adds to **202**. The amidyl radical **201C** may couple to the reduced  $\text{Mn(dpm)}_2$  and the resulting manganese carbazate **201D** reacts subsequently with the silane to regenerate the catalyst **195A** and to liberate products **203**.

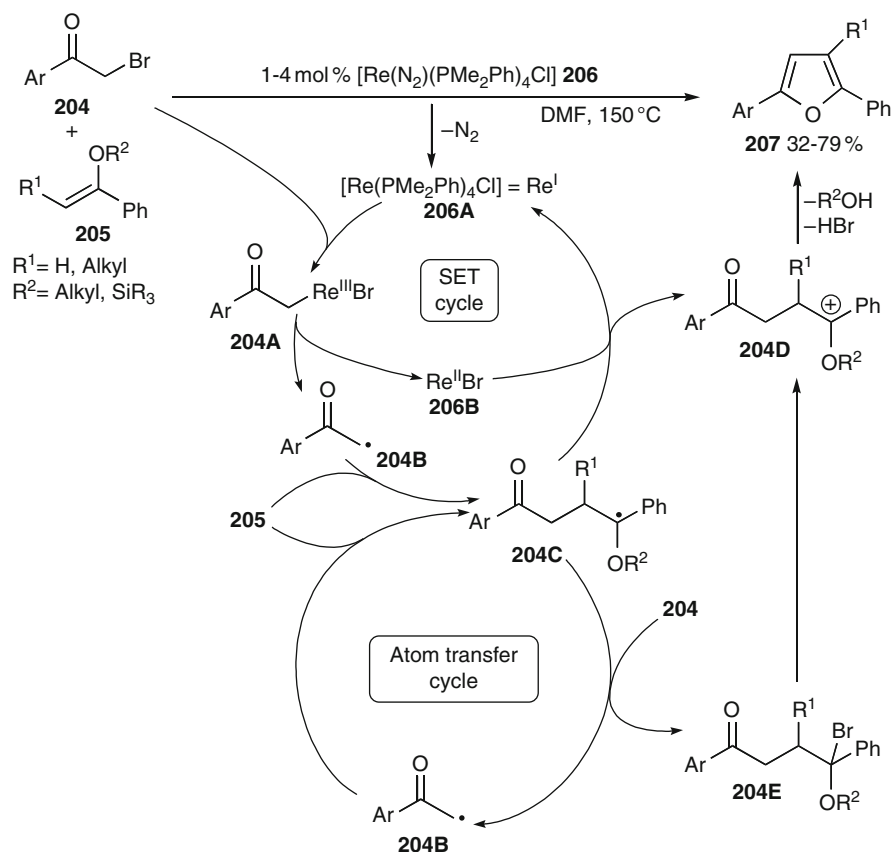
Alkenes can be cleaved to aldehydes by 5 mol% of a  $(\text{salen})_2\text{Mn}$  complex in the presence of air and thiophenols in 13–98% yield. The reaction involves an initial

thiyl radical addition to the olefin and trapping by oxygen. The resulting peroxy radical is in turn most likely transformed to an alkoxy radical by the catalyst and undergoes  $\beta$ -fragmentation to form the most stable radical. The reaction can also be performed starting from the corresponding disulfide under photostimulation [198].

## 10 Rhenium-Catalyzed Radical Reactions

Kondo and coworkers studied the alkoxyacylation of alkyl iodides **152** catalyzed by a large number of metal carbonyl complexes [258]. Among them 4 mol%  $\text{Re}_2(\text{CO})_{10}$  was highly active giving 77% yield of ester **154** (cf. Fig. 41).

Narasaka and coworkers reported radical-polar crossover addition/cyclization reactions of phenacyl bromides **204** and electron-rich alkenes such as (silyl) enol ethers **205**, catalyzed by the rhenium(I) complex **206** (Fig. 57) [302]. The active catalyst **206A** formed after thermal nitrogen elimination from **206** reduced **204** either directly or by oxidative addition/homolysis via rhenium enolate **204A** to



**Fig. 57** Rhenium(I)-catalyzed radical-polar crossover addition/cyclization reactions

$\alpha$ -carbonyl radical **204B**. This adds to enol ethers **205**. From electron-rich adduct radical **204C** two pathways to products **207** were proposed. In a SET cycle, **204C** would be oxidized to a carbocation **204D** by Re(II) complex **206B**, thus regenerating the catalyst **206A**, which enters the next cycle. On the other hand, abstraction of a bromine atom from the substrate **204** is possible, from which an atom transfer radical addition cycle starts, in which the rhenium complex **206** acted merely as an initiator. The resulting labile bromo ether **204E** should convert easily to carbocation **204D** by bromide elimination. No matter what pathway was followed the resulting intermediate **204D** cyclizes in a polar Paal–Knorr synthesis giving furan derivatives **207** in 32–79% yield. With TBS silyl enol ethers, the cyclizations are apparently slower and 1,4-dicarbonyl compounds result, sometimes as a mixture with **207**. The method was applied to the synthesis of the lignan furoguaiacin.

The Re(III) complex  $\text{Re}(\text{PPh}_3)_2(\text{MeCN})\text{Cl}_3$  (2 mol%) catalyzes the ATRA of tetrachloromethane or bromotrichloromethane to terminal alkenes in 39–76% yield [303].  $\beta$ -Pinene suffered a cyclobutylcarbiny radical ring opening, thus supporting the free radical mechanism. With 1,*n*-dienes double addition was found, while 1,3-dienes gave the 1,4-addition product. Internal alkenes were almost inert under the reaction conditions. 1,6-Dienes **158** underwent a tandem radical addition/cyclization reaction to cycles **159** in 64–87% yield with 3–6:1 *cis*-diastereoselectivity (cf. Fig 43). This compares well to the results obtained with the most frequently used catalyst  $\text{Ru}(\text{PPh}_3)_3\text{Cl}_2$  (see Part 2, Sects. 3.3.1 and 3.3.2).

Recently Geiger and coworkers found that the electrochemically generated  $\text{CpRe}(\text{CO})_3$  cation catalyzes the [2+2] cycloaddition of unactivated alkenes [304]. The reaction proceeds via SET oxidation of the olefin to the corresponding radical cation, addition, cyclization, and back electron transfer (BET), which can occur either from the reduced catalyst or the alkene.

## 11 Transition Metal-Catalyzed Radical Reactions According to Reaction Type

The following table provides an overview over the most common reaction types that were conducted with different metals of different oxidation states. This list summarizes only reaction types that are catalyzed by more than one metal.

Reaction type	Part	Metal catalyst	Section
Alkoxy carbonylation	1	Mn(–I), Mn(0)	9.1
	3	Pd(0)	3.4
	3	Pt(0)	4
Amination (Nitrenoid)	2	Fe(II), Fe(III)	2.6, 2.8
	2	Ru(II)	3.7
	2	Co(II)	5.6
	3	Cu(I), Cu(II)	5.8

(continued)

Atom transfer radical addition (ATRA)	1	Ti(0)	3.1
	1	Mo(0), Mo(I)	7
	1	Mn(II)	9.3.1
	2	Fe(0), Fe(II)	2.2.1, 2.4
	2	Ru(II)	3.3.1
	2	Os(II)	4
	2	Rh(I)	6
	2	Ir(I)	7
	3	Ni(II)	2.9
	3	Pd(0)	3.1
	3	Pt(0), Pt(II)	4
	3	Cu(0), Cu(I)	5.1, 5.2
	3	Ru(II)-Rh(III), Ru(II)-Rh(I)	8.5
Atom transfer radical cyclization (ATRC)	1	Mn(0)	9.1
	1	Re	10
	2	Fe(II)	2.4
	2	Ru(II)	3.3.2
	3	Pd(0)	3.2
	3	Cu(I)	5.3
Barbier reaction	1	Ti(III)	3.3.1
	3	Cr(II)-Co(II)	8.2
Biaryl coupling	2	Fe(II)	2.5
	2	Co(II)	5.11
Carbonylation	1	W	8
	2	Ru(0)	3.1
	2	Rh(I)	6
	2	Ir(I)	7
	3	Pd(0)	3.4, 3.5
C-H-Activation/coupling	3	Ni(0)	2.2
	3	Pd(II)	3.7
Cross-coupling (Hiyama-type)	3	Ni(0)	2.1
Cross-coupling (Kumada-type)	1	V(III)	5.2
	2	Low-valent Fe	2.1.1, 2.1.2
	2	Co(0)/Co(I)	5.2.1
	3	Ni(0)/Ni(II)	2.1
	3	Pd(0)	3.3
	3	Ag(0)	6.1
	2	Low-valent Fe	2.1.1
	3	Ni(0)/Ni(I)	2.1
Cross-coupling (Negishi-type)	3	Ag(0)	6.1
	2	Low-valent Fe	2.1.1
	3	Ni(0)	2.1
Cross-coupling (Suzuki-type)	3	Pd(0)	3.3, 3.4
	3	Ni(0)	2.1
	3	Pd(0)	3.3, 3.4
Cross-coupling (Stille-type)	3	Ni(0)	2.1
	3	Pd(0)	3.1

(continued)

[2+2] Cycloaddition	1	Re	10
	2	Fe(III)	2.7.2
	2	Co(II)	5.4
Heck reaction (Redox-neutral radical addition)	3	Cu(I)	5.6, 5.7
	1	Ti(II)	3.2
	2	Co(0)/Co(I)	5.2.2
Hydrofunctionalization of olefins	2	Co(I)	5.3
	3	Ni(0)	2.3
	1	Mn(II), Mn(III)	9.5
Minisci reaction	2	Co(II)	5.7
	2	Fe(II)	2.5
Oxidative cleavage	3	Ag(II)	6.3
	1	V(IV, V)	5.3
	1	Mn(III)	9.4
Oxidative dimerization	2	Ru(III)	3.6
	3	Cu(II)	5.12
	3	Mn(II)-Co(II)	8.3
	1	V	5
Oxonium ylide rearrangement (Stevens rearrangement)	2	Fe	2
	3	Cu	5
	3	Ag	6
Photocatalysis	2	Rh(II)	6
	3	Cu(II)	5.11
Photoredox catalysis	1	W	8
	2	Ru(0)	3.1
	2	Rh(I)	6
	2	Ir(I)	7
Pinacol coupling	2	Ru(II)	3.2
	2	Ir(III)	7
Radical addition (oxidative)	1	Ti	3
	1	V, Nb, Ta	5
	1	Cr	6
	3	Au(0)	7
	1	Mn(III)	9.3.2
Radical addition (redox-neutral)	2	Fe(0), Fe(II), Fe(III)	2.2.2, 2.4, 2.7.1, 2.8
	2	Co(II)	5.9
	3	Cu(I), Cu(II)	5.4, 5.12
	3	Ag(I)	6.2
	1	Ti(II)	3.2
Radical addition (reductive)	2	Fe(II), Fe(III)	2.5, 2.8
	2	Ru(II)	3.4
	2	Rh(I)	6
Radical addition (oxidative)	1	Mn(II)	9.3.1
	2	Co(I)	5.3.1
	3	Ni(0), Ni(I)	2.3, 2.6
	3	Mn(II)-Co(II)	8.3

(continued)

Radical cyclization (oxidative)	1	Mn(III)	9.4
	2	Fe(III)	2.7.2
	2	Ru(III)	3.6
	2	Co(II)	5.10
	3	Cu(II)	5.12
Radical cyclization (Redox-neutral, Heck-type)	3	Ag(I)	6.2
	1	Mn(0)	9.2
	2	Low-valent Fe	2.1.3
	2	Fe(I)	2.3
	2	Co(0)/Co(I)	5.2.4
Radical cyclization (Reductive)	2	Co(I)	5.3
	1	Ti(II), Ti(III)	3.2, 3.3.2
	1	Zr(II)	4
	1	Cr(I), Cr(II)	6.2, 6.3
	2	Co(I)	5.3
	3	Ni(0), Ni(I)	2.4, 2.7
	3	Cu(I)	5.9
Reductive cleavage of peroxides	3	Mn(II)-Cu(I)	8.4
	2	Ru(II)	3.5
	2	Co(II)	5.8
	2	Rh(I)	6
	3	Pd(II)	3.6
Tandem addition/cyclization	1	Re	10
	2	Fe(I)	2.3
	2	Co(II)	5.5
	3	Ag(I)	6.2
Tandem ATRA/ATRC	1	Mn(0)	9.1
	2	Fe(0), Fe(II)	2.2.1, 2.4
	2	Ru(II)	3.3.3
	3	Cu(I)	5.3
Tandem radical addition/cross-coupling	3	Cu(I)	5.3
	1	Ti(II)	3.2
	2	Co(0)/Co(I)	5.2.3
Tandem radical cyclization	3	Ni(0)	2.3
	1	Ti(III)	3.3.2
	1	Mn(III)	9.4
	2	Fe(III)	2.7.3
	2	Co(I)	5.3
	3	Ni(I)	2.7
Tandem cyclization/addition reaction	3	Cu(I)	5.9
	2	Co(I)	5.3.2
	3	Ni(0)	2.4
	3	Pd(0)	3.5
	3	Mn(II)-Cu(I)	8.4
Tandem radical cyclization/cross-coupling	2	Low-valent Fe	2.1.3
	2	Co(0)/Co(I)	5.2.5
	3	Ni(0)	2.4
	3	Pd(0)	3.5
	3	Ag(0)	6.1

---



**Acknowledgments** This manuscript is dedicated to Professor Dr. Bernd Giese, a pioneer of preparative radical chemistry and early contributor to this topic, on the occasion of his 70th birthday. Generous funding by the Institute of Organic Chemistry and Biochemistry, Academy of Sciences of the Czech Republic (Z4 055 0506), and the Grant Agency of the Czech Republic (203/09/1936) is gratefully acknowledged. I thank my group for critical reading of the manuscript and many helpful comments and discussions. I apologize to all colleagues for the omissions of their work that were necessary due to space constraints of the manuscript.

## References

1. Cornils B, Herrmann WA, Muhler M, Wong C-H (eds) (2008) *Catalysis from A to Z*. Weinheim, A concise encyclopedia. Wiley-VCH
2. van Leeuwen PWNM (ed) (2004) *Homogeneous catalysis. Understanding the art*. Kluwer, Dordrecht
3. Diederich F, Stang PJ (eds) (1998) *Metal-catalyzed cross-coupling reactions*. Wiley-VCH, Weinheim
4. de Meijere A, Diederich F (eds) (2004) *Metal-catalyzed cross-coupling reactions*, 2nd edn. Weinheim, Wiley-VCH
5. Beller M, Bolm C (eds) (2004) *Transition metals for organic synthesis*. Wiley-VCH, Weinheim
6. Dyker G (ed) (2005) *Handbook of C-H transformations*. Wiley-VCH, Weinheim
7. Ackermann L (ed) (2009) *Modern arylation methods*. Wiley-VCH, Weinheim
8. Marek I (ed) (2002) *Titanium and zirconium in organic synthesis*. Wiley-VCH, Weinheim
9. Plietker B (ed) (2008) *Iron catalysis in organic chemistry*. Wiley-VCH, Weinheim
10. Cahiez G, Moyeux A (2010) *Chem Rev* 110:1435
11. Tamaru Y (ed) (2005) *Modern organonickel chemistry*. Wiley-VCH, Weinheim
12. Krause N (ed) (2002) *Modern organocopper chemistry*. Wiley-VCH, Weinheim
13. S-i M (ed) (2004) *Ruthenium in organic synthesis*. Wiley-VCH, Weinheim
14. Evans PA (ed) (2005) *Modern rhodium-catalyzed organic reactions*. Wiley-VCH, Weinheim
15. Tsuji J (2004) *Palladium reagents and catalysts – new perspectives for the 21st century*. Wiley, Chichester
16. Harmata M (ed) (2010) *Silver in organic chemistry*. Wiley, Hoboken
17. Oro LA, Claver C (eds) (2009) *Iridium complexes in organic synthesis*. Wiley-VCH, Weinheim
18. Fürstner A (2009) *Chem Soc Rev* 38:3208
19. Fossey J, Lefort D, Sorba J (1995) *Free radicals in organic chemistry*. Wiley, New York
20. Curran DP, Porter NA, Giese B (1996) *Stereochemistry of radical reactions*. Weinheim, VCH
21. Giese B, Kopping B, Göbel T, Dickhaut J, Thoma G, Kulicke KJ, Trach F (1996) *Org React* 48:301
22. Melikyan GG (1997) *Org React* 49:427
23. Renaud P, Sibi MP (eds) (2001) *Radicals in organic synthesis*, vol 1+2. Wiley-VCH, Weinheim
24. Sibi MP, Manyem S, Zimmerman J (2003) *Chem Rev* 103:3263
25. Zard SZ (2003) *Radical reactions in organic synthesis*. Oxford Univ Press, New York
26. *Radicals in synthesis I: methods and mechanisms* (2006) *Topics Curr Chem* 263
27. *Radicals in synthesis II: complex molecules* (2006) *Topics Curr Chem* 264
28. Procter DJ, Flowers RA II, Skrydstrup T (2009) *Organic synthesis using samarium diiodide*. RSC, Cambridge
29. Rowlands GJ (2009) *Tetrahedron* 65:8603
30. Rowlands GJ (2010) *Tetrahedron* 66:1593

31. Kochi JK (1974) *Acc Chem Res* 7:351
32. Lappert MF, Lednor PW (1976) *Adv Organomet Chem* 14:345
33. Kochi JK (1978) *Organometallic mechanisms and catalysis*. Academic, New York
34. Kochi JK (1980) *Pure Appl Chem* 52:571
35. Kochi JK (1986) *J Organomet Chem* 300:139
36. Kochi JK (2002) *J Organomet Chem* 653:11
37. Iqbal J, Bhatia B, Nayyar NK (1994) *Chem Rev* 94:519
38. Hartwig JF (2010) *Organotransition metal chemistry. From bonding to catalysis*. University Science, Sausalito
39. McGiarrigle EM, Gilheany DG (2005) *Chem Rev* 105:1563
40. Ortiz de Montellano PR (ed) (2005) *Cytochrome P450 structure, mechanism, and biochemistry*. Kluwer/Plenum, New York
41. Ortiz de Montellano PR (2010) *Chem Rev* 110:932
42. Firmansjah L, Fu GC (2007) *J Am Chem Soc* 129:11340
43. Netherton MR, Fu GC (2005) *Top Organomet Chem* 14:85
44. Cardenas DJ (2003) *Angew Chem Int Ed* 42:384
45. Stille JK, Lau KSY (1977) *Acc Chem Res* 10:434
46. Chirik PJ, Wieghardt K (2010) *Science* 327:794
47. de Bruin B, Hettterscheid DGHK, Koekkoek AJJ, Grutzmacher H (2007) *Prog Inorg Chem* 55:247
48. de Bruin B, Hettterscheid DGH (2007) *Eur J Inorg Chem* 211
49. Dzik WI, Reek JNH, de Bruin B (2008) *Chem Eur J* 14:7594
50. Hettterscheid DGH, Kaiser J, Reijerse E, Peters TPJ, Thewissen S, Blok ANJ, Smits JMM, de Gelder R, de Bruin B (2005) *J Am Chem Soc* 127:1895
51. Hettterscheid DGH, Bens M, de Bruin B (2005) *Dalton Trans* 979
52. Studer A (2001) *Chem Eur J* 7:1159
53. Fischer H (2001) *Chem Rev* 101:3581
54. Espenson JH (1992) *Acc Chem Res* 25:222
55. Masarwa A, Meyerstein D (2004) *Adv Inorg Chem* 55:271
56. Torraca KE, McElwee-White L (2000) *Coord Chem Rev* 206:469
57. Kharasch MS, Jensen EV, Urry WH (1945) *Science* 102:128
58. Asscher M, Vofsi D (1963) *J Chem Soc* 1887
59. Minisci F (1975) *Acc Chem Res* 8:165
60. Severin K (2006) *Curr Org Chem* 10:217
61. Eckenhoff WT, Pintauer T (2010) *Catal Rev* 52:1
62. Matyjaszewski K, Xia JH (2001) *Chem Rev* 101:2921
63. Matyjaszewski K (2009) *ACS Symposium Series*, vol 1024. ACS, Washington, DC
64. Müller AHE, Matyjaszewski K (2009) *Controlled and living polymerizations*. Wiley-VCH, Weinheim
65. Kamigaito M, Ando T, Sawamoto M (2001) *Chem Rev* 101:3689
66. Ouchi M, Terashima T, Sawamoto M (2009) *Chem Rev* 109:4963
67. Smith KM, McNeil WS, Abd-El-Aziz AS (2010) *Macromol Chem Phys* 211:10
68. Reid SJ, Baird MC (2003) *Dalton Trans* 3975
69. Reid SJ, Baird MC (2004) *J Organomet Chem* 689:1257
70. Fischer PJ, Neary MC, Heerboth AP, Sullivan KP (2010) *Organometallics* 29:4562
71. Hasanayn F, Gozem S (2008) *Organometallics* 27:5426
72. Hasanayn F, Nsouli NH, Al-Ayoubi A, Goldman AS (2008) *J Am Chem Soc* 130:511
73. Kaim W (2001) *ESR spectroscopy of inorganic and organometallic radicals*. In: Balzani V (ed) *Electron transfer in chemistry*, vol 2. Wiley-VCH, Weinheim, p 976
74. Rieger AL, Rieger PH (2004) *Organometallics* 23:154
75. Van Doorslaer S, Caretti I, Fallis IA, Murphy DM (2009) *Coord Chem Rev* 253:2116
76. Allen RB, Lawler RG, Ward HR (1973) *J Am Chem Soc* 95:1692
77. Kramer AV, Labinger JA, Bradley JS, Osborn JA (1974) *J Am Chem Soc* 96:7145

78. Lehr GF, Lawler RG (1984) *J Am Chem Soc* 106:4048
79. Kalai T, Balog M, Jeko J, Hubbell WL, Hideg K (2002) *Synthesis* 2365
80. Kalai T, Bognar B, Jeko J, Hideg K (2006) *Synthesis* 2573
81. Kalai T, Jeko J, Berente Z, Hideg K (2006) *Synthesis* 439
82. Lagunas A, Mairata i Payeras A, Jimeno C, Pericas MA (2005) *Org Lett* 7:3033
83. Chan KS, Li XZ, Dzik WI, de Bruin B (2008) *J Am Chem Soc* 130:2051
84. Vogler T, Studer A (2008) *Adv Synth Catal* 350:1963
85. Vogler T, Studer A (2008) *Org Lett* 10:129
86. Kirchberg S, Fröhlich R, Studer A (2009) *Angew Chem Int Ed* 48:4235
87. Kirchberg S, Fröhlich R, Studer A (2010) *Angew Chem Int Ed* 49:6877
88. Albeniz AC, Espinet P, Lopez-Fernandez R, Sen A (2002) *J Am Chem Soc* 124:11278
89. Giovannini R, Stüdemann T, Dussin G, Knochel P (1998) *Angew Chem Int Ed Engl* 37:2387
90. Giovannini R, Stüdemann T, Devasagayaraj A, Dussin G, Knochel P (1999) *J Org Chem* 64:3544
91. Newcomb M (1993) *Tetrahedron* 49:1151
92. Newcomb M, Toy PH (2000) *Acc Chem Res* 33:449
93. Terao J, Watanabe H, Ikumi A, Kuniyasu H, Kambe N (2002) *J Am Chem Soc* 124:4222
94. Terao J, Todo H, Begum SA, Kuniyasu H, Kambe N (2007) *Angew Chem Int Ed* 46:2086
95. Terao J, Naitoh Y, Kuniyasu H, Kambe N (2007) *Chem Commun* 825
96. Wang J, Tong X, Xie X, Zhang Z (2010) *Org Lett* 12:5370
97. Necas D, Katora M (2007) *Curr Org Chem* 11:1566
98. Wender PA, Takahashi H, Witulski B (1995) *J Am Chem Soc* 117:4720
99. Hayashi M, Ohmatsu T, Meng Y-P, Saigo K (1998) *Angew Chem Int Ed* 37:837
100. Bart SC, Chirik PJ (2003) *J Am Chem Soc* 125:886
101. Ford L, Jahn U (2009) *Angew Chem Int Ed* 48:6386
102. Recupero F, Punta C (2007) *Chem Rev* 107:3800
103. Eames J, Watkinson M (2001) *Angew Chem Int Ed* 40:3567
104. Andrus MB, Lashley JC (2002) *Tetrahedron* 58:845
105. Punniyamurthy T, Velusamy S, Iqbal J (2005) *Chem Rev* 105:2329
106. Punniyamurthy T, Rout L (2008) *Coord Chem Rev* 252:134
107. Katsuki T (2002) *Adv Synth Catal* 344:131
108. Xia Q-H, Ge H-Q, Ye C-P, Liu Z-M, Su K-X (2005) *Chem Rev* 105:1603
109. Baleizao C, Garcia H (2006) *Chem Rev* 106:3987
110. Li C-J, Li Z (2006) *Pure Appl Chem* 78:935
111. Li C-J (2009) *Acc Chem Res* 42:335
112. Scheuermann CJ (2010) *Chem Asian J* 5:436
113. Yoo W-J, Li C-J (2010) *Topics Curr Chem* 292:281
114. Sud A, Sureshkumar D, Klussmann M (2009) *Chem Commun* 3169
115. Li Y-Z, Li B-J, Lu X-Y, Lin S, Shi Z-J (2009) *Angew Chem Int Ed* 48:3817
116. Han W, Ofial AR (2009) *Chem Commun* 5024
117. Han W, Ofial AR (2009) *Chem Commun* 6023
118. Han W, Mayer P, Ofial AR (2010) *Adv Synth Catal* 352:1667
119. Zimmerman J, Sibi MP (2006) *Topics Curr Chem* 263:107
120. Desimoni G, Faita G, Jorgensen KA (2006) *Chem Rev* 106:3561
121. Miyabe H, Takemoto Y (2007) *Chem Eur J* 13:7280
122. Yoshioka E, Kohtani S, Miyabe H (2009) *Heterocycles* 79:229
123. Juan MC, Justicia J, Oller-Lopez JL, Oltra JE (2006) *Topics Curr Chem* 264:63
124. Barrero AF, Quílez del Moral JF, Sánchez EM, Arteaga JF (2006) *Eur J Org Chem* 1627
125. Fürstner A (1998) *Pure Appl Chem* 70:1071
126. Ephritikhine M (1998) *Chem Commun* 2549
127. Ladipo FT (2006) *Curr Org Chem* 10:965
128. Chatterjee A, Joshi NN (2006) *Tetrahedron* 62:12137
129. Hirao T (2007) *Topics Curr Chem* 279:53

130. Burchak ON, Py S (2009) *Tetrahedron* 65:7333
131. Fürstner A, Hupperts A (1995) *J Am Chem Soc* 117:4468
132. Davis CR, Burton DJ, Yang Z-Y (1995) *J Fluorine Chem* 70:135
133. Kablaoui NM, Hicks FA, Buchwald SL (1997) *J Am Chem Soc* 119:4424
134. Terao J, Kambe N (2006) *Bull Chem Soc Jpn* 79:663
135. Terao J, Saito K, Nii S, Kambe N, Sonoda N (1998) *J Am Chem Soc* 120:11822
136. Nii S, Terao J, Kambe N (2000) *J Org Chem* 65:5291
137. Terao J, Saito K, Nii S, Kambe N, Sonoda N (1998) *Tetrahedron Lett* 39:9697
138. Terao J, Kato Y, Kambe N (2008) *Chem Asian J* 3:1472
139. Terao J, Watabe H, Miyamoto M, Kambe N (2003) *Bull Chem Soc Jpn* 76:2209
140. Nii S, Terao J, Kambe N (2004) *J Org Chem* 69:573
141. Fujii Y, Terao J, Kato Y, Kambe N (2008) *Chem Commun* 5836
142. Gansäuer A (1998) *Synlett* 801
143. Gansäuer A, Lauterbach T, Narayan S (2003) *Angew Chem Int Ed* 42:5556
144. Gansäuer A, Fan C-A, Keller F, Karbaum P (2007) *Chem Eur J* 13:8084
145. Gansäuer A, Justicia J, Fan C-A, Worgull D, Piestert F (2007) *Topics Curr Chem* 279:25
146. Fernandez-Mateos A, Teijon PH, Clemente RR, Gonzalez RR (2008) *Synlett* 3208
147. Gansäuer A, Ndene N, Lauterbach T, Justicia J, Winkler I, Mück-Lichtenfeld C, Grimme S (2008) *Tetrahedron* 64:11839
148. Kosal AD, Ashfeld BL (2010) *Org Lett* 12:44
149. Rosales A, Oller-Lopez JL, Justicia J, Gansäuer A, Oltra JE, Cuerva JM (2004) *Chem Commun* 2628
150. Estevez RE, Justicia J, Bazdi B, Fuentes N, Paradas M, Choquesillo-Lazarte D, Garcia-Ruiz JM, Robles R, Gansäuer A, Cuerva JM, Oltra JE (2009) *Chem Eur J* 15:2774
151. Justicia J, Sancho-Sanz I, Alvarez-Manzaneda E, Oltra JE, Cuerva JM (2009) *Adv Synth Catal* 351:2295
152. Hirao T, Hatano B, Asahara M, Muguruma Y, Ogawa A (1998) *Tetrahedron Lett* 39:5247
153. Zhou L, Hirao T (2003) *J Org Chem* 68:1633
154. Beckwith ALJ, Schiesser CH (1985) *Tetrahedron* 41:3925
155. Spellmeyer DC, Houk KN (1987) *J Org Chem* 52:959
156. Friedrich J, Walczak K, Dolg M, Piestert F, Lauterbach T, Worgull D, Gansäuer A (2008) *J Am Chem Soc* 130:1788
157. Gansäuer A, Worgull D, Knebel K, Huth I, Schnakenburg G (2009) *Angew Chem Int Ed* 48:8882
158. Gansäuer A, Greb A, Huth I, Worgull D, Knebel K (2009) *Tetrahedron* 65:10791
159. Gansäuer A, Piestert F, Huth I, Lauterbach T (2008) *Synthesis* 3509
160. Gansäuer A, Fleckhaus A, Lafont MA, Okkel A, Kotsis K, Anoop A, Neese F (2009) *J Am Chem Soc* 131:16989
161. Gansäuer A, Shi L, Otte M (2010) *J Am Chem Soc* 132:11858
162. Gansäuer A, Shi L, Keller F, Karbaum P, Fan C-A (2010) *Tetrahedron Asymmetry* 21:1361
163. Hemmerling M, Sjöholm A, Somfai P (1999) *Tetrahedron Asymmetry* 10:4091
164. Sjöholm A, Hemmerling M, Pradeille N, Somfai P (2001) *J Chem Soc Perkin Trans* 1:891
165. Williams GM, Gell KI, Schwartz J (1980) *J Am Chem Soc* 102:3660
166. Williams GM, Schwartz J (1982) *J Am Chem Soc* 104:1122
167. Fujita K, Yorimitsu H, Oshima K (2004) *Chem Rec* 4:110
168. Fujita K, Nakamura T, Yorimitsu H, Oshima K (2001) *J Am Chem Soc* 123:3137
169. Fujita K, Yorimitsu H, Oshima K (2004) *Bull Chem Soc Jpn* 77:1727
170. Yoshida S, Yorimitsu H, Oshima K (2007) *J Organomet Chem* 692:3110
171. Hirao T (1997) *Chem Rev* 97:2707
172. Hirao T, Takeuchi H, Ogawa A, Sakurai H (2000) *Synlett* 1658
173. Xu X, Hirao T (2005) *J Org Chem* 70:8594
174. Sun J, Dai Z, Li C, Pan X, Zhu C (2009) *J Organomet Chem* 694:3219
175. Hon S-W, Li C-H, Kuo J-H, Barhate NB, Liu Y-H, Wang Y, Chen C-T (2001) *Org Lett* 3:869

176. Chu C-Y, Hwang D-R, Wang S-K, Uang B-J (2001) *Chem Commun* 980
177. Barhate NB, Chen C-T (2002) *Org Lett* 4:2529
178. Chu C-Y, Uang B-J (2003) *Tetrahedron Asymmetry* 14:53
179. Somei H, Asano Y, Yoshida T, Takizawa S, Yamataka H, Sasai H (2004) *Tetrahedron Lett* 45:1841
180. Takizawa S, Katayama T, Sasai H (2008) *Chem Commun* 4113
181. Takizawa S (2009) *Chem Pharm Bull* 57:1179
182. Luo Z, Liu Q, Gong L, Cui X, Mi A, Jiang Y (2002) *Angew Chem Int Ed* 41:4532
183. Luo Z, Liu Q, Gong L, Cui X, Mi A, Jiang Y (2002) *Chem Commun* 914
184. Liu Q-Z, Xie N-S, Luo Z-B, Cui X, Cun L-F, Gong L-Z, Mi A-Q, Jiang Y-Z (2003) *J Org Chem* 68:7921
185. Guo Q-X, Wu Z-J, Luo Z-B, Liu Q-Z, Ye J-L, Luo S-W, Cun L-F, Gong L-Z (2007) *J Am Chem Soc* 129:13927
186. Takizawa S, Rajesh D, Katayama T, Sasai H (2009) *Synlett* 1667
187. Mizuno H, Sakurai H, Amaya T, Hirao T (2006) *Chem Commun* 5042
188. Zhou L, Hirao T (2000) *Tetrahedron Lett* 41:8517
189. Yasuda S, Yorimitsu H, Oshima K (2008) *Bull Chem Soc Jpn* 81:287
190. Kirihara M, Takizawa S, Momose T (1998) *J Chem Soc Perkin Trans* 1:7
191. Kirihara M, Ichinose M, Takizawa S, Momose T (1998) *Chem Commun* 1691
192. Kirihara M, Kakuda H, Ichinose M, Ochiai Y, Takizawa S, Mokuya A, Okubo K, Hatano A, Shiro M (2005) *Tetrahedron* 61:4831
193. Kulinkovich OG (2003) *Chem Rev* 103:2597
194. Hirao T (1996) *Topics Curr Chem* 178:99
195. Russell GA (1957) *J Am Chem Soc* 79:3871
196. Miyamoto S, Martinez GR, Medeiros MHG, DiMascio P (2003) *J Am Chem Soc* 125:6172
197. Son S, Toste FD (2010) *Angew Chem Int Ed* 49:3791
198. Baucherel X, Uziel J, Juge S (2001) *J Org Chem* 66:4504
199. Hashmi ASK (1996) *J Prakt Chem* 338:491
200. Avalos M, Babiano R, Cintas P, Jimenez JL, Palacios JC (1999) *Chem Soc Rev* 28:169
201. Fürstner A (1999) *Chem Rev* 99:991
202. Smith KM (2006) *Coord Chem Rev* 250:1023
203. Fürstner A, Shi N (1996) *J Am Chem Soc* 118:12349
204. Kuroboshi M, Tanaka M, Kishimoto S, Goto K, Mochizuki M, Tanaka H (2000) *Tetrahedron Lett* 41:81
205. Hargaden GC, Guiry PJ (2007) *Adv Synth Catal* 349:2407
206. Ocampo R, Dolbier WR (2004) *Tetrahedron* 60:9325
207. Svatos A, Boland W (1998) *Synlett* 549
208. Groth U, Jung M, Vogel T (2004) *Synlett* 1054
209. Halterman RL, Porterfield JP, Mekala S (2009) *Tetrahedron Lett* 50:7172
210. Takenaka N, Xia G, Yamamoto H (2004) *J Am Chem Soc* 126:13198
211. Groth U, Jung M, Vogel T (2005) *Chem Eur J* 11:3127
212. Volla CMR, Markovic D, Laclef S, Vogel P (2010) *Chem Eur J* 16:8984
213. MacLeod KC, Conway JL, Patrick BO, Smith KM (2010) *J Am Chem Soc* 132:17325
214. Ash CE, Hurd PW, Darensbourg MY, Newcomb M (1987) *J Am Chem Soc* 109:3313
215. Gandolfi O, Cais M (1977) *J Organomet Chem* 125:141
216. Bland WJ, Davis R, Durrant JLA (1984) *J Organomet Chem* 260:C75
217. Bland WJ, Davis R, Durrant JLA (1985) *J Organomet Chem* 280:95
218. Shvo Y, Green R (2003) *J Organomet Chem* 675:77
219. Tang L, Papish ET, Abramo GP, Norton JR, Baik M-H, Friesner RA, Rappe A (2003) *J Am Chem Soc* 125:10093
220. Choi J, Tang L, Norton JR (2007) *J Am Chem Soc* 129:234
221. Smith DM, Pulling ME, Norton JR (2007) *J Am Chem Soc* 129:770
222. Hartung J, Pulling ME, Smith DM, Yang DX, Norton JR (2008) *Tetrahedron* 64:11822

223. Hackmann C, Schäfer HJ (1993) *Tetrahedron* 49:4559
224. MacLeod KC, Patrick BO, Smith KM (2010) *Organometallics* 29:6639
225. Barma DK, Kundu A, Baati R, Mioskowski C, Falck JR (2002) *Org Lett* 4:1387
226. Franz JA, Linehan JC, Birnbaum JC, Hicks KW, Alnajjar MS (1999) *J Am Chem Soc* 121:9824
227. Le Grogneq E, Claverie J, Poli R (2001) *J Am Chem Soc* 123:9513
228. Maria S, Stoffelbach F, Mata J, Daran JC, Richard P, Poli R (2005) *J Am Chem Soc* 127:5946
229. Susuki T, Tsuji J (1970) *J Org Chem* 35:2982
230. Davis R, Khazal NMS, Bitterwolf TE (1990) *J Organomet Chem* 397:51
231. Mori Y, Tsuji J (1972) *Tetrahedron* 28:29
232. Hayes TK, Freyer AJ, Parvez M, Weinreb SM (1986) *J Org Chem* 51:5501
233. Hayes TK, Villani R, Weinreb SM (1988) *J Am Chem Soc* 110:5533
234. Lee GM, Parvez M, Weinreb SM (1988) *Tetrahedron* 44:4671
235. Lee GM, Weinreb SM (1990) *J Org Chem* 55:1281
236. Yang H, Wang H, Zhu C (2007) *J Org Chem* 72:10029
237. Tzirakis MD, Lykakis IN, Orfanopoulos M (2009) *Chem Soc Rev* 38:2609
238. Jaynes BS, Hill CL (1993) *J Am Chem Soc* 115:12212
239. Jaynes BS, Hill CL (1995) *J Am Chem Soc* 117:4704
240. Zheng Z, Hill CL (1998) *Chem Commun* 2467
241. Dondi D, Fagnoni M, Molinari A, Maldotti A, Albini A (2004) *Chem Eur J* 10:142
242. Dondi D, Cardarelli AM, Fagnoni M, Albini A (2006) *Tetrahedron* 62:5527
243. Dondi D, Ravelli D, Fagnoni M, Mella M, Molinari A, Maldotti A, Albini A (2009) *Chem Eur J* 15:7949
244. Dondi D, Fagnoni M, Albini A (2006) *Chem Eur J* 12:4153
245. Angioni S, Ravelli D, Emma D, Dondi D, Fagnoni M, Albini A (2008) *Adv Synth Catal* 350:2209
246. Esposti S, Dondi D, Fagnoni M, Albini A (2007) *Angew Chem Int Ed* 46:2531
247. Ravelli D, Zema M, Mella M, Fagnoni M, Albini A (2010) *Org Biomol Chem* 8:4158
248. Protti S, Ravelli D, Fagnoni M, Albini A (2009) *Chem Commun* 7351
249. Tzirakis MD, Orfanopoulos M (2009) *J Am Chem Soc* 131:4063
250. Tzirakis MD, Alberti MN, Orfanopoulos M (2010) *Chem Commun* 46:8228
251. Cahiez G, Duplais C, Buendia J (2009) *Chem Rev* 109:1434
252. Snider BB (1996) *Chem Rev* 96:339
253. Nishino H (2006) *Topics Heterocycl. Chem* 6:39
254. Demir AS, Emrullahoglu M (2007) *Curr Org Synth* 4:321
255. Snider BB (2009) *Tetrahedron* 65:10738
256. Liu W, Groves JT (2010) *J Am Chem Soc* 132:12847
257. Kang S-K, Baik T-G, Jiao XH, Lee Y-T (1999) *Tetrahedron Lett* 40:2383
258. Kondo T, Sone Y, Tsuji Y, Watanabe Y (1994) *J Organomet Chem* 473:163
259. Kondo T, Tsuji Y, Watanabe Y (1988) *Tetrahedron Lett* 29:3833
260. Fukuyama T, Nishitani S, Inouye T, Morimoto K, Ryu I (2006) *Org Lett* 8:1383
261. Ryu I (2001) *Chem Soc Rev* 30:16
262. Ryu I (2002) *Chem Rec* 2:249
263. Gilbert BC, Kalz W, Lindsay CI, McGrail PT, Parsons AF, Whittaker DTE (1999) *Tetrahedron Lett* 40:6095
264. Gilbert BC, Kalz W, Lindsay CI, McGrail PT, Parsons AF, Whittaker DTE (2000) *J Chem Soc Perkin Trans* 1:1187
265. Huther N, McGrail PT, Parsons AF (2002) *Tetrahedron Lett* 43:2535
266. Huther N, McGrail PT, Parsons AF (2004) *Eur J Org Chem*:1740
267. Nakao J, Inoue R, Shinokubo H, Oshima K (1997) *J Org Chem* 62:1910
268. Inoue R, Nakao J, Shinokubo H, Oshima K (1997) *Bull Chem Soc Jpn* 70:2039
269. Uchiyama M, Matsumoto Y, Nakamura S, Ohwada T, Kobayashi N, Yamashita N, Matsumiya A, Sakamoto T (2004) *J Am Chem Soc* 126:8755

270. Kinoshita H, Kakiya H, Oshima K (2000) *Bull Chem Soc Jpn* 73:2159
271. Tayama O, Nakano A, Iwahama T, Sakaguchi S, Ishii Y (2004) *J Org Chem* 69:5494
272. Nohair K, Lachaise I, Paugam J-P, Nedelec, J-Y (1992) *Tetrahedron Lett* 33:213
273. Nedelec JY, Nohair K (1991) *Synlett* 659
274. Shundo R, Nishiguchi I, Matsubara Y, Hirashima T (1990) *Chem Lett* 2285
275. Shundo R, Nishiguchi I, Matsubara Y, Hirashima T (1991) *Tetrahedron* 47:831
276. Warsinsky R, Steckhan E (1994) *J Chem Soc Perkin Trans 1*:2027
277. Linker T, Kersten B, Linker U, Peters K, Peters E-M, von Schnering HG (1996) *Synlett* 468
278. Qian C-Y, Nishino H, Kurosawa K, Korp JD (1993) *J Org Chem* 58:4448
279. Rahman MT, Nishino H, Qian C-Y (2003) *Tetrahedron Lett* 44:5225
280. Rahman MT, Nishino H (2003) *Tetrahedron* 59:8383
281. Kumabe R, Nishino H (2004) *Tetrahedron Lett* 45:703
282. Shundo R, Nishiguchi I, Matsubara Y, Toyoshima M, Hirashima T (1991) *Chem Lett* 185
283. Coleman JP, Hallcher RC, McMackins DE, Rogers TE, Wagenknecht JH (1991) *Tetrahedron* 47:809
284. Bar G, Parsons AF, Thomas CB (2000) *Tetrahedron Lett* 41:7751
285. Yamada T, Iwahara Y, Nishino H, Kurosawa K (1993) *J Chem Soc Perkin Trans 1*:609
286. Kumabe R, Nishino H, Yasutake M, Nguyen V-H, Kurosawa K (2001) *Tetrahedron Lett* 42:69
287. Asahi K, Nishino H (2005) *Tetrahedron* 61:11107
288. Asahi K, Nishino H (2008) *Eur J Org Chem* 2404
289. Kulinkovich OG, Astashko DA, Tyvorskii VI, Ilyina NA (2001) *Synthesis* 1453
290. Inoki S, Kato K, Isayama S, Mukaiyama T (1990) *Chem Lett* 1869
291. Magnus P, Payne AH, Hobson L (2000) *Tetrahedron Lett* 41:2077
292. Magnus P, Westlund N (2000) *Tetrahedron Lett* 41:9369
293. Magnus P, Hobson LA, Westlund N, Lynch V (2001) *Tetrahedron Lett* 42:993
294. Magnus P, Gazzard L, Hobson L, Payne AH, Rainey TJ, Westlund N, Lynch V (2002) *Tetrahedron* 58:3423
295. Schindler CS, Bertschi L, Carreira EM (2010) *Angew Chem Int Ed* 49:9229
296. Magnus P, Payne AH, Waring MJ, Scott DA, Lynch V (2000) *Tetrahedron Lett* 41:9725
297. Magnus P, Scott DA, Fielding MR (2001) *Tetrahedron Lett* 42:4127
298. Magnus P, Waring MJ, Scott DA (2000) *Tetrahedron Lett* 41:9731
299. Sato M, Gunji Y, Ikeno T, Yamada T (2004) *Chem Lett* 33:1304
300. Waser J, Gaspar B, Nambu H, Carreira EM (2006) *J Am Chem Soc* 128:11693
301. Waser J, Carreira EM (2004) *Angew Chem Int Ed* 43:4099
302. Koga Y, Kusama H, Narasaka K (1998) *Bull Chem Soc Jpn* 71:475
303. Grigg R, Devlin J, Ramasubbu A, Scott RM, Stevenson P (1987) *J Chem Soc Perkin Trans 1*:1515
304. Chong D, Stewart M, Geiger WE (2009) *J Am Chem Soc* 131:7968

# Radicals in Transition Metal Catalyzed Reactions? Transition Metal Catalyzed Radical Reactions? – A Fruitful Interplay Anyway

## Part 2. Radical Catalysis by Group 8 and 9 Elements

Ullrich Jahn

**Abstract** This review summarizes the current status of transition metal catalyzed reactions involving radical intermediates in organic chemistry. This part focuses on radical-based methods catalyzed by group 8 and group 9 metal complexes. Reductive and redox-neutral coupling methods catalyzed by low-valent metal complexes as well as catalytic oxidative C–C bond formations are reviewed.

**Keywords** Addition · Catalysis · Cross-coupling · Cyclization · Electron transfer · Radicals · Transition metals

### Contents

1	Introduction .....	192
2	Iron-Catalyzed Radical Reactions .....	192
2.1	Low-Valent Iron-Catalyzed Reactions .....	193
2.2	Fe(0)–Fe(I) Catalysis: Radical Additions .....	206
2.3	Fe(I)–Fe(II) Catalysis .....	209
2.4	Fe(II)–Fe(III) Catalysis: Kharasch Additions and Atom Transfer Cyclizations ....	210
2.5	Fe(II)–Fe(III) Catalysis: Radical Additions and Cyclizations .....	212
2.6	Fe(II)–Fe(III) Catalysis: Nitrenoid Cyclizations .....	216
2.7	Fe(III)–Fe(II) Oxidative Catalysis .....	217
2.8	Fe(III)–Fe(IV) Catalysis .....	221
2.9	Miscellaneous .....	223
3	Ruthenium-Catalyzed Radical Reactions .....	224
3.1	Ru(0)–Ru(I)–Ru(II) Catalysis .....	224
3.2	Oxidative or Reductive Photoredox Catalysis Using Ru(II) Complexes .....	225

---

For Part 1, see [1]

U. Jahn (✉)

Institute of Organic Chemistry and Biochemistry, Academy of Sciences of the Czech Republic,  
Flemingovo namesti 2, 16610 Prague 6, Czech Republic  
e-mail: [jahn@uochb.cas.cz](mailto:jahn@uochb.cas.cz)



3.3	Ru(II)–Ru(III) Catalysis .....	232
3.4	Ru(II)-Catalyzed Alkylative Coupling Reactions of Alcohols .....	243
3.5	Ru(II)-Catalyzed Cleavage of Peroxides and Epoxides .....	243
3.6	Ruthenium-Catalyzed Oxidative Cyclizations .....	245
3.7	Miscellaneous .....	246
4	Osmium-Catalyzed Radical Reactions .....	246
5	Cobalt Catalysis .....	247
5.1	Co(0)–Co(I) Catalysis .....	247
5.2	Co(0)–Co(I)–Co(II) Catalysis .....	247
5.3	Co(I)–Co(II)–Co(III) Catalysis .....	261
5.4	Co(I)–Co(II)–Co(III) Catalysis in Radical Cycloadditions .....	275
5.5	Co(II)–Co(III) Catalysis: Cyclopropanation .....	276
5.6	Co(II)–Co(III) Catalysis: Intra- and Intermolecular C–H Amination of Hydrocarbons .....	280
5.7	Co(II)–Co(III) Catalysis: Hydrocobaltation/Functionalization of Alkenes .....	282
5.8	Co(II)–Co(III) Catalysis: Reductive 1,2-Dioxine Ring Opening and Tandem Reactions Involving It .....	291
5.9	Co(II)–Co(III) Catalysis: Radical Additions .....	295
5.10	Co(II)–Co(III) Catalysis: Radical Cyclizations .....	299
5.11	Miscellaneous .....	301
6	Rhodium-Catalyzed Radical Reactions .....	302
7	Iridium-Catalyzed Radical Reactions .....	308
8	Transition Metal-Catalyzed Radical Reactions According to Reaction Type .....	311
	References .....	311

## 1 Introduction

This review is divided into three parts. For a general introduction to the topic see Sects. 1 and 2 in Part 1. The basic reactivity patterns and the general methods to conduct radical-catalyzed reactions and to analyze the involved intermediates are discussed there. Processes catalyzed by metals of group 4 to group 7 are discussed in Sects. 3–10 of the first part. Synthetic methodology employing group 10 and 11 catalysts as well as reactions catalyzed by bimetallic catalytic systems are covered in the third part. A general overview of the scope and limitations of this review is provided in Part 1 (Part 1, Sect. 2.8). The available methodology to form (or cleave) one or more C–C bonds and/or C–heteroatom bonds is the main focus of this manuscript.

## 2 Iron-Catalyzed Radical Reactions

Recently, iron catalysis gained general importance. Its catalytic chemistry has been summarized ([2]; recent reviews [3, 4]). Iron(II) and iron(III) salts have a long history in radical chemistry. The former are moderately active in atom-transfer reactions as well as initiators for the Fenton reaction with hydrogen peroxide or hydroperoxides (reviews [5–12]). Important applications of this principle are the Kharasch–Sosnovsky reaction (the allylic oxidation of olefins) [13], which often

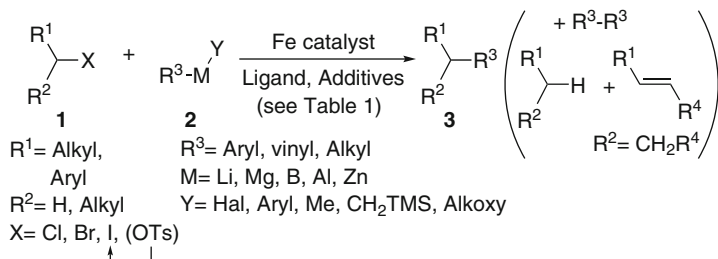
capitalizes on Fenton-type initiation to generate hydroxyl or alkoxy radicals, or the Minisci reaction to alkylate heteroarenes homolytically [14–16]. Iron(III) salts can be used stoichiometrically in oxidative dimerizations of enolates, phenolates, and electron-rich arenes (reviews [17, 18]). Iron-catalyzed asymmetric naphtholate dimerizations were developed very recently [19, 20]. Organometallic compounds can also be dimerized catalytically [21]. High-valent iron complexes are used extensively by Nature to catalyze oxidation reactions. The workhorse is cytochrome P450 (selected reviews [22–27]). As a synthetic counterpart, Barton developed Gif oxidation chemistry (reviews [28–31]).

## 2.1 *Low-Valent Iron-Catalyzed Reactions*

The most prominent reactions catalyzed by low-valent iron species involving radical intermediates are cross-coupling reactions of alkyl halides (recent reviews [32–35]) and atom transfer radical reactions. In cross-coupling reactions the oxidation state of the catalytically active species can vary significantly depending on the reaction conditions; very often it is not known exactly. To facilitate a summary, all iron-catalyzed cross-coupling reactions are treated together and involved oxidation states, where known, are mentioned at the example. In contrast, iron-catalyzed Kharasch reactions will be treated at the oxidation state of the iron precursors.

### 2.1.1 **Iron-Catalyzed Cross-Coupling Reactions of Alkyl Halides with Organometallic Reagents**

The alkylation of secondary alkyl halides by carbon nucleophiles represents a challenge in organic synthesis, since classical  $S_N2$  conditions lead to side reactions and yields are often low. Generally, transition metal-catalyzed cross-couplings represent a viable alternative, but for alkyl halides classical oxidative addition is much more difficult compared to alkenyl or aryl halides, since the activating effect of the adjacent unsaturation is lacking. Recently this obstacle was overcome and today transition metal catalyzed couplings of alkyl halides offer an effective alternative for the synthesis of branched alkanes or arylalkanes [32–35]. Among the available coupling reactions, iron-catalyzed processes often proceed via radical intermediates. Kharasch first noted the involvement of radicals when studying Fe-, Co-, and Ni-catalyzed homocouplings of aryl Grignard reagents using alkyl halides as stoichiometric oxidants [36]. Later studies by Kochi point clearly to the involvement of radicals in iron-catalyzed reactions of Grignard reagents with alkyl halides, although the active catalyst remained unclear [37]. These results were confirmed in later studies by CIDNP [38, 39]. In contrast, radicals do not seem to be involved in iron-catalyzed alkylations of vinyl bromides by alkyl Grignard reagents [37, 40, 41]. In Heck reactions of aryl iodides catalyzed by 10 mol%  $FeCl_2$  radicals are also unlikely to be involved [42]. Wunderlich and Knochel recently published the



**Fig. 1** Iron-catalyzed cross-coupling of alkyl halides with organometallic compounds

alkylation of diaryliron compounds by alkyl halides [43]. This process is, however, stoichiometric in iron, but catalyzed by nickel impurities in iron (see Part 3, Sect. 2.1). Thus, coupling reactions involving  $sp^2$ -electrophiles generally proceed by classical catalytic cycles.

Nakamura et al. provided the first evidence for the involvement of radicals in iron-catalyzed alkylation reactions of aryl Grignard reagents **2** (M=Mg) with secondary alkyl chlorides, bromides, and iodides **1**, which afforded alkylarenes **3** in 67–96% yield (Fig. 1, Table 1, entry 1) [44]. The conditions are mild and functional group tolerance is good, but a large excess of TMEDA and slow addition of the Grignard reagent was required. Primary alkyl halides were less useful, while tertiary alkyl halides did not afford products. Small amounts of biaryls and products resulting from reductive and  $\beta$ -hydride elimination were also observed in many coupling reactions.

Fürstner reported in parallel coupling reactions using 5 mol% of the isolated ferrate(–II) catalyst  $[\text{Li}(\text{TMEDA})]_2[\text{Fe}(\text{C}_2\text{H}_4)_4]$  **4** in THF (Fig. 2) (entry 2) [45, 46]. Primary and secondary alkyl bromides and iodides and allylic halides worked well, while alkyl chlorides and tertiary alkyl iodides were inert. Many sensitive functionalities like ester, nitrile, isocyanate, epoxide, and amine groups are tolerated.

Nagano and Hayashi found  $\text{Fe}(\text{acac})_3$  to be an active catalyst for the coupling of alkyl bromides **1** with aryl Grignard reagents **2** in ether (entry 3) [47]. Though no mechanistic evidence was provided, the similarity of the system suggests a radical process. An aryl triflate was inert under the reaction conditions in ether, but coupled with alkyl Grignard reagents, using the same catalyst in THF/NMP.

The Bedford group used 2.5 mol% of salen catalyst **5** to couple primary and secondary alkyl halides with aryl Grignard reagents in good to moderate yield (Fig. 2, entry 4) [48]. In parallel, coupling reactions using simple amines like triethylamine or DABCO as ligands in catalytic quantities were studied. The yields were similar to those obtained with excess TMEDA. The latter could also be used in catalytic amounts, but in somewhat lower yield (entries 5, 6) [49]. With 5-hexenyl bromide cyclic and acyclic products were found in similar yields of 30 and 22% (cf. Part 1, Fig. 8). This indicates that cyclization and coupling compete with an approximate rate constant of ca.  $10^5 \text{ mol}^{-1} \text{ s}^{-1}$  for this catalytic system.

For large scale preparations Cahiez and coworkers developed a simple process based on catalytic amounts of  $\text{Fe}(\text{acac})_3$  and catalytic amounts of a combination of

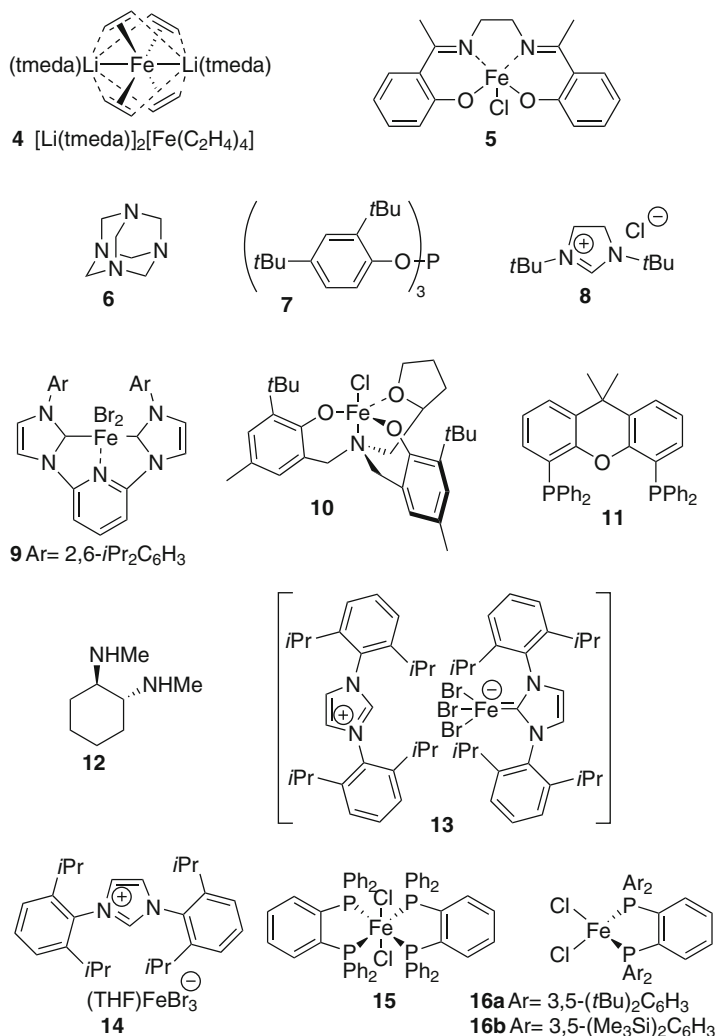
**Table 1** Iron catalyzed alkylations of organometallic reagents **2** by alkyl halides **1**

Entry	R <sup>3</sup>	Y	M	Fe source	Ligand/additives	Yield (%)	Ref.
1	Ar	Br	Mg	FeCl <sub>3</sub> (5 mol%)	TMEDA (excess)	45–99	[44]
2	Ar	Br	Mg, Li	<b>4</b> (5 mol%)	–	56–96	[45, 46]
3	Ar	Br	Mg	Fe(acac) <sub>3</sub> (5 mol%)	–	32–73	[47]
4	Ar	Br	Mg	<b>5</b> (2.5 mol%)	–	56–90	[48]
5	Ar	Br	Mg	FeCl <sub>3</sub> (5 mol%)	NEt <sub>3</sub> (10 mol%)	66–85	[49]
6	Ar	Br	Mg	FeCl <sub>3</sub> (5 mol%)	DABCO (5 mol%)	40–100	[49]
7	Ar	Br	Mg	Fe(acac) <sub>3</sub> (5 mol%)	TMEDA/ <b>6</b> (10/5 mol%)	39–94	[50] <sup>a</sup>
8	Ar	Br	Mg	[(FeCl <sub>3</sub> ) <sub>2</sub> (tmeda) <sub>3</sub> ] (1.5 mol%)	–	75–92	[50]
9	Ar	Br	Mg	FeCl <sub>3</sub> (5 mol%)	PCy <sub>3</sub> or dpph (10 or 5 mol%)	31–85	[51]
10	Ar	Br	Mg	FeCl <sub>3</sub> (5 mol%)	<b>7</b>	47–88	[51]
11	Ar	Br	Mg	FeCl <sub>3</sub> (5 mol%)	<b>8</b> or <b>9</b>	45–89	[51]
12	Ar	Br	Mg	FeCl <sub>3</sub> (5 mol%)	PEG	30–92	[52]
13	Ar	Br	Mg	<b>10</b> (5 mol%)	–	30–99	[53]
14	Alkenyl	Br	Mg	Fe(acac) <sub>3</sub> (5 mol%)	TMEDA, <b>6</b>	48–84	[54]
15	Alkenyl	Br	Mg	FeCl <sub>3</sub> (5–10 mol%)	TMEDA	40–98	[55]
16	Alkyl	Br	Mg	Fe(OAc) <sub>2</sub> (3 mol%)	<b>11</b>	8–64	[56]
17	Ar	Cl	Mg <sup>b</sup>	FeCl <sub>3</sub> (5–10 mol%)	<b>12</b>	20–80	[57]
18	Ar	Br	Mg	<b>13</b> (0.5 mol%); <b>14</b> (3 mol%)	–	74–96	[58]
19	Ar	Br	Mg <sup>c</sup>	FeCl <sub>3</sub> (5 mol%)	TMEDA	20–80	[59]
20	Ar	Ar <sup>d</sup>	Zn <sup>e</sup>	FeCl <sub>3</sub> (5 mol%)	TMEDA	72–99	[60]
21	Ar	Ar <sup>d</sup>	Zn <sup>e</sup>	FeCl <sub>3</sub> (1 mol%)	TMEDA	13–95	[61]
22	Ar	Ar <sup>d</sup>	Zn <sup>e</sup>	<b>15</b> (5 mol%)	–	58–93	[62]
23	Ar	Ar <sup>d</sup>	Zn <sup>e</sup>	<b>15</b> (3 mol%) <sup>f</sup>	–	69–92	[63]
24	Alkenyl	Alkenyl <sup>d</sup>	Zn <sup>e</sup>	FeCl <sub>3</sub> (5 mol%)	TMEDA	73–99	[64]
25	Ar	Me	Zn <sup>e</sup>	Fe(acac) <sub>3</sub> (10 mol%)	(CH <sub>2</sub> Br) <sub>2</sub> <sup>g</sup>	31–79	[65]
26	Ar	Ar	BAr <sub>2</sub>	<b>15</b> (5 mol%)	Zn(C <sub>6</sub> H <sub>4</sub> OMe) <sub>2</sub>	38–88	[66]
27	Ar	Bu	Bpin <sup>h</sup>	<b>16a,b</b> (10 mol%)	–	65–99	[67]
28	Ar	Ar	AlAr <sup>c</sup>	<b>15</b> (3 mol%)	–	55–96	[68]

<sup>a</sup>Large scale preparation<sup>b</sup>TMPMgCl-LiCl used for generation of the arylmagnesium reagent<sup>c</sup>In situ generation of Grignard reagent from both halides<sup>d</sup>The non-transferable Me<sub>3</sub>SiCH<sub>2</sub> group can be used instead<sup>e</sup>Mg(II) ions mandatory (Entries 20, 21, 22 not investigated but present)<sup>f</sup>In situ generation of the catalyst from FeCl<sub>3</sub> and ligand<sup>g</sup>Role as an oxidant to generate **1** in situ<sup>h</sup>Lithium borate complex used

10 mol% TMEDA and 5 mol% hexamethylenetetramine (HMTA) **6** (Fig. 2, entry 7) [50]. The isolated stable complex [(FeCl<sub>3</sub>)<sub>2</sub>(tmeda)<sub>3</sub>] also proved to be an efficient catalyst (entry 8) [50].

Bedford and colleagues found that phosphines, diphosphines, arsines, and bulky triaryl phosphites are convenient ligands [51]. Best results were obtained with



**Fig. 2** Catalysts and ligands used in iron-catalyzed cross-coupling reactions with alkyl halides

tricyclohexylphosphine or bis(diphenylphosphinyl)hexane (dpph) ligands, which provided the coupled products in good yield (entry 9).  $\text{FeCl}_3$  proved to be a more selective precatalyst than  $\text{FeCl}_2$ . A variety of trialkyl and triaryl phosphites were found to be active ligands in the coupling. Best results were obtained with bulky triaryl phosphites, such as tris(2,4-di-*tert*-butylphenyl) phosphite **7** (entry 10). NHC ligands, such as **8** or complex **9**, were competitive or superior in the iron-catalyzed coupling processes (entry 11). Pincer complex **9** failed, however, to catalyze the reaction of an alkyl chloride, while the in situ generation of an (NHC)iron complex from **8** gave a good yield in the coupling of chlorides; it was, however, not useful for the coupling of primary alkyl bromides. Tertiary alkyl halides did not couple.

Even iron nanoparticles, which may also be generated in several of the  $\text{FeCl}_3$ -catalyzed reactions discussed before, are catalytically active in the coupling of primary and secondary alkyl halides **1** with aryl Grignard reagents **2** (entry 12) [52]. The best system proved to be 5 mol%  $\text{FeCl}_3$  supported on predried polyethylene glycol (PEG) having a molecular weight of  $14,000 \text{ g mol}^{-1}$  in a ratio of Fe:PEG monomer of 1:1–2.5 giving iron nanoparticles of 7–13 nm diameter. With this catalyst alkylarenes **3** were formed in 30–92% yield. The activity of the catalyst is only slightly reduced on storage.

Kozak and coworkers reported catalyst **10** to be the most active among a number of related trigonal-bipyramidal iron complexes in the cross-coupling of primary and secondary alkyl halides (entry 13) [53].

A notable feature in all these coupling protocols is that the coupling rates of iron-phosphorus systems, of the (salen)iron complex **5**, the  $\text{Fe}(\text{acac})_3$  catalyst, and catalyst **10** with respect to the alkyl halide are rather uncommonly bromide > iodide > chloride (entries 3, 4, 9, 13), whereas the reactivity order for iron-amine catalyst systems is iodide > bromide > chloride (entries 1, 5, 6).

The reactivity of vinyl Grignard reagents is similar. In fact Cahiez and colleagues as well as Cossy and coworkers reported iron catalyzed cross-couplings of alkenyl Grignard reagents with alkyl halides **1** (entries 14, 15) [54, 55]. All possible geometric isomers of alkenyl Grignard reagents react well in the coupling reactions and the stereochemistry of the alkene unit is fully retained during the coupling. Ester, nitrile, carbamate, acetal, or alkyne functions are tolerated in the alkyl halide unit, but Cossy noted that the ester function has to be remote from the reacting halide function, since product mixtures result with bromoacetates or 3-bromopropionates. Alkyl chlorides and aryl halides were inert under their reaction conditions [55]. The method was applied to the synthesis of a fragment of the natural product spirangien A [69] and to the introduction of the isopropenyl group in a formal total synthesis of allokainic acid [70].

Even alkyl Grignard reagents can be coupled with alkyl halides **1** using iron catalysis with the xantphos ligand **11** (entry 16) [56]. The yields are acceptable for primary alkyl bromides. Secondary alkyl halides reacted only in low yield.

Tran and Daugulis expanded the range of applicable arylmagnesium reagents considerably (entry 17) [57]. A directed *ortho*-metalation/Kumada coupling strategy was devised to access functionalized alkylarenes and alkylhetarenes **3**. Functionalized arylmagnesium halides that are easily available using Knochel's mixed lithium magnesium tetramethylpiperidide base couple to alkyl bromides in the presence of 5–10 mol% of  $\text{FeCl}_3$  and 13–25 mol% of *rac*- $N,N'$ -dimethylcyclohexan-1,2-diamine **12** giving 44–92% yield of coupling products.

Recently, Gao and colleagues characterized the anionic  $\text{Fe}(\text{NHC})$  complexes **13** and **14** by X-ray crystallography and tested them in Kumada-type reactions of alkyl bromides **1** with phenylmagnesium bromide (entry 18) [58]. With **13**, catalyst loadings of 0.5 mol% suffice to obtain the coupling product in 89% yield. No slow addition of the aryl Grignard reagent was necessary. The simpler complex **14** is somewhat less active, but 74% yield of **3** was obtained at 3 mol% catalyst loading. A comparison of the catalytic activity of **13** with Bedford's NHC catalyst

**9** (entry 11) showed that the former anionic complexes are considerably more active.

Very recently von Wangelin-Jacobi et al. found that the use of preformed Grignard reagents is not necessary in the cross-coupling (entry 19) ([59]; highlight [71]). The reaction proceeds apparently by initial formation of an alkyl Grignard reagent followed by a transmetalation generating the aryl Grignard compound **2** in situ, which couples using 5 mol% of FeCl<sub>3</sub>. The reaction requires TMEDA as an additive. The functional group tolerance of the alkyl bromide and aryl bromide coupling partners is, however, lower as compared to the other catalytic systems.

The methodology is not limited to Kumada-type coupling reactions. Nakamura reported that diarylzinc reagents obtained by transmetalation of aryllithium or Grignard reagents are even more effective in such couplings with respect to functional group tolerance and simplicity of experimental setup, since no slow addition of reagents is necessary (entry 20) [60]. It is worth mentioning that the presence of magnesium ions was mandatory and that only one aryl unit is transferred to the substrate. Arylzinc halides are unreactive. If the aryl unit in Ar<sub>2</sub>Zn is valuable, mixed aryl(trimethylsilylmethyl)zinc reagents can be used to obtain arylalkanes **3** in high yield. Ester, nitrile, or alkyne functions are tolerated under the reaction conditions.

These studies were extended later to the coupling of primary, secondary, and tertiary alkyl tosylates with diarylzinc reagents generated in situ from aryl Grignard or aryllithium reagents with the ZnI<sub>2</sub>(tmEDA) complex (entry 21) [61]. The reactions proceed catalyzed by FeCl<sub>3</sub> in the presence of TMEDA in 13–95% yield. The outcome was dependent on the transmetalation conditions. Since tosylates are much less easily reduced than halides, it was suggested that iodide ions substitute the tosylate first and a radical was generated only subsequently by SET reduction.

Bedford and coworkers used bis(*ortho*-phenylenediphosphine)iron(II) complex **15** to catalyze the Negishi coupling of diarylzinc reagents with benzylic halides to give diarylmethanes in 58–95% yield (entry 22) [62]. For these more activated electrophiles a distinction between two-electron or radical pathways could not be made. If the aryl substituent was valuable, the trimethylsilylmethyl group was used as a dummy ligand at the organozinc reagent. The organozinc compounds were only active if at least catalytic amounts of a magnesium salt were present in the mixture. Its role consists most likely of promoting formation of a zincate complex in a Schlenk-type equilibrium. This facilitates transmetalation of the diarylzinc reagent to an aryliron species at the initial stage of the reaction. The resulting aryliron complex was proposed to be prone to dissociation to a cationic aryliron(II) species and to formation of a mixed zincate-iron(II) complex, both stabilizing the Fe(II) oxidation state during the coupling. Complex **15** is otherwise reduction-sensitive as most other precatalysts used in Kumada-type couplings above. The formation of a dark mixture, which shows much diminished catalytic activity, was observed on treatment of **15** with an aryl Grignard reagent in the absence of zinc compounds.

Fluorinated arylzinc reagents can also be applied provided that **15**, either isolated or generated in situ, was used as the catalyst precursor (entry 23) [63].

This allowed the synthesis of alkylpolyfluoroarenes in 69–92% yield. Nitrile, acetal, and aryl bromide functionalities were compatible with the reaction conditions. Hatakeyama and coworkers also extended the Negishi-type coupling methodology to vinyl zinc reagents (entry 24) [64]. Their reaction with primary and secondary alkyl chlorides or bromides using 5 mol% FeCl<sub>3</sub> and an excess of TMEDA provided 73–99% yield of alkylated olefins. Aryl bromides, esters, nitriles, and amides are tolerated in the method. The TMSCH<sub>2</sub> functionality can be used as a dummy ligand. It should be noted that the reaction is stereospecific with respect to the vinylzinc. Complete retention of olefin geometry was observed. Vinyl Grignard reagents are much less suited under the reaction conditions.

Cahiez reported chemoselective cross-coupling reactions of aryl(methyl)zinc reagents with dialkylzinc compounds catalyzed by Fe(acac)<sub>3</sub> using 1,2-dibromoethane as the stoichiometric oxidant. Alkylarenes **3** were obtained in 31–79% yield (entry 25) [65]. Ester and amide functionalities are tolerated by the method. The reaction may involve the initial oxidation of the alkylzinc reagent to an alkyl bromide by dibromoethane and subsequent cross-coupling. When Knochel's magnesium–iodine exchange was applied to the generation of the arylzinc reagent from aryl iodides, coformed isopropyl iodide participated in the coupling in 33% yield, while 55% of the desired coupling product was formed. When 3-pentylmagnesium chloride was applied instead, the more hindered 3-pentyl iodide did not interfere with the desired coupling. The homocoupling of mixed isopropyl(phenyl)zinc proceeded in 58% yield. 2-Octyl bromide reacted equally cleanly with isopropyl(phenyl)zinc to give 89% of 2-octylbenzene and 11% of the alkyl–alkyl coupling product.

Bedford and coworkers disclosed iron-catalyzed Suzuki–Miyaura-type coupling reactions of benzyl bromides with sodium tetraphenylborate in the presence of 5 mol% **15** as the catalyst and 10 mol% of dianisylzinc as a promoter. No reaction occurred in its absence. The coupling furnished 38–88% yield of **3** (entry 26) [66]. The transformation proceeds probably by initial B–Zn transmetalation. The resulting arylzinc transfers the aryl group to the iron catalyst as in the Negishi couplings above. An aryliron(I) complex was proposed to be formed initially.

Iron-catalyzed Suzuki–Miyaura coupling reactions were also reported by Nakamura and colleagues (entry 27) [67]. Alkyl halides **1** and mixed pinacol aryl(butyl)borates, generated in situ from arylboronates and butyllithium, were used as the reagents and 10 mol% of the iron complexes **16a** or **16b** as the catalysts. The addition of 20 mol% of MgBr<sub>2</sub> was essential for the success of the reaction. Products **3** were isolated in 65–99% yield. The methodology tolerates ester and nitrile functions. The reaction starts probably by initial boron–iron transmetalation to generate a diaryliron(II) complex.

Arylaluminum compounds generated in situ from aryl Grignard reagents and aluminum trichloride couple with primary and secondary alkyl bromides or chlorides catalyzed by 3 mol% of complex **15** in 55–96% yield (entry 28) [68]. Best results were achieved with the ate complex generated from 1 equiv. of AlCl<sub>3</sub> and 4 equiv. of the Grignard reagent or 1:3 mixtures of AlCl<sub>3</sub> and the corresponding



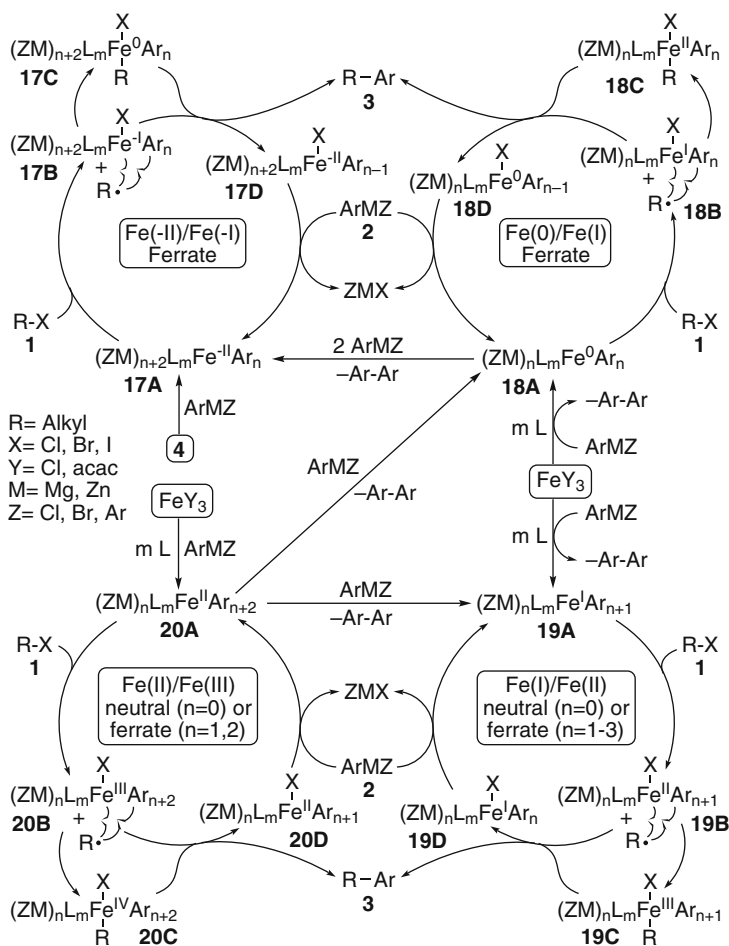
Grignard reagent, which favor ate complex formation in equilibrium as determined by NMR spectroscopy. The reaction tolerates ester functions.

A number of similar alkylations were reported, but no involvement of radicals was pointed out [72–77] or was not proven [75]. Shi and coworkers ascribed a radical mechanism to the coupling of alkyl Grignard reagents with vinyl pivalates [76]. Jacobi von Wangelin found that *tert*-butylmagnesium chloride served as a reducing reagent but not as a coupling partner in iron-catalyzed reaction of alkyl halides providing the corresponding hydrocarbons in 79–93% yield [77].

What is known about the nature of this cross-coupling family, the mechanistic course, and the active catalysts? In early studies of the reaction of alkyl Grignard reagents with vinyl bromides Kochi proposed Fe(0)–Fe(II) (**18A–D**) or Fe(I)–Fe(III) (**19A–D**) catalytic cycles, in which the iron species transmetalates the Grignard reagent fast (Fig. 3) [41]. Bogdanovic proposed a gross structure of [Fe(MgCl)<sub>2</sub>] (an inorganic Grignard reagent) and thus an Fe(-II) species as the active catalyst when iron salts are treated with 4 equiv. of alkyl Grignard reagents [78]. Thus reductive elimination is apparently very fast for most organoiron intermediates after transmetalation (for an exception see below). This catalyst is able to insert easily in aryl chlorides. Fürstner and coworkers reported cross-couplings of alkyl Grignard reagents with aryl halides and invoked [Fe(MgCl)<sub>2</sub>] as the active catalyst [79]. The same group provided more comprehensive structural insight to iron catalysis in these cross-coupling reactions and identified a nucleophilic ferrate manifold that mostly reacts without radical involvement and a low-valent iron manifold [46]. Both Ph<sub>4</sub>FeLi<sub>2</sub> and Ph<sub>4</sub>FeLi<sub>4</sub> complexes were structurally characterized, which points to the involvement of Fe(0) or Fe(II) ate complexes if an excess of Grignard reagent is present in the reaction mixture. Me<sub>4</sub>FeLi<sub>2</sub> was also structurally characterized and showed a pronounced ability to trigger SET reduction reactions of ketones [80].

From a comparison of the coupling of alkyl bromides **1** with aryl Grignard reagents **2** with different catalysts it can be concluded that all provided essentially the same result, although the required reaction temperatures and times varied (Table 1, entries 1–3, 5, 6, 8, and 9). The catalytic system using **4** is the fastest of all. That the most electron-rich complex is the best electron donor to generate radicals is a likely explanation. An Fe(-II)/Fe(-I) manifold (**17A–D**) accounts for the observed results (Fig. 3, Table 1, entry 2). Whether other catalyst systems can reach this redox state under the reaction conditions remains open. However, other low-valent redox manifolds, such as the Fe(0)/Fe(I) or Fe(I)/Fe(II) manifolds (**18A–D**, **19A–D**), are also viable and may account for the reactivity differences.

Nakamura's [44] and Bedford's [51] catalytic experiments support low-valent iron catalysts based on the fact that biaryls were formed indicating that reductive elimination of diaryliron species is facile producing low-valent Fe(0) or Fe(I) species **18A** or **19A**, which are the active catalysts. Bedford noticed the formation of dark colored reaction mixtures upon addition of the aryl Grignard reagent in all cross-coupling reactions using phosphines as the ligands supporting low-valent iron species as the active catalysts. For the coupling using the FeCl<sub>3</sub>/dpph catalyst,



**Fig. 3** Catalytic manifolds in iron-catalyzed cross-coupling reactions of alkyl halides **1** with organometallic species **2**

the formation of iron nanoparticles was proven by a TEM investigation [52]. Cahiez proposed a ferrate mechanism, in which the (amine)iron(III) precatalyst is reduced to an Fe(0) or Fe(I) complex **18A** or **19A** and biphenyl by the Grignard reagent [50].

Nagashima et al. showed that not only are low-valent pathways possible, but that Fe(II)/Fe(III) catalysis (**20A–D**) also operates [81]. In a detailed mechanistic investigation of the  $FeCl_3$ /TMEDA-catalyzed coupling of Grignard reagents the neutral complex  $Mes_2Fe(TMEDA)$  obtained by reaction of  $FeCl_3$ , TMEDA, and mesitylmagnesium bromide was characterized by X-ray crystallography. When this complex was subjected to octyl bromide, mesityliron bromide complexed by TMEDA was isolated in ca. 90% yield and also characterized by X-ray crystallography. Octylmesitylene was formed in 76% yield. An individual reaction of

mesityliron bromide with octyl bromide revealed that the conversion was significantly slower. This suggests that, at least for sterically hindered aryl groups, the diaryliron(II) complex is the active catalyst, which reduces the alkyl bromide to the corresponding radical. The reaction course is supported by the fact that almost no biaryl, typical for the generation of low-valent iron complexes (see above), was formed. Radical clock experiments with 5-hexenyl bromide gave only the acyclic coupling product (cf. Part 1, Fig. 8), while cyclopropylmethyl bromide gave 17% of cyclopropylmethylarene and 55% of 3-butenylarene resulting from ring opening of an intermediate cyclopropylcarbinyl radical ( $k = 1.3 \times 10^8 \text{ s}^{-1}$ ) [82, 83]. From this, the rate constant for coupling of the intermediate radical should amount to approximately  $10^7 \text{ mol}^{-1} \text{ s}^{-1}$ . Results obtained with iron complexes **15** and **16** also support an Fe(II)–Fe(III) catalytic cycle via **20A–D** more than low-valent iron catalyzed cycles via **17**, **18**, or **19**, respectively (entries 22, 23, 26–28) [62, 63, 67]. Organozinc reagents are apparently less activated to reduce iron(II) to low-valent iron complexes [62].

Most of the studies point to another important factor influencing the cross-couplings – the involvement of ate complexes. Organometallic ate complexes increase the rate of transmetalation to iron and are thus generally desired. The increased electron density of organoferrates facilitates the SET process generating the alkyl radical in contrast to neutral iron complexes. The ferrate manifold is therefore related to a higher reactivity in the cross-coupling [45, 46, 50], but sometimes a lower selectivity was attributed to this manifold. For the Fe(0)/Fe(I), Fe(I)/Fe(II), and Fe(II)/Fe(III) redox couples neutral and/or ferrate intermediates are possible. Slow addition techniques [44] or the use of sterically demanding complexes, such as **15a–c**, proved successful to prevent ferrate complex formation and to promote neutral pathways instead [62, 63, 67, 68].

Thus, for most of the catalytic systems, multiple pathways occurring at several formal iron oxidation states can be formulated. Common to all seems that SET reduction of **1** by the respective iron catalyst **17A–20A**, followed by halide dissociation, generates an alkyl radical and the oxidized iron species **17B–20B**. The alkyl radical may couple subsequently directly with the bound aryl group leading to a reduced iron halide **17D–20D** and the coupling product **3**. Alternatively, coupling with the oxidized aryliron species to an intermediate alkyl(aryl)iron complex **17C–20C** is possible, from which reductive elimination to product **3** and the reduced iron catalyst **17D–20D** occurs. The active catalysts **17A–20A** are regenerated by transmetalation with excess of the organometallic compound. A traditional oxidative addition is less likely, since typical groups that follow two-electron pathways, such as sulfonates, are unreactive in these iron-catalyzed cross-coupling reactions unless substitution by a halide is possible. Based on experiments with organoiron complexes it cannot be excluded completely, however, that radicals are only generated after formal oxidative addition and/or transmetalation by homolysis [46, 84]. Future studies must aim to dissect these manifolds further to build a rational foundation for these useful couplings.

The proposed alkyl radicals were detected in almost all couplings by typical probe reactions, such as the opening of cyclopropylcarbinyl radicals as well as radical 5-exo cyclizations of 5-hexenyl bromide, which proceed in competition to coupling (cf. Part 1, Fig. 8) [44–46, 49, 51, 52, 56, 60, 63, 64, 67, 69]. Stereochemical probe reactions, such as the racemization of optically active alkyl halides,<sup>1</sup> and the convergent formation of *trans*-disubstituted 1-aryl-4-*tert*-butylcyclohexanes from individual *cis*- and *trans*-4-*tert*-butylcyclohexyl bromides, gave hints on the involvement of radicals in the process (cf. Part 1, Fig. 9) [44–46, 60, 63]. It should be noted, however, that probe reactions are subtle. Cyclopropylcarbinyl radical ring opening reactions, the formation of *trans*-4-*tert*-butylcyclohexyl derivatives, and the racemization of optically active bromides, reliably occur and suggest radical intermediates. Intended radical 5-exo cyclizations do not always provide cyclized materials. This is due to a subtle kinetic balance of bimolecular coupling of the acyclic radical with the organoiron species and radical 5-exo cyclization. While typically fast Ueno-Stork-type cyclizations of halo ethers are useful reactions (see below), simple 5-hexenyl radical cyclizations often furnished mixtures of cyclized and uncyclized compounds [49, 51, 52]. In some cases direct coupling was considerably faster than cyclization, which may be traced to the higher coupling activity of the intermediate aryliron species [44–46].

### 2.1.2 Low-Valent Iron Catalysis: 1,5-Hydrogen Transfer/Kumada Coupling

Although the involvement of radicals in iron-catalyzed coupling reactions with aryl iodides was considered unlikely [42], Nakamura et al. reported a sequence of 1,5-hydrogen transfer and Kumada or Negishi-type coupling of a number of *N*-(*ortho*-iodobenzyl) *N,N*-dialkylamines **21** giving dibenzylic amines **22**, where radical intermediates are probably involved (Fig. 4) [85]. In analogy to alkyl halide coupling reactions, the sequence starts with transmetalation of the iron complex by the organometallic reagent and reductive elimination to a low-valent iron species **23A**. This complex triggers iodine abstraction from **21** leading to aryl radical **21A**, which stabilizes to  $\alpha$ -amino radical **21B** by 1,5 hydrogen transfer. This couples with the oxidized aryliron species **23B** to complex **21C**, which undergoes reductive elimination to products **22** in moderate to excellent yield. Cross-over reactions of deuterated and non-deuterated compounds point to a strictly intramolecular hydrogen transfer, suggesting that it occurs in the coordination sphere or at least in the vicinity of the iron complex.

---

<sup>1</sup>The racemization of optically active halides in the coupling process may, however, also be a result of the configurational lability of organoiron intermediates.

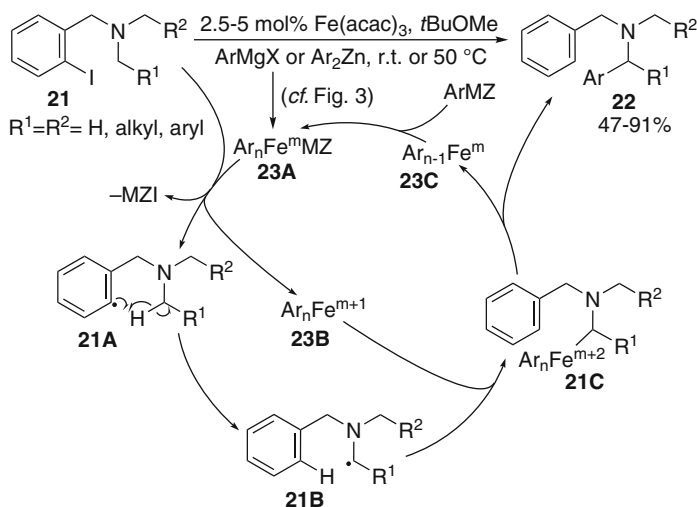
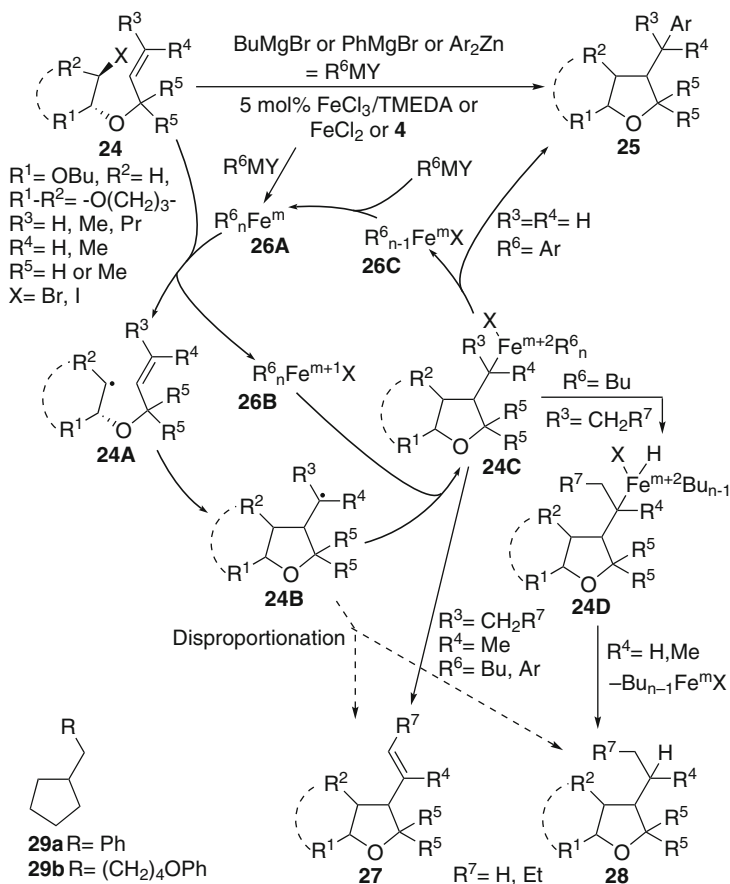


Fig. 4 Iron-catalyzed domino 1,5-hydrogen transfer/Kumada coupling

### 2.1.3 Low-Valent Iron Catalysis: Radical Cyclizations and Tandem Processes

Although Grignard reagents are known to trigger radical 5-exo cyclizations on their own [86], Oshima's group was the first to report iron-catalyzed radical cyclizations of haloacetaldehyde acetals **24** using phenyl or butyl Grignard reagents as the terminal reductants (Fig. 5, Table 2) [87]. After addition of the Grignard solution to  $\text{FeCl}_2$  a dark reaction mixture resulted, indicating a low-valent iron species as the active catalyst (cf. Fig. 3). The cyclization outcome was dependent on the structure of the alkene unit in **24** and the Grignard reagent. With phenylmagnesium bromide and acetals carrying di- and trisubstituted alkene units, 2-alkoxy-4-alkenyltetrahydrofurans **27** were obtained in moderate to good yields (entry 1). When butylmagnesium bromide was used, almost equimolar mixtures of alkyltetrahydrofurans **27** and alkenyl tetrahydrofurans **28** result (entry 2). Allyl and propargyl acetals generating primary and vinylic radicals provide, in contrast, reduced products **28** in 29–83% yield. Aryl radical cyclizations were also triggered by this catalyst system in good yields (cf. Part 1, Fig. 45). In no case was coupling with the Grignard reagent in a Kumada-type process yielding **25** observed.

Fürstner and coworkers reported radical cyclization reactions of **24** involving allyl, prenyl, or 3-phenylpropargyl acetal units using isolated catalyst **4** and phenylmagnesium bromide [45, 46]. Product **25** was isolated from the corresponding allyl acetal as the exclusive product in a tandem radical cyclization/Kumada coupling process (entry 3). The cyclization also proceeded smoothly with a prenyl substituent in **24**. Here, product **27** was formed in good yield, but no coupling product **25** was found (entry 4). Attempted tandem radical 5-exo cyclization/Kumada coupling reactions of 5-hexenyl bromide to cycle **29** did not proceed.



**Fig. 5** Radical 5-exo cyclizations and 5-exo cyclization/coupling sequences of iodo acetals

Nakamura disclosed tandem radical 5-exo cyclization/Negishi coupling reactions of **24** catalyzed by the  $\text{FeCl}_3/\text{TMEDA}$  catalyst system giving benzylbutyrolactols **25** in 73–86% (entry 5) [60]. The reaction can also be applied to fluorinated arylzinc reagents provided that **15** was used as the catalyst precursor (entry 6) [63]. Bedford's and Chai's groups reported successful 5-exo cyclization/Kumada coupling sequences with 5-hexenyl bromide giving **29a,b** (entries 7, 8) [52, 56].

The results indicate that a low-valent iron species **26A** is generated from the iron precursor first as described above. This leads to reductive generation of radicals **24A** via SET, which is efficient with all substrates **24** and catalyst systems. The cyclizations to radical **24B** proceed smoothly for the fast cyclizing  $\beta$ -iodo ethers, but for the slower cyclizing 5-hexenyl bromide (cf. Part 1, Fig. 8) cross-coupling of the initial radical may compete. The cyclized alkyl radicals **24B** couple most likely with the oxidized organoiron species **26B** resulting in cyclopentylmethyliron

**Table 2** Iron catalyzed radical 5-exo cyclization/cross-coupling reactions with organometallic reagents

Entry	R <sup>1</sup>	R <sup>2</sup>	R <sup>3</sup>	R <sup>4</sup>	R <sup>6</sup>	Y	M	Fe source	Product	Yield (%)	Ref.
1	BuO	H	Me, Pr	H, Me	Ph	Br	Mg	FeCl <sub>2</sub> (5 mol%)	<b>27</b>	36–83	[87]
2	BuO	H	Me	H, Me	Bu	Br	Mg	FeCl <sub>2</sub> (5 mol%)	<b>27/28</b> ca 1:1	41–88	[87]
3	-O(CH <sub>2</sub> ) <sub>3</sub> -	H		H	Ph	Br	Mg	<b>4</b> (1 mol%)	<b>25</b>	85	[45, 46]
4	-O(CH <sub>2</sub> ) <sub>3</sub> -	Me		Me	Ph	Br	Mg	<b>4</b> (1 mol%)	<b>27</b>	77	[45, 46]
5	BuO	H	H	H	Ar	Ar	Zn	Fe(acac) <sub>3</sub> (5 mol%), TMEDA	<b>25</b>	32–73	[60]
6	BuO	H	H	H	Ar	Ar	Zn	<b>15</b> (3 mol%)	<b>25</b>	85	[63]
7 <sup>a</sup>	H	H	H	H	Ph	Br	Mg	FeCl <sub>3</sub> (5 mol%), PEG	<b>29a</b>	56	[52]
8 <sup>a</sup>	H	H	H	H	Alk	Br	Mg	Fe(OAc) <sub>2</sub> (3 mol%), <b>11</b> (6 mol%)	<b>29b</b>	51	[56]

<sup>a</sup>5-Hexenyl bromide as precursor

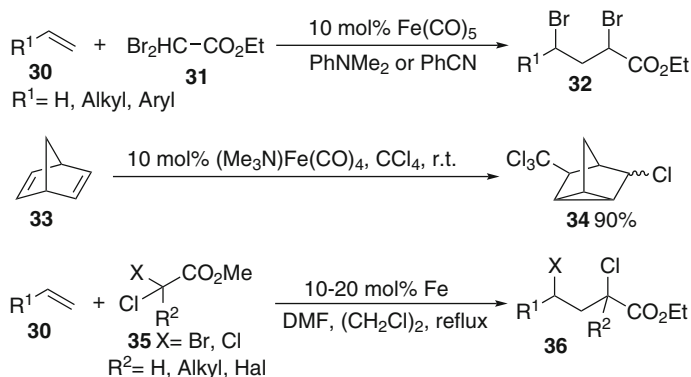
species **24C**. The substitution pattern at the cyclopentane ring and the iron center significantly determines the stabilization pathways to the products. For primary organoiron complexes bearing an aryl substituent at iron (R<sup>3</sup>=R<sup>4</sup>=H, R<sup>6</sup>=Ar), reductive elimination to coupling products **25** prevails in good yields. Tertiary iron species with iron-bound aryl substituents (R<sup>3</sup>=R<sup>4</sup>=alkyl, R<sup>6</sup>=Ar) are subject to selective β-hydride elimination leading to **27**, while mixtures of **27** and **28** are formed when the iron-bound substituent R<sup>6</sup> is an alkyl group. From intermediate **24C** competing β-hydride elimination is likely. This process leads to **27** when it occurs at the branched cyclopentylalkyl group. In competition β-hydride elimination from the iron-bound alkyl group R<sup>6</sup> proceeds, leading to hydride complex **24D**. Subsequent reductive elimination affords **28**. A potential disproportionation of tertiary radicals **24B** should not play a role, because both aryl and alkyliron species should give the same product distribution of **27** and **28**.

2-Chloro-1,6-heptadienes underwent alkylation/5-exo cyclization reactions in the presence of alkylaluminum reagents catalyzed by 5 mol% FeCl<sub>3</sub> in the presence of PPh<sub>3</sub> or DPEphos affording 2-alkylmethylenecyclopentanes in 30–80% yield. A polar two-electron mechanism was formulated for the reaction, but radicals may be involved [88].

## 2.2 Fe(0)–Fe(I) Catalysis: Radical Additions

### 2.2.1 Atom Transfer Radical Additions

Nesmeynov's and Freidlina's groups studied Kharasch additions of methyl dibromoacetate **31** to olefins **30** furnishing 2,4-dibromoesters **32** thoroughly in the 1960s and 1970s (Fig. 6) (review [89]). The preferred catalyst was iron



**Fig. 6** Kharasch additions catalyzed by low-valent iron species

pentacarbonyl. *N,N*-Dimethylaniline or benzonitrile are useful as ligands. Lactonization can also be promoted under the reaction conditions. Terent'ev and coworkers reported more recently ATRC of allylic dibromo and trichloroacetates using  $\text{Fe}(\text{CO})_5$  as the catalyst and DMF or proline as additives [90, 91]. Elzinga and Hogeveen published Kharasch additions of  $\text{CCl}_4$  to simple olefins **30** catalyzed by 10 mol% of  $(\text{Me}_3\text{N})\text{Fe}(\text{CO})_4$  or  $\text{Fe}_2(\text{CO})_9$  at room temperature in 10–95% yields [92]. Norbornadiene **33** gave the tricyclic derivative **34** resulting from a radical addition/3-exo cyclization/ligand transfer process in 90% yield, while bicyclobutanes underwent radical addition/cyclopropylcarbinyl radical ring opening sequences to bicyclo[3.1.0]hexene derivatives. Iron pentacarbonyl could also be used with  $\text{Cl}_3\text{CBr}$ . The catalysts are, however, prone to deactivation by precipitation of insoluble iron species.

Gasanov and coworkers studied the efficiency of  $\text{M}_3(\text{CO})_{12}$  ( $\text{M} = \text{Fe, Ru, Os}$ ) in the presence and absence of DMF as a ligand and found that the efficiency of the catalyst decreases in the order  $\text{Fe} > \text{Ru} > \text{Os}$  [93]. DMF activates all three systems. Its role was attributed to the generation of mononuclear complexes by ligand exchange, which are more active than the trinuclear complexes. The authors proposed that the radicals remain in the vicinity of the metal during the addition process. Even simple iron filings (20 mol%) catalyzed the ATRA of 2-bromo-2-chloroesters **35** to simple terminal olefins **30** in 48–84% yield [94]. 2, 2-Dichloroesters reacted in the presence of 10 mol% iron filings in 6–81% yield [95]. Trichloroacetate or trichloroacetamides can also be applied and gave the 2,2,4-trihalogenated esters or amides **36** in 18–89% yield. DMF also proved to be crucial as a cosolvent in these reactions. They are inhibited by oxygen, hydroquinone, and 1,4-dinitrobenzene.

All these reactions proceed most likely by initial activation of the iron(0) species by a ligand exchange with the activating additives, such as amines, benzonitrile or DMF (Fig. 7). Thus generated mononuclear iron complexes bearing a labile ligand are activated to form coordinatively unsaturated iron complexes **37A**. These species reduce the polyhalo compounds to radicals **38A**, which add to olefins **30** or **33**.



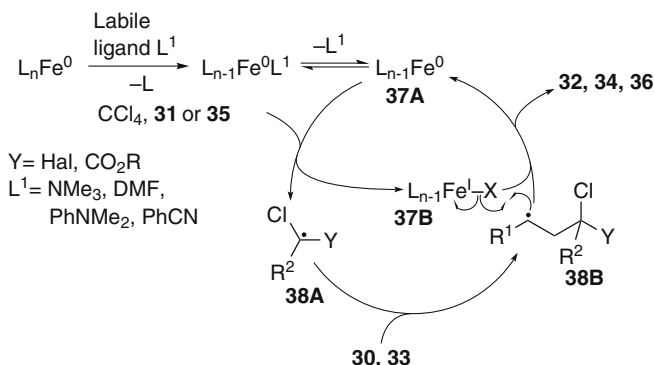


Fig. 7 Catalytic cycle of Kharasch additions catalyzed by iron(0) complexes

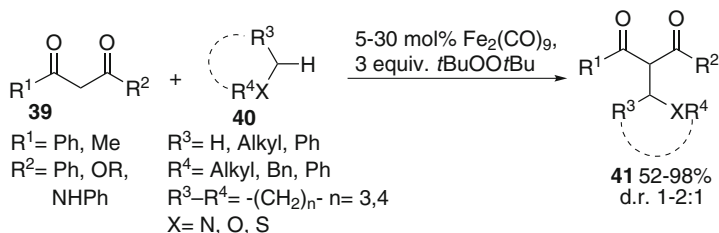


Fig. 8 Iron-catalyzed coupling reactions of  $\beta$ -dicarbonyl compounds with ethers, sulfides or tertiary amines

The adduct radicals **38B** can undergo direct ligand transfer from the Fe(I) complex **37B** to products **32**, **34**, or **36** and regenerate catalyst **37A**. Alternatively, it was proposed that **38B** couples with the Fe(I) metal center **37B** to an organoiron(II) species, which would be subject to reductive elimination.

## 2.2.2 Oxidative Radical Additions

Li and coworkers published addition reactions of ethers, sulfides, or tertiary amines **40** to  $\beta$ -dicarbonyl compounds **39** (Fig. 8) [96].  $Fe_2(CO)_9$  proved to be the catalyst of choice and di-*tert*-butyl peroxide the optimal oxidant.  $\alpha$ -Functionalized  $\beta$ -dicarbonyl compounds **41** were isolated in 52–98% yield. Although the details of the catalytic cycle remain unclear, it seems to be likely that the peroxide is reductively cleaved by the Fe(0) catalyst leading to an Fe(I) complex and a *tert*-butoxyl radical, which abstracts the  $\alpha$ -hydrogen atom of **40**. Addition of the resulting radical to the free enol form of **39** or the corresponding iron enolate of **39** may subsequently occur. It remains unclear, however, whether the main catalytic reaction proceeds on an Fe(0)–Fe(I) oxidation stage or whether further oxidation of initially formed Fe(I) rather leads to an Fe(II) catalyst. This cannot be excluded,

since it is known that a number of related reactions proceed clearly based on an Fe(II)–Fe(III) catalytic cycle (see Sect. 2.5) (reviews [97–100]). In fact, Fe(OAc)<sub>2</sub> was only slightly less active than Fe<sub>2</sub>(CO)<sub>9</sub> in the same reaction.

### 2.3 Fe(I)–Fe(II) Catalysis

Suzuki and Tsuji reported the first Kharasch addition/carbonylation sequences to synthesize halogenated acid chlorides from olefins, carbon tetrachloride, and carbon monoxide catalyzed by [CpFe(CO)<sub>2</sub>]<sub>2</sub> [101]. Its activity is comparable to or better than that of the corresponding molybdenum complex (see Part 1, Sect. 7). Davis and coworkers determined later that the reaction does not involve homolysis of the dimer to a metal-centered radical, which reduces the organic halide, but that radical generation occurs from the dimeric catalyst after initial dissociation of a CO ligand and subsequent SET [102]. The reaction proceeds otherwise as a typical metal-catalyzed atom transfer process (cf. Part 1, Fig. 37, Part 2, Fig. 7).

Hilt and coworkers developed radical addition/cyclization sequences of styrene oxides **42** and styrenes, dienes, 1,3-enynes, and acrylates **43** catalyzed by three catalyst systems: (A) 20 mol% of the Fe(dppe)Cl<sub>2</sub> complex [103], (B) FeCl<sub>2</sub> in the presence of 10 mol% PPh<sub>3</sub>/10 mol% NHC **44** [103], or (C) 20 mol% of (salen)iron(II) complex **45** (Fig. 9) [104, 105]. In all three methods NEt<sub>3</sub> and zinc were used as

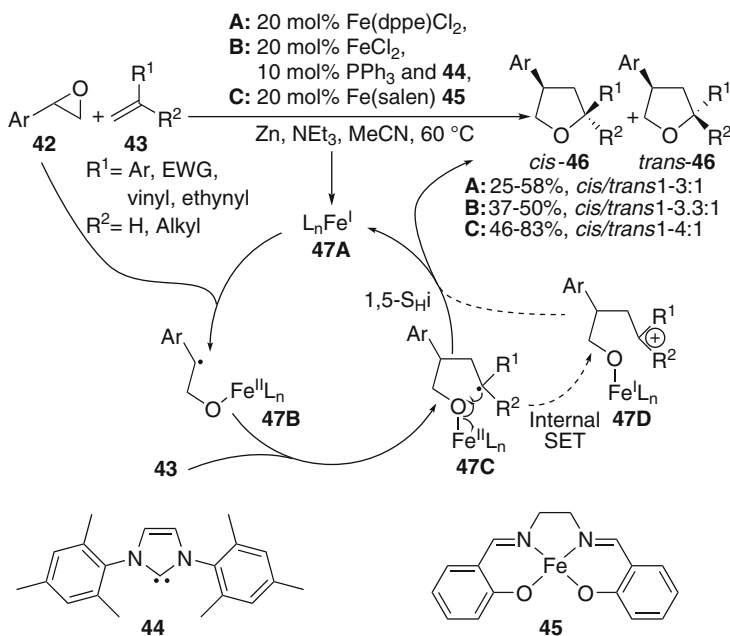


Fig. 9 Iron(I)-catalyzed addition-cyclization sequences

the base and stoichiometric reducing agent. Catalyst systems (A) and (B) gave moderate yields of tetrahydrofurans **46** at best [103, 106], while with catalyst **45** significant improvements of the yield to 48–84% were achieved [105]. The *cis*-diastereoselectivity of the process is low to moderate. The reaction was extended to annulations using cyclic olefins, which gave bicyclic tetrahydrofurans in 19–69% yield. Depending on the alkene structure, low to excellent diastereoselectivities were observed. The reaction is thought to proceed by initial reduction of the iron(II) catalyst to iron(I) species **47A**. This electron-rich intermediate triggers SET reduction of the epoxide in **42** similarly to titanocene(III) complexes (see Part 1, Sect. 3.3.2) to give iron-coordinated benzylic radicals **47B**, which add to the terminal double bond of olefins **43**. The resulting alkyl radical **47C** is ideally suited to undergo a 1,5-S<sub>H</sub>i reaction leading to the products **46** and catalyst **47A**, ready to enter the next cycle. Similar 1,5-S<sub>H</sub>i termination steps were also observed for titanocene chloride-catalyzed reactions (see Part 1, Sect. 3.3.2). Initially, an internal electron transfer from **47C** to iron(I)-coordinated carbocation **47D** and a subsequent intramolecular nucleophilic trapping by the iron alkoxide was proposed. While such a pathway may occur for radicals **47C** having strongly electron-releasing substituents, it would be highly unlikely for acceptor-substituted radicals, such as those resulting from addition to acrylates. Moreover, the very weakly oxidizing properties of iron(II) compounds suggest the absence of such a process.

## 2.4 Fe(II)–Fe(III) Catalysis: Kharasch Additions and Atom Transfer Cyclizations

Minisci discovered the strongly beneficial effect of iron catalysts on the course of Kharasch additions and traced it to the ability of Fe(II) to generate radicals reductively and the much higher rate constant of ligand transfer from FeCl<sub>3</sub> compared to chlorine transfer from CCl<sub>4</sub> (review [107]). In 1963 Asscher and Vofsi reported Kharasch additions of CCl<sub>4</sub> to olefins **48** catalyzed by 1 mol% FeCl<sub>3</sub> providing 1,1,1,3-tetrachloroalkanes **49** in 14–96% yield (Fig. 10) [108]. They discussed in principle the still accepted catalytic cycle (cf. Fig. 7, Fe(II) instead of Fe(0)). Catalytic amounts of diethylammonium chloride proved to be a useful additive in these reactions increasing the yields. Cupric chloride gave higher yields than FeCl<sub>3</sub> due to the slower ligand transfer with the latter.

Brace reported atom transfer radical addition/cyclization sequences of 1,6-dienes **50** with CCl<sub>4</sub> using 1 mol% FeCl<sub>3</sub> as the catalyst and benzoin as the reducing

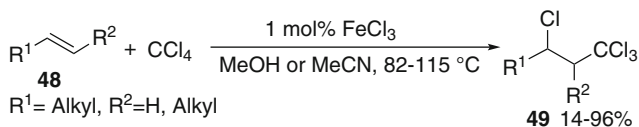
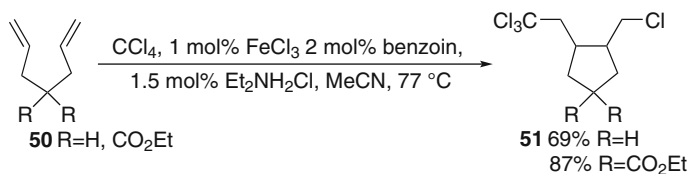
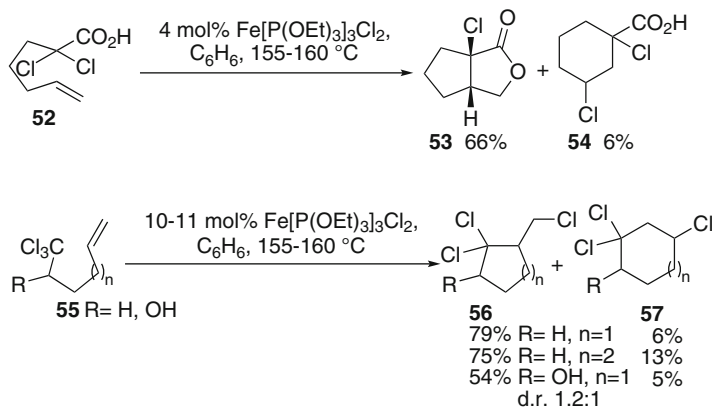


Fig. 10 Iron(II)-catalyzed Kharasch addition reactions



**Fig. 11** Tandem addition/cyclization sequences catalyzed by Fe(II)

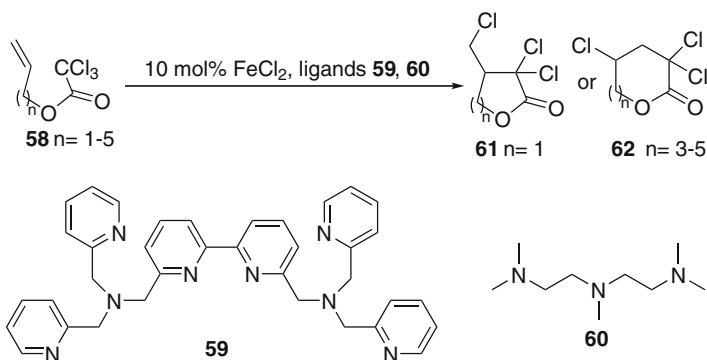


**Fig. 12** Weinreb's ATRC catalyzed by iron(II) complexes

agent for generation of the active Fe(II) catalyst and diethylammonium chloride as an additive (Fig. 11) [109, 110]. Cyclic products **51** were obtained in 69% and 87% yield as a *cis/trans*-mixture. Tsai and coworkers applied this methodology to the synthesis of non-natural carbanucleosides; however, double addition of  $\text{CCl}_4$  competed to a large extent [111].

Freidlina et al. used 10 mol% of  $\text{FeCl}_3$  and 40 mol% of *N,N*-dimethylaniline to promote Kharasch additions of methyl dibromoacetate, methyl 2,2-dibromopropionate, methyl tribromoacetate, or dibromomalonate to acceptor-substituted olefins (cf. Fig. 6) [89]. Either linear addition products **32** or lactones were obtained in 23–60% and 43–48% yield, respectively.

ATRC of alkyl 2,2-dichloro-6-heptenoates catalyzed by 3.7–12 mol%  $\text{Fe[P(OEt)}_3\text{]}_3\text{Cl}_2$  provided 1-chloro-2-(chloromethyl)cyclopentanecarboxylates in 63–85% yield as a 1.8–5.3:1 *trans/cis*-diastereomeric mixture (cf. Part 1, Fig. 38 **133**→**134**–**137**) [112, 113]. Small amounts of 6-endo cyclization products were also detected, but only traces of lactones, if at all. The corresponding free carboxylic acids, such as **52**, gave in contrast 66–91% of lactones **53** together with small amounts of 6-endo cyclization product **54** (Fig. 12). Simpler 2-bromo- or 2-chloro-6-heptenoates furnished 48–93% of cyclized products under similar conditions [114]. The *cis/trans*-selectivity was not high for most acyclic substrates, but lactonization was facile for most *cis*-derivatives under the reaction conditions.



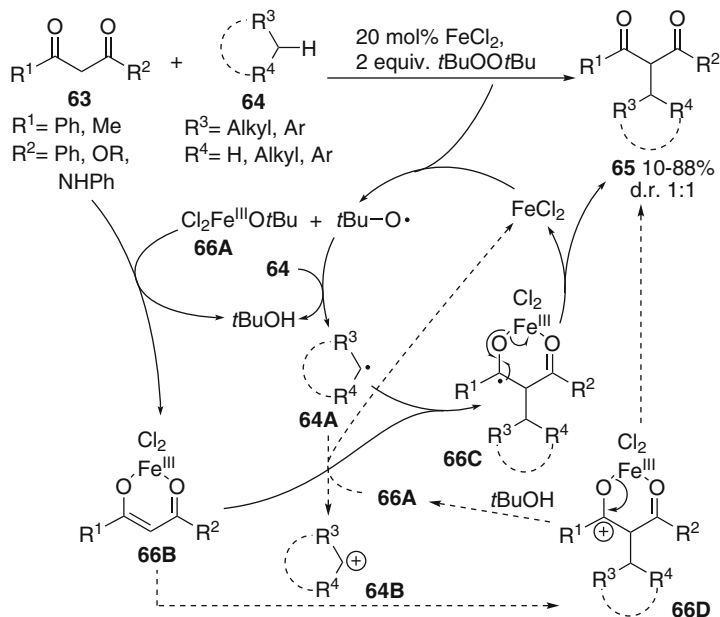
**Fig. 13** Iron(II)-catalyzed ATRC of trichloroacetates

Annulation reactions also proceeded in 72–88% yield with moderate to excellent diastereoselectivity. Even simple 1,1,1-trichloro-5-hexenes or 6-heptenes **55** gave chlorinated carbocycles **56** in 54–79% yields [115]. Approximately 10% of products **57** resulting from 6-endo or 7-endo cyclizations were also isolated.

By use of chelating tri- and tetramines **59** or **60** Kharasch additions can be performed in 65–75% yield using 0.3–10 mol% FeCl<sub>2</sub> as the catalyst (Fig. 13) [116, 117]. The same catalysts are very efficient to promote otherwise difficult ATRC of  $\omega$ -alkenyl trichloroacetates **58** providing five-membered lactone **61** by 5-exo cyclization in 55% yield and eight- to ten-membered lactones **62** by 8–10-endo cyclizations in 34–50% yield, respectively. Even  $\omega$ -allyl oligo(ethyleneoxy) trichloroacetates underwent radical macrolactonization reactions in 56–60% yield with 10 mol% of catalyst.

## 2.5 Fe(II)–Fe(III) Catalysis: Radical Additions and Cyclizations

Li and coworkers merged the iron-catalyzed Fenton reaction and the capability of iron to chelate  $\beta$ -dicarbonyl compounds **63** to an efficient radical addition protocol to synthesize  $\alpha$ -branched alkyl- $\beta$ -dicarbonyl compounds **65** in 10–88% yield (Fig. 14) [118, 119]. The reaction course can be rationalized by initial cleavage of the peroxide bond of the stoichiometric oxidant di-*tert*-butyl peroxide by the iron catalyst (20 mol%) to generate a *tert*-butoxyl radical, which abstracts a hydrogen atom from substrates **64**. Cogenerated iron(III) compound **66A** complexes  $\beta$ -dicarbonyl compounds **63** leading to chelate **66B**. Radicals **64A** add in the next step to **66B** forming radical **66C**, which liberates the Fe(II) catalyst and the alkylation product **65**. Interference of a catalytic cycle involving cationic intermediates is also possible (dashed arrows). In this process, oxidation of radical **64A** by iron(III) complex **66A** forms carbocation **64B** and regenerates the iron(II) catalyst, which is able to start a new catalytic cycle. Concomitantly, addition of cation **64B** to iron enolate **66B** forming intermediate **66D** may proceed. Product **65**

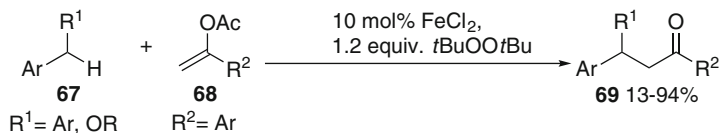


**Fig. 14** Radical additions by Fenton-type initiation

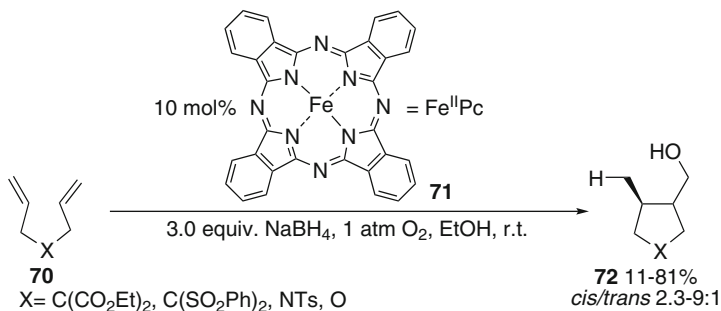
and iron complex **66A** are released by solvolysis with *tert*-butanol. The latter cycle seems to be viable, although only for sufficiently electron-rich benzylic substrates; less oxidizable benzylic radicals and secondary alkyl radicals should react at the radical stage. Needless to say, the active catalyst can also be a complex formed initially from  $\text{FeCl}_2$  and **63**.

Indoles can be used as radical acceptors instead of **63** [120, 121]. Simple and twofold reactions giving either 3-alkylindoles [120] or 1,1-bis(3-indolyl)alkanes [121] were observed in 16–72% and 54–90% yield, respectively. In both methods the indole is subject to radical addition in 3-position. The resulting  $\alpha$ -amino radical undergoes a further oxidation and deprotonation to the 3-substituted indole. In the case of twofold additions, the second indole unit is introduced by a subsequent polar Friedel–Crafts-type alkylation.

A cross-coupling of  $\beta$ -dicarbonyl compounds **63** with phenols furnishing benzofurans using di-*tert*-butyl peroxide as stoichiometric oxidant was reported recently [122]. The same authors recently found that  $\alpha$ -hydroxy ketones can be used to alkylate phenols using a  $\text{FeCl}_2/(t\text{BuO})_2$  catalytic system [123]. The methodology provides aryl  $\alpha$ -diketones in 51–88% yield and likely proceeds by initial hydrogen abstraction and subsequent SET oxidation of the corresponding  $\alpha$ -hydroxy ketones to  $\alpha$ -keto aldehydes, which undergo polar Friedel–Crafts alkylation at the phenols. The intermediate benzylic alcohols are oxidized to  $\alpha$ -diketones under the reaction conditions. The reaction course is supported by control experiments demonstrating the polar alkylation of phenols by  $\alpha$ -keto aldehydes and the dimerization of the initially formed ketyl radicals in the absence of phenols.



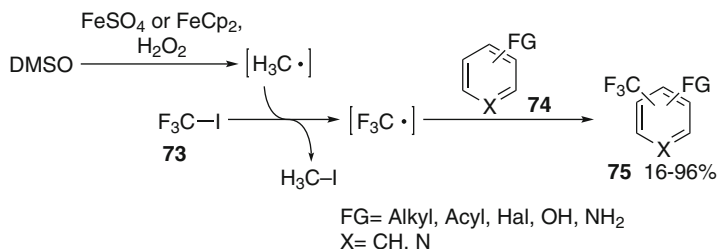
**Fig. 15** Iron(II)-catalyzed addition of alkylarenes to enol acetates



**Fig. 16** Oxygenative radical cyclizations of dienes catalyzed by (phthalocyanine)iron complex **71**

Shi and coworkers found that vinyl acetates **68** are viable acceptors in addition reactions of alkylarenes **67** catalyzed by 10 mol% FeCl<sub>2</sub> in the presence of di-*tert*-butyl peroxide (Fig. 15) [124]. β-Branched ketones **69** were isolated in 13–94% yield. The reaction proceeded with best yields when the vinyl acetate **68** was more electron deficient, but both donor- and acceptor-substituted 1-arylviny acetates underwent the addition reaction. These reactivity patterns and the observation of dibenzyls as side products support a radical mechanism, which starts with a Fenton process as described in Fig. 14. Hydrogen abstraction from **67** forms a benzylic radical, which stabilizes by addition to **68**. SET oxidation of the resulting electron-rich α-acyloxy radical by the oxidized iron species leads to reduced iron catalyst and a carbocation, which stabilizes to **69** by acyl transfer to *tert*-butanol. However, a second SET oxidation of the benzylic radical to a benzylic cation prior to addition followed by a polar addition to **68** cannot be excluded completely for the most electron-rich substrates.

(Phthalocyanine)iron **71** (10 mol%) proved to be a suitable catalyst to promote oxygenative radical cyclizations of 1,6-dienes **70** to hydroxy-substituted cycles **72** using sodium borohydride as the hydrogen source and oxygen (Fig. 16) [125]. In analogy to related manganese- or cobalt-catalyzed hydrofunctionalization reactions of olefins (see Part 1, Sect. 9.5 and Part 2, Sect. 5.7) catalyst **71** is probably transformed initially to an iron(III) hydride complex by NaBH<sub>4</sub>, which adds to one of the alkene functions of substrate **70**. The resulting alkyliron(III) species was proposed to be oxidized by oxygen to an alkyl radical and an iron(III) peroxy complex, which may be in equilibrium with starting **71**. Thus generated alkyl radical undergoes a 5-*exo* cyclization. The resulting alkyl radical is trapped by oxygen to give a peroxy radical, which couples to **71**. The resulting iron(III)



**Fig. 17** Iron-catalyzed radical trifluoromethylation for arenes

peroxide is cleaved reductively to product **72** (cf. Fig. 20). Catalyst **71** is probably regenerated by reductive dehydration with excess borohydride. Precedence for a hydroferration was provided by Okamoto and coworkers, who disclosed a single example of an iron-catalyzed hydration of styrenes, which proceeds in analogy to the cobalt-catalyzed reaction (see Sect. 5.7) [126].

Iron(II)-catalyzed Fenton-type radical generation was applied in Minisci reactions [14]. Perfluoroalkyl radical additions to arenes were reported by Minisci and coworkers using substoichiometric amounts of the Fenton system  $\text{FeSO}_4/\text{H}_2\text{O}_2/\text{DMSO}$  [127]. However, conversions were moderate. Kino and coworkers were able to reduce the amount of catalyst to 30 mol% and obtained a large number of trifluoromethylarenes and hetarenes **75** in 16–96% yield (Fig. 17) [128]. The reaction proceeds by generation of hydroxyl radicals from  $\text{FeSO}_4$  and  $\text{H}_2\text{O}_2$ , addition to DMSO, and fragmentation of a methyl radical, which abstracts iodine from trifluoromethyl iodide **73**. The trifluoromethyl radical formed adds to the arene **74**, and SET oxidation of the resulting cyclohexadienyl radical by Fe(III) and deprotonation complete the catalytic cycle. Similar alkylations were reported more recently by Maslankiewicz [129] and Duncton et al. [130].

Iron-catalyzed aryl radical additions to arenes were very recently developed (review [131]). Charette and coworkers reported cross-coupling reactions of aryl iodides **76** to arenes **77** catalyzed by 5 mol%  $\text{Fe}(\text{OAc})_2$  using bathophenanthroline **78** as the ligand and  $\text{KO}t\text{Bu}$  as the base (Fig. 18) [132]. The reaction works well for electron-poor and electron-rich aryl iodides as well as for heteroaryl iodides, giving biaryls **79** in 43–93% yield. The arenes **77** mostly consisted of benzene, but alkylated arenes and aryl ethers can also be employed in 28–81% yield. Most likely a (phenanthroline)iron complex, such as **80A**, is generated initially. This serves to reduce **76** reversibly to an aryl radical **76A**, which probably remains in the vicinity of the iron(III) complex. This allows addition to **77** present in large excess. The resulting arylcyclohexadienyl radical **76B** may stabilize by iodine transfer or SET oxidation by the cogenerated Fe(III) species and subsequent fast deprotonation by the base furnishing products **79**. A kinetic isotope effect (KIE) of 1.04 shows that hydrogen transfer is not rate limiting. Complete inhibition by TEMPO or galvinoxyl supports the reaction course. A related method using LiHMDS as a base and *N,N*-dimethylethylenediamine as a ligand gave similar results although a mechanism was not proposed [133].



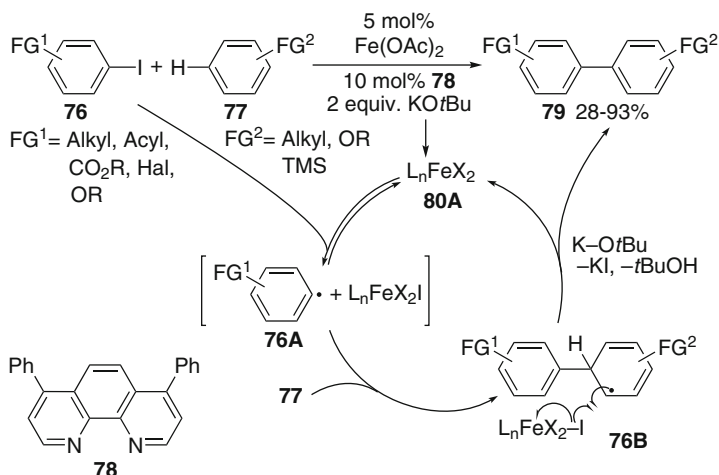


Fig. 18 Iron(II)-catalyzed arylation by aryl iodides

## 2.6 Fe(II)–Fe(III) Catalysis: Nitrenoid Cyclizations

Bach reported iron(II)-catalyzed chloroaminations, which proceed via radicals (Fig. 19). Allylic carbonyl azides **81a** react with 10 mol% FeCl<sub>2</sub> in the presence of stoichiometric amounts of TMSCl to 4-(1-chloroalkyl)oxazolidin-2-ones **82a** in 33–84% yield [134–136]. The cyclization was *trans*-selective, while the preferred relative configuration to the exocyclic chloride stereocenter was *threo*. Propargylic carbonyl azides **81b** cyclized to (*Z*)-chloroalkylidene and chloroarylidene oxazolidin-2-ones **82b** in 81–99% yield [137]. The reaction proceeds probably by cleavage of the azide function to dinitrogen and an iron-bound nitrenoid **81A**. This valence tautomeric nitrenoid, which can be depicted either as iron(III) amidyl or iron(II) nitrene species **81B**, behaves more like an amidyl radical, which cyclizes in a 5-exo manner to the alkene or alkyne units generating radical **81C**. Chlorine transfer from the dichloroiron group occurs preferentially with *threo*-diastereoselectivity for alkyl radicals and with *cis*-orientation to the amine unit for vinyl radicals indicating an intramolecular delivery. The catalyst is subsequently liberated by reaction with chlorotrimethylsilane. Attempts to prove the radical intermediacy by intercepting radical **81C** by a 5-exo cyclization failed, showing that intramolecular ligand transfer is considerably faster [135]. The method was also applied to the amidoglycosylation of glycols, resulting in 2-amido glycosyl chlorides with good to exclusive β-selectivity [138, 139]. γ,δ-Unsaturated carboxylic acids were similarly converted to 5-(1-chloroalkyl)lactams in 57–81% yield in a one-pot operation via the corresponding acid chloride and carbonyl azide intermediates [140].

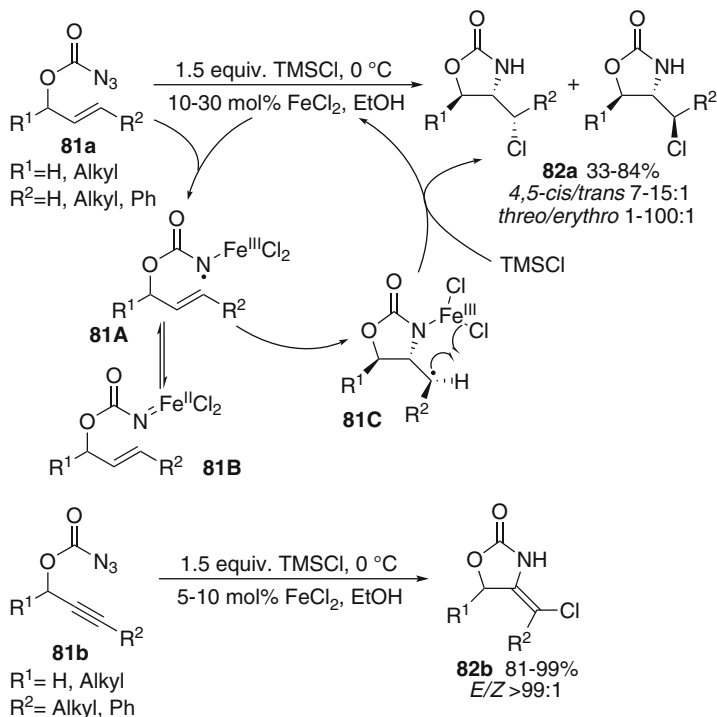
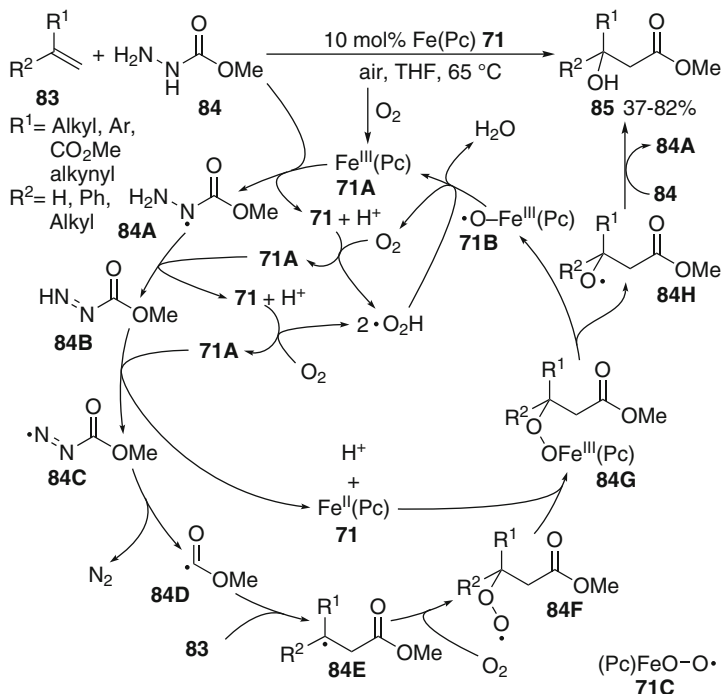


Fig. 19 Iron(II)-catalyzed intramolecular vicinal difunctionalization of alkenes or alkynes

## 2.7 *Fe(III)–Fe(II) Oxidative Catalysis*

### 2.7.1 Oxidative Radical Addition Reactions

Very recently, Taniguchi reported aerobic iron(III)-catalyzed radical hydroxycarboxylation reactions of olefins **83**. Alkyl carbazates **84** were used as the precursors and 10 mol% of (phthalocyanine)iron(II) **71** served as the catalyst (Fig. 20) [141]. Precatalyst **71** was oxidized probably by air to the corresponding iron(III) species **71A**. This oxidizes the alkyl carbazate **84** in a number of SET oxidation/deprotonation steps via **84A** and **84B** to azo radical **84C**. Fragmentation of nitrogen provides the crucial alkoxy carbonyl radical **84D**, which adds to **83** forming radical **84E**. This subsequently couples with oxygen. The resulting peroxy radical **84F** reacts with the reduced iron(II) complex **71**. Thus formed iron peroxide **84G** fragments to alkoxy radical **84H** and an iron(III) oxyl species **71B**. Alkoxy radical **84H** can subsequently serve to abstract hydrogen from **84** starting the next catalytic cycle (not shown for clarity). The iron oxyl complex **71B** can be reduced to the active catalyst **71A** by hydrogen transfer from cogenerated hydroperoxy radicals or **84**. An iron peroxy complex **71C** may also be formed reversibly and may contribute to the catalytic cycle by acting as a hydrogen atom acceptor.

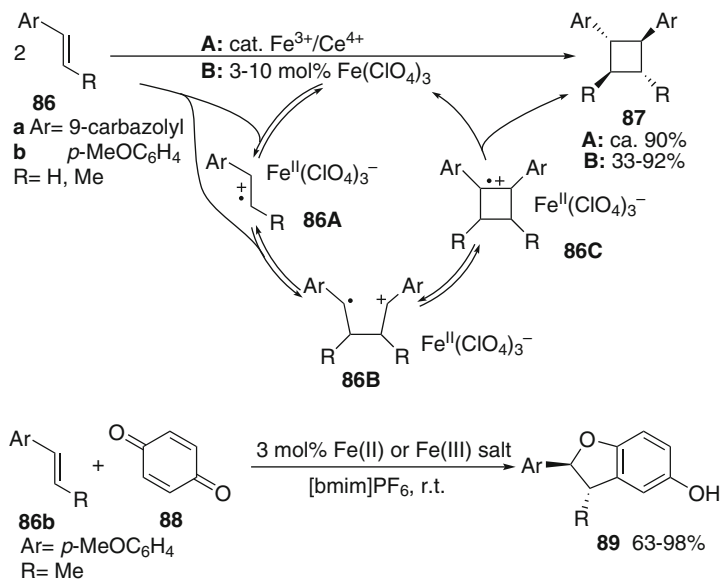


**Fig. 20** Oxidative radical hydroxycarboxylation reactions catalyzed by (phthalocyanine)iron (The depiction of the hydroperoxyl radical is formal to account for the correct proton and electron balance. Another formal hydroperoxyl radical (not shown for clarity) results from coupling of the initially generated superoxide and the proton resulting from formation of the azo radical)

### 2.7.2 Radical Cation [2+2] and [3+2] Cycloadditions

Bauld and coworkers studied the [2+2] cycloaddition of *N*-vinyl carbazoles **86a** and electron-rich styrenes **86b** catalyzed by iron(III) catalysts **A** or **B** in the presence of 2,2'-bipyridine as a ligand, which was reported originally by Ledwith and coworkers (Fig. 21) [142, 143]. Deuterium-labeling studies provided support for the stepwise nature of the process, consisting of reversible SET oxidation of the electron-rich olefin to a radical cation **86A**. Nucleophilic addition of excess **86** leads to distonic radical cation **86B**, which cyclizes to cyclobutane radical cation **86C**. Back electron transfer affords cyclobutanes **87** and regenerates the catalyst. Photoelectron transfer catalysis gave essentially the same result, thus supporting the pathway.

Itoh and colleagues reported more recently that *trans*-anethole **86b** underwent an analogous [2+2] cycloaddition to cyclobutanes **87** in 21–78% yield with complete *trans*-selectivity when 5–10 mol%  $\text{Fe}(\text{ClO}_4)_3$  was used as the catalyst [144]. Some ligands were tested and it was found that chiral BOX-type ligands, induced only



**Fig. 21** Iron-catalyzed [2+2] and [3+2] cycloadditions of electron-rich alkenes

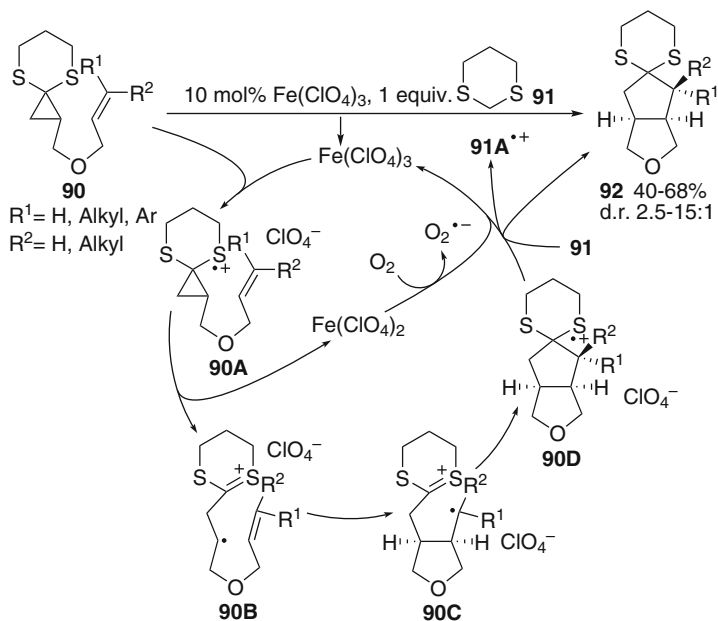
marginal ees, which is in line with the mechanistic proposal that the catalyst serves as a mere oxidant generating radical cation **86A**, but is not involved in the subsequent bond-forming step to **86B**. The reaction initially produced a 59:41 mixture of two diastereomers, which isomerizes slowly to the *all-trans*-isomer **87**. This indicates that the overall process **86B**→**86C** is reversible until all material is converted to the thermodynamic product **87** with *all-trans*-stereochemistry. The yield was improved to 92% when an Al<sub>2</sub>O<sub>3</sub>-supported iron(III) catalyst was used.

A similar, but overall [3+2] radical cation cycloaddition process involving alkoxyalkenes **86b** and benzoquinone **88** was subsequently developed (Fig. 21). *trans*-Dihydrobenzofurans **89** were produced in 33–94% yield catalyzed by 3 mol% Fe(ClO<sub>4</sub>)<sub>3</sub> [145]. The reaction can be performed in ionic liquids using 3 mol% FeCl<sub>3</sub>, FeCl<sub>2</sub>, or Fe(BF<sub>4</sub>)<sub>2</sub>. Compounds **89** formed with these catalysts in 63–98% yield. A stepwise process involving radical cation **86A** is likely, since the (*Z*)-isomer gave *trans*-product **89** exclusively. The reactions with Fe(III) salts probably proceed similarly by initial SET oxidation of **86b**. Coformed Fe(II) salt reduces **88** to its semiquinone radical anion, thus regenerating the catalyst. The analogous transformations applying iron(II) salts as catalysts are thought to involve initial SET reduction of **88** generating a semiquinone radical anion and an iron(III) catalyst, which oxidizes **86b** to radical cation **86A**. This is trapped by benzoquinone or its radical anion either in a [2+2] or a [3+2] cycloaddition mode. The former leads to an oxetane intermediate, which transforms to **89** by ring opening and recyclization, while the latter provides **89** directly.

### 2.7.3 Radical Cation Cyclizations

The SET oxidation of neutral molecules gives radical cations. Metal catalyzed radical cation reactions are so far not well developed in comparison to metal-mediated reactions, mainly because back-electron transfer (BET) by the reduced catalyst is hard to accomplish. Nakamura et al. reported a first iron-catalyzed bicyclization reaction of (allyloxymethyl)cyclopropanone dithioketals **90** to bicyclic 2-oxabicyclo[3.3.0]octanone dithioketals **92** in 40–68% yield (Fig. 22) [146]. The catalyst system of choice proved to be 10 mol% of ferric perchlorate in the presence of air and stoichiometric amounts of 1,3-dithiane **91**. The reaction is most likely initiated by SET oxidation of the thioketal unit in **90** to the corresponding radical cation **90A**. This triggers fast ring opening of the cyclopropane ring to distonic radical cation **90B**, which is suitably positioned for a 5-exo radical cyclization to the allyl ether unit. The resulting alkyl radical **90C** attacks the thionium ion in another 5-exo cyclization providing bicyclic thiyl radical cation **90D**. The reduced Fe(II) catalyst is reoxidized by air. The superoxide radical anion thus generated is able to reduce the thiyl radical cation of **90D** to **92**, but the selectivity is not high enough and side reactions occur. Therefore, 1,3-dithiane **91** proved to be the more efficient sacrificial reductant leading to its radical cation **91A<sup>•+</sup>**.

Wang and colleagues found that 10 mol% of FeCl<sub>3</sub> catalyzed the intramolecular oxidative cyclization of acceptor-substituted (*E*)- and (*Z*)-stilbenes **93** to



**Fig. 22** Iron(III)-catalyzed oxidative radical cation cyclizations (only major diastereomer **92** shown)

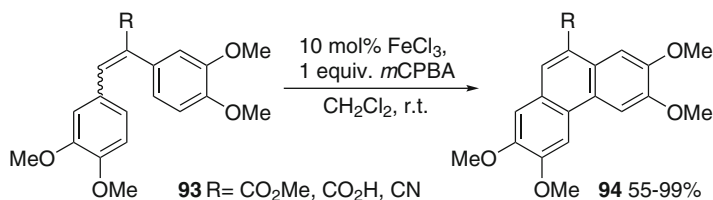


Fig. 23 Oxidative cyclizations of stilbenes catalyzed by  $\text{FeCl}_3$

phenanthrenes **94** using *m*CPBA as the stoichiometric oxidant (Fig. 23) [147]. Products **94** were formed in 55–99% yield. An ESR investigation showed the involvement of radical cations. Moreover, the reaction was inhibited by TEMPO. The course of the reaction is therefore best described by SET oxidation of the aromatic ring forming a delocalized radical cation, in which the double bond geometry is not fixed anymore. Intramolecular addition of the other arene unit leads to a distonic radical cation, which stabilizes by further SET oxidation to a cyclohexadienyl cation and rearomatization by deprotonation. The Fe(III) catalyst is regenerated by *m*CPBA. Oxidative dimerizations of phenols are also possible using this catalyst system.

## 2.8 Fe(III)–Fe(IV) Catalysis

Recently Liu and coworkers used (porphyrin)iron(III) chloride complex **96** to promote 1,5-hydrogen transfer/ $S_{\text{H}}1$  reactions of aryl azides **95**, which provided indolines or tetrahydroquinolines **97** in 72–82% yield (Fig. 24) [148]. The reaction starts probably with the formation of iron nitrenoids **95A** from **95**. These diradicaloids undergo a 1,5- or 1,6-hydrogen transfer from the benzylic position of the *ortho*-side chain. The resulting benzylic radicals **95B** react subsequently with the iron(IV) amide unit in an  $S_{\text{H}}1$  reaction, which liberates the products **97** and regenerates the catalyst. *N,N*-Dialkyl-*ortho*-azidobenzamides reacted similarly in 63–83% yield. For hydroxy- or methoxy-substituted indolines **97** ( $\text{R}^2 = \text{OH}$  or  $\text{OMe}$ ) elimination of water or methanol occurred from the initial products **97** under the reaction conditions giving indoles **98** in 74–78% yield.

Zhang and coworkers recently reported a hydrohydroxyalkylation of alkenes **100** by primary alcohols **99** catalyzed by 15 mol%  $\text{FeCl}_3$  in the absence of ligands affording secondary alcohols **101** in 48–93% yield (Fig. 25) [149]. The reaction is thought to occur by hydrogen atom abstraction from alcohol **99** via transition state **99A** by the iron(III) catalyst generating a ketyl radical-iron(IV) pair **99B**, in which the alkene is activated by complexation to iron. Radical addition leads to benzylic radical **99C**. Hydrogen transfer regenerates the catalyst and gives the product alcohols **101**. The radical mechanism was supported by crossover experiments using mixtures of two different alcohols, one of which was fully deuterated in

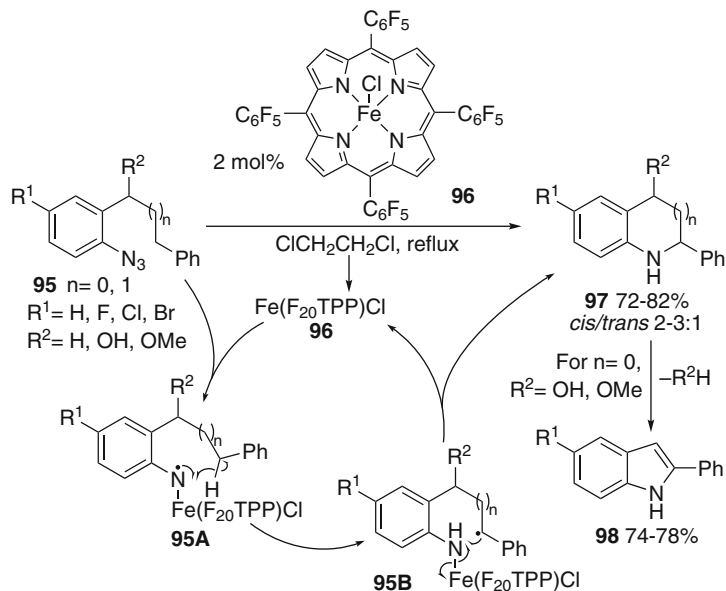


Fig. 24 Iron-catalyzed hydrogen transfer/ $S_{\text{HI}}$  cyclizations of nitrenoids

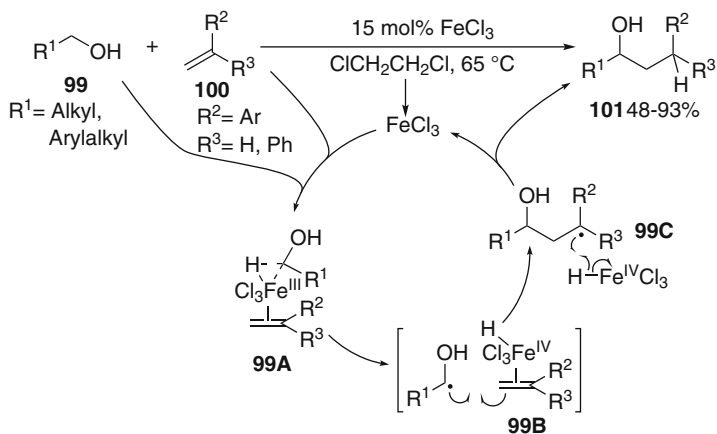
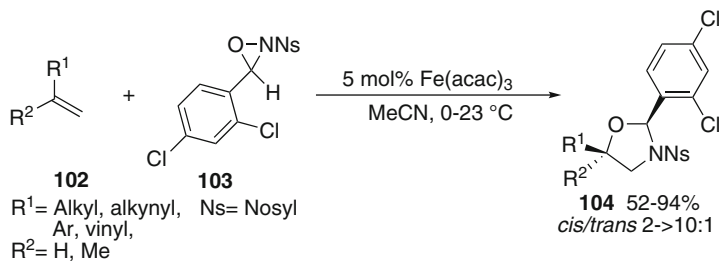


Fig. 25 Iron-catalyzed coupling of alcohols to olefins

$\alpha$ -position. Mixtures of deuterated and non-deuterated compounds resulted revealing that hydrogen transfer is intermolecular. An electrophilic addition mechanism was excluded since no deuterium incorporation was found, when *O*-deuterated alcohols or  $\text{D}_2\text{O}$  were used. Addition of thiophenol inhibited the reaction.

While working on Cu(II)-catalyzed aminohydroxylation reactions (see Part 3, Sect. 5.13) Williamson and Yoon found that oxaziridines **103** gave oxazolidines



**Fig. 26** Iron-catalyzed aminohydroxylation reactions

**104** on reaction with styrenes, 1,3-dienes, 1,3-enynes, or even simple olefins **102** and 5 mol% of Fe(acac)<sub>3</sub>. The reactions occurred in 52–94% yield with exclusive regioselectivity (Fig. 26) [150]. The products are regioisomeric to those in the corresponding copper(II)-catalyzed reactions. Although no mechanistic proposal was made, the reactions may occur similarly to the Cu(II)-catalyzed radical reactions involving oxaziridines (see Part 3, Sect. 5.13 for the mechanistic scheme). Ring opening of **103** by the iron(III) catalyst provides an iron(IV) oxide-bound aminyl radical, which adds to **102**. A 1,5-S<sub>H</sub>i reaction at the Fe(IV) oxide unit provides the products **104** and releases the Fe(III) catalyst. It can, however, not be excluded that the reaction proceeds on the Fe(II)/Fe(III) redox stage by initial reduction of the catalyst and subsequent reductive Fenton-type ring opening of the oxaziridine ring.

## 2.9 Miscellaneous

FeCl<sub>2</sub> was applied as a catalyst in the isomerization of isoxazoles to acylazirines, which proceeds by reductive cleavage of the N–O bond, 3-exo cyclization, and oxidation of the resulting ketyl radical by Fe(III) [151]. Noyori and coworkers studied the reductive cleavage of 3,6-dihydro-1,2-dioxines catalyzed by Fe(PPh<sub>3</sub>)<sub>3</sub>Cl<sub>2</sub> and observed similar selectivity and activities as with the corresponding ruthenium complex (see Sect. 3.5) [152]. Blanco and coworkers reported an oxidative cleavage of bicyclic bridgehead cyclopropanols to bicyclic hydroperoxides catalyzed by 4 mol% of Fe(acac)<sub>3</sub> in the presence of daylight and air in 35–68% yield. The reaction proceeds similarly to the vanadium-catalyzed process (cf. Part 1, Sect. 5.3 **103** → **105/106**) [153, 154]. A photochemically promoted CpFe<sup>+</sup>-catalyzed Bergman cyclization of enediynes using 1,4-cyclohexadiene or terpinene as hydrogen donors was reported by O'Connor and colleagues [155]. Ligand-centered radical intermediates were proposed in iron(II)-catalyzed cycloisomerization reactions of 1,6-enynes to retain an Fe(II) oxidation state; however, carbon-centered radical intermediates may be unlikely in the catalytically active species [156].



### 3 Ruthenium-Catalyzed Radical Reactions

Ruthenium catalysts found many applications in C–C bond formation reactions (selected reviews [157–161]). Ruthenium occurs mostly in oxidation states +2 and +3, but lower as well as higher oxidation states can easily be reached. Thus ruthenium compounds are frequently used in oxidative transformations proceeding by either single or two electron transfer pathways (selected reviews [162–164]). It has long been known that ruthenium complexes can be used for the photoactivation of organic molecules (selected reviews [165, 166]). Ruthenium complexes are applied as catalysts in controlled or living radical polymerizations [167–169].

#### 3.1 *Ru(0)–Ru(I)–Ru(II) Catalysis*

Boese and Goldman investigated the photocarbonylation of cyclohexane **105** cocatalyzed by  $d^8$  metal complexes, such as **106**, and aromatic ketones, like acetophenone **107** or benzophenone, as sensitizers (Fig. 27) [170]. The transformation furnished cyclohexanecarbaldehyde **108**. The formation of **108** was

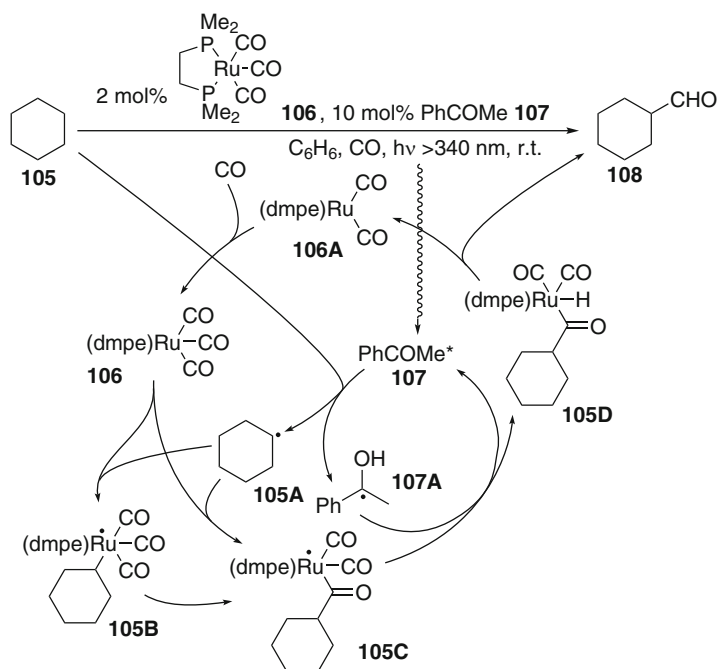


Fig. 27 Ruthenium(0)/phenone-cocatalyzed photocarbonylation of hydrocarbons

rationalized by initial excitation of the ketone catalyst **107** by  $>340$  nm light. The resulting triplet abstracts a hydrogen atom from **105**. The resulting alkyl radical **105A** subsequently attacks the 18e catalyst **106** (dmpe = bis(dimethylphosphinyl)ethane) either at the carbonyl ligand leading to 17e (acyl)ruthenium(I) complex **105C** or at the metal center generating 19e alkylruthenium(I) intermediate **105B**, which is subject to migratory insertion of a CO ligand resulting in **105C**. The metal-centered radical **105C** can in turn abstract a hydrogen atom from initially formed ketyl radical **107A** leading to ruthenium(II) hydrido complex **105D**. Reductive elimination liberates the coordinatively unsaturated complex **106A** and the product **108**. The mechanism was recently supported by a computational investigation of the reaction course. The addition pathway of the alkyl radical to bound CO ( $\rightarrow$ **105C**) is energetically preferred over radical coupling to the metal ( $\rightarrow$ **105B**) [171].

Kondo and coworkers studied the alkoxyacylation of alkyl iodides catalyzed by a large number of metal carbonyl complexes [172, 173]. Among them 4 mol%  $\text{Ru}_3(\text{CO})_{12}$  was highly active giving 82% yield of esters (cf. Part 1, Fig. 41 **152** $\rightarrow$ **154**). Gasanov and coworkers studied the efficiency of  $\text{M}_3(\text{CO})_{12}$  (M=Fe, Ru, Os) as catalysts for Kharasch additions in the presence and absence of DMF as a ligand and found that the efficiency decreases in the order Fe>Ru>Os [93]. DMF activates all three systems. Its role was attributed to the generation of mononuclear complexes by ligand exchange, which are more active than the trinuclear complexes. The authors proposed that the radicals remain in the vicinity of the metal during the addition process.

### 3.2 Oxidative or Reductive Photoredox Catalysis Using Ru(II) Complexes

It has long been known that Ru(II) complexes undergo efficient metal-to-ligand charge transfer (MLCT) on excitation with visible light [165, 166]. This behavior was widely used in supramolecular and materials chemistry. However, applications of this principle in organic chemistry remained scarce until recently (reviews [174, 175]). In early studies Whitten and others demonstrated that  $\text{Ru}(\text{bipy})_3\text{Cl}_2$  is reduced by tertiary amines, such as triethylamine to Ru(I) species. Moreover, the strongly reducing  $\alpha$ -amino radical was also able to reduce  $\text{Ru}(\text{bipy})_3\text{Cl}_2$  [176]. Fukuzumi and coworkers found that phenacyl bromides, irrespective of their electronic structure, were reduced by 10-methyl-9,10-dihydroacridine [177]. The course of the reaction depended on the acidity of the medium. In neutral medium oxidation of the dihydroacridine prevailed and Ru(I) resulted, while under acidic conditions the organic substrate was reduced directly leading to oxidation of Ru(II) to Ru(III). Based on these principles, both reductive and oxidative photocatalytic synthetic methodology involving radical processes was developed (reviews [174, 175]).

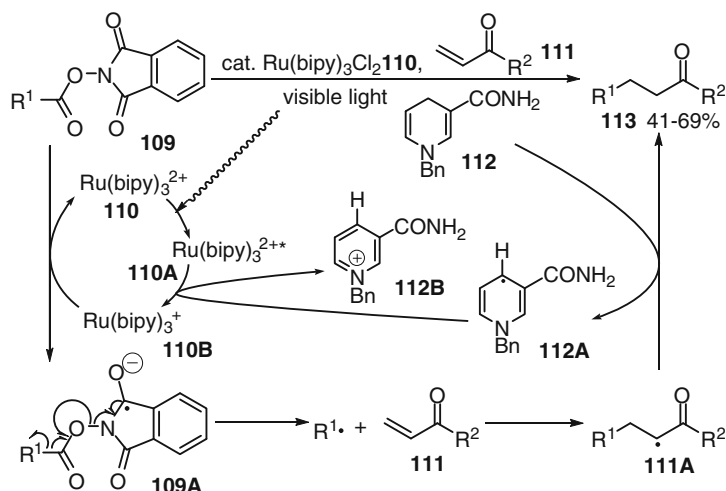


Fig. 28 Photoredox-catalyzed radical addition reactions

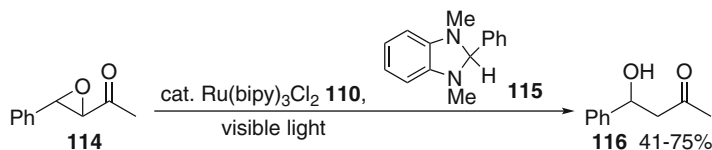
### 3.2.1 Ru(I)–Ru(II) Catalysis: Reductive Photoredox Reactions

Cano-Yalo and Deronzier reported the first application photoredox catalysis to organic reactions. Diazonium salts derived from 2,3-diphenylacrylate undergo a Pschorr reaction giving phenanthrenecarboxylates [178].

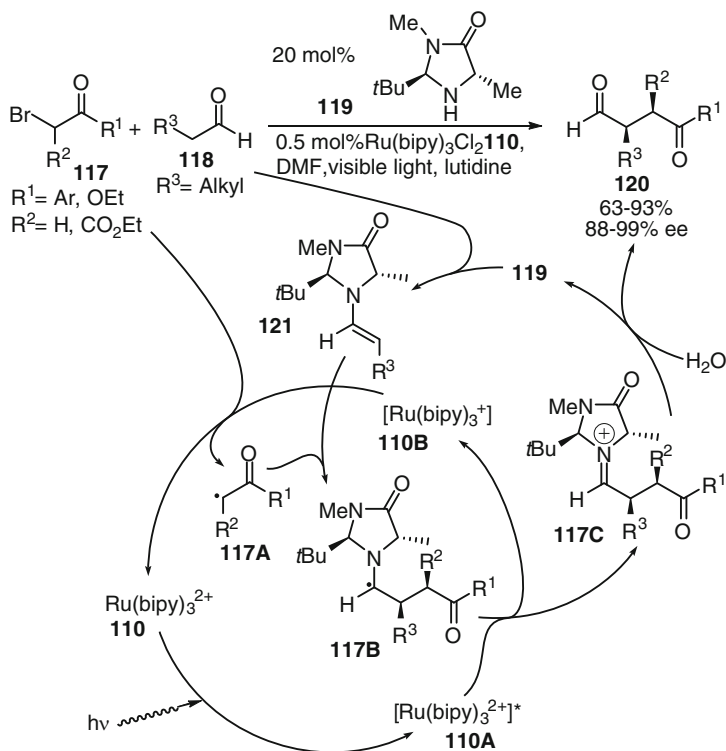
A few years later, Okada and colleagues investigated reductive radical additions of *N*-(acyloxy)phthalimides **109** to  $\alpha,\beta$ -unsaturated carbonyl compounds **111** catalyzed by  $\text{Ru}(\text{bipy})_3\text{Cl}_2$  **110** (Fig. 28) [179]. *N*-Benzyl-1,4-dihydropyridin-2(1H)-one **112** served as the initial reducing agent for the photoexcited ruthenium catalyst **110A**. Ru(I) catalyst **110B** thus generated reduces the phthalimide to its radical anion **109A**, which releases a carboxyl radical by  $\beta$ -fragmentation. Decarboxylation of the latter forms the alkyl radical, which undergoes addition to **111**. Adduct radical **111A** stabilizes by hydrogen abstraction from **112** furnishing products **113** in 41–69% yield. The cogenerated pyridyl radical **112A** subsequently serves as the reducing agent for the ruthenium catalyst to allow turnover. Similar conditions were later applied to catalyze radical reduction reactions of **109** mediated by *t*BuSH [180] or selenylation reactions using diphenyl diselenide as the reagent [181].

Hasegawa and colleagues recently reported the reductive ring opening of epoxy ketones **114** to 3-hydroxy ketones **116** catalyzed by 1 mol% of **110** (Fig. 29). Dihydrobenzimidazole **115** served as a reducing agent acting similarly to **112** [182].

Nicewicz and MacMillan merged later photoredox catalysis and asymmetric organocatalysis to an efficient approach to the otherwise difficult asymmetric  $\alpha$ -alkylation of aldehydes **118** by activated alkyl bromides **117** (Fig. 30) [183]. The concept of face differentiation at the  $\alpha$ -position of aldehydes via chiral enamines **121** provides the basis for the method. This allows the formation of functionalized

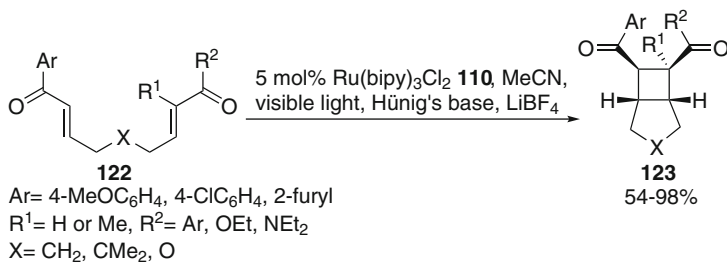


**Fig. 29** Photoredox-catalyzed ring opening reactions of epoxy ketones



**Fig. 30** Asymmetric aldehyde alkylation using organocatalyst **119** and reductive photoredox catalysis

aldehydes **120** in good yields and enantioselectivity. The reaction proceeds by two linked catalytic cycles. The ruthenium complex **110** (0.5 mol%) in the first one was excited by visible light to the excited Ru(II) catalyst **110A**. This will be initially reduced by an electron donor (such as **119** or **121**) to Ru(I) catalyst **110B**, whose reduction potential of  $-1.33$  V vs SCE is sufficient to reduce alkyl bromides **117** to electrophilic alkyl radicals **117A**. In the second, the imidazolidinone organocatalyst **119** (20 mol%) condenses with aldehydes **118** to enamines **121**. Radicals **117A**, whose concentration is much lower, add to **121** leading to  $\alpha$ -amino radicals **117B**. These electron-rich species reduce the excited Ru(II) complex **117A** in the other

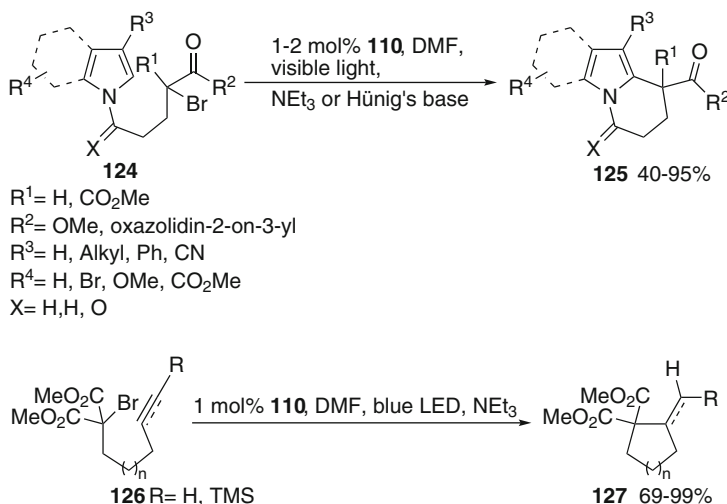


**Fig. 31** Photoredox-catalyzed intramolecular [2+2] cycloadditions

cycle to the active Ru(I) complex **110B** forming iminium ions **117C**, which hydrolyze to product aldehydes **120** and free organocatalyst **119**. A household light bulb is sufficient to trigger the process. The catalytic cycles are supported by the fact that the reactions do not occur in the absence of light or either catalyst. When the enamine **121** was cyclopropyl-substituted, no ring-opened product was isolated. This lends strong support to the fact that the enamine **121** is not undergoing SET redox processes to a significant extent.

In parallel Yoon reported intramolecular [2+2] cycloaddition reactions of tethered bis(enone)s **122** catalyzed by **110** in the presence of Hünig's base (Fig. 31) [184]. The photoexcited Ru(II) complex **110A** is reduced here under the reaction conditions by the amine (cf. Figs. 28 and 30). The resulting Ru(I) complex **110B** transfers an electron to the LUMO of **122**. A 5-exo cyclization of the resulting radical anion leads to a distonic radical anion, which cyclizes to form the four-membered ring. The final ketyl radical anion is oxidized by the amine radical cation or the ruthenium complex **110** to bicycles **123**. Products were isolated in yields of 54–98% as *meso*-diastereomers. Lithium tetrafluoroborate proved to be essential in two ways – first by increasing the solubility of the ruthenium complex by anion exchange and second to enhance the electron-accepting ability of the enone function by coordination. The method is limited to aromatic ketone functions – aliphatic carbonyl compounds do not react. The group extended this method to intermolecular cycloadditions provided that aromatic enones were used as one of the substrates under identical conditions [185]. The method worked best when the aromatic enones did not bear sterically too demanding  $\beta$ -substituents and the addition acceptors were terminal and not easily reducible. The products were isolated in 53–88% yield and with >10:1 *trans,trans*-diastereoselectivity.

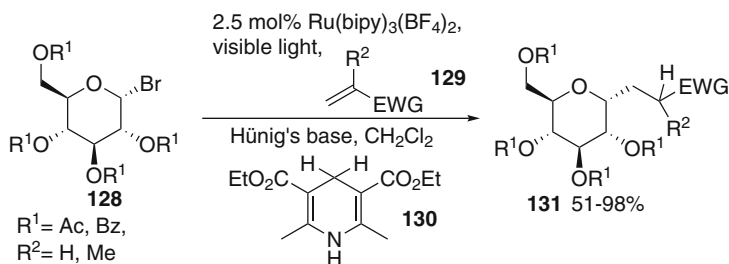
Stephenson and coworkers applied reductive photoredox catalysis to trigger radical 6-exo cyclizations of  $\omega$ -pyrrole or  $\omega$ -indole-substituted  $\alpha$ -bromocarbonyl compounds **124** [186] as well as radical 5-exo cyclizations of 2-bromo-2-(4-pentenyl)malonates **126** (Fig. 32) [187]. These cyclization processes provide bi- or tricyclic products **125** or cyclopentanecarboxylates **127** in moderate to excellent yields. The initial radical was formed with reduced ruthenium catalyst **110B** generated similarly as above from **110** and a sacrificial amine



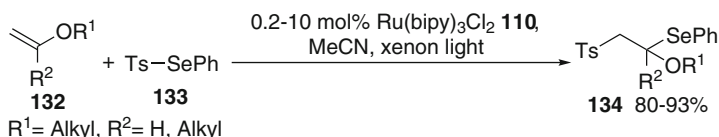
**Fig. 32** Photoredox-catalyzed radical cyclization reactions

(cf. Figs. 28 and 30). For the final stabilization of the cyclized radical to aromatic products **125** under the reductive conditions, several scenarios can be envisioned. SET oxidation of the cyclic radical by the ruthenium(II) complex and subsequent deprotonation may lead to **125**. The cyclic radical may also undergo bromine abstraction from the starting material thus starting an atom transfer chain reaction, in which the catalyst may act only as an initiator. A third mechanistic option consists of ligand transfer from the initially formed Ru(II)Br intermediate, as commonly observed in Ru-catalyzed Kharasch additions (see Sect. 3.3.1), and final HBr elimination seems to be less likely here, since such a process should also occur in cyclizations of **126** to **127**, but was never observed. For those substrates, the cyclized radical stabilizes exclusively by reduction. Either SET reduction of the cyclized radical/protonation or hydrogen abstraction from the solvent DMF or NEt<sub>3</sub> are viable pathways for this process. An iridium complex can also be used to catalyze these reductive cyclizations (see Sect. 7). Intermolecular radical additions of bromomalonate to indoles or pyrroles succeeded in 40–92% yield [188]. Triethylamine was not suitable as a reducing agent here, since charge recombination and radical reduction compete in these more challenging intermolecular additions. *N,N*-Diphenyl-*para*-anisidine was more convenient since it forms a more stable aminium radical cation, which is not a reductant but may rather act as a cooxidant for the benzylic radical formed after addition. Radical reductions were also performed using this methodology [189, 190].

Gagne and coworkers showed that Giese additions of glycosyl bromides **128** to  $\alpha,\beta$ -unsaturated carbonyl compounds **129** can be successfully performed using reductive photoredox catalysis (Fig. 33) [191]. Double addition of **129** competed to a considerable extent under standard conditions, indicating that reduction of the



**Fig. 33** Photoredox-catalyzed Giese additions



**Fig. 34** Ru(II)-catalyzed seleno sulfonation of enol ethers

radical resulting after addition was inefficient. The use of Hantzsch ester **130** as an external hydrogen donor led to superior results. Under optimized conditions applying 5 mol% of  $[\text{Ru}(\text{bipy})_3](\text{BF}_4)_2$ , 3 equiv. of Hünig's base, and 2 equiv. of both **129** and **130**, 51–98% of addition products **131** were isolated.

### 3.2.2 Ru(II)–Ru(III) Catalysis: Reductive Photoredox Reactions

Barton and colleagues described the seleno sulfonation of terminal enol ethers **132** with phenylselenyl toluenesulfonate **133** using 0.2–10 mol% of **110** and irradiation by xenon light (Fig. 34) [192].  $\beta$ -Sulfonyl selenoacetals **134** were obtained in 80–93% yields. Methyl acrylate can also be used, but the catalyst amount needed to promote the radical addition has to be 10 mol%. The reaction is thought to proceed by SET reduction of **133** by photoexcited **110**. Its fragmentation forms a ruthenium(III) phenylselenide and tosyl radical, which adds to **132**. The resulting  $\alpha$ -alkoxy radical was proposed by the authors to form product **134** by an  $\text{S}_{\text{H}}2$  process. The reaction thus proceeds as a radical chain reaction with **110** being only an initiator. A more active role of **110** may also be envisaged in that the initially formed Ru(III) catalyst may oxidize the adduct  $\alpha$ -alkoxy radical easily to an alkoxy-carbenium ion, which is subsequently trapped by the selenide anion. This process would regenerate **110** and allow initiation of a new catalytic cycle. Such a cycle is reminiscent of oxidative photoredox catalysis or the ability of ruthenium complexes to catalyze the Kharasch addition (see Sect. 3.3). A few other ruthenium complexes were also studied and gave similar results.

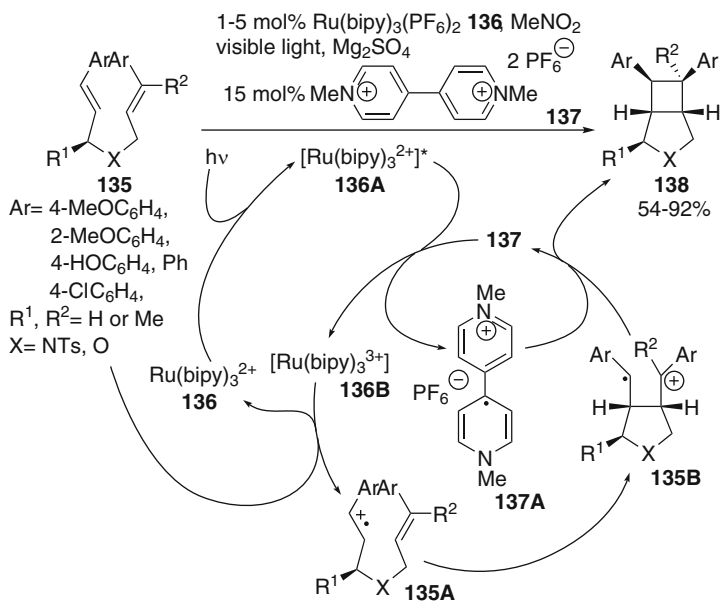


Fig. 35 Oxidative photoredox catalysis using Ru(bipy)<sub>3</sub>(PF<sub>6</sub>)<sub>2</sub> (anions omitted for clarity)

### 3.2.3 Ru(II)–Ru(III) Catalysis: Oxidative Photoredox Catalysis

Yoon and coworkers reported oxidative intramolecular [2+2] cycloadditions of dienes **135** using 1–5 mol% of Ru(bipy)<sub>3</sub>(PF<sub>6</sub>)<sub>2</sub> **136** as a photocatalyst (Fig. 35) [193]. In this method the photoexcited Ru(II) complex **136A** donates an electron to methylviologen **137** serving as a sacrificial oxidant. Ru(III) complex **136B** thus generated oxidizes electron-rich olefins **135** to radical cations **135A**. They are activated for [2+2] cycloadditions leading to distonic radical cations **135B** (see Part 1, Sect. 10 and Part 2, Sect. 2.7.2). These reactive intermediates cyclize rapidly to cyclobutane radical cations, which are reduced by methylviologen radical cation **137A** (or **136**) to bicycles **138**. The yields amount to 54–92% yield and the *meso*-diastereoselectivity is excellent. The mechanism is supported by the fact that (*E*)- and (*Z*)-cinnamyl ether give the same diastereoselectivity in the cycloaddition.

Koike and Akita applied 2 mol% of **136** to organocatalytic  $\alpha$ -oxygenation reactions of enamines or aldehydes with stable free radical TEMPO [194]. Photosensitization of Ru(II) generates a strong oxidant, which triggers the SET oxidation of the enamine formed as an intermediate. The resulting enamine radical cation reacts with TEMPO to form an  $\alpha$ -oxygenated iminium ion intermediate. After hydrolysis  $\alpha$ -oxygenated aldehydes result. This example occurs apparently at the oxidative Ru(II)–Ru(I) manifold. The reoxidation of the resulting Ru(I) complex was, however, not considered.



### 3.3 Ru(II)–Ru(III) Catalysis

#### 3.3.1 Atom Transfer Radical Additions

Due to the facile interconversion of Ru(II) and Ru(III) oxidation states, atom transfer reactions are easily possible. Ru(PPh<sub>3</sub>)<sub>3</sub>Cl<sub>2</sub> was recognized early as one of the most efficient Kharasch addition catalysts (Fig. 36) [195]. Since then the field has grown considerably and many examples of Ru(PPh<sub>3</sub>)<sub>3</sub>Cl<sub>2</sub>-catalyzed atom transfer radical additions (ATRA) were developed, which were reviewed recently [196]. Kamigata and coworkers developed a number of ATRA of sulfonyl chlorides catalyzed by Ru(PPh<sub>3</sub>)<sub>3</sub>Cl<sub>2</sub> [197]. Anderson and coworkers determined the scope of olefins **139** in the Ru(PPh<sub>3</sub>)<sub>3</sub>Cl<sub>2</sub>-catalyzed ATRA with CCl<sub>4</sub>, ethyl trichloroacetate, and chloromalonate **140** in detail recently [198]. Terminal and internal olefins reacted in moderate to excellent yields. Additions to electron-rich as well as electron-poor olefins proceeded. Additions using less reactive trichloroacetate esters also took place, but sometimes in somewhat lower yield. For more electron-rich cinnamyl alcohol-based olefins, addition/cyclization to butyrolactones prevailed (cf. Part 1, Fig. 37). Chloromalonate and phenacyl chloride reacted very slowly.

The mechanism of the addition was initially controversially discussed. Bland and coworkers showed in a kinetic study that radical intermediates are likely to be involved. This was also supported by crossover experiments using CCl<sub>4</sub> and CBr<sub>4</sub> [199]. The catalytic cycle can best be described by initial ligand dissociation from the Ru(II) precatalyst. The coordinatively unsaturated Ru(II) complex **142A** triggers SET reduction of the polyhaloalkane **140** generating a halomethyl radical **140A** and a ruthenium(III) complex **142B**. Radical addition of **140A** to olefins **139** leads to a more nucleophilic alkyl radical **140B**, which is subject to a fast ligand transfer from the electrophilic Ru(III) complex **142B**. In some cases the radicals may not be completely free, but caged to the complex.

Subsequently, many other mononuclear ruthenium complexes were successfully tested as catalysts (Fig. 37). Several catalyst classes were reviewed recently

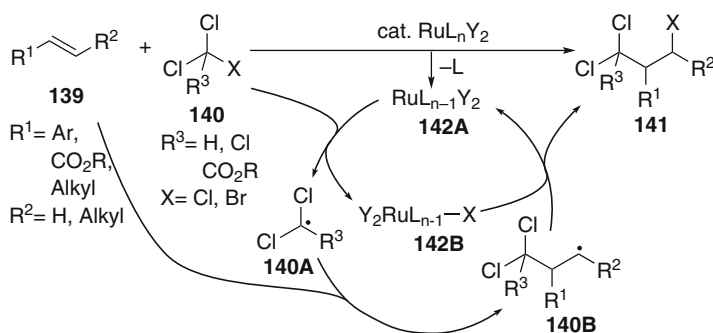


Fig. 36 Ruthenium(II)-catalyzed Kharasch additions

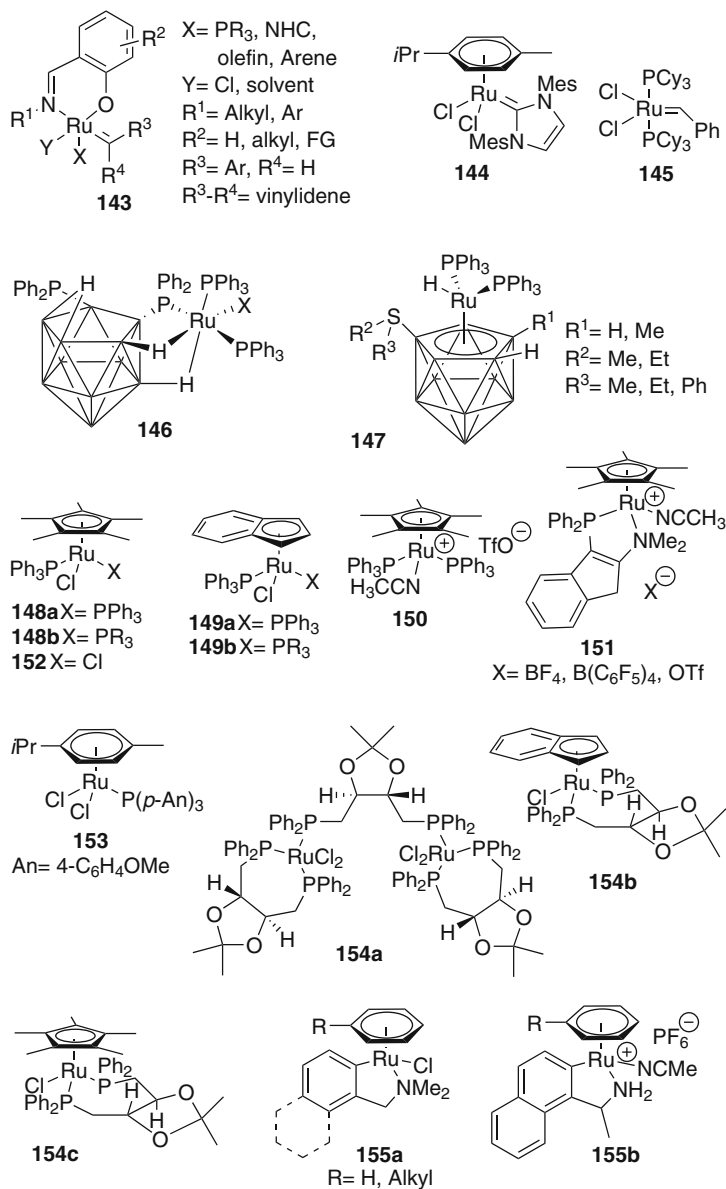


Fig. 37 Mononuclear ruthenium catalysts for Kharasch additions

[200–202], such as (salen)Ru complexes **143**, developed by Verpoort and coworkers (reviews [203, 204]), ruthenium-NHC complexes **144**, investigated by Noels and colleagues [205], and other structural motifs. Therefore only the general advances are summarized here.

Grubbs' first generation metathesis catalyst **145** was found to be an active catalyst for the Kharasch addition, provided its metathesis activity for the chosen olefin is low [206]. Snapper and coworkers found at the same time that the Grubbs I olefin metathesis catalyst is efficient for the Kharasch addition of less activated halides, such as  $\text{CHCl}_3$ , 1,1,1-trichloroethane, or ethyl trichloroacetate, to olefins like styrenes, acrylates, or acrolein [207, 208].

Demonceau and colleagues reported that 0.3 mol% of a complex of ruthenium(II) with an anionic carboranephosphine ligand **146** catalyzed the Kharasch addition of  $\text{CCl}_4$  to a range of electronically different olefins in 60–99% yield [209]. The same group developed on this basis (carbollide)Ru(II) complexes **147** with different substitution patterns on the sulfonium and carbollide unit to finetune the redox properties of the cyclopentadiene-like ligand [210, 211]. The results showed that ideal catalysts for the Kharasch addition of  $\text{CCl}_4$  to styrene or methyl methacrylate should have an intermediate redox potential to activate the reduced and the oxidized species in the catalytic cycle. With these catalysts turnover frequencies (TOF) of 1,880 and 1,500  $\text{h}^{-1}$  and total turnover numbers (TTN) of 4,200 and 9,000 were achieved.

Simal et al. introduced  $\text{Cp}^*\text{Ru}(\text{PPh}_3)_2\text{Cl}$  **148a** as an efficient Kharasch addition catalyst, which is applicable even for less activated halides, such as chloroform under very mild conditions [212, 213]. The related (indenyl)Ru( $\text{PPh}_3$ )<sub>2</sub>Cl **149a** can also be used, but is not suited for additions of  $\text{CHCl}_3$ . On this basis Frost and coworkers studied complexes **148b** and **149b** having two different phosphine groups coordinated to ruthenium. It was shown that they catalyzed the Kharasch addition of  $\text{CCl}_4$  to styrene similarly with TOF of up to 1,060  $\text{h}^{-1}$  [214]. Complexes **148b** with  $\text{Cp}^*$  ligands were the most active, while the corresponding indenyl complexes **149b** were much less potent. Tris(pyrazolyl)borate ruthenium complexes were not useful. ATRA using  $\text{CHCl}_3$  and tosyl chloride were performed in 93–99% and 33–96% yields, respectively. The TOF for both reactions were, however, considerably lower. Sawamoto and colleagues reported very recently an efficient template-controlled ATRA of methacrylic acid using 4 mol% of (indenyl) ruthenium complex **149a** [215, 216].

The Kharasch additions using **148** and **149** start by dissociation of a phosphine ligand from the catalysts. To avoid this step, Severin and coworkers introduced a related cationic catalyst **150** [217], which was obtained by ligand and anion exchange of precursor **148a**. Catalyst **150** displayed a much higher stability than the former and promoted the ATRA of  $\text{CCl}_4$  to a range of different olefins at 0.33 mol% catalyst loading in 67–97% yield. Chloroform also reacted efficiently with styrene under similar conditions. Cationic ruthenium complexes **151** based on aminoindenylphosphine ligands were reported by Stradiotto and colleagues [218]. They found that 0.05 mol% of the catalysts was sufficient to promote the addition of  $\text{CCl}_4$  to styrenes in 48–95% yield. Methyl methacrylate or 1-hexene, in contrast, gave the products only in low yields. However, addition of 5 mol% of AIBN was useful to allow efficient catalysis by 0.02 mol% of **151** providing the addition products in 66 and 99% yield, respectively.

A significant side product in Kharasch additions using  $\text{CCl}_4$  is  $\text{C}_2\text{Cl}_6$  formed by radical-radical coupling. This results in an increase of formation of unproductive  $\text{Cp}^*\text{Ru}(\text{PPh}_3)\text{Cl}_2$  **152** in the reaction mixture during Kharasch additions catalyzed by **148a** and thus in catalyst deactivation. To overcome this problem, Severin and coworkers added small amounts of radical starter azobis(isobutyronitrile) (AIBN) [219]. Its role consists of slow generation of isobutyronitrile radicals by thermal homolysis, which reduce **152** by ligand transfer back to **148a**. It then became obvious that much more stable **152** could be used as a precatalyst, which would be activated in situ to the coordinatively unsaturated Ru(II) catalyst by AIBN. Indeed, 0.005–0.5 mol% **152** proved to be a very active catalyst for ATRA of  $\text{CCl}_4$ , trichloroacetic acid, and even less activated  $\text{CHCl}_3$ , ethyl dichloroacetate, or tosyl chloride to electronically different olefins at 60 °C in 75–98% yield. The turnover numbers in these reactions amount to 1,300–1,700.

The use of AIBN has the disadvantage that chloroisobutyronitrile is an organic byproduct that may potentially contaminate the desired products. Therefore, magnesium was introduced as an alternative innocent reducing agent [220]. Under these conditions ATRA of  $\text{CCl}_4$  or chloroform with styrenes or acrylates gave 48–92% yield applying only 0.05–0.5 mol% of **152**. 1-Decene or  $\alpha$ -methylstyrene reacted with  $\text{CCl}_4$  in 81% and 96% yield, respectively. They were, however, not suitable substrates with chloroform. Trichloroacetate, dichloroacetate, or tosyl chloride added under similar conditions resulting in 52–97% yield using 0.1 mol% of **152**. Various other  $\text{Cp}^*\text{Ru}(\text{II})$  or  $\text{Cp}^*\text{Ru}(\text{III})$  catalysts were also tested, but gave inferior results. Oe and Uozumi developed on this basis a resin-supported version of catalyst **152**, in which the catalyst is anchored to the polymer via the phosphine ligand. This catalyst can be recycled several times [221].

A recent study showed that **152** behaves mechanistically different from other catalysts in addition reactions of more activated halides **140**, such as trichloroacetate to styrene [222]. After initial reduction to Ru(II), chlorine abstraction from substrates **140** is in contrast to all other ruthenium complexes not the rate limiting step (cf. Fig. 36). ESR spectroscopic investigations support this fact. The subsequent addition to styrene becomes rate limiting, while the final ligand transfer step is fast and concentration-independent. For less activated substrates **140**, however, chlorine abstraction becomes rate-determining again. Moreover, the Ru(III) complex itself can enter an, albeit considerably slower Ru(III)–Ru(IV) Kharasch addition cycle, when the reaction was performed in the absence of magnesium. This cycle operates, however, for only the most easily reducible halides, such as trichloroacetate.

Demonceau and colleagues studied (*p*-cymene)Ru(PAr<sub>3</sub>)Cl<sub>2</sub> complexes **153** and found that those having an electron-rich triarylphosphine ligand were especially active for the ATRA of  $\text{CCl}_4$  to simple 1-alkenes, which are notoriously difficult Kharasch addition substrates [223]. The yields decrease with increasing electron-deficiency of the arene unit in the phosphine ligand. The addition products were obtained under optimized conditions (0.3 mol% catalyst, 85 °C) in 82–99% yield. Styrene also reacted smoothly, while methyl methacrylate afforded considerable amounts of oligomers besides the desired product **141**. In a subsequent study it was

shown that **153** is comparable to  $\text{Ru}(\text{PPh}_3)_3\text{Cl}_2$  in its catalytic activity and that the use of microwave irradiation led to considerably improved yields in the Kharasch reactions [224]. Especially with acrylates the conversion to the desired products was much higher and the formation of oligomers decreased. Microwave irradiation had, on the other hand, a more moderate effect on the much less efficient addition of  $\text{CHCl}_3$  to alkenes.

Based on earlier applications Kamigaito and coworkers investigated asymmetric Kharasch additions using (diop)Ru(II) complexes **154a–c** [225]. All three mediated the ATRA of  $\text{BrCCl}_3$  to styrene in quantitative yield between 25 and 60 °C. The enantiomeric excess in the ligand transfer step amounted to 21–30% ee for **154a** and 15–23% ee for **154b**, respectively, while **154c** afforded a racemic product. These results show that bromine atom transfer can in principle be performed asymmetrically; future efforts must concentrate on finding more efficient catalysts with respect to face differentiation. Methyl (meth)acrylate reacted with  $\text{CCl}_4$  in high yield catalyzed by **154c**, but also without asymmetric induction. With **154a** and **154b** the yields were somewhat lower. The indenyl complex **154b** was slightly more selective. The differential asymmetric induction of **154a–c** was rationalized by the fact that in 18e complex **154c** one phosphine unit of the diop ligand must dissociate for bromine abstraction, which leads to a flexible monodentate system in the ligand transfer step, prohibiting face differentiation. In 16e complex **154a** and 18e complex **154b**, which can easily transform by indenyl  $\eta^5 \rightarrow \eta^3$  ring slippage to a 16e complex, the asymmetric environment induced by the ligand is preserved even in the oxidized form, thus resulting in noticeable enantioselectivity.

Very recently, Parkhomenko et al. used cycloruthenated complexes **155a** and **155b** to catalyze the Kharasch addition of  $\text{Cl}_3\text{CBr}$  to styrene, methyl methacrylate, acrylate, and 1-hexene in high yields [226]. The reaction with  $\text{CCl}_4$ , on the other hand, required microwave irradiation for all complexes and substrates to achieve moderate to good yields.

Besides mononuclear, dinuclear complexes were also applied successfully as Kharasch addition catalysts (Fig. 38) [200, 201]. Ruthenium amidinate complex

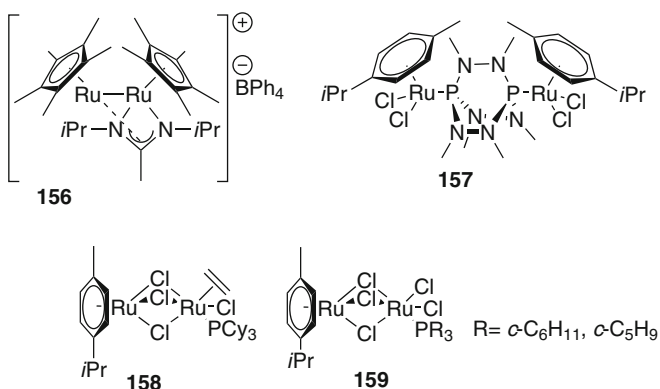


Fig. 38 Dinuclear ruthenium catalysts for ATRA

**156** is active in room temperature ATRA reactions of chlorinated pyrrolidones to alkenes [227]. It was subsequently demonstrated that 0.5 mol% of dinuclear ruthenium complex **157** having a bridging THDP ligand is an active catalyst for the Kharasch addition of  $\text{BrCCl}_3$  to simple olefins in water [228]. The yields ranged from 66–84%. The activity of the catalyst is strongly reduced in organic solvents. The catalyst is, in contrast to related rhodium and iridium catalysts, not useful in additions to internal alkenes and styrenes (see Sects. 6 and 7). Dinuclear chloro-bridged Ru(II)–Ru(II) complexes **158** and Ru(II)–Ru(III) complexes **159** were also tested for their activity in Kharasch additions [229]. In the presence of magnesium as a reductant for excess Ru(III), both catalyst types were active at loadings of 0.05–0.2 mol%. Especially Ru(II)–Ru(III) dinuclear complexes **159** combine stability and catalytic activity. Several electronically different alkenes react smoothly with  $\text{CCl}_4$  or trichloroacetate in 61–99% yield, but only styrene reacted cleanly in 74% yield with  $\text{CHCl}_3$  using the tricyclopentylphosphine complex. Dinuclear Ru(II)–Rh(III) complexes are also active in Kharasch addition reactions (see Part 3, Sect. 8.5).

Zakarian's group reported very recently a radical trichloromethylation related to ATRA (Fig. 39) [230]. They generated preformed titanium imide enolates **160A** from *N*-acyloxazolidinones **160** and subjected them to ATRA conditions using  $\text{Cl}_3\text{CBr}$  and 7 mol% of  $\text{Ru}(\text{PPh}_3)_3\text{Cl}_2$  as the catalyst. According to theoretical calculations, such titanium enolates display valence tautomerism, in which a titanium(III)- $\alpha$ -carbonyl biradical **160B** contributes besides classical **160A** strongly to the electronic structure

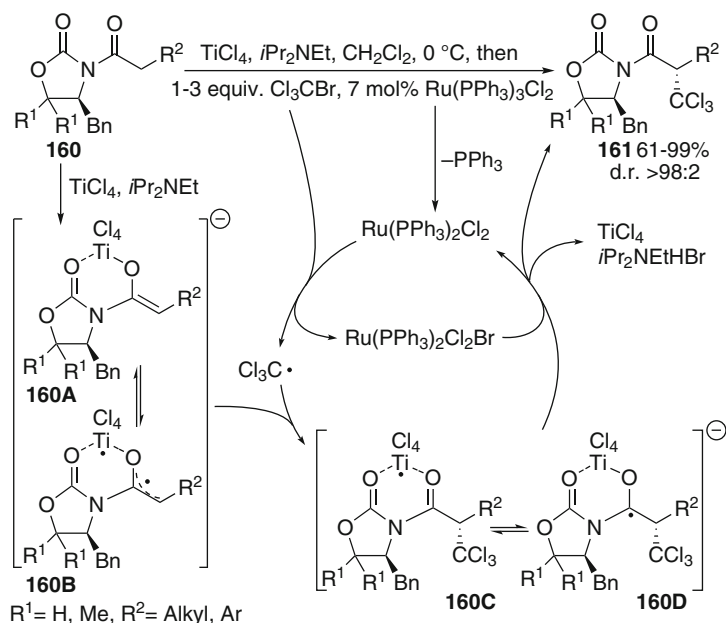


Fig. 39 Ruthenium-catalyzed radical addition reactions to titanate enolates

of the enolate [231]. Therefore **160B** represents a persistent radical (reviews [232, 233]), which is prone to coupling with the transient trichloromethyl radical resulting from reductive radical generation by the Ru(II) complex. This leads to a Ti(III)-complexed imide/Ti(IV)-ketyl radical valence tautomeric pair **160C/D**, which is oxidized by the coformed Ru(III) complex. The  $\alpha$ -(trichloromethyl) imides **161** were formed in 61–99% yield with diastereomeric ratios of  $>98:2$ . The scope was extended to the use of Simal's catalyst **148a**, which also allowed dichloromethylation reactions. The method was applied to the total synthesis of neodysidenin and the di- and trichloroleucine containing sintokamides [234].

### 3.3.2 Ru(II)–Ru(III) Catalysis: Atom Transfer Radical Cyclizations (ATRC)

Ruthenium-catalyzed ATRC were studied extensively (reviews [196, 201, 235]) after Nagashima's first reports on the cyclization of *N*-allyltrichloroacetamides **162** ( $R^1=X=Cl$ ) to chlorinated pyrrolidones **163** using  $Ru(PPh_3)_3Cl_2$  as the catalyst (Fig. 40) [236–238]. The cyclization reactions were compared to those catalyzed by the  $CuCl/bipy$  system (see Part 3, Sect. 5.3) [239, 240]. The ruthenium catalyst was required in considerably less quantity (5 vs 30 mol%), but required higher temperatures (50–140 °C vs r.t.–80 °C) to achieve comparable yields. Other amides were also successfully cyclized. Rachita and Slough investigated the diastereoselectivity of cyclizations of *N*-allyl-2,2-dichloroamides **162** ( $R^1=alkyl$ ,  $X=Cl$ ) catalyzed by 3 mol% of  $Ru(PPh_3)_3Cl_2$  and found the diastereomeric ratio to switch from a 4:1 *trans/cis*-selectivity to a 100:1 *cis/trans*-selectivity with increasing size of substituent  $R^2$  [241]. The related monochloropropionamide **162** ( $R^1=Me$ ,  $X=H$ ) also cyclizes with a 4:1 *trans*-selectivity in 56% yield. It was shown that the diastereomers of **163** ( $X=Cl$ ) epimerize under the influence of the ruthenium catalyst by a chlorine abstraction/ligand transfer process [242]. Recently Sutherland et al. reported the ATRC of a chiral cyclohexenyl trichloroacetamide to a chiral bicyclic lactam catalyzed by  $Ru(PPh_3)_3Cl_2$  in 75% yield as a single diastereomer [243].

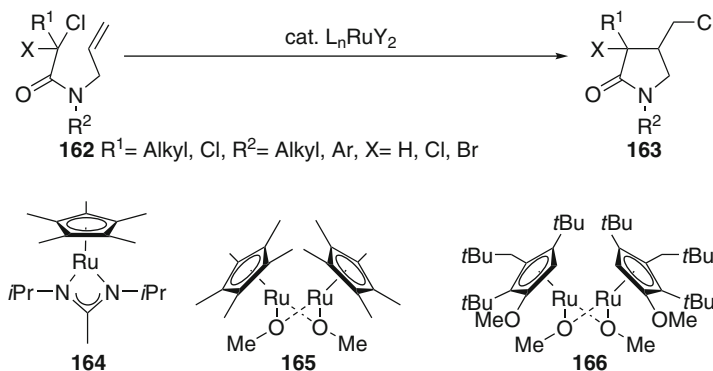
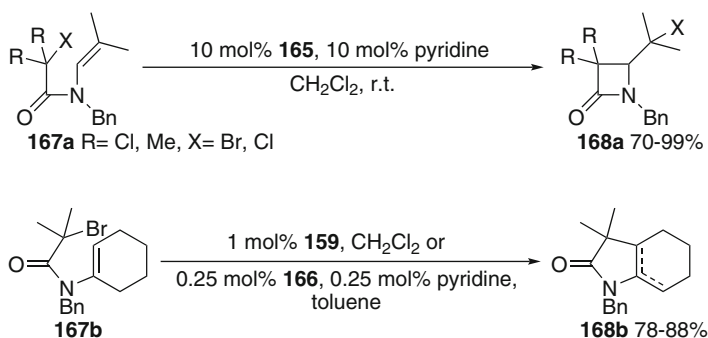


Fig. 40 Ruthenium(II)-catalyzed atom transfer radical cyclizations

More recently, a number of new ruthenium catalysts were tested for ATRC of *N*-allyltrichloroacetamides **162** and related compounds. The Grubbs I catalyst **145** gave pyrrolidones **163** in 70–84% yield [244]. A further study using *N,N*-diallyltrichloroacetamide revealed that at room temperature ring closing metathesis (RCM) is the preferred process, while ATRC is efficient at higher temperatures [245]. Moreover, based on the fact that **145** is thermally labile, it was shown that the catalyst initially activated for metathesis transformed into an activated ATRC catalyst by sacrificial RCM followed by addition of the ATRC substrate. Alternatively, a simple thermal denaturation of **145** suffices to turn it into an ATRC catalyst. Even alkene systems, amenable to RCM, become substrates for ATRC after catalyst pretreatment in good yield.

Severin reported that 0.05–5 mol% of **152** in the presence of magnesium catalyzed 5-exo cyclizations and even the significantly slower 5-endo and 9-endo cyclizations of dichloroacetamides,  $\alpha$ -bromoamides, or trichloroacetates in 66–94% yield [220].

(Amidinate)Ru complex **164** triggers cyclizations of **162** [235, 246]. However, dinuclear amidinate complexes **156** proved to be even more active promoting the ATRC at room temperature [227, 247]. Standard copper catalysts (see Part 3, Sect. 5.3) required higher temperatures and sometimes higher catalyst loading to be active. Related dinuclear methoxide complexes **165** were effective for the ATRC of *N*-allyldichloroacetamides at room temperature in the presence of pyridine [248]. 3-Chloro-4-(chloromethyl)pyrrolidones were isolated in 76–99% yield with 4–6:1 *trans/cis*-selectivity. In the absence of the amine ligand the yields were considerably lower.  $\alpha$ -Bromoamides or trichloroacetamides **167a** can even be cyclized in the demanding 4-exo mode to  $\beta$ -lactams **168a** in 70–99% yield (Fig. 41). The ease of cyclization for these substrates and the preferred *trans*-diastereoselectivity were explained by the enhanced complexation ability of coordinatively unsaturated complex **165** to the carbonyl oxygen. This favors a conformation facilitating cyclization and forces the olefin acceptor in an orientation to avoid steric interactions with the coordinated catalyst. Pyridine probably assists the dissociation of the dinuclear precatalyst to the active mononuclear catalyst.



**Fig. 41** Ruthenium-catalyzed demanding radical cyclization reactions



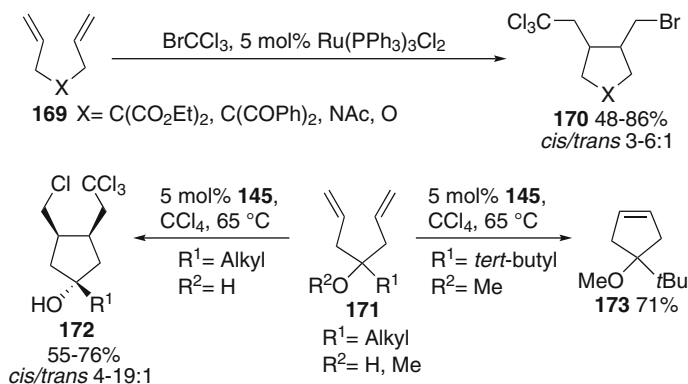
Sterically more demanding binuclear ruthenium complex **166** proved to be an efficient catalyst for ATRC in the presence of catalytic amounts of pyridine [249]. *N*-Allyltrichloroacetamide and *N*-allyldichloroacetamide **162** as well as cinnamyl trichloroethyl ether cyclized at room temperature using 0.25–2.5 mol% of the catalyst in 60–88% yield. *N*-Cyclohexenyl- $\alpha$ -bromoisobutyramide **167b** underwent a slow 5-endo cyclization to hexahydroindole **168b** in good yield. With 3-oxa-5-hexenyl trichloroacetate even a 9-endo cyclization was observed in 65% yield using 1 mol% **166** at 60 °C. Dinuclear Ru(II)–Ru(II) complexes **158** and Ru(II)–Ru(III) complexes **159** were also tested for their activity in ATRC [229]. In the presence of magnesium as a reducing agent for excess Ru(III), both catalyst types were active at loadings of 1–10 mol%. Especially Ru(II)–Ru(III) dinuclear complexes **159** combine stability and catalytic activity. *N*-Allyltrichloroacetamide, *N*-allyldichloroacetamide **162**, or cinnamyl trichloroethyl ether underwent 5-exo cyclizations, while *N*-cyclohexenyl  $\alpha$ -bromoisobutyramide **167b** cyclized to **168b** in a 5-endo manner in 58–92% yield at room temperature. A 9-endo cyclization of 3-oxa-5-hexenyl trichloroacetate proceeded in contrast with 10 mol% **159** at 80 °C in only 15% yield.

Weinreb reported 5-exo carbocyclization reactions of 2,2-dichloro-6-heptenoates to a nearly equimolar *trans/cis*-diastereomeric mixture of 1-chloro-2-(chloromethyl)cyclopentancarboxylates in 61–77% yield catalyzed by 2–8 mol% of Ru(PPh<sub>3</sub>)<sub>3</sub>Cl<sub>2</sub> (cf. Part 1, Sect. 7, Fig. 38 **133**→**135**+**136**) [112, 113]. Cyclizations to alkyne and diene units as well as annulations to bicyclic systems were also possible in good yield. 2-Bromo- or 2-chloro-6-heptenoates were also applied under similar conditions resulting in 69–85% of cyclized products [114]. The *cis/trans*-selectivity was not high for most acyclic substrates, but lactonization was facile for most *cis*-derivatives under the reaction conditions. Annulation reactions also proceeded in 75–88% yield with moderate to excellent diastereoselectivity. Even simple 1,1,1-trichloro-5-hexenes or 6-heptenes **55** underwent similar cyclizations providing carbocycles **56** and **57** in 50–79% yields (cf. Fig. 12) [115]. Approximately 10% of products resulting from 6-endo or 7-endo cyclizations were also isolated.

Lactone-forming reactions are also feasible. Radical 12-endo cyclizations of trichloroacetates tethered to imidazolones proceeded in 48–92% yields catalyzed by 10 mol% Ru(PPh<sub>3</sub>)<sub>3</sub>Cl<sub>2</sub>. A Lewis acid cocatalyst, probably organizing the chain, was mandatory to achieve good yields [250]. Quayle found that 5 mol% of the Grubbs I catalyst **145** catalyzes the ATRC of allylic trichloroacetates, such as **58** ( $n = 1$ ), to give 4-(chloroalkyl)-3,3-dichlorobutyrolactones **61** in 25–75% yields (cf. Fig. 13) [244].

### 3.3.3 Ruthenium(II)-Catalyzed Tandem Reactions Involving Kharasch Additions/Cyclizations

Grigg reported tandem radical addition/5-exo cyclization reactions of bromotrichloromethane and 1,6-dienes **169** catalyzed by 5 mol% Ru(PPh<sub>3</sub>)<sub>3</sub>Cl<sub>2</sub> (Fig. 42).

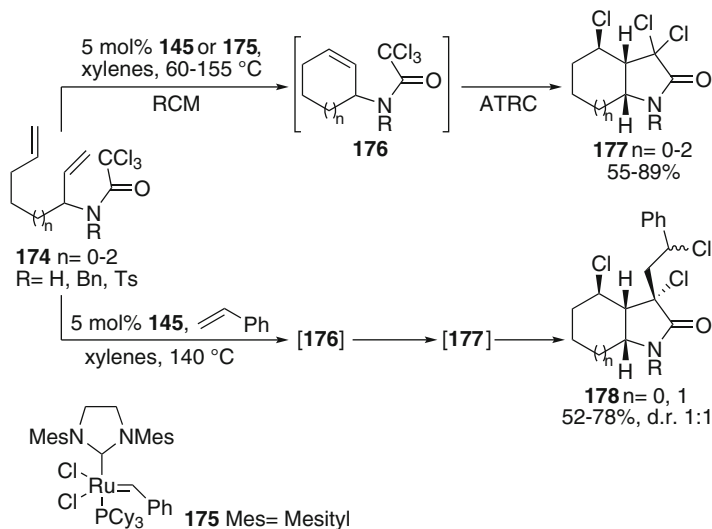


**Fig. 42** Tandem addition/cyclization sequences of 1,6-dienes and  $\text{CCl}_4$

The reactions gave 48–86% yield of **170** and proceeded with 3–6:1 *cis*-diastereoselectivity [251]. 6-exo or 7-exo cyclizations were not possible, double addition taking place instead. Similar cyclizations of 4-hydroxy-substituted 1,6-dienes **171** with  $\text{CCl}_4$  were performed by Schmidt and coworkers using the Grubbs I catalyst **145**. Carbocycles **172** were obtained in 55–76% yield and good to excellent *cis*-diastereoselectivity [252]. RCM was not observed at all. This surprising result was rationalized by the fact that the free hydroxy group blocks the necessary coordination site for olefins in **145**, thus preventing RCM, while electron transfer to reduce  $\text{CCl}_4$  is still possible. When the hydroxy group was protected as a methyl ether, the normal RCM selectivity over ATRC was restored and cyclopentene **173** was formed in 71% yield. Structurally similar diallylsilanes did not cyclize but underwent double ATRA.

Snapper designed tandem RCM/ATRC reactions of *N*-dienyl trichloroacetamides **174** and related 1,1,1-trichloroalkanes (not shown) catalyzed by the Grubbs I catalyst **145** (Fig. 43) [253]. The reactions proceed by initial ring closing metathesis to provide cyclic alkenes **176**, which undergo ATRC under the reaction conditions. The yields of bicycles **177** range from 55 to 89%. Tandem RCM/ATRA processes are also possible in 65–83% when olefins were added that do not undergo metathesis easily. Catalyst **145** also allowed tandem RCM/ATRC/ATRA processes starting from **174**, providing bicyclic products **178** in 52 and 78% yield, respectively. In this study, the Grubbs I catalyst **145** was reported to be considerably more effective than the Grubbs II catalyst **175**.

*N*-Dienyltrichloroacetamide **174** ( $n = 0$ ,  $\text{R} = \text{H}$ ) was, however, subsequently also subject to tandem RCM/ATRC catalyzed by the Grubbs II catalyst **175** (Fig. 43) [254]. The yield of **177** in this reaction was reported to be 82–91%, showing that catalyst **175** is also effective in such tandem processes. Tandem cross-metathesis/ATRC reactions of *N*-allyltrichloroacetamides with styrenes catalyzed by **175** produced rather low yields of trichlorinated lactams [254]. Almost at the same time Schmidt and Pohler reported similar tandem RCM/ATRC sequences of 1,6-dienyl trichloroacetates with 5 mol% of **175** and of 1,7-dienyl trichloroacetates



**Fig. 43** Tandem RCM/ATRC and tandem RCM/ATRC/ATRA reactions catalyzed by the Grubbs catalysts

using **145**. In both cases bicyclic lactones were isolated in 61 and 62% yield [255]. The Grubbs II catalyst **175** was much more active in RCM to five-membered rings and also proved potent in the cyclization step with similar efficiency as **145**. For unsubstituted substrates concomitant dehydrochlorination and isomerization of the generated alkene was observed. On the other hand, **145** was not suitable to catalyze the tandem RCM/ATRC of 1,6-heptadien-3-yl trichloroacetate [254]. Only a bimetallic catalytic system of **145** and a Cu(I) catalyst worked efficiently. Moreover, it was shown that in cyclohexenyl trichloroacetate a [3,3]-rearrangement competes under the reaction conditions.

Very recently Sutherland and coworkers merged the Pd-catalyzed Overman rearrangement with RCM and ATRC (Fig. 44) [256]. Treatment of dienols **179** with trichloroacetonitrile in the presence of 10 mol%  $\text{Pd}(\text{MeCN})_2\text{Cl}_2$  afforded the non-isolated trichloroacetimidate **180**, which underwent the [3,3] rearrangement to *N*-dienyltrichloroacetamides **174**. They were immediately subjected to the RCM/ATRC sequence using 10 mol% of **145**. When chiral cobalt complex (*S*)- or (*R*)-**181** was used as the catalyst for the Overman rearrangement, indolinones **177** were isolated in 51–70% yields and 89–94% ee.

Kharasch additions result in 1,3-dihalohydrocarbons. The products are thus suitable to be converted to cyclopropanes under reductive conditions. Severin recently developed a ruthenium-catalyzed Kharasch addition/magnesium-promoted cyclization sequence of ethyl dichloroacetate, dichloroacetamide, or dichloroacetonitrile with olefins **182** in the presence of magnesium (Fig. 45) [257]. Using 1 mol% of **152** the Kharasch addition/cyclopropanation sequences provided a simple access to cyclopropanes **184** via adduct **183** in 51–74% yield. The reactions can also be

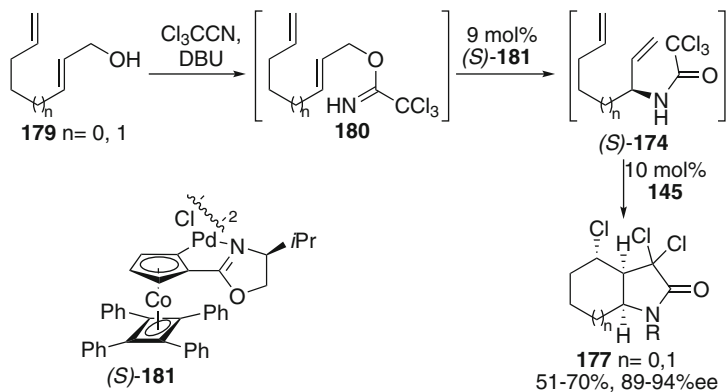


Fig. 44 Ruthenium-catalyzed tandem Overman rearrangement/RCM/ATRC reactions

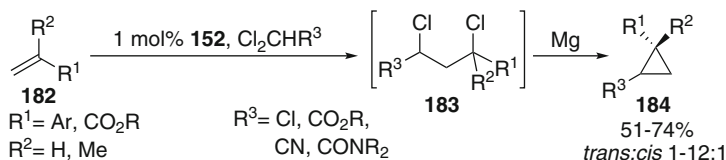


Fig. 45 Tandem Kharasch addition/cyclopropanation reactions

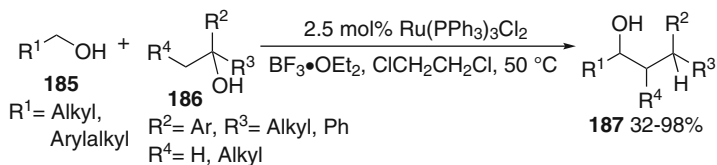
performed intramolecularly; thus *N*-allyltrichloroacetamides provided bicyclic nitrogen heterocycles in 57–65% yield.

### 3.4 *Ru(II)*-Catalyzed Alkylative Coupling Reactions of Alcohols

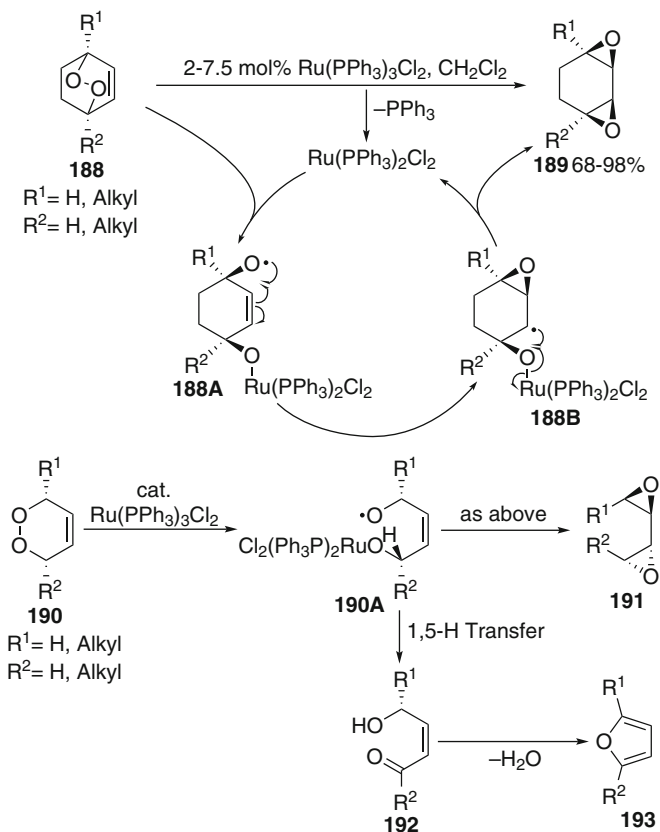
It was recently shown by Zhang and coworkers that  $\text{Ru}(\text{PPh}_3)_3\text{Cl}_2$  is a suitable catalyst for the alkylative coupling of tertiary alcohols **186** to primary alcohols **185** leading to branched alcohols **187** in 32–98% yield (Fig. 46) [258]. The reaction required the presence of a Lewis acid, such as  $\text{BF}_3 \cdot \text{OEt}_2$ . It mediates the dehydration of the tertiary alcohol to a 1,1-disubstituted alkene, which coordinates the ruthenium catalyst. The further course is likely to be similar to the corresponding iron- or rhodium-catalyzed reactions (see Sects. 2.8 and 6).

### 3.5 *Ru(II)*-Catalyzed Cleavage of Peroxides and Epoxides

Shortly after Footes initial report on cobalt catalyzed reactions (see Sect. 5.8), Noyori and coworkers found that  $\text{Ru}(\text{PPh}_3)_3\text{Cl}_2$  catalyzes the reductive cleavage of endoperoxides (Fig. 47) [152, 259]. While 1,2-dioxanes provided a mixture of



**Fig. 46** Ruthenium-catalyzed coupling of primary and tertiary alcohols



**Fig. 47** Ruthenium-catalyzed ring opening reactions of endoperoxides

products consisting mainly of 1,5-hydrogen transfer- and  $\beta$ -fragmentation-derived products and diols in various ratios, bicyclic 3,6-dihydro-1,2-dioxines **188** afforded diepoxides **189** in 68–98% yield. The reaction can be explained by initial SET reduction of the peroxide bridge, 3-exo cyclization of the resulting alkoxy radical **188A** to the adjacent double bond, and a subsequent 1,3- $\text{S}_{\text{H}}1$  reaction of the alkyl radical **188B** at the ruthenium alkoxide thus regenerating the catalyst and forming products **189**. Monocyclic endoperoxides **190** gave

diepoxides **191** only in low to moderate yields. Instead the reaction provided furans **193**, often in good yields (34–76%) [152]. For these substrates, 1,5-hydrogen transfer competes successfully with 3-exo cyclization in alkoxy radical **190A**, thus leading to (*Z*)-4-hydroxyenones **192**, which cyclize to furans **193** (see also Sect. 5.8). The analogous iron and osmium complexes showed similar efficiency.

### 3.6 Ruthenium-Catalyzed Oxidative Cyclizations

Katsuki et al. found that (salen)(nitrosyl)ruthenium(III) **195** complexes undergo a facile photochemical cleavage of the nitrosyl ligand to generate a coordinatively unsaturated (salen)Ru<sup>III</sup>Cl complex (Fig. 48) [260]. Phenols **194** coordinate to this complex. The resulting ruthenium(III) phenolate is easily oxidized by oxygen to a Ru(IV) complex. Ligand-to-metal charge transfer of the coordinated phenol provides a valence tautomeric ruthenium(III)-coordinated radical cation of **194**. This is subject to a 5-endo cyclization to the central alkene unit. Further oxidation of the benzylic radical generates a benzylic carbocation, which is trapped by the adjacent phenolic hydroxy group to give dibenzotetrahydrofurofurans **196** in 24–87% yield. Despite the sterically very demanding ligand in **195**, the ee remained

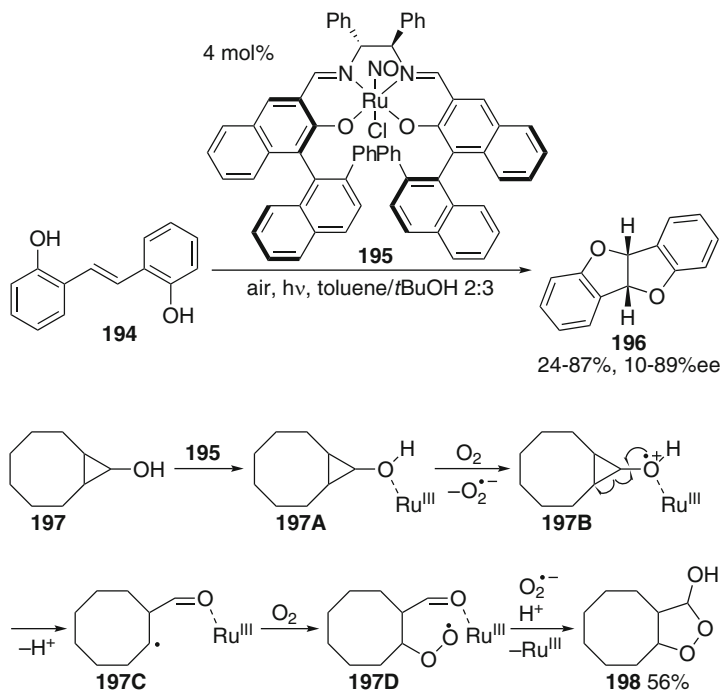
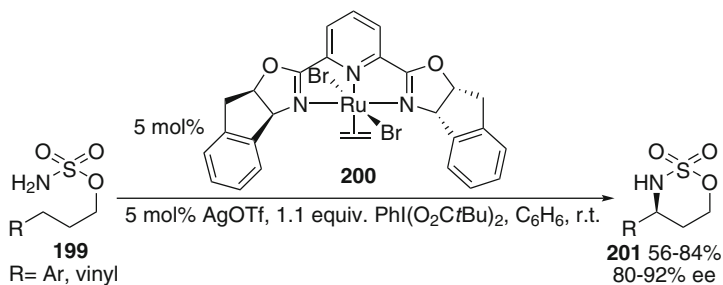


Fig. 48 Ru(III)-catalyzed oxidative cyclizations and fragmentations



**Fig. 49** Ruthenium-catalyzed C–H amination reactions

moderate. The reaction mechanism is supported by UV/vis-spectroscopic monitoring of the catalyst during the reaction and by probe reactions. This was the cleavage of bicyclo[6.1.0]nonanol **197** to endoperoxy hemiacetal **198** [261]. It results from coordination of **197** to the Ru(III) complex leading to **197A**, which is oxidized by oxygen to a valence tautomeric oxygen radical cation **197B**. This intermediate undergoes cyclopropane ring opening and deprotonation to coordinated  $\beta$ -oxo radical **197C**. Coupling of this radical to oxygen gives peroxy species **197D**, which on cyclization and reduction by superoxide forms the endoperoxy hemiacetal **198** in 56% yield.

### 3.7 Miscellaneous

Ruthenium complexes, such as **200**, catalyze C–H amination reactions of **199**, in which radical pathways are likely to operate, in good yields and enantioselectivities (Fig. 49) [262].

Other radical-based transformations are ruthenium-catalyzed oxidative dimerizations of phenols [263] and reductive dimerizations [264]. The isomerization of chiral *cis*-epoxides to *trans*-epoxides catalyzed by 2–10 mol%  $\text{TpRu}(\text{py})_2\text{Cl}$  proceeds at 100 °C in 95–98% yields with inversion of configuration [265]. A radical or  $\text{S}_{\text{N}}2$  mechanism was discussed for this process.

## 4 Osmium-Catalyzed Radical Reactions

There are only very few applications of osmium complexes in radical chemistry. Gasanov and coworkers studied the efficiency of  $\text{M}_3(\text{CO})_{12}$  ( $\text{M}=\text{Fe}, \text{Ru}, \text{Os}$ ) in Kharasch addition reactions in the presence and absence of DMF as a ligand and found that the efficiency of the catalyst decreases in the order  $\text{Fe} > \text{Ru} > \text{Os}$  [93]. DMF activates all three systems. Its role was attributed to the generation of

mononuclear complexes by ligand exchange, which are more active than the trinuclear complexes.

Noyori and coworkers studied the reductive cleavage of 3,6-dihydro-1,2-dioxines catalyzed by  $\text{Os}(\text{PPh}_3)_3\text{Cl}_2$  and observed a similar selectivity and activity as the for the corresponding iron and ruthenium complexes (cf. Fig. 47) [152].

Severin compared the activity of 0.02–0.1 mol% of  $\text{Cp}^*\text{Os}(\text{PPh}_3)\text{Br}_2$  in Kharasch additions to that of related catalyst  $\text{Cp}^*\text{Ru}(\text{PPh}_3)\text{Cl}_2$  **152** using reductive activation by magnesium (cf. Figs. 36 and 37) [266]. The ruthenium complex **152** performed better than the osmium complex. The lower activity of the osmium complex may be attributed to the more facile formation of olefin complexes. Such a (styrene)Os complex was isolated and characterized. This complex was even less efficient in Kharasch additions. Both complexes, **152** and  $\text{Cp}^*\text{Os}(\text{PPh}_3)\text{Br}_2$ , behaved similarly in ATRC of allylic trichloroethyl ethers or *N*-allyldichloroacetamides. Complex **152** gave slightly better results.

## 5 Cobalt Catalysis

Nature demonstrates that transition metals can be very effective in catalyzing transformations, which are impossible to accomplish otherwise under physiological conditions. The prime example is vitamin  $\text{B}_{12}$ , whose resting state is adenosylcobalamine(III) (reviews [267–273]). On homolysis it triggers a variety of radical reactions crucial to the living world. This inspired the interest of chemists and led to a number of applications. More recently, interest shifted to catalysis by low-valent cobalt complexes.

### 5.1 *Co(0)–Co(I) Catalysis*

Kondo and coworkers studied the alkoxyacylation of alkyl iodides catalyzed by a large number of metal carbonyl complexes [172, 173]. Among them 5 mol%  $\text{Co}_2(\text{CO})_8$  was highly active giving 76% yield of esters (cf. Part 1, Sect. 9.1, Fig. 41).

### 5.2 *Co(0)–Co(I)–Co(II) Catalysis*

#### 5.2.1 Kumada Cross-Coupling Reactions

The homocoupling of aryl Grignard reagents triggered by organic halides in the presence of catalytic quantities of cobalt chloride or other transition metal halogenides was studied initially by Kharasch and Fields in 1941 [36]. They



observed high yields of biaryls and attributed the catalytic effect of  $\text{CoCl}_2$  to single electron transfer and the involvement of radicals. Similar experiments with alkyl Grignard reagents led mostly to the formation of disproportionation products, also pointing to the involvement of radicals [274]. Cobalt regained interest in cross-coupling reactions only recently (reviews [275–277]) and the methodology development paralleled that of the related iron-catalyzed process (see Sect. 2.1.1).

Oshima reported the cross-coupling of primary, secondary, or tertiary alkyl halides **202** with allylic Grignard reagents **203** catalyzed by the  $\text{CoCl}_2(\text{dppp})$  catalyst (Fig. 50, Table 3, entry 1) [278, 279]. The dppp ligand **205b** proved to be the most effective among several chelating diphosphine ligands **205**. This method proved to be especially suitable for the coupling of difficult tertiary alkyl halides. Best yields were obtained with alkyl iodides; the corresponding bromides gave similar yields but required longer reaction times. Alkyl chlorides often gave only low yields, while aryl bromides did not react. Acetal units were tolerated in these reactions, but amide and ester functionalities were not. The allylic fragment was varied and branched products were strongly preferred with crotyl Grignard reagents, while nearly equal mixtures of linear and branched products were found with prenyl-type Grignard reagents. Attempted asymmetric Grignard cross-coupling

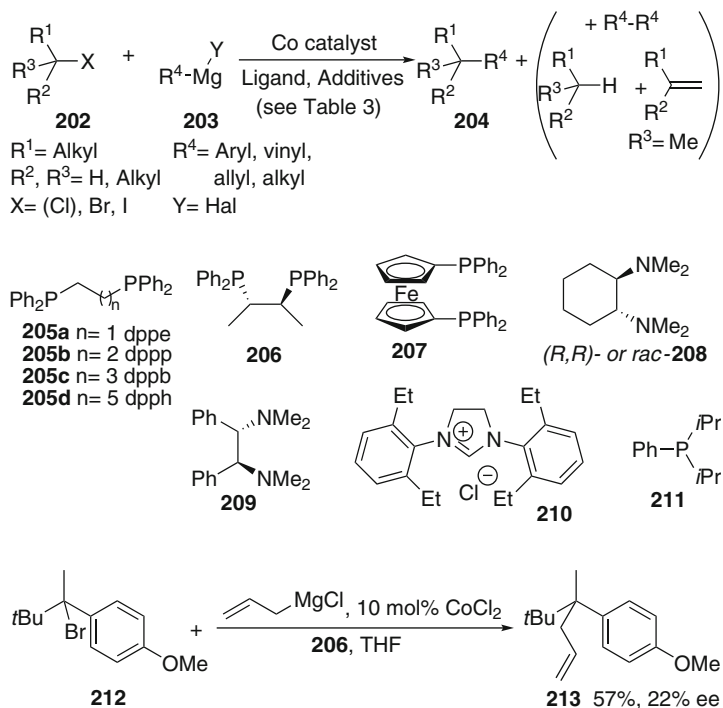


Fig. 50 Cobalt-catalyzed cross-coupling of alkyl halides with Grignard reagents

**Table 3** Cobalt-catalyzed cross-coupling reactions

Entry	R <sup>4</sup>	Y	M	Co source	Yield (%)	Ref.
1	Allylic	Cl	Mg	Co(dppp)Cl <sub>2</sub> (10 mol%)	30–84	[278, 279]
2	Bn	Cl	Mg	Co(dppp)Cl <sub>2</sub> (10 mol%)	37–70	[279]
3	Ar	Br	Mg	Co(dppp)Cl <sub>2</sub> (10 mol%)	33–67	[280]
4	Ar	Br	Mg	CoCl <sub>2</sub> / <b>208</b> or <b>209</b> (5 mol%)	43–99	[281]
5	Alkynyl, TMSvinyl	Br	Mg	Co(acac) <sub>3</sub> /TMEDA (20–40 mol%)	54–90	[282]
6	R <sub>3</sub> SiCH <sub>2</sub>	Cl	Mg	CoCl <sub>2</sub> / <b>210</b> (5 mol%)	79	[283]
7	Alkyl	Br	Mg	CoCl <sub>2</sub> ·2LiI/TMEDA or <i>rac</i> - <b>208</b> (5 mol%)	45–98	[284]
8	Ar	Br	Mg	Co(acac) <sub>3</sub> /TMEDA or <i>rac</i> - <b>208</b> (5 mol%)	79–98	[285]
9	Ar	Br	Mg <sup>a</sup>	CoCl <sub>2</sub> / <i>rac</i> - <b>208</b> (5 mol%)	39–85	[286]
10	Ar	Br	Mn <sup>b</sup>	CoBr <sub>2</sub> / <b>211</b> or bipy (10 mol%)	56–96	[287]

<sup>a</sup>In situ generation of Grignard reagent from both halides

<sup>b</sup>Used as stoichiometric reducing agent for CoBr<sub>2</sub>

using **212** and the chiraphos ligand **206** resulted in up to 22% ee in the product **213**. Benzylic Grignard reagents were also applicable in the alkylation (entry 2). From most of the reactions, small amounts of alkenes and alkanes derived from **202** as well as biaryls derived from homocoupling of the Grignard reagents **203** were detected as byproducts.

In 2006, Oshima's group reported the Kumada-type coupling of primary alkyl bromides **202** with aryl Grignard reagents **203** catalyzed by 10 mol% of the Co(dppp)Cl<sub>2</sub> complex (entry 3) [280]. Other ligands, such as dppe **205a**, dpfp **207**, or other diphosphine ligands, were essentially ineffective. The reaction is sensitive to the steric demand of the Grignard reagents. *ortho*-Substituted aryl Grignard reagents were unreactive in the coupling process. Alkyl iodides and secondary alkyl bromides were less suitable in the coupling reaction. However, the conditions are compatible with various sensitive functionalities, such as ester or acetal groups. Mechanistic experiments under stoichiometric conditions using dppe **205a** as the ligand showed that 4 equiv. of phenyl Grignard reagent were necessary to generate the active catalyst and that an 1 equiv. of biphenyl was formed.

In a parallel study, it was found that chelating chiral diamines **208** or **209** are well suited as ligands to promote Kumada-type couplings of primary and secondary alkyl halides **202** with aryl Grignard reagents **203** (entry 4) [281]. This reaction was applicable to alkyl bromides and alkyl iodides, while alkyl chlorides gave only low yields. Acetal and ester functions are tolerated. A notable feature is the stereoretentive arylation of *trans*- $\alpha$ -bromo acetals with excellent diastereoselectivity. The involvement of radicals is supported by the stereoconvergent formation of *exo*-phenylnorbornane from both *endo*- or *exo*-bromonorbornane (cf. Part 1, Fig. 9) and radical 5-*exo* cyclizations (see below).

The cobalt-catalyzed radical Kumada coupling was extended to 1-silylvinyl- and silylethynylmagnesium compounds (entry 5) [282]. Co(acac)<sub>3</sub> in the presence of TMEDA, which served as a ligand and solvent, proved to be the catalyst of choice; however, a rather high loading of 20–40 mol% was required. The reaction

proceeded in good yields with primary and secondary alkyl bromides and iodides, while alkyl chlorides afforded the coupling products only in low yields. Tertiary alkyl halides failed to react and the coupling was limited to silylated vinyl and alkynyl Grignard reagents. Acetals and sulfonamides are compatible under the reaction conditions. 3-Bromobutyrolactols and 2-bromocyclopentyl silyl ethers gave the products with exclusive *trans*-selectivity. The intermediacy of radicals is supported by the fact that both *endo*- and *exo*-bromonorbornane gave the coupled product with high *exo*-diastereoselectivity (cf. Part 1, Fig. 9) and by radical 5-*exo* cyclizations (see below).

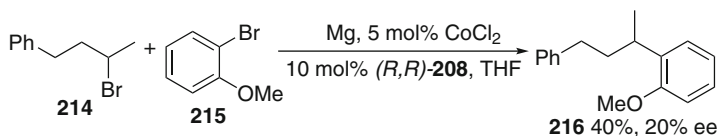
A single example of a coupling reaction of a primary alkyl iodide with (allyldimethylsilylmethyl)magnesium chloride was reported by Oshima in the presence of a Co(NHC) catalyst generated in situ from imidazolium salt **210** and CoCl<sub>2</sub> (entry 6) [283]. The reaction is, however, not useful for secondary iodides, since β-hydride elimination prevailed.

A year later Cahiez reported the first generally applicable alkyl–alkyl Kumada coupling catalyzed by the complex CoCl<sub>2</sub>•2LiI and TMEDA or **208** as the ligand (entry 7) [284]. The reaction works well for primary and secondary alkyl bromides and primary alkyl Grignard reagents. Aliphatic ester, amide, or keto functions are tolerated under the reaction conditions. Tertiary alkyl halides as well as secondary and tertiary Grignard reagents are not applicable in this method.

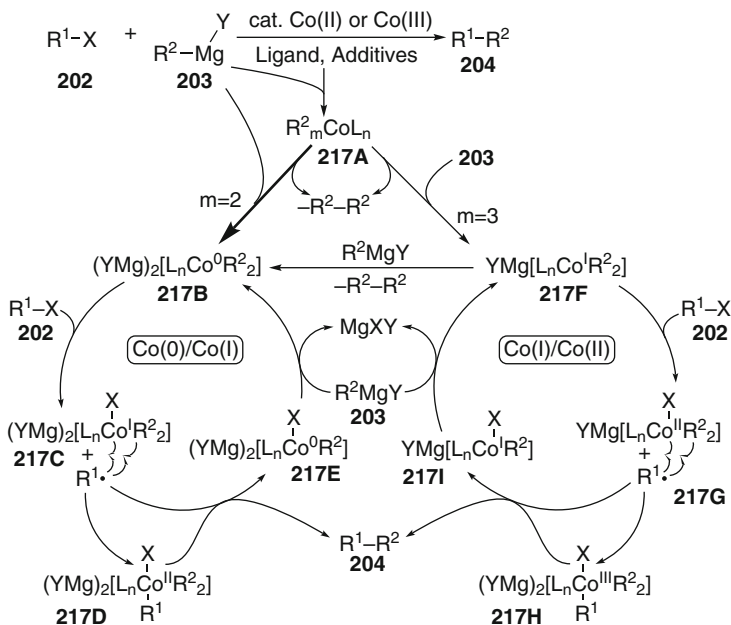
In 2009, Cahiez described a very chemoselective cobalt-catalyzed Kumada coupling of primary and secondary alkyl bromides with aryl Grignard reagents, in which ester, nitrile, and keto functions are tolerated (entry 8) [285]. The optimal catalyst for the coupling consisted of Co(acac)<sub>3</sub> and TMEDA or **208** as the ligands. This method even allows the coupling of a number of *ortho*-substituted aryl Grignard reagents in good yields. Alkyl chlorides, alkyl tosylates, and tertiary alkyl bromides are, however, not applicable under the conditions.

Similar to the iron-catalyzed magnesium-promoted direct coupling reactions (see Sect. 2.1.1), Jacobi von Wangelin and colleagues developed a direct coupling of aryl halides with alkyl halides (entry 9) [286]. Chelating amine ligands accelerate the reactions, while monodentate amines induced low activity. An advantage of this method compared to iron-catalyzed processes is that only a catalytic amount of the amine ligand is necessary. Thus 5 mol% of CoCl<sub>2</sub> and 10 mol% of **208** promoted the formation of alkylarenes in 39–85% yield. The formation of biaryls was less than 15%. When (*R,R*)-**208**, racemic (3-bromobutyl)benzene **214**, and 2-bromoanisole **215** were employed, chiral product **216** was obtained with an enantiomeric excess of 20% (Fig. 51). Chlorides gave only low yields in the coupling. The results suggest an initial SET reduction of the (amine)Co(II) complex to a Co(0) ate species by the in situ-formed Grignard reagent similar to the results described before.

Amatore and Gosmini designed a cobalt-catalyzed process, which does not even rely on in situ formation of an organometallic component (entry 10) [287]. Using 10 mol% of CoBr<sub>2</sub> and diisopropyl(phenyl)phosphine **211** or 2,2'-bipyridine as the ligand and manganese as the stoichiometric reducing agent, cross-coupling reactions of aryl and alkyl halides proceeded smoothly in 56–96% yield.



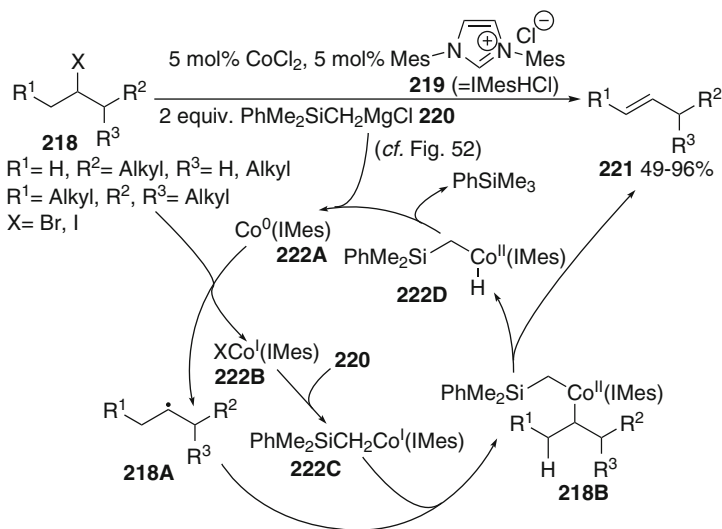
**Fig. 51** Asymmetric Co-catalyzed Kumada-type cross-coupling reactions



**Fig. 52** Catalytic cycles for cobalt-catalyzed cross-coupling reactions

Ester, nitrile, or ketone functions are tolerated in the method. Aryl chlorides can be applied with only slightly decreased yields. For 3-bromopropionate the bipyridine ligand was mandatory for the success of the reaction. The involvement of radicals is supported by ring opening occurring when cyclopropylmethyl bromide was used as the substrate (cf. Part 1, Fig. 8).

Based on the preparative and mechanistically oriented results, the reaction can be assumed to start with a transmetalation of the initial Co(II) or Co(III) compound by the Grignard reagent **203** to an organocobalt species **217A** (Fig. 52). Reductive elimination and addition of excess **203** leads to cobalt(0) ate complex **217B**. This is the most likely catalyst to trigger SET reduction of the alkyl halide **202** to generate the alkyl radical, which may be either free or caged with the cobalt(I) complex **217C**. It was proposed that this radical couples subsequently with **217C** to cobalt(II) species **217D** in analogy to results obtained for tandem cyclization/Kumada reactions (see below). Reductive elimination from this mixed complex affords the cross-coupling product **204** and a reduced neutral cobalt species **217E**. On the other



**Fig. 53** Cobalt-catalyzed dehydrohalogenation reactions of alkyl halides to olefins **221**

hand, the radical formed may attack the aryl ligand directly leading to product **204** and reduced species **217E**, which regenerates the active catalyst by ligand exchange with **203**. However, it cannot be excluded that some coupling reactions follow a Co(I)–Co(II) catalytic cycle, in which a cobalt(I) complex **217F** is generated initially that reduces **202**. Coupling of the resulting radical via **217G** and **217H** leads also to products **204** and Co(I) species **217I**, which closes the catalytic cycle by ligand exchange with **203**.

Similar reaction conditions can also be used to effect dehydrohalogenation reactions of alkyl halides **218** to the corresponding olefins **221** (Fig. 53) [288]. The reaction of alkyl iodides or bromides with 5 mol% of  $\text{CoCl}_2$  and the imidazolium chloride (IMesHCl) **219** in the presence of (dimethylphenylsilyl)methylmagnesium chloride **220** provided terminal alkenes with excellent regioselectivity under very mild conditions in short reaction times. The transformation proceeds most likely by SET reduction of **218** to radical **218A** by in situ-generated Co(0) complex **222A**. This leads to a cobalt(I) complex **222B**, which reacts with excess of Grignard reagent **220** to form alkylcobalt(I) complex **222C**. Its coupling with **218A** provides a mixed dialkylcobalt(II) complex **218B**, which undergoes  $\beta$ -hydride elimination to **221**. Catalyst **222A** is regenerated from coformed **222D** by reductive elimination of phenyltrimethylsilane. The reaction is selective for the kinetic Hofmann product, since the *syn*-selective  $\beta$ -hydride elimination usually shows a good preference for proceeding through the least encumbered transition state. Tosylates and mesylates are completely inert under the reaction conditions, lending further support to a radical mechanism.

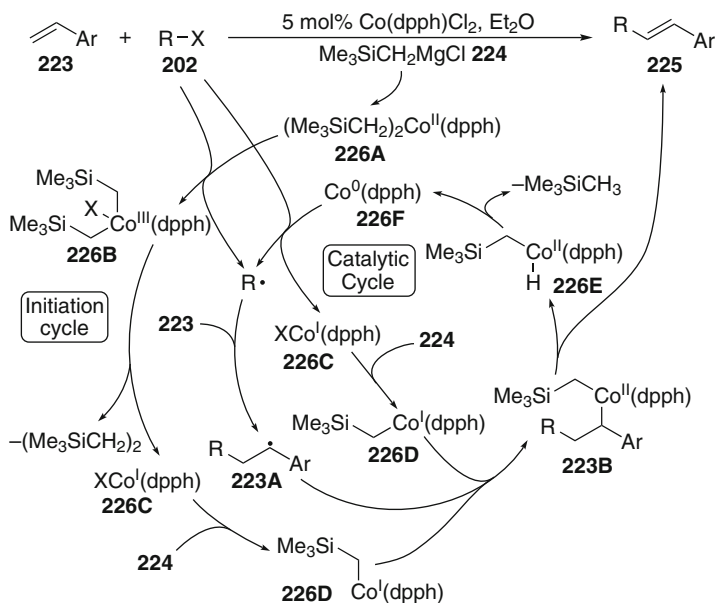


Fig. 54 Cobalt-catalyzed Heck reactions of alkyl halides and styrenes

### 5.2.2 Radical Addition/ $\beta$ -Hydride Elimination: A Radical Heck Reaction

When styrenes **225** were treated with alkyl halides **202** in the presence of cobalt catalysts generated from cobalt(II) chloride and a chelating diphosphine in the presence of a non-transferable Grignard reagent, such as trimethylsilylmethylmagnesium chloride **224**, arylalkenes **225** were isolated (Fig. 54) [289]. Primary, secondary, and tertiary alkyl halides can be employed; the reactions proceed especially well with alkyl bromides. Alkyl iodides and alkyl chlorides required higher temperatures to achieve good yields. Chelating diphosphines were mandatory to achieve reasonable reactions rates; 1,6-bis(diphenylphosphino)hexane **205d** was the optimal ligand. Electron-rich and electron-poor styrenes were applicable. Ester and amide functionalities at the arene ring are tolerated. The intermediacy of free radicals is supported by the use of cyclopropylmethyl bromide, which afforded the ring-opened addition product exclusively in 50% yield (cf. Part 1, Fig. 8). Moreover, diastereomerically pure cyclohexane-derived bromo ethers reacted with low diastereoselectivity in favor of the stereoretentive *trans*-product, while the corresponding conformationally less flexible five-membered derivative gave 2-styrenylcyclopentyl ethers with high *trans*-diastereoselectivity. Mechanistic investigations showed that the  $\text{CoCl}_2(\text{dppe})$  complex reacts first with **224** giving a complex of gross structure **226A**, which may exist as monomer or dimer [290]. SET reduction of the alkyl halide generates cobalt(III) complex **226B**, which undergoes fast reductive elimination of 1,2-bis(trimethylsilyl)ethane to give

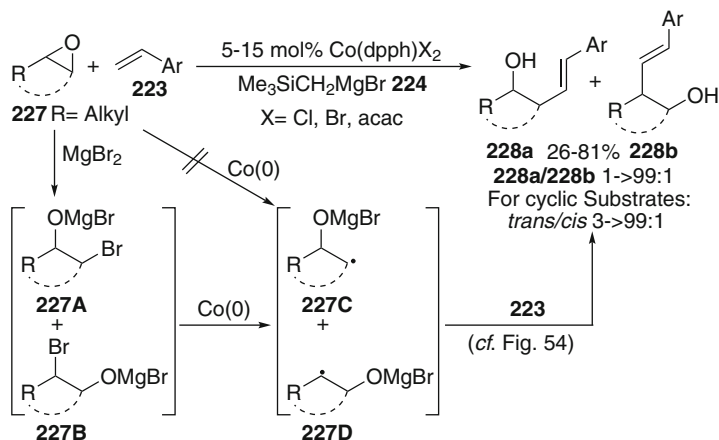
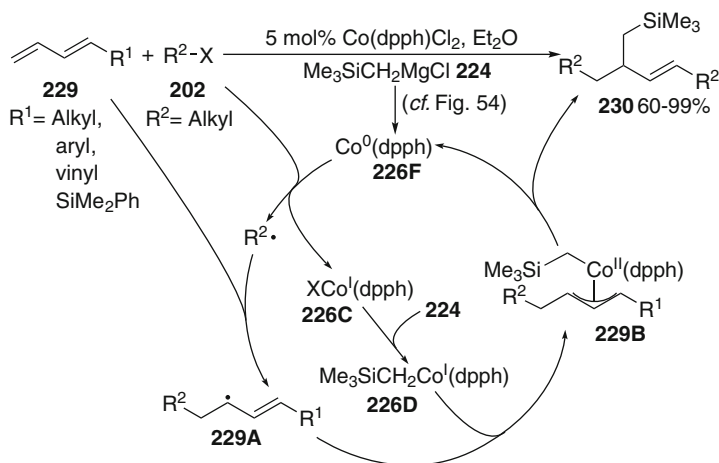


Fig. 55 Cobalt-catalyzed Heck reactions using epoxides

cobalt(I) complex **226C**. This reacts with excess **224** to  $[\text{Co}(\text{CH}_2\text{TMS})(\text{dpph})]$  **226D**. This complex can couple easily with benzylic radical **223A** resulting from addition of the alkyl radical to styrene **223**. The resulting cobalt(II) complex **223B** is subject to typical  $\beta$ -hydride elimination affording the product **225** and cobalt hydride complex **226E**, from which the active  $\text{Co}(0)(\text{dpph})$  catalyst **226F** is generated by reductive elimination of tetramethylsilane. This more electron-rich complex will then carry the catalytic cycle for the Heck reaction by SET reduction of **202**. It may, however, also be possible that a more electron-rich  $[\text{Co}(\text{CH}_2\text{TMS})(\text{dpph})]\text{MgCl}$  ate complex performs the SET reduction as proposed for other coupling reactions (see above).

Oshima's group later reported that epoxides are also competent precursors in Co-catalyzed radical addition/ $\beta$ -hydride elimination reactions (Fig. 55) [291]. When epoxides **227** were treated with styrenes **223**, trimethylsilylmethylmagnesium bromide **224**, and catalytic amounts of  $\text{CoCl}_2$ ,  $\text{CoBr}_2$ , or  $\text{Co}(\text{acac})_3$ , and diphosphine **205d**, homocinnamyl alcohols **228** were isolated in 26–81% yield. From symmetric cyclic epoxides, such as cyclopentene or cycloheptene oxide, *trans*-2-styrenyl cycloalkanols resulted as the exclusive products, while cyclohexene oxide provided a ca. 3:1 *trans/cis*-mixture of coupling products irrespective of the cobalt precursor. Larger cyclic epoxides failed to react. Unsymmetrical acyclic epoxides gave regioisomeric mixtures of coupling products **228a** and **228b**, in which **228a** often predominates. The reaction sequences were also extended to aziridines, which provided homocinnamylamines in 36 and 73% yield with very similar diastereo- and regioselectivities. The results exclude a direct reductive ring opening of **227** to  $\beta$ -hydroxyalkyl radicals **227C/D** by the low-valent cobalt complex, as it is common for instance in analogous titanocene chloride-catalyzed reactions (see Part 1, Sect. 3.3.2), since this would provide the more stable internal radicals **227D** exclusively. Based on this fact and a brief study of the competitive polar ring opening of epoxides by magnesium halides, the following



**Fig. 56** Cobalt-catalyzed tandem radical addition/cross-coupling reactions

course is more likely: MgBr<sub>2</sub> resulting from the Schlenk equilibrium of the Grignard reagent opens the epoxide in a S<sub>N</sub>2-type reaction forming regioisomeric bromo alkoxide intermediates **227A** and **227B**. Their SET reduction by the initially generated low-valent cobalt catalyst (cf. Fig. 54) leads to radicals **227C** and **227D**, which add to **223**. The resulting benzylic radicals react to products **228a** and **228b** according to the mechanism outlined in Fig. 54.

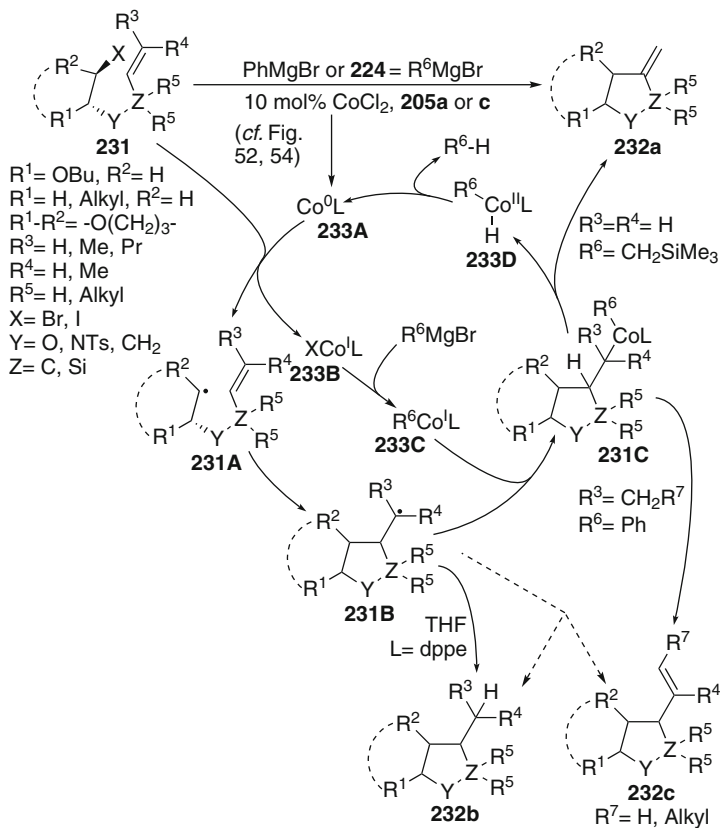
### 5.2.3 Radical Addition/Kumada Coupling Reactions

Oshima's group reported a tandem radical addition/Kumada-type cross-coupling catalyzed by the Co(dpph)Cl<sub>2</sub> complex (Fig. 56) [292]. Upon reaction of 1,3-dienes **229** with alkyl bromides **202** and trimethylsilylmethylmagnesium chloride **224**, homoallylic silanes **230** were formed in good yields. The reactions proceed by reductive generation of alkyl radicals induced by low-valent cobalt complex **226F** followed by addition to the terminus of diene **229**. The resulting allylic radical **229A** couples with cobalt intermediate **226D** leading to (allyl)cobalt complex **229B**, from which products **230** form by reductive elimination. The reaction course is supported by isolation of the product resulting from complete ring opening of cyclopropylmethyl bromide (cf. Part 1, Fig. 8) and by 5-exo radical cyclizations (see below).

### 5.2.4 Radical Cyclizations

Allylic β-iodo ethers, allylic β-iodo amines, or α-iodo acetals **231** (Z=C) unsubstituted at the alkene unit (R<sup>3</sup>=R<sup>4</sup>=H) cyclized when CoCl<sub>2</sub> and chelating





**Fig. 57** Co(0)-catalyzed radical cyclizations

diphosphines were used as catalyst and trimethylsilylmethylmagnesium chloride **224** as the reductant (Fig. 57) [290, 293]. The product distribution can be steered between unsaturated and saturated THF derivatives **232a** and **232b**, respectively, by choice of the ligand. While dppb **205c** leads to the formation of the 4-unsaturated THF derivatives **232a** in 74–94% yield, dppe **205a** favors the production of reduced **232b** in 74% yield together with 8% of **232a**. Trimethylsilylmethylmagnesium chloride **224** was essential for the success of the cyclizations.

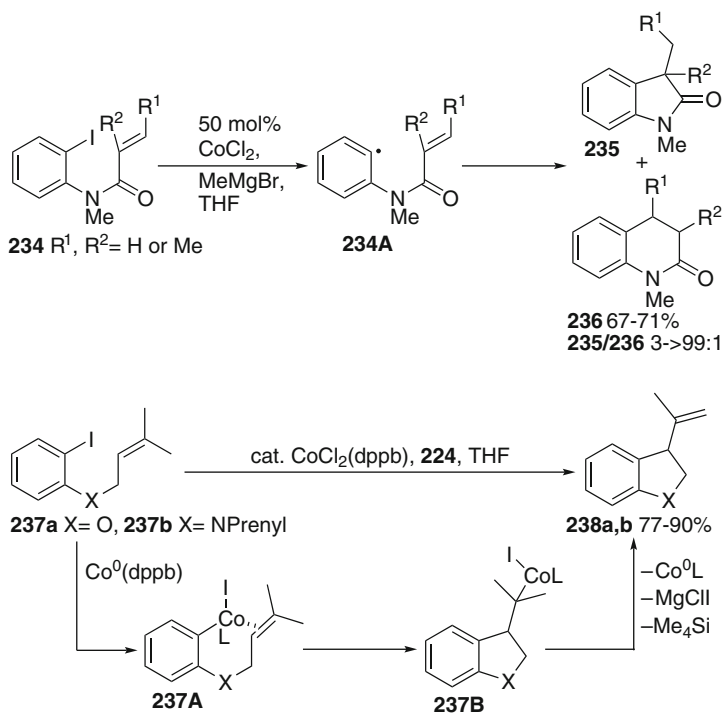
When 2-iodoalkyl vinylsilyl ethers **231** ( $\text{Z}=\text{Si}$ ) were reacted with **224** in the presence of the  $\text{Co}(\text{dppb})\text{Cl}_2$  catalyst, silatetrahydrofurans **232a** ( $\text{Z}=\text{Si}$ ) were isolated [294]. When substrates **231** with substituted allyl groups ( $\text{R}^3$  and/or  $\text{R}^4=\text{alkyl}$ ) were treated with catalytic amounts of  $\text{Co}(\text{dppe})\text{Cl}_2$  and **224** or phenylmagnesium bromide, a 5-exo cyclization proceeded and tetrahydrofurans **232c** with exocyclic alkenyl units were isolated in 58–89% yield. For substrates with disubstituted alkene acceptors ( $\text{R}^3=\text{alkyl}, \text{R}^4=\text{H}$ ), the formation of 18% of reduced tetrahydrofuran **232b** was also observed [280, 295].

The cyclization reactions can be assumed to occur by in situ generation of the respective Co(0) catalyst **233A** by the Grignard reagent as discussed before (cf. Figs. 52 and 54). This triggers SET reduction of **231** to radicals **231A**. A 5-exo radical cyclization proceeded to **231B**. The structure of the latter and the ligands at the cobalt(I) complex **233C** formed by ligand exchange from **233B** determine the further course significantly. The Co(I)(dppb) complex bearing the silylmethyl unit couples efficiently with primary radicals **231B** ( $R^3=R^4=H$ ) leading to cobalt(II) complex **231C**. Subsequent  $\beta$ -hydride elimination provides products **232a**. Catalyst **233A** is regenerated by reductive elimination from coformed cobalt hydride **233D**. The analogous organocobalt dppe complex seems to couple much more slowly with cyclized radical **231B**, which therefore stabilizes by hydrogen transfer from the solvent THF and gives product **232b** preferentially. This rationalization is supported by the fact that almost no deuterium incorporation was found when the reaction mixtures were quenched by deuterium oxide. The phenylmagnesium bromide derived cobalt dppe complex **233C** ( $R^6=Ph$ ) couples apparently quickly enough even with substituted **231B** ( $R^3$  and/or  $R^4=alkyl$ ).  $\beta$ -Hydride elimination occurs predominately or exclusively at the exocyclic alkyl groups from the resulting organocobalt complex **231C** leading to tetrahydrofurans **232c**. The formation of **232b** from **231** ( $R^3=alkyl$ ,  $R^4=H$ ) indicates that some disproportionation may take place from secondary radical **231B** (dashed arrows).

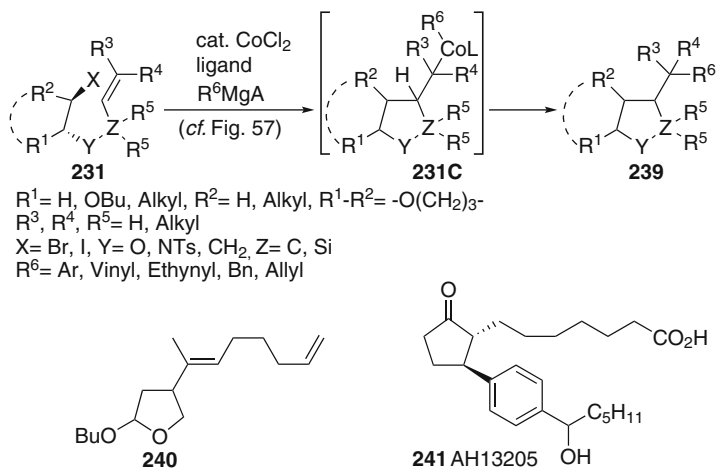
*N*-(*ortho*-Iodoaryl)  $\alpha,\beta$ -unsaturated amides, such as **234**, cyclized using a combination of methylmagnesium bromide as a reducing agent and  $CoCl_2$  as a catalyst (Fig. 58) [296]. Oxindoles **235** were isolated in 67 and 71% yield for  $R^2=H$ . When  $R^2$  was substituted some 6-endo cyclization product **236** was also formed. The authors attributed these results to an aryl radical cyclization reaction and subsequent hydrogen abstraction from the solvent THF. In stark contrast, Oshima and coworkers investigated catalytic cyclizations of aryl iodides **237a,b** using the  $Co(dppb)Cl_2$  complex and trimethylsilylmethylmagnesium chloride **224** [290, 293]. Under these conditions the formation of 3-alkenyldihydrobenzofurans or indolines **238a,b** was observed in 77–90% yield. It was found that aryl iodides are by far the most efficient precursors for these reactions. The authors rationalized the results by proposing the accepted two-electron catalytic cycle commonly observed in Heck reactions. Oxidative addition of the low-valent cobalt catalyst and subsequent migratory insertion of **237A** leads to **237B**. This proposal was supported by the application of similar (*E*)- and (*Z*)-vinyl iodides. A cyclization is not possible with these substrates, but the cross-coupling proceeded with retention of alkene configuration, thus ruling out a vinyl radical. Overall, there remains an ambiguity in the reactivity of aryl iodides toward low-valent cobalt complexes. Future studies should address this point.

### 5.2.5 Tandem Radical Cyclization/Cross-Coupling or Heck Reactions

Oshima provided a number of examples of cobalt-catalyzed tandem radical 5-exo cyclization/cross-coupling reactions (Fig. 59, Table 4). Allyl  $\alpha$ -haloaldehyde



**Fig. 58** Cyclizations of aryl iodides catalyzed by low-valent cobalt complexes



**Fig. 59** Low-valent cobalt-catalyzed radical cyclization/Kumada coupling reactions

**Table 4** Cobalt-catalyzed radical cyclization/cross-coupling reactions

Entry	R <sup>6</sup>	A	Co source	Yield	Ref.
1	Ar	Br	CoCl <sub>2</sub> (dppe) (5 mol%)	21–84	[280, 295]
2	Allyl, Bn	Cl	CoCl <sub>2</sub> (dppp) (5 mol%)	77–100	[278, 279]
3	Ar	Br	CoCl <sub>2</sub> , ( <i>R,R</i> )- <b>208</b> (5 mol%)	26–84	[281]
4	Alkynyl, TMSvinyl	Br	Co(acac) <sub>3</sub> , TMEDA (20–40 mol%)	30–78	[282]
5	Ar	Br	CoCl <sub>2</sub> , <i>rac</i> - <b>208</b> (5 mol%)	41–93	[283, 294]
6	R <sub>3</sub> SiCH <sub>2</sub> , Alkynyl	Cl	CoCl <sub>2</sub> , <b>210</b> (5 mol%)	67–81	[283, 297]

acetals **231** underwent tandem radical 5-exo cyclization/Kumada coupling reactions with aryl Grignard reagents catalyzed by CoCl<sub>2</sub> and **205a** affording mono- or bicyclic benzylic tetrahydrofuran derivatives **239** (entry 1) [280, 295]. Reactions with *ortho*-substituted aryl Grignard reagents proceed only in low yields. The coupling is limited to unsubstituted allyl units (R<sup>3</sup>=R<sup>4</sup>=H). It was demonstrated in stoichiometric experiments that 4 equiv. of phenylmagnesium bromide were necessary to generate the catalytically active species, and that 1 equiv. of biphenyl was formed, from which the authors concluded that the actual catalyst should have the gross structure of a 17-electron Co(0) ate complex (MgBr)<sub>2</sub>[Co(0)(dppe)Ph<sub>2</sub>] (cf. Fig. 52).

Allylic Grignard reagents reacted with **231** in the presence of 5 mol% CoCl<sub>2</sub> and dppp **205b** in 77–100% yield to 2-alkoxy-4-homoallylic tetrahydrofurans **239** (entry 2) [278, 279]. With this less demanding Grignard reagent the cross-coupling proceeded even with substituted allylic termini (R<sup>3</sup>=R<sup>4</sup>=alkyl). The radical nature of the cyclization is strongly supported by the use of cyclopropyl-substituted allylic acetal (R<sup>3</sup>=cyclopropyl, R<sup>4</sup>=Me), which underwent the cross-coupling only after ring opening of the cyclopropylcarbinyl radical giving **240**. When the radical cyclization/cross-coupling reaction was performed in ether instead of standard THF at room temperature, the cyclization proceeded reliably; however, reductive elimination from organocobalt intermediate **231C** was retarded and thus a subsequent intramolecular nucleophilic attack at the acetal group with formation of a cyclopropane derivative prevailed (not shown) [279].

5-exo Radical cyclizations followed by coupling with aryl Grignard reagents took place mostly in good yields in the presence of catalytic amounts of CoCl<sub>2</sub> and chiral ligand (*R,R*)-**208** (entry 3) [281]. This catalytic system was also applicable to annulation reactions and, in contrast to most other iron- and cobalt-based systems, even promoted cross-couplings at secondary radical centers. This strategy was applied to the synthesis of the therapeutically important prostaglandin analog AH 13205 **241**. In line with a radical mechanism for the cyclization, in which the asymmetric environment of the catalyst does not play a role, products **239** or **241** were racemic.

Similar radical 5-exo cyclization/cross-coupling reactions were performed with **231** and 2-trimethylsilylethynyl and 1-trimethylsilylvinyl Grignard reagents using Co(acac)<sub>3</sub> as the precatalyst and TMEDA as the ligand and solvent (entry 4) [282]. The reaction sequences gave moderate to good yields of the cyclization/coupling products **239**. The observed diastereoselectivities were similar to those in

traditional tributyltin hydride-mediated reactions. When the initial products **239** were butyrolactol derivatives, they were immediately subjected to Jones oxidation, giving the corresponding lactones in 30–78% yield. This catalyst system allowed the coupling of secondary alkylcobalt species after cyclization. The spectrum of applicable Grignard reagents is, however, limited to the silyl substituted ones. Alkyl or aryl substituted vinyl and alkynyl Grignard reagents failed to react.

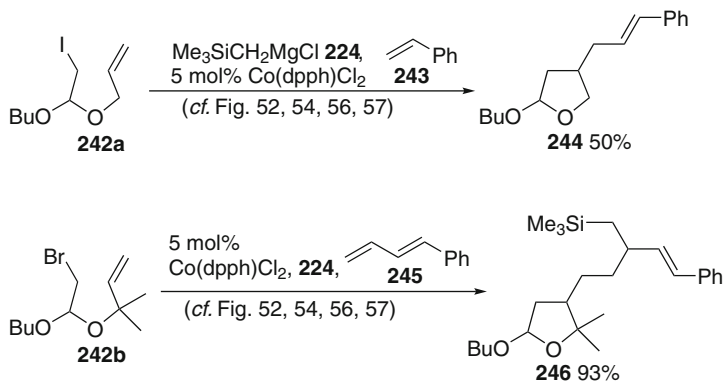
Easily available 2-iodoalkyl vinylsilyl ethers **231** ( $Z=Si$ ) were subjected to tandem radical 5-exo cyclization/Kumada cross-coupling reactions using aryl Grignard reagents and the complex from  $CoCl_2$  and **208** as the catalyst (entry 5) [283, 294]. Silaoxacyclopentane derivatives **239** ( $Z=Si$ ) were obtained in 41–93% yield as a 1:1 mixture of diastereomers at the newly formed stereocenter. This method allows the application of *ortho*-substituted aryl Grignard reagents in acceptable yield. A subsequent Tamao–Fleming oxidation gave access to 1,3-diols. This method was used to synthesize a human CCR5 receptor antagonist.

When (allyldimethylsilyl)methyl or (dimethylphenylsilyl)methyl Grignard reagents were reacted with several 5-hexenyl iodide-type substrates in the presence of a  $Co(NHC)$  catalyst generated from  $CoCl_2$  and imidazolium salt **210**, a smooth tandem radical 5-exo cyclization/Kumada coupling took place giving (2-silylethyl)-substituted cyclic products **239** ( $R^6=CH_2SiMe_2R$ ), which were easily converted to 2-hydroxyethyl-substituted cycles under Tamao–Fleming conditions (entry 6) [283, 297]. Similarly, a 2-iodoethyl (vinyl dimethylsilyl) ether ( $Z=Si$ ) provided the cyclic alcohols with phenylsilyl Grignard reagent **220** as the coupling partner in 65% yield. Alkynyl Grignard reagents are also suitable reaction partners affording propargylic products in 68–85% yield. Bromide cyclization precursors were less reactive. The ethylated NHC ligand **210** was optimal among a number of NHC ligands and these were the only ligands among a number of phosphine and amine ligands which promoted the sequences efficiently.

The course of the reaction is similar to the cross-coupling reactions discussed before (see above, Figs. 52, 54, and 57). Initially a cobalt(0) catalyst of gross structure  $[R_2^6CoL](MgBr)_2$  is generated by addition of four equivalents of the Grignard reagents. Only this complex is competent to trigger SET reduction of **231**. Radical **231A** so formed cyclizes and couples subsequently with the resulting cobalt(I) species. Reductive elimination from complex **231C** finally affords cross-coupling product **239**.

### 5.2.6 Tandem Radical 5-exo Cyclization/Heck Reactions or Tandem Radical Cyclization/Allylic Substitution Reactions

Oshima's group reported the first example of a tandem radical cyclization/intermolecular Heck reaction in 2002 (Fig. 60) [289]. Iodoacetaldehyde allyl acetal **242a** was treated with styrene **243**, catalytic amounts of  $CoCl_2(dppe)$ , and trimethylsilylmethylmagnesium chloride **224** as a stoichiometric reducing agent. 4-Cinnamylbutyrolactol **244** was isolated in 50% yield (cf. Fig. 54).



**Fig. 60** Cobalt-catalyzed tandem reactions involving radical cyclizations

A tandem radical 5-exo cyclization/radical addition/allylic substitution reaction was subsequently described [292]. Allylic  $\alpha$ -bromo acetal **242b** cyclized cobalt-catalyzed. Addition to diene **245** and subsequent coupling with coformed organocobalt(I) species generates an allylcobalt complex, which undergoes reductive elimination to cyclic product **246** in 93% yield (cf. Fig. 56).

### 5.3 *Co(I)–Co(II)–Co(III) Catalysis*

#### 5.3.1 Radical Additions and Tandem Reactions with Radical Additions as the Initial Step

Radical reactions involving cobalt(I) catalysis find their model in Nature, which uses vitamin B<sub>12</sub> **247** extensively for catalyzing difficult transformations [267–273]. This served as an early inspiration to use cobalt complexes as mediators and catalysts for radical reactions [268, 298].

Giese and coworkers determined on the basis of experimental results obtained by Scheffold et al. [268, 299] that addition reactions of alkyl bromides **249** to  $\alpha,\beta$ -unsaturated nitriles or esters **248** catalyzed by cobalamine **247** are free radical reactions (Fig. 61) [300]. This conclusion was based on the similar *cis/trans*-selectivities in addition reactions of the 4-*tert*-butylcyclohexyl radical to different electron-poor alkenes **248** using **247** as a catalyst on one hand and classical tributyltin hydride conditions on the other. The kinetics of the radical addition was determined.

Radical additions of primary, secondary, and tertiary alkyl bromides **249** to diethyl mesaconate **248** catalyzed by 5 mol% vitamin B<sub>12a</sub> **247** (X=OH<sub>2</sub>) proceeded in yields of 63–90% [301]. Deuteration experiments and comparison to similar addition processes support that **247** is initially reduced to cobalt(I) complex **253A**. This reacts with **249** giving an alkylcobalamin(III) intermediate



formation depended strongly on the catalyst amount. In the presence of higher concentrations of cobalt species the desired addition product **252** arises predominately. When the concentration of **247** was kept low and a suitable radical acceptor was present in radical **248A**, even a slow 7-endo cyclization occurred in reasonable yield.

Rusling et al. performed electrochemically and light mediated radical additions of alkyl iodides to cyclohexenone in conductive microemulsions catalyzed by 20 mol% of **247** in 14–81% yield [303]. Radical allylations of alkyl bromides **249** with allyl sulfides, sulfones, or phosphates catalyzed by 5 mol% of cobalt (iminate) complex **250** in the presence of zinc as reducing agent proceeded in 52–85% yield [304].

In a more recent study  $\text{Co}(\text{dppe})\text{I}_2$  was used as a catalyst for reductive additions of primary, secondary, and tertiary alkyl bromides or iodides **249** to alkyl acrylates, acrylonitrile, methyl vinyl ketone, or vinylsulfone **248** in an acetonitrile/water mixture using zinc as a stoichiometric reducing agent [305]. The yields of the resulting esters **252** were mostly good. The authors tested radical probes, such as cyclopropylmethyl bromide or 6-bromo-1-hexene (cf. Part 1, Fig. 8). However, the latter did not cyclize, but isomerized during addition, while the former afforded complicated mixtures. On this basis the authors proposed a traditional two-electron mechanism to be operative; the results do not, however, exclude a radical-based  $\text{Co}(\text{I})$  catalytic cycle convincingly (Fig. 61).

Branchaud and Detlefsen disclosed the addition of  $\alpha$ -bromo esters or alkyl bromides **254** to styrene **243** catalyzed by (dimethylglyoximate) $\text{Co}(\text{III})\text{Cl}$  **255** (Fig. 62) [306]. The in situ-generated cobalt(I) complex reacted with **254** to give an organocobalt complex (cf. Fig. 61). Subsequent homolysis of the labile alkylcobalt(III) complex generated the radical, which adds to styrene **243**. The resulting benzylic radical is trapped by  $\text{Co}(\text{II})$  forming alkylcobalt(III) complex **254A**, which undergoes  $\beta$ -hydride elimination to arylalkenes **256**. The active  $\text{Co}(\text{I})$  catalyst is regenerated by  $\text{Zn}$  added as a stoichiometric reductant. The reactions gave moderate yields of the coupling products.

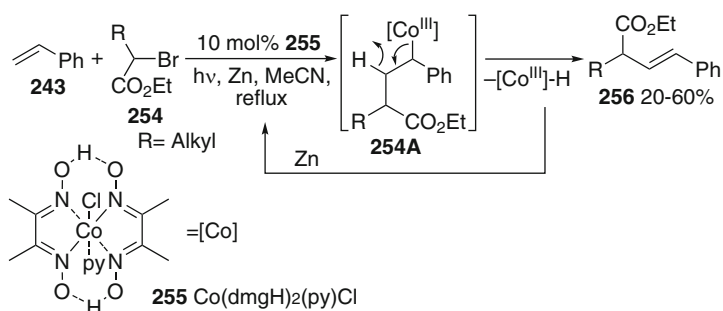
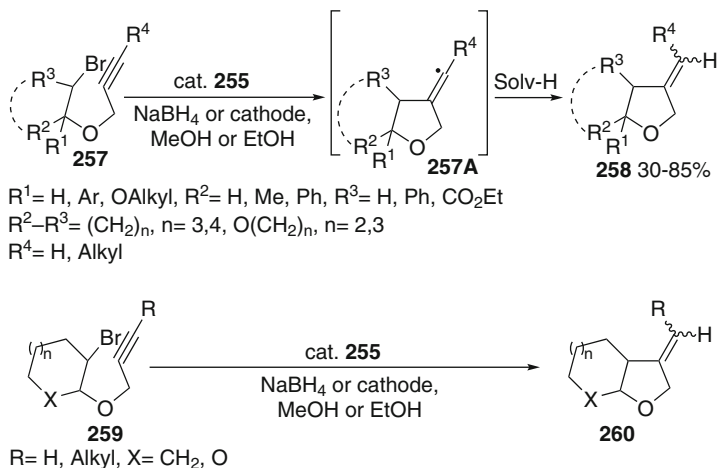


Fig. 62  $\text{Co}(\text{I})$ -catalyzed Heck reactions of alkyl halides with styrene



### 5.3.2 Co(I)–Co(II)–Co(III) Catalysis: Radical Cyclizations Catalyzed by Cobaloxime and Related Complexes

Early examples of catalytic radical cyclizations were provided by Okabe and coworkers, who subjected 2-bromoethyl propargyl ethers or bromoacetaldehyde propargyl acetals **257** to complex **255** as a catalyst and sodium borohydride as the stoichiometric reducing agent (Fig. 63, Table 5, entry 1) [307, 308].



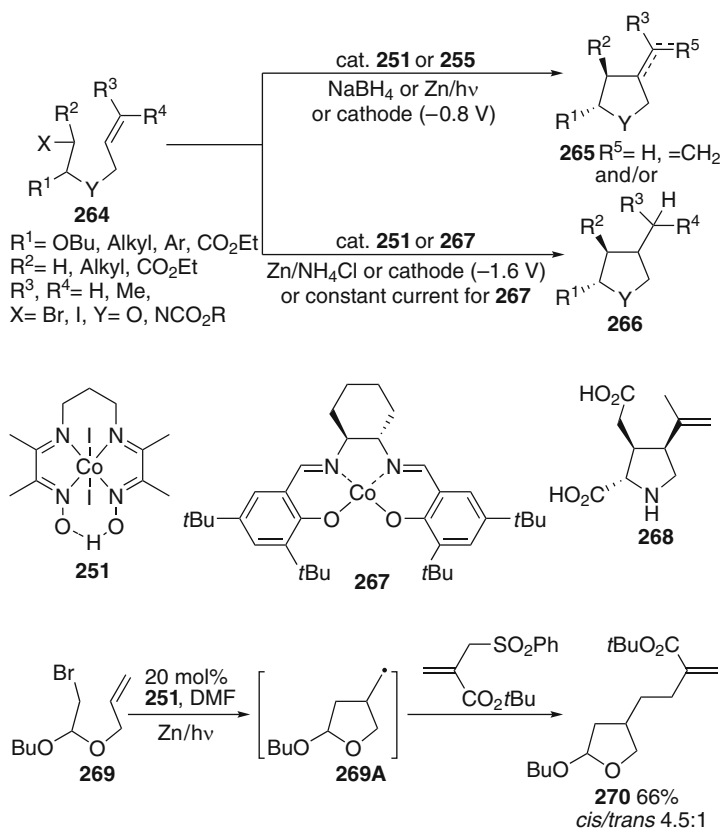
**Fig. 63** Co(I)-catalyzed radical 5-exo cyclization of bromo ethers

**Table 5** Cobalt(I)-catalyzed radical 5-exo cyclizations of alkyl halides

Entry	Educt	Catalyst	Reducing agent	Product	Yield	Ref.
1	<b>257</b>	<b>255</b> (6 mol%)	NaBH <sub>4</sub>	<b>258</b>	48–85	[307, 308]
2	<b>259</b>	<b>255</b> (50 mol%)	Cathode	<b>260</b>	35–87	[309, 310]
3	<b>259</b>	<b>255</b> (5 mol%)	NaBH <sub>4</sub>	<b>260</b>	35–95	[311]
4	<b>257,259</b>	<b>255</b> (6 mol%)	NaBH <sub>4</sub>	<b>258, 260</b>	50, 57	[312, 313]
5	<b>261</b>	<b>255</b> (N.S.) <sup>a</sup>	NaBH <sub>4</sub>	<b>262, (263)</b>	40–71	[314, 315]
6	<b>261</b>	<b>255</b> or <b>247</b> (8–12 mol%)	Cathode	<b>262, (263)</b>	60–70	[316, 317]
7	<b>264</b>	<b>255</b> (20 mol%)	NaBH <sub>4</sub>	<b>265</b>	50–80	[318]
8	<b>264</b>	<b>251</b> (1–40 mol%)	Zn or cathode	<b>265</b> or <b>266</b>	25–99	[304]
9	<b>264</b>	<b>267</b> (20 mol%)	Cathode	<b>266</b>	70	[319]
10	<b>271</b>	<b>255</b> (5–22 mol%)	Cathode	<b>272</b>	47–76	[320]
11	<b>273</b>	<b>274</b> (3 mol%)	NaBH <sub>4</sub>	<b>275a,b</b>	50–84	[321, 322]
12	<b>276</b>	<b>274</b> (3 mol%)	NaBH <sub>4</sub>	<b>277</b>	30–80	[323, 324]
13	<b>278</b>	<b>247</b> (N.S)	Cathode	<b>279</b>	70	[325]
14	<b>281, 285</b>	<b>247</b> (0.75–4.6 mol%)	Cathode	<b>283, 287</b>	55, 63	[326, 327]
15	<b>261</b>	<b>247</b> (1–20 mol%)	Cathode, light	<b>262</b> and/or <b>263</b>	50–74	[328]
16	<b>288</b>	<b>247</b> (10 mol%)	Cathode	<b>289</b>	65	[329]
17	<b>290</b>	<b>247</b> (10 mol%)	Ti(citrate)	<b>291</b> or <b>292</b>	54–82	[330]

<sup>a</sup>N.S. = Not specified

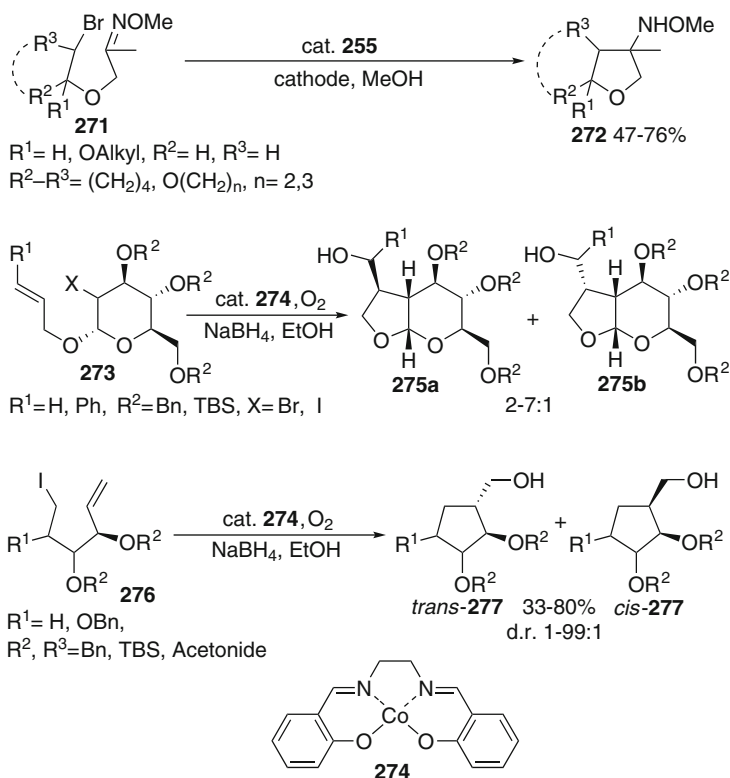




**Fig. 65** Cobalt(I)-catalyzed cyclizations to alkenes

cobalt concentration (20–40 mol%) provided the unsaturated compounds **265** with good to high selectivity. Using stronger reducing conditions, such as zinc/ $\text{NH}_4\text{Cl}$  or a more negative potential of  $-1.6 \text{ V}$  in the presence of dodecylthiol, and a low cobalt concentration (1–5 mol%) led to saturated products **266** in good yield. This divergent behavior can be used to couple radical cyclizations with radical allylation. Bromo acetal **269** cyclizes in the presence of 20 mol% of **251** with zinc as the reductant in DMF to radical **269A**. A subsequent radical allylation using 2-(*tert*-butoxycarbonyl)allyl sulfone gave functionalized butyrolactol **270** in 66% yield and with a 4.5:1 *cis/trans*-diastereoselectivity.

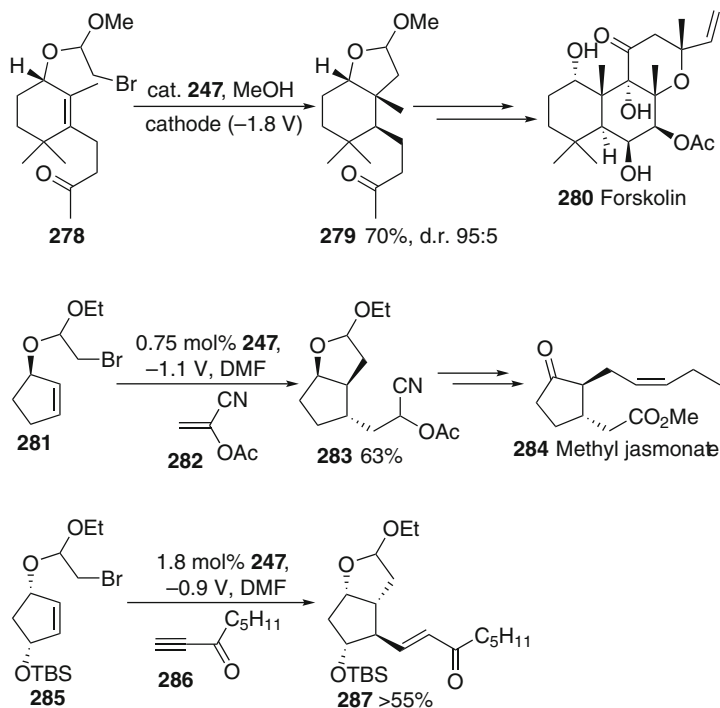
A 3-allyloxy-2-bromo ester **264** ( $\text{Y} = \text{O}$ ,  $\text{R}^2 = \text{CO}_2\text{Et}$ ) cyclized similarly using 20 mol% of (salen)Co complex **267** as a catalyst under reductive electrochemical conditions at a carbon fiber cathode and a sacrificial aluminum anode under constant current conditions. Tetrahydrofurancarboxylates **266** were isolated in 70% yield and a good 6:1 *cis/trans*-selectivity (entry 9) [319].



**Fig. 66** Cobalt-catalyzed radical cyclizations of using other radical acceptors and termination reagents

Not only alkenes but also oxime ethers proved to be suitable radical acceptors in cobaloxime-catalyzed radical 5-exo cyclizations (Fig. 66, entry 10) [320]. Bromo acetals **271**, easily generated by bromoetherification of enol ethers with hydroxy acetone oxime ethers, furnished 3-alkoxyaminotetrahydrofuran derivatives **272** in 47–76% yield using 5–22 mol% **255** and sacrificial zinc electrodes for electrochemical regeneration of the Co(I) catalyst. The cyclization diastereoselectivity is mostly good to excellent, although the relative configuration at the newly generated alkoxyamine center was not established.

A number of cyclic and sugar-derived halo acetals **273** were subjected to radical 5-exo cyclizations catalyzed by a cobalt salen catalyst **274** with  $\text{NaBH}_4$  as the stoichiometric reductant but in the presence of air (entry 11) [321, 322]. Under these conditions, bicyclic oxygenated tetrahydrofurans **275a** were obtained in 50–84% yield. Diastereomeric isomers **275b** were isolated as the minor components. The yields were similar to those obtained with tributyltin hydride. The oxygen concentration proved to be important, since air gave better yields



**Fig. 67** Vitamin B<sub>12</sub>-catalyzed radical cyclizations in natural product synthesis

than pure oxygen. 5-exo Cyclizations of oxygenated 5-hexenyl iodides **276** afforded carbapentoses **277** in 30–80% yield under similar conditions (entry 12) [323, 324].

### 5.3.3 Co(I)–Co(II)–Co(III) Catalysis: Radical Cyclizations Catalyzed by Vitamin B<sub>12</sub> and Derivatives

Inspired by Nature, hydroxocobalamin **247** (X=OH) itself or modified vitamin B<sub>12</sub> derivatives (review [331]) were probed as catalysts for radical cyclizations. This methodology is mediated by light and electrochemical or chemical reduction to close the catalytic cycle. It was applied to total syntheses of forskolin **280** by Pattenden [325] (Fig. 67, entry 13) as well as of jasmonate **284** and prostaglandin precursors **287** by Scheffold (entry 14) [326, 327]. Starting materials were bromoacetaldehyde cyclohexenyl or cyclopentenyl acetals **278**, **281**, or **285**, which cyclized in the presence of **247** to annulated butyrolactols **279**, **283**, or **287**. In the forskolin synthesis the cyclized radical was reduced directly, while a radical addition ensued in the presence of acetoxyacrylonitrile **282** or ynone **286** in

the syntheses leading to **283** and **287**. The reactions work with catalyst loadings of 0.75–4.6 mol% of **247**.

Rusling, Fry, and colleagues reported cyclizations of **261** to **262** and/or **263** catalyzed efficiently by **247** in microemulsions (see Fig. 64, entry 15) [328]. At higher catalyst concentration, the unsaturated product **262** was formed with high selectivity. When a more negative potential was applied and the catalyst load was reduced to 1 mol%, the saturated product **263** was strongly favored.

Katsumata and colleagues disclosed electrochemically mediated vitamin B<sub>12</sub>-catalyzed tandem radical cyclizations (Fig. 68, entry 16) [329]. Bromoacetaldehyde dienyl acetal **288** reacted in a 5-exo/5-exo cyclization sequence applying electrochemically reduced vitamin B<sub>12</sub> **247** as the catalyst. Ester **289** was isolated in 65% yield as a mixture of four diastereomers after oxidation of the lactol.

More recently, van der Donk and coworkers reported radical cyclizations catalyzed by vitamin B<sub>12</sub> using titanium(III) citrate as a stoichiometric reducing agent (Fig. 69, entry 17) [330]. Here *N*-allylic 2-(isopropenyl) pyrroles **290** or allyl 2-phenylallyl ethers serve as the starting material in tandem hydrocobaltation/radical 5-exo cyclization sequences giving dihydropyrrolizine derivatives **291** or **292**. The mechanistic course is not completely clear. However, it is assumed that the reactions start with an initial hydrocobaltation of the isopropenyl unit in the presence of the allylic alkene (see Sect. 5.7). The benzylic cobalt intermediate is subject to homolysis of the very weak cobalt–carbon bond and initiates the radical 5-exo cyclization. Interestingly, the fate of the cyclized radical is dependent on the

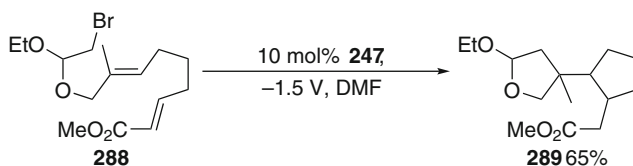


Fig. 68 Cobalamine-catalyzed tandem 5-exo/5-exo radical cyclization

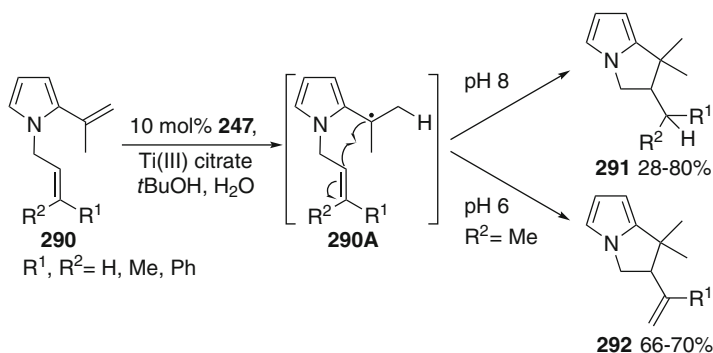


Fig. 69 Vitamin B<sub>12</sub>-catalyzed radical 5-exo cyclization reactions

pH of the solution. At pH 6 unsaturated alkenyl dihydropyrrolizines **292** were formed selectively, while at pH 8 the saturated heterocycles **291** are the major products. This is explained by the fact that the reduction of cobalamine(II) to cobalamine(I) is dependent on the reducing power of Ti(III). At lower pH Ti(III) is a weaker reducing agent. Thus, coupling of persistent Co(II) with the cyclized radical followed by  $\beta$ -hydride elimination prevails under these conditions leading to **292**. At higher pH the persistent radical cobalamine(II) is removed quickly from the reaction mixture by reduction to cobalamine(I). The cyclized radical thus stabilizes by hydrogen abstraction from the solvent affording product **291**. A limitation of this method is that only arylalkenes undergo the required initial hydrocobaltation.

### 5.3.4 Cobalt(I)-Catalyzed Aryl Radical 5-exo Cyclizations

Pattenden and coworkers studied the cyclization of allyl *ortho*-iodophenyl ether **293a** (R=H) catalyzed by (salen)cobalt complex **294** (Fig. 70) [317]. Dihydrobenzofuran **295a** (R=H) was obtained in a moderate 45% yield.

Jacobsen–Katsuki-type chiral (salen)cobalt(II) complex **267** (10 mol%) was used by Dunach and coworkers to catalyze electrochemical radical 5-exo cyclizations of *ortho*-bromophenyl allyl ethers **293a,b** to dihydrobenzofurans **295a,b** (and **296a,b**) [332]. Constant current or constant potential conditions

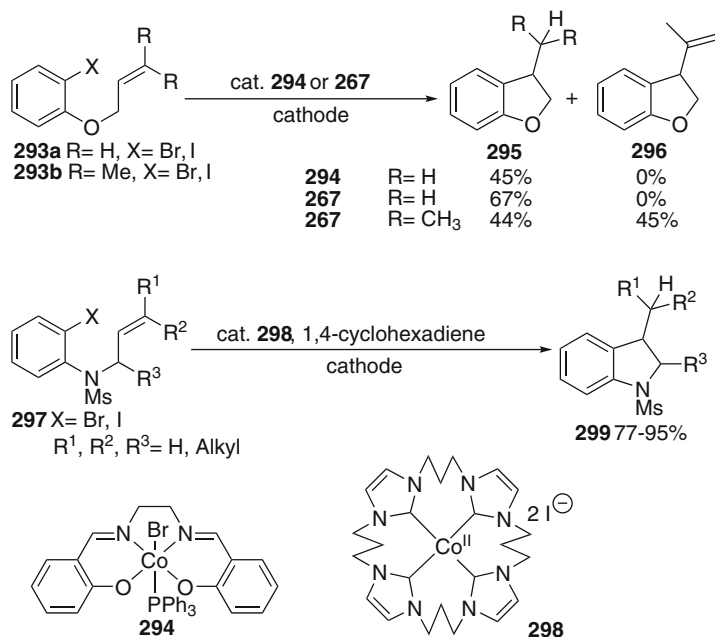


Fig. 70 Electrochemically mediated cobalt-catalyzed aryl radical 5-exo cyclizations

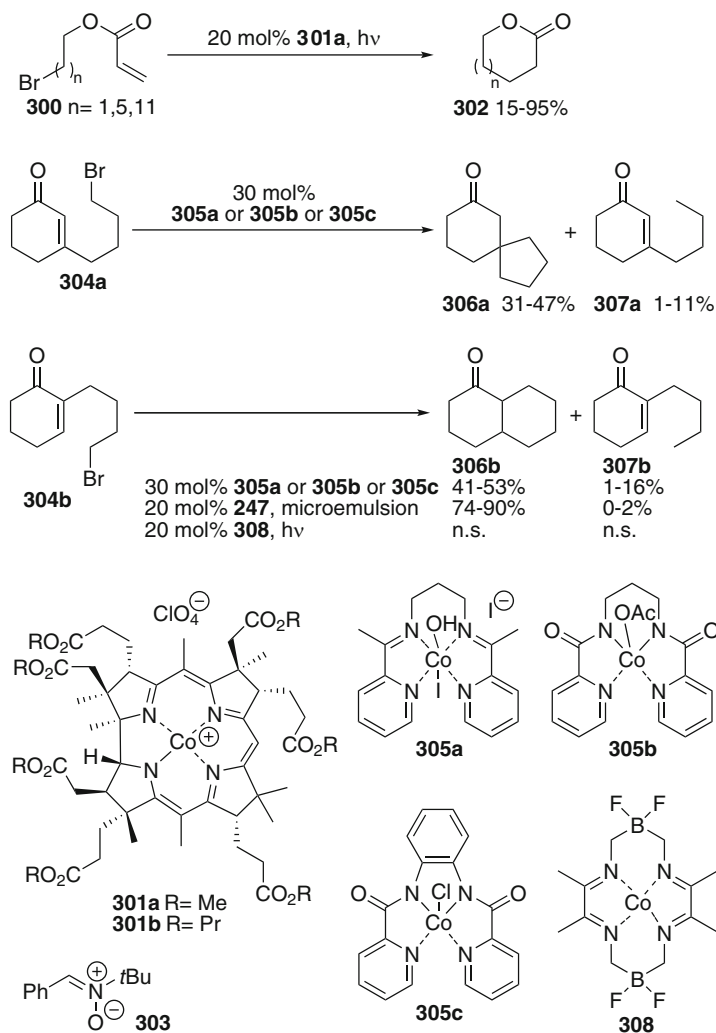
using carbon felt or RVC cathodes, respectively, were applied in DMF to reduce cobalt(II) complex **267** to its Co(I) oxidation state. This allows reductive cleavage of the aryl bromide. The generation of an aryl radical may take place by two pathways. On one hand two-electron oxidative addition of the reduced Co(I) complex to the aryl bromide and subsequent homolysis of the resulting arylcobalt(III) to the Co(II) catalyst **267** and an aryl radical can be envisaged. On the other hand a direct single-electron reductive cleavage of the aryl bromide to an aryl radical is also possible. The controlled potential electrolysis showed that only one electron transfer occurred under the reaction conditions, thus supporting a direct reductive aryl radical generation. Cyclization predominates but the formation of some reduced aryl ether was also observed. For allyl ether **293a** hydrogen abstraction resulting in formation of the reduced product dominates giving **295a** in 67% yield. Disproportionation leading to 3-methylbenzofuran competes only to a minor extent if at all. The cyclized radical derived from the corresponding prenyl ether **293b** disproportionates under the reaction conditions giving isopropyl and isopropenyl dihydrobenzofurans **295b** and **296b** in almost equal proportions in 45–89% yields. For both cyclizations the maximum enantiomeric excess achieved with enantiomerically pure catalyst **267** was 16% ee, indicating that there is not much interaction of the catalyst with the aryl radical in the cyclization transition state. No conversion was observed in the absence of the catalysts.

Recently, Murphy and colleagues introduced new cobalt complexes featuring a macrocyclic tetrakis(NHC) ligand. Complexes, such as **298**, form a very stable Co(I)/Co(II) redox couple. Lower and higher oxidation states cannot be achieved due to the constrained ligand geometry [333]. This complex catalyzed aryl radical 5-exo cyclizations of *N*-allyl-*ortho*-iodoanilines **297** to indolines **299** in 70–95% yield using electrochemical recycling of the catalyst and 1,4-cyclohexadiene as a stoichiometric reducing agent for the cyclized radical. Similar catalytic cyclizations of aryl bromides required heating to 90 °C to achieve the electron transfer. Aryl chlorides were inert. The reaction proceeds by SET reduction of aryl iodides by the Co(I) catalyst, similar to stoichiometric aryl radical cyclizations developed before by Pattenden [298].

### 5.3.5 Other Radical Cyclizations

Hisaeda and coworkers subsequently reported radical (macro)cyclizations of  $\omega$ -bromoalkyl acrylates **300** catalyzed by modified vitamin B<sub>12</sub> **301a** under photolytic conditions (Fig. 71) [334]. The active Co(I) catalyst is generated by electroreduction at platinum cathodes and subsequently substitutes the halide in **300**. The resulting organocobalt(III) intermediate was characterized by UV and MS techniques in the dark. Photolysis triggers 6-endo, 10-endo, or 16-endo cyclizations affording the products **302** in 95, 15, and 43% yield, respectively. The reaction was inhibited by addition of the radical trap PBN **303** and the derived radical adducts were detected by ESR-spectroscopy.





**Fig. 71** Co(I)-catalyzed radical cyclizations (n.s. = not specified)

Ozaki and coworkers studied a number of cobalt and nickel complexes as electrocatalysts in reductive cyclizations, of which **305a–c** were the most effective [335].  $\omega$ -Bromoalkyl cyclohexenones **304a** or **304b** underwent radical 5-exo, 6-exo, or 6-endo cyclizations depending on the substitution pattern of the enone unit to give either spirocyclohexanones **306a** or decalinones **306b** in moderate yields. Major side products were the uncyclized reduced compounds **307a** or **307b**, respectively.

Light-stimulated radical 6-endo cyclizations of **304b** catalyzed by vitamin B<sub>12</sub> **247** with electrochemical regeneration of the catalyst gave 74–90% yield of

bicyclic product **306b** [303, 336]. Vitamin B<sub>12</sub>-modified electrodes can also be used [337]. When similar conditions were applied to analogous 5-endo cyclizations, yields were, as expected, very low. However, reactions at a more negative potential promoted further reduction to a carbanion, which cyclized in an intramolecular conjugate addition in good yield [338].

### 5.3.6 Radical Ring Expansion Reactions

In analogy to enzymatic reactions catalyzed by vitamin B<sub>12</sub>, Murakami investigated ring expansion reactions of 2-methylcyclopentan-1,3-dione **309a** and 3-methylpyrrolidone **309b** to cyclohexan-1,4-dione **310a** and 2-piperidone **310b**, respectively (Fig. 72) [339]. Both rearrangements proceed efficiently in almost quantitative yield in an ammonium salt vesicle catalyzed by 1.7 mol% of vitamin B<sub>12</sub> heptapropyl ester **301b**. A vanadium trichloride/oxygen system served the dual role of mediating the hydrogen abstraction reaction from the substrates, generating the alkyl radicals that couple with the Co(II) complex. At the same time, V(III) serves as the stoichiometric reducing agent for Co(III).

Ring expansions of 1-(bromomethyl)-2-oxocycloalkanecarboxylates **311a** catalyzed by 0.65 mol% of hydrophobically modified vitamin B<sub>12</sub> perchlorate **301a** were subsequently developed by Hisaeda and colleagues [340]. Constant potential conditions (−1.5 V vs SCE) were applied to reduce **301a** initially to the corresponding Co(I) complex. Substitution of the bromide in **311a** gives an organocobalt(III) intermediate, which cleaved to the radical and the active Co(I or II) catalyst under the reductive conditions. 3-exo Cyclization to the carbonyl and

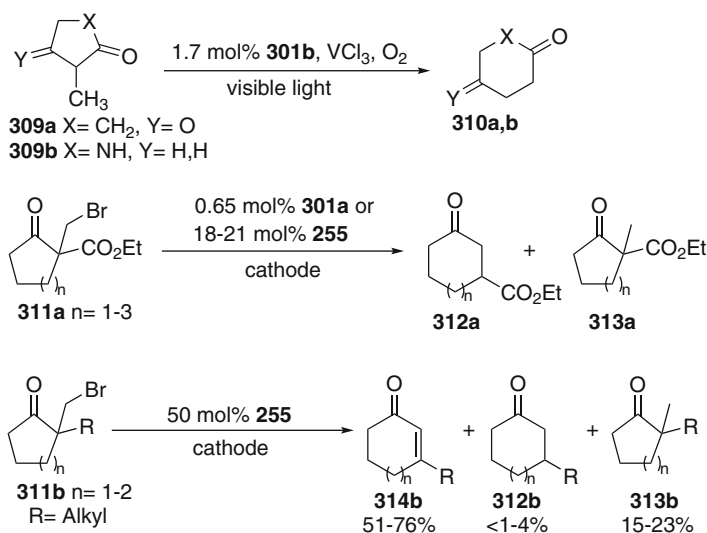


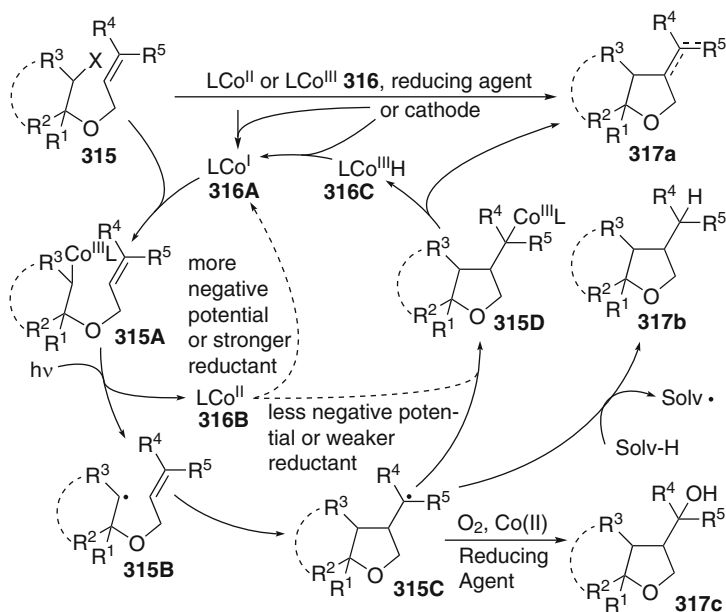
Fig. 72 Cobalt-catalyzed ring expansion reactions of carbonyl compounds

alternative cyclopropyloxy radical ring opening leads to the ring-expanded products **312a** in moderate yield together with the directly reduced derivatives **313a**.

Kawafuchi et al. reported the ring expansion of 2-(bromomethyl)cyclopentanones **309a** and **311a** ( $n = 1$ ) to cyclohexan-1,4-dione derivatives **310a** and **312a**, respectively, using 18–21 mol% of cobaloxime(II) **255** in 56–74% yields [341]. The catalyst was electrochemically regenerated.

Inokuchi and colleagues reported related cobalt-catalyzed radical ring expansion of (bromomethyl)cycloalkanones **311b** using significantly higher concentration (50 mol%) of cobalt catalyst **255**, which led to cycloalkanones **314b** [342]. The active catalyst was (re)generated electrochemically. The reduced products **312b** and **313b** were formed as byproducts. In accord with the results by Giese and others, the formation of unsaturated products **314b** prevails using high cobalt catalyst concentrations (see above).

All cyclizations discussed in Sects. 5.3.2–5.3.5 occur by a unified mechanism (Fig. 73). In an initial step the cobalt(II) or (III) precatalyst **316** is reduced chemically or electrochemically to an active cobalt(I) catalyst **316A**. These highly nucleophilic species undergo a substitution with alkyl halides **315**, leading to alkylcobalt(III) intermediates **315A**. These complexes can be isolated and characterized and were used in stoichiometric cyclizations [298]. They are, however, very sensitive to light and form radicals **315B** and cobalt(II) complexes **316B** on irradiation. For aryl halides (not shown) radical generation can occur either



**Fig. 73** Mechanism of cobalt(I)-catalyzed radical cyclizations (Anions at cobalt in **315** and **316** omitted for clarity)

similarly by oxidative addition followed by homolysis or by direct reductive aryl radical generation triggered by electron-rich **316A**.

Radicals **315B** cyclize under the reaction conditions forming radicals **315C**. In the ring expansion reactions in Fig. 72, the initially formed radical **315B** cyclizes in a 3-exo process and stabilizes by a transannular cyclopropyloxy radical ring opening (not shown). The amount of catalysts **316** and the strength of the reducing conditions determine the fate of **315C** significantly. When mild reducing conditions and higher catalyst loadings are applied, coupling of cyclized radical **315C** with paramagnetic **316B** prevails. The resulting organocobalt(III) species **315D** undergoes a typical  $\beta$ -hydride elimination affording unsaturated products **317a** as the major products. The concomitantly formed cobalt hydride species **316C** is transformed to active cobalt catalyst **316A** under the reducing conditions. Under stronger reducing conditions and using low catalyst amounts, cobalt(II) species **316B** is reduced faster to **316A** and cannot further interact with radicals **315C**. They consequently stabilize most often by hydrogen abstraction from the solvent or external reducing agents, such as 1,4-cyclohexadiene, to reduced cyclic products **317b**. Alternatively radical coupling of **315C** with oxygen was also used, which leads to products **317c**.

#### 5.4 Co(I)–Co(II)–Co(III) Catalysis in Radical Cycloadditions

Krische and coworkers developed intramolecular [2+2] cycloadditions of bis(enones) **318** catalyzed by 10 mol% of Co(dpm)<sub>2</sub> **319** using PhSiMeH<sub>2</sub> as the stoichiometric reducing agent (Fig. 74) [343, 344]. *cis*-Diacylbicyclo[3.2.0]heptanes **320** were isolated in 48–73% yield. The reaction is limited to substrates that have one easily reducible aroyl unit in the molecule, otherwise intramolecular Michael addition is observed as the major pathway. The reaction was proposed to proceed by reduction of **318** to a Co(I) species **319A** by the silane. This species is able to reduce phenyl or furyl-substituted **318** to an anionic (oxyallyl)cobalt(III) species **318A**, which is valence tautomeric to a cobalt(II)-complexed radical anion **318B**. This manifold undergoes a 5-exo cyclization, leading to a cobalt(III) enolate, which may exist as an equilibrium between oxyallyl and C-centered forms **318C** and **318D**. The intermediacy of this equilibrating pair is supported by the fact that the isomeric (*Z*)-enone substrates give the same product **320**, in which both benzoyl units orient to the sterically less encumbered convex face. Facile reductive elimination leads to **320** as a single diastereomer and closes the catalytic cycle with regeneration of **319A**. The mechanism is supported by similar cathodic reductive cycloadditions, which lead to the same products. Yield and diastereoselectivity were lower though, which may be a result of the lacking template effect of the cobalt center under the electrochemical conditions [345]. When the stronger reducing agent PhSiH<sub>3</sub> or more electron-rich enones were applied the course of the reaction switched to a two-electron hydrometalation/Michael addition pathway promoted by a cobalt hydride species.

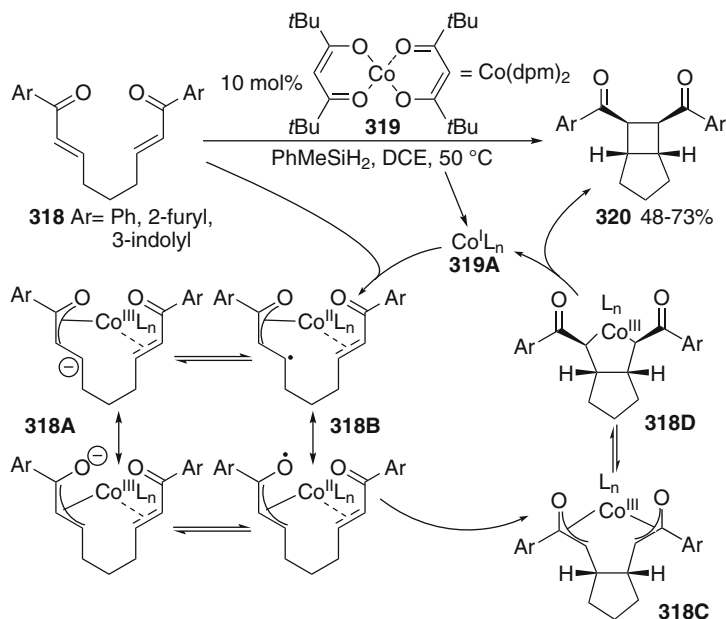
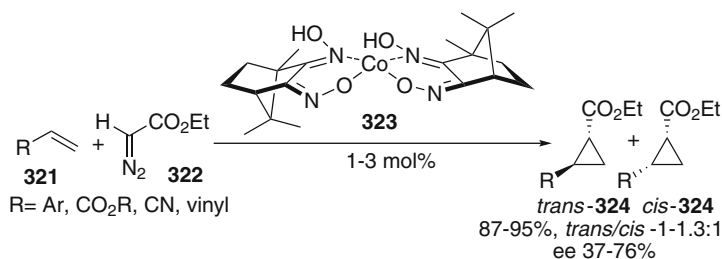


Fig. 74 Co-catalyzed intramolecular [2+2] cycloadditions (L=dpm)

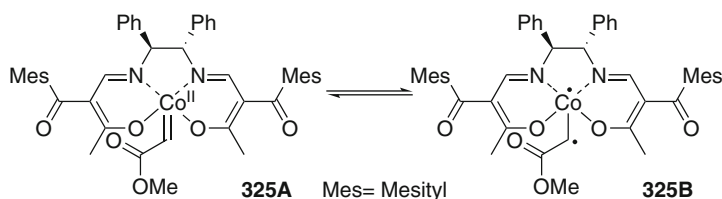
## 5.5 Co(II)–Co(III) Catalysis: Cyclopropanation

Cobalt-catalyzed cyclopropanations are one of the few well-developed reaction types, in which ligand-centered radicals are generated and react with neutral molecules. Nakamura and colleagues reported the first cyclopropanations of styrenes or dienes **321** with alkyl diazoacetates **322** catalyzed by 1.7–10 mol% bis(camphorquinonedioximate)Co(II) complex **323** under very mild conditions (Fig. 75) [346, 347]. Cyclopropanes **324** were isolated in 87–95% yield and moderate to good enantiomeric excess. The *cis/trans*-ratio was, on the other hand, very low. In contrast to most other typical cyclopropanation methods almost no dimerization of the diazo compound was observed. The reaction did not work well with electron-deficient alkenes, such as acrylates or acrylonitrile. The corresponding Co(III) complex was completely inactive while the analogous Co(I) complex was considerably slower. NMR experiments indicated that a paramagnetic species was present throughout the reaction and the Co(II) center remains unchanged at the end. Based on the kinetics, a two-electron catalytic cycle was proposed and the mode of enantioselection discussed. This method was later expanded by several groups using salen and oximate ligands [348, 349].

Much later, Ikeno and coworkers provided IR-spectroscopic evidence that Co(II) carbene complexes **325** exhibit considerable single bond character (Fig. 76). This complex can be depicted best as a valence tautomeric pair **325A** and **325B**, in which



**Fig. 75** Catalytic cyclopropanation using a cobalt camphor quinone oximate complex

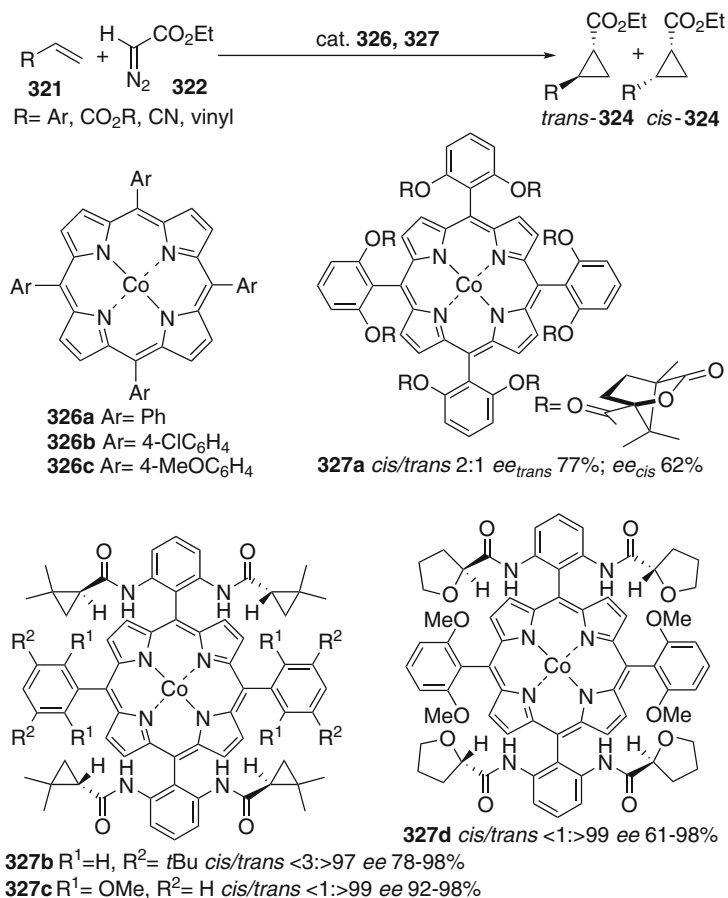


**Fig. 76** Valence tautomeric (salen)cobalt carbene complexes **325**

the latter is significant [350]. The radical character of (porphyrin)cobalt(II) complexes has already been exploited in the 1990s in living radical polymerizations. The kinetics of the addition of radicals to cobalt(II) complexes were determined. The rate constants amounted to approximately  $10^7 \text{ M}^{-1} \text{ s}^{-1}$  [351–354].

In 2003, Cenini and coworkers reported (tetraarylporphyrin)cobalt(II) complexes **326** as efficient catalysts (1 mol%) for cyclopropanations. In the absence of air, styrenes **321** underwent an efficient cyclopropanation with ethyl diazoacetate **322** giving cyclopropanes **324** in 65–99% yield with 3–5:1 *trans/cis* ratios (Fig. 77) [348]. Simple olefins and more hindered diazoesters did not react. With diazoacetate and hydrocarbons, such as cyclohexane or benzene, C–H insertion took place furnishing cyclohexyl- or phenylacetate. In line with Ikono's proposal the cyclopropanation reaction was considerably slowed down in the presence of TEMPO, though not completely inhibited. Based on a kinetic analysis a two-electron catalytic cycle with a bridged carbene unit was formulated, however.

In parallel, Zhang and coworkers reported similar results using the same catalysts [349]. They showed that cobalt complexes **326** are much more active than related iron, ruthenium or rhodium porphyrin complexes. Cyclopropanes **324** (R=Ar) were isolated for a number of styrene derivatives in 89–99% yield. On the other hand the *trans/cis*-ratio was, at ca. 3:1, the worst compared to Fe and Ru porphyrin catalysts. The *trans*-selectivity was improved by addition of nitrogen ligands, such as *N*-methylimidazole or pyridines. An asymmetric variant using complex **327a** was developed. The enantio- and diastereoselectivities were, however, moderate [349]. The transformation was proposed to proceed via a radical complex being similar to **325B**. Based on these results vitamin B<sub>12</sub> derivatives **247** were applied [355]. 2-Arylcyclopropanecarboxylates **324**

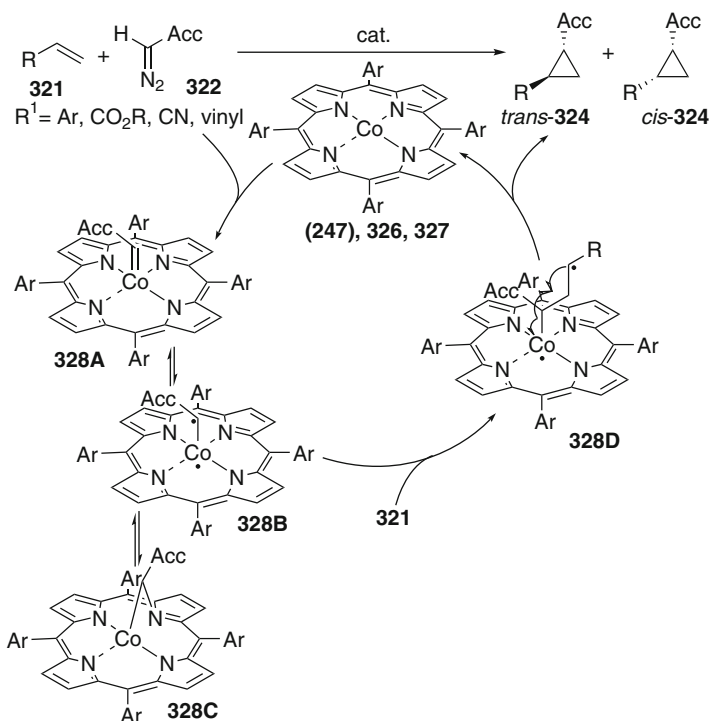


**Fig. 77** (Tetraarylporphyrin)cobalt cyclopropanation catalysts

(R=Ar) were isolated in good yield (70–98%) as diastereomeric mixtures, in which the *cis*-isomers predominated (ca. 2:1). The *ee* values for **324** amounted to 55–66%.

Zhang's group developed highly active chiral (porphyrin)cobalt(II) complexes **327b–d**, which catalyzed the cyclopropanation reactions of styrenes [356–358] and even of  $\alpha,\beta$ -unsaturated esters or nitriles [358, 359] by diazoacetates. Nitro-diazoacetates [360] or sulfonyldiazomethane [361] also proved to be useful in asymmetric cyclopropanation reactions of styrenes, acrylic derivatives, and in some cases even simple olefins with good to high *de* and moderate to excellent *ee* (highlight [362]).

Chiral binaphthyl-bridged [*meso*-tetrakis(2-aminophenyl)porphyrin]cobalt or polymer-supported chiral (salen)Co complexes also catalyzed the cyclopropanation of styrenes albeit so far with lower diastereo- and enantioselectivities [363, 364].



**Fig. 78** Mechanistic rationale for the cobalt-catalyzed cyclopropanation

Recently de Bruin, Zhang, and coworkers studied the mechanistic course of these cyclopropanation reactions in detail and the following course is most likely (Fig. 78) [365]. According to ESR and mass spectrometric investigations and supported by the earlier trapping reactions by TEMPO it is assumed that the (porphyrin)Co(II) complexes **247**, **326**, and **327** coordinate the diazoester **322** first leading to a nitrogen containing intermediate complex (not shown). After its fragmentation a carbene complex **328A** results, which has strong biradical character as shown in valence tautomer **328B** at the cobalt-bound carbon atom. Moreover, this complex can stabilize by bridging to the porphyrin ligand as shown in **328C**. Structure **328B** has, according to a DFT investigation, the lowest barrier to add to olefin **321**. The resulting radical **328D** forms the cyclopropane ring in a favorable 1,3- $S_H1$  reaction, in which the two substituents are located *anti* to each other. The face selectivity is determined by hydrogen bonding of the amide substituent in the cobalt complex with the acceptor unit of the bound carbenoid in the transition state. The radical character of **328B** explains the very low tendency for dimerization of **322** very well, which is common with other metal catalysts. The *trans*-selectivity observed and the very slow reduction of the bound diazoacetate in case of slow cyclopropanation are also accommodated by the mechanistic proposal.



## 5.6 Co(II)–Co(III) Catalysis: Intra- and Intermolecular C–H Amination of Hydrocarbons

Cenini and coworkers investigated the intermolecular amination of alkylarenes by aryl azides catalyzed by (porphyrin)Co(II) **326** initially and found that mixtures of benzylic amines and imines result from linear alkylarenes, while only benzylic amines were formed from branched alkylarenes [366, 367]. In stoichiometric experiments between the catalyst and the azide the corresponding azobenzene results, which suggests the involvement of a nitrene intermediate. TEMPO inhibited the reaction. A blank experiment showed that TEMPO does not react with Co(TPP) **326a**. Kinetic investigations were in line with the involvement of a radical-like species. The transition state for the amination was, however, proposed to consist of an azide-cobalt complex, which inserts into the benzylic C–H bond. More recently Zhang and colleagues applied modified (tetraarylporphyrin)Co(II) complex **326d** as the catalyst and bromoamine T **330** as the nitrogen source in intermolecular C–H aminations of alkylarenes **329** (Fig. 79) [368]. A cobalt nitrenoid complex is generated initially, from which amination reactions of alkylarenes yielding benzylic amines **331a** succeeded in 14–73% yield. Very recently it was shown that Troc azide **332** is a suitable nitrene precursor in benzylic C–H amination reactions [369]. Troc-Protected benzylic amines **331b** were isolated in 69–92% yield.

Zhang and coworkers reported recently that (porphyrin)cobalt(II) complexes are suitable for intramolecular amination of C–H bonds. Initially, *ortho*-substituted arylsulfonyl azides **333a** were subjected to 2 mol% of Co(TPP) **326a**. Benzosultams **334a** were formed in 87–99% yield (Fig. 80) [370]. When substrates **333** with longer R<sup>1</sup> chains were used, mixtures of five- and six-membered sultams

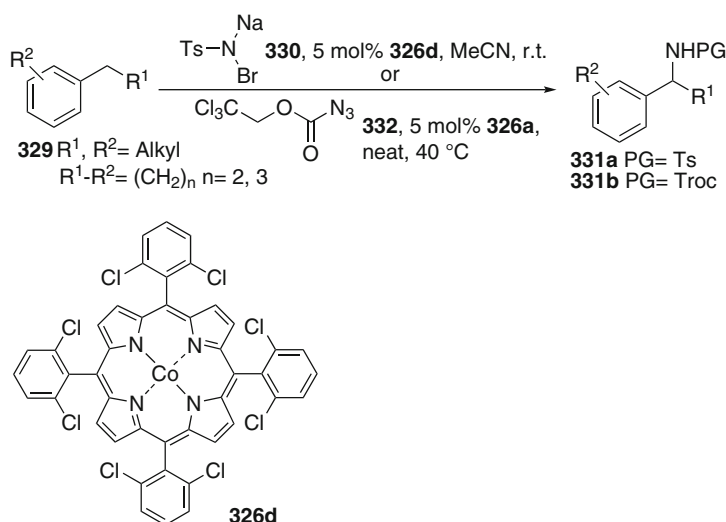
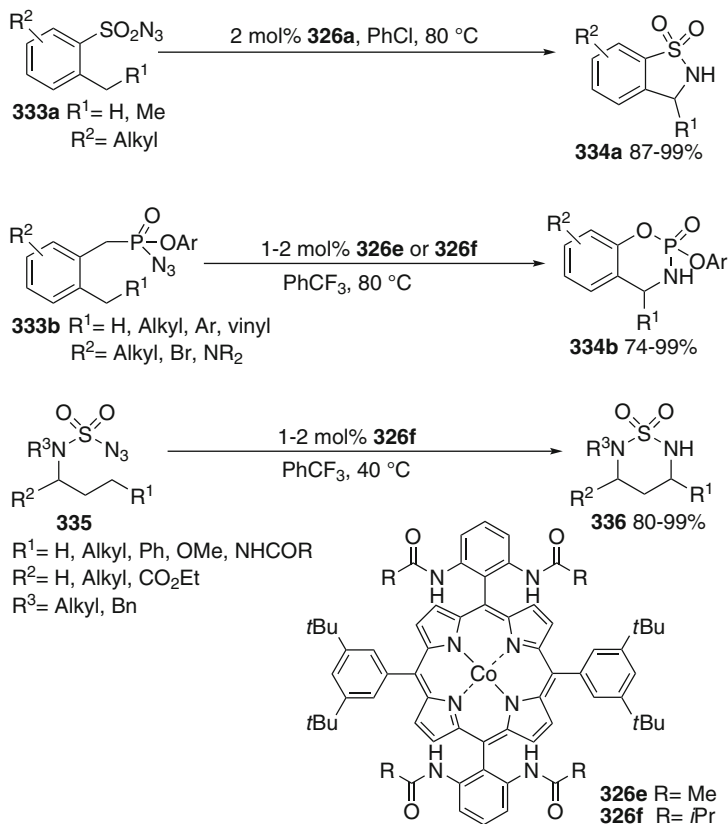


Fig. 79 Cobalt porphyrin-catalyzed intermolecular C–H amination reactions



**Fig. 80** (Porphyrin)cobalt-catalyzed intramolecular C–H amination reactions

resulted, in which **334a** prevailed to some extent. The cobalt catalyst **326a** gave the best yield among all third row transition metal porphyrin complexes. The method was later extended to *ortho*-alkylphenyl phosphoryl azides **333b** [371]. For these substrates 1–2 mol% of substituted (tetraarylporphyrin)Co(II) complexes **326e** or **326f** proved to be the optimal catalysts. 1,3,2-Oxazaphosphorinanes **334b** were isolated in 74–99% yield. When the benzylic position was blocked in **333**, the C–H insertion took place at the homobenzylic position in 37–99% yield (not shown).

Alkyl sulfamoyl azides **335** are convenient substrates for the synthesis of aliphatic 1,3-diamines [372]. Cobalt complex **326f** catalyzed the process providing **336** in 80–95% yield. When (1-methylcyclopropyl)methylamine was used as the substrate, ring opening of the cyclopropane was observed, suggesting the involvement of a cyclopropylcarbinyl radical (cf. Part 1, Fig. 8). When the amination was tried with enantiomerically enriched precursors, a loss of ee was found suggesting that the reactions occur through a planar intermediate. A plausible course for these aminations involves the generation of a (porphyrin)cobalt nitrenoid radical, which is able to abstract a suitably located hydrogen atom (for a similar mechanistic

scheme, see Fig. 24). The resulting carbon radical attacks the cobalt amide in a 1,5-, 1,6-, or 1,7-S<sub>H</sub>i reaction releasing the products and liberating the catalyst **326**. Similar asymmetric aziridination reactions of arylalkenes were developed using trichloroethoxysulfonyl azide catalyzed by **327d** in 43–95% yield and 80–99% ee. Simple olefins reacted less efficiently [373].

## 5.7 Co(II)–Co(III) Catalysis: Hydrocobaltation/Functionalization of Alkenes

Okamoto et al. disclosed a hydration reaction of styrenes **337** ( $R^1 = \text{Ar}$ ,  $R^2 = R^3 = \text{H}$ ) leading to benzylic alcohols **341** in 78–98% yield using 1 mol% (tetraphenylporphyrinato)cobalt(II) **326a** and stoichiometric amounts of tetraalkylammonium boranates in the presence of oxygen in 1984 (Fig. 81, Table 6, entry 1) [126]. Higher-substituted arylalkenes reacted much more slowly. The yields ranged between 14 and 98%, while simple alkenes remained unaffected. The  $\text{Co}(\text{dmgH})_2(\text{py})\text{Cl}$  complex **255** also gave good results, but the rate of reaction and conversion was

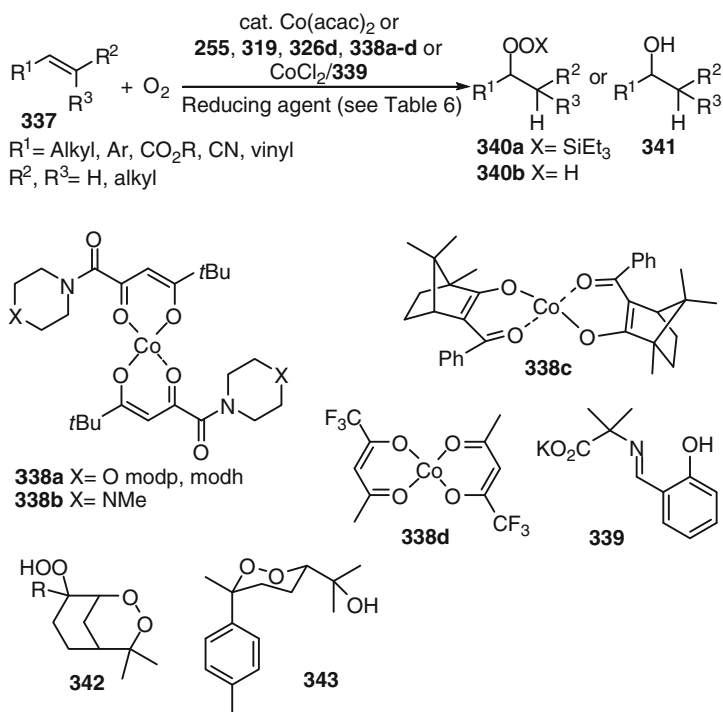


Fig. 81 Cobalt-catalyzed hydration of alkenes

**Table 6** Cobalt-catalyzed hydrofunctionalization reactions of olefins

Entry	Reagent	Product	Catalyst	Additive	Reducing agent	Yield	Reference
1	Oxygen	<b>341</b>	(TPP)Co <b>326a</b> (0.9 mol%)	–	Et <sub>4</sub> NBH <sub>4</sub>	14–98	[126]
2	Oxygen	<b>340a</b>	<b>338a</b> (5 mol%)	cat. <i>t</i> BuOOH	Et <sub>3</sub> SiH	75–99	[374, 375]
3	Oxygen	<b>340a</b>	<b>338a</b> (5 mol%)	cat. <i>t</i> BuOOH	Et <sub>3</sub> SiH	58–89	[376–380]
4	Oxygen	<b>340a</b>	<b>338a</b> (N.S.) <sup>a</sup>	–	Et <sub>3</sub> SiH	54–90	[381]
5	Oxygen	<b>340a</b>	Co(acac) <sub>2</sub> (10 mol%)	–	Et <sub>3</sub> SiH	61–74	[382, 383]
6	Oxygen	<b>340a</b>	Co(acac) <sub>2</sub> (N.S.)	–	Et <sub>3</sub> SiH	40–90 <sup>b</sup>	[384]
7	Oxygen	<b>340a</b>	Co(dpm) <sub>2</sub> <b>319</b> or <b>338c</b> (N.S.)	–	Et <sub>3</sub> SiH	68–90	[385]
8	Oxygen	<b>340a</b>	Co(dpm) <sub>2</sub> <b>319</b>	–	Et <sub>3</sub> SiH	45–78	[386, 387]
9	Oxygen	<b>340b</b>	<b>326d</b> (0.1 mol%)	–	Et <sub>3</sub> SiH	49–92	[388]
10	Oxygen	<b>341</b> <sup>c</sup>	Co(acac) <sub>2</sub> (5 mol%)	cat. <i>t</i> BuOOH	Et <sub>3</sub> SiH	50–83	[375]
11	Oxygen	<b>341</b>	<b>338d</b> (5 mol%)	–	Et <sub>3</sub> SiH	53–87	[389]
12	Oxygen	<b>341</b>	Co(acac) <sub>2</sub> (5 mol%)	–	PhSiH <sub>3</sub>	64–93	[390]
13	Oxygen	<b>341</b>	CoCl <sub>2</sub> or Co(NO <sub>3</sub> ) <sub>2</sub> / <b>339</b> (12 mol%)	–	PhSiH <sub>3</sub>	–	[391]
14	Oxygen	<b>341</b>	Co(acac) <sub>2</sub> or <b>338d</b> (20 mol%)	–	<i>i</i> PrOH	37–91	[392–394]
15	NO	<b>345</b>	<b>255</b> (20 mol%)	–	Et <sub>4</sub> NBH <sub>4</sub>	33–69	[395]
16	NO	<b>345</b> , <b>346</b>	Co(eobe) <b>344</b> (5 mol%)	–	Et <sub>3</sub> SiH	67–96	[396]
17	BuONO	<b>345</b>	(TPP)Co <b>326a</b> (0.3 mol%)	–	Et <sub>3</sub> SiH	31–94	[397]
18	<b>348</b>	<b>350</b>	<b>349a</b> or <b>b</b> (2.5–5 mol%)	–	PhSiH <sub>3</sub>	60–98	[391, 398, 399]
19	<b>352a–d</b>	<b>354</b>	Co(BF <sub>4</sub> ) <sub>2</sub> •6H <sub>2</sub> O (6 mol%), <b>353</b> (6 mol%)	30 mol% <i>t</i> BuOOH	PhSiH <sub>3</sub> or (Me <sub>2</sub> HSi) <sub>2</sub> O	39–90	[391, 400]
20	<b>352e,f</b>	<b>354</b>	Co(BF <sub>4</sub> ) <sub>2</sub> •6H <sub>2</sub> O (6 mol%), <b>353</b> (6 mol%)	cat. <i>t</i> BuOOH	(Me <sub>2</sub> HSi) <sub>2</sub> O	48–99	[401]
21	<b>356</b>	<b>358</b>	<b>357a</b> or <b>b</b> (1 mol%)	cat. <i>t</i> BuOOH	PhSiH <sub>3</sub>	55–99	[402]
22	<b>359</b>	<b>360</b>	<b>357a</b> (2 mol%)	–	PhSiH <sub>3</sub>	33–95	[403]
23	<b>361</b>	<b>362</b>	Co(BF <sub>4</sub> ) <sub>2</sub> •6H <sub>2</sub> O (6–12 mol%), <b>353</b> (6–12 mol%) or <b>357a</b> (2–8 mol%)	For <b>353</b> cat. <i>t</i> BuOOH	PhSiH <sub>3</sub>	67–96	[404]
24	PhSSPh	<b>364</b>	Co(eobe) <b>344</b> (10 mol%)	–	PhSiH <sub>3</sub>	31–71	[405]

<sup>a</sup>N.S. = Not specified<sup>b</sup>Isolated yields of 1,2,4-trioxanes after condensation of crude silyl peroxide with aldehydes<sup>c</sup>In situ reduction of intermediate hydroperoxide by Na<sub>2</sub>S<sub>2</sub>O<sub>3</sub>

lower. The isolation of small amounts of dimerization products and ketones support the occurrence of radical intermediates.

Mukaiyama subsequently reported a cobalt-catalyzed silyl peroxidation of alkenes giving products **340a** with exclusive Markovnikov regioselectivity using molecular oxygen in 75–99% yield (entry 2). The  $\text{Co}(\text{modp})_2$  complex **338a** proved to be the best catalyst among a number of cobalt  $\beta$ -diketonate complexes, while  $\text{Et}_3\text{SiH}$  was the reducing agent of choice [374, 375]. It was later found that an induction period observed with several precatalysts could be overcome by addition of substoichiometric amounts of *tert*-butyl hydroperoxide [375].

In a recent mechanistic study it was shown that *tert*-butyl hydroperoxide acts most likely as a precursor for the formation of a cobalt peroxide intermediate (entry 3) [376]. The intermediacy of radicals during the formation of silyl peroxides **340a** is supported by the occurrence of a cyclopropylcarbinyl radical ring opening, when the reaction was conducted with vinylcyclopropane as the olefin (cf. Part 1, Fig. 8). A systematic investigation of the silanes showed that sterically non-demanding ones are the most efficient hydride sources. Among them  $\text{Et}_3\text{SiH}$  was the most effective [377]. Other silanes led to an increase in the formation of alcohols **341** and free hydroperoxides **340b**. Tokuyasu et al. extended the investigations to Co-catalyzed tandem radical peroxidation/peroxyl radical cyclization sequences to give oxygenated endoperoxides, such as **342** [378].

The relative rates of the cobalt-catalyzed silyl peroxidation reactions were determined for different substitution patterns of **337**. Terminal alkenes are the least reactive substrates. The reaction is sensitive to steric factors. 1,1-Disubstituted olefins convert most easily, while tri- and tetrasubstituted alkenes transform more slowly. Both electron-rich and electron-poor alkenes are substrates in the silyl peroxidation; however, both types react more slowly than styrenes [379]. These reaction conditions were also applied to the silyl peroxidation of several 1,1-disubstituted alkenes bearing alcohol or peroxy functionalities in the molecule [380].

The silyl peroxidation method was used in the total synthesis of peroxide containing natural products. Xu and coworkers applied this methodology to a total synthesis of all four diastereomers of Yingzhaosu C **343** (entry 4) [381].  $\text{Co}(\text{modp})_2$  **338a** worked better than  $\text{Co}(\text{acac})_2$  and the silyl peroxidation reaction was more efficient using a protected instead of a free alcohol function (90 vs 54% yield). Oh and Kang applied this method to the silyl peroxidation of several terminal and 1,2-disubstituted simple olefins **337** using 10 mol% of  $\text{Co}(\text{acac})_2$ , oxygen and  $\text{Et}_3\text{SiH}$  in dichloroethane or ethanol (entry 5) [382]. The latter was better and the resulting silyl peroxides **340a** were formed in 61–74% yield. Free alcohols are tolerated by the method. The reaction proceeded, however, without diastereoselectivity when a chiral allylic alcohol was used under identical conditions [383]. 2-Arylallylic alcohols undergo the desired silyl peroxidation (entry 6) [384]. The resulting tertiary benzylic silyl peroxides **340a** were cyclized *in situ* with aldehydes and ketone affording 1,2,4-trioxanes in 40–90% yield.

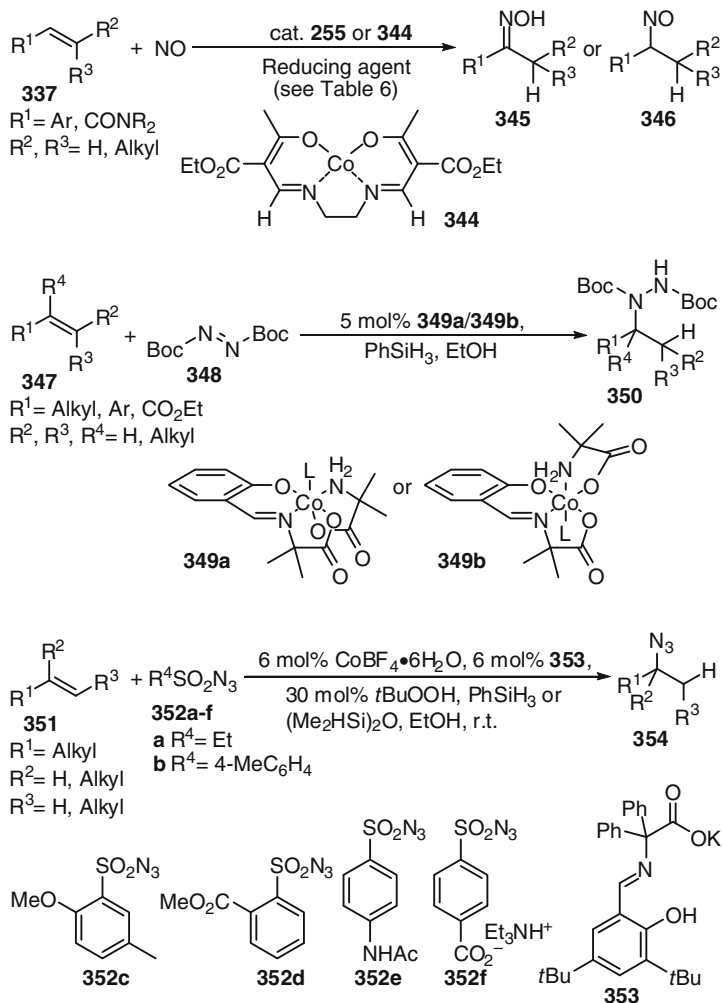
O'Neill and coworkers recently introduced the  $\text{Co}(\text{dpm})_2$  catalyst **319** to make the silyl peroxidation more effective (entry 7) [385]. It gives consistently higher yields (68–90%) than  $\text{Co}(\text{acac})_2$  (5–80%). The catalyst tolerates free alcohol functions well.

A camphor-derived 1,3-diketone complex **338c** worked well (55–80% yield), but no asymmetric induction was observed. One-pot reactions to access 1,2,4-trioxanes were also effective using the new catalysts. Dussault and coworkers used **319** to catalyze the silyl peroxidation of 3-methyl-3-butenol in ethanol in 45% yield (entry 8) [386]. Some silylation of the alcohol function was also found under the reaction conditions. Similar double silyl peroxidation reactions were performed with trisubstituted olefins in 52–78% yield using **319** as the catalyst [387].

Sugamoto and colleagues developed a hydroperoxidation of 1,3-dienes and especially diunsaturated carbonyl compounds catalyzed by (porphyrin)Co(II) complex **326d** (entry 9) [388]. The reaction worked with only 0.1–1 mol% of the cobalt catalyst and triethylsilane as the optimal reducing agent. This reaction was applicable to acrylates giving  $\alpha$ -hydroperoxy esters **340b** in 72–89% yield, while 2,4-dienoates, 2,4-dienals, 2,4-dienones, or nitrodienes reacted in 49–92% yields. The reaction is regioselective for the distal double bond of the conjugated system affording  $\gamma$ -hydroperoxy- $\alpha,\beta$ -unsaturated carbonyl compounds exclusively. Styrenes were converted to benzylic hydroperoxides **340b**. However, in this case ketones formed as byproducts. Simple olefins were not applicable. Thus this and Mukaiyama's methods (see above) are complementary to each other. Deuteration studies using  $\text{Et}_3\text{SiD}$  and *i*PrOD or *i*PrOH led to deuterium incorporation into the substrate, while no D-incorporation was found with *i*PrOD alone. An EPR investigation showed that dienes coordinate to the cobalt-porphyrin complex, while simple alkenes do not. This led to a slightly different mechanistic proposal compared to that suggested for other cobalt complexes (see below). Here, a cobalt-diene complex is proposed to form initially, which abstracts hydrogen from the silane giving an (allyl)Co(III)(porphyrin) complex. The addition of a cobalt hydroperoxide to the olefin is unlikely based on the deuteration and EPR evidence. Unfortunately, however, an investigation of the interaction of the cobalt complex with triethylsilane, definitely ruling out an initial hydrocobaltation, was not reported.

The anti-Markovnikov hydration of  $\alpha,\beta$ -unsaturated esters to provide  $\alpha$ -hydroxy esters **341** ( $\text{R}^1=\text{CO}_2\text{R}$ ) succeeded in 50–83% yield when the intermediate hydroperoxide was reduced by sodium thiosulfate (entry 10) [375]. An exception also pointing to the involvement of radicals was ethyl cinnamate, where the reaction occurred with completely opposite regioselectivity.

The oxygenation reactions could also be performed so that direct conversion of olefins **337** to alcohols **341** by reductive cleavage of the silyl peroxide to the alcohol was promoted (entry 11) [389]. This was achieved by use of bis(trifluoroacetylacetonato)cobalt(II) **338d** as the catalyst and triethylsilane as the reducing agent. Alcohols were isolated in 53–87% yield. For terminal alkenes the formation of some ketone was also observed in 10–29% yield. When phenylsilane was used under similar conditions, somewhat better results were achieved (entry 12) [390]. Structurally diverse alcohols were isolated in 64–93% yield, but 3–24% of ketones were still formed in competition with the desired alcohol **341**. Thus reductive peroxide cleavage is only moderately faster than eliminative cleavage leading to the ketone. Carreira demonstrated that cobalt(II) complexes derived from  $\text{CoCl}_2$  and amino acid-derived salicylidene imines **339** catalyzed the hydration of conjugated enynes to propargylic



**Fig. 82** Cobalt-catalyzed addition of nitrogen functionalities to olefins

alcohols in the presence of  $\text{PhSiH}_3$  as a reductant. The product alcohols **341** were obtained by a reductive workup using  $\text{Na}_2\text{S}_2\text{O}_3$  (entry 13) [391].

The direct conversion of alkenes **337** to secondary alcohols **341** was also achieved using an excess of sacrificial secondary alcohol, such as isopropanol, as the hydrogen source (entry 14) [392–394]. Although the mechanistic details are not completely understood, it is likely that the reaction follows a similar course involving hydrocobaltation/oxygen trapping and reduction (see below). In addition to products **341** and the corresponding ketones, which were formed in similar ratios as before, 2 equiv. of water were also detected.

The introduction of nitrogen is possible under similar conditions (Fig. 82). Styrenes **337** ( $\text{R}^1 = \text{Ar}$ ,  $\text{R}^2 = \text{R}^3 = \text{H}$ ) reacted with nitrous oxide and  $\text{Et}_4\text{NBH}_4$  in the

presence of 13–25 mol% of (py)Co(dmgH)<sub>2</sub>Cl complex **255** to acetophenone oximes **345** in 33–69% yield (entry 15) [395]. The reaction is limited to terminal styrenes. Stilbene, indene, and related compounds do not react.

$\alpha,\beta$ -Unsaturated amides underwent the typical hydrocobaltation (entry 16) [396]. Subsequent homolysis and trapping by nitrogen monoxide provided the corresponding  $\alpha$ -nitroso amides **346**, which tautomerize to the hydroxyimino amides **345**. The yields range from 67 to 96%. The method is, however, limited to amides. A more general protocol involves a hydrocobaltation/nitrosation using butyl nitrite. However, this method probably does not involve radicals, but proceeds more likely according to an S<sub>N</sub>2 process [406, 407].

Styrenes, enolates, and dienolates **337** can be nitrosated using (tetraphenylporphyrin)cobalt(II) **326a** as the catalyst (entry 17). Under these conditions oximes **345** were isolated in 31–94% yield. The mechanistic details of this reaction remain to be elucidated [397].

Carreira and coworkers recently developed intermolecular cobalt-catalyzed hydrohydrazination and hydroazidation reactions, which proceed via radical intermediates with complete regioselectivity. Capitalizing on the hydration results above, a high-yielding intermolecular hydrohydrazination with a good substrate scope was developed (entry 18) [391]. The olefin hydrohydrazination proceeded with best results using a mixture of the amino acid-derived cobalt Schiff base complexes **349a,b** as the catalyst, phenylsilane as the reducing agent, and di-*tert*-butyl azodicarboxylate **348** as the nitrogen source [398]. The reaction works for a broad spectrum of mono-, di-, and trisubstituted alkenes **347** bearing keto, bromide, hydroxy, or acetal functions furnishing alkyl hydrazines **350** in 60–98% yield [391]. Styrenes and vinyl-substituted heterocycles gave the Markovnikov products in 40–85% yield. Vinylpyrrole was an exception. Attempts to conduct the hydrohydrazination asymmetrically with Evans' auxiliary failed, but a pantolactone ester gave moderate diastereoselectivity. Mechanistic experiments support the reaction course. The formation of completely deuterated products when PhSiD<sub>3</sub> was used supports an initial hydrocobaltation as in the hydration reaction (see below). The occurrence of a significant kinetic isotope effect of 2.2 supports the hydrocobaltation to be the rate-determining step of the overall catalytic cycle. The involvement of radical intermediates was shown by ring opening of vinylcyclopropane during the reaction and by the occurrence of radical 5-exo cyclizations at the faster end of the kinetic scale in good yields (cf. Part 1, Fig. 8). Slower cyclopropylcarbinyl radical ring opening and 5-exo cyclization probes led in contrast mostly to ring-closed and ring-opened hydrazination products, respectively. From these values a rate constant for the addition of the radical to the azodicarboxylate of ca.  $1.5\text{--}2 \times 10^8 \text{ mol}^{-1} \text{ s}^{-1}$  was derived. The hydrohydrazination of dienes and enynes was also possible and proceeded for most substrates regioselectively in a 1,2-fashion giving allylic hydrazines in 27–90% yield [399]. The mechanistic situation may, however, be more complicated, since an allylcobalt species results after hydrocobaltation, which may furnish the product through other reaction channels.

The corresponding hydroazidation of olefins **351** proceeded best by use of an in situ-generated complex from 6 mol% Co(BF<sub>4</sub>)<sub>2</sub>•6H<sub>2</sub>O and salicylidene



diphenylglycine ligand **353**,  $\text{PhSiH}_3$ , or tetramethyldisiloxane as a reducing agent and ethylsulfonyl or tosyl azide **352a,b** as the azide transfer reagents (entry 19) [391, 400]. A substoichiometric amount of *tert*-butyl hydroperoxide was also necessary in this reaction to obtain good yields of alkyl azides **354**. They ranged from 39 to 90% under optimized conditions. Phenylsilane gave somewhat lower yields. For sterically more demanding alkenes, arylsulfonyl azides **352c** and **352d** gave considerably better yields. The sulfonyl azides react apparently somewhat slower than other substrates with the initially generated radicals, since reduced hydrocarbon products were also formed to some extent. A further study demonstrated that commercially available 4-acetamidobenzenesulfonyl azide **352e** and especially sodium or triethylammonium 4-azidosulfonylbenzoate **352f** were better azide sources allowing the synthesis of tertiary azides **354** from 1,1-disubstituted alkenes in 48–99% yield (entry 20) [401]. The reaction tolerates many functionalities and is applicable to the functionalization of amino acid derivatives.

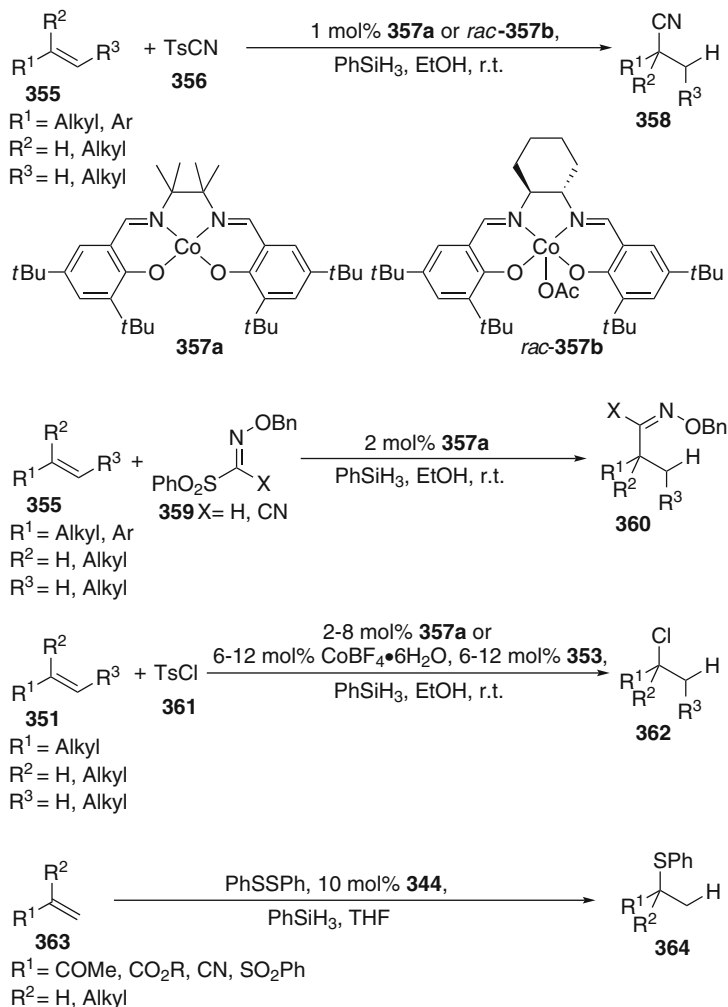
Similar reaction conditions allowed the preparation of  $\alpha$ -branched nitriles (Fig. 83). When mono-, di-, and trisubstituted olefins **355** bearing functionalities, such as esters, aldehydes, ketones, amides, or alcohols, were reacted with tosyl cyanide **356** and phenylsilane in the presence of 1 mol% of the (salen)Co catalysts **357a** or **357b** the corresponding nitriles **358** were isolated in 55–99% yield (entry 21) [402]. Although no mechanistic evidence was provided, the reaction may be assumed to proceed similarly as the hydroazidation.

Very recently it was shown that sulfonyl oximes **359** are suitable reagents for the addition of oxime functions to olefins **355** (entry 22) [403]. This C–C bond-forming reaction proceeded for a wide range of terminal and 1,1-disubstituted substrates with formal Markovnikov selectivity using catalytic amounts of **357a**. Branched oximes **360** were isolated in 33–95% yield.

Tosyl chloride **361** can be applied similarly (entry 23) [404]. Here the best cobalt complex was dependent on the structure of the starting olefin. For terminal alkenes 2 mol% of the (salen)Co complex **357a** was preferred. Secondary alkyl chlorides were obtained with complete regioselectivity in 73–94% yield, while the catalyst derived from  $\text{Co}(\text{BF}_4)_2$  and *N*-salicylidene diphenylglycinate **353** proved to be better for the hydrochlorination of 1,1-disubstituted olefins (entry 22). Tertiary alkyl chlorides **362** were obtained in 67–96% yield. The reaction conditions are mild so that acid- and base-sensitive protecting groups are compatible.

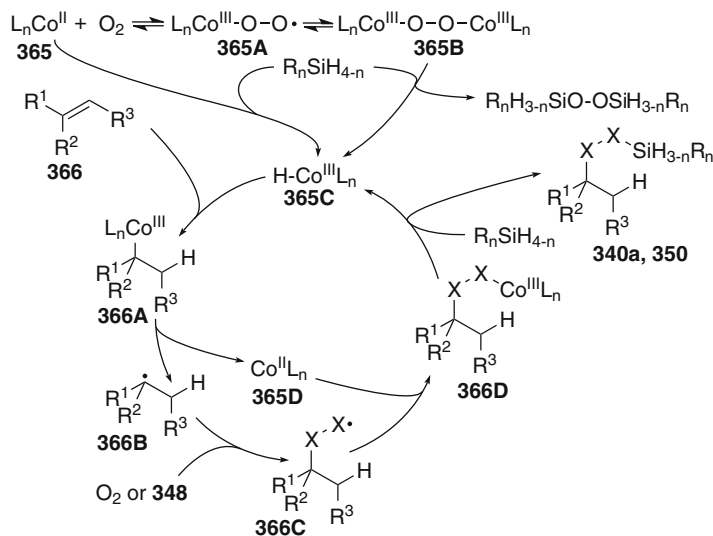
Sulfide groups can also be introduced by this methodology (entry 24) [405]. Simpkins and coworkers found that the reaction of acceptor-substituted alkenes **363** with diphenyl disulfide in the presence of 10 mol% of  $\text{Co}(\text{eobe})_2$  **344** and  $\text{PhSiH}_3$  as the stoichiometric hydrogen source furnished 31–71% of  $\alpha$ -(phenylthio) carbonyl compounds **364**. The intermediacy of radicals was proven by a 5-exo cyclization occurring in competition to the  $\text{S}_{\text{H}}2$  reaction at sulfur.

The mechanism of the cobalt-catalyzed hydrofunctionalizations can be rationalized as follows. Common to all protocols is the generation of a cobalt(III) hydride complex **365C** from a cobalt(II) precursor **365** (Fig. 84). A major difference lies in the generation of **365C**. In the presence of oxygen (entries 1–14), the reaction starts most likely by oxidation of **365** to Co(III) peroxide complexes **365A**



**Fig. 83** Cobalt-catalyzed hydrosulfenylation, hydrochlorination, and C–C bond formation

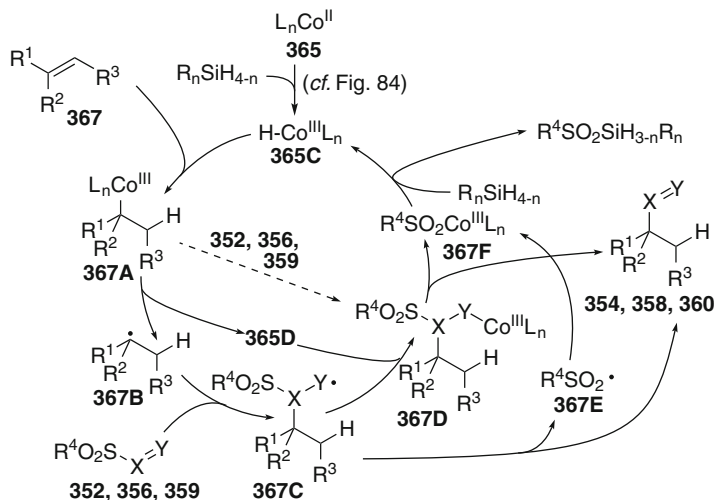
and **365B** by oxygen (see also Sect. 5.9). The resulting complex is reduced by the silane to the active cobalt hydride complex **365C** and a disilyl peroxide. In all other methods, oxygen has to be excluded. The silane forms the cobalt hydride complex **365C** most likely directly or by assistance of additives, such as *tert*-butyl hydroperoxide. Thus generated complex **365C** adds probably in a concerted asynchronous fashion to the olefin **366**. The regioselectivity for the formation of branched organocobalt(III) compounds **366A** is quite high. These organocobalt(III) species undergo homolysis to radicals **366B** with extraordinary ease. This is in line with the reactivity of organocobaloxime(III) intermediates (see Sect. 5.3). For the resulting alkyl radicals **366B**, several pathways are open.



**Fig. 84** Catalytic cycle of cobalt catalyzed hydroperoxidation and hydrohydrazination reactions (Anions at cobalt omitted for clarity)

In the presence of oxygen radical **366B** is trapped to peroxy radical **366C** ( $X=O$ ), which couples with persistent cobalt(II) species **365D** forming cobalt(III) peroxide **366D** ( $X=O$ ). Transmetalation by excess silane provides silyl peroxides **340a**. When boranates are used instead, the intermediate peroxides are cleaved under the reaction conditions to alcohols **341**. The latter can be easily obtained from **340** using common reducing agents. In the hydrohydrazination reaction, alkyl radical **366B** adds to azodicarboxylate **348**. The hydrazinyl radical **366C** ( $X=NBoc$ ) so formed couples with **365D** to cobalt hydrazide intermediate **366D** ( $X=NBoc$ ). Co-Si transmetalation regenerates catalyst **365C** and leads to a silyl hydrazide, which forms product **350** by reaction with the alcohol solvent or on hydrolysis during workup.

The reactions involving sulfonyl azides **352**, sulfonyl cyanides **356**, or sulfonyl oximes **359** proceed initially similarly as the hydrohydrazination reaction (Fig. 85). Hydrocobaltation of olefin **367** by cobalt(III) hydride **365C** is followed by homolysis of the alkylcobalt complex **367A**. The resulting radical **367B** adds to radical acceptors **352**, **356**, or **359**. The ability of radicals to attack these compounds was amply demonstrated by extensive investigations of the Renaud and Kim groups (reviews [408, 409]). Radicals **367C** thus formed can stabilize on one hand by coupling with persistent Co(II) complex **365D** leading to cobalt(III) complexes **367D**, from which an elimination of cobalt(III) sulfinate **367F** can occur that affords products **354**, **358** or **360**. On the other, it is well known that radicals like **367C** undergo very facile  $\beta$ -fragmentation reactions leading directly to products **354**, **358**, or **360** and sulfonyl radicals **367E**. They can also couple with **365D** providing cobalt(III) sulfinate **367F**. A third alternative consists of a coordination of **352**, **356**, or **359** to alkylcobalt compound **367A** and subsequent migratory insertion



**Fig. 85** Catalytic cycle of hydroazidation, hydrocyanation and hydrooximation reactions (Anions at cobalt omitted for clarity)

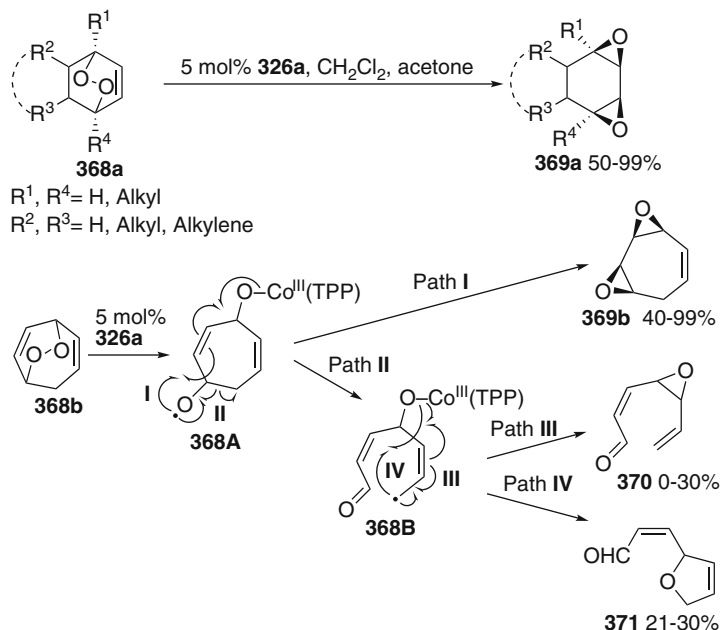
into the cobalt–carbon bond furnishing intermediate **367D** (dashed arrow). The active catalyst **365C** is reformed by reduction of cobalt sulfinate **367F** by the silane.

The hydrochlorination and hydrosulenylation reactions giving **362** or **364** can also be explained easily by  $S_{H2}$  reactions of radical **367B** with TsCl or PhSSPh.

## 5.8 Co(II)–Co(III) Catalysis: Reductive 1,2-Dioxine Ring Opening and Tandem Reactions Involving It

Footo and coworkers reported the first reductive ring opening reactions of mono- and bicyclic unsaturated endoperoxides **368a** applying 5 mol% of cobalt(tetraphenylporphyrin) **326a** (Fig. 86) [410]. Initially the peroxide linkage cleaves reductively and the resulting alkoxy radical is subject to a 3-exo cyclization to the adjacent alkene unit, followed by a 1,3- $S_{H1}$  reaction that liberates the catalyst and the diepoxide products **369a** (cf. Fig. 47), which were isolated in 50–99% as single diastereomers.

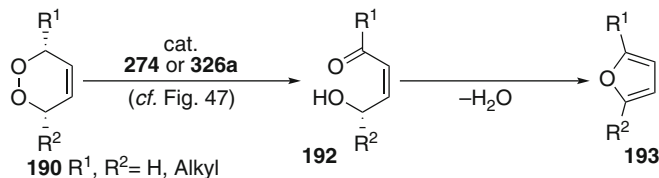
Balci and coworkers used this method to introduce multiple epoxide units in endoperoxides derived from cycloheptatrienes, such as **368b**, providing compounds **369b** via **368A** according to path I in 40–99% yield [411]. This pathway is exclusive when the conformation of radical **368A** does not allow the overlap of the alkoxy radical with the  $\beta$ -C–C bond, which would promote fragmentation (see below). This holds for several cyclopentane-annulated cycloheptadiene endoperoxide analogous to **368b**, which provided the diepoxides of type **369b** selectively in 73–82% yield [412], and for geminal dialkyl-substituted derivatives [413]. For most conformationally more flexible



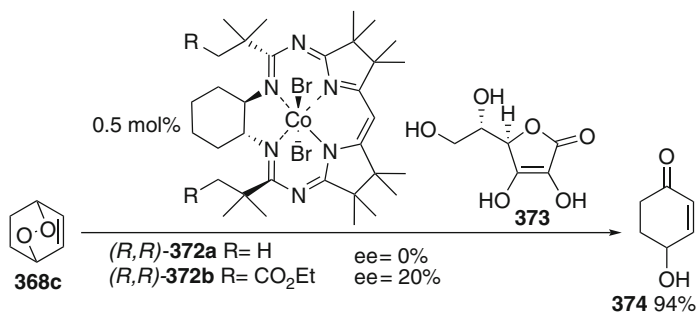
**Fig. 86** Reductive cleavage of unsaturated endoperoxides by cobalt(tetraphenylporphyrin)

compounds of type **368b**, however, up to 30% of epoxy aldehydes **370** were formed as byproducts. They result from competing  $\beta$ -fragmentation of the initial alkoxy radical **368A** to a stabilized allylic radical **368B** (Path II). On one hand this can be subject to a further 1,3- $\text{S}_{\text{H}}$  reaction giving epoxy aldehydes **370** (Path III) [413–415]. On the other, when tropone ketal endoperoxides were used, 70% of the expected diepoxide **369b** was isolated and, additionally, 30% of tetrahydrofuran **371** was formed, which resulted from a 1,5- $\text{S}_{\text{H}}$  reaction of allylic radical **368B** (Path IV) [416]. Cyclobutanone-annulated endoperoxides reacted similarly and gave 61% of the corresponding diepoxide **369b** and 21% of tetrahydrofuran aldehyde **371** [417]. Saturated bicyclic endoperoxides reacted much less selectively, since epoxide formation,  $\beta$ -fragmentation, and reduction competed (see also Sect. 3.5) [418]. A further fragmentation/recyclization mode was reported for a dihydropyridazine fused cycloheptatriene-derived endoperoxide [419].

O'Shea and Foote investigated in parallel to studies by Noyori (see Sect. 3.5) the cleavage of monocyclic 3,6-dihydro-1,2-dioxines **190** catalyzed by 5–10 mol% of CoTPP **326a** or (salen)Co **274**, which gave furan derivatives **193** (Fig. 87) [420]. Square-planar low-spin cobalt complexes are a prerequisite for successful conversion. These reactions proceed similarly to the corresponding ruthenium-catalyzed reactions via 1,5-hydrogen transfer leading to (*Z*)-4-hydroxyenones **192**, which cyclize to give furans **193** in almost quantitative yield (cf. Fig. 47).



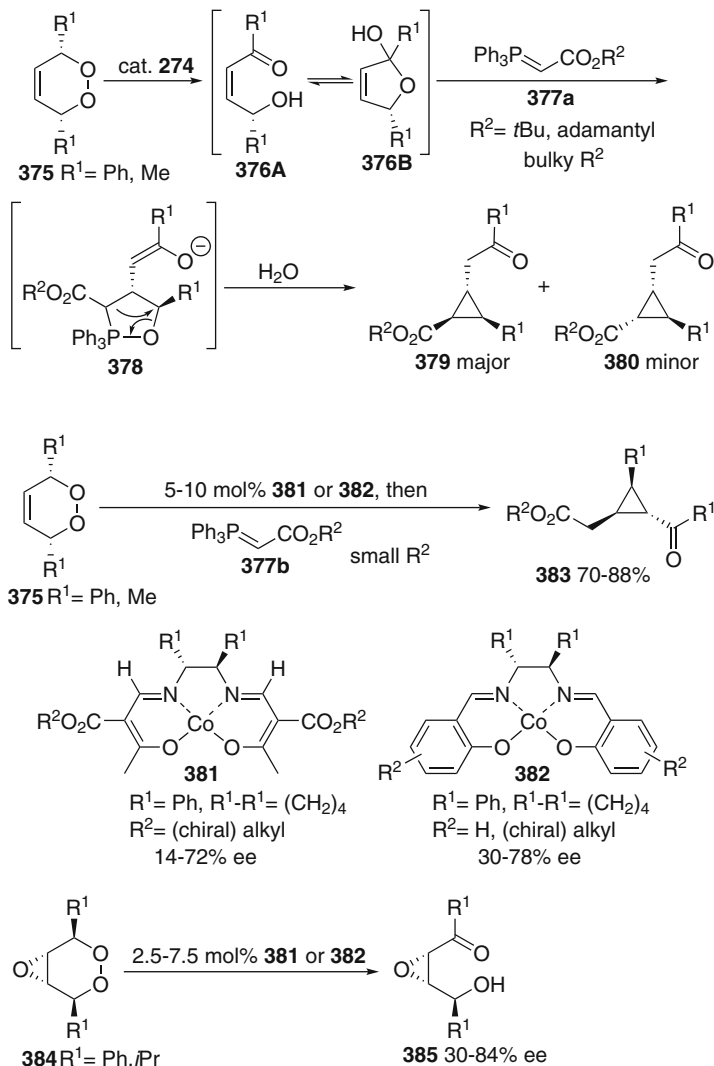
**Fig. 87** Furans by cobalt-catalyzed cleavage/recyclization of endoperoxides



**Fig. 88** Asymmetric reductive ring opening of bicyclic endoperoxide **368c**

Scheffold et al. demonstrated that 0.5 mol% of cobalt(III) complexes (*R,R*)-**372** after in situ reduction to the corresponding Co(II) complex by vitamin C **373**, catalyzed the reductive ring opening of parent dioxabicyclo[2.2.2]octene **368c** to 4-hydroxy-2-cyclohexenone **374** with up to 20% ee (Fig. 88) [421]. Özer and colleagues subjected **368c** annulated with a pyridazine unit to Co(TPP) **326a** and isolated a product analogous to **374** [419].

Taylor and coworkers used (salen)Co(II) complex **274** to catalyze a tandem sequence of reductive peroxide cleavage/1,5-hydrogen transfer/phosphorus ylide conjugate addition/intramolecular  $S_N$  reactions starting from 1,2-dioxines **375** (Fig. 89) [422–424]. Initial reductive cleavage of **375** by the Co(II) complex generates (*Z*)-4-hydroxyenone **376A**, which is in equilibrium with its hemiketal **376B**. This mixture undergoes a conjugate addition of the phosphorus ylide **377a** bearing a bulky ester group, followed by formation of phosphaoxacyclopentane **378**. Phosphine oxide elimination yields cyclopropanes **379** and **380** in 67–91% yield. *meso*-3,6-Dihydro-1,2-dioxines **375** can be desymmetrized using 5 mol% of chiral (salen)Co or ( $\beta$ -ketiminato)Co complexes **381** or **382** [425]. Enantiomerically enriched **376A/376B** mixtures were formed, which transform to alternative cyclopropanes **383** by use of a phosphorus ylide bearing sterically non-demanding ester groups in 70–88% yield and 14–78% ee. The authors extended this methodology to racemic diastereoselective and asymmetric tandem ring opening/Michael addition/lactonization reactions affording butyrolactones in 56–97% yield and 77–82% ee. The induction remains unclear since the structure and assigned configuration of used **381** are contradictory [426].



**Fig. 89** Cobalt-catalyzed reductive ring opening reactions of monocyclic endoperoxides

The same ring opening methodology was also applied to 4,5-epoxy-1,2-dioxanes **384** using 2.5–7.5 mol% of (salen)Co(II) complexes **381** or **382**. Yields of 77–96% for 2,3-epoxy-4-hydroxy ketones **385**, which exist in equilibrium with their cyclic hemiacetals, were obtained [427]. The desymmetrization succeeded with 30–84% ee. Analogous reductive ring opening reactions of 4,5-dihydroxy-1,2-dioxanes gave 2,3,4-trihydroxy ketones with mixed results [428]. Some substrates reacted in excellent yields, others decomposed under the reaction conditions. When the diol function was protected as an acetonide or carbonate, the reaction provided the products, which

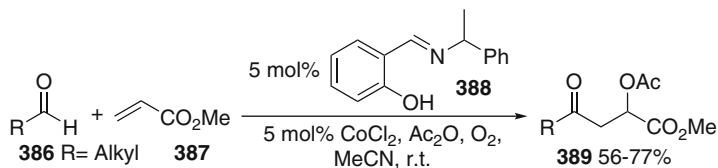
were isolated as an anomeric mixture of furanoses in yields of 80–99%. Attempted desymmetrization resulted only in 20–26% ee. 3,6-Unsymmetrically disubstituted 1,2-dioxines coordinate the cobalt catalyst preferentially at the least hindered position [429]. Thus, the alkoxy radical is generated at the more hindered position. For 6-unsubstituted dioxines 4-hydroxyenals arise with approximately 2–>20:1 regioselectivity, while 3,6-disubstituted 1,2-dioxines afford the isomeric products with less selectivity.

Isoxazolines are related to 1,2-dioxines in that they are also prone to reductive ring opening. Ishikawa and colleagues found that *N*-benzylisoxazolines form 2-acylaziridines by SET reduction/ring opening and recyclization of the resulting aminyl radical to the cobalt enolate [430].

### 5.9 Co(II)–Co(III) Catalysis: Radical Additions

Cobalt complexes derived from Schiff bases **388** catalyzed the hydroxyacylation of electron-deficient alkenes (Fig. 90) [431, 432]. Thus, methyl acrylate **387** reacted with aliphatic aldehydes **386** in the presence of 5 mol% of the in situ generated catalyst, molecular oxygen, and acetic anhydride to 2-acyloxy-4-oxoesters **389** in 56–77% yield. When acetic anhydride was omitted, the yields of products were lower and mixtures of the free hydroxy compounds and acylated compounds resulting from Tishchenko reactions were obtained. Electron-rich alkenes did not undergo the transformation, since the addition of the acyl radical is much slower. The acylcobalt species inserts oxygen instead and acts as an epoxidation catalyst.

Ishii and coworkers subsequently reported acetylation reactions of adamantane **390** by diacetyl **391** catalyzed by 0.0025 mol% Co(OAc)<sub>2</sub> in acetic acid in an oxygen atmosphere (Fig. 91) [433]. The reaction gave a mixture of mono- and diacetyladamantane **392** and **393** in 51 and 14% yield, respectively. Oxygenated adamantane **394** was formed as a side product. The cobalt catalyst is supposed to act only as an initiator in this reaction, since no reaction took place with cobalt(III) in the absence or presence of oxygen or by Co(II) in the absence of oxygen. No reaction occurred also in the absence of **391** showing that the Co(II)–O<sub>2</sub> system is unable to abstract hydrogen atoms from **390**. Increasing the amount of Co(OAc)<sub>2</sub> up to 0.5 mol% did not lead to a better yield, but decreased it. The reaction is thought to proceed by initial formation of a Co(III)–O<sub>2</sub> complex **395** from Co(OAc)<sub>2</sub> and



**Fig. 90** Cobalt-catalyzed hydroxyacylation reactions of acrylates



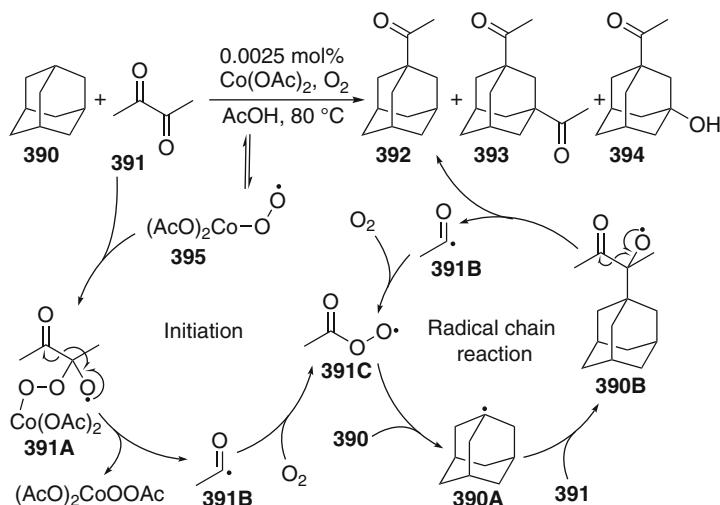


Fig. 91 Co(II)-catalyzed acetylation of adamantane

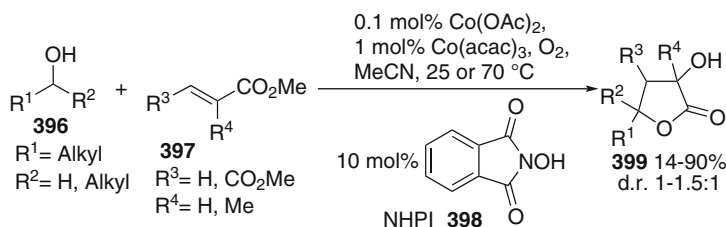
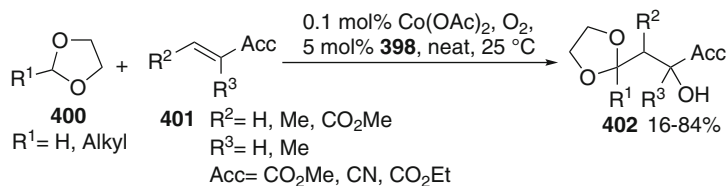


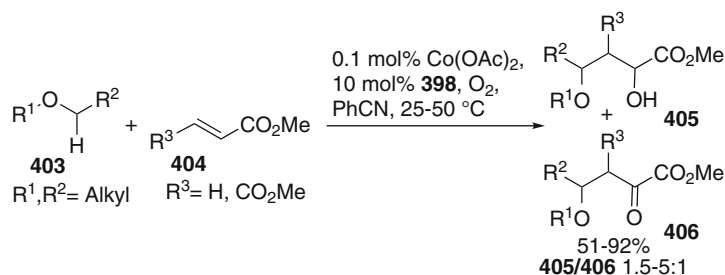
Fig. 92 Cobalt(II)/NHPI-cocatalyzed ketyl radical additions

oxygen. This species may add to **391** triggering its fragmentation to cobalt(III) and acetyl radical **391B**. This radical is known to couple almost diffusion-controlled with oxygen. The resulting acetylperoxy radical **391C** is activated to abstract a hydrogen atom from the tertiary position of **390** giving adamantyl radical **390A**, which adds to excess **391**. The alkoxy radical **390B** thus formed fragments easily to chain-carrying **391B** and product **392**. Side product **393** forms similarly from **392**.

In parallel the cocatalysis of cobalt compounds with *N*-hydroxyphthalimide **398** was developed extensively for oxidative radical reactions [434]. Ishii and colleagues showed that these conditions can be used in radical additions (Fig. 92). Ketyl radicals generated by hydrogen abstraction from secondary alcohols **396** add to  $\alpha,\beta$ -unsaturated esters **397** affording 2,4-dihydroxy esters, which cyclized to lactones **399** under the reactions conditions [435]. Using 0.1 mol% of Co(OAc)<sub>2</sub>, 1 mol% of Co(acac)<sub>3</sub>, and 10 mol% of **398** under 1 atm of oxygen, the cyclic products **399** were isolated in 14–90% yield. As observed for similar reactions, Co(III) alone needs an induction period (see below).



**Fig. 93** 2-Hydroxy-4-oxo carboxylic acid derivatives by Co/NHPI-catalyzed radical additions



**Fig. 94** Radical addition reactions of ethers to  $\alpha,\beta$ -unsaturated carbonyl compounds

Similar reactions were performed with dioxolanes **400** bearing abstractable hydrogen atoms in the 2-position (Fig. 93) [436]. Radical addition to acceptors **401** and oxygenation gave protected 2-hydroxy-4-oxo carbonyl compounds **402** in 16–84% yield. For these substrates a catalyst system of 0.1 mol%  $\text{Co(OAc)}_2$  and 5 mol% **398** proved to be sufficient to achieve good yields. Low yields were only obtained with  $\beta$ -alkyl-substituted substrates **401**. Methyl vinyl ketone undergoes a fragmentation under the reaction conditions.

Ethers **403** are likewise reactive under these conditions (Fig. 94). Mixtures of  $\alpha$ -hydroxy esters **405** and  $\alpha$ -keto esters **406** resulted from **404** in 51–92% yield using 0.1 mol%  $\text{Co(OAc)}_2$  and 10 mol% of **398** [437]. Ethers having secondary and tertiary hydrogen atoms react selectively at the tertiary position. When methacrolein was applied, the  $\alpha$ -hydroperoxy aldehyde formed initially underwent a fragmentation of the formyl group under the reaction conditions resulting in a ketone (not shown).

Hydrocarbons **407** can be used as precursors in hydroxyalkylation reactions of  $\alpha,\beta$ -unsaturated carbonyl compounds **408** in the presence of molecular oxygen (Fig. 95) [438]. The reactions are catalyzed by 0.3–1 mol%  $\text{Co(acac)}_3$  and 30 mol% **398**. Alkylated  $\alpha$ -hydroxy carbonyl compounds **409** and  $\alpha$ -keto carbonyl compounds **410** were obtained in 42–98% yield in a 1–100:1 ratio. The reactions showed a considerable induction period.  $\text{Co(acac)}_2$ , in contrast, initiated the reaction very quickly, but conversion soon ceased. The success using the unreactive Co(III) complex consists of gradual reduction to catalytically active Co(II).

Even the addition of silyl radicals derived from silanes **411** to  $\alpha,\beta$ -unsaturated carbonyl compounds **401** leading to  $\beta$ -silyl esters or nitriles **412** can be promoted under similar conditions in 42–74% yield (Fig. 96) [439].

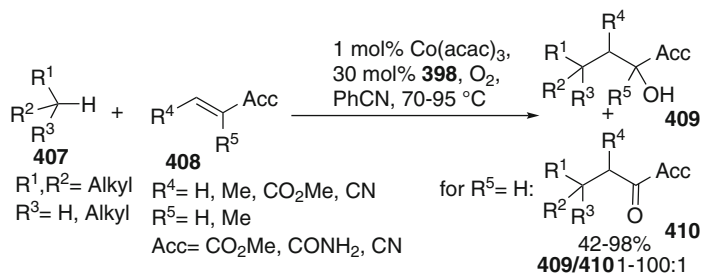


Fig. 95 Cobalt/NHPI-catalyzed addition of hydrocarbons to  $\alpha,\beta$ -unsaturated carbonyl compounds

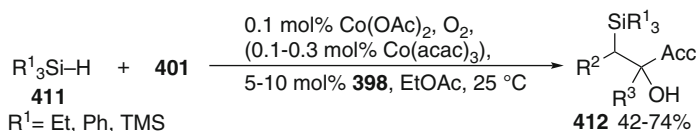


Fig. 96 Oxygenative silylation of  $\alpha,\beta$ -unsaturated carbonyl compounds

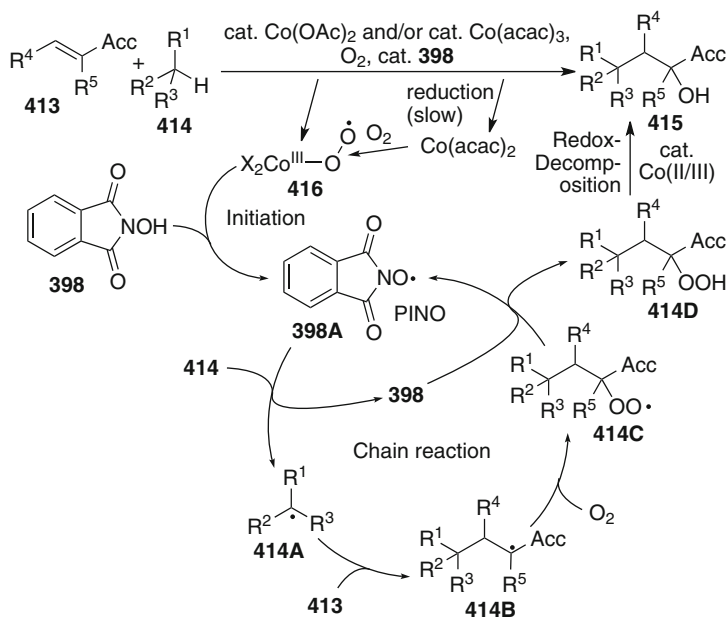


Fig. 97 Reaction course of cobalt-catalyzed radical addition/oxygenation reactions

The reactions are thought to proceed by initial formation of a cobalt(III)-oxygen complex **416** from  $\text{CoX}_2$  and  $\text{O}_2$  (Fig. 97). The induction period observed in many reactions involving  $\text{Co(acac)}_3$  can be traced to its initial slow reduction to  $\text{Co(acac)}_2$ . Complex **416** initiates the radical reaction by hydrogen abstraction

from NHPI **398** to generate phthalimide *N*-oxyl (PINO) **398A**. This oxygen-centered radical is responsible for the subsequent hydrogen abstraction reaction from substrates **414**. The resulting electron-rich alkyl radical **414A** adds to the radical acceptor **413**. The adduct radical **414B** couples with oxygen to peroxy radical **414C**. The latter is reduced by catalytic redox decomposition by the Co(II)/Co(III) couple to the product alcohols **415** [440, 441]. Not surprisingly, the diastereoselectivity of oxygen trapping is low. Further reaction steps, such as lactonization to compounds **399**, may follow the radical reaction. The formation of the  $\alpha$ -keto esters **406** or **410** can be explained by a hydrogen abstraction reaction from **405** or **409** by PINO **398A** and further oxidation. In a number of other applications the catalytic system Co(II)/O<sub>2</sub> is applied as an initiator for *N*-hydroxyphthalimide-catalyzed oxidation reactions [434]. Since cobalt is not otherwise interacting in the radical process, these reactions are not covered here.

### 5.10 Co(II)–Co(III) Catalysis: Radical Cyclizations

Mukaiyama et al. transformed the Co(II)-catalyzed hydrofunctionalizations (see Sect. 5.7) to intramolecular oxidative alkoxy radical cyclizations by omission of the silane (Fig. 98). 4-Penten-1-ols **417** (R<sup>2</sup>=H) cyclized in the presence of 20 mol%

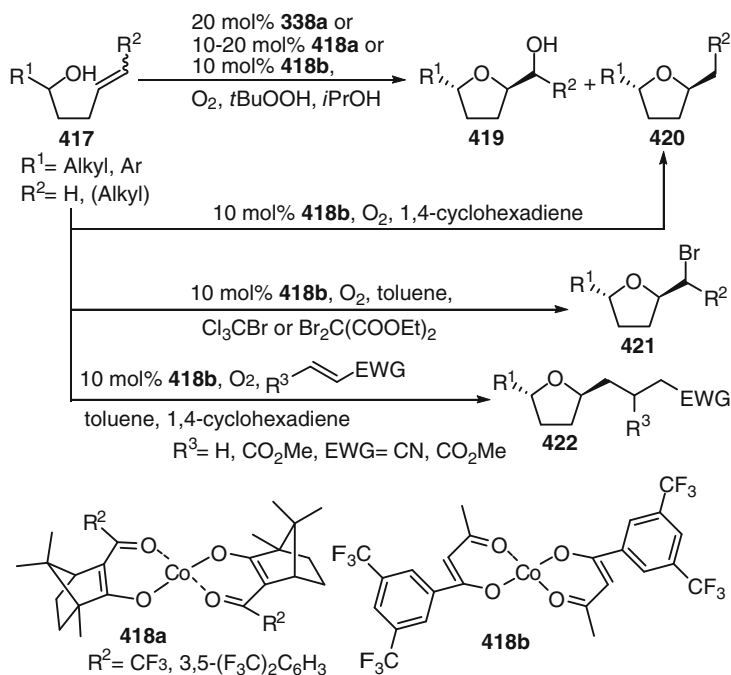


Fig. 98 Cobalt-catalyzed alkoxy radical cyclization reactions

Co(modp)<sub>2</sub> **338a**, oxygen, *tert*-butyl hydroperoxide, and isopropanol to 2-hydroxymethyltetrahydrofurans **419** in 53–79% yield with exclusive *trans*-selectivity [442]. Reduced tetrahydrofurans **420** were isolated as a side product. This method was applied in total syntheses of annonaceous acetogenins [443], such as gigantetrocin A [444, 445], asimilobin [446, 447], mucocin [448, 449], or bullatacin [450], as well as of the algal natural product aplysiallene [451].

Hartung used 10 mol% of cobalt complexes bearing 1,3-diketone ligands **418** to catalyze oxidative radical 5-exo cyclizations of 1-substituted 4-pentenols **417** (R<sup>2</sup>=H) in the presence of oxygen and isopropanol as the solvent. 2-(Hydroxymethyl)tetrahydrofurans **419** were obtained in 56–76% yield as pure *trans*-isomers [452]. Side products coformed were **420**, acetone, and minor amounts of overoxidized products resulting from further reactions with **418**. When substrates **417** (R<sup>2</sup>=alkyl) were used, low to moderate yields resulted [453]. The reactions gave higher yields of reduced product **420** when cyclohexadiene was used as an external radical trap. With disubstituted **417** (R<sup>1</sup>, R<sup>2</sup>=alkyl) products **419** were isolated only in low yield; dioxygenated acyclic materials were formed instead [452]. The cobalt peroxide probably acts as a better epoxidation reagent with these more electron-rich substrates. Hartung and coworkers later performed similar cyclizations in the presence of radical trapping agents other than oxygen with good chemo- and stereoselectivity [454]. 4-Pentenols cyclized in the presence of 1–30 mol% of cobalt(II) complex **418b** in 70–88% yield to 2-methyltetrahydrofurans **420** using 1,4-cyclohexadiene as the radical trap. Bromotrichloromethane provided bromomethyltetrahydrofurans **421** in 22–96% yield. A large excess of radical trapping agent was, however, necessary to avoid competing oxygenation. The cyclizations generally occurred with high diastereoselectivity. A cyclopropyl-terminated alkene afforded the ring opened product exclusively, thus supporting the radical cyclization course (cf. Part 1, Fig. 8). Even tandem radical cyclization/addition reactions of **417** with acrylonitrile or dimethyl fumarate were possible furnishing functionalized alkyltetrahydrofurans **422** in 41 and 51% yield. Pagenkopf and coworkers introduced the complex Co(nmp)<sub>2</sub> **338b** [455]. It catalyzed the oxidative cyclizations in good yield and has the advantage that workup and product isolation were facilitated by aqueous acid treatment of the reaction mixture or *N*-methylation of the catalyst after the reaction.

The cyclization reactions of 4-pentenols **417** were proposed to proceed via initial formation of cobalt peroxy complex **423A** from precatalysts **423** (see also Sect. 5.9) (Fig. 99). This complex coordinates the substrates **417** forming valence tautomeric complexes **417A/B**. Intramolecular hydrogen transfer generates valence tautomeric alkoxy radical/alkoxide-radical cation pair **417C/D**. Cyclization provides an alkyl radical, which may exist either complexed (**417E**) or free (**417F**). From both species compounds **419–422** are formed by oxygenation, reduction, bromine transfer, or addition reactions. The active catalyst is regenerated by sequential reduction of the final hydroperoxycobalt(III) complex by isopropanol giving acetone, water, and cobalt(III) hydroxide **423B**. Its further reduction by isopropanol leads to starting cobalt(II) complex **423**.

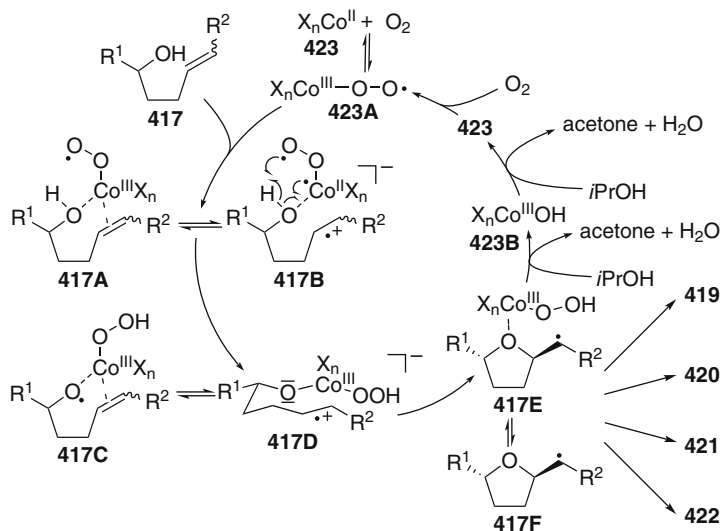


Fig. 99 Catalytic cycle of the cobalt-catalyzed cyclization to tetrahydrofurans

## 5.11 Miscellaneous

A reduction of chlorocyclopropanes by  $\text{CoCl}_2(\text{dppe})$  was reported; however, radical involvement was not proven [74]. van der Donk and colleagues described radical dimerization reactions catalyzed by vitamin B<sub>12</sub> [456]. Carbonylative ring expansion reactions of chiral oxazolines to 1,4-dihydro-1,3-oxazin-6-ones with preferential inversion of configuration using 5 mol% of a  $\text{Co}_2(\text{CO})_8/\text{AIBN}$  catalytic system were found by Jia and coworkers. Radical intermediates were proposed to be involved [457, 458]. Scheffold and coworkers demonstrated that epoxides undergo asymmetric ring opening catalyzed by 1 mol% hydroxycobalamine hydrochloride **247** [459]. The reaction gave a mixture of enantiomerically enriched 2-cyclopentanol and cyclopentanone in addition to cyclopentene. The reaction proceeds by nucleophilic opening of the epoxide by the reduced Co(I) and subsequent homolysis. Aziridines [460] and cyclopropanes [461] also undergo ring opening by cobalamine(I) **247**. Recently, a direct coupling of aryl iodides with arenes catalyzed by 10 mol%  $\text{Co}(\text{acac})_3$  and DMEDA or phenanthroline was reported to give 69–71% biaryls. The mechanism is probably similar to the corresponding iron-catalyzed protocol (cf. Fig. 18) [462]. Kharasch addition reactions applying (amine)Co(II) were reported. The reaction proceeds well for terminal alkenes, but led to predominant telomerization with typical vinyl monomers [463].

## 6 Rhodium-Catalyzed Radical Reactions

Rhodium catalysis is very well developed with respect to its two-electron catalysis [464]. Applications involving radicals are rather rare. Similar to the cobalt-catalyzed processes, the reductive cleavage of endoperoxides **424** proceeds with rhodium(I) catalysts. Hagenbuch and Vogel reported the formation of bicyclic hydroxymethyl enals **425** catalyzed by 3.8 mol%  $[\text{Rh}(\text{CO})_2\text{Cl}]_2$  (Fig. 100) [465, 466].

Sakakura and colleagues investigated the photochemical carbonylation of linear hydrocarbons **426** catalyzed by  $[\text{Rh}(\text{CO})(\text{PMe}_3)_2\text{Cl}]$  and found a high selectivity for the formation of linear aldehydes **427** (Fig. 101) [467]. The applied light wavelength was very important. Irradiation with near-UV light at ca 365 nm led to selective formation of the aldehyde. A specific radical involvement was, however, not discussed by the authors. A later mechanistic study reported that this photocarbonylation occurs by at least two pathways. The major linear aldehyde is formed by a photochemical process, while the minor branched aldehyde was produced by a competing radical process [468]. The synthesis of acetaldehyde by methane photocarbonylation under similar conditions was also accomplished recently [469].

Boese and Goldman investigated the photocarbonylation of cyclohexane **105** cocatalyzed by aromatic ketones, such as acetophenone or benzophenone, and  $d^8$  metal complexes, such as  $[\text{Rh}(\text{CO})(\text{PR}_3)_2\text{Cl}]$  (cf. Fig. 27) [170]. The formation of cyclohexancarbaldehyde **108** was rationalized similarly as the process catalyzed by a ruthenium complex (see Sect. 3.1). The ketone catalyst abstracts a hydrogen atom from the substrate after photoexcitation by  $>340\text{-nm}$  light. The resulting alkyl radical either attacks the bound carbonyl ligand of the Rh(I) complex leading to an (acyl)rhodium(II) complex or adds first to the metal center generating an alkyrhodium(II) intermediate, which is subject to migratory insertion of a CO ligand. According to a computational investigation both radical addition pathways are energetically feasible for this 16e complex [171]. The resulting Rh-centered radical abstracts a hydrogen atom from the initially formed ketyl radical leading to rhodium(III) hydride complex. Reductive elimination regenerates the Rh(I) catalyst and liberates the aldehyde **108**. Analogous photocarbonylations of arenes do not occur by a radical mechanism [470].

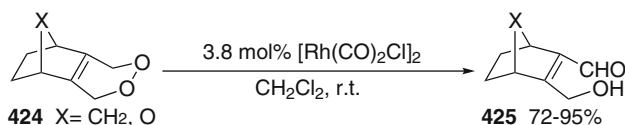


Fig. 100 Rh(I)-catalyzed cleavage of endoperoxides

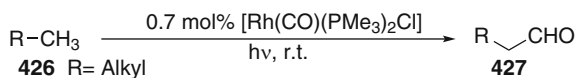
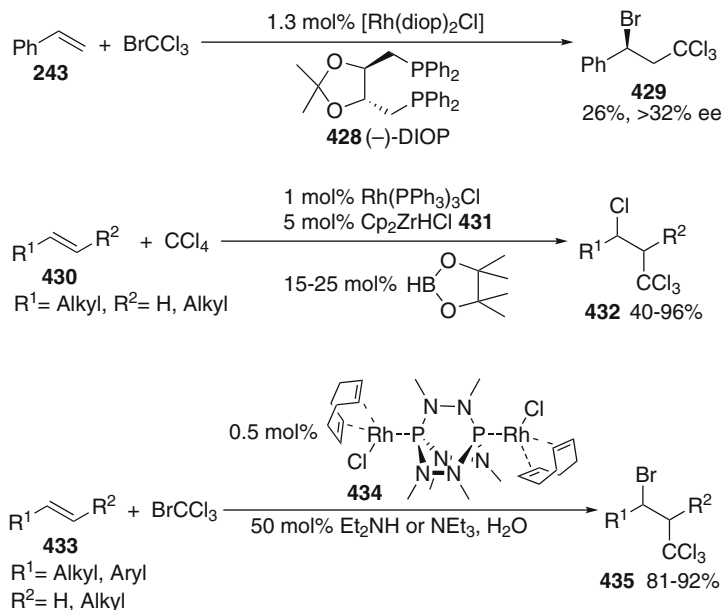


Fig. 101 Rhodium-catalyzed photocarbonylation of hydrocarbons to aldehydes



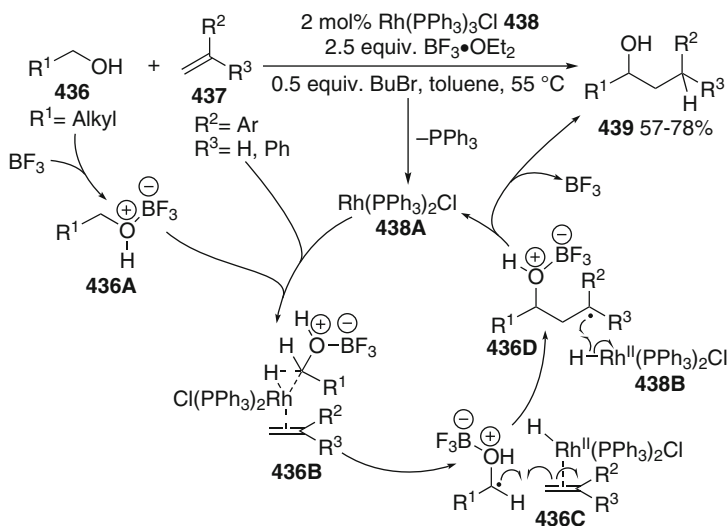
**Fig. 102** Rhodium(I)-catalyzed Kharasch addition reactions

In 1981 Murai and colleagues reported the first asymmetric Rh-catalyzed Kharasch additions of bromotrichloromethane to styrene **243** (Fig. 102). Using 1.3 mol% (–)-diopRhCl **428**, 26% of (*S*)-1-bromo-3,3,3-trichloro-1-phenylpropane **429** was isolated having an ee value of 32% [471]. Based on these observations Cable and colleagues conducted Kharasch additions of  $\text{BrCCl}_3$  to styrene [472]. They isolated a product resulting from oxidative addition of the  $[\text{Rh}(\text{CO})(\text{PMe}_3)_2\text{Cl}]$  catalyst to  $\text{Cl}_3\text{CBr}$ . The resulting Rh(III) complex also catalyzed the addition. Crossover experiments using  $\text{CCl}_4$  and  $\text{CBr}_4$  did not indicate scrambling and the reaction with 1,5-cyclooctadiene did not lead to transannular cyclization (cf. Part 1, Fig. 38), but gave the simple addition product. Therefore, a two-electron mechanism was proposed. However, this evidence does not exclude a radical mechanism rigorously, since the reactivity difference of  $\text{CCl}_4$  and  $\text{CBr}_4$  is significant and ligand transfer may be faster than transannular 5-exo cyclization for cyclooctadiene.

Pereira and Srebnik added tetrachloromethane to alkenes **430** catalyzed by the Wilkinson complex and Schwartz reagent **431** mediated by pinacolborane [473]. The mechanism of the reaction leading to **432** was proposed not to involve radicals, which was supported by failure of inhibition by galvinoxyl or BHT.

Recently, Severin reported the Kharasch addition of several mixed rhodium(I)–ruthenium(II) and rhodium(III)–ruthenium(II) catalysts (see Part 3, Sect. 8.5). It was also demonstrated that 0.5 mol% of dinuclear rhodium(I) complex **434** having a bridging THDP ligand is an active catalyst for the Kharasch addition of  $\text{BrCCl}_3$  to simple olefins **433** in water [228]. The yields of adducts **435** ranged from 81 to 92%.





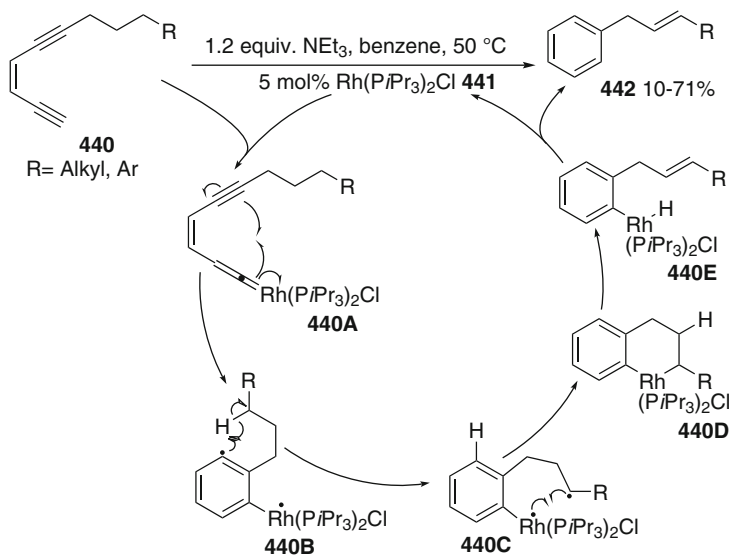
**Fig. 103** Radical additions of alcohols to styrenes catalyzed by the Wilkinson complex **438**

The addition of substoichiometric amounts of amines as promoters proved to be useful. The catalyst can be applied in additions to internal alkenes and styrenes. The simpler [Rh(cod)Cl]<sub>2</sub> complex displayed a considerably lower activity under otherwise identical conditions.

Shi et al. found that primary alcohols **436** add to arylalkenes **437** using 2 mol% of the Wilkinson complex **438** as the catalyst and boron trifluoride as a Lewis acid activator (Fig. 103) [474]. Butyl bromide proved to be suitable as an additive to prevent competitive Friedel–Crafts alkylation reactions. Crossover experiments using  $\alpha$ -deuterated and non-deuterated alcohols led to mixtures of compounds proving that dissociation of an intermediate generated from the alcohol occurred. Radical scavengers like TEMPO or benzoquinone inhibited the reaction. It was proposed that the initial step is a C–H insertion of the complex generated from coordinatively unsaturated **438A** and **437** into the BF<sub>3</sub>-complexed alcohol **436A** via **436B**. Homolysis of the resulting Rh(III) complex (not shown) to a Rh(II) complex-ketyl radical pair **436C**, which may be caged, takes place subsequently. Radical addition to the coordinated alkene ligand followed by dissociation and hydrogen transfer from the rhodium(II) hydride complex **438B** to benzylic radical **436D** complete the catalytic cycle affording 3-aryl alcohols **439** in 57–78% yield. The radical addition to the alkene ligand of **436C** may alternatively result in an alkylrhodium(III) hydride complex, from which reductive elimination occurs (not shown).

A reverse mode of radical addition reactions is also possible, in which a ligand-centered radical would add to a radical acceptor [475]. Catalytic applications of such a process are so far missing.

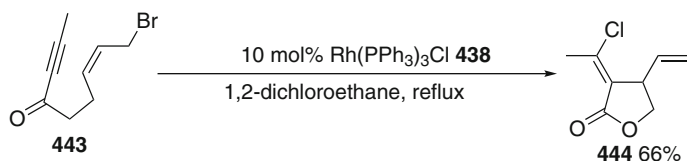
The more coordinatively unsaturated Rh(I) complex **441** was shown to be a catalyst in tandem metalla Myers–Saito cyclization/hydrogen transfer sequences of



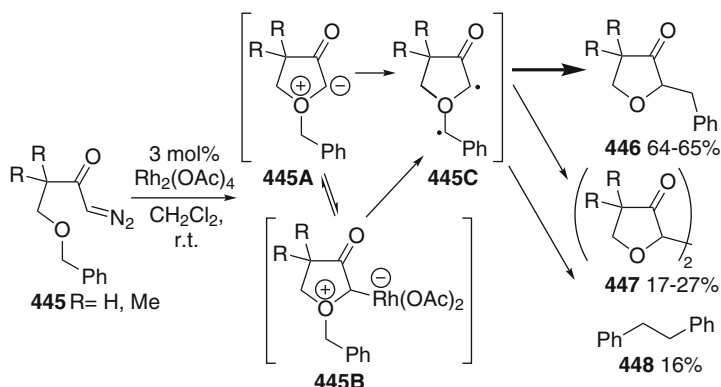
**Fig. 104** Rhodium-catalyzed Myers–Saito cyclization reactions

enediynes **440** providing allylarenes **442** in 10–71% yield (Fig. 104) [476, 477]. Compounds **440**, typically substrates for Bergman cyclization reactions (selected reviews [478, 479]), are transformed here by coupling to the catalyst **441** to (vinylidene)rhodium complexes **440A**, which represent metallacyclopentadienes. They cycloisomerize under the reaction conditions to aryl-rhodium biradical species **440B**. The highly reactive aryl radical stabilized by 1,5-, 1,6-, or 1,7-hydrogen transfer resulting in alkyl-rhodium 1,6- or 1,7-biradical pairs **440C**. Intramolecular coupling affords the rhodacycles **440D**. The substituent R determines the further fate. If R ≠ H, β-hydride elimination followed by reductive elimination prevails giving **442**. If R = H, annulated arenes were formed by reductive elimination from **440D** (not shown).

Wang and colleagues recently discovered rhodium-catalyzed halogen exchange processes during halogenative cycloisomerization reactions of (*Z*)-4-bromocrotyl butynoates **443** (Fig. 105) [480]. When this reaction was performed in 1,2-dichloroethane as the solvent, 3-(1-chloroethylidene)-4-vinylbutyrolactone **444** was formed as the product instead of the expected bromo compound. A reverse result was obtained when the corresponding allylic chloride was subjected to 10 mol% of the Wilkinson complex **438** and excess of 3-(phenoxy)propyl bromide. In control experiments it was shown that simple allylic chlorides or bromides undergo the halogen exchange quickly under identical conditions; thus it occurs prior to cycloisomerization to **444**. This unexpected reaction course was rationalized by SET oxidation of the Wilkinson catalyst and formation of an allylic radical from the allylic halide. The Rh(II)-allyl radical pair couples and the resulting mixed chloride-bromide rhodium complex is subject to reductive elimination of the allylic



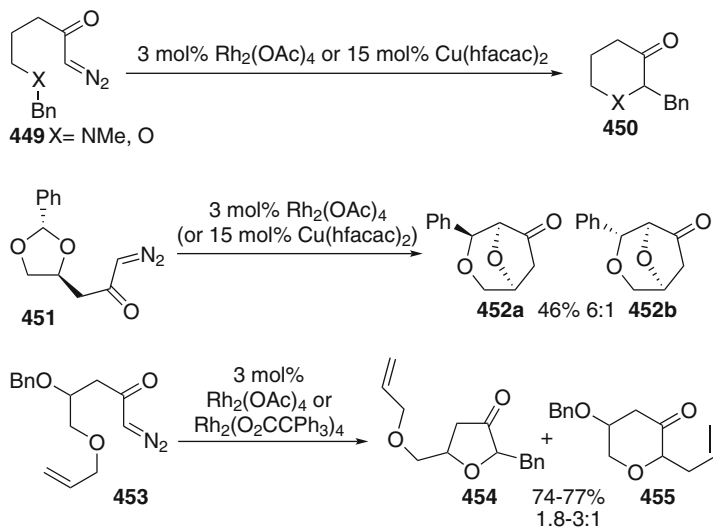
**Fig. 105** Rh-catalyzed halogen exchange/cycloisomerization sequence



**Fig. 106** Rhodium(II)-catalyzed oxonium ylide rearrangements of diazoketones **445**

chloride instead of the expected bromide. A parallel similar halogen exchange with solvent molecules drives the halogen content in the allylic halide toward that in the solvent. Control experiments using 4-hydroxyTEMPO showed complete inhibition of the reaction. Since this may not be conclusive (see Part 1, Sect. 2.5), 2-phenylcyclopropylmethyl bromide was subjected to the reaction conditions (cf. Part 1, Fig. 8). 1-Phenyl-1,3-butadiene was the exclusive product suggesting a radical ring opening of the reductively generated cyclopropylmethyl radical. Coupling of the resulting benzylic radical with Rh(II) and  $\beta$ -hydride elimination complete the reaction. Since cyclopropylmethylrhodium complexes are also known to undergo ring opening in a concerted fashion, providing 2-phenylbutadienes (review [481–484]), the product 1-phenyl-1,3-butadiene supports a radical mechanism.

While [2,3]-onium ylide rearrangements proceed most often by concerted pathways (review [485]), [1,2]-onium ylide rearrangements (Stevens rearrangements) often involve radical intermediates (recent reviews [486, 487]). Benzyl ether-substituted diazoketone **445** underwent a  $[\text{Rh}(\text{OAc})_2]_2$ -catalyzed formation of oxonium ylide **445A**/[1,2]-shift leading to tetrahydrofuran-3-ones **446** as the major product (Fig. 106) [488]. The isolation of dimers **447** and **448** suggests a radical pair **445C** formed from either free ylide **445A** or bound oxonium rhodate **445B**, which suffers mostly an in-cage collapse to product **446**. Out of cage diffusion led to **447** and **448**. West and coworkers subsequently demonstrated that diazoketones bearing



**Fig. 107** Onium ylide rearrangements catalyzed by rhodium(II) carboxylates

ether functions at larger distance were also subject to oxonium ylide formation/[1,2]-shift providing medium-sized bicyclic ethers [489]. In a substrate amenable to [1,2]- and [2,3]-rearrangements, the product from the latter process was obtained exclusively.

Studies aimed at the comparison of Rh(II) and Cu(II)-catalyzed onium ylide reactions of diazoketones **449** using 3 mol% of the former and 15 mol% of the latter led to the conclusion that the copper-catalyzed process provides the better yields and selectivities for [1,2]-rearrangement products **450** (Fig. 107) [490, 491]. In the rhodium-catalyzed process, 1,5-C–H insertion may compete. The diastereoselectivity with both catalysts is in some cases similar, in others the Rh-catalyzed process is more selective. Analogous reactions of acetal **451** provided a mixture of stereoisomers **452a** and **452b** at the benzylidene position, supporting a stepwise process. The authors proposed that the involved intermediate was either a 1,6-biradical or the corresponding ion pair.

Competition experiments with substrates **453** bearing different ether substituents in  $\beta$ - and  $\gamma$ -position showed that the formation of five-membered oxonium ylides leading to tetrahydrofuran-3-ones **454** is preferred over six-membered providing tetrahydropyran-3-ones **455** with Rh(II)-catalysts [492]. Copper catalysts showed a contrasting behavior (see Part 3, Sect. 5.11). In an attempt to access the zaragozic acid core by an oxonium ylide [1,2]-rearrangement, a selective reaction was observed using  $\text{Rh}_2(\text{OAc})_4$ , while the analogous Cu-catalyzed process was less selective [493]. Asymmetric rhodium-catalyzed Stevens-type rearrangements of allylic oxonium ylides having a different substitution pattern in the 3-position occurred in competition to a preferred [2,3] rearrangement as the degree of substitution in the 3-position increased. A moderate enantioselectivity was observed for the [1,2] rearrangement product, suggesting the collapse of the radical pair in the

solvent cage [494]. It must be stated here that for most of the examples biradical or metal assisted ion pair-based mechanisms may operate. No systematic studies distinguishing these pathways unambiguously have been conducted so far.

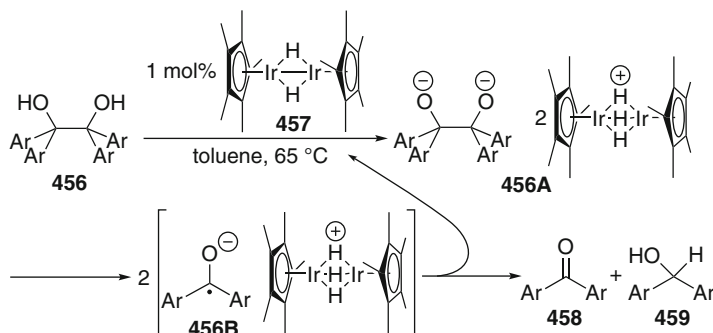
[Rh(OAc)<sub>2</sub>]<sub>2</sub> was shown to catalyze the addition of aldehydes to azodicarboxylates [495]. The products of a hydroacylation *N*-acylhydrazines were formed in 45–97% yield using 1.5–2 mol% of the catalyst. The reaction was inhibited by 10 mol% of the radical scavenger 4,4'-dithiobis(2,6-di-*tert*-butylphenol); a catalytic cycle was, however, not proposed. Recently, Zalatan and Du Bois found that 3 mol% [Rh(OAc)<sub>2</sub>]<sub>2</sub> catalyzed a Hofmann–Löffler–Freitag reaction of 3-arylpropyl sulfamates mediated by NaOCl/NaBr as the stoichiometric oxidants [496]. Cyclic sulfamates were isolated in 10–85% yield. The reaction was proposed to proceed via 1,6-hydrogen transfer of an amidyl radical; the role of the catalyst remained unclear, however. The same group showed that rhodium(II)-catalyzed nitrenoid C–H insertions occur by a concerted mechanism based on the fact that Newcomb's ultrafast cyclopropane radical probes [82, 83] gave no ring-opened materials. On the other hand it was shown that radical processes initiated by SET reduction could proceed when the catalyzed concerted C–H insertion becomes slow [497].

## 7 Iridium-Catalyzed Radical Reactions

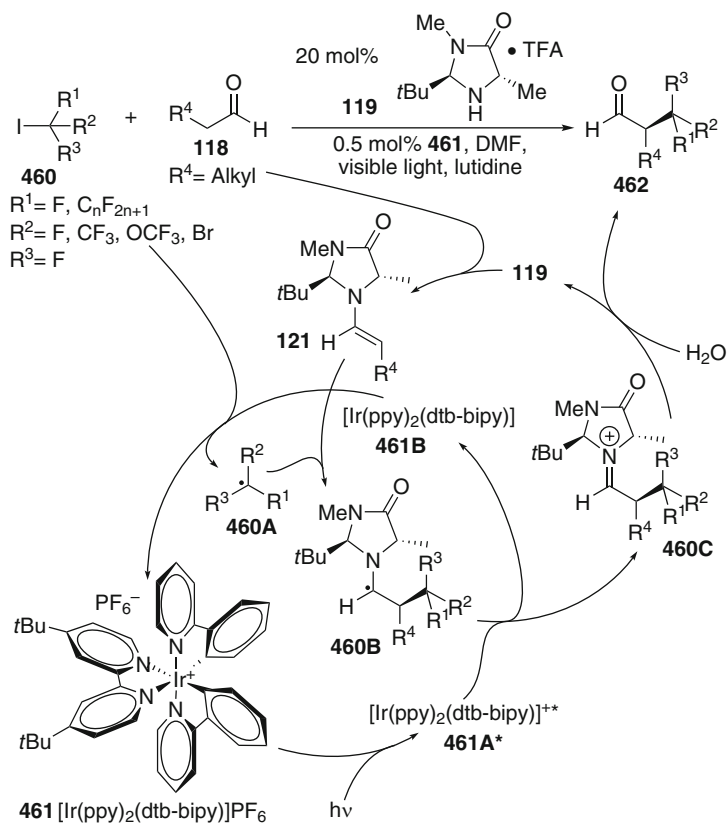
Although iridium complexes are known to generate [498, 499] and to accommodate ([475, 500]; see also [501–503]) radicals, their potential to catalyze radical processes has not been widely explored so far. Boese and Goldman investigated the photocarbonylation of cyclohexane **105** cocatalyzed by aromatic ketones, such as acetophenone or benzophenone, and d<sup>8</sup> metal complex [Ir(CO)<sub>2</sub>(PMe<sub>3</sub>)<sub>2</sub>Cl] (see Sects. 3.1 and 6) [170]. They rationalized the formation of aldehyde **108** by a hydrogen atom from the substrate after photoexcitation by >340-nm light. The resulting alkyl radical should attack the bound carbonyl ligand of the 18e Ir(I) complex leading directly to an (acyl)iridium(II) complex. This 17e metal-centered radical can abstract a hydrogen atom from initially formed ketyl radical leading to iridium(III) hydride complex, thus regenerating the ketone catalyst. Reductive elimination liberates the Ir(I) catalyst and aldehyde **108**.

It was recently demonstrated that 0.5 mol% of a dinuclear iridium(I) complex having a bridging THDP ligand and being analogous to rhodium complex **434** is an active catalyst for the Kharasch addition of BrCCl<sub>3</sub> to simple olefins **433** in water (cf. Fig. 102) [228]. The yields of addition products **435** ranged from 53 to 92%. The addition of amines as promoters in substoichiometric amounts proved to be useful. It is, however, somewhat less active than the corresponding **434**. The simpler complex [Ir(cod)Cl]<sub>2</sub> displayed a considerably lower activity under otherwise identical conditions.

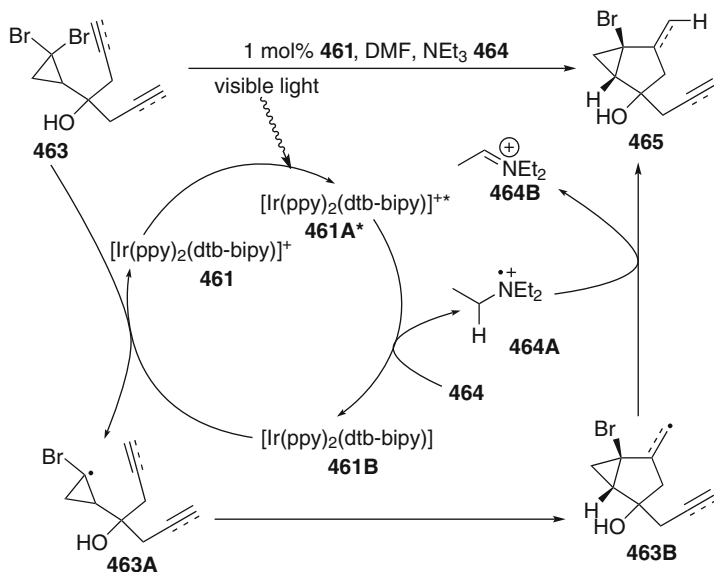
Hou and colleagues reported the cleavage of benzopinacol **456** to a mixture of benzophenone **458** and benzhydrol **459** catalyzed by 1 mol% of the iridium(II) hydride complex [Cp\*IrH]<sub>2</sub> **457** (Fig. 108) [504]. The catalyst deprotonates **456** to



**Fig. 108** Iridium-catalyzed retro-pinacol reactions



**Fig. 109** Organocatalytic photoredox-catalyzed alkylation of aldehydes



**Fig. 110** Visible light-mediated iridium-catalyzed radical cyclization reactions

ion pair **456A** triggering the retro-pinacol reaction. The resulting ketyl radical anion **456B** is subject to hydrogen transfer, proton transfer, and electron transfer leading to the products **458** and **459**.

Based on their earlier investigations into organocatalytic photoredox catalysis, MacMillan and coworkers applied iridium(III) complex  $[\text{Ir}(\text{ppy})_2(\text{dtb-bipy})]\text{PF}_6$  **461** as a photocatalyst in organocatalytic asymmetric perfluoroalkylation reactions of aldehydes **118** (Fig. 109) [505]. The reactions are thought to be initiated by photoexcitation of **461** followed by reduction of photoexcited **461A\*** by the enamine **121** or organocatalyst **119**. Ir(II) complex **461B** thus generated ( $-1.51$  V vs SCE in  $\text{CH}_3\text{CN}$ ) is able to reduce the perfluoroalkyl iodides **460** to the corresponding radicals **460A**, which add to the enamine **121** formed in situ from aldehyde **118** and imidazolidinone **119**. The radical attacks **121** *anti*-selective to the shielding methyl group resulting in  $\alpha$ -amino radical **460B**. This will be oxidized by the Ir(III) complex **461A\*** to an iminium ion **460C**. This process regenerates the photocatalyst **461B**. Iminium ion **460C** is subject to hydrolysis under the reaction conditions.  $\alpha$ -Fluoroalkylated aldehydes were obtained in 61–89% yield with an enantiomeric excess of 90–99%. Similar photoredox-catalyzed benzylation reactions of aldehydes **118** with benzylic bromides using **461** as the catalyst gave 2-substituted 3-phenylpropionaldehydes in 68–94% yield and 87–97% ee [506].

Stephenson and coworkers applied complex **461** to trigger reductive radical 5-exo cyclizations of suitably substituted bromides, such as **463**, for whom  $\text{Ru}(\text{bipy})_3\text{Cl}_2$  **110** is not a sufficiently strong reducing agent (Fig. 110) [187]. Triethylamine **464** served to reduce photoexcited  $[\text{Ir}(\text{ppy})_2(\text{dtb-bipy})]\text{PF}_6$  **461A\*** to Ir(II) species **461B**, which triggered the generation of radical **463A** by reductive electron transfer to

**463.** A subsequent 5-exo cyclization forms radical **463B**, which was proposed to stabilize to **465** by reduction by coformed aminium radical cation **464A**. However, the solvent DMF or  $\text{NEt}_3$  **464** are also viable hydrogen atom sources to reduce **463B**. The higher reduction potential of **461** compared to  $\text{Ru}(\text{bipy})_3\text{Cl}_2$  **110** thus allows one to exploit less easily reducible radical precursors. A similar principle was used to oxidize amines to iminium ions, such as **464B**, and to apply them in aza-Henry reactions with nitroalkanes [507].

## 8 Transition Metal-Catalyzed Radical Reactions According to Reaction Type

A table providing an overview over the most common reaction types that were conducted with different metals of different oxidation states can be found in Part 1, Sect. 11. This list summarizes only reaction types that are catalyzed by more than one metal.

**Acknowledgments** This manuscript is dedicated to the memory of Professor Dr. Jay K. Kochi, a pioneer of transition metal and radical chemistry. Generous funding of the work by the Institute of Organic Chemistry and Biochemistry, Academy of Sciences of the Czech Republic (Z4 055 0506), and the Grant Agency of the Czech Republic (203/09/1936) is gratefully acknowledged. I thank my group for critical reading of the manuscript and many helpful comments and discussions. I apologize to all colleagues for the omissions of their work that were necessary due to space constraints of the manuscript.

## References

1. Jahn U (2011) Radicals in transition metal catalyzed reactions? Transition metal catalyzed radical reactions? – a fruitful interplay anyway. Part 1. Radical catalysis by Group 4 – Group 7 elements. *Top Curr Chem*. doi:10.1007/128\_2011\_261
2. Plietker B (ed) (2008) Iron catalysis in organic chemistry. Wiley-VCH, Weinheim
3. Bauer EB (2008) *Curr Org Chem* 12:1341
4. Bolm C, Legros J, Le Paih J, Zani L (2004) *Chem Rev* 104:6217
5. Sawyer DT, Sobkowiak A, Matsushita T (1996) *Acc Chem Res* 29:409
6. Walling C (1998) *Acc Chem Res* 31:155
7. MacFaul PA, Wayner DDM, Ingold KU (1998) *Acc Chem Res* 31:159
8. Goldstein S, Meyerstein D (1999) *Acc Chem Res* 32:547
9. Costas M, Chen K, Que L (2000) *Coord Chem Rev* 200:517
10. Gozzo F (2001) *J Mol Cat A Chem* 171:1
11. Dunford HB (2002) *Coord Chem Rev* 233:311
12. Masarwa A, Rachmilovich-Calis S, Meyerstein N, Meyerstein D (2005) *Coord Chem Rev* 249:1937
13. Punniyamurthy T, Velusamy S, Iqbal J (2005) *Chem Rev* 105:2329
14. Punta C, Minisci F (2008) *Trends Heterocycl Chem* 13:1
15. Minisci F, Vismara E, Fontana F (1989) *Heterocycles* 28:489
16. Minisci F, Vismara E, Fontana F (1989) *J Org Chem* 54:5224
17. Csaky AG, Plumet J (2001) *Chem Soc Rev* 30:313



18. Sarhan AAO, Bolm C (2009) *Chem Soc Rev* 38:2730
19. Egami H, Katsuki T (2009) *J Am Chem Soc* 131:6082
20. Egami H, Matsumoto K, Oguma T, Kunisu T, Katsuki T (2010) *J Am Chem Soc* 132:13633
21. Cahiez G, Chaboche C, Mahuteau-Betzer F, Ahr M (2005) *Org Lett* 7:1943
22. Ortiz de Montellano PR (ed) (2005) *Cytochrome P450 structure, mechanism, and biochemistry*. Kluwer/Plenum, New York
23. Ortiz de Montellano PR (2010) *Chem Rev* 110:932
24. Munro AW, Girvan HM, McLean KJ (2007) *Nat Prod Rep* 24:585
25. Watanabe Y, Nakajima H, Ueno T (2007) *Acc Chem Res* 40:554
26. Zhang R, Newcomb M (2008) *Acc Chem Res* 41:468
27. Yin G (2010) *Coord Chem Rev* 254:1826
28. Perkins MJ (1996) *Chem Soc Rev* 25:229
29. Barton DHR (1996) *Chem Soc Rev* 25:237
30. Barton DHR (1998) *Tetrahedron* 54:5805
31. Stavropoulos P, Celenligil-Cetin R, Tapper AE (2001) *Acc Chem Res* 34:745
32. Frisch AC, Beller M (2005) *Angew Chem Int Ed* 44:674
33. Sherry BD, Fürstner A (2008) *Acc Chem Res* 41:1500
34. Rudolph A, Lautens M (2009) *Angew Chem Int Ed* 48:2656
35. Nakamura E, Yoshikai N (2010) *J Org Chem* 75:6061
36. Kharasch MS, Fields EK (1941) *J Am Chem Soc* 63:2316
37. Tamura M, Kochi J (1971) *J Am Chem Soc* 93:1487
38. Allen RB, Lawler RG, Ward HR (1973) *J Am Chem Soc* 95:1692
39. Lehr GF, Lawler RG (1984) *J Am Chem Soc* 106:4048
40. Neumann SM, Kochi JK (1975) *J Org Chem* 40:599
41. Smith RS, Kochi JK (1976) *J Org Chem* 41:502
42. Loska R, Volla CMR, Vogel P (2008) *Adv Synth Catal* 350:2859
43. Wunderlich SH, Knochel P (2009) *Angew Chem Int Ed* 48:9717
44. Nakamura M, Matsuo K, Ito S, Nakamura E (2004) *J Am Chem Soc* 126:3686
45. Martin R, Fürstner A (2004) *Angew Chem Int Ed* 43:3955
46. Fürstner A, Martin R, Krause H, Seidel G, Goddard R, Lehmann CW (2008) *J Am Chem Soc* 130:8773
47. Nagano T, Hayashi T (2004) *Org Lett* 6:1297
48. Bedford RB, Bruce DW, Frost RM, Goodby JW, Hird M (2004) *Chem Commun* 2822
49. Bedford RB, Bruce DW, Frost RM, Hird M (2005) *Chem Commun* 4161
50. Cahiez G, Habiak V, Duplais C, Moyeux A (2007) *Angew Chem Int Ed* 46:4364
51. Bedford RB, Betham M, Bruce DW, Danopoulos AA, Frost RM, Hird M (2006) *J Org Chem* 71:1104
52. Bedford RB, Betham M, Bruce DW, Davis SA, Frost RM, Hird M (2006) *Chem Commun* 1398
53. Chowdhury RR, Crane AK, Fowler C, Kwong P, Kozak CM (2008) *Chem Commun* 94
54. Cahiez G, Duplais C, Moyeux A (2007) *Org Lett* 9:3253
55. Guerinot A, Reymond S, Cossy J (2007) *Angew Chem Int Ed* 46:6521
56. Dongol KG, Koh H, Sau M, Chai CLL (2007) *Adv Synth Catal* 349:1015
57. Tran LD, Daugulis O (2010) *Org Lett* 12:4277
58. Gao H-H, Yan C-H, Tao X-P, Xia Y, Sun H-M, Shen Q, Zhang Y (2010) *Organometallics* 29:4189
59. Czaplik WM, Mayer M, von Wangelin AJ (2009) *Angew Chem Int Ed* 48:607
60. Nakamura M, Ito S, Matsuo K, Nakamura E (2005) *Synlett* 1794
61. Ito S, Fujiwara Y-i, Nakamura E, Nakamura M (2009) *Org Lett* 11:4306
62. Bedford RB, Huwe M, Wilkinson MC (2009) *Chem Commun* 600
63. Hatakeyama T, Kondo Y, Fujiwara Y-i, Takaya H, Ito S, Nakamura E, Nakamura M (2009) *Chem Commun* 1216
64. Hatakeyama T, Nakagawa N, Nakamura M (2009) *Org Lett* 11:4496

65. Cahiez G, Foulgoc L, Moyeux A (2009) *Angew Chem Int Ed* 48:2969
66. Bedford RB, Hall MA, Hodges GR, Huwe M, Wilkinson MC (2009) *Chem Commun* 6430
67. Hatakeyama T, Hashimoto T, Kondo Y, Fujiwara Y, Seike H, Takaya H, Tamada Y, Ono T, Nakamura M (2010) *J Am Chem Soc* 132:10674
68. Kawamura S, Ishizuka K, Takaya H, Nakamura M (2010) *Chem Commun* 46:6054
69. Guerinot A, Lepesqueux G, Sable S, Reymond S, Cossy J (2010) *J Org Chem* 75:5151
70. Yamada KI, Sato T, Hosoi M, Yamamoto Y, Tomioka K (2010) *Chem Pharm Bull* 58:1511
71. Fürstner A (2009) *Angew Chem Int Ed* 48:1364
72. Brinker UH, König L (1983) *Chem Ber* 116:882
73. Bica K, Gaertner P (2006) *Org Lett* 8:733
74. Nishii Y, Wakasugi K, Tanabe Y (1998) *Synlett* 67
75. Rao Volla CM, Vogel P (2008) *Angew Chem Int Ed* 47:1305
76. Li B-J, Xu L, Wu Z-H, Guan B-T, Sun C-L, Wang B-Q, Shi Z-J (2009) *J Am Chem Soc* 131:14656
77. Czaplak WM, Grupe S, Mayer M, von Wangelin AJ (2010) *Chem Commun* 46:6350
78. Bogdanovic B, Schwickardi M (2000) *Angew Chem Int Ed* 39:4610
79. Fürstner A, Leitner A, Mendez M, Krause H (2002) *J Am Chem Soc* 124:13856
80. Fürstner A, Krause H, Lehmann CW (2006) *Angew Chem Int Ed* 45:440
81. Noda D, Sunada Y, Hatakeyama T, Nakamura M, Nagashima H (2009) *J Am Chem Soc* 131:6078
82. Newcomb M (1993) *Tetrahedron* 49:1151
83. Newcomb M, Toy PH (2000) *Acc Chem Res* 33:449
84. Hölzer B, Hoffmann RW (2003) *Chem Commun* 732
85. Yoshikai N, Mieczkowski A, Matsumoto A, Ilies L, Nakamura E (2010) *J Am Chem Soc* 132:5568
86. Inoue A, Shinokubo H, Oshima K (2000) *Org Lett* 2:651, and cited refs
87. Hayashi Y, Shinokubo H, Oshima K (1998) *Tetrahedron Lett* 39:63
88. Necas D, Katora M, Cisarova I (2004) *Eur J Org Chem* 1280
89. Freidlina RK, Velichko FK (1977) *Synthesis* 145
90. Terent'ev AB, Vasil'eva TT, Kuzmina NA, Ikonnikov NS, Orlova SA, Mysov EI, Belokon YN (1997) *Russ Chem Bull* 46:2096
91. Terent'ev AB, Vasil'eva TT, Kuz'mina NA, Mysov EI, Belokon YN (1997) *Russ Chem Bull* 46:764
92. Elzinga J, Hogeveen H (1980) *J Org Chem* 45:3957
93. Gasanov RG, Dolgushin FM, Yanovsky AI, Klemenkova ZS, Lokshin BV, Petrovskii PV, Rybinskaya MI (1997) *Russ Chem Bull* 46:1125
94. Forti L, Ghelfi F, Pagnoni UM (1996) *Tetrahedron Lett* 37:2077
95. Forti L, Ghelfi F, Libertini E, Pagnoni UM, Soragni E (1997) *Tetrahedron* 53:17761
96. Li Z, Yu R, Li H (2008) *Angew Chem Int Ed* 47:7497
97. Li C-J, Li Z (2006) *Pure Appl Chem* 78:935
98. Li C-J (2009) *Acc Chem Res* 42:335
99. Scheuermann CJ (2010) *Chem Asian J* 5:436
100. Yoo W-J, Li C-J (2010) *Topics Curr Chem* 292:281
101. Susuki T, Tsuji J (1970) *J Org Chem* 35:2982
102. Davis R, Durrant JLA, Khazal NMS, Bitterwolf TE (1990) *J Organomet Chem* 386:229
103. Hilt G, Bolze P, Kieltisch I (2005) *Chem Commun* 1996
104. Hilt G, Walter C, Bolze P (2006) *Adv Synth Catal* 348:1241
105. Hilt G, Bolze P, Harms K (2007) *Chem Eur J* 13:4312
106. Hilt G, Bolze P, Kieltisch I (2006) *Chem Commun* 1673 (correction)
107. Minisci F (1975) *Acc Chem Res* 8:165
108. Asscher M, Vofsi D (1963) *J Chem Soc* 1887
109. Brace NO (1967) *J Org Chem* 32:2711
110. Brace NO (1969) *J Org Chem* 34:2441

111. Tsai J-Y, Bouhadir KH, Zhou J-L, Webb TR, Sun Y, Shevlin PB (2003) *J Org Chem* 68:1235
112. Hayes TK, Freyer AJ, Parvez M, Weinreb SM (1986) *J Org Chem* 51:5501
113. Hayes TK, Villani R, Weinreb SM (1988) *J Am Chem Soc* 110:5533
114. Lee GM, Parvez M, Weinreb SM (1988) *Tetrahedron* 44:4671
115. Lee GM, Weinreb SM (1990) *J Org Chem* 55:1281
116. de Campo H, Lastecoueres D, Verlhac JB (1998) *Chem Commun* 2117
117. de Campo H, Lastecoueres D, Verlhac J-B (2000) *J Chem Soc Perkin Trans 1* 575
118. Li Z, Cao L, Li C-J (2007) *Angew Chem Int Ed* 46:6505
119. Zhang Y, Li C-J (2007) *Eur J Org Chem* 4654
120. Ghobrial M, Harhammer K, Mihovilovic MD, Schnurch M (2010) *Chem Commun* 46:8836
121. Guo X, Pan S, Liu J, Li Z (2009) *J Org Chem* 74:8848
122. Guo X, Yu R, Li H, Li Z (2009) *J Am Chem Soc* 131:17387
123. Guo X, Li W, Li Z (2010) *Eur J Org Chem* 5787
124. Song C-X, Cai G-X, Farrell TR, Jiang Z-P, Li H, Gan L-B, Shi Z-J (2009) *Chem Commun* 6002
125. Taniguchi T, Goto N, Nishibata A, Ishibashi H (2010) *Org Lett* 12:112
126. Okamoto T, Oka S (1984) *J Org Chem* 49:1589
127. Bravo A, Bjørsvik H-R, Fontana F, Ligouri L, Mele A, Minisci F (1997) *J Org Chem* 62:7128
128. Kino T, Nagase Y, Ohtsuka Y, Yamamoto K, Uraguchi D, Tokuhisa K, Yamakawa T (2010) *J Fluorine Chem* 131:98
129. Maslankiewicz A, Michalik E, Ciunik Z (2008) *J Heterocycl Chem* 45:527
130. Duncton MAJ, Estiarte MA, Johnson RJ, Cox MJ, O'Mahony DJR, Edwards WT, Kelly MG (2009) *J Org Chem* 74:6354
131. Lei A, Liu W, Liu C, Chen M (2010) *Dalton Trans* 39:10352
132. Vallee F, Mousseau JJ, Charette AB (2010) *J Am Chem Soc* 132:1514
133. Liu W, Cao H, Lei A (2010) *Angew Chem Int Ed* 49:2004
134. Bach T, Schlummer B, Harms K (2000) *Chem Commun* 287
135. Bach T, Schlummer B, Harms K (2001) *Chem Eur J* 7:2581
136. Danielec H, Klugge J, Schlummer B, Bach T (2006) *Synthesis* 551
137. Bach T, Schlummer B, Harms K (2000) *Synlett* 1330
138. Churchill DG, Rojas CM (2002) *Tetrahedron Lett* 43:7225
139. Chung HW, Lee GS, Chung BY (2002) *Bull Korean Chem Soc* 23:1325
140. Kluegge J, Herdtweck E, Bach T (2004) *Synlett* 1199
141. Taniguchi T, Sugiura Y, Zaimoku H, Ishibashi H (2010) *Angew Chem Int Ed* 49:10154
142. Bell FA, Crellin RA, Fujii H, Ledwith A (1969) *J Chem Soc Chem Commun* 251
143. Bauld NL, Gao D (2000) *J Chem Soc Perkin Trans 2* 191
144. Ohara H, Itoh T, Nakamura M, Nakamura E (2001) *Chem Lett* 624
145. Ohara H, Kiyokane H, Itoh T (2002) *Tetrahedron Lett* 43:3041
146. Ohara H, Kudo K, Itoh T, Nakamura M, Nakamura E (2000) *Heterocycles* 52:505
147. Wang K, Lu M, Yu A, Zhu X, Wang Q (2009) *J Org Chem* 74:935
148. Liu Y, Wei J, Che C-M (2010) *Chem Commun* 46:6926
149. Zhang S-Y, Tu Y-Q, Fan C-A, Zhang F-M, Shi L (2009) *Angew Chem Int Ed* 48:8761
150. Williamson KS, Yoon TP (2010) *J Am Chem Soc* 132:4570
151. Auricchio S, Bini A, Pastormerlo E, Truscillo AM (1997) *Tetrahedron* 53:10911
152. Suzuki M, Ohtake H, Kameya Y, Hamanaka N, Noyori R (1989) *J Org Chem* 54:5292
153. Morisson V, Barnier J-P, Blanco L (1999) *Tetrahedron Lett* 40:4045
154. Barnier J-P, Morisson V, Blanco L (2001) *Synth Commun* 31:349
155. O'Connor JM, Friese SJ, Rodgers BL (2005) *J Am Chem Soc* 127:16342
156. Sylvester KT, Chirik PJ (2009) *J Am Chem Soc* 132:8772
157. Murahashi S-i (ed) (2004) *Ruthenium in organic synthesis*. Wiley-VCH, Weinheim
158. Naota T, Takaya H, Murahashi S-I (1998) *Chem Rev* 98:2599
159. Trost BM, Frederiksen MU, Rudd MT (2005) *Angew Chem Int Ed* 44:6630
160. Alcaide B, Almendros P, Luna A (2009) *Chem Rev* 109:3817

161. Cossy J, Arseniyadis S, Meyer C (eds) (2010) *Metathesis in natural product synthesis*. Wiley-VCH, Weinheim
162. Arends IWCE, Kodama T, Sheldon RA (2004) Oxidation using ruthenium catalysts. In: Bruneau C, Dixneuf PH (eds) *Ruthenium catalysts and fine chemistry*. Springer, Berlin, p 277
163. Lam WWY, Man WL, Lau TC (2007) *Coord Chem Rev* 251:2238
164. Murahashi SI, Zhang D (2008) *Chem Soc Rev* 37:1490
165. Dürr H, Bossmann S (2001) *Acc Chem Res* 34:905
166. Balzani V, Bergamini G, Marchioni F, Ceroni P (2006) *Coord Chem Rev* 250:1254
167. Kamigaito M, Ando T, Sawamoto M (2001) *Chem Rev* 101:3689
168. Ouchi M, Terashima T, Sawamoto M (2009) *Chem Rev* 109:4963
169. Ouchi M, Terashima T, Sawamoto M (2008) *Acc Chem Res* 41:1120
170. Boese WT, Goldman AS (1992) *J Am Chem Soc* 114:350, and cited refs
171. Hasanayn F, Nsouli NH, Al-Ayoubi A, Goldman AS (2008) *J Am Chem Soc* 130:511
172. Kondo T, Sone Y, Tsuji Y, Watanabe Y (1994) *J Organomet Chem* 473:163
173. Kondo T, Tsuji Y, Watanabe Y (1988) *Tetrahedron Lett* 29:3833
174. Yoon TP, Ischay MA, Du J (2010) *Nat Chem* 2:527
175. Zeitler K (2009) *Angew Chem Int Ed* 48:9785
176. DeLaive PJ, Sullivan BP, Meyer TJ, Whitten DG (1979) *J Am Chem Soc* 101:4007, and cited refs
177. Fukuzumi S, Mochizuki S, Tanaka T (1990) *J Phys Chem* 94:722
178. Cano-Yalo H, Deronzier A (1984) *J Chem Soc Perkin Trans* 2:1093
179. Okada K, Okamoto K, Morita N, Okubo K, Oda M (1991) *J Am Chem Soc* 113:9401
180. Okada K, Okubo K, Morita N, Oda M (1992) *Tetrahedron Lett* 33:7377
181. Okada K, Okubo K, Morita N, Oda M (1993) *Chem Lett* 2021
182. Hasegawa E, Takizawa S, Seida T, Yamaguchi A, Yamaguchi N, Chiba N, Takahashi T, Ikeda H, Akiyama K (2006) *Tetrahedron* 62:6581
183. Nicewicz DA, MacMillan DWC (2008) *Science* 322:77
184. Ischay MA, Anzovino ME, Du J, Yoon TP (2008) *J Am Chem Soc* 130:12886
185. Du J, Yoon TP (2009) *J Am Chem Soc* 131:14604
186. Tucker JW, Narayanam JMR, Krabbe SW, Stephenson CRJ (2010) *Org Lett* 12:368
187. Tucker JW, Nguyen JD, Narayanam JMR, Krabbe SW, Stephenson CRJ (2010) *Chem Commun* 46:4985
188. Furst L, Matsuura BS, Narayanam JMR, Tucker JW, Stephenson CRJ (2010) *Org Lett* 12:3104
189. Narayanam JMR, Tucker JW, Stephenson CRJ (2009) *J Am Chem Soc* 131:8756
190. Borak JB, Falvey DE (2009) *J Org Chem* 74:3894
191. Andrews RS, Becker JJ, Gagne MR (2010) *Angew Chem Int Ed* 49:7274
192. Barton DHR, Csiba MA, Jaszberenyi JC (1994) *Tetrahedron Lett* 35:2869
193. Ischay MA, Lu Z, Yoon TP (2010) *J Am Chem Soc* 132:8572
194. Koike T, Akita M (2009) *Chem Lett* 38:166
195. Matsumoto H, Nakano T, Nagai Y (1973) *Tetrahedron Lett* 5147
196. Nagashima H (2004) Ruthenium-promoted radical reactions. In: Murahashi S-i (ed) *Ruthenium in organic synthesis*. Wiley-VCH, Weinheim, p 333
197. Kamigata N, Shimizu T (1997) *Rev Heteroatom Chem* 17:1
198. Mume E, Munslow IJ, Källström K, Andersson PG (2007) *Collect Czech Chem Commun* 72:1005
199. Bland WJ, Davis R, Durrant JLA (1985) *J Organomet Chem* 280:397
200. Delaude L, Demonceau A, Noels AF (2004) *Top Organomet Chem* 11:1551
201. Severin K (2006) *Curr Org Chem* 10:217
202. Edlin CD, Faulkner J, Fengas D, Helliwell M, Knight CK, House D, Parker J, Preece I, Quayle P, Raftery J, Richards SN (2006) *J Organomet Chem* 691:5375
203. Drozdak R, Allaert B, Ledoux N, Dragutan I, Dragutan V, Verpoort F (2005) *Adv Synth Catal* 347:1721

204. Drozdak R, Allaert B, Ledoux N, Dragutan I, Dragutan V, Verpoort F (2005) *Coord Chem Rev* 249:3055
205. Delaude L, Demonceau A, Noels AF (2006) *Curr Org Chem* 10:203
206. Simal F, Demonceau A, Noels AF (1999) *Tetrahedron Lett* 40:5689
207. Tallarico JA, Malnick LM, Snapper ML (1999) *J Org Chem* 64:344
208. Lee BT, Schrader TO, Martin-Matute B, Kauffman CR, Zhang P, Snapper ML (2004) *Tetrahedron* 60:7391
209. Simal F, Sebillé S, Demonceau A, Noels AF, Nunez R, Abad M, Teixidor F, Vinas C (1999) *Tetrahedron Lett* 40:5347
210. Tutusaus O, Vinas C, Nunez R, Teixidor F, Demonceau A, Delfosse S, Noels AF, Mata I, Molins E (2003) *J Am Chem Soc* 125:11830
211. Tutusaus O, Delfosse S, Demonceau A, Noels AF, Vinas C, Teixidor F (2003) *Tetrahedron Lett* 44:8421
212. Simal F, Wlodarczak L, Demonceau A, Noels AF (2000) *Tetrahedron Lett* 41:6071
213. Simal F, Wlodarczak L, Demonceau A, Noels AF (2001) *Eur J Org Chem* 2689
214. Nair RP, Kim TH, Frost BJ (2009) *Organometallics* 28:4681
215. Ida S, Terashima T, Ouchi M, Sawamoto M (2009) *J Am Chem Soc* 131:10808
216. Ida S, Ouchi M, Sawamoto M (2010) *J Am Chem Soc* 132:14748
217. Quebatte L, Scopelliti R, Severin K (2005) *Eur J Inorg Chem* 3353
218. Lundgren RJ, Rankin MA, McDonald R, Stradiotto M (2008) *Organometallics* 27:254
219. Quebatte L, Thommes K, Severin K (2006) *J Am Chem Soc* 128:7440
220. Thommes K, Icli B, Scopelliti R, Severin K (2007) *Chem Eur J* 13:6899
221. Oe Y, Uozumi Y (2008) *Adv Synth Catal* 350:1771
222. Fernandez-Zumel MA, Thommes K, Kiefer G, Sienkiewicz A, Pierzchala K, Severin K (2009) *Chem Eur J* 15:11601
223. Richel A, Demonceau A, Noels AF (2006) *Tetrahedron Lett* 47:2077
224. Borguet Y, Richel A, Delfosse S, Leclerc A, Delaude L, Demonceau A (2007) *Tetrahedron Lett* 48:6334
225. Iizuka Y, Li Z, Satoh K, Kamigaito M, Okamoto Y, Ito J-i, Nishiyama H (2007) *Eur J Org Chem* 782
226. Parkhomenko K, Barloy L, Sortais JB, Djukic JP, Pfeffer M (2010) *Tetrahedron Lett* 51:822
227. Motoyama Y, Hanada S, Niibayashi S, Shimamoto K, Takaoka N, Nagashima H (2005) *Tetrahedron* 61:10216
228. Diaz-Alvarez AE, Crochet P, Zablocka M, Duhayon C, Cadierno V, Majoral J-P (2008) *Eur J Inorg Chem* 786
229. Wolf J, Thommes K, Briel O, Scopelliti R, Severin K (2008) *Organometallics* 27:4464
230. Beaumont S, Ilardi EA, Monroe LR, Zakarian A (2010) *J Am Chem Soc* 132:1482
231. Moreira IDR, Bofill JM, Anglada JM, Solsona JG, Nebot J, Romea P, Urpi F (2008) *J Am Chem Soc* 130:3242
232. Studer A (2001) *Chem Eur J* 7:1159
233. Fischer H (2001) *Chem Rev* 101:3581
234. Gu Z, Zakarian A (2010) *Angew Chem Int Ed* 49:9702
235. Nagashima H, Kondo H, Hayashida T, Yamaguchi Y, Gondo M, Masuda S, Miyazaki K, Matsubara K, Kirchner K (2003) *Coord Chem Rev* 245:177
236. Nagashima H, Wakamatsu H, Itoh K (1984) *J Chem Soc Chem Commun* 652
237. Nagashima H, Ara K-i, Wakamatsu H, Itoh K (1985) *J Chem Soc Chem Commun* 518
238. Nagashima H, Wakamatsu H, Ozaki N, Ishii T, Watanabe M, Tajima T, Itoh K (1992) *J Org Chem* 57:1682
239. Nagashima H, Ozaki N, Seki K, Ishii M, Itoh K (1989) *J Org Chem* 54:4497
240. Nagashima H, Ozaki N, Ishii M, Seki K, Washiyama M, Itoh K (1993) *J Org Chem* 58:464
241. Rachita MA, Slough GA (1993) *Tetrahedron Lett* 34:6821
242. Slough GA (1993) *Tetrahedron Lett* 34:6825
243. Swift MD, Donaldson A, Sutherland A (2009) *Tetrahedron Lett* 50:3241

244. Quayle P, Fengas D, Richards S (2003) *Synlett* 1797
245. Faulkner J, Edlin CD, Fengas D, Preece I, Quayle P, Richards SN (2005) *Tetrahedron Lett* 46:2381
246. Nagashima H, Gondo M, Masuda S, Kondo H, Yamaguchi Y, Matsubara K (2003) *Chem Commun* 442
247. Motoyama Y, Gondo M, Masuda S, Iwashita Y, Nagashima H (2004) *Chem Lett* 33:442
248. Motoyama Y, Hanada S, Shimamoto K, Nagashima H (2006) *Tetrahedron* 62:2779
249. Dutta B, Scopelliti R, Severin K (2008) *Organometallics* 27:423
250. Katahira T, Ishizuka T, Matsunaga H, Kunieda T (2001) *Tetrahedron Lett* 42:6319
251. Grigg R, Devlin J, Ramasubbu A, Scott RM, Stevenson P (1987) *J Chem Soc Perkin Trans 1* 1515
252. Schmidt B, Pohler M, Costisella B (2004) *J Org Chem* 69:1421
253. Seigal BA, Fajardo C, Snapper ML (2005) *J Am Chem Soc* 127:16329
254. Edlin CD, Faulkner J, Quayle P (2006) *Tetrahedron Lett* 47:1145
255. Schmidt B, Pohler M (2005) *J Organomet Chem* 690:5552
256. McGonagle FI, Brown L, Cooke A, Sutherland A (2010) *Org Biomol Chem* 8:3418
257. Thommes K, Kiefer G, Scopelliti R, Severin K (2009) *Angew Chem Int Ed* 48:8115
258. Zhang S-Y, Tu Y-Q, Fan C-A, Jiang Y-J, Shi L, Cao K, Zhang E (2008) *Chem Eur J* 14:10201
259. Suzuki M, Noyori R, Hamanaka N (1982) *J Am Chem Soc* 104:2024
260. Masutani K, Irie R, Katsuki T (2002) *Chem Lett* 36
261. Shimizu H, Onitsuka S, Egami H, Katsuki T (2005) *J Am Chem Soc* 127:5396
262. Milczek E, Boudet N, Blakey S (2008) *Angew Chem Int Ed* 47:6825
263. Matsushita M, Kamata K, Yamaguchi K, Mizuno N (2005) *J Am Chem Soc* 127:6632
264. Li Y, Kijima T, Izumi T (2003) *J Organomet Chem* 687:12
265. Lo C-Y, Pal S, Odedra A, Liu R-S (2003) *Tetrahedron Lett* 44:3143
266. Fernandez-Zumel MA, Kiefer G, Thommes K, Scopelliti R, Severin K (2010) *Eur J Inorg Chem* 3596
267. Schrauzer GN (1976) *Angew Chem Int Ed Engl* 15:417
268. Scheffold R, Abrecht S, Orlinski R, Ruf H-R, Stamouli P, Tinembart O, Walder L, Weymuth C (1987) *Pure Appl Chem* 59:363
269. Kräutler B, Arigoni D, Golding BT (eds) (1998) *Vitamin B12 and B12 proteins*. Wiley-VCH, Weinheim
270. Banerjee R (1999) *Chemistry and biochemistry of B12*. Wiley, Chichester
271. Banerjee R (2003) *Chem Rev* 103:2083
272. Brown KL (2005) *Chem Rev* 105:2075
273. Butler PA, Kräutler B (2006) *Topics Organomet Chem* 17:1
274. Kharasch MS, Hambling JK, Rudy TP (1959) *J Org Chem* 63:303
275. Shinokubo H, Oshima K (2004) *Eur J Org Chem* 2081
276. Oshima K (2008) *Bull Chem Soc Jpn* 81:1
277. Cahiez G, Moyeux A (2010) *Chem Rev* 110:1435
278. Tsuji T, Yorimitsu H, Oshima K (2002) *Angew Chem Int Ed* 41:4137
279. Ohmiya H, Tsuji T, Yorimitsu H, Oshima K (2004) *Chem Eur J* 10:5640
280. Ohmiya H, Wakabayashi K, Yorimitsu H, Oshima K (2006) *Tetrahedron* 62:2207
281. Ohmiya H, Yorimitsu H, Oshima K (2006) *J Am Chem Soc* 128:1886
282. Ohmiya H, Yorimitsu H, Oshima K (2006) *Org Lett* 8:3093
283. Someya H, Ohmiya H, Yorimitsu H, Oshima K (2007) *Tetrahedron* 63:8609
284. Cahiez G, Chaboche C, Duplais C, Giulliani A, Moyeux A (2008) *Adv Synth Catal* 350:1484
285. Cahiez G, Chaboche C, Duplais C, Moyeux A (2009) *Org Lett* 11:277
286. Czaplik WM, Mayer M, Jacobi von Wangelin A (2009) *Synlett* 2931
287. Amatore M, Gosmini C (2010) *Chem Eur J* 16:5848
288. Kobayashi T, Ohmiya H, Yorimitsu H, Oshima K (2008) *J Am Chem Soc* 130:11276
289. Ikeda Y, Nakamura T, Yorimitsu H, Oshima K (2002) *J Am Chem Soc* 124:6514

290. Affo W, Ohmiya H, Fujioka T, Ikeda Y, Nakamura T, Yorimitsu H, Oshima K, Imamura Y, Mizuta T, Miyoshi K (2006) *J Am Chem Soc* 128:8068
291. Ikeda Y, Yorimitsu H, Shinokubo H, Oshima K (2004) *Adv Synth Catal* 346:1631
292. Mizutani K, Shinokubo H, Oshima K (2003) *Org Lett* 5:3959
293. Fujioka T, Nakamura T, Yorimitsu H, Oshima K (2002) *Org Lett* 4:2257
294. Someya H, Kondoh A, Sato A, Ohmiya H, Yorimitsu H, Oshima K (2006) *Synlett* 3061
295. Wakabayashi K, Yorimitsu H, Oshima K (2001) *J Am Chem Soc* 123:5374
296. Clark AJ, Davies DI, Jones K, Millbanks C (1994) *J Chem Soc Chem Commun* 41
297. Someya H, Ohmiya H, Yorimitsu H, Oshima K (2007) *Org Lett* 9:1565
298. Pattenden G (1988) *Chem Soc Rev* 17:361
299. Scheffold R, Dike M, Dike S, Herold T, Walder L (1980) *J Am Chem Soc* 102:3642
300. Giese B, Hartung J, He J, Hüter O, Koch A (1989) *Angew Chem Int Ed Engl* 28:325
301. Erdmann P, Schäfer J, Springer R, Zeitz HG, Giese B (1992) *Helv Chim Acta* 75:638
302. Auer L, Weymuth C, Scheffold R (1993) *Helv Chim Acta* 76:810
303. Gao J, Rusling JF, Zhou D-l (1996) *J Org Chem* 61:5972
304. Giese B, Erdmann P, Göbel T, Springer R (1992) *Tetrahedron Lett* 33:4545
305. Shukla P, Hsu Y-C, Cheng C-H (2006) *J Org Chem* 71:655
306. Branchaud BP, Detlefsen WD (1991) *Tetrahedron Lett* 32:6273
307. Okabe M, Abe M, Tada M (1982) *J Org Chem* 47:1775
308. Okabe M, Tada M (1982) *J Org Chem* 47:5382
309. Torii S, Inokuchi T, Yukawa T (1985) *J Org Chem* 50:5875
310. Inokuchi T, Kawafuchi H, Aoki K, Yoshida A, Torii S (1994) *Bull Chem Soc Jpn* 67:595
311. Last K, Hoffmann HMR (1989) *Synthesis* 901
312. Tabatabaieian K, Mamaghani M, Ghanadzadeh A, Riahi A (2006) *Mendeleev Commun* 16:33
313. Tabatabaieian K, Mamaghani M, Navai-Dyva T (2002) *Russ J Org Chem* 38:210
314. Ladlow M, Pattenden G (1984) *Tetrahedron Lett* 25:4317
315. Begley MJ, Ladlow M, Pattenden G (1988) *J Chem Soc Perkin Trans 1* 1095
316. Bhandal B, Pattenden G, Russell JJ (1986) *Tetrahedron Lett* 27:2299
317. Bhandal B, Patel VF, Pattenden G, Russell JJ (1990) *J Chem Soc Perkin Trans 1* 2691
318. Baldwin JE, Li C-S (1987) *J Chem Soc Chem Commun* 166
319. Dunach E, Esteves AP, Medeiros MJ, Olivero S (2004) *Tetrahedron Lett* 45:7935
320. Inokuchi T, Kawafuchi H (2001) *Synlett* 421
321. Bamhaoud T, Prandi J (1996) *J Chem Soc Chem Commun* 1229
322. Mayer S, Prandi J, Bamhaoud T, Bakkas S, Guillou O (1998) *Tetrahedron* 54:8753
323. Desire J, Prandi J (1997) *Tetrahedron Lett* 38:6189
324. Desire J, Prandi J (2000) *Eur J Org Chem* 3075
325. Hutchinson JH, Pattenden G, Myers PL (1987) *Tetrahedron Lett* 28:1313
326. Busato S, Tinembart O, Zhang Z-d, Scheffold R (1990) *Tetrahedron* 46:3155
327. Busato S, Scheffold R (1994) *Helv Chim Acta* 77:92
328. Carrero H, Gao J, Rusling JF, Lee C-W, Fry AJ (1999) *Electrochim Acta* 45:503
329. Katsumata A, Takasu K, Ihara M (1999) *Heterocycles* 51:733
330. McGinley CM, Relyea HA, van der Donk WA (2006) *Synlett* 211
331. Hisaeda Y, Nishioka T, Inoue Y, Asada K, Hayashi T (2000) *Coord Chem Rev* 198:21
332. Dunach E, Esteves AP, Medeiros MJ, Pletcher D, Olivero S (2004) *J Electroanal Chem* 566:39
333. Park SR, Findlay NJ, Garnier J, Zhou SZ, Spicer MD, Murphy JA (2009) *Tetrahedron* 65:10756
334. Shimakoshi H, Nakazato A, Hayashi T, Tachi Y, Naruta Y, Hisaeda Y (2001) *J Electroanal Chem* 507:170
335. Ozaki S, Nakanishi T, Sugiyama M, Miyamoto C, Ohmori M (1991) *Chem Pharm Bull* 39:31
336. Campbell CJ, Haddleton DM, Rusling JF (1999) *Electrochem Commun* 1:618
337. Njue CK, Rusling JF (2002) *Electrochem Commun* 4:340
338. Gao J, Rusling JF (1998) *J Org Chem* 63:218

339. Murakami Y, Hisaeda Y, Ohno T, Matsuda Y (1988) *Chem Lett* 621
340. Hisaeda Y, Takenaka J, Murakami Y (1997) *Electrochim Acta* 42:2165
341. Kawafuchi H, Inokuchi T (2002) *Tetrahedron Lett* 43:2051
342. Inokuchi T, Tsuji M, Kawafuchi H, Torii S (1991) *J Org Chem* 56:5945
343. Baik T-G, Luis AL, Wang L-C, Krische MJ (2001) *J Am Chem Soc* 123:6716
344. Wang L-C, Jang H-Y, Roh Y, Lynch V, Schultz AJ, Wang X, Krische MJ (2002) *J Am Chem Soc* 124:9448
345. Roh Y, Jang H-Y, Lynch V, Bauld NL, Krische MJ (2002) *Org Lett* 4:611
346. Nakamura A, Konishi A, Tatsuno Y, Otsuka S (1978) *J Am Chem Soc* 100:3443
347. Nakamura A, Konishi A, Tsujitani R, Kudo M-a, Otsuka S (1978) *J Am Chem Soc* 100:3449
348. Penoni A, Wanke R, Tollari S, Gallo E, Musella D, Ragaini F, Demartin F, CENINI S (2003) *Eur J Inorg Chem* 1452 and cited refs
349. Huang L, Chen Y, Gao G-Y, Zhang XP (2003) *J Org Chem* 68:8179, and cited refs
350. Ikeno T, Iwakura I, Yamada T (2002) *J Am Chem Soc* 124:15152
351. Wayland BB, Poszmik G, Mukerjee SL, Fryd M (1994) *J Am Chem Soc* 116:7943
352. Gridnev AA, Ittel SD, Fryd M, Wayland BB (1996) *Organometallics* 15:222
353. Gridnev AA, Ittel SD, Wayland BB, Fryd M (1996) *Organometallics* 15:5116
354. Shaham N, Marsawa A, Matana Y, Cohen H, Meyerstein D (2002) *Eur J Inorg Chem* 87
355. Chen Y, Zhang XP (2004) *J Org Chem* 69:2431
356. Chen Y, Fields KB, Zhang XP (2004) *J Am Chem Soc* 126:14718
357. Chen Y, Zhang XP (2007) *J Org Chem* 72:5931
358. Ruppel JV, Gauthier TJ, Snyder NL, Perman JA, Zhang XP (2009) *Org Lett* 11:2273
359. Chen Y, Ruppel JV, Zhang XP (2007) *J Am Chem Soc* 129:12074
360. Zhu S, Perman JA, Zhang XP (2008) *Angew Chem Int Ed* 47:8460
361. Zhu S, Ruppel JV, Lu H, Wojtas L, Zhang XP (2008) *J Am Chem Soc* 130:5042
362. Doyle MP (2009) *Angew Chem Int Ed* 48:850
363. Fantauzzi S, Gallo E, Rose E, Raoul N, Caselli A, Issa S, Ragaini F, CENINI S (2008) *Organometallics* 27:6143
364. Caselli A, Buonomenna MG, de Baldironi F, Laera L, Fantauzzi S, Ragaini F, Gallo E, Golemme G, CENINI S, Drioli E (2010) *J Mol Catal A Chem* 317:72
365. Dzik WI, Xu X, Zhang XP, Reek JNH, de Bruin B (2010) *J Am Chem Soc* 132:10891
366. CENINI S, Gallo E, Penoni A, Ragaini F, Tollari S (2000) *Chem Commun* 2265
367. Ragaini F, Penoni A, Gallo E, Tollari S, Gotti CL, Lapadula M, Mangioni E, CENINI S (2003) *Chem Eur J* 9:249
368. Harden JD, Ruppel JV, Gao G-Y, Zhang XP (2007) *Chem Commun* 4644
369. Lu H, Subbarayan V, Tao J, Zhang XP (2010) *Organometallics* 29:389
370. Ruppel JV, Kamble RM, Zhang XP (2007) *Org Lett* 9:4889
371. Lu H, Tao J, Jones JE, Wojtas L, Zhang XP (2010) *Org Lett* 12:1248
372. Lu H, Jiang H, Wojtas L, Zhang XP (2010) *Angew Chem Int Ed* 49:10192
373. Subbarayan V, Ruppel JV, Zhu S, Perman JA, Zhang XP (2009) *Chem Commun* 4266
374. Isayama S, Mukaiyama T (1989) *Chem Lett* 573
375. Isayama S (1990) *Bull Chem Soc Jpn* 63:1305
376. Tokuyasu T, Kunikawa S, Masuyama A, Nojima M (2002) *Org Lett* 4:3595
377. Wu J-M, Kunikawa S, Tokuyasu T, Masuyama A, Nojima M, Kim H-S, Wataya Y (2005) *Tetrahedron* 61:9961
378. Tokuyasu T, Kunikawa S, Abe M, Masuyama A, Nojima M, Kim H-S, Begum K, Wataya Y (2003) *J Org Chem* 68:7361
379. Tokuyasu T, Kunikawa S, McCullough KJ, Masuyama A, Nojima M (2005) *J Org Chem* 70:251
380. Ito T, Tokuyasu T, Masuyama A, Nojima M, McCullough KJ (2003) *Tetrahedron* 59:525
381. Xu X-X, Dong H-Q (1994) *Tetrahedron Lett* 35:9429
382. Oh CH, Kang JH (1998) *Tetrahedron Lett* 39:2771
383. Oh CH, Kim HJ, Wu SH, Won HS (1999) *Tetrahedron Lett* 40:8391



384. O'Neill PM, Pugh M, Davies J, Ward SA, Park BK (2001) *Tetrahedron Lett* 42:4569
385. O'Neill PM, Hindley S, Pugh MD, Davies J, Bray PG, Park BK, Kapu DS, Ward SA, Stocks PA (2003) *Tetrahedron Lett* 44:8135
386. Ahmed A, Dussault PH (2004) *Org Lett* 6:3609
387. Ghorai P, Dussault PH, Hu C (2008) *Org Lett* 10:2401
388. Sugamoto K, Matsushita Y-i, Matsui T (1998) *J Chem Soc Perkin Trans 1* 3989
389. Isayama S, Mukaiyama T (1989) *Chem Lett* 569
390. Isayama S, Mukaiyama T (1989) *Chem Lett* 1071
391. Waser J, Gaspar B, Nambu H, Carreira EM (2006) *J Am Chem Soc* 128:11693
392. Mukaiyama T, Isayama S, Inoki S, Kato K, Yamada T, Takai T (1989) *Chem Lett* 449
393. Inoki S, Kato K, Takai T, Isayama S, Yamada T, Mukaiyama T (1989) *Chem Lett* 515
394. Kato K, Yamada T, Takai T, Inoki S, Isayama S (1990) *Bull Chem Soc Jpn* 63:179
395. Okamoto T, Kobayashi K, Oka S, Tanimoto S (1987) *J Org Chem* 52:5089
396. Kato K, Mukaiyama T (1990) *Chem Lett* 1395
397. Sugamoto K, Hamasuna Y, Matsushita Y-i, Matsui T (1998) *Synlett* 1270
398. Waser J, Carreira EM (2004) *J Am Chem Soc* 126:5676
399. Waser J, Gonzalez-Gomez JC, Nambu H, Huber P, Carreira EM (2005) *Org Lett* 7:4249
400. Waser J, Nambu H, Carreira EM (2005) *J Am Chem Soc* 127:8294
401. Gaspar B, Waser J, Carreira EM (2007) *Synthesis* 3839
402. Gaspar B, Carreira EM (2007) *Angew Chem Int Ed* 46:4519
403. Gaspar B, Carreira EM (2009) *J Am Chem Soc* 132:13214
404. Gaspar B, Carreira EM (2008) *Angew Chem Int Ed* 47:5758
405. Friend CL, Simpkins NS, Anson M, Polywka MEC (1998) *Tetrahedron* 54:2801
406. Kato K, Mukaiyama T (1990) *Chem Lett* 1917
407. Kato K, Mukaiyama T (1991) *Bull Chem Soc Jpn* 64:2948
408. Panchaud P, Chabaud L, Landais Y, Ollivier C, Renaud P, Zigmantas S (2004) *Chem Eur J* 10:3606
409. Kim S (2004) *Adv Synth Catal* 346:19
410. Boyd JD, Foote CS, Imagawa DK (1980) *J Am Chem Soc* 102:3641
411. Balci M, Sütbeyaz Y (1983) *Tetrahedron Lett* 24:311
412. Celik M, Akbulut N, Balci M (2000) *Helv Chim Acta* 83:3131
413. Sütbeyaz Y, Secen H, Balci M (1988) *J Org Chem* 53:2312
414. Balci M, Sütbeyaz Y (1983) *Tetrahedron Lett* 24:4135
415. Sengül ME, Balci M (1997) *J Chem Soc Perkin Trans 1* 2071
416. Coskun A, Güney M, Dastan A, Balci M (2007) *Tetrahedron* 63:4944
417. Sengul ME, Simsek N, Balci M (2000) *Eur J Org Chem* 1359
418. Balci M, Akbulut N (1985) *Tetrahedron* 41:1315
419. Özer G, Saracoglu N, Balci M (2003) *J Org Chem* 68:7009
420. O'Shea KE, Foote CS (1989) *J Org Chem* 54:3475
421. Härter R, Weymuth C, Scheffold R, Engel P, Linden A (1993) *Helv Chim Acta* 76:353
422. Avery TD, Geatrex BW, Taylor DK, Tiekink ERT (2000) *J Chem Soc Perkin Trans 1* 1319
423. Avery TD, Taylor DK, Tiekink ERT (2000) *J Org Chem* 65:5531
424. Avery TD, Fallon G, Geatrex BW, Pyke SM, Taylor DK, Tiekink ERT (2001) *J Org Chem* 66:7955
425. Avery TD, Jenkins NF, Kimber MC, Lupton DW, Taylor DK (2002) *Chem Commun* 28
426. Geatrex BW, Kimber MC, Taylor DK, Fallon G, Tiekink ERT (2002) *J Org Chem* 67:5307
427. Geatrex BW, Jenkins NF, Taylor DK, Tiekink ERT (2003) *J Org Chem* 68:5205
428. Robinson TV, Taylor DK, Tiekink ERT (2006) *J Org Chem* 71:7236
429. Geatrex BW, Taylor DK (2005) *J Org Chem* 70:470
430. Ishikawa T, Kudoh T, Yoshida J, Yasuhara A, Manabe S, Saito S (2002) *Org Lett* 4:1907
431. Bhatia S, Punniyamurthy T, Bhatia B, Iqbal J (1993) *Tetrahedron* 49:6101
432. Punniyamurthy T, Bhatia B, Iqbal J (1994) *J Org Chem* 59:850
433. Kishi A, Kato S, Sakaguchi S, Ishii Y (1999) *Chem Commun* 1421

434. Recupero F, Punta C (2007) *Chem Rev* 107:3800
435. Iwahama T, Sakaguchi S, Ishii Y (2000) *Chem Commun* 613
436. Hirano K, Iwahama T, Sakaguchi S, Ishii Y (2000) *Chem Commun* 2457
437. Hirano K, Sakaguchi S, Ishii Y (2002) *Tetrahedron Lett* 43:3617
438. Hara T, Iwahama T, Sakaguchi S, Ishii Y (2001) *J Org Chem* 66:6425
439. Tayama O, Iwahama T, Sakaguchi S, Ishii Y (2003) *Eur J Org Chem* 2286
440. Turra N, Neuenschwander U, Baiker A, Peeters J, Hermans I (2010) *Chem Eur J* 16:13226, and cited refs
441. Sheldon RA, Kochi JK (1981) *Metal-catalyzed oxidation of organic compounds*. Academic Press, New York
442. Inoki S, Mukaiyama T (1990) *Chem Lett* 67
443. Tian S-K, Wang Z-M, Jiang J-K, Shi M (1999) *Tetrahedron Asymmetry* 10:2551
444. Wang Z-M, Tian S-K, Shi M (1999) *Tetrahedron Asymmetry* 10:667
445. Wang Z-M, Tian S-K, Shi M (2000) *Chirality* 12:581
446. Wang Z-M, Tian S-K, Shi M (1999) *Tetrahedron Lett* 40:977
447. Wang Z-M, Tian S-K, Shi M (2000) *Eur J Org Chem* 349
448. Evans PA, Cui J, Gharpure SJ, Polosukhin A, Zhang H-R (2003) *J Am Chem Soc* 125:14702
449. Takahashi S, Kubota A, Nakata T (2002) *Angew Chem Int Ed* 41:4751
450. Zhao H, Gorman JST, Pagenkopf BL (2006) *Org Lett* 8:4379
451. Wang J, Pagenkopf BL (2007) *Org Lett* 9:3703
452. Menendez Perez B, Schuch D, Hartung J (2008) *Org Biomol Chem* 6:3532
453. Menendez Perez B, Hartung J (2009) *Tetrahedron Lett* 50:960
454. Schuch D, Fries P, Dönges M, Menendez Perez B, Hartung J (2009) *J Am Chem Soc* 131:12918
455. Palmer C, Morra NA, Stevens AC, Bajtos B, Machin BP, Pagenkopf BL (2009) *Org Lett* 11:5614
456. Shey J, McGinley CM, McCauley KM, Dearth AS, Young BT, van der Donk WA (2002) *J Org Chem* 67:837
457. Xu H, Jia L (2003) *Org Lett* 5:1575
458. Xu H, Gladding JA, Jia L (2004) *Inorg Chim Acta* 357:4024
459. Bonhote P, Scheffold R (1991) *Helv Chim Acta* 74:1425
460. Zhang ZD, Scheffold R (1993) *Helv Chim Acta* 76:2602
461. Troxler T, Scheffold R (1994) *Helv Chim Acta* 77:1193
462. Sun C-L, Li H, Yu D-G, Yu M, Zhou X, Lu X-Y, Huang K, Zheng S-F, Li B-J, Shi Z-J (2010) *Nature Chem* 2:1044
463. Kotora M, Adamek F, Hajek M (1993) *Catal Lett* 18:345
464. Evans PA (ed) (2005) *Modern rhodium-catalyzed organic reactions*. Wiley-VCH, Weinheim, and cited refs
465. Hagenbuch J-P, Vogel P (1980) *J Chem Soc Chem Commun* 1062
466. Hagenbuch J-P, Birbaum J-L, Metral J-L, Vogel P (1982) *Helv Chim Acta* 65:887
467. Sakakura T, Sodeyama T, Sasaki K, Wada K, Tanaka M (1990) *J Am Chem Soc* 112:7221
468. Rosini GP, Zhu K, Goldman AS (1995) *J Organomet Chem* 504:115
469. Kazimerczuk R, Wozniowski T, Borowiak M, Zimmnicka E, Zwolinski K, Rogulski Z, Trzeciak A, Ostrowski S, Dobrowolski JC, Skupinski W (2007) *Tetrahedron Lett* 48:7046
470. Rosini GP, Boese WT, Goldman AS (1994) *J Am Chem Soc* 116:9498
471. Murai S, Sugise R, Sonoda N (1981) *Angew Chem Int Ed Engl* 20:475
472. Cable CJ, Adams H, Bailey NA, Crosby J, White C (1991) *J Chem Soc Chem Commun* 165
473. Pereira S, Srebnik M (1996) *J Am Chem Soc* 118:909
474. Shi L, Tu Y-Q, Wang M, Zhang F-M, Fan C-A, Zhao Y-M, Xia W-J (2005) *J Am Chem Soc* 127:10836
475. de Bruin B, Hettterscheid DGHK, Koekkoek AJJ, Grützmacher H (2007) *Prog Inorg Chem* 55:247
476. Ohe K, Kojima M-a, Yonehara K, Uemura S (1996) *Angew Chem Int Ed Engl* 35:1823

477. Manabe T, Yanagi S-i, Ohe K, Uemura S (1998) *Organometallics* 17:2942
478. Wang KK (1996) *Chem Rev* 96:207
479. Klein M, Walenzyk T, König B (2004) *Collect Czech Chem Commun* 69:945
480. Wang J, Tong X, Xie X, Zhang Z (2010) *Org Lett* 12:5370
481. Necas D, Katora M (2007) *Curr Org Chem* 11:1566
482. Wender PA, Takahashi H, Witulski B (1995) *J Am Chem Soc* 117:4720
483. Hayashi M, Ohmatsu T, Meng Y-P, Saigo K (1998) *Angew Chem Int Ed* 37:837
484. Bart SC, Chirik PJ (2003) *J Am Chem Soc* 125:886
485. Wee AGH (2006) *Curr Org Synth* 3:499
486. Vanecko JA, Wan H, West FG (2006) *Tetrahedron* 62:1043
487. Sweeney JB (2009) *Chem Soc Rev* 38:1027
488. Eberlein TH, West FG, Tester RW (1992) *J Org Chem* 57:3479
489. West FG, Eberlein TH, Tester RW (1993) *J Chem Soc Perkin Trans* 1:2857
490. West FG, Naidu BN, Tester RW (1994) *J Org Chem* 59:6892
491. Tester RW, West FG (1998) *Tetrahedron Lett* 39:4631
492. Marmsäter FP, Vanecko JA, West FG (2004) *Org Lett* 6:1657
493. Brogan JB, Zercher CK (1998) *Tetrahedron Lett* 39:1691
494. Kitagaki S, Yanamoto Y, Tsutsui H, Anada M, Nakajima M, Hashimoto S (2001) *Tetrahedron Lett* 42:6361; correction: Kitagaki S, Yanamoto Y, Tsutsui H, Anada M, Nakajima M, Hashimoto S (2001) *Tetrahedron Lett* 42:7715
495. Lee D, Otte RD (2004) *J Org Chem* 69:3569
496. Zalatan DN, Du Bois J (2009) *Synlett* 143
497. Fiori KW, Du Bois J (2007) *J Am Chem Soc* 129:562
498. Labinger JA, Osborn JA (1980) *Inorg Chem* 19:3230
499. Labinger JA, Osborn JA, Coville NJ (1980) *Inorg Chem* 19:3236, and cited ref
500. de Bruin B, Hettterscheid DGH (2007) *Eur J Inorg Chem* 211
501. Dzik WI, Reek JNH, de Bruin B (2008) *Chem Eur J* 14:7594
502. Hettterscheid DGH, Kaiser J, Reijerse E, Peters TPI, Thewissen S, Blok ANJ, Smits JMM, de Gelder R, de Bruin B (2005) *J Am Chem Soc* 127:1895
503. Hettterscheid DGH, Bens M, de Bruin B (2005) *Dalton Trans* 979
504. Hou Z, Koizumi T-a, Fujita A, Yamazaki H, Wakatsuki Y (2001) *J Am Chem Soc* 123:5812
505. Nagib DA, Scott ME, MacMillan DWC (2009) *J Am Chem Soc* 131:10875
506. Shih H-W, Vander Wal MN, Grange RL, MacMillan DWC (2010) *J Am Chem Soc* 132:13600
507. Condie AG, Gonzalez-Gomez JC, Stephenson CRJ (2010) *J Am Chem Soc* 132:1464

# Radicals in Transition Metal Catalyzed Reactions? Transition Metal Catalyzed Radical Reactions?: A Fruitful Interplay Anyway

## Part 3: Catalysis by Group 10 and 11 Elements and Bimetallic Catalysis

Ullrich Jahn

**Abstract** This review summarizes the current status of transition metal catalyzed reactions involving radical intermediates in organic chemistry. This part focuses on radical-based methods catalyzed by group 10 and group 11 metal complexes. Reductive and redox-neutral C–C bond formations catalyzed by low-valent metal complexes as well as catalytic oxidative methods are reviewed. Catalytic processes which rely on the combination of two metal complexes are also covered.

**Keywords** Catalysis · Transition metals · Radicals · Electron transfer · Cross-coupling · Addition · Cyclization

### Contents

1	Introduction .....	324
2	Nickel Catalysis .....	325
2.1	Low-Valent Nickel-Catalyzed Cross-Coupling Reactions of Alkyl Halides ....	326
2.2	Ni(0)–Ni(I)–Ni(II) Catalysis: Coupling Reactions of Alkyl Halides with Unsubstituted Arenes .....	340
2.3	Ni(0)–Ni(I)–Ni(II) Catalysis: Radical Addition Reactions .....	341
2.4	Ni(0)–Ni(I)–Ni(II) Catalysis: Radical cyclizations .....	347
2.5	Ni(0)–Ni(II)–Ni(I)–Ni(III) Catalysis: Cross-Coupling .....	350
2.6	Ni(I)–Ni(II) Catalysis: Radical Additions .....	353
2.7	Ni(I)–Ni(II) Catalysis: Radical Cyclizations .....	354
2.8	Ni(I)–Ni(II)–Ni(III) Catalysis: Conjugate Addition Reactions .....	360

---

For Part 1, see [1]; for Part 2, see [2]

U. Jahn (✉)

Institute of Organic Chemistry and Biochemistry, Academy of Sciences of the Czech Republic,  
Flemingovo namesti 2, 16610 Prague 6, Czech Republic  
e-mail: [jahn@uochb.cas.cz](mailto:jahn@uochb.cas.cz)

2.9	Ni(II)–Ni(III)–(Ni(IV)) Catalysis: Radical Additions .....	360
2.10	Ni(II)–Ni(I) Catalysis: Oxidative Rearrangement .....	362
3	Pd-Catalyzed Radical Reactions .....	363
3.1	Pd(0)–Pd(I) Catalysis: Atom Transfer Radical Additions .....	363
3.2	Pd(0)–Pd(I) Catalysis: Atom Transfer Cyclizations .....	368
3.3	Pd(0)–Pd(I)–Pd(II) Catalysis: Cross-Coupling Reactions .....	369
3.4	Pd(0)–Pd(I)–Pd(II) Catalysis: Carbonylation and Carbonylation/Coupling Reactions .....	372
3.5	Pd(0)–Pd(I)–Pd(II) Catalysis: Radical Cyclizations .....	375
3.6	Pd(II)–Catalyzed Ring Opening of Endoperoxides .....	379
3.7	Pd(II)–Pd(III)–Pd(IV) Catalysis .....	379
4	Pt-Catalyzed Radical Reactions .....	382
5	Copper-Catalyzed Radical Reactions .....	384
5.1	Cu(0)-Catalyzed Atom Transfer Radical Addition Reactions .....	384
5.2	Cu(I)-Catalyzed Atom Transfer Radical Addition Reactions .....	385
5.3	Cu(I)-Catalyzed Atom Transfer Radical Cyclization Reactions .....	387
5.4	Cu(I)–Cu(II) Catalysis: Other Radical Additions .....	393
5.5	Cu(I)–Cu(II) Catalysis: Ullmann Reactions .....	395
5.6	Cu(I)–Cu(II) Catalysis: Electron Transfer in Conjugate Addition Reactions ...	397
5.7	Cu(I)-Catalyzed Photochemical [2+2] Photocycloaddition Reactions .....	399
5.8	Cu(I)–Cu(II) Catalysis: Amination of Hydrocarbons .....	399
5.9	Cu(I)–Cu(II) Catalysis: Radical Reactions Triggered by Oxaziridine Ring Opening .....	401
5.10	Cu(I)–Cu(II) Catalysis: Diamination Reactions Triggered by Diaziridinone Ring Opening .....	403
5.11	Cu(II) Catalysis: [1,2]-Onium Ylide Rearrangements (Stevens Rearrangements)	406
5.12	Cu(II)–Cu(I) Oxidative Catalysis: Oxidative Cleavage Reactions and Cyclizations of Amides .....	411
5.13	Cu(II)–Cu(III) Catalysis: Ring Opening Reactions of Oxaziridines .....	415
5.14	Miscellaneous .....	418
6	Silver-Catalyzed Radical Reactions .....	419
6.1	Ag(0)–Ag(I) Catalysis: Cross-Coupling and Addition Reactions .....	419
6.2	Ag(I)/Ag(0)-Catalyzed Addition and Cyclization Reactions .....	424
6.3	Ag(II)–Ag(I) Catalysis: Minisci Reactions .....	425
7	Gold-Catalyzed Radical Reactions .....	428
8	Bimetallic Catalysis .....	429
8.1	Ti(III)–Rh(I) Catalysis .....	429
8.2	Cr(II)–Co(II) Catalysis .....	431
8.3	Mn(II)–Co(II) Catalysis .....	434
8.4	Mn(II)–Cu(I) Catalysis .....	437
8.5	Ru(II)–Rh(III) Catalysis .....	438
9	Concluding Remarks .....	439
10	Transition Metal-Catalyzed Radical Reactions According to Reaction Type .....	440
	References .....	441

## 1 Introduction

This review is divided into three parts. For a general introduction to the topic see Sects. 1 and 2 in Part 1. The basic reactivity patterns and the general methods to conduct radical-catalyzed reactions and to analyze the involved intermediates are discussed there. Processes catalyzed by metals of group 4 to group 7 are reviewed in

Sects. 3–10 of the first part. Synthetic methodology employing group 8 and 9 catalysts is covered in the second part. A general overview on the scope and limitations of this review is provided in Part 1 (Part 1, Sect. 2.8). The available methodology to form (or cleave) one or more C–C bonds and/or C–heteroatom bonds is the main focus of this manuscript.

## 2 Nickel Catalysis

Nickel catalysis is a very active field in organometallic and organic chemistry (selected reviews [3–7]). Complexes of all oxidation states are active in two-electron transfer processes, such as oxidative addition or reductive elimination as well as in single electron transfer initiating radical reactions. Through these processes, oxidation states from Ni(0) to Ni(III) can be easily accessed under mild conditions. Occasionally, Ni(IV) intermediates were also proposed. Apart from the vast number of Ni(II) complexes, a number of organonickel(I) complexes were characterized by X-ray crystallography and their potency as active species in catalytic cycles tested [8–10]. Either radical or two-electron reactivity was observed. Recently, the structure of some alkylnickel(III) complexes was also structurally elucidated [11].

(Cyclam)Ni(II) complexes react readily with methyl radicals [12]. The resulting (cyclam)Ni(III)–CH<sub>3</sub> intermediates transform with excess radiolytically generated methyl radicals to ethane and reform the initial Ni(II) complex. The kinetics was determined.

Inhibition and stereochemical and radical clock experiments pointed to the involvement of radicals as intermediates in stoichiometric coupling reactions of (allyl)nickel(II) halides with alkyl halides [13, 14], initially reported by Semmelhack and Corey [15]. In contrast, vinyl halides reacted with retention of stereochemistry, thus supporting a two-electron coupling pathway starting with oxidative addition [16]. In an attempt to unify all observed results for all organic halides, Hegedus and Thompson proposed a two-electron oxidative addition and exchange pathway explaining the experimental observations, including the observed radical clock experiments. However, the differential oxidative addition rates of saturated and unsaturated organic halides, favoring SET for the former and oxidative addition or S<sub>N</sub>2 for the latter, were not taken into account. Kinetic investigations were moreover conducted only with iodobenzene as the substrate, but not with alkyl halides. Finally, the exchange pathways proposed for stoichiometric experiments are less likely under catalytic conditions, where concentrations of active species are significantly lower. Other nickel(II) complexes act as SET reductants to alkyl halides and trigger radical reactions [17].

Most often, nickel complexes are preactivated by initial reduction to Ni(0) or Ni(I) for C–C bond forming reactions. The reducing agent and ligands at the initial Ni(II) precatalyst determine the reduction course significantly (reviews [18–20]). Organometallic compounds are good reducing agents and lead very often to Ni(0) intermediates. In contrast, electroreduction is dependent on the applied ligand and

the applied potential. Macrocyclic porphyrin, cyclam, or salen-type nickel complexes are mostly reduced to paramagnetic nickel(I) intermediates, while nickel phosphine, amine, or diamine complexes, such as Ni(bipy)<sub>3</sub>X<sub>2</sub>, lead to diamagnetic Ni(0) intermediates on electroreduction in one or two consecutive electron transfer steps [21, 22]. This reduction behavior contributes in part subsequently to the two-electron vs. radical reactivity of the catalysts.

When aryl halides were applied in catalytic coupling reactions, the mechanistic evidence points to initial SET reduction by low-valent nickel phosphine species (selected investigations in [23, 24]). The competition of cage collapse to ArNi(PR<sub>3</sub>)<sub>2</sub>X vs. dissociation of the aryl halide radical anion to a free radical and Ni(I) complexes determines the cross-coupling manifolds. Thus, Ni(0)–Ni(II) and Ni(I)–Ni(III) catalytic cycles can occur interwoven with each other and a distinction may be difficult. Common to both is that the coupling process with aryl halides is likely to occur by a two-electron oxidative addition/reductive elimination pathway.

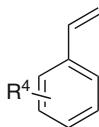
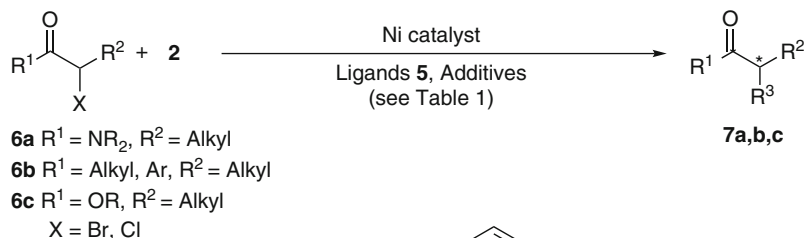
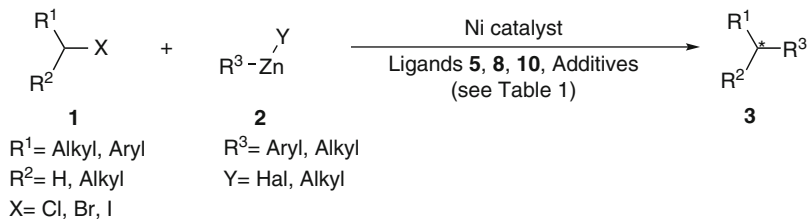
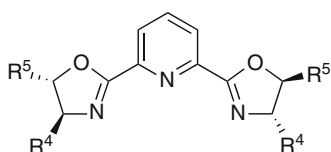
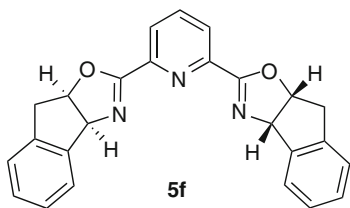
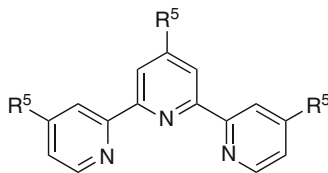
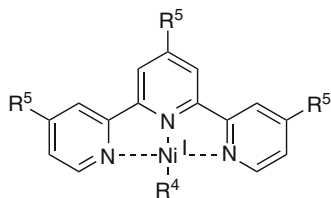
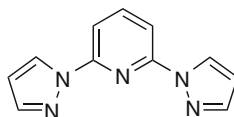
Nickel catalysts display significant accelerating effects in reactions mediated by SmI<sub>2</sub> [25], such as aza-pinacol coupling reactions of imines [26, 27].

## 2.1 Low-Valent Nickel-Catalyzed Cross-Coupling Reactions of Alkyl Halides

The current knowledge about Ni-catalyzed coupling reactions reveals the following general patterns. The coupling of aryl or vinyl halides with alkylzinc reagents and probably other alkylmetal derivatives occurs according to a classical two-electron catalytic cycle [28]. These reactions are not inhibited by BHT, while TEMPO reacts irreversibly with the organozinc or organonickel compounds to alkoxyamines. Apparently these reactions occur according to a Ni(I)–Ni(III) catalytic cycle. DFT calculations of the elementary steps support this notion. The Ni-catalyzed coupling of alkyl halides **1** with organometallic reagents has been studied in detail recently (Fig. 1) (recent reviews [29–33]). A clear dichotomy was observed in these reactions. Those employing amine or phosphine ligands point to the involvement of radical intermediates. Terao and colleagues reported in contrast the coupling of alkyl halides or alkyl tosylates with alkyl Grignard reagents catalyzed by NiCl<sub>2</sub> in the presence of butadiene and other 1,3-dienes as ligands [34–37]. Experiments using cyclopropylmethyl bromide or 6,6-diphenyl-5-hexenyl fluoride (cf. Part 1, Fig. 8) afforded only ring-closed product for the former and linear coupling products for the latter, thus supporting a two-electron coupling mechanism, which is based on a Ni(II) ate catalyst.

Very often, however, the actual oxidation state of the catalysts in the individual coupling examples is not known exactly. Therefore, all cross-coupling reactions are treated together and it must be kept in mind that most of the applied nickel compounds represent only precatalysts.

Nickel complexes seem to be especially suited to catalyze cross-coupling reactions, in which both partners are sp<sup>3</sup>-hybridized. Scott and coworkers noted

**4a** R<sup>4</sup> = *m*- or *p*-CF<sub>3</sub>**4b** R<sup>4</sup> = *p*-F**5a** R<sup>4</sup> = *s*Bu, R<sup>5</sup> = H**5b** R<sup>4</sup> = *i*Pr, R<sup>5</sup> = H**5c** R<sup>4</sup>, R<sup>5</sup> = H**5d** R<sup>4</sup> = BnCH<sub>2</sub>, R<sup>5</sup> = H**5e** R<sup>4</sup> = CH<sub>2</sub>OMe, R<sup>5</sup> = Ph**5f****8a** R<sup>5</sup> = H**8b** R<sup>5</sup> = *t*Bu**9a** R<sup>4</sup> = Me, R<sup>5</sup> = H**9b** R<sup>4</sup> = I, R<sup>5</sup> = H**9c** R<sup>4</sup> = Me, R<sup>5</sup> = *t*Bu**9d** R<sup>4</sup> = I, R<sup>5</sup> = *t*Bu**10****Fig. 1** Nickel-catalyzed Negishi coupling reactions of alkyl halides **1** with organozinc reagents **2**



the formation of dimers of alkyl halides bearing no  $\beta$ -hydrogen atoms during alkyl–alkyl coupling reactions and attributed them to radical intermediates [38]. Knochel described cross-coupling reactions of alkyl iodides **1** with diorganozinc compounds or arylzinc halides **2** catalyzed by  $\text{Ni}(\text{acac})_2$  giving hydrocarbons **3** with [39–42] or without [43] cocatalysis by trifluoromethylstyrenes **4** (Fig. 1, Table 1, entry 1). It was observed that the reactions were inhibited by 1,4-dinitrobenzene. Clean cross-coupling but no cyclization of 7-iodo-2-heptenoate (see below) was observed. Based on these facts, the authors did not exclude a radical involvement during the process, but a two-electron mechanism was favored.

Fu reported a number of Negishi-type reactions of alkyl halides **1** catalyzed by nickel complexes. Radical intermediates were not mentioned in an initial report on alkyl–alkyl Negishi couplings of primary or secondary alkyl bromides or iodides **1** with alkylzinc halides **2** catalyzed by 4 mol% of  $[\text{Ni}(\text{cod})_2]$  and 8 mol% of (*s*Bu)-PyBOX ligand **5a** (entry 2) [44]. Racemic  $\alpha$ -bromo amides **6a** can be coupled when 10 mol%  $\text{NiCl}_2 \cdot \text{DME}$  and 13 mol% of (*R*)-*i*Pr-PyBOX **5b** were used as the catalyst. Primary alkylzinc bromides gave 51–90% yield and 77–96% ee for the  $\alpha$ -branched amides **7a** (entry 3) [45]. Nitrile, imide, and acetal functions were tolerated in the method. Ligand **5a** gave in contrast only very low yields. The reaction is sensitive to steric factors, since branched bromo amides and secondary alkylzinc reagents could not be applied. The authors excluded a kinetic resolution mechanism. This methodology was applied to the asymmetric synthesis of enantiomerically enriched 1-substituted indanes from racemic 1-bromo or 1-chloro indanes and primary alkylzinc bromides in 39–89% yield and 91–99% ee (entry 4) [46]. Chloride, nitrile, ester, keto, acetal, and imide functions are tolerated. Racemic 1-phenylethyl bromide reacted similarly in 63% yield, but the ee of the coupling product amounted only to 75%.

In parallel, Vicic and coworkers studied alkyl–alkyl cross-coupling reactions of alkyl iodides with alkyl zinc reagents catalyzed by  $\text{Ni}(\text{terpy})$  complexes (entry 5) [8]. In an initial publication it was shown that the complex  $(\text{TMEDA})\text{NiMe}_2$  underwent a ligand exchange reaction with terpy **8a** with formation of a  $(\text{terpy})\text{Ni}(\text{I})\text{Me}$  complex **9a**; 5 mol% of this complex catalyzed the cross-coupling reaction in 60–65% yield. In a stoichiometric experiment it was shown that the product mixture consisted of the hydrocarbon and the Ni(I) complex  $(\text{terpy})\text{NiI}$  **9b**. The in situ generated Ni(I) complex **9b** from  $\text{Ni}(\text{cod})_2$ , terpy **8a** and MeI was similarly active in cross-coupling reactions. Homocoupling products were observed in minor amounts. Cyclopropylmethyl iodide afforded the ring-opened product in substantial amounts (cf. Part 1, Fig. 8). In a subsequent study using deuterated and non-deuterated complexes it was determined that the formation of  $(\text{terpy})\text{Ni}^{\text{I}}\text{Me}$  **9a** occurs by a non-radical pathway, most likely by comproportionation of unstable  $(\text{terpy})\text{Ni}(0)$  and  $(\text{terpy})\text{NiMe}_2$  [47]. To gain detailed insight into the couplings, complexes **9a–d** were structurally characterized [9]. Reaction of an alkyl iodide with Ni(I) complex **9c** leads to the corresponding isolable ionic (*t*Bu<sub>3</sub>-terpy)Ni(II)Me halide complex. Reaction of this material with an alkylzinc reagent **2** hardly proceeded, while that of methyl Ni(I) complex **9c** and an alkyl halide **1** gave 90% of the cross-coupling product **3**.

In preparative experiments it was shown that 5 mol% of **9a–d** were effective to catalyze the cross-coupling. The tri(*tert*-butyl)terpy complexes **9c,d** proved to be

**Table 1** Nickel-catalyzed cross-coupling reactions

Entry	R <sup>3</sup>	M	Y	Catalyst/ligand	Additive	Yield [%] (% ee)	Ref.
1	Ar, Alkyl	Zn	Hal, Alkyl	Ni(acac) <sub>2</sub> (10 mol%)	<b>4</b>	66–92	[39–43]
2	Alkyl	Zn	Br	Ni(cod) <sub>2</sub> (4 mol%), <b>5a</b> (8 mol%)	–	62–91	[44]
3	Alkyl	Zn	Br	NiCl <sub>2</sub> •DME (10 mol%), <b>5b</b> (13 mol%)	–	51–90 (77–96)	[45]
4	Alkyl	Zn	Br	NiBr <sub>2</sub> •diglyme (10 mol%), <b>5b</b> (13 mol%)	–	39–89 (91–99)	[46]
5	Alkyl	Zn	Br	<b>9a–d</b> (5 mol%)	–	60–65	[8, 47]
6	Alkyl	Zn	Br	Ni(py) <sub>4</sub> Cl <sub>2</sub> (10 mol%), <b>5a</b> (10 mol%)	–	59–79	[48]
7	Alkyl	Zn	Br	NiCl <sub>2</sub> (10 mol%), <b>5c</b> (15 mol%)	–	40–76	[49, 50]
8	Ar	Zn	Br	Ni(cod) <sub>2</sub> (10 mol%), <i>t</i> Bu <sub>3</sub> -terpy <b>8b</b> (15 mol%)	–	40–83	[50]
9	Alkyl	Zn	Br	NiCl <sub>2</sub> •DME (5 mol%), <b>5d</b> (5.5 mol%)	–	54–97 (69–98)	[51]
10	Alkyl	Zn	Br	NiCl <sub>2</sub> •DME (10 mol%), <b>8a</b> (10 mol%) or <b>10</b>	–	63–97	[52]
11	Ar	Zn	Et	NiCl <sub>2</sub> •DME (3 mol%), <b>5f</b> (3.9 mol%)	–	39–92 (92–94)	[53]
12	Ar	Zn	I	NiCl <sub>2</sub> •DME (5 mol%), <b>5e</b> (6.5 mol%)	–	71–93 (72–96)	[54]
13	<b>11a</b>			Ni(cod) <sub>2</sub> (4 mol%), <b>12</b> (8 mol%)	KO <i>t</i> Bu	44–91	[55]
14	<b>11a</b>			NiI <sub>2</sub> (6 mol%), <b>14</b> (6 mol%)	NaHMDS or KHMDS	68–92	[56]
15	<b>11a</b>			Ni(PPh <sub>3</sub> ) <sub>4</sub> (5 mol%)	K <sub>3</sub> PO <sub>4</sub>	55–95	[57]
16	<b>11b</b>			NiCl <sub>2</sub> •DME (6 mol%), <b>15</b> (8 mol%)	KO <i>t</i> Bu, <i>i</i> BuOH	64–94	[58]
17	<b>11b</b>			Ni(cod) <sub>2</sub> (10 mol%), ( <i>R,R</i> )- <b>16a</b> (12 mol%)	KO <i>t</i> Bu, <i>i</i> BuOH	62–86 (40–94)	[59]

(continued)

Table 1 (continued)

Entry	R <sup>3</sup>	M	Y	Catalyst/ligand	Additive	Yield [%] (% ee)	Ref.
18	<b>11b</b>			NiBr <sub>2</sub> •diglyme (6 mol%), <i>rac</i> - <b>16b</b> (8 mol%)	KO <i>t</i> Bu, <i>i</i> BuOH	53–86	[60]
19	<b>11b</b>			NiBr <sub>2</sub> •diglyme (10 mol%), ( <i>S,S</i> )- <b>16b</b> (12 mol%)	KO <i>t</i> Bu, <i>n</i> -C <sub>6</sub> H <sub>13</sub> OH	54–82 (90–98)	[61]
20	<b>11c</b>			NiBr <sub>2</sub> •diglyme (8 mol%), ( <i>S,S</i> )- <b>16a</b> (10 mol%)	KO <i>t</i> Bu, <i>i</i> BuOH	70–89 (84–94)	[62]
21	Ar	Si	F	NiBr <sub>2</sub> •diglyme (6.5 mol%), <b>12</b> (7.5 mol%)	CsF	60–86	[63]
22	Ar	Si	F	NiCl <sub>2</sub> •DME (10 mol%), <b>22</b> (15 mol%)	CsF, cat. LiHMDS	59–92	[64]
23	Ar, vinyl	Si	OMe	NiCl <sub>2</sub> •DME (10 mol%), ( <i>S,S</i> )- <b>16b</b> (12 mol%)	TBAT	64–84 (75–99)	[65]
24	Alkyl, Ar	Mg	Cl, Br	Ni(dppf)Cl <sub>2</sub> (10 mol%)	–	42–94	[66]
25	Ar	Mg	Br	NiCl <sub>2</sub> (5 mol%), <b>23</b> (10 mol%)	–	60–84	[67]
26	Alkyl	Mg	Cl	<b>24a</b> (1–12 mol%)	–	39–88	[68–70]
27	Ar	Mg	X	<b>24a</b> (1–12 mol%)	TMEDA		[71]
28	Ar	Mg	Br	NiCl <sub>2</sub> •DME (7 mol%), <b>25a</b> or <b>b</b> (9 mol%)	–	70–91 (72–95)	[72]
29	Alkynyl	Cu	–	<b>24a</b> (5 mol%), CuI (3 mol%)	Cs <sub>2</sub> CO <sub>3</sub> , NaI or Bu <sub>4</sub> NI <sup>a</sup>	57–89	[73]
30	Alkynyl	In	Alkynyl	NiBr <sub>2</sub> •diglyme (10 mol%), <b>5b</b> (13 mol%)	–	35–70 (77–87)	[74]
31	Ar	Sn	Cl	NiCl <sub>2</sub> (10 mol%), <b>26</b> (15 mol%)	KO <i>t</i> Bu, <i>i</i> BuOH, <i>i</i> BuOH	47–86	[75]
32	Vinyl	Zr	Cp <sub>2</sub> Cl	NiCl <sub>2</sub> •DME (3 mol%), <b>25c</b> (3.6 mol%)	–	74–95 (80–98)	[76]
33	Ar	Fe	Ar	Ni content in 98% FeCl <sub>2</sub>	TMPMgCl•LiCl	65–88	[77]

<sup>a</sup>For in situ Finkelstein exchange

optimal to achieve high yields. Structural studies of complexes **9** showed that the Ni(I) complexes carry much of their spin density at the ligand according to ESR spectral investigations [47]. A whole range of structurally related ligands were studied with respect to their ability to promote alkyl–alkyl Negishi couplings; however, complexes **9** proved to be optimal.

Negishi-type cross-coupling reactions of primary and secondary alkyl iodides **1** and alkylzinc bromides **2** proceeded with 10 mol% of Ni(py)<sub>4</sub>Cl<sub>2</sub>/(*s*Bu)-PyBOX **5a** (entry 6) [48]. Based on calculations, an alkylNi(I)(PyBOX) complex is formed by initial SET reduction, which carries much of the spin density in the ligand, similar to Vicic's catalysts **9**. Based on this result a Ni(I)–Ni(II)–Ni(III) catalytic cycle was proposed to operate.

Gagne and colleagues applied Fu's method to alkyl–alkyl Negishi coupling reactions of glycosyl halides (entry 7) [49, 50]. Using 10 mol% of NiCl<sub>2</sub> and 15 mol% of the unsubstituted PyBOX ligand **5c**, moderate β-diastereoselectivity for glucosyl and galactosyl bromides was observed, while mannosyl bromide reacted with good α-selectivity. The yields of coupling products amounted to 40–76%. Glycals, which are commonly formed according to an E1cB mechanism, were detected only in 3–25% yield. The study was also extended to Vicic's catalyst **9** derived from terpy **8**, which provided methyl C-glucoside with MeZnI exclusively as the β-anomer in 60% yield (entry 8) [50]. An extension to other alkylzinc halides was, however, not possible. Ligand **8b** proved to be the catalyst of choice for the coupling of glycosyl bromides with arylzinc halide•LiCl complexes. Glucosyl bromides afforded aryl glucosides in 30–83% yield and good to excellent β-selectivity. The PyBOX ligands **5** were not effective in promoting the cross-coupling. Glycosyl chlorides gave only low yields of coupling products. Mannosyl bromides reacted with the PhZnI•LiCl complex using both Ni(PyBOX) and Ni(terpy) catalysis; the former, however, provided a significantly higher diastereoselectivity in favor of the α-anomer. These results were taken as evidence that the catalytic cycles with the Ni(PyBOX) and Ni(terpy) catalysts differ but that radical processes are involved. The methodology was applied to the total synthesis of the C-glycosidic natural product Salmochelin SX [50].

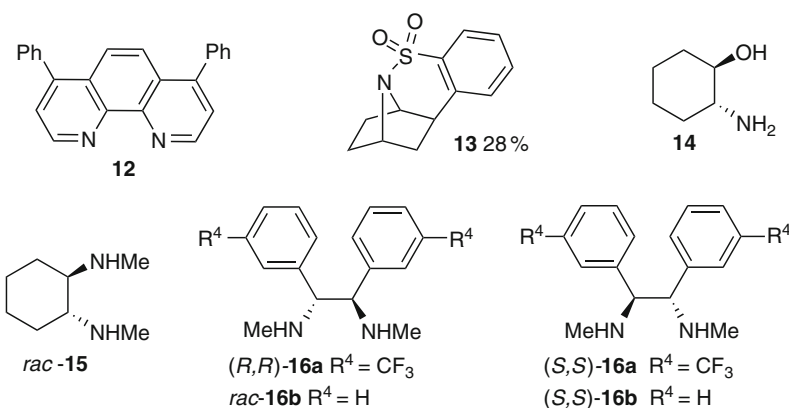
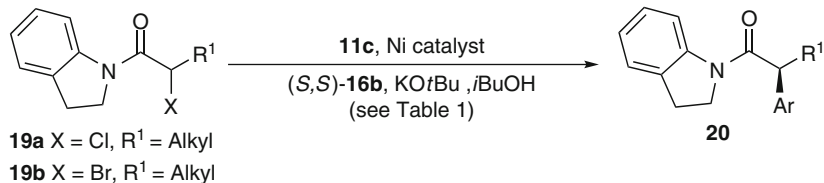
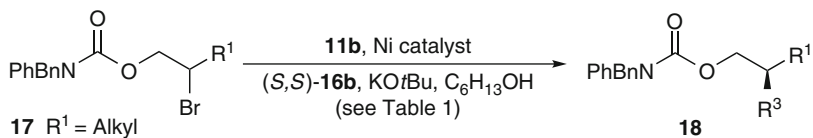
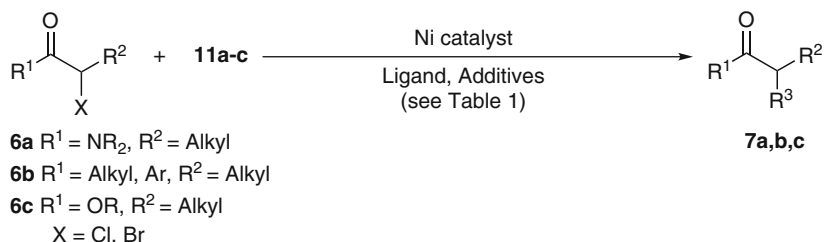
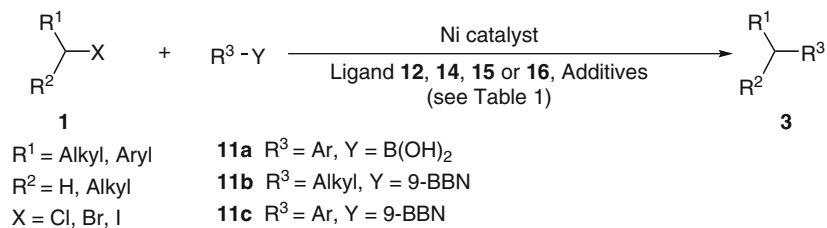
Similar coupling reactions were also reported for 1,3-disubstituted allylic chlorides using a catalyst generated from NiCl<sub>2</sub>•DME and ligand **5d** (entry 9). Unsymmetrical allylic chlorides reacted often with good regioselectivity when the two termini are sufficiently differentiated [51]. Propargylic chlorides or bromides were transformed to products **3** with primary and secondary organozinc reagents in the presence of 10 mol% of a catalyst composed of NiCl<sub>2</sub>•DME and **8a** (entry 10) [52]. The reaction is limited to alkynes bearing bulky groups at the alkyne terminus. If the alkylzinc is sterically more demanding, 2,6-bis(pyrazol-1-yl)pyridine **10** proved to be the more efficient ligand. The methodology was applied to the total synthesis of the terpene α-cembra-2,7,11-triene-4,6-diol. An asymmetric propargylation of aryl(ethyl)zinc reagents was developed using 3 mol% of NiCl<sub>2</sub>•DME and 3.9 mol% of indane-based PyBOX ligand **5f** (entry 11) [53]. The reaction gave 1-substituted propargylarenes in 39–92% yield and 84–94% ee. The aryl group of phenyl(ethyl)zinc obtained by transmetalation of phenylboronic acid

with diethylzinc was transferred selectively. It must be mentioned that the more activated allylic and propargylic halides may also react by a two-electron oxidative addition/transmetalation/reductive elimination pathway.

Fu's group showed more recently that  $\alpha$ -bromo ketones **6b** can be coupled with arylzinc halides catalyzed by 5 mol% NiCl<sub>2</sub>·DME and 6.5 mol% of PyBOX ligand **5e** with good asymmetric induction providing benzylic ketones in 71–93% yield and 72–96% ee (entry 12) [54]. The lower ee values were obtained with *ortho*-substituted aryl bromo ketones, while *ortho*-substituted arylzinc reagents as well as  $\alpha$ -branched bromo ketones did not react.

A significant effort was made to develop nickel-catalyzed alkyl–aryl Suzuki–Miyaura coupling reactions (Fig. 2). When primary and secondary alkyl bromides or iodides **1** reacted with aryl or vinylboronic acids **11a** catalyzed by 4 mol% [Ni(cod)<sub>2</sub>] and 8 mol% of bathophenanthroline **12**, alkylarenes **3** were isolated in 44–91% yield (entry 13) [55]. The stereoconvergent formation of *exo*-alkylnorbornanes (cf. Part 1, Fig. 9) from either *exo*- or *endo*-norbornyl bromide with phenylboronic acid indicated the involvement of radical intermediates. PyBOX ligand **5a** was ineffective. These conditions were subsequently applied to access biologically active epibatidine analogs from 7-bromo-2-azabicycloheptanes and aryl and hetarylboronic acids **11a** [78, 79]. *syn/anti*-Mixtures of 7-(het)aryl-2-azanorbornanes were isolated in 30–50% yield. The formation of isomeric products from diastereomerically pure starting materials supports the occurrence of radicals in the process; however, it was also shown that base-mediated epimerization contributes to the overall stereochemical outcome. Armstrong et al. designed around the same time a total synthesis of epibatidine itself and of analogs using a similar nickel-catalyzed alkyl–aryl Suzuki cross-coupling [80]. Starting materials were the isomeric 7-protected *endo*- or *exo*-2-bromo-7-azabicyclo[2.2.1]heptanes, which underwent clean cross-coupling using 10 mol% of Ni(cod)<sub>2</sub> and 20 mol% of **12** in the presence of KO<sup>t</sup>Bu. Both isomeric bromides having a Boc protecting group led to the same *exo*-cross-coupling product, which is in line with a radical mechanism, though the yields varied significantly. A 7-*N*-tosyl-protected precursor afforded in contrast the tricyclic product **13** albeit only in 28% yield. The formation of this product supports a radical pathway strongly, since its formation can be rationalized only by reductive radical generation by the Ni(0) catalyst, a subsequent radical 6-*endo* cyclization and rearomatization by hydrogen abstraction.

Based on these results, *trans*-2-aminocyclohexanol **14** was devised as a suitable ligand for promoting Suzuki–Miyaura coupling reactions of primary and secondary alkyl chlorides, bromides, or iodides **1** with **11a** in the presence of NaHMDS or KHMDS as a base (entry 14) [56]. Branched alkylarenes were isolated in 68–92% yield. The reaction course was supported by the stereoconvergent preparation of *exo*-arylnorbornanes from either *exo*- or *endo*-norbornyl bromides (cf. Part 1, Fig. 9) and by radical cyclizations. Duncton and colleagues applied this method to accomplish cross-coupling reactions of 3-iodooxetanes with arylboronic acids **11a** [81]. Using 6 mol% of NiI<sub>2</sub> and 6 mol% of **14**, 35–69% of 3-aryloxetanes were isolated. Heteroaromatic boronic acids were not applicable under the reaction conditions, suggesting that they block necessary coordination sites at the catalyst



**Fig. 2** Nickel-catalyzed alkyl–alkyl and alkyl–aryl Suzuki–Miyaura coupling reactions

competitively. Small amounts of biaryls were isolated in most cases probably resulting from initial reduction of the Ni(II) precatalyst.

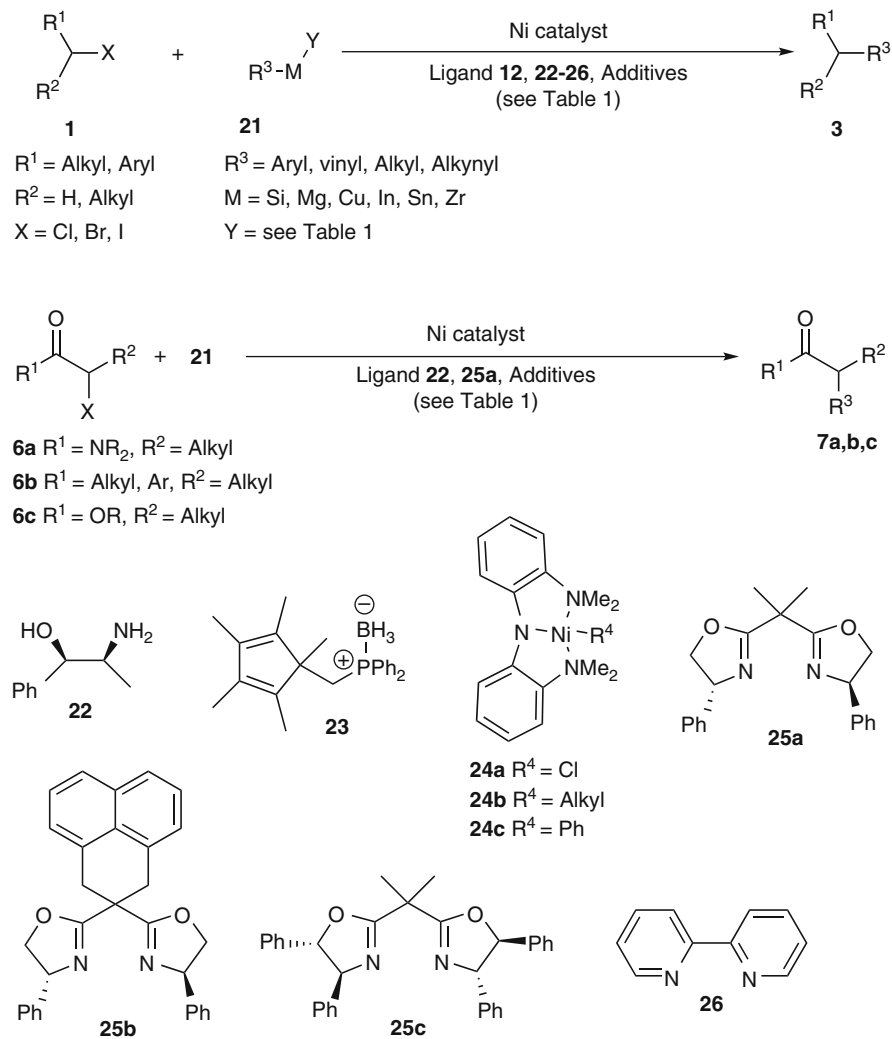
Liu and coworkers found almost at the same time that 5 mol% Ni(PPh<sub>3</sub>)<sub>4</sub> catalyzed the Suzuki–Miyaura coupling of **11a** with  $\alpha$ -bromo esters, amides, or ketones **6a–c** resulting in arylacetic acid derivatives **7a,c** in 55–95% yield (entry 15) [57].  $\alpha$ -Chloroketones **6b** reacted in 60–75% yield to benzylic ketones **7b**.

Suzuki alkyl–alkyl coupling reactions were developed by Fu's group [58]. A combination of 6 mol% of NiCl<sub>2</sub>•DME and 8 mol% of racemic *trans*-*N,N'*-dimethylcyclohexan-1,2-diamine **15** proved to be optimal for the coupling of secondary alkyl bromides or primary alkyl iodides **1** with 9-alkyl-9-BBN **11b** in the presence of KO*t*Bu as a base (entry 16). The products were isolated in 64–94% yield. The involvement of radicals is supported by the stereoconvergent formation of *exo*-alkylnorbornanes from the individual *exo*- or *endo*-norbornyl bromides (cf. Part 1, Fig. 9). An asymmetric variant, which is applicable to secondary homobenzylic bromides, was developed in Fu's group (entry 17) [59]. Using 10 mol% of Ni(cod)<sub>2</sub> and 12 mol% of 1,2-diarylethylene diamine ligand (*R,R*)-**16a** afforded 62–86% of  $\beta$ -branched alkylarenes displaying ee values of 40–94%. The lower values in the ee range result probably from competitive coordination of ether substituents to the nickel catalyst. The method was extended to alkyl–alkyl Suzuki coupling reactions applying alkyl chlorides and **11b** using 6 mol% NiBr<sub>2</sub>•diglyme as the precatalyst and 8 mol% *rac*-*N,N'*-dimethyl-1,2-diphenylethylenediamine **16b** as the ligand in diisopropyl ether (entry 18) [60]. Under these conditions, 53–83% of products were isolated. Alkyl bromides and iodides also couple. Competition experiments revealed a >15:1 reactivity order in the initial rates of iodide:bromide and bromide:chloride, respectively. Very recently, Owston and Fu disclosed that carbamate protected bromohydrins **17** undergo asymmetric alkyl–alkyl Suzuki coupling reactions with **11b** in the presence of KO*t*Bu as the base catalyzed by 10 mol% NiBr<sub>2</sub>•diglyme and 12 mol% of **16b** (entry 19) [61].  $\beta$ -Branched carbamates **18** were isolated in 54–82% yield with 90–98% ee. An anisoyl-protected bromohydrin also reacted in good yield, but with diminished ee. Chlorohydrins and 3-bromoalkyl carbamates are applicable as substrates. For the latter the trifluoromethyl-substituted ligand (*S,S*)-**16a** furnished the product in better yield and ee.

Recently an asymmetric alkyl–aryl Suzuki–Miyaura coupling reaction of racemic  $\alpha$ -chloro amides **19a** with 9-aryl-9-BBN **11c** catalyzed by 8 mol% NiBr<sub>2</sub>•diglyme as the precatalyst and 10 mol% (*S,S*)-1,2-bis(3-trifluoromethyl)-*N,N'*-dimethylethylenediamine (*S,S*)-**16a** as the ligand was found (entry 20) [62]. The reaction occurred under very mild conditions using KO*t*Bu as the base and *i*BuOH as an additive at –5°C in 70–89% yield and 84–94% ee. In contrast to all other methodology reported before, in which the starting  $\alpha$ -halo carbonyl compound **6** remained racemic throughout the course of the reaction, in the present case a kinetic resolution of *N*-(2-chloropropionyl)indolines **19a** occurred leaving the starting material with substantial ee at intermediate conversions. The corresponding bromopropionamide **19b**, however, remained racemic at any point of the reaction. Control experiments showed that the overall oxidative addition process is irreversible, since the ee of the starting material **19a** remained constant throughout the reactions when both enantiomers

were reacted individually. The formation of the coupling product **20** is, however, stereoconvergent, since both enantiomers of **19a** led to the same enantiomer of **20** with identical ee. Thus the mechanism of generation of the alkylnickel intermediate during the coupling of **19a** seems to be different from all other cross-coupling reactions before.

Hiyama coupling reactions applying primary and secondary alkyl bromides or iodides **1** and aryltrifluorosilanes **21** ( $M = \text{SiF}_3$ ) catalyzed by 6.5 mol%  $\text{NiBr}_2 \cdot \text{DME}$  and 7.5 mol% bathophenanthroline **12** are viable to obtain branched



**Fig. 3** Hiyama, Kumada–Corriu, Stille, Sonogashira, and other nickel-catalyzed coupling reactions



alkylarenes **3** in 60–86% yield (entry 21) (Fig. 3) [63]. CsF proved to be mandatory as an activator. Ester, nitrile, ketone, or amide functions are tolerated in the reactions. Both *exo*- and *endo*-norbornyl bromide gave *exo*-phenylnorbornane in 96:4 and 94:6 selectivity (cf. Part 1, Fig. 9). Small amounts of biphenyl were detected indicating the in situ reduction of Ni(II). The scope of this reaction could be extended when norephedrine **22** (12 mol%) was applied with 10 mol% of NiCl<sub>2</sub>•DME (entry 22) [64]. Simple secondary alkyl bromides or iodides **1** coupled with aryltrifluorosilanes in 59–89% yield.  $\alpha$ -Bromo amides,  $\alpha$ -bromo ketones,  $\alpha$ -bromo esters **6a–c**, and even  $\alpha$ -bromo phosphonates or  $\alpha$ -bromo nitriles were coupled under identical conditions in 60–92% yield. Excess CsF proved to be necessary as a promoter. An enantioselective coupling protocol for racemic  $\alpha$ -bromo esters **6c** and aryl or vinyl trimethoxysilanes **21** (M = Si(OMe)<sub>3</sub>) was also developed (entry 23) [65]. Using a catalyst assembled from 10 mol% NiCl<sub>2</sub>•DME and 12 mol% of (*S,S*)-**16b**  $\alpha$ -aryl and  $\alpha$ -vinyl-branched esters **7c** were obtained in 64–84% yield and 75–99% ee (highlight [82]). The reactions work best with 2,6-di-*tert*-butyl-4-methylphenyl (BHT) esters. The enantioselectivity of the reactions is sensitive to the steric bulk of the alkyl chain as more branched esters tend to give lower ee values.

Nickel-catalyzed Kumada-couplings are also viable (highlight [83]). Yuan and Scott reported the first examples of alkyl-Kumada coupling reactions employing neopentyl-type iodides **1** and alkyl or aryl Grignard reagents **21** (M = Mg) in the presence of 10 mol% Ni(dppf)Cl<sub>2</sub> (entry 24) [66]. The cross-coupling products **3** were isolated in 42–94% yield. Some dimerization and reduction of the alkyl iodide were observed in the coupling reactions with alkyl Grignard reagents indicating the involvement of radical intermediates. Oshima et al. developed ligand **23** for the coupling reactions of primary alkyl bromides or iodides with aryl Grignard reagents (entry 25) [67]. With 5 mol% of NiCl<sub>2</sub> the formation of alkylarenes **3** was observed in 60–84% yield. Secondary alkyl bromides and alkyl chlorides are much less reactive. The reaction course is supported by isolation of the ring-opened product in 58% yield when cyclopropylmethyl bromide was applied as the substrate (cf. Part 1, Fig. 8).

Recently Hu and colleagues reported the cross-coupling of Grignard reagents with dichloromethane or chloroform catalyzed by 1–12 mol% of nickel pincer complex **24a** (entry 26) [68]. The reactions occurred rapidly under very mild conditions (–20°C for 0.5 h) and gave the corresponding hydrocarbons in 23–81% yield. Aryl halides were inert under the reaction conditions, and thus the catalytic system is uniquely suited for alkyl–alkyl couplings. The reaction proceeds by initial alkylation of nickel complex **24a** leading to isolable alkylnickel(II) complex **24b**. The corresponding ethyl complex was characterized by X-ray crystallography. Based on these results, the scope of alkyl–alkyl Kumada coupling reactions of alkyl bromides with alkyl Grignard reagents catalyzed by nickel pincer complex **24a** was studied [69, 70]. Functionalized hydrocarbons are accessible in 56–99% yield applying 3 or 9 mol% of the catalyst in dimethylacetamide at –35°C for 30 min. Primary and secondary alkyl iodides or bromides reacted efficiently with linear or  $\beta$ -branched Grignard reagents. Competition experiments proved iodides more reactive than bromides and primary iodides slightly more reactive

than secondary. Alkyl chlorides were inert. Benzylic Grignard reagents gave only low yields, while secondary and tertiary Grignard reagents failed to react. The methodology tolerates ester, nitrile, ketone, and acetal functions. The ring opening of cyclopropylmethyl bromide and retardation in the presence of TEMPO support a Ni(II)–Ni(III)–Ni(IV) catalytic cycle involving free radicals. It was later shown that branched Grignard reagents undergo isomerization under the reaction conditions, since linear coupling products were observed as the sole products [84]. This indicates that branched Grignard reagents are transmetalated fast by nickel pincer complex **24a** and that  $\beta$ -hydride elimination and hydronickelation are faster than SET reduction of the alkyl halide.

Conditions to catalyze alkyl–aryl Kumada couplings were also reported (entry 27) [71]. When THF was applied as a solvent and TMEDA was used as an additive, 3 mol% of **24a** sufficed to promote the formation of alkyl(het)arenes **3** from primary and secondary alkyl iodides or bromides **1** in 51–99% yield. Alkyl chlorides and isopropyl halides gave only low yields, while tertiary alkyl iodides and *ortho*-substituted Grignard reagents did not afford the desired products. The protocol is applicable to alkyl halides bearing ester, nitrile, amide, carbamate, acetal, or fluoride substituents. The reactions with ketones were substrate-dependent. Knochel's method for the preparation of functionalized aryl Grignard reagents by halogen–magnesium exchange using *i*PrMgCl and the corresponding aryl halides can also be applied, giving 27–99% of coupling products. Stoichiometric control experiments showed that the air-stable arylnickel complex **24c** can be isolated after workup. It acts as a competent catalyst. The intermediacy of radicals was also shown here by the exclusive isolation of ring-opened products when cyclopropylmethyl bromide was applied in the coupling reaction (cf. Part 1, Fig. 8)

More recently, Lou and Fu reported the first asymmetric Kumada coupling reactions of racemic aryl  $\alpha$ -bromoalkyl ketones **6b** with aryl Grignard reagents catalyzed by 7 mol% NiCl<sub>2</sub>•DME and 9 mol% of diphenyl-BOX ligand **25a** under very mild conditions (entry 28) [72]. The resulting benzylic ketones **7b** were isolated in 72–91% yield and 72–95% ee. Nitrile, ester, trifluoromethyl, and halo functions as well as indole units are well tolerated under the reaction conditions. *ortho*-Substituted Grignard reagents or *ortho*-substituted aryl ketones reacted in good yield, but the ee of the products **7b** amounted only to 80% and 72%, respectively.  $\alpha$ -Bromo dialkyl ketones transformed only with modest enantioselectivity. Good ee values were, however, achieved by use of sterically more demanding ligand **25b**. Alkyl benzyl ketones **7b** were obtained under these conditions in 70–90% yield and with 73–90% ee.

Based on these results, conditions for alkyl–Sonogashira coupling reactions were developed. Primary alkyl halides reacted with terminal alkynes catalyzed by 5 mol% of complex **24a** and CuI in the presence of substoichiometric amounts of NaI for bromides or Bu<sub>4</sub>NI for alkyl chlorides (entry 29) [73]. The latter serves to catalyze the in situ generation of more reactive alkyl iodides under the reaction conditions. The internal alkyne products were isolated in 57–89% yield. The Sonogashira coupling can also be combined to the Kumada reaction described above.  $\alpha,\omega$ -Chloroalkyl bromides underwent the Kumada coupling first selectively

at the more reactive bromide function, followed by the Sonogashira coupling step of the chloride in 69–86%.

Cairo and colleagues coupled racemic benzylic bromides **1** with alkynylindium compounds **21** (M=In) catalyzed by a nickel complex generated from 10 mol% NiBr<sub>2</sub>•diglyme and 13 mol% of (*S,S*)-**5b** (entry 30) [74]. Reasonable to good ee values of 77–87% were observed for the benzyl alkyne products. The isolated yields were, however, a rather moderate 35–70%.

Stille coupling reactions of alkyl halides with aryltrichlorostannanes catalyzed by 10 mol% NiCl<sub>2</sub> and 15 mol% proceeded in 47–86% yield (entry 31) ([75]; highlight [85]). The intermediacy of radicals was proven by the stereoconvergent *exo*-selective coupling of the diastereomeric norbornyl bromides (cf. Part 1, Fig. 9) and radical cyclizations. Ni(cod)<sub>2</sub>, NiBr<sub>2</sub>, or NiBr<sub>2</sub>•diglyme could be used as precatalysts with similar efficiency. The reaction requires, however, a rather large excess of KO<sup>t</sup>Bu as a base.

Lou and Fu demonstrated that vinylzirconium reagents are also viable coupling partners for  $\alpha$ -bromo ketones **6b** providing access to  $\beta,\gamma$ -unsaturated ketones (entry 32) [76]. Using 3 mol% of NiCl<sub>2</sub>•DME and 3.6 mol% of BOX ligand **25c** as the catalyst furnished 74–95% yield of coupling products **7b** with 80–98% ee. Chloride, nitrile, ester, or trifluoromethyl functionalities are tolerated under the reaction conditions. The interaction of the catalyst with the substrate is the determining factor for the asymmetric induction, as  $\alpha'$ -residing stereocenters did not influence the sense and extent of asymmetric induction (catalyst control).  $\alpha$ -Bromo dialkyl ketones were coupled with similar results.

Wunderlich and Knochel recently published the alkylation of diaryliron compounds by alkyl iodides or benzyl chloride **1** (entry 33) [77]. The reaction works well with 98% pure FeCl<sub>2</sub>•2LiCl but not with 99.998% pure metal salt. Addition of other transition metal salts showed that nickel contained in the FeCl<sub>2</sub> of 98% purity is the likely catalyst. Alkylarenes **3** were obtained in 65–88% yield. The method tolerates ester, nitrile, fluoride, or chloride substituents. Although the use of 5-hexenyl iodide did not provide a cyclized product, the initial formation of radicals cannot be excluded safely.

There is good evidence that all presented nickel-catalyzed coupling reactions of alkyl halides involve the generation of radical intermediates. However, the catalytic cycles through which the individual coupling reactions proceed may vary with respect to the oxidation state, the electronic and steric structure of the precatalyst, the strength of the reducing agents in the reaction mixture, and the nucleophilicity of the coupling partner. It is well known that nickel(II) amine or phosphine precatalysts may be reduced easily to Ni(0) or Ni(I) complexes. Nickel(II) pincer complexes, such as **24a**, are, in contrast, not reduced to low-valent nickel species due to their coordination geometry [71]. A number of alkyl and arylnickel complexes in the oxidation states +I and +II, such as **9a,c** or **24b,c**, were structurally characterized and their catalytic competence was determined [8, 9, 47, 68, 69]. Moreover, some complexes, such as **9** (or those derived from pyBOX **5**), are able to form valence tautomeric structures **9A** and **9B** having ligand-centered radicals and regular metal oxidation states (Fig. 4) [47].

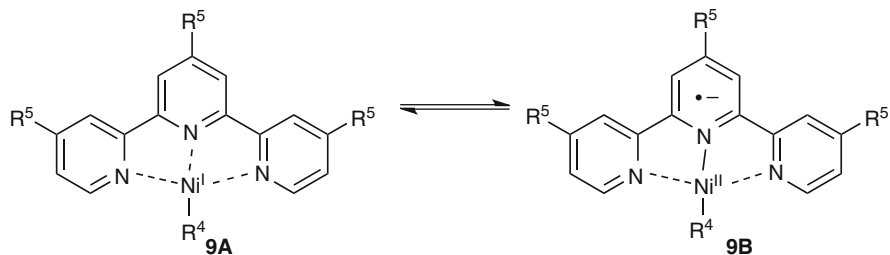


Fig. 4 Valence tautomeric (terpy)Ni(I) complexes

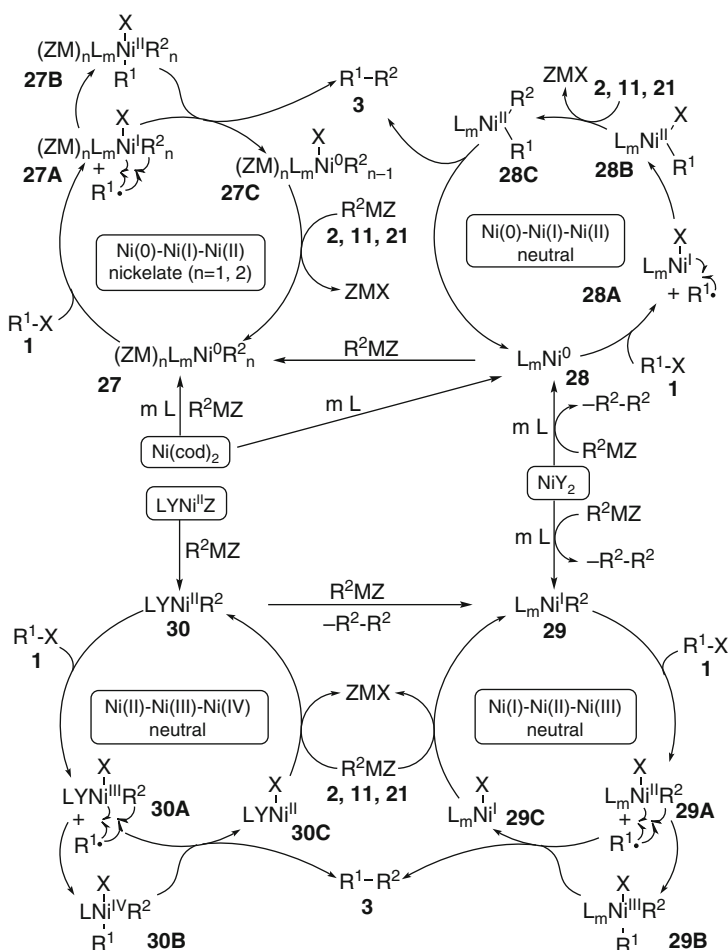


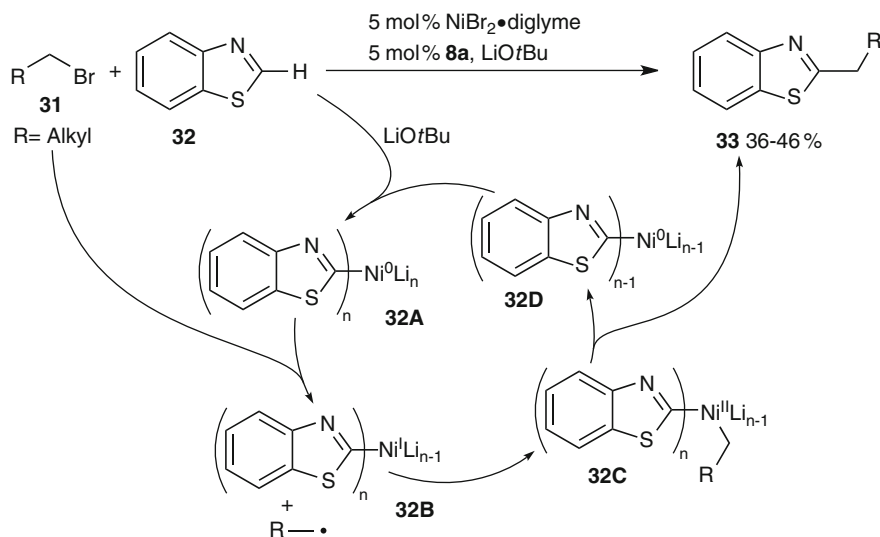
Fig. 5 Catalytic cycles of nickel-catalyzed cross-coupling reactions

Thus, catalytic reactions can occur variably at Ni(0)–Ni(I)–Ni(II), Ni(I)–Ni(II)–Ni(III), and Ni(II)–Ni(III)–Ni(IV) oxidation states (Fig. 5). Some precatalysts are able to form ate complexes, which are catalytically active. Thus neutral and anionic catalytic cycles are possible. Common to most of them is that at first an ate complex **27** or organonickel complexes **29**, **30** are formed from the nickel precatalysts and the nucleophilic organometallic component. Only these more electron-rich species are able to reduce alkyl halides **1** to radicals. These couple with the oxidized complexes **27A**, **29A**, or **30A**. This may occur either directly at the bound organic residue of these complexes providing products **3** directly. Alternatively, attack at the metal leading to diorganonickel complexes **27B**, **29B**, or **30B** is possible. Reductive elimination of the latter generates products **3** and reduced metal complexes **27C**, **29C**, or **30C**, which are able to reenter the catalytic cycle by transmetalation with the organometallic nucleophile.

For neutral nickel(0) complexes **28** another cycle operates. It should be electron-rich enough to reduce **1** giving a radical and nickel(I) complex **28A**. Coupling may precede transmetalation and leads to organonickel(II) complex **28B**. This is subject to transmetalation by the nucleophile. The resulting diorganonickel(II) **28C** is finally subject to reductive elimination giving product **3** and the reduced nickel catalyst **28**. The mechanistic course of the reactions is also supported by a theoretical investigation [86]. In principle, the catalytic cycles may even interchange, since the oxidation states can be modulated by the organometallic components. Overall these catalytic cycles are similar to those of the corresponding iron- or cobalt-catalyzed cross-coupling reactions (see Part 2, Sects. 2.1.1 and 5.2).

## 2.2 *Ni(0)–Ni(I)–Ni(II) Catalysis: Coupling Reactions of Alkyl Halides with Unsubstituted Arenes*

Recently, the cross-coupling of unactivated arenes with different aryl compounds moved to the center of interest. These reactions proceed mostly by two-electron catalytic cycles. Yao et al. developed very recently a method to couple unfunctionalized (benz)oxazoles or benzothiazoles with alkyl bromides **31** (Fig. 6) [87]. While the corresponding oxazoles react palladium-catalyzed according to a two-electron catalytic cycle, benzothiazole **32** did not afford a product under palladium catalysis. However, when a catalyst prepared from 5 mol% NiBr<sub>2</sub>•diglyme/terpy **8a** was applied together with excess LiOtBu as the base, the coupling reaction to 2-alkylbenzothiazoles **33** was observed in moderate yield. The reaction course may be explained by a base-assisted oxidative addition of an initially generated Ni(0) complex to **32** forming an ate complex **32A**. This electron-rich species mediates the reductive generation of the alkyl radical, which couples to the cogenerated Ni(I) species **32B**. The mixed alkylnickel(II) complex **32C** undergoes reductive elimination affording the product **33** and the active catalyst **32D**. The participation of radical intermediates is supported by radical



**Fig. 6** Nickel-catalyzed alkylation of benzothiazole via C–H insertion

5-exo cyclization and cyclopropylcarbinyl radical ring opening reactions (cf. Part 1, Fig. 8).

Hu and colleagues reported in parallel similar coupling reactions of electron-poor and electron-rich heterocycles with alkyl halides applying 5 mol% catalyst **24a** and 5 mol% CuI [88]. Complex **24a** served only as a precatalyst, the actual catalytically active species seeming to be a low-valent nickel species devoid of the ligand according to NMR investigations. CuI is not mandatory, but facilitates the process. Alkylhetarenes were formed in 44–86% yield.

### 2.3 Ni(0)–Ni(I)–Ni(II) Catalysis: Radical Addition Reactions

Nickel(0) phosphine complexes are very well suited to catalyze radical reactions (Fig. 7). In 1988, Lebedev and coworkers found a nickel-catalyzed addition of aryl and alkyl halides **34** to olefins **35** [89]. Using a catalytic system composed of 5 mol% NiCl<sub>2</sub>, 10 mol% of PPh<sub>3</sub>, zinc as the stoichiometric reducing agent, and pyridine as a ligand and base, styrenes **35** gave stilbenes (48–86%) or 1-aryllkenes **36** (11–65%), while acrylates gave hydrocinnamates (30–62%) or aliphatic esters (36–41%) as the products. No mechanistic evidence was provided. The authors attributed all reactions occurring according to the accepted two-electron catalytic cycle starting with Ni(0) generated by reduction with Zn. It can be assumed, however, that alkyl halides react rather by initial SET reduction as observed with other low-valent nickel catalysts. It is interesting to note that benzylic nickel intermediates resulting from addition to styrene underwent facile β-hydride

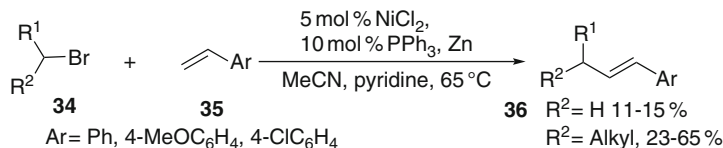


Fig. 7 Radical addition of alkyl bromides to styrenes

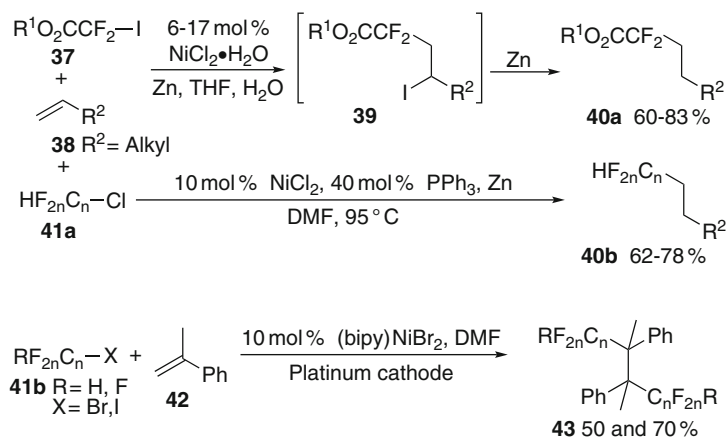


Fig. 8 Nickel-catalyzed fluoroalkylations of olefins

elimination, while the nickel enolate resulting after addition to the acrylate proved to be stable towards this process. Catalyst liberation proceeds by enolate protonation. Therefore addition of water proved to be beneficial in these reactions.

Yang and Burton studied reductive radical additions of iododifluoroacetate **37** to olefins **38** and dienes catalyzed by 6–17 mol% of a catalyst generated from NiCl<sub>2</sub> and stoichiometric amounts of zinc in the presence of water (Fig. 8) [90, 91]. Olefins gave the reductive addition products **40a** in 60–83% yield, while 1,5-hexadiene or 1,8-nonadiene provided double addition products exclusively in 55% and 73% yield. 1,7-Hexadiene gave an inseparable mixture of the expected acyclic double addition product and a tandem addition/cyclization product, in which the former dominated. The radical nature of the addition is supported by inhibition of the reaction by *para*-dinitrobenzene. The reaction proceeds probably via initially formed atom transfer product **39**, which is subsequently reduced by nickel(0) and zinc. This is supported by deuterium incorporation, when D<sub>2</sub>O was used instead of water. No deuterium incorporation was observed with THF-d<sub>8</sub>, thus ruling out hydrogen transfer from the solvent.

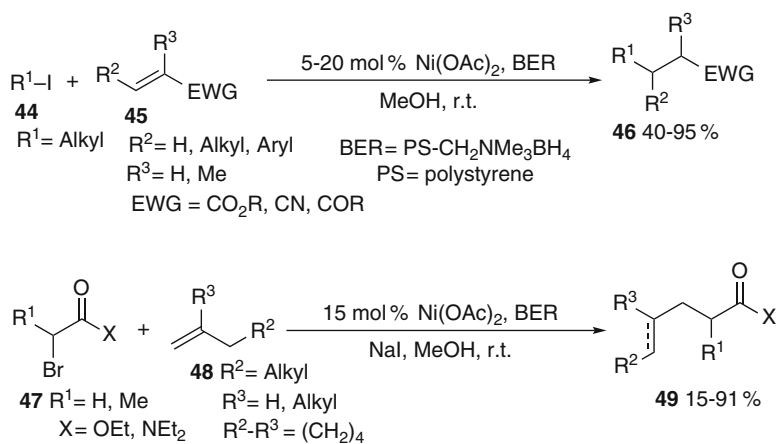
Huang and Chen applied a catalyst generated in situ from 10 mol% of NiCl<sub>2</sub>, 40 mol% of triphenylphosphine, and stoichiometric amounts of zinc to promote similar reductive radical additions of perfluoroalkyl chlorides **41a** to olefins **38** in DMF as the solvent (Fig. 8) [92]. The reaction works for electron-rich and electron-

poor olefins. Products **40b** were isolated in 62–78% yield. Alkynes gave fluorinated alkenes in 51–75% yield as an *E/Z*-mixture. Electron-rich arenes and heteroarenes furnished perfluoroalkylarenes in 56–78% yield. The reactions were inhibited by hydroquinone and *para*-dinitrobenzene. The reaction course is supported by the occurrence of radical 5-exo cyclizations and by earlier reports that Ni(PPh<sub>3</sub>)<sub>4</sub> catalyzes the addition of perfluoroalkyl radicals to enamines [93], arenes, and heteroarenes [94, 95]. The reaction works well with all group 10M(PPh<sub>3</sub>)<sub>4</sub> complexes. The nickel complex is the most reactive.

Electrochemical catalyst regeneration was tested for addition reactions of perfluoroalkyl halides **41b** to  $\alpha$ -methylstyrene **42** (Fig. 8) [96]. Dimers **43** were isolated in 50% and 70% yield, respectively, using 6–10 mol% of Ni(bipy)Br<sub>2</sub> as the catalyst in a divided cell at –1.2 V at a platinum cathode. Under these conditions the Ni(II) complex is first reduced to Ni(0).

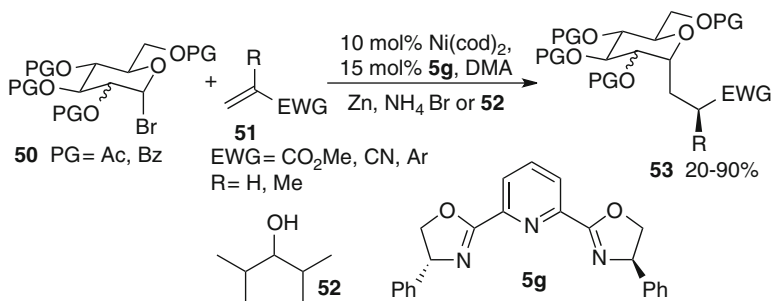
Yoon used 5–20 mol% of Ni(OAc)<sub>2</sub> as a precatalyst to promote Giese additions of alkyl iodides **44** to  $\alpha,\beta$ -unsaturated esters, ketones or nitriles **45** (Fig. 9) [97, 98]. The reactions tolerate  $\beta$ -substituted radical acceptors. The addition products **46** were isolated in 40–95% yield. The reaction proceeds by initial reduction of Ni(OAc)<sub>2</sub> to Ni(0) mediated by the polystyrene-based borohydride exchange resin (BER). Cyclizations were not observed with suitable substrates, indicating that reduction is considerably faster. Similar reductive addition reactions of alkyl halides to acrylates, acrylonitrile, or methyl vinyl ketone catalyzed by 15–20 mol% of NiCl<sub>2</sub>·6H<sub>2</sub>O using zinc as the stoichiometric reducing agent were also reported by Sustmann and colleagues [99]. Aryl and vinyl bromides reacted analogously under identical conditions.

The addition of  $\alpha$ -carbonyl radicals derived from bromo esters **47** to olefins **48** proceeded smoothly using 7.5–15 mol% of Ni(OAc)<sub>2</sub> [100]. The reaction furnished reduced esters and amides **49** in 15–91% yield. Reactions to 1,2-disubstituted



**Fig. 9** Nickel-catalyzed radical addition reactions mediated by borohydride exchange resins (BER)



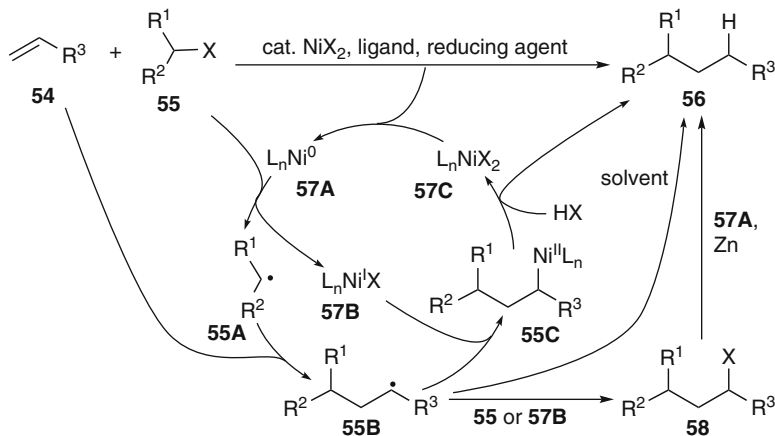


**Fig. 10** Glycosyl radical additions catalyzed by nickel complexes

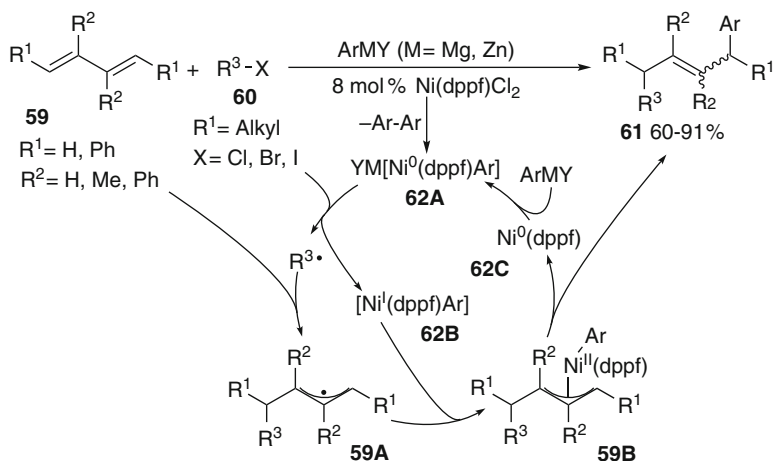
alkenes were generally lower yielding and required higher temperatures. When methylenecyclohexane ( $R^2-R^3=(CH_2)_4$ ) was employed, unsaturated carbonyl compounds were isolated, suggesting an atom transfer addition followed by in situ-dehydrohalogenation leading to unsaturated products.

Gagne et al. found recently that glycosyl bromides **50** are subject to Giese radical additions to acceptor-substituted olefins **51** applying 10 mol% of a catalyst generated from  $Ni(cod)_2$  and (*S,S*)-Ph-PyBOX **5g**, zinc as a reducing agent, and ammonium bromide or alcohols as a proton source (Fig. 10) [101]. The reductive coupling products **53** were isolated in 20–90% yield as  $\alpha$ -anomers. Styrenes substituted by strong acceptor substituents in four-position were also suitable substrates giving the addition products in 65–72% yield, while more electron-rich styrenes were poor acceptors, resulting in low yields. For methacrylates the stereocenter at the  $\alpha$ -position to the ester could also be controlled by application of a bulky alcohol, such as **52**, as the proton source. The results indicate that the adduct radical couples with the nickel(I) complex forming a nickel(II) enolate, which liberates the product **53** by hydrolysis. Other acceptors also worked well, although the extent of stereocontrol of protonation was very dependent on the substrate. The radical nature of the addition step is supported by the reaction of 2-vinylcyclopropanedicarboxylate, which gave exclusively the corresponding ring-opened product with complete  $\alpha$ -selectivity (cf. Part 1, Fig. 8). Marsden and colleagues disclosed a similar nickel(I)-catalyzed approach before (see Sect. 2.6).

The catalytic cycle of all these addition reactions can be described by initial chemical or electrochemical reduction of the Ni(II) precatalyst to a nickel(0) intermediate **57A** (Fig. 11). This species triggers SET reduction of the alkyl halide **55**. The so generated alkyl radical **55A** adds to the alkene or alkyne acceptor **54**. For the resulting radical **55B** three stabilization pathways were suggested dependent on the conditions. It may either be subject to atom transfer giving haloalkane **58**, which is further reduced to product **56** under the reaction conditions. Direct reduction of **55B** by hydrogen transfer from the solvent was also proposed as a stabilization pathway. There is also evidence that radical **55B** may convert to organonickel species **55C** by coupling with nickel(I) complex **57B**. Protonation subsequently liberates the product



**Fig. 11** Catalytic cycle of nickel-catalyzed reductive radical addition reactions



**Fig. 12** Nickel-catalyzed three-component coupling of 1,3-dienes, alkyl halides and organometallic reagents

and provides the oxidized catalyst **57C**, which is finally reduced back to the active Ni(0) species **57A** by sacrificial reducing agents.

Terao and Kambe showed a dichotomy in the reactivity of nickel complexes (review [102]). While nickel diene complexes reacted primarily via two-electron pathways [34–37], nickel phosphine complexes promote radical addition reactions [103].

Radical addition/cross-coupling products **61** were obtained in 60–91% yield when Ni(dppf)Cl<sub>2</sub> was applied as a catalyst in reactions of alkyl halides **60** with 2,3-disubstituted dienes **59** and aryl Grignard or arylzinc reagents (Fig. 12). Competition experiments of *n*-, *sec*-, and *tert*-butyl bromide with 2,3-dimethylbutadiene





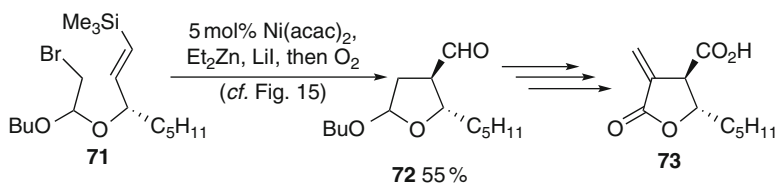
reduced to radicals **67A** by the nickel(0) catalyst **70A** generated from Ni(acac)<sub>2</sub> and Et<sub>2</sub>Zn. A subsequent 5-exo cyclization leads to radicals **67B**, which react further with nickel(I) species **70B** to organonickel species **67C**. A transmetalation leads to organozinc species **67D**. Alternatively, a S<sub>H</sub>2 reaction of **67B** at Et<sub>2</sub>Zn will also provide **67D**. These stable species are transmetalated by addition of the CuCN·2LiCl complex to the corresponding organocopper species **67E**, which react subsequently with activated allylic halides, Michael acceptors, or acid chlorides **68a–d** to provide functionalized butyrolactols **69** in 60–75% yield and good to high diastereoselectivity. Annulations succeeded with high *endo*-selectivity. The diastereoselectivity can be explained by a Beckwith–Houk transition state. *N*-Allyl-β-iodo amines cyclized to pyrrolidines under similar conditions.

Bromoacetaldehyde acetals cannot be applied directly under the reaction conditions. However, when anhydrous LiI was used as an additive the cyclizations proceeded smoothly, probably by an initial Finkelstein reaction [107].

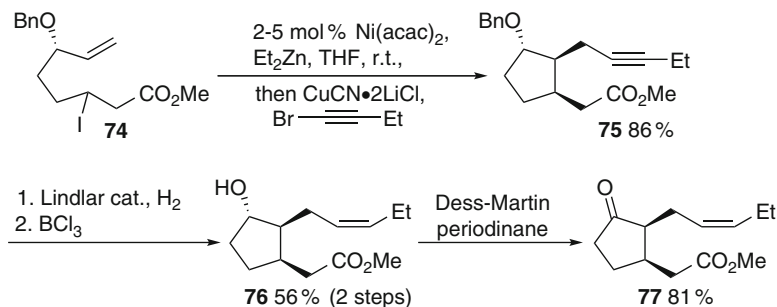
A similar cyclization was applied as the key step in a formal total synthesis of (–)-methylenolactocin **73** (Fig. 16) [108]. Subjecting bromoacetaldehyde 3-trimethylsilylallyl acetals **71** to 5 mol% of Ni(acac)<sub>2</sub>, 25 mol% of LiI, and Et<sub>2</sub>Zn gave cyclized organozinc species analogous to **67D**, which were functionalized subsequently to a number of butyrolactol derivatives. To obtain the target molecule **73**, the organozinc was oxidized by oxygen giving aldehyde **72** in 55% yield.

Similar conditions were also suitable for carbocyclization reactions. Although organozinc compounds undergo uncatalyzed intramolecular carbocyclization reactions, which might proceed via radical intermediates [109], Knochel and coworkers discovered subsequently that Ni(0) complexes catalyze such radical cyclizations efficiently [110, 111]. This methodology was applied to the stereocontrolled synthesis of methyl epijasmonate **77** and methyl curcubate **76** (Fig. 17). Methyl 3-iodo-7-octenoate **74** cyclized using 2.5 mol% Ni(acac)<sub>2</sub> and 2.0 equiv. of Et<sub>2</sub>Zn via a Beckwith–Houk transition state with high *cis*-diastereoselectivity. This transition state may be enforced by the metal components in the reaction mixture. The resulting cyclopentylmethylzinc species was transmetalated to the more reactive organocopper compound, which underwent cross-coupling with 1-bromobutyne affording **75** in 86% yield. A few standard steps led to the natural products **76** and **77**.

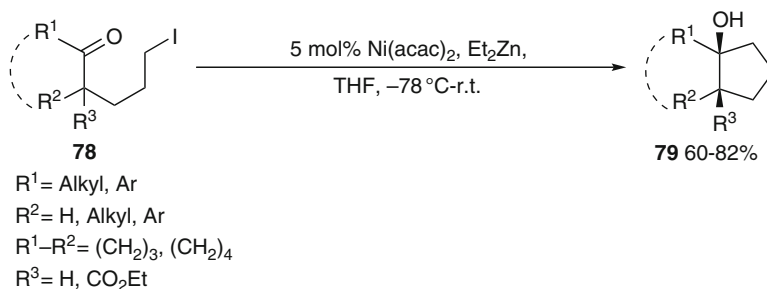
When 5-iodo ketones **78** were subjected to 5 mol% Ni(acac)<sub>2</sub> and stoichiometric amounts of Et<sub>2</sub>Zn, cyclopentanols **79** were obtained in 60–82% yield (Fig. 18) [112]. The reaction is thought to be initiated by reductive radical generation by the



**Fig. 16** Nickel(0)-catalyzed radical cyclization/oxygenation sequence in a formal total synthesis of (–)-methylenolactocin **73**



**Fig. 17** Total synthesis of methyl curcubate **76** and methyl epijasmonate **77** via a radical-polar 5-exo cyclization/alkylation sequence

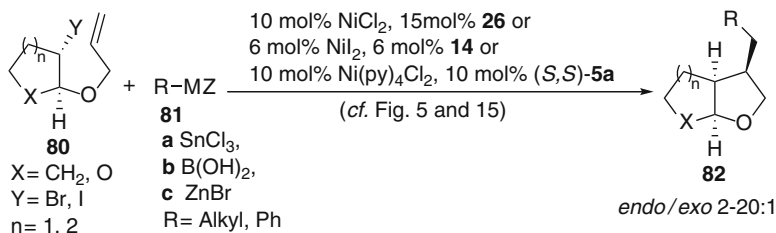


**Fig. 18** Ni(0)-catalyzed  $\text{Et}_2\text{Zn}$  mediated cyclizations of 5-iodo ketones to cyclopentanols

Ni(0) catalyst. A radical 5-exo cyclization to the potentially zinc or nickel-complexed ketone provides an alkoxy radical that combines with the co-produced Ni(I) species. A transmetalation to a zinc alkoxide regenerates the catalyst and forms the zinc cyclopentoxide, from which products **79** are liberated on hydrolysis. A bimetallic Cu(I)–Mn(II) system provided similar results (see Sect. 8.4). Analogous samarium diiodide-mediated reactions require in contrast stoichiometric amounts of the reducing agent and are less diastereoselective [26, 27].

$\beta$ -Allyloxy tellurides also underwent similar radical 5-exo cyclizations catalyzed by 7 mol% of  $\text{Ni(acac)}_2$  and 2 equiv. of  $\text{Et}_2\text{Zn}$  [113]. The reaction proceeded with high *cis*-selectivity in 56% yield. In contrast to the reactions of 5-hexenyl iodides shown above, 5-exo cyclization reactions of 5-hexynyl iodides were proposed to proceed by a two-electron pathway consisting of alkyne coordination/oxidative addition/intramolecular carbonickelation and reductive elimination, resulting in alkylidenecyclopentanes [114].

Powell, Maki, and Fu reported a Ni-catalyzed tandem radical 5-exo cyclization/Stille coupling reaction (Fig. 19) [75]. When allylic bromo ethers **80** were subjected to a reaction with trichlorophenylstannane **81a** in the presence of 10 mol%  $\text{NiCl}_2$  and 15 mol% of bipy **26**, bicyclic phenyl-substituted products **82** were isolated in 57–67% yield and moderate to excellent *endo*-diastereoselectivity. Suzuki–Miyaura-type coupling reactions of **80** with arylboronic acids **81b** worked similarly in 69–87%



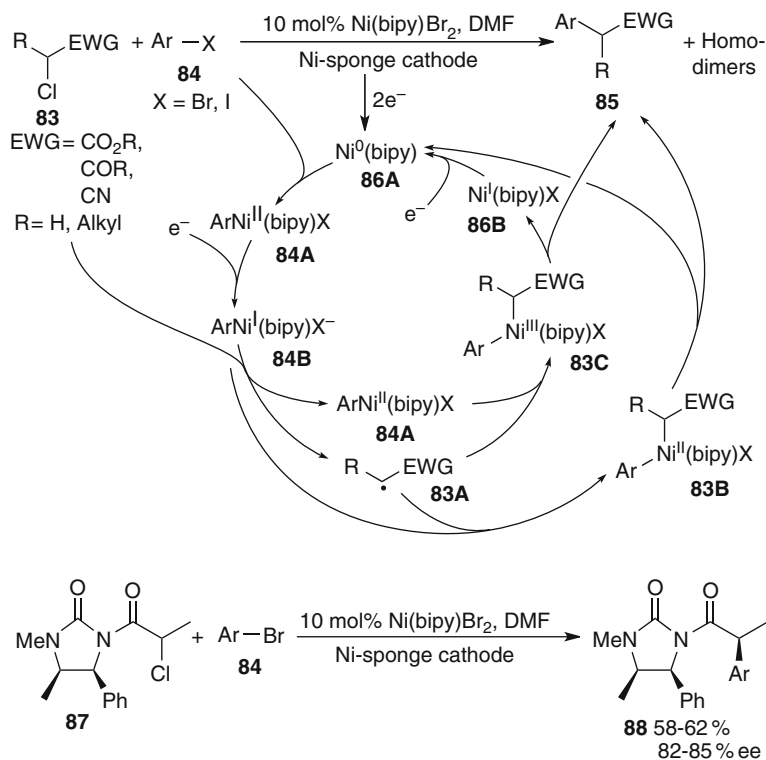
**Fig. 19** Nickel-catalyzed tandem radical cyclization/cross-coupling reactions

yield and 2–20:1 *endo*-diastereoselectivity using 6 mol% of NiI<sub>2</sub> and *trans*-2-aminocyclohexanol **14** [56].

Cardenas et al. reported subsequently tandem radical 5-*exo* cyclization/Negishi coupling reactions of iodo allylacetals **80** and other 5-*exo* cyclization substrates with alkylzinc reagents **81c** catalyzed by 10 mol% Ni(py)<sub>4</sub>Cl<sub>2</sub> and 10 mol% of PyBOX ligand (*S,S*)-**5a** giving cyclic cross-coupling products **82** in 46–94% yield [48]. In the absence of a ligand or with phenanthroline as the ligand, only an iodinated cyclization product (R=I) was obtained, which underwent coupling with the organozinc reagent **81c** furnishing **82** under identical conditions. The method is applicable to substrates bearing ester or acetal functions. In the presence of TEMPO the typical oxygenation product of the organozinc reagent was obtained. The rate for cross-coupling was estimated to be approximately 10<sup>7</sup> mol<sup>-1</sup> s<sup>-1</sup> on the basis that cyclizations with known rate constants of ≤ 9 × 10<sup>6</sup> s<sup>-1</sup> did not proceed but gave acyclic products exclusively. The course of the reaction was proposed to start with a SET reduction of the Ni(II) precatalyst to a Ni(I) catalyst (cf. Fig. 5). The latter reduces the iodide to the corresponding radical, which cyclizes. Coupling with coformed alkyl Ni(II) leads to a Ni(III) intermediate (cf. Fig. 15), which undergoes reductive elimination. It can, however, not be discarded that a Ni(0)–Ni(I)–Ni(II) catalytic cycle operates.

## 2.5 Ni(0)–Ni(II)–Ni(I)–Ni(III) Catalysis: Cross-Coupling

As mentioned in the introduction to this section, catalytic cycles of cross-couplings may occur interwoven, involving different oxidation states of nickel. Durandetti studied electrochemically mediated nickel-catalyzed cross-coupling reactions of  $\alpha$ -chloro esters or ketones **83** with aryl halides **84** (Fig. 20) [115]. Using ca. 10 mol% Ni(bipy)Br<sub>2</sub>, a nickel sponge cathode and an aluminum anode under constant current conditions, benzyl ketones or arylacetates **85** were isolated in 34–80% and 51–85% yields, respectively. To avoid the formation of larger amounts of biaryls or 1,4-dicarbonyl compounds resulting from reductive homocoupling of the components, the alkyl halide had to be added by syringe pump, since it reacted faster with the nickel complex than the aryl halide. The reaction can best be



**Fig. 20** Nickel-catalyzed arylation of  $\alpha$ -chloro carbonyl compounds

described by initial reduction of the catalyst to the corresponding Ni(0) complex **86A**. Oxidative addition of the aryl halide provides an arynickel(II) species **84A**, which can be reduced to the corresponding Ni(I) complex **84B** under the reductive electrolysis conditions. Arylnickel(I) **84A** is able to act as a SET reducing agent toward **83**. The resulting  $\alpha$ -carbonyl radical **83A** may either couple with **84A** or **84B** leading to mixed diorganonickel(II or III) complexes **83B** or **83C**, from which reductive elimination occurs. The reaction mechanism is supported by the formation of racemic arylacetate **85** from enantiomerically pure  $\alpha$ -chloropropionate **83**. The reaction was also performed with ester and amide auxiliary-substituted chloropropionate [116]. The obtained des for most auxiliaries, such as menthyl esters or Evans oxazolidinones, were low to moderate. Chiral imidazolidinones **87** coupled with **84** furnishing 2-arylpropionimides **88** in 58–62% yield and with 92–93% de.

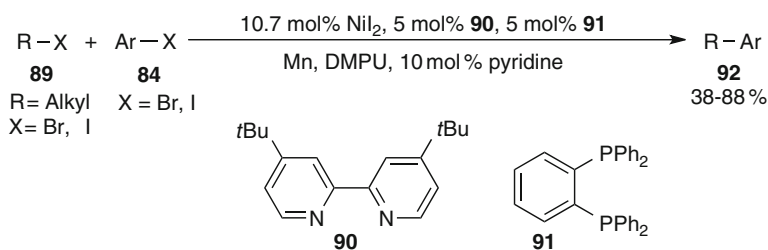
The scope was also extended to vinyl halides [117]. These substrates couple with retention of the double bond geometry, indicating that no SET or radicals are involved during oxidative addition. The coupling proceeds as above, giving  $\beta,\gamma$ -unsaturated esters or ketones in 44–88% yield. For these substrates, no involvement of radicals was proposed, but based on the similarity of the process to those



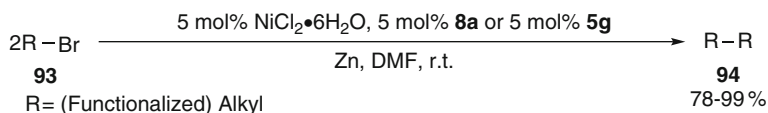
described above, they cannot be excluded from the discussion, especially since an enantiomerically pure chloroester gave the racemic product [118]. A similar coupling process, in which manganese was used as a stoichiometric reducing agent for Ni(bipy)Br<sub>2</sub> (7 mol%), was developed. Aryl bromides or iodides coupled to  $\alpha$ -chloro esters in 40–88% yield. Aryl chlorides provided only 20% yield of  $\alpha$ -aryl esters [119]. Ni(bipy)Br<sub>2</sub> catalyzed the dimerization of alkyl or benzyl halides, which may be formed by a radical process, while reductive additions of aryl halides catalyzed by the same complex occur probably by a two-electron process [120].

Weix and colleagues found recently that cross-coupling reactions of alkyl bromides or iodides **89** with aryl bromides or iodides **84** are possible under nickel catalysis giving alkylarenes **92** in 38–88% yield (Fig. 21) [121]. Optimal conditions consisted of 10.7 mol% of NiI<sub>2</sub>, 5 mol% of 4,4'-di-*tert*-butylbipyridine **90**, and 5 mol% of 1,2-bis(diphenylphosphinyl)benzene **91** as ligands and 10 mol% of pyridine. Manganese served as the stoichiometric reducing agent. The reactions proceed probably by a catalytic cycle similar to that of the electrochemically mediated couplings (cf. Fig. 20). The nickel precatalyst is initially reduced to a Ni(0) complex. Oxidative addition to the aryl halide provides probably an arylnickel(II) species **84A**. This intermediate might be reduced to an arylnickel(I) intermediate **84B**, which triggers SET reduction of **89**. Coupling of the resulting radical, followed by reductive elimination, gives the product and a Ni(I) complex, which can be re-activated by further reduction to Ni(0).

Leigh and coworkers developed in parallel a Ni-catalyzed reductive homocoupling of alkyl halides **93** toward an efficient synthesis of rotaxanes (Fig. 22) [122]. In model studies 5–12 mol% of the Ni(II) precatalyst and terpy **8a** or (*R,R*)-Ph-PyBOX **5g** sufficed for the coupling of alkyl halides under normal conditions, under which 78–99% of dimers **94** were obtained. A macrocyclic Ni(PyBOX) complex, which has to be present stoichiometrically due to its function as the wheel, serves as the precatalyst in the rotaxane synthesis. Initial reduction of



**Fig. 21** Nickel-catalyzed reductive cross-coupling of aryl and alkyl halides



**Fig. 22** Leigh's reductive coupling of functionalized alkyl halides

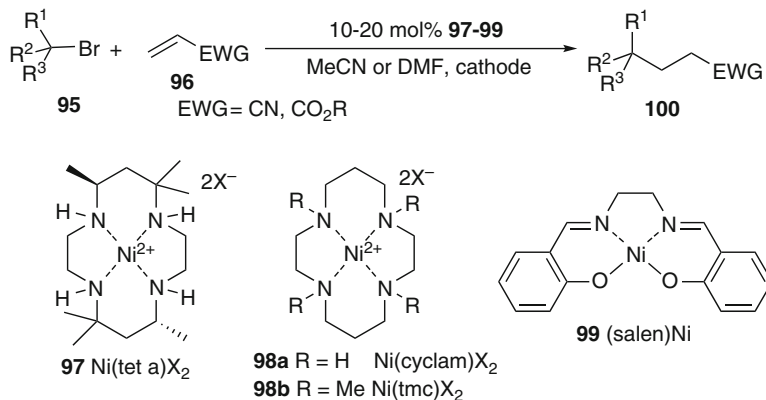


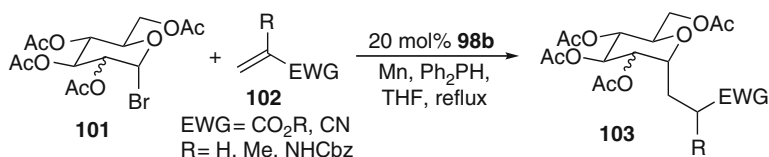
Fig. 23 Nickel-catalyzed electrochemically mediated reductive radical addition reactions

the Ni(II) precatalyst to Ni(0) by sacrificial zinc gives a Ni(0) species, which activates the alkyl halide by twofold reduction. The resulting alkylnickel(II) complex was proposed to be reduced to an alkylnickel(I) complex, similarly to the reactions reported by Durandetti [115–120] (cf. Fig. 20) or Vicic et al. [9, 47]. A second SET reduction-coupling process provides a dialkylnickel(III) complex, from which reductive elimination to the coupling product **94** occurs.

## 2.6 Ni(I)–Ni(II) Catalysis: Radical Additions

Electrochemical methods are well suited to (re)generate active nickel catalysts for radical additions. First reductive addition reactions of alkyl halides **95** to α,β-unsaturated carbonyl compounds **96** were mostly mediated by Ni(tet a)(ClO<sub>4</sub>)<sub>2</sub> **97** and thought to proceed via a two-electron pathway (Fig. 23) [123]. After exploring the potential of such nickel complexes as catalysts in dimerization reactions, the radical nature was recognized and a catalytic radical addition methodology using (salen)Ni complex **99** was developed [124]. Since then this electrocatalytic radical approach to compounds of type **100** developed as an alternative to tin hydride-mediated radical additions. The field was reviewed recently [19]. Typical electrocatalysts are cyclam-type nickel(II) compounds, such as **97** [125] or **98a,b**, which are electrochemically easily reduced to the corresponding Ni(I) complexes at –0.9 to –1.3 V vs. SCE. Both **95** and **96** are electrochemically inactive at this potential.

Similar reactions can also be conducted using cheap metals as stoichiometric reducing agents. Marsden et al. described the radical addition of glycosyl bromides **101** to acrylates or acrylonitriles **102** catalyzed by 20 mol% Ni(tmc)(BF<sub>4</sub>)<sub>2</sub> **98b** in the presence of diphenylphosphine as the hydrogen donor and manganese metal as the reducing agent (Fig. 24) [126]. The yields of C-glycosides **103** range from 49% to 98% and the stereoselectivity of the reaction amounted to 95:5 for the α-anomer.



**Fig. 24** Nickel(I)-catalyzed reductive glycosyl radical addition reactions

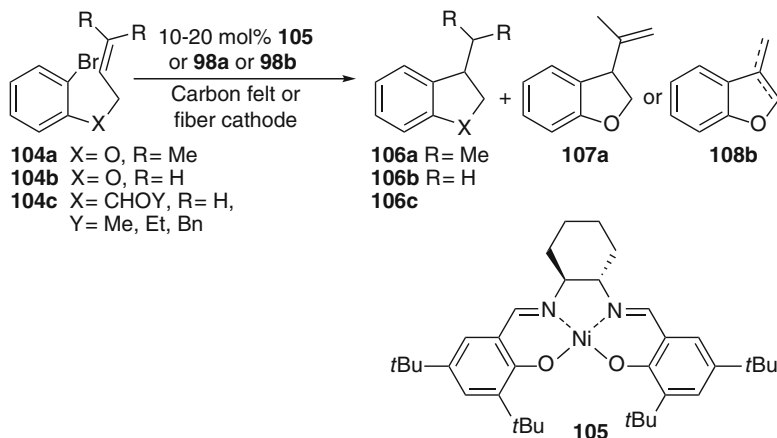
Not unexpectedly, no asymmetric induction was observed in the reduction step of the adduct radical. This reaction works only for acceptor-substituted alkenes; even styrene did not react with the highly nucleophilic glycosyl radical. Gagne and colleagues later disclosed a similar nickel-catalyzed approach (see Sect. 2.3).

Several electrochemically mediated Ni-catalyzed addition reactions with aryl halides were reported, but their mechanism is not fully clarified. Using 10 mol% of NiBr<sub>2</sub> as a catalyst, heteroaryl halides were added to  $\alpha,\beta$ -unsaturated carbonyl compounds affording  $\beta$ -aryl carbonyl compounds in 15–86% yield [127]. These addition reactions seem to proceed rather by classical Ni(0)–Ni(II) or Ni(I)–Ni(III) catalytic cycles than by a radical catalysis mechanism.

## 2.7 Ni(I)–Ni(II) Catalysis: Radical Cyclizations

Reductive radical cyclization and tandem radical addition/cyclization reactions catalyzed by Ni(II) complexes, such as Ni(cyclam)(ClO<sub>4</sub>)<sub>2</sub> **98a**, were studied starting in the 1990s by Ozaki's group [128]. The reaction conditions are applicable to alkyl and aryl halides bearing suitable positioned olefin units. Iodides and bromides can be used; in some cases even aryl chlorides were successfully applied. The field was reviewed recently, and thus only more recent results are summarized here [19, 20].

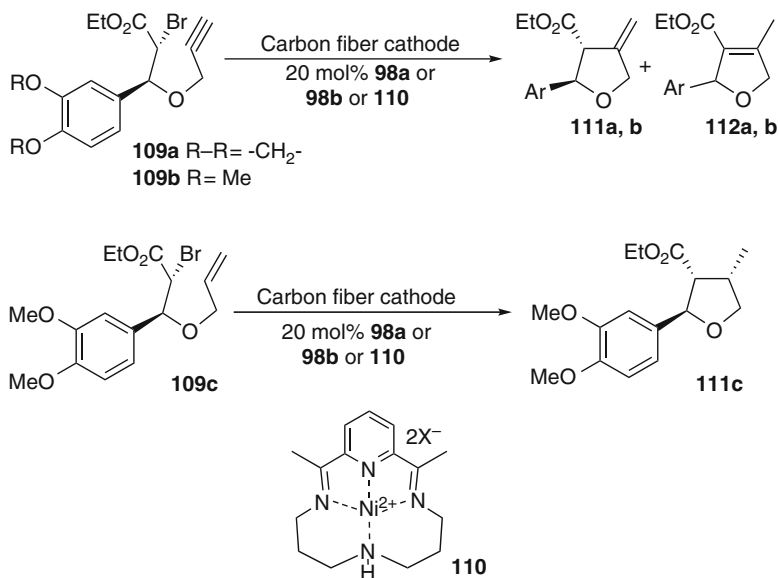
Jacobsen–Katsuki-type chiral (salen)nickel(II) complex **105** (10 mol%) was used by Dunach and coworkers to catalyze electrochemical radical 5-exo cyclizations of allylic *ortho*-bromophenyl ethers **104a** and **104b** to dihydrobenzofurans **106** (Fig. 25) [129]. Constant current or constant potential conditions using carbon felt or reticulated vitreous carbon (RVC) cathodes, respectively, were applied in DMF to reduce the nickel(II) complex **105** to its Ni(I) oxidation state. Ether **104a** afforded isopropyl and isopropenyl dihydrobenzofurans **106a** and **107a** in the presence of nickel complex **105** in a ratio of 2–5:1 in 60–76% yields. This result is in contrast to that with the corresponding cobalt complex, where almost perfect disproportionation was observed. Hydrogen abstraction resulting in formation of the reduced product dominates for allyl ether **104b** giving **106b** in 52% yield. Disproportionation leading to 3-methylenedihydrobenzofuran or 3-methylbenzofuran **108b** competes to some extent. The maximum enantiomeric excess observed for both cyclizations was 13% ee, indicating that there is almost no interaction of the catalyst with the substrate during the cyclization. Both substrates were themselves inactive under the electrolysis conditions in the absence of the



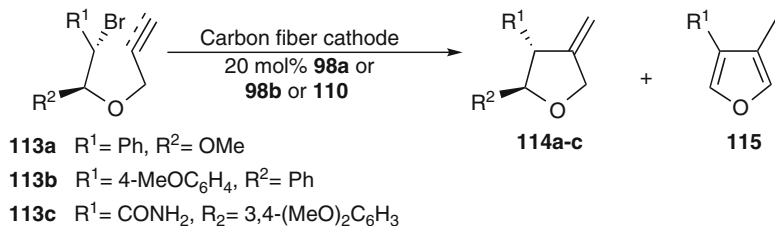
**Fig. 25** Nickel(I)-catalyzed radical 5-exo cyclization of haloarenes

catalysts. The controlled potential electrolysis showed that only one SET step occurred during the process, supporting the notion that SET is only involved in radical generation but not after cyclization. Oxygen-substituted *ortho*-bromo homoallylbenzenes **104c** are convenient starting materials for electrochemically mediated radical 5-exo cyclization reactions catalyzed by nickel complexes **98a** or **98b** [130]. Using 10 mol% of the catalysts, 48–83% of indanes **106c** were isolated. The corresponding aryl chlorides were considerably less reactive; the yield of the isolated indanes amounted to 14–68%. The diastereoselectivity was, as expected, low. The major side product was the acyclic reduced product, which results possibly from hydrogen abstraction from the solvent DMF.

2-Bromo-3-propargyloxy ester **109a** or 3-allyloxy-2-bromo ester **109c** cyclized similarly using 20 mol% of Ni complexes **98a,b** or **110** as catalysts under reductive electrochemical conditions at a carbon fiber cathode and a sacrificial metal anode in 38–77% yield (Fig. 26). The initial *exo*-methylenetetrahydrofuran **111a** isomerized partly under the reaction conditions to the more stable 2,5-dihydrofuran derivative **112a**. Tetrahydrofuran **111c** was obtained with good 8–10:1 3,4-*cis/trans*-selectivity [131]. Esteves and colleagues performed similar cyclizations with substrates **109a** using substoichiometric amounts of Ni(tmc) $X_2$  **98b** resulting in 63–81% yield of **111a** [132]. Some isomerized dihydrofuran **112a** was also found. Allyloxy ester **109c** cyclized in excellent yield and with good diastereoselectivity to **111c**. Similar cyclizations of **109a,b** were also conducted in aqueous/hydrocarbon microemulsions using 10–25 mol% of **98b** as the catalyst. The cyclized tetrahydrofurans **111a,b** were obtained in 67–100% yield with *trans*-selectivity under controlled potential conditions at RVC or carbon felt cathodes [133]. The amounts of isomerized product **112a,b** were under optimized condition considerably less than in an organic solvent (3–99:1). The corresponding allyl ether **109c** gave in contrast only 43–55% yield of **111c** but excellent diastereoselectivity. This indicates that hydrogen transfer from the medium is more difficult for alkyl radicals in microemulsions.



**Fig. 26** Electrochemical mediated nickel-catalyzed cyclizations of esters **109**



**Fig. 27** Reductive nickel(I)-catalyzed radical cyclizations of bromo propargyl ethers **113**

2-Bromoalkyl propargyl ethers **113a–c** were also subject to reductive radical cyclizations by nickel complexes **98a,b** or **110** under constant current conditions (Fig. 27) [134]. Tetrahydrofurans **114a–c** were isolated in 13–99% yield. Best yields (76–99%) were achieved with the Ni(tmc) $\text{X}_2$  catalyst **98b** using a zinc anode in DMF. When controlled potential conditions and vitreous carbon cathodes in DMF were applied, bromo ethers **113a–c** underwent the 5-exo cyclization reactions catalyzed by 10–25 mol% **98b** much more efficiently giving **114a–c** in high yield. No products **112** or **115** resulting from base-mediated isomerization were detected [135]. These conditions are milder than constant current electrolyses, during which apparently considerable quantities of electrogenerated bases are formed, which lead to isomerized side products. Addition of a proton donor, such as hexafluoroisopropanol, had no effect on the reaction.

Aqueous ethanolic solutions are a very convenient medium to perform cyclizations of  $\beta$ -bromo propargyl ethers **113a,b** or 2-bromo-3-propargyloxy esters **109a–c** using

electrochemical regeneration of the Ni(tmc)Br<sub>2</sub> catalyst **98b** [136]. The catalyst concentration was varied between 10 and 40 mol%. Under these conditions almost quantitative yields of 4-methylenetetrahydrofurans **114a,b** were obtained, while 61–92% of tetrahydrofuran-3-carboxylates **111a,b** were isolated. The remainder of the material proved to be isomerized dihydrofuran **112a,b** (6–24%). 3-Allyloxy-2-bromo ester **109c** cyclized to **111c** in 47–86% yield with 91:9–94:6 *cis*-diastereoselectivity. The optimal catalyst concentration was 30–40 mol% for this substrate. Only one SET reduction step is involved in the overall process. The same reductive cyclizations can also be performed in ethanol or ethanol/water mixtures under constant current conditions in 69–97% and 61–75% yield, respectively [137].

Recently, Chaminade and coworkers reported Ni-catalyzed electrochemically mediated radical 5-*exo* cyclization reactions of *N*-allyl- $\alpha$ -bromo amides **116** (Fig. 28) [138]. Among the catalysts tested **98a** and **98b** were the best in DMF as the solvent, but the cyclized products **117** were obtained in moderate yields of. For *N,N*-diallylamides **116** (R<sup>2</sup>=Allyl), overreduction of the extra alkenyl unit competed under the reaction conditions. Using ethanol instead gave considerably better results and pyrrolidones **117** were isolated in 49–99% yield. Reduction of the allyl group could, however, not be prevented under these conditions.

Katsumata and colleagues reported the first electrochemically mediated Ni(I)-catalyzed tandem radical cyclization reactions [139]. A bromoacetaldehyde dienyl acetal or the corresponding enynyl acetal underwent tandem 5-*exo*/5-*exo* cyclization reactions in the presence of Ni(cyclam) complex **98a** under electrochemical reductive conditions (see Part 2, Sect. 5.3.3, Fig. 68). Bicyclic esters were isolated in 35% and 72% yields as a mixture of two and four diastereomers, respectively.

All these cyclizations can be rationalized as follows (Fig. 29). The nickel catalysts **97–99**, **105**, or **110** are reduced under the conditions of the electrolysis at potentials of ca. –0.95 to –1.4 V vs SCE to the corresponding nickel(I) complexes **120A**. Organic halides **118** are not reduced at these potentials. The electron-rich nickel(I) species **120A** can react with organic halides **118** in two ways. A two-electron oxidative addition may proceed initially leading to organonickel(III) intermediates **118A**, which are prone to homolysis providing radicals **118B**. Halides **118** can, on the other hand, be reduced directly to radicals **118B** and the starting Ni(II) catalyst **120B**. It is likely that aryl halides react preferentially by the former pathway and alkyl halides rather by the latter. Radicals **118B** cyclize under the reaction conditions to radicals **118C**. It was shown that in many cases only one

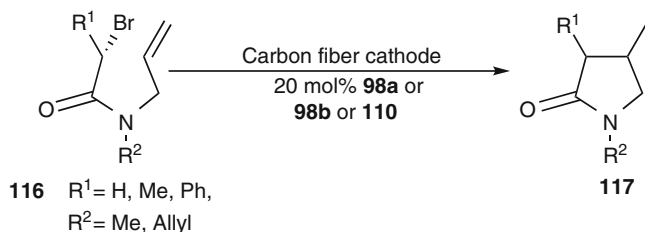


Fig. 28 Nickel-catalyzed cyclization of *N*-allyl  $\alpha$ -bromo amides

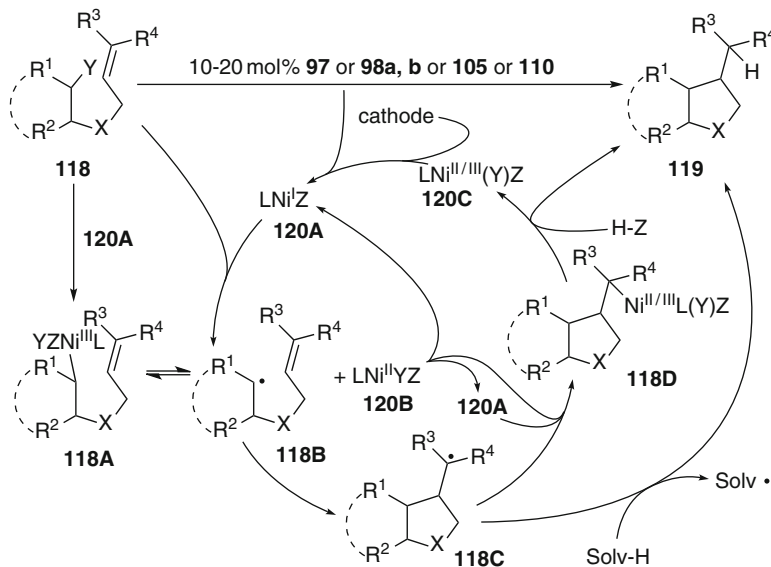
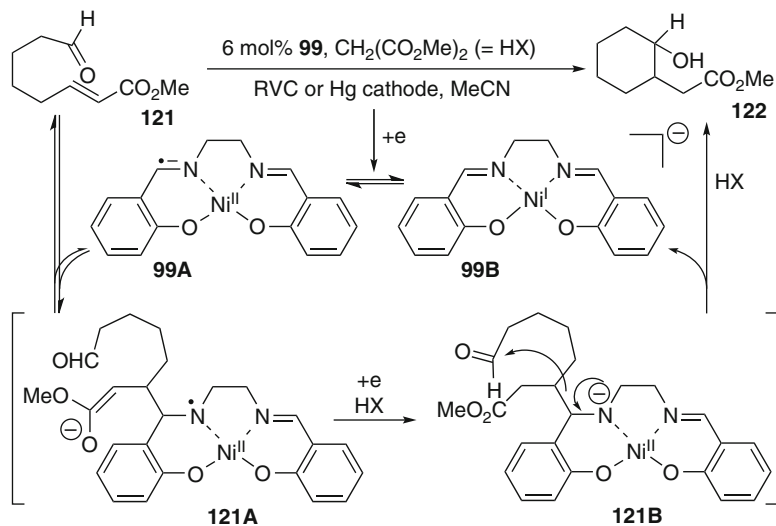


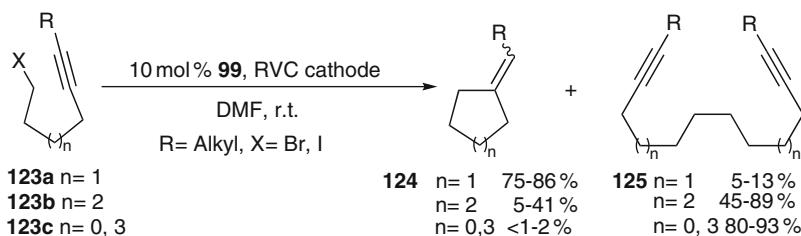
Fig. 29 Catalytic cycle of Ni(I)-catalyzed electroreductive cyclization reactions

electron per molecule of substrate was transferred in the overall electrolysis. This is in accord with the fact that radicals **118C** stabilize by hydrogen abstraction from the medium giving the products **119** directly. The resulting Ni(II) species is in this case reduced back to **120A** at the cathode. When two electrons were sequentially transferred in the process, the cyclized radical is subject to coupling with either the nickel(II) species **120B** or **120A** leading to organonickel intermediates **118D**, which are transformed to products **119** by protonation.

Little and coworkers reported reductive cyclizations of  $\omega$ -oxo enoates **121** catalyzed by 6 mol% Ni(salen) complex **99** (Fig. 30) [140]. Cyclic esters or nitriles **122** were isolated in 60–94% yield. To explain the experimental results the authors invoked the active participation of a reduced valence tautomeric complex pair **99A/99B**, in which ligand-centered radical anion **99A** is significant. This complex will add in a conjugate addition to the enoate function of **121**. Further SET reduction and protonation of the enolate unit in the complexed aminyl radical of adduct **121A** generates amide anion **121B**. The ligand-bound amide triggers the cleavage of the ligand-substrate bond, regenerating the nickel(I) catalyst **99A/B** and enabling cyclization to the aldehyde unit in a concerted or stepwise fashion. Some competing deprotonation of the aldehyde function followed by intramolecular Michael addition was observed, thus supporting the competitive action of the amide in **121B** as a base. An analogous acetophenone-derived salen complex triggered no reductive cyclization, but only intramolecular Michael addition, probably due to its steric hindrance. The corresponding cobalt complex was inactive.



**Fig. 30** Reductive cyclizations of  $\omega$ -oxo enoates catalyzed by (salen)Ni complex **99**



**Fig. 31** Reductive radical cyclization reactions of alkynyl halides catalyzed by Ni(I) complexes

Ischay and coworkers studied the reaction behavior of alkynyl halides **123** under reductive conditions catalyzed by 10 mol% of **99** (Fig. 31). 5-Hexynyl halides **123a** ( $n = 1$ ) underwent efficient radical 5-exo cyclizations giving **124a** in 75–86% yield [141]. The dimer **125a** and the fully reduced alkyne (not shown) were isolated in low yield. Attempted 4-exo or 6-exo cyclizations failed, but gave the dimers **125** in 80–89% yield. In a subsequent study it was shown that radical 6-exo cyclizations could also be triggered from **123b** ( $n = 2$ ) using similar conditions [142]. The yields of cyclic compounds **124b** were considerably lower (33–41%) and dimerization of the alkyl radical prevailed, furnishing **125b** in 45–51% yield. Cyclization reactions of **123c** in the 4-exo and 7-exo mode were not possible and the acyclic dimers **125c** ( $n = 0, 3$ ) were isolated as the major products in 81–93% yield. The cyclization reactions proceed probably by initial SET reduction of catalyst **99** to the valence tautomeric complex pair **99A/B**. SET reduction of **123** followed by 5-exo cyclization gave the cyclized vinylic radical, which stabilized to **124** by hydrogen abstraction from the solvent. The involvement valence tautomer **99A** was also observed during dimerization [143] or reduction reactions of alkyl iodides [144].



## 2.8 Ni(I)–Ni(II)–Ni(III) Catalysis: Conjugate Addition Reactions

Schwartz and coworkers reported the Ni(acac)<sub>2</sub>/DIBAL-H system as a convenient catalyst for conjugate addition reactions of vinylzirconium species **126** to  $\alpha,\beta$ -unsaturated ketones **127** (Fig. 32) [145–147]. Based on the amount of isobutane evolved during reduction of Ni(II), the active catalyst was suggested to be a Ni(I) species **129A**. This reduced **127** to radical anion **127A**. Coupling with Ni(II) generates a formal dianion **127B** bearing a Ni(III) center. Transmetalation with **126** leads to Ni(III) intermediate **127C**, which undergoes reductive elimination to the active Ni(I) catalyst **129A** and vinylated enolate **127D**. Protonation liberates products **128**.

Nadal and colleagues recently reported a Ni-catalyzed carbonylative Pauson–Khand-like [2+2+1] cycloaddition of allyl halides and alkynes in the presence of carbon monoxide and iron as the stoichiometric reducing agent [148]. The reaction was proposed to occur via reductively generated Ni(I)-radical like species; free radicals were, however, considered unlikely.

## 2.9 Ni(II)–Ni(III)–(Ni(IV)) Catalysis: Radical Additions

Nickel pincer complexes **132** are convenient catalysts for the Kharasch addition of tetrachloromethane or other perhaloalkanes **131** to methyl methacrylate **130**

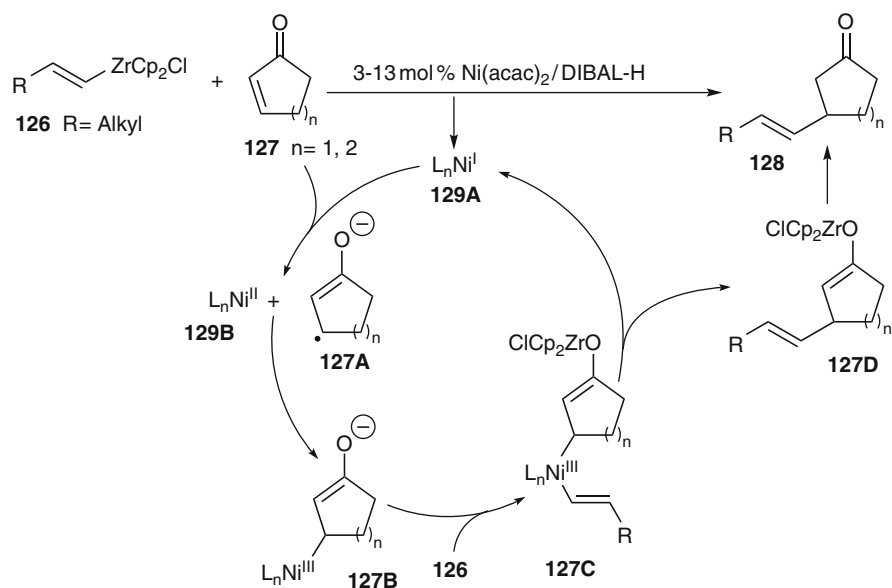


Fig. 32 Ni(I)-catalyzed conjugate additions of vinylzirconocenes to  $\alpha,\beta$ -unsaturated ketones

(Fig. 33) [149]. In the presence of a large excess of the perhaloalkane, exclusive atom transfer radical addition (ATRA) was observed with 0.3 mol% of **132**, while controlled atom transfer radical polymerization (ATRP) prevailed at low  $\text{CCl}_4$  concentration. The reaction was proposed to occur by formation of an equilibrium mixture of intermediate nickel(III) chloride and nickel(IV) complexes ( $\text{X}=\text{Cl}$ ) **132A** and **132B**, respectively. In parallel, dendrimer-based arylnickel pincer-type catalysts (review [150]) were developed. The nickel catalytic sites were connected to the dendrimer by long-chain carbamate linkers [151]. Catalyst **134a** catalyzed the Kharasch addition of tetrachloromethane to methyl methacrylate in high yield and TOF of 167. The influence of different dendritic units and the density of nickel units on the dendritic surface was investigated [152, 153]. The Kharasch addition reaction was proposed to occur by generation to the trichloromethyl radical, which remains in the coordination sphere of the cogenerated nickel(III) complex as shown for **132A**. In the presence of the olefin, radical addition and ligand transfer take place. When the nickel units on the surface of the dendrimer are too close to each other, the efficiency of catalysis decreases. The reason is that the initially formed Ni(III) units apparently interact more efficiently with surrounding Ni(II) units than with the transient radicals in solution; the ligand transfer efficiency thus decreases. Since radicals cannot stabilize by ligand transfer, they undergo oligomerization and

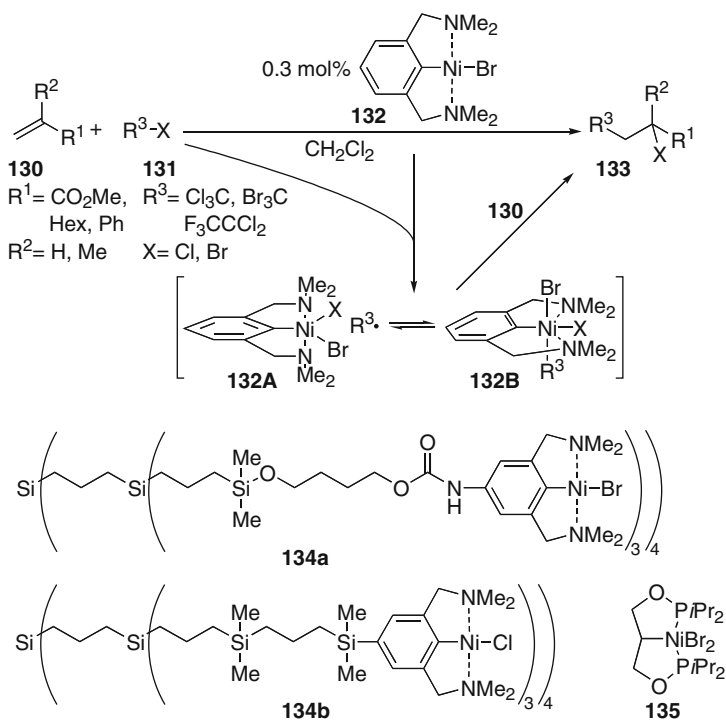


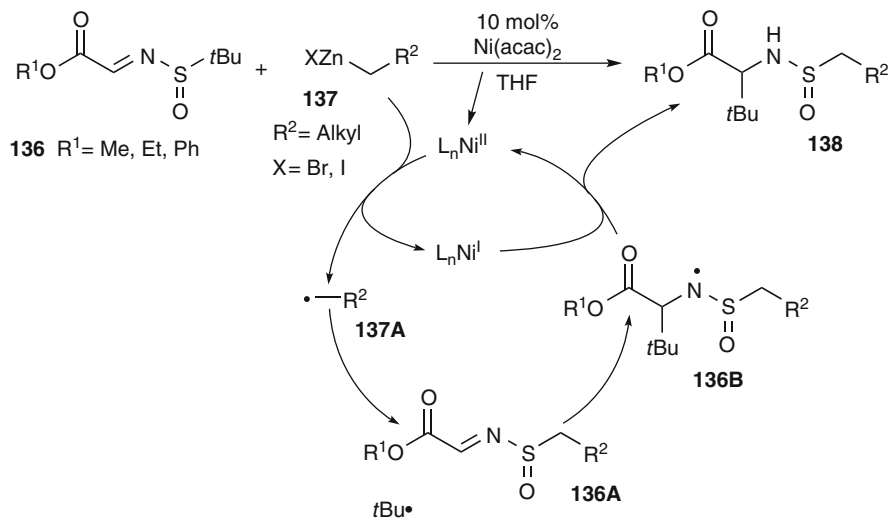
Fig. 33 Nickel-catalyzed Kharasch addition reactions

other typical processes. At the same time irreversible oxidation of the catalyst becomes predominant. This leads to a decrease of the catalytic activity and eventually to precipitation. If the spacer length increases, such as in **134b**, an increase of the efficiency of ATRA is again observed.

Pandarus and Zargarian developed propane-1,3-diol-based diphosphinite pincer nickel(III) complex **135** as a catalyst for Kharasch additions of olefins with  $\text{CCl}_4$  [154, 155]. Only 0.1 mol% of the complex catalyzed the reaction of several olefins, such as styrene, methyl (meth)acrylate, acrolein, or acrylonitrile, in 65–97% yield.

## 2.10 Ni(II)–Ni(I) Catalysis: Oxidative Rearrangement

Sun and coworkers reported 1,3-rearrangements of the sulfur substituent in acceptor-substituted *N-tert*-butylsulfinyl imines **136** catalyzed by 10 mol% of  $\text{Ni}(\text{acac})_2$  (Fig. 34) [156]. The aim of the study was to obtain branched *N*-sulfinylamines by addition of alkylzinc reagents **137**; however, *tert*-leucine derivatives **138** were isolated instead in 47–92% yield. The reaction was proposed to proceed by oxidative generation of radicals **137A** by the nickel catalyst. Addition to the sulfur atom, followed by  $\beta$ -fragmentation of the more stable *tert*-butyl radical, leads to *N*-alkylsulfinylimines **136A**, to which the resulting *tert*-butyl radical adds. Thus formed sulfinylaminyl radicals **136B** stabilize to products **138** either by hydrogen abstraction from the solvent or reoxidation of the coformed Ni(I) intermediate. Further investigations are necessary to prove the mechanistic course of this useful



**Fig. 34** Nickel-catalyzed 1,3-rearrangement of *tert*-butylsulfinyl imines with organozinc bromides

transformation, because other alternatives, such as a radical chain reaction triggered by trace amounts of oxygen, may also be a viable pathway.

### 3 Pd-Catalyzed Radical Reactions

The interaction of alkyl halides and palladium complexes has been studied since the 1970s in several labs [157]. It was shown that alkyl radicals result from the reaction of isopropyl iodide and Pd(PET<sub>3</sub>)<sub>3</sub> [158]. Alkyl radicals are also formed from reduction of alkyl iodides at palladated cathodes [159, 160]. The application of alkyl halides in coupling reactions was for long not considered very useful, since two-electron oxidative addition of Pd(0) to alkyl halides is rather slow compared to aryl and vinyl halides. Moreover, once an alkylpalladium species is generated, β-hydride elimination is facile leading to olefins as side or even major products [161]. More recently, however, it was shown that alkyl halides are useful in palladium catalyzed processes. On one hand they serve well as precursors for palladium-catalyzed radical transformations. On the other they can be activated by an S<sub>N</sub>2 process in the presence of proper ligands. Ligand design also allows the stabilization of alkylpalladium complexes and in turn their use in cross-coupling reactions, which occur by a two-electron process. This was shown by using chiral precursors in the coupling, which proceeded by stereoinversion or retention, respectively [29–33, 162–165].

Recently oxidative catalysis using high-valent palladium complexes has received more attention. A number of Pd(I) and Pd(III) complexes were characterized recently, which occur as dimers [166–169]. The oxidation of dialkylpalladium(II) complexes by SET oxidants was also investigated [170]. Reductive elimination is facilitated from oxidatively generated Pd(III) or Pd(IV) but does not involve carbon radical intermediates. Oxygen inserts on the other hand into dimethylpalladium complexes according to a radical chain mechanism leading to (methylperoxy)methylpalladium complexes [171]. It was shown that Pd(III) complexes are subject to facile reactions with radicals and photolytic radical generation [168].

#### 3.1 Pd(0)–Pd(I) Catalysis: Atom Transfer Radical Additions

Tsuji and colleagues investigated Kharasch addition reactions of CCl<sub>4</sub>, Cl<sub>3</sub>CBr, or methyl trichloroacetate to olefins in much detail [172, 173]. A catalyst system of Pd(OAc)<sub>2</sub>/PPh<sub>3</sub> in a ratio of 1:2 was applied in additions to simple terminal or 1,1-disubstituted olefins **139**, which gave the products **140** in 20–90% yield (Fig. 35). K<sub>2</sub>CO<sub>3</sub> was necessary as a base and the reactions worked best under an atmosphere of carbon monoxide. This suggests a Pd(0) species as the active catalyst. No incorporation of CO was observed. Prochiral olefins gave very similar

diastereoselectivities under classical free radical and palladium-catalyzed conditions, thus supporting a radical mechanism for these catalyzed reactions.

When the CO pressure was increased to 40 bar and alcohols were added, carbonylative additions took place giving mixtures of  $\beta$ -trichloromethylated esters **141** and simple Kharasch addition products **140** [174, 175]. The reactions are supposed to involve addition of the reductively generated trichloromethyl radical to **139** (cf. Part 1, Sect. 7, Fig. 37; Part 2, Sect. 2.2.1, Fig. 6; Part 2, Sect. 3.3.1, Fig. 36). The resulting radical can couple to the coformed palladium(I) complex followed by migratory insertion of CO and substitution by the alcohol. Alternatively, it may add directly to a bound CO ligand followed by substitution by the alcohol (see Sect. 3.4). Allylic alcohols **142** reacted with  $\text{CCl}_4$  catalyzed by 1 mol%  $\text{Pd}(\text{OAc})_2$  and 2 mol%  $\text{P}(o\text{-tol})_3$  affording 3,3,3-trichloromethylketones **144** in 39–87% yield [176, 177]. The reactions are thought to proceed by an initial Kharasch addition to the allylic alcohol. Indeed, halohydrins **143** were formed exclusively at 40°C. Monitoring the reactions at 60–80°C indicated an initial build-up of Kharasch addition products **143**, which transformed at more elevated temperatures to ketones **144**. Thus, more demanding phosphine ligands promote oxidative addition to the carbon–chlorine bond in **143**, which is followed by  $\beta$ -hydride elimination leading to ketones **144**.

Oshima reported more recently mild Kharasch additions of  $\text{Cl}_3\text{CBr}$  to olefins **139** catalyzed by a combination of 2 mol%  $\text{Pd}(\text{PhCN})_2\text{Cl}_2/\text{dppf}$  in the presence of diethylamine as a base in an aqueous–organic biphasic medium [178]. Terminal functionalized alkenes gave the addition products **140** in 39–93% yield. Internal

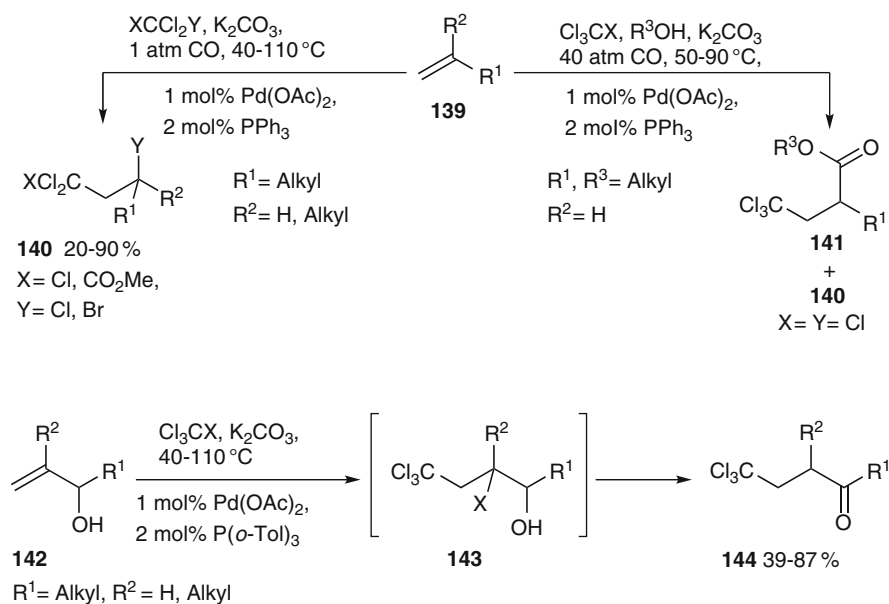
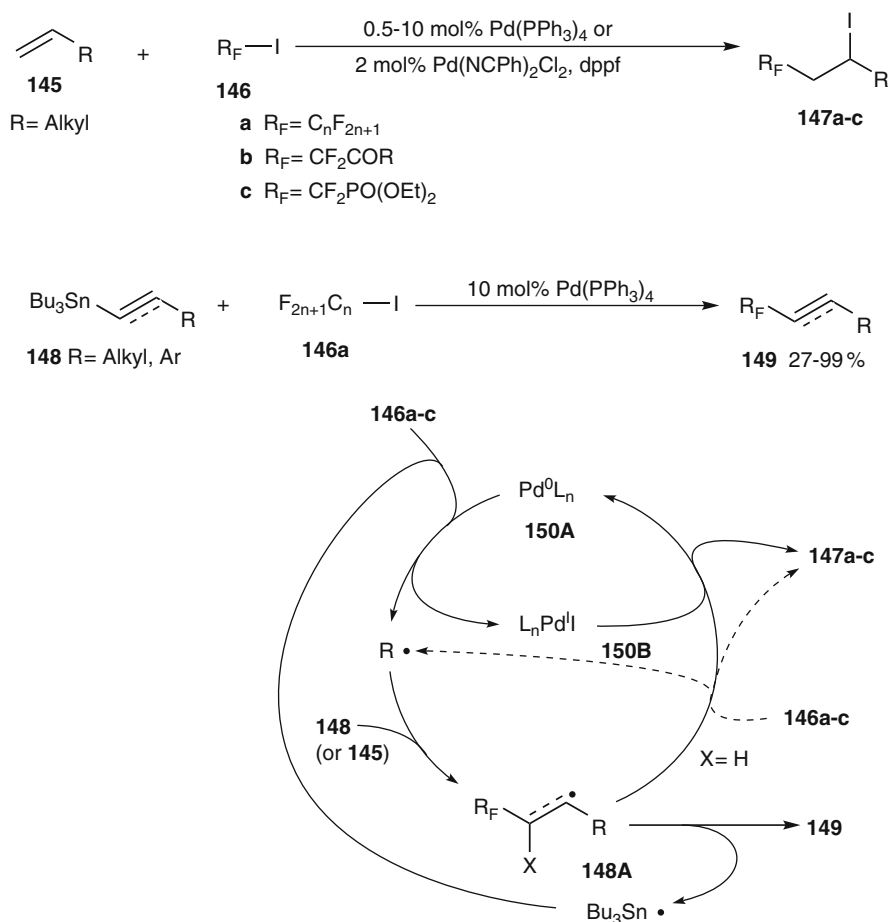


Fig. 35 Pd(0)-catalyzed Kharasch additions

alkenes reacted sluggishly. 1,6-Dienes were subject to tandem addition/radical 5-exo cyclization sequences providing halogenated cycles in 43–80% yield and 3–4:1 *cis/trans*-selectivity (cf. Part 2, Sect. 3.3.3, Fig. 42, **169**→**170**).

Chen and coworkers [179] as well as Ishihara et al. [180] investigated atom transfer radical additions of perfluoroalkyl iodides **146a** to olefins **145** catalyzed by Pd(PPh<sub>3</sub>)<sub>4</sub> starting in the middle of the 1980s (Fig. 36). Adding 0.5–1 mol% of the catalyst to a neat mixture of **146a** and **145** or 5–10 mol% to a hexane solution of the components led to fast reactions at room temperature giving iodides **147a** in 34–97% yield. Perfluoroalkyl bromides provided only low yields. A Pd(II) complex as the catalyst precursor required the presence of an amine or another base, probably to reduce Pd(II) to catalytically active Pd(0). The failure to detect Heck-type reaction products and the high thermal stability of (perfluoroalkyl)palladium(II) complexes rule out a two-electron catalytic cycle involving them. A radical mechanism is likely



**Fig. 36** Pd(0)-catalyzed atom transfer radical addition reactions

based on inhibition and spin trapping/ESR experiments using phenyl *tert*-butyl nitron (PBN) or 2-nitrosoisobutane. The occurrence of a cyclization reaction when diallyl ether **65** was used as the substrate supports a radical pathway too.

Qiu and Burton studied the reaction of  $\alpha,\alpha$ -difluoro- $\alpha$ -iodo ketones **146b** with alkenes **145** in the presence of 1.5–3 mol% of Pd(PPh<sub>3</sub>)<sub>4</sub> [181, 182]. A smooth atom transfer radical addition occurred under neat conditions providing  $\alpha,\alpha$ -difluoro- $\gamma$ -iodo ketones **147b** in 50–93% yield. Tandem radical addition/5-*exo* cyclization/iodine transfer reactions of diallyl ether **65** or diallyl malonate proceeded in 66–80% yield. The palladium catalyst acts most likely only as an initiator. When a catalytic system of 1.3–3 mol% Pd(PPh<sub>3</sub>)<sub>4</sub> and 6–20 mol% NiCl<sub>2</sub>·6H<sub>2</sub>O was applied in the presence of zinc as a stoichiometric reducing agent, reductive radical additions leading to  $\alpha,\alpha$ -difluoro ketones succeeded in 68–82% yield (cf. Fig. 8). Atom transfer radical additions of difluoroiodomethylphosphonate **146c** catalyzed by 2 mol% of Pd(PPh<sub>3</sub>)<sub>4</sub> at room temperature provided phosphonates **147c** in 63–91% yield [183]. A tandem radical addition/5-*exo* cyclization/atom transfer sequence succeeded in 82% yield when diallyl ether **65** was used as the substrate.

Matsubara and colleagues established Stille-type coupling reactions of perfluoroalkyl halides **146a** with allyl, alkynyl, or vinyl stannanes **148** catalyzed by 10 mol% of Pd(PPh<sub>3</sub>)<sub>4</sub> (Fig. 36) [184]. The reaction gave perfluoroalkylated olefins or alkynes **149** in 27–99% yield. The former were obtained as pure (*E*)-isomers, irrespective of the configuration of the precursor. Based on the similarity to other addition reactions, a radical mechanism was proposed. Shimizu and Fuchikami later reported very similar transformations of  $\beta$ -fluorinated alkyl iodides catalyzed by 10 mol% of Pd(PPh<sub>3</sub>)<sub>2</sub>Cl<sub>2</sub> or Pd(PPh<sub>3</sub>)<sub>4</sub> giving formal coupling products **149** in 41–97% yield [185]. The authors proposed a two-electron mechanism for these reactions. The similarity of the conditions to other Pd(0)-catalyzed additions suggests, however, rather a radical pathway. This is also supported by the fact that an (*E,Z*)-mixture of 2-phenylvinylstannane provided the (*E*)-product **149** exclusively, while two-electron Stille coupling reactions should occur with retention of configuration at the alkene. Carbonylation/addition sequences provided ketones in 29–97% yield.

All these reactions were proposed to proceed by reductive generation of perfluoroalkyl radicals from **146** induced by palladium(0) species **150A**. Addition of this radical to alkenes **145** or stannanes **148** leads to radicals **148A**. Depending on the conditions, this radical can undergo a ligand transfer from cogenerated Pd(I)I intermediate **150B** thus forming products **147** and the active Pd(0) catalyst (solid arrows). For several reactions, only an initiator function of the palladium catalyst was proposed (dashed arrows). Here atom transfer to radical **148A** by the starting iodide **146**, which is present in large excess compared to the palladium catalyst, results in an overall chain reaction. A classical chain reaction with Pd(PPh<sub>3</sub>)<sub>4</sub> as an initiator was also proposed in the reactions involving **148**. After formation of radical **148A** a  $\beta$ -fragmentation ensues, which leads to formal Stille coupling products **149** and a stannyl radical, which carries the chain.

Oshima showed subsequently that 2 mol% of a Pd(0) catalyst generated from Pd(PhCN)<sub>2</sub>Cl<sub>2</sub> and dppf was active as a catalyst for ATRA of perfluoroalkyl iodides





compete to a significant extent in the reactions of norbornadiene and cyclooctene, respectively (cf. Part 2, Sect. 2.2.1, Fig. 6 33→34).

### 3.2 Pd(0)–Pd(I) Catalysis: Atom Transfer Cyclizations

Mori and Ban developed cyclizations of *N*-allylic iodoacetamides **158a** and 3- or 4-(allylamino)-2-halo esters **161** catalyzed by 10 mol% of Pd(PPh<sub>3</sub>)<sub>4</sub> giving 4-halomethyl-2-pyrrolidones **159a** [187, 188] or 4-halomethylpyrrolidin-3-carboxylates **162** [189, 190], respectively, in moderate to good yields (Fig. 39). This methodology was extended to 6-exo cyclizations of 4-(allylamino)-2-iodo ketones [191] and 7-endo cyclizations of β-lactams [192]. In many reactions unsaturated products similar to **160** were formed as side products. A traditional two-electron catalytic cycle was proposed to operate, although some unusual reactivity patterns in organopalladium chemistry were noted: (1) oxidative addition of Pd(0) to alkyl halides and (2) reductive elimination from an alkylpalladium halide is faster than β-hydride elimination. Control experiments applying an independently generated authentic palladium enolate showed that: (1) in contrast to the cyclizations above, preferential β-hydride elimination and only little cyclization

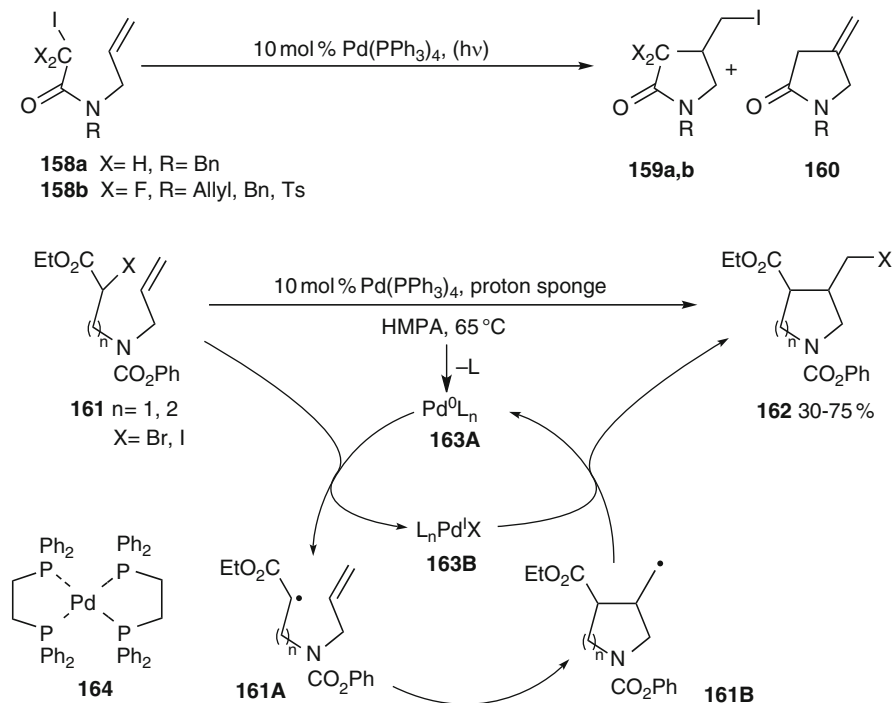


Fig. 39 Pd-catalyzed iodine atom transfer cyclization reactions

occurred and (2) the small part of cyclized material proved to be **160** resulting from  $\beta$ -hydride elimination, but not iodinated product **159**.

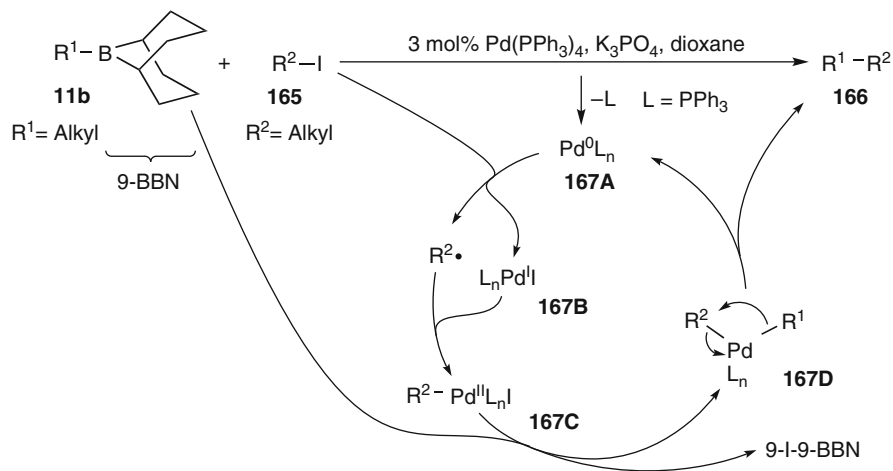
Curran and Chang realized that Mori's and Ban's results were very similar to iodine transfer radical cyclizations and investigated the cyclization of several structurally different  $\alpha$ -iodo esters under typical radical atom transfer conditions (10 mol%  $\text{Bu}_6\text{Sn}_2$ ,  $h\nu$ ) and palladium catalysis (10 mol%  $\text{Pd}(\text{dppe})_2$  **164**) [193]. Virtually identical product ratios were obtained. They concluded that Mori's and Ban's Pd-catalyzed ene-halo cyclizations are better described by a radical mechanism, which involves initial generation of  $\alpha$ -carbonyl radicals **161A** by reductive SET mediated by Pd(0) species **163A**. A subsequent radical cyclization forms **161B**, from which the product is formed by iodine transfer from Pd(I) species **163B**. Unsaturated compounds, such as **160**, may arise from some competing coupling of the cyclized radicals **161B** with the palladium atom of **163B** and subsequent  $\beta$ -hydride elimination. An allylic iodide showed in contrast a very different reactivity under the two conditions.

Nagashima and colleagues showed subsequently that 5–10 mol% of  $\text{Pd}(\text{PPh}_3)_4$  catalyzed atom transfer radical cyclizations (ATRC) of *N*-allyl-difluoroiodoacetamides **158b** in fluorescent lab light at ambient temperature [194]. Under these conditions, 34–98% yield of cyclized compounds **159b** were obtained. No reaction occurred in the dark, while it was considerably slower in the absence of the catalyst. The low yield of 34% in one example ( $\text{R}=\text{Bn}$ ) is due to the unfavorable rotational barrier in the substrate, which cannot be influenced by the presence of the catalyst.

### 3.3 Pd(0)–Pd(I)–Pd(II) Catalysis: Cross-Coupling Reactions

Castle and Widdowson were first to disclose alkyl–alkyl Kumada coupling reactions catalyzed by  $\text{Pd}(\text{dppf})\text{Cl}_2$  [195]. This report was later questioned and corrected by Scott [196]. Matsubara and colleagues established formal Stille-type coupling reactions of perfluoroalkyl halides with allyl, alkynyl, or vinyl stannanes catalyzed by 10 mol% of  $\text{Pd}(\text{PPh}_3)_4$ , which have to be considered, however, better as radical addition/elimination reactions rather than as coupling reactions (see Sect. 3.1) [184].

Direct Suzuki coupling reactions of alkyl iodides **165** with 9-alkyl-9-BBN **11b** yielding hydrocarbons **166** were performed in 45–71% yield in the presence of 3 mol%  $\text{Pd}(\text{PPh}_3)_4$  and  $\text{K}_3\text{PO}_4$  as a base (Fig. 40) [197]. These reactions are not affected by light as similar carbonylation reactions (see Sect. 3.4). Based on the formation of a 1:2 mixture of cyclized and uncyclized coupling products from 5-hexenyl iodide, a radical catalytic cycle was proposed. In line with other results, the Pd(0) catalyst **167A** reduces **165** to a radical, which couples subsequently with the palladium(I) intermediate **167B**. Transmetalation of the resulting alkylpalladium(II) complex **167C** by **11b** gives a diorganopalladium species **167D**, which is subject to reductive elimination. The formation and stability of compound **167C** seems to be yield limiting, since alkenes and alkanes generated



**Fig. 40** Alkyl-alkyl cross-coupling reactions catalyzed by Pd(0) complexes

from **165** by  $\beta$ -hydride and reductive eliminations are the major side products. Side products arising from **11b** were in contrast observed only to a very minor extent. Both  $Pd(PPh_3)_4$  and 9-BBN derivatives **11b** are unique for this process, since neither other Pd(0) catalysts nor other organometallic components (boranes, stannanes, organozinc or Grignard reagents) provided a product under similar conditions.

Lipshutz and colleagues presented recently palladium-catalyzed direct coupling reactions of alkyl iodides and vinyl bromides or iodides catalyzed by 1 mol%  $Pd(\text{amphos})Cl_2$  in the presence of zinc and TMEDA in a biphasic aqueous/poly(ethylene glycol tocopheryl sebacate) reaction medium [198]. Internal olefins were obtained in 51–95% yield. For aryl-substituted (*E*)-vinyl bromides, retention of double bond geometry was observed, while different degrees of isomerization occurred for (*Z*)-isomers, which may indicate the intervention of a radical addition process in the course of the coupling process. Alkyl-substituted (*Z*)-vinyl halides were transformed in contrast with retention of alkene geometry. Aryl halides also reacted [199].

A number of Pd(0)-catalyzed alkyl cross-couplings using alkyl halides, such as Suzuki–Miyaura [200, 201], Negishi [202, 203], or Stille [204] couplings, were reported. These reactions might proceed via radical intermediates based on substrates, catalysts, and the observed product spectrum, but mechanistic information is so far lacking. In contrast, Fu's catalytic coupling reactions of alkyl halides involve an initial  $S_N2$  process to generate the alkylpalladium intermediate [162, 163]. Pd(0)-catalyzed coupling of alkyl tosylates with Grignard reagents in the presence of 1,3-diene ligands disclosed by Terao and colleagues proceed by a two-electron catalytic cycle based on the formation of a ring-closed coupling product when cyclopropylmethyl bromide was used (cf. Part 1, Fig. 8) [36, 205].

Manolikakes and Knochel provided recently evidence that aryl–aryl Kumada-coupling reactions can be accelerated dramatically by involving radical intermediates (Fig. 41) [206]. When aryl Grignard reagents **173** were generated by a magnesium–iodine exchange from aryl iodides **169** and isopropylmagnesium chloride an almost instantaneous coupling reaction with aryl bromides **168** was observed under very mild conditions using either 2 mol% of PEPPSI **170** or a catalyst generated from 2 mol% Pd(OAc)<sub>2</sub> and 3 mol% S-Phos **171a**. The reaction worked for a wide variety of aryl and heteroaryl bromides or iodides and Grignard

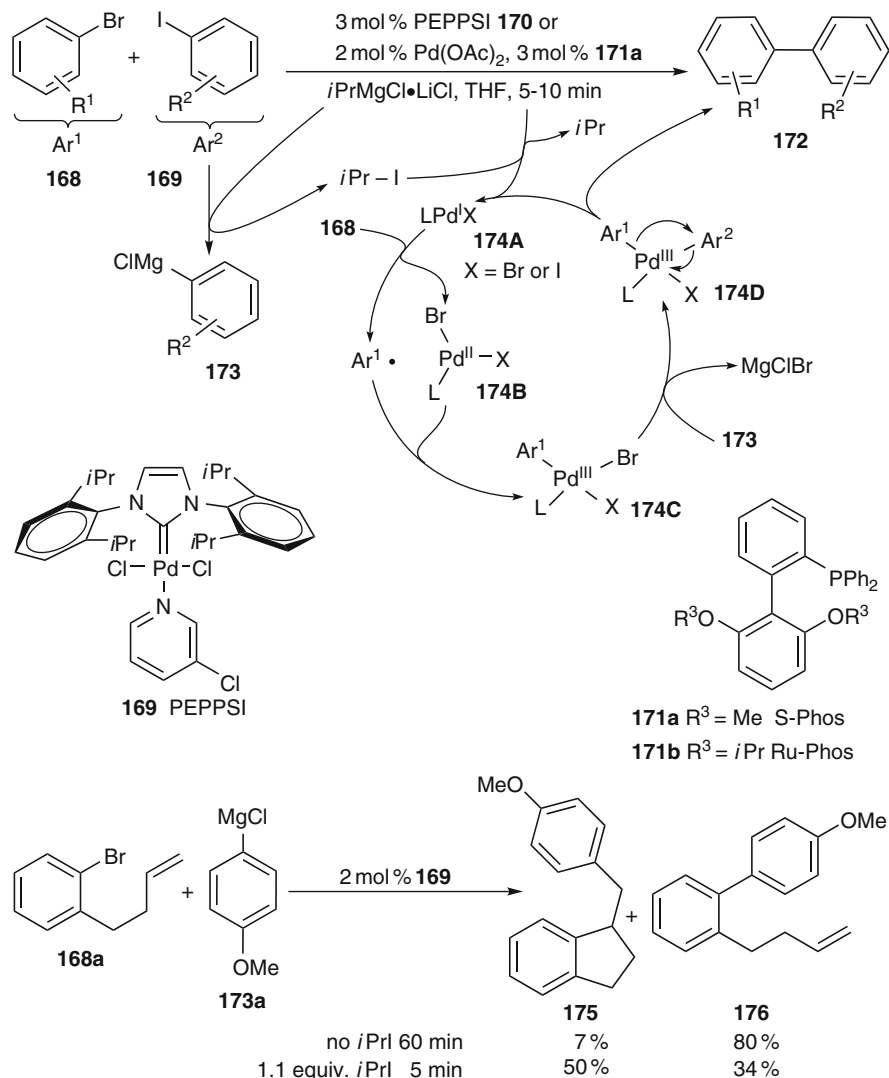


Fig. 41 Aryl–aryl Kumada couplings facilitated by isopropyl iodide

reagents and afforded biaryls **172** in 74–98% yield. Sensitive functionality, for example ester or nitrile groups, is tolerated.

Control experiments using *ortho*-(3-butenyl)bromobenzene **168a** and **173** showed that the reaction proceeded only slowly in the absence of *i*PrI, which is the coproduct during the formation of the Grignard reagent **173**. The major product was direct coupling product **176** and only very little cyclization to **175** occurred. In the presence of *i*PrI the reaction was finished in 5 min and 50% of benzy lindane **175** was formed in addition to 34% of **176**. On the other hand introduction of the 3-butenyl side chain into the Grignard reagent afforded only biaryl **172** but no cyclic product at all.

Based on these findings the authors proposed that the palladium(0) catalysts are oxidized to Pd(I) intermediates **174A** by *i*PrI in the initiation step. This species is able to abstract a bromine atom from aryl bromide **168** generating an aryl radical and Pd(II) complex **174B**. The aryl radical couples to **174B** leading to an arylpalladium(III) species **174C**, which transmetalates with the aryl Grignard reagent **173**. Reductive elimination from the diarylpalladium(III) species **174D** regenerates the palladium(I) catalyst **174A** and liberates the product **172**.

The acceleration by isopropyl iodide was also found in Negishi coupling reactions. When aryl Grignard reagents **173** formed initially from aryl iodides **169** and *i*PrMgCl were transmetalated by ZnCl<sub>2</sub>·2LiCl prior to coupling catalyzed by 1 mol% Pd(dba)<sub>2</sub> and 2 mol% RuPhos **171b**, biaryls **172** [207] which may contain cyano, ester, keto, fluoro, chloro, trifluoromethyl, amino, and hydroxy-groups, were isolated in 73–97% yield. Acidic *para*-bromophenylacetates or -acetonitriles are also applicable in very good yields using this protocol. A few alkylzinc reagents were also applied and coupled in 67–79% yield.

### 3.4 Pd(0)–Pd(I)–Pd(II) Catalysis: Carbonylation and Carbonylation/Coupling Reactions

Urata and coworkers developed alkoxycarbonylation, carboxylation [208], as well as aminodicarbonylation reactions [31, 209] of fluoroalkyl iodides catalyzed by Pd(0) or Pd(II) proceeding at 80–100 C under 30–50 atm CO pressure. Fluorinated carboxylic acids, esters, or  $\alpha$ -keto amides were isolated in moderate to good yields. In the aminodicarbonylation reactions variable amounts of fluorinated amides were formed as byproducts. Although no mechanistic information was provided, the reactions may occur by initial SET reduction of the iodide by the initially generated Pd(0) complex in analogy to Pd-catalyzed couplings as well as radical addition and cyclization reactions (see Sects. 3.1–3.3, and 3.5).

Ryu and coworkers subsequently reported photochemically initiated radical alkoxycarbonylation reactions of alkyl iodides **177** using 5 mol% of Pd(PPh<sub>3</sub>)<sub>4</sub> as the catalyst (Fig. 42) [210]. The reaction proceeds by light-stimulated reductive generation of an alkyl radical by the palladium(0) catalyst **179A**. This radical has three options to react further. Direct addition to CO forms the acyl radical **177A**.

This radical can couple with cogenerated Pd(I) complex **179B** giving rise to acylpalladium(II) complex **177B**. On the other hand, addition of the alkyl radical to the CO ligand coordinated at palladium of 17-electron valence tautomeric Pd(I) complex pair **179C/179D** is also viable. The third pathway consists of coupling of the radical with the coordinatively unsaturated metal center of **179C/179D** leading to complex **179E**. Migratory insertion of CO subsequently provides **177B**. According to a computational investigation, coupling to palladium-bound CO is the only energetically feasible pathway in 18-electron palladium(0) complexes besides direct radical addition to CO, while in coordinatively unsaturated 16-electron palladium(0) complexes addition to both the metal and the CO ligand are

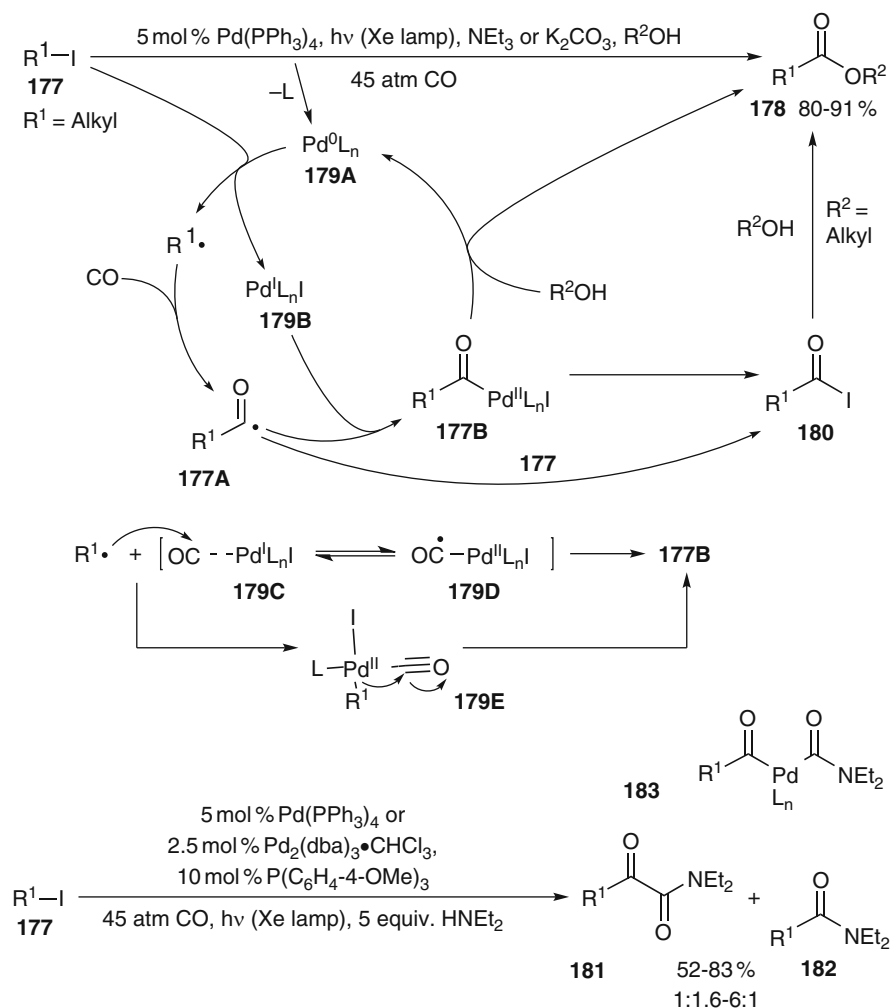


Fig. 42 Photochemically mediated Pd-catalyzed alkoxy and aminocarbonylation reactions

favorable [211]. No matter what path is followed, acylpalladium species **177B** results. Products **178** can subsequently form from **177B** via ligand substitution with alcohols. An alternative reductive elimination from **177B** or an atom transfer from **177** to acyl radical **177A** resulting in acyl iodides **180** cannot be completely excluded. Alcoholysis of the latter would provide products **178**.

Analogous aminocarbonylations of **177** furnished mixtures of mono- and dicarbonylation products **181** and **182** in 52–91% yield [209, 210]. The formation of **181** is surprising, since it is known that non-metal-catalyzed radical carbonylations give hardly any dicarbonylation products of type **181** (reviews [212, 213]). Analogous radical carbonylations catalyzed by  $\text{Mn}_2(\text{CO})_{10}$  do not give double carbonylation products as well (see Part 1, Sect. 9.1) [214, 215]. The formation of  $\alpha$ -keto amides **181** supports the intermediacy of (acyl)(carbamoyl)palladium complexes **183**, which undergo reductive elimination. This carbonylation methodology was applied to the total synthesis of the lignan hinokinin and the red pepper component dihydrocapsaicin.

The aminocarbonylation reaction of secondary alkyl iodides **177** affording **182** succeeded in the ionic liquid  $[\text{bmim}]\text{NTf}_2$  in 44–87% yield [216]. Double carbonylation products **181** were formed only to a small extent under these conditions. Tertiary alkyl iodides gave lower yields of monocarbonylation products **182** (38–61%). With adamantyl iodide 33% of double carbonylation product **181** was also formed. Primary alkyl iodides reacted only slowly under the conditions and gave mixtures of carbonylation, double carbonylation, and simple amination products in low yield.

Suzuki and coworkers found that Pd(0)-catalyzed light-promoted carbonylation/cross-coupling reactions of alkyl iodides **177** with carbon monoxide and in situ generated 9-alkyl-9-BBN **11b** afforded ketones **184** in 50–76% yield (Fig. 43) [217]. The reaction is applicable to primary, secondary, and tertiary alkyl iodides **177**. Functional groups, such as nitrile, acetal, and ester units, are tolerated. It was suggested that light irradiation facilitates ligand dissociation from the Pd(0) catalyst, which in turn accelerates SET reduction of **177** to a radical. This may react to acylpalladium(II) species **177B** following one of the three alternative pathways (cf. Fig. 42). The acyl complex transmetalates the borane **11b** and releases the products **184** by reductive elimination in the final step. The intermediacy of free alkyl radicals is supported by the isolation of a cyclopentylmethyl ketone in 60% yield, when 5-hexenyl iodide was applied as the substrate (cf. Part 1, Fig. 8).

Very recently Ryu and coworkers disclosed radical carbonylation/Sonogashira coupling sequences (Fig. 44) [218]. The reaction is applicable to primary, secondary, and tertiary alkyl iodides **177**, and terminal aryl or alkyl alkynes **185**. Alkynyl

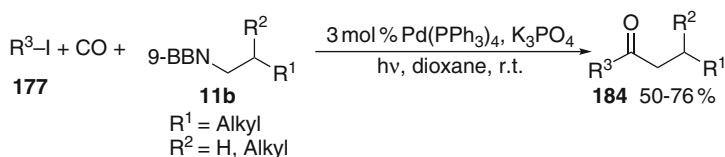
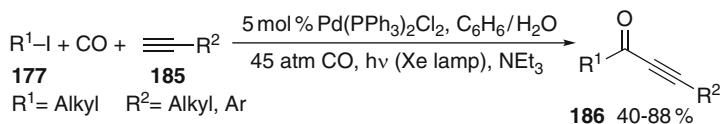


Fig. 43 Palladium-catalyzed tandem carbonylation/Suzuki coupling reactions



**Fig. 44** Tandem carbonylation/Sonogashira coupling sequences of alkyl halides

ketones **186** were isolated in 40–88% yield. When cyclopropylmethyl iodide was applied only the linear product was isolated in 42% yield (*cf.* Part 1, Fig. 8). The reaction was proposed to occur by initial light-assisted SET reduction of **177**. The resulting radical forms an acylpalladium species **177B** (*cf.* Fig. 42). This intermediate coordinates **185** leading to an acylpalladium acetylide, which forms product **186** by reductive elimination.

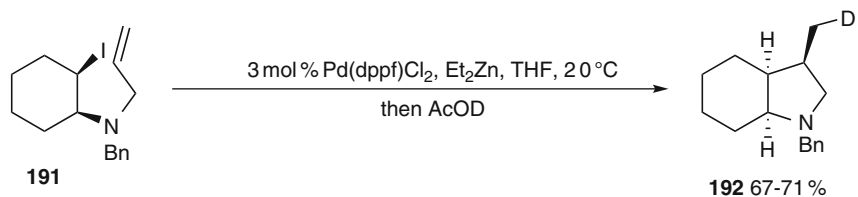
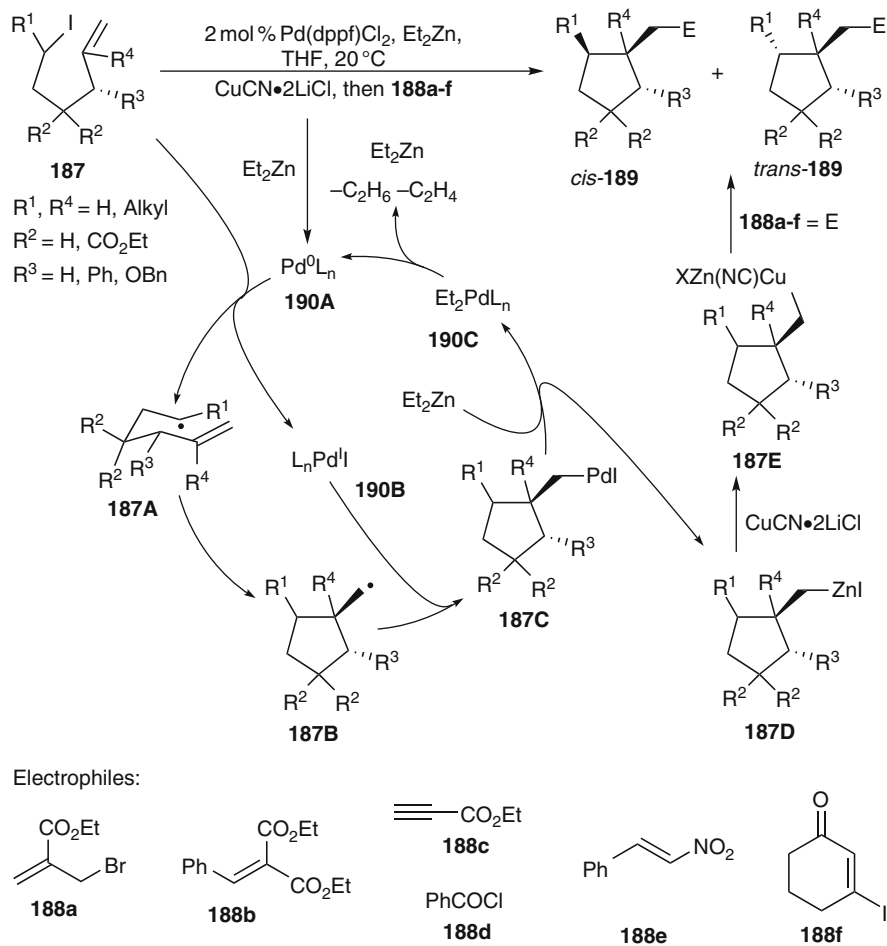
### 3.5 Pd(0)–Pd(I)–Pd(II) Catalysis: Radical Cyclizations

While studying Pd(II) and Ni(II) catalyzed alkyl exchange reactions of alkyl iodides at Et<sub>2</sub>Zn, Knochel and coworkers noted that these reactions were inhibited by nitrobenzene and did not work with alkyl sulfonates as substrates [219]. They reasoned that this alkyl exchange reaction is a process involving radical intermediates. They demonstrated subsequently that 1.5–3 mol% of Pd(dppf)Cl<sub>2</sub> catalyzed cyclization/(conjugate) addition sequences of a number of 5-hexenyl iodide substrates **187** in the presence of the CuCN·2LiCl complex with electrophiles **188a–f** (Fig. 45) [111, 220]. Diversely functionalized cyclopentane derivatives **189** were obtained in 41–90% yield. The method tolerates ester and nitrile functions in **187**.

When using stereochemically more elaborate precursors **187** a close relationship to free-radical cyclization reactions with respect to their diastereoselectivity was noted. Thus, 4-substituted 5-hexenyl iodides reacted with good *trans*-selectivity, while 1-substituted derivatives gave moderate *cis*-selectivity that is dependent on the size of the substituent. Tandem cyclizations provided bicyclo[3.3.0]octanes or angular triquinanes in 63–85% yields. Even cyclization reactions to  $\alpha,\beta$ -unsaturated esters or ketones proceeded in 52–73% yield. *N*-Allyl- $\beta$ -iodo amine **191** cyclized stereoselectively to annulated pyrrolidine **192** under similar conditions [107]. Substrates having a  $\beta$ -pivaloyloxy substituent cyclized cleanly, thus indicating that  $\beta$ -acyloxymetal intermediates, which are prone to facile E1cB reactions, are not present in the process. The radical nature of the cyclization is also supported by the fact that individual *exo*- and *endo*-bicyclo[4.1.0]heptyl bromides gave exclusively the *exo*-coupling product, which is not in accord with either oxidative addition or S<sub>N</sub>2 pathways.

The course of the reactions was rationalized by initial reduction of the Pd(II) precatalyst to a Pd(0) species **190A** by diethylzinc. This electron-rich complex reduces the alkyl iodide **187** to a radical **187A**, which undergoes cyclization to the alkene unit. The diastereoselectivity of the cyclizations can be explained by a Beckwith–Houk





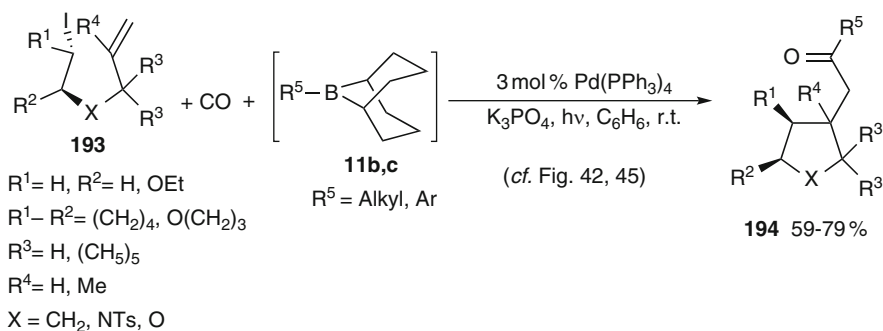
**Fig. 45** Pd-catalyzed diethylzinc mediated radical cyclization/addition or substitution sequences

transition state [221, 222]. The resulting radical **187B** couples to cogenerated Pd(I) intermediate **190B**. So formed cyclic organopalladium(II) complex **187C** transmetalates with Et<sub>2</sub>Zn to release a diethylpalladium species **190C** and cyclopentylmethylzinc intermediate **187D**, which can be functionalized in multiple ways. Iodination or silylation leads to heteroatom-substituted cyclic products (not shown).

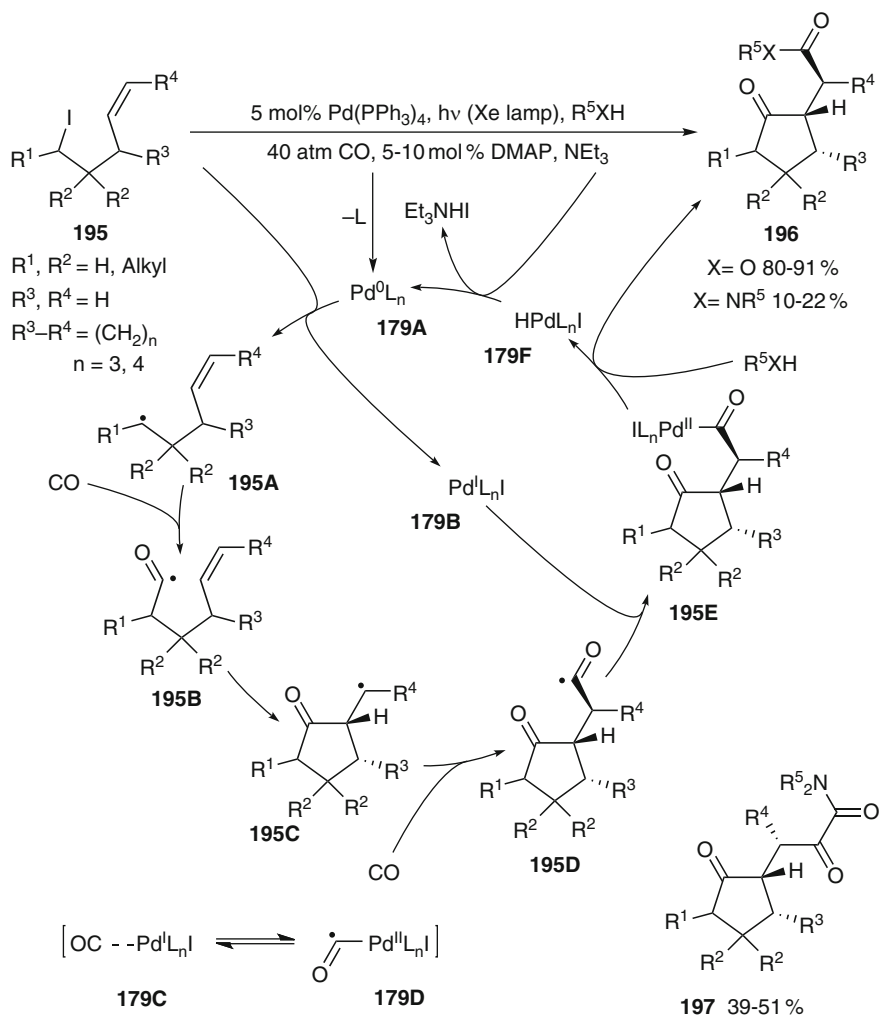
Transmetalation of the organozinc compound by copper(I) leads to more nucleophilic alkylcopper intermediates **187E**, which undergo Michael addition reactions or allylic substitutions with electrophiles **188** providing products **189** easily. This procedure allows a difunctionalization of the alkene unit in the starting materials **187**. The coformed diethylpalladium(II) species **190C** regenerates **190A** by  $\beta$ -hydride and reductive elimination. Substrates, in which radicals **187B** being secondary resulted after cyclization, gave only reduced cyclic products, but no reaction with **188**.

Miyaura and colleagues published a tandem radical cyclization/carbonylation/cross-coupling methodology to construct cycloalkyl ketones **194** (Fig. 46) [223]. Structurally different 5-hexenyl iodides **193** and related  $\beta$ -iodo amines or ethers reacted with 9-alkyl- or 9-aryl-9-BBN **11b,c** in the presence of 3 mol% Pd(PPh<sub>3</sub>)<sub>4</sub> and anhydrous K<sub>3</sub>PO<sub>4</sub> to afford cyclopentylmethyl ketones **194** as well as related tetrahydrofurans or pyrrolidines substituted with a 2-oxoalkyl side chain in 59–79% yield. The reactions are initiated by reductive electron transfer from the Pd(0) catalyst to **193** generating an alkyl radical, which cyclizes (cf. Figs. 42 and 45). The cyclized radical couples with coformed Pd(I) and the resulting (alkyl)Pd(II) complex is subsequently subject to migratory insertion of carbon monoxide. The reaction sequence to **194** continues by transmetalation with **11** and reductive elimination. Analogous 6-exo cyclizations were not efficient.

Ryu and colleagues developed radical carbonylation chemistry extensively [212]. Based on this highly selective photochemically mediated carbonylative radical cyclizations of 4-pentenyl iodides **195** catalyzed by 5 mol% of Pd(PPh<sub>3</sub>)<sub>4</sub> were discovered (Fig. 47) [224]. The reactions proceed by initial photostimulated reductive generation of an alkyl radical **195A** by the palladium catalyst **179A**. This adds to CO leading to acyl radical **195B**, which is now able to cyclize in a 5-exo process leading to cyclopentanone radical **195C**. A second carbonylation provides acyl radical **195D**, which can combine with Pd(I)I **179B** present in the reaction medium. The coupling partner for **195C** can also be the valence tautomeric pair **179C/179D**. The resulting acylpalladium intermediate **195E** undergoes a substitution by alcohols or amines according to the established mechanism to give the ester

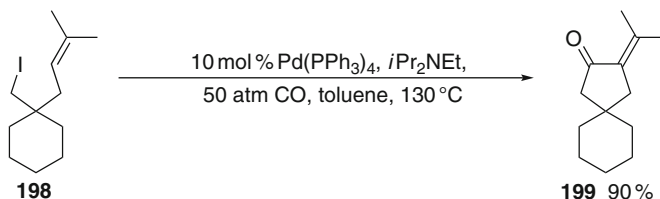


**Fig. 46** Light-stimulated palladium-catalyzed tandem radical cyclization/carbonylation/Suzuki–Miyaura coupling reactions



**Fig. 47** Photostimulated Pd(0)-catalyzed carbonylative radical cyclizations

or amide products **196** and a palladium hydride species **179F**, which re-forms the Pd(0) catalyst **179A** by dehydroiodination. A remarkable feature of the overall process is that the lifetime of the transient radicals **195A–D** can be increased by a reversible coupling to a persistent Pd(I) species **179B**. No reaction was observed in the absence of irradiation. That acylpalladium species **195E** are involved is supported by the isolation of significant quantities of dicarbonylation product **197**, which results from reductive elimination of diacylpalladium species **183** (cf. Fig. 42). Very recently, a similar tandem carbonylation/5-exo cyclization/carbonylation/Sonogashira-type coupling reaction of **195**, CO, and alkynes catalyzed by 5 mol% of Pd(PPh<sub>3</sub>)<sub>2</sub>Cl<sub>2</sub> was reported [218].



**Fig. 48** Pd(0)-catalyzed thermal carbonylative Heck-type cyclization reactions

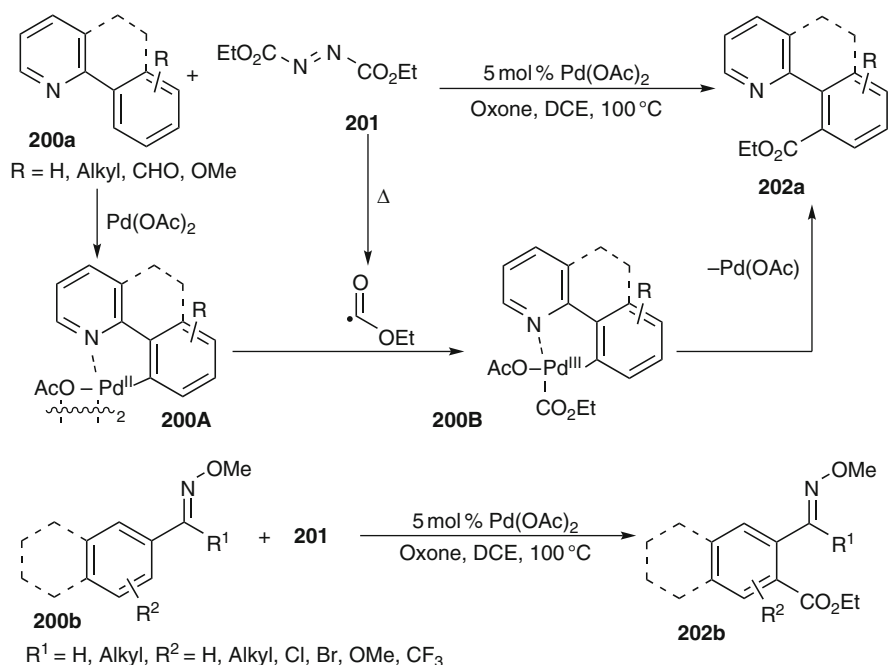
Bloome and Alexanian presented very recently a thermal variant of such carbonylative radical cyclizations (Fig. 48) [225]. When 4-pentenyl iodides, such as **198**, were subjected to 10 mol% of Pd(PPh<sub>3</sub>)<sub>4</sub> in the presence of Hünig's base under 50 bar of CO at 130°C, bi- or spirocyclic ketones resulted in 55–91% yield as illustrated by **199**. An experiment in the presence of TEMPO (cf. Part 1, Fig. 7, **17**) produced 17% of acyclic trapping product together with 65% of cyclic material. This suggests the initial reductive generation of alkyl radicals and Pd(I)I, which add carbon monoxide to provide an acyl radical (cf. Figs. 42 and 47). A radical 5-exo cyclization followed by coupling with the coformed persistent Pd(I) intermediate leads to a Pd(II) species that stabilizes to the product by β-hydride elimination.

### 3.6 Pd(II)-Catalyzed Ring Opening of Endoperoxides

Noyori and colleagues investigated the ring opening of unsaturated mono- and bicyclic endoperoxides catalyzed by 5–10 mol% of Pd(PPh<sub>3</sub>)<sub>4</sub> [226, 227]. Similarly to the cobalt-catalyzed reactions, (*Z*)-4-hydroxy enones resulted as the main products, which were accompanied by (*Z*)-2-ene-1,4-diols and diepoxides. The latter are formed as the major products under either ruthenium or cobalt catalysis (see Part 2, Sects. 3.5 and 5.8). Both two-electron and radical mechanisms were considered for this transformation. Saturated bicyclic endoperoxides gave mixtures of cyclic 4-hydroxy ketones and 1,4-diols and their formation may be a result of a radical process [227, 228].

### 3.7 Pd(II)–Pd(III)–Pd(IV) Catalysis

Catalysis by high-valent palladium complexes rose recently into the focus of research (review [229]). In an attempt to apply azodicarboxylates as C–H amination reagents, Yu, Chan, and colleagues discovered that the reaction of 2-arylpyridines **200a** or oxime ethers **200b** with diethyl azodicarboxylate (DEAD) **201** catalyzed by 5 mol% of Pd(OAc)<sub>2</sub> gave benzoic acid esters **202a** or **202b** instead (Fig. 49) [230]. The reactions required a stoichiometric oxidant. Oxone, Cu(OAc)<sub>2</sub>, or K<sub>2</sub>S<sub>2</sub>O<sub>8</sub> proved to be best. Arylcarboxylates **202a** or **202b** were isolated in 78–87% and



**Fig. 49** Pd(II)-catalyzed alkoxyacylation of arenes by diethyl azodicarboxylate

27–85% yields, respectively. The reactions proceed probably by initial cyclopalladation to the *ortho*-C–H bond of the substrates leading to arylpalladium(II) species **200A**. DEAD **201** decomposes under the reaction conditions to an alkoxyacyl radical, which may stabilize by addition to arylpalladium intermediate **200A** resulting in acylpalladium(III) complex **200B**. Under the oxidative conditions, a palladium(IV) complex may also be reached. Reductive elimination furnishes **202a** or **202b** and a Pd(I) or Pd(II) complex. The former will be reoxidized to regenerate the active Pd(II) catalyst.

The same group reported subsequently an arylation methodology based on substrates **200a** or **200b** and diaryl peroxides **203** catalyzed by 5–10 mol% of Pd(OAc)<sub>2</sub> (Fig. 50) [231]. Arylated products **204** were formed in 54–84% yield based on conversion of **200a**. When dianisoyl peroxide **203** (R<sup>2</sup>=4-OMe) was used, in which the decarboxylation is retarded, *ortho*-aryloxy arene **205** was formed in 90% yield. The reaction course can be described similarly as above by an initial cyclopalladation of substrates **200**. Thermal homolysis generates aryloxy radicals, which decarboxylate to aryl radicals. They couple most likely with the arylpalladium(II) intermediate **200A** giving diarylpalladium(III) species **200C**, from which reductive elimination to the product **204** proceeds. The resulting Pd(I) species can be reoxidized by peroxide **203**. When decarboxylation is slow, the corresponding aryloxy radical couples with **200A**, which leads to product **205** via reductive elimination.

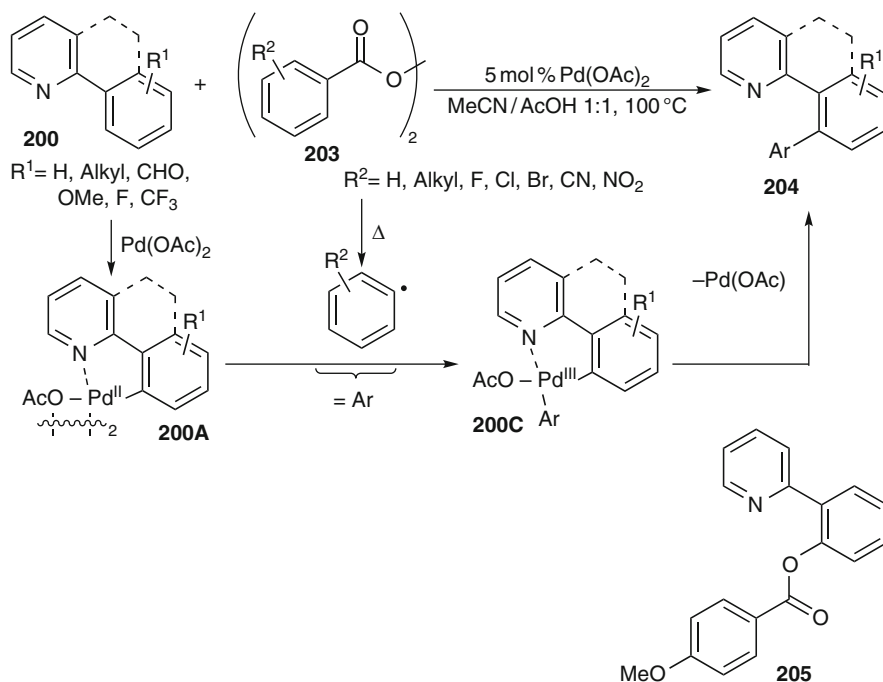
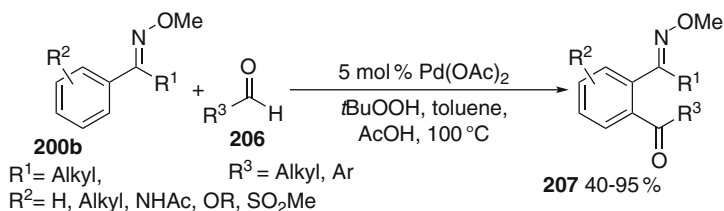


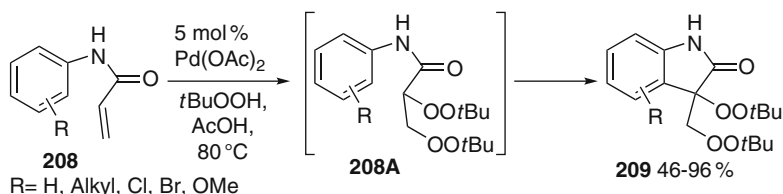
Fig. 50 Pd-catalyzed oxidative C–H arylation using aryl peroxides

Li's group reported a similar coupling protocol for dialkyl peroxides catalyzed by 10 mol% of  $\text{Pd(OAc)}_2$  [232]. The reactions provided mixtures of *ortho*-methyl and *ortho,ortho'*-dimethylarenes in 55–76% yield. No kinetic isotope effect was found, since in an *ortho*-monodeuterated arene the hydrogen and deuterium atoms were exchanged in a 1:1 ratio. An oxidative addition of Pd(0) or Pd(II) to the peroxide linkage resulting in a Pd(II) or Pd(IV) dialkoxide was proposed to be likely. A polar elimination of the corresponding ketone generates a methylpalladium(III or IV) species, from which reductive elimination to the methylated arenes proceeds. However, a mechanism based on *tert*-butoxyl radicals was also considered.

Similar conditions were applied to effect Pd-catalyzed acylation reactions (Fig. 51). When aryl ketone oxime ethers **200b** were treated with aliphatic or aromatic aldehydes **206** in the presence of 5 mol%  $\text{Pd(OAc)}_2$ , acetic acid, and *tert*-butyl hydroperoxide at 100°C, functionalized aryl ketones **207** resulted in 40–95% yield [233]. Ascorbic acid retarded the transformation. The reaction can be rationalized by a cyclometalation of the oxime ether leading to arylpalladium(II) intermediate similar to **200A**. *tert*-Butyl hydroperoxide may be cleaved reductively by the palladium compound to generate a *tert*-butoxyl radical, which abstracts the formyl hydrogen atom of the aldehyde leading to an acyl radical. Its coupling with the cyclometalated complex **200A** generates an acylpalladium(III or IV) intermediate. Reductive elimination yields product **207** and a palladium(I or II) species, which is reoxidized to the active Pd(II) catalyst. Li and coworkers reported



**Fig. 51** Pd(II)-catalyzed acylation of arenes



**Fig. 52** Pd(II)-catalyzed tandem bis(peroxidation)/cyclization reactions of *N*-arylacrylamides

independently closely related results for 2-arylpyridines and benzoquinolines [234]. A similar Pd(II)–Pd(IV) cycle was proposed, but radicals were not mentioned.

Recently An et al. disclosed a palladium(II)-catalyzed bis(peroxidation)/cyclization method for the synthesis of 3-(peroxymethyl)-3-peroxyoxindoles **209** from *N*-arylacrylamides **208** (Fig. 52) [235]. Using 5 mol% of Pd(OAc)<sub>2</sub> in the presence of *tert*-butyl hydroperoxide, 46–96% of products **209** were obtained. The reactions were proposed to involve a Pd-catalyzed radical bis(peroxidation) of the acrylic unit [236] followed by a two-electron directed cyclometalation/reductive elimination reaction of intermediate bis(peroxide) **208A**.

## 4 Pt-Catalyzed Radical Reactions

Alkyl radicals result from the reaction of alkyl iodides or acyl halides and Pt(0) complexes, such as Pt(PET<sub>3</sub>)<sub>3</sub>, as evidenced by spin trapping and ESR spectroscopy [237, 238]. Inhibition and CIDNP studies gave a similar result for simple alkyl iodides [158]. Benzyl bromide also reacts by a SET mechanism according to CIDNP measurements, while benzyl chloride affords the oxidative addition product without observing a CIDNP effect. This is in line with the fact that bromine abstraction is more facile than that of chlorine by a factor of 10<sup>4</sup>; thus for the latter an S<sub>N</sub>2 process leading to benzylplatinum chloride is more favorable. The rate constants for coupling of neopentyl, primary, and secondary alkyl radicals with the Pt(PPh<sub>3</sub>)<sub>3</sub> complex was estimated to 10<sup>1</sup>, 10<sup>6</sup>, and 2 × 10<sup>-1</sup> M<sup>-1</sup> s<sup>-1</sup>, respectively [239]. Optically active α-chloropropionate gave a racemic C-centered platinum enolate exclusively, indicating a SET pathway via the corresponding radical

intermediate. The rate of reaction of platinum complexes with secondary alkyl bromides was shown to be dependent on their coordinative saturation. The highest reactivity was observed for Pt(PEt<sub>3</sub>)<sub>2</sub>, while Pt(PEt<sub>3</sub>)<sub>4</sub> was inactive. The oxidative addition of platinum(II) complexes to sulfonyl halides gave strong ESR spectra of spin adducts of sulfonyl radicals with nitroso-2,3,5,6-tetramethylbenzene, while for acyl halides no ESR signal was observed [238]. A recent study of the kinetic isotope effects in the reaction of ethyl iodide with (bipy)PtMe<sub>2</sub> revealed that the oxidative addition of ethyl iodide is finely balanced between S<sub>N</sub>2 and electron transfer pathways [240]. To obey the observed second order kinetics the radicals generated would have to be caged. When the reactions were conducted in benzene in normal lab light, a radical pathway seemed to account better for the observed product spectrum. Some platinum(III) complexes were recently structurally characterized [241].

There are relatively few Pt-catalyzed radical reactions known. Kondo and coworkers investigated a number of platinum complexes in photochemically stimulated alkoxy-carbonylations and aminocarbonylations of primary, secondary, or tertiary alkyl iodides (cf. Part 1, Sect. 9.1, Fig. 41, Part 3, Sect. 3.4 177→178) [214, 215]. Pt(CO)<sub>2</sub>(PPh<sub>3</sub>)<sub>2</sub> showed the highest activity giving 63–84% yield of esters or amides **182** (cf. Fig. 42). The intermediacy of radicals was proven by spin trapping by nitrosodurene and ESR spectroscopy. In a kinetic study, it was found that the transformation is a radical process, but no iodine transfer chain reaction. Even though the presence of radicals was strongly supported, there was no inhibition of the process by BHT. Analogous thermal methoxy-carbonylation reactions of alkyl iodides under a CO pressure of 70 bar at 120°C gave 56–76% of esters **178** [242]. Formylation reactions providing aldehydes succeeded under similar conditions in 51–86% yield. The process does not occur according to a β-hydride elimination/hydroformylation sequence. The authors favored, however, a two-electron mechanism for these reactions. A similar carbonylation/arylation method was also reported [243].

Huang and Zhou investigated radical addition reactions of perfluoroalkyl iodides **146a** to tertiary amines **155** catalyzed by Pt(PPh<sub>3</sub>)<sub>4</sub> (cf. Fig. 38) [93]. Fluoroalkylenamines **156** were obtained in 40–50% yield accompanied by 40–50% of the corresponding reduced perfluoroalkane **157**. The reaction was proposed to occur similarly as the palladium-catalyzed process. The reaction works well with all group 10 M(PPh<sub>3</sub>)<sub>4</sub> complexes. The nickel compound is the most reactive followed by the corresponding palladium complex. This reactivity order can be traced to their first ionization potentials.

Zazybin et al. studied Kharasch addition reactions of tetrachloromethane to terminal alkenes catalyzed by a number of Pt(II) complexes [244, 245]. Pt(PPh<sub>3</sub>)<sub>2</sub>I<sub>2</sub> and Me<sub>2</sub>Pt(PPh<sub>3</sub>)<sub>2</sub> gave highest yields of addition products. Both are, however, unstable and transform easily to Pt(PPh<sub>3</sub>)<sub>2</sub>Cl<sub>2</sub> under the reaction conditions. The addition of K<sub>2</sub>CO<sub>3</sub> as the base increased the yields. Benzoquinone inhibited the reaction completely. The kinetics for the radical addition catalyzed by these complexes was determined. Cyclohexene reacted approximately an order of magnitude slower than 1-hexene ( $k = 1.19 \times 10^3 \text{ l}^2 \text{ mol}^{-2} \text{ s}^{-1}$ ) using Pt(PPh<sub>3</sub>)<sub>2</sub>Cl<sub>2</sub>. Based



on this information a catalytic cycle that is similar to the corresponding molybdenum, iron, ruthenium, nickel, palladium, and copper-catalyzed Kharasch additions can be formulated (cf. Part 1, Sect. 7; Part 2, Sects. 2.2.1, 2.4, and 3.3; Part 3, Sects. 2.9, 3.1, and 5.1).

Liu and colleagues developed a number of Bergman-type cyclization reactions leading to arene derivatives.  $\text{PtCl}_2$  (5 mol%) proved to be the catalyst of choice providing the cyclization products in 46–86% yield [246]. A valence tautomeric platinum biradical–carbenoid pair was considered, while for related cyclizations with nucleophiles present in the reaction mixture two-electron pathways were favored by the authors [247, 248].

## 5 Copper-Catalyzed Radical Reactions

Copper(I) compounds are applied as stoichiometric promoters in a number of radical processes, such as the Hofmann–Löffler–Freitag (review [249]), Meerwein arylation (recent review [250]), Pschorr cyclization (recent review [251]), and other radical reactions. Radical intermediates were detected in copper-catalyzed alkylations (see for example [252]) and conjugate additions (see for example [253]). Many Cu(I)-catalyzed cross-dehydrogenative couplings involve transient radicals (reviews [254–257]). Catalytic Kharasch–Sosnovsky reactions using copper(I) catalysts were developed (reviews [258–262]). Copper(II) compounds and especially  $\text{Cu}(\text{OAc})_2$  are frequently applied as stoichiometric co-oxidants in  $\text{Mn}(\text{OAc})_3$ -promoted radical cyclizations (recent reviews [263–267]). Copper(II)-promoted radical cation cyclizations were summarized [268]. Other examples of copper(II)-mediated reactions involving radicals are oxidative dimerizations of enolates to 1,4-dicarbonyl compounds (review [269]). Organometallics can also be coupled by copper reagents, but radical as well as non-radical pathways are possible. Due to the recent interest in biaryls and binaphthols as chiral ligands in asymmetric synthesis, catalytic asymmetric oxidative dimerizations of organometallics and phenols moved to the center of interest (recent reviews [270–273]). Catalytic oxidative functionalization reactions using  $\text{Cu}(\text{OAc})_2$  were reported for the directed introduction of halide, hydroxy, amino, or sulfide functions to arenes [274]. Copper-catalyzed aziridination reactions were reviewed. Two-electron and radical pathways are possible (review [275]).

### 5.1 *Cu(0)-Catalyzed Atom Transfer Radical Addition Reactions*

Copper powder was frequently applied in (super)stoichiometric amounts to trigger reductive radical addition reactions. Yang and Burton described the addition of difluoroiodoacetates **37** to olefins **210** in the absence of a solvent in the presence of 10–20 mol% copper powder (Fig. 53) [276, 277]. The method tolerates sensitive

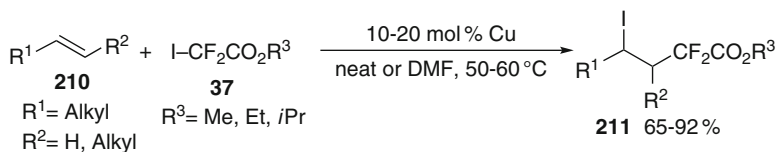


Fig. 53 Copper powder-catalyzed iodine transfer radical additions

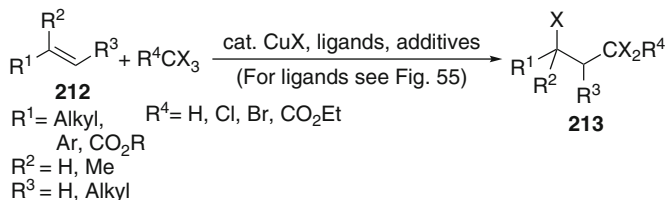


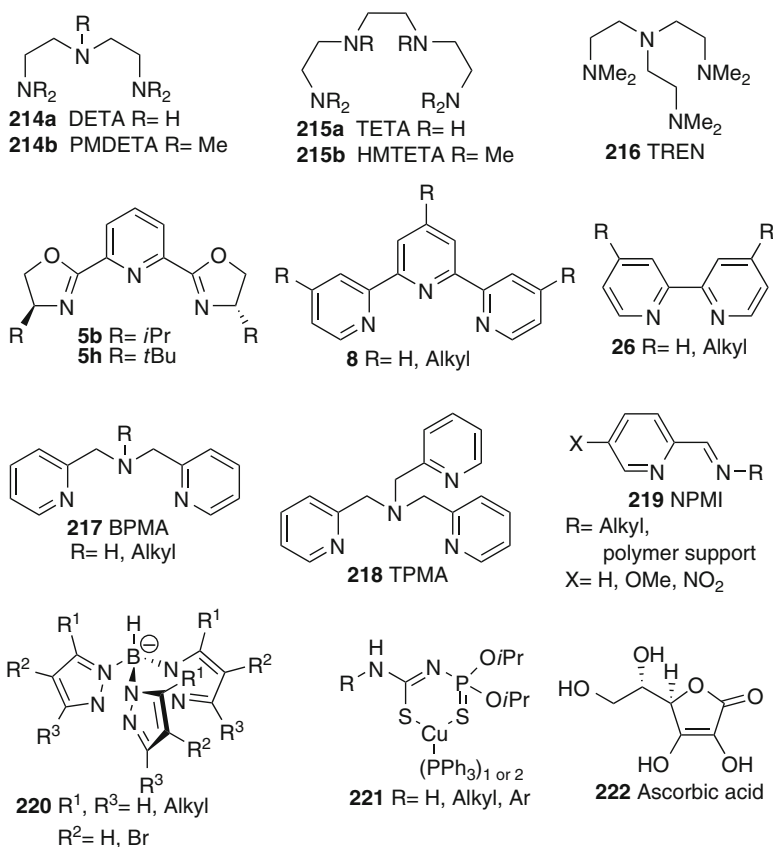
Fig. 54 Cu(I)-catalyzed ATRA

functionality, such as ketones or epoxides. 2,2-Difluoro-4-iodo esters **211** were isolated in 65–92% yield. Internal alkenes also reacted in good yield, although the reaction times were considerably longer. A tandem radical addition/5-exo cyclization sequence with diallyl ether **65** gave the product in 82% yield, thus supporting the radical process. Kitagawa and coworkers disclosed ATRA of methyl iododifluoroacetate to terminal and internal olefins **210** catalyzed by 30 mol% copper in DMF providing 2,2-difluoro-4-iodo esters **211** in 42–88% yield [278].

## 5.2 Cu(I)-Catalyzed Atom Transfer Radical Addition Reactions

In 1963 Asscher and Vofsi reported the first Kharasch additions of  $\text{CCl}_4$  to olefins **212** catalyzed by 1 mol%  $\text{CuCl}_2$ . Products **213** were obtained in 42–92% yield (Fig. 54) [279]. In principle they proposed the still accepted mechanism (see Part 2, Sects. 2.2.1, 2.4, and 3.3). Catalytic amounts of diethylammonium chloride proved to be a useful additive in these reactions, increasing the yields. Cupric chloride gave higher yields than  $\text{FeCl}_3$ , probably because the former is a better chlorine donor. Shortly afterwards, Murai disclosed ATRA of trichloroacetates to **212**. The addition products were isolated in low to moderate yield using 2–3 mol% of  $\text{CuCl}$  or  $\text{Cu}_2\text{O}$  [280].

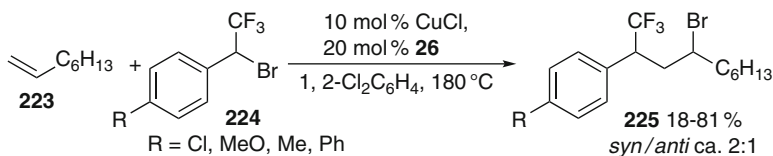
Subsequently copper-catalyzed ATRA reactions were developed continuously and the progress was reviewed thoroughly (reviews [281–286]). Therefore, only selected recent examples are highlighted here. A number of ligands (Fig. 55), such as TMEDA, aliphatic tri- and tetramines **214**, **215**, or **216**, PyBOX derivatives **5**, bipyridines **26**, terpyridines **8**, bis- or tris(2-pyridylmethyl)amines **217** and **218**, picolinaldehyde imines **219**, tris(pyrazolyl)borates **220**, or thionophosphates **221** [287], were applied successfully. Phenanthrolines or the bis(TPMA) ligand (cf. Part 2, Fig. 13) also proved valuable to perform ATRA under mild conditions at



**Fig. 55** Ligands and additives for Cu-catalyzed ATRA

low catalyst loading. The kinetics of these addition reactions was determined [281–286]. Polymer-supported copper catalysts using variants of these ligands were developed [285, 286, 288–290].

The progress of ATRA development was very much inspired and went in parallel with that of the copper-catalyzed ATRP, which is mechanistically closely related [284, 291]. For a long time, a drawback was that the catalyst loadings remained high with 5–30 mol%. A solution to this problem proved to be the addition of agents, which reduce the amount of accumulating unproductive oxidized catalyst (compare also developments in the related Ru-catalyzed ATRA, Part 2, Sect. 3.3) [284–286]. Typical radical starters, such as AIBN or V-70 (azobis-(4-methoxy-2,4-dimethylvaleronitrile)) generate radicals thermally, which are subject to ligand transfer from the oxidized copper species, thus regenerating the active catalysts. This method enables ATRA of CCl<sub>4</sub> to simple olefins at substrate-catalyst ratios of up to 10,000:1 (TON = 7,200) and of CBr<sub>4</sub> to styrene or methyl methacrylate ratios of up to 200,000:1 (TON > 150,000) [284]. Since these radical



**Fig. 56** ATRA of benzylic bromides to olefins

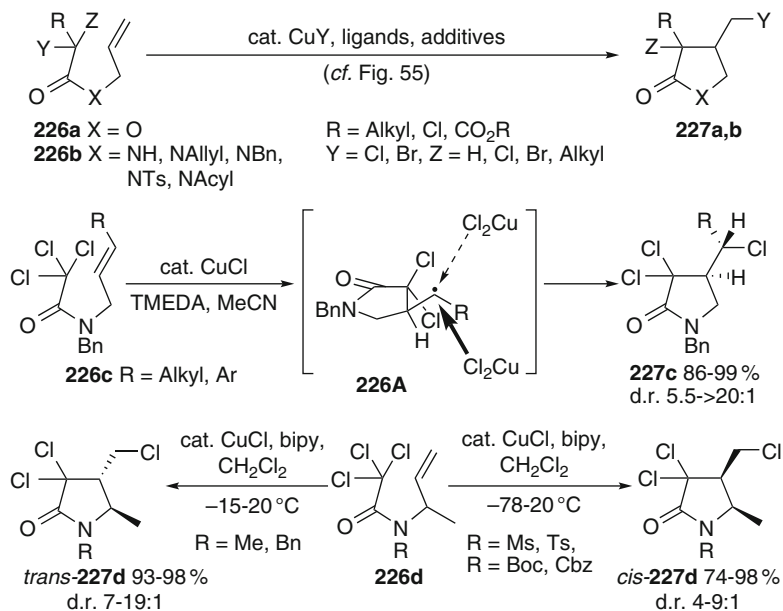
initiators can also trigger undesired polymerization of sensitive vinyl monomers, alternative reducing agents were introduced very recently. Pintauer reported ascorbic acid **222** as a very suitable reducing agent for accumulating Cu(II) in Kharasch additions without being a radical initiator [292]. Although **222** was not as efficient as the azo initiators, amounts of 1–7 mol% suffice to achieve high conversion and turnover numbers with less than 1 mol% of Cu(TPMA)Cl as the catalyst. Additions of CBr<sub>4</sub> work with full conversion even at substrate:catalyst ratios of up to 20,000:1.

Okano and coworkers accomplished ATRA of very deactivated (1-bromo-2,2,2-trifluoroethyl)benzenes **224** with 1-octene **223** in the presence of 10 mol% CuCl and 20 mol% bipy **26** and obtained 18–81% of the atom transfer addition products **225** as a 2:1 *syn/anti* mixture (Fig. 56) [293].

### 5.3 Cu(I)-Catalyzed Atom Transfer Radical Cyclization Reactions

Nagashima et al. reported the first 5-exo ATRC of allylic trichloroacetates **226a** (R<sup>1</sup>=Y=Z=Cl). Chlorinated butyrolactones **227a** were isolated in 38–78% yield with 30 mol% of CuCl as the catalyst at 140 °C (Fig. 57) [294]. *N*-Allylic trichloroacetamides **226b** (R<sup>1</sup>=Y=Z=Cl, NR<sup>2</sup>=H, Allyl, Bn) were transformed to pyrrolidones **227b** in 57–90% yield using CuCl in acetonitrile [295]. Subsequently ATRC reactions were applied widely. The progress of the methodology was reviewed thoroughly [281–286, 296], so that only selected examples are highlighted.

Copper-catalyzed 5-exo ATRC are similar to Ru-catalyzed cyclizations (see Part 2, Sect. 3.3.2). A standard CuCl/bipy system is required at a considerably higher catalyst loading of typically 30 mol% compared to 5 mol% of Ru(PPh<sub>3</sub>)<sub>3</sub>Cl<sub>2</sub> [297, 298]. The ruthenium catalyst in contrast requires higher reaction temperatures of 50–140 °C compared to 20–80 °C for the copper catalyst to achieve comparable yields. More recently Nagashima and coworkers compared the reactivity of a ruthenium amidinate catalyst (cf. Part 2, Fig. 38, **156**) to that of copper-catalysts in ATRC of trichloroacetamides and ATRA reactions of pyrrolidones **227**. They found that the ruthenium catalyst and the CuCl/bipy systems were similarly active in ATRC of **226b** to **227b** at room temperature, but the former was more active in ATRA between **227** and styrene [299, 300]. A number of ligand systems were introduced recently to improve these 5-exo cyclization reactions (see Fig. 55). It



**Fig. 57** Cu-catalyzed ATRC – basic and stereochemical features

was recently also shown that DMF acts as a ligand in ATRC. This allowed reduction of the catalyst loadings to 5 mol% and the temperature to 60–100 °C compared to reactions run in acetonitrile [301].

The diastereoselectivity of ligand transfer was studied with substrates **226c** bearing substituted allylic radical acceptors (Fig. 57) [302]. An additional chiral center is introduced at the exocyclic position of **227c**. The observed moderate to excellent diastereoselectivity can be explained by a preferred ligand transfer from the less hindered face to strain-biased radical **226A**. The methodology is also applicable to annulation reactions using cyclic radical acceptors [303]. Ligand transfer to the resulting cyclic radicals occurs preferentially or exclusively at the convex face.

In substrates **226d** bearing 1-substituted allyl groups a switch of diastereoselectivity depending on the nitrogen substituent was observed. Ruthenium and copper catalysts provided **227d** with typical good to excellent *trans*-selectivity for *N*-alkyl-substituted amides [297, 298]. For *N*-acyl or *N*-sulfonyl substituted *N*-allyl trichloroacetamides **226d** a 4–9:1 *cis*-selectivity was observed in products **227d**.

Not only trichloroacetate or trichloroacetamide systems can be applied. Weinreb and coworkers reported a few copper-catalyzed 5-exo ATRC of 2,2-dichloro-3-oxo-6-heptenoates using 3.2 mol% CuCl and PPh<sub>3</sub> as a ligand [304]. A 1.6:1 mixture of regioisomeric 5-exo and 6-endo products was obtained with low diastereoselectivity. 5-exo Annulations and 6-exo cyclizations gave the products with 1 and 2.7 mol% Cu catalyst in 82–99% and 91% yield, respectively. Ghelfi and colleagues found that dichloroacetaldehyde-derived mixed *O*-allylic acetals served

well in 5-exo ATRC using the CuCl/PMDETA catalyst system [305]. Dichlorinated butyrolactols were isolated in 84–93% yield as a mixture of four diastereomers.

5-exo ATRC was applied in the total synthesis of chaetomelic anhydrides A and C [306–308], (±)-botryodiplodin acetate [309], tyromycin A [310], quercus lactones [311], or (*Z*)-pulchellalactam [312, 313]. Lignan analogs with a butyrolactone unit [314] and the eunicellin core [315] were approached similarly.

Applications of Cu-catalyzed 4-exo [316], 5-endo [317], or 6-endo [316] types and even medio- and macrocyclization reactions work well [285, 296].

Cu-catalyzed ATRC of *N*-allyl-bromo or iododifluoroacetamides **158b** were studied by Nagashima and colleagues (Fig. 58) [194]. The reactions proceeded most efficiently applying 10 or 30 mol% of a complex generated in situ from CuI and bipy **26** and using substrates with electron-withdrawing groups at the nitrogen atom. This lowers the rotational barrier of the amide and facilitates reaching the cyclization transition state. Difluorinated pyrrolidones **159b** were isolated in 34–92% yield. The lower yields result from cyclizations of substrates having an *N*-benzyl substituent. Other common copper complexes and Ru(PPh<sub>3</sub>)<sub>3</sub>Cl<sub>2</sub> (see Part 2, Sect. 3.3.2) gave worse results, but Pd(PPh<sub>3</sub>)<sub>4</sub> was applied successfully as a catalyst (see Sect. 3.2).

Tandem ATRA/ATRC of 1,6-dienes with CCl<sub>4</sub> were devised using copper catalysis (see Part 2, Sect. 3.3.3, Fig. 42, **169**→**170**) [284–286, 296]. Very high substrate/catalyst ratios can be achieved when these reactions were performed in the presence of catalytic amounts of azo initiators AIBN or V-70 or ascorbic acid **222** to reduce accumulating Cu(II) back to Cu(I) [285, 286, 292]. Tandem ATRC/ATRC of indoles **228** were tested recently; the yields of tetracyclic spiro benzoindolizidines **229**, however, remained moderate (Fig. 59) [318].

Quayle and colleagues recently introduced (NHC)Cu(I) complexes as catalysts for tandem ATRC (Fig. 60) [319]. When the imidazolium salt **231**, CuCl, and *ortho*-allylphenyl trichloroacetate **230** were heated in dichloroethane the eight-membered lactone **230B** was obtained in good yield accompanied by minor amounts of annulated arene **233**. Under microwave heating the latter becomes the exclusive product. This annulation reaction proved to be rather general giving naphthalenes, phenanthrenes, and higher arenes **233** in 34–91% yield as single isomers. The reaction starts with reductive generation of radical **230A**. An 8-endo cyclization to the allyl group followed by ligand transfer from the coformed copper(II) complex provides the 8-membered lactone **230B**. With this catalyst a subsequent generation of radical **230C** is possible, which triggers a 4-exo cyclization leading to tricyclic ring system **230D**, from which CO<sub>2</sub> extrusion to semihydrogenated compounds

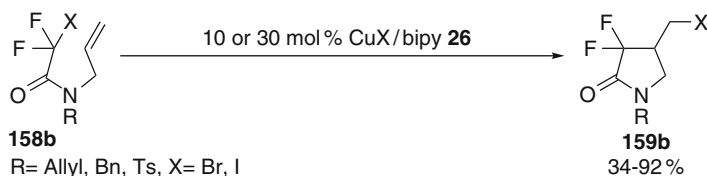


Fig. 58 Fluorinated pyrrolidones by Cu-catalyzed ATRC of difluoroacetamides **158b**

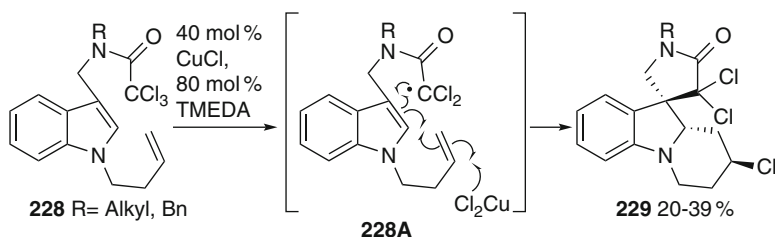


Fig. 59 Cu(I)-catalyzed tandem ATRC/ATRC

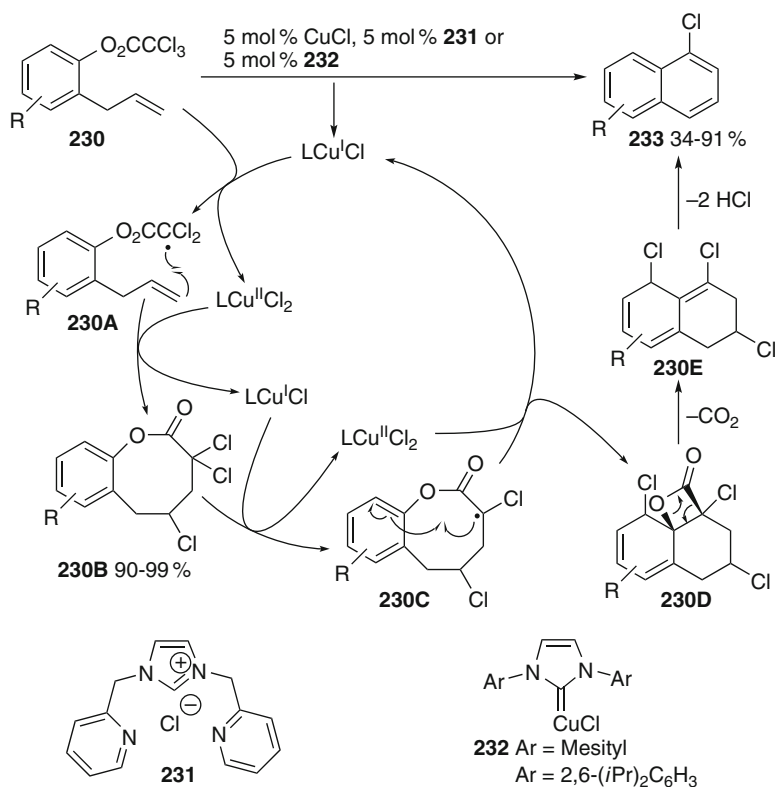


Fig. 60 Tandem ATRC/ring contraction/elimination reactions

**230E** is facile. Dehydrochlorination provides the aromatic products **233**. An alternatively possible HCl elimination/electrocyclization/decarboxylation pathway was excluded, since lactone **230B** was thermally stable under the reaction conditions in the absence of the catalyst. (NHC)Cu(I) catalyst **232** gave comparable or better yields than **231** in these ATRC/ring contraction sequences, while other (NHC)Cu(I) complexes provided considerably lower yields [320]. Chlorinated cyclic compounds arising from ATRC can also be transformed to chlorinated furans [321].

Göttlich and coworkers devised Cu(I)-catalyzed ATRC of *N*-chloro amines. When *N*-chloro-4-pentenylamines **234a** were treated with 10 mol% of CuCl, 3-chloropiperidines **237** resulted in 55–77% yield (Fig. 61) [322, 323]. The yields of the cyclization products **237** were dependent on the Lewis acidity of the copper salts. The yields dropped with more Lewis-acidic copper salts, such as CuPF<sub>6</sub>. Moderate to good yields were achieved by addition of chelating ligands, such as tetramethyl-1,2-cyclohexanediamine **235** or bipy **26**. The diastereoselectivity of the cyclization increased considerably at the same time [323]. The reactions start with reductive generation of aminyl radicals **234A**, which are likely coordinated by Lewis-acidic Cu(II) salts (**234B**). A radical 5-exo cyclization proceeds subsequently via a Beckwith–Houk transition state and leads to pyrrolidinylmethyl radicals **234C**. Facile chlorine transfer from coformed Cu(II) salts furnishes the products and regenerates the catalyst. 2-(Chloromethyl)pyrrolidines **236a** were detected as the primary products by NMR spectroscopy. They rearrange, however, under the reaction conditions via bicyclic aziridinium ions **236A** to **237**. A corresponding 6-exo cyclization gave in contrast 2-(chloromethyl)piperidine in 53% yield, but no ring-expanded product was formed. Similar cyclizations were

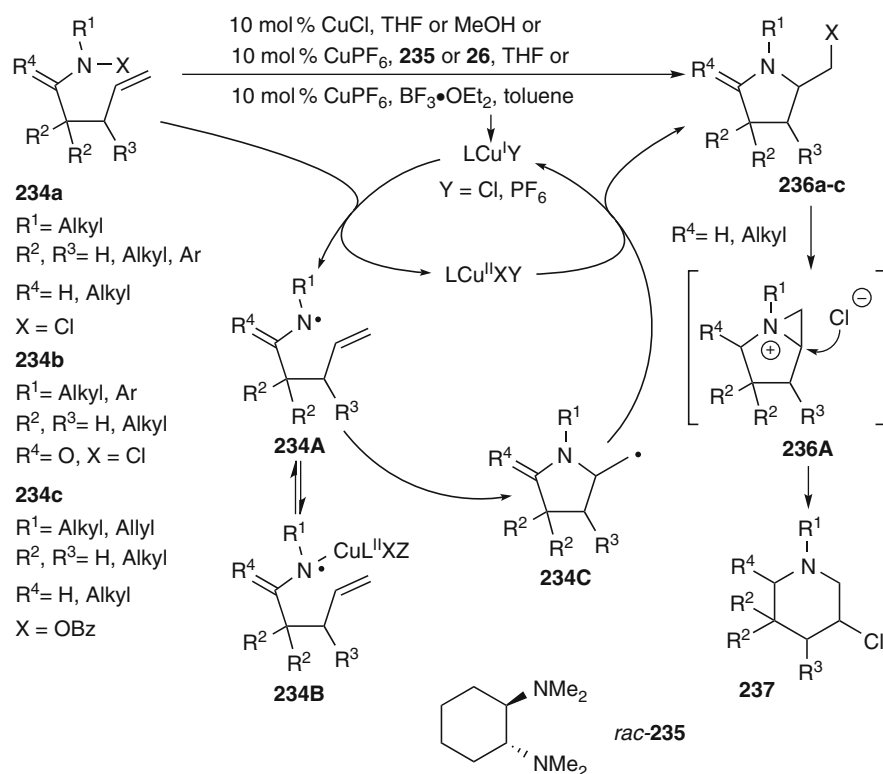


Fig. 61 Copper(I)-catalyzed ATRC of *N*-acyloxy or *N*-chloro amines or amides



also mentioned by Somfai and colleagues [324]. *N*-Chloro-4-pentenoic amides **234b** cyclized analogously in the presence of 10 mol% of CuCl in MeOH and afforded 5-(chloromethyl)-2-pyrrolidones **236b** in 63–96% yield [325]. *N*-Benzoyloxy-4-pentenylamines **234c** cyclized to 2-(benzoyloxymethyl)pyrrolidines **236c**, but required much higher temperatures and the addition of stoichiometric amounts of  $\text{BF}_3 \cdot \text{OEt}_2$  to achieve yields of 39–79% [326]. No rearrangement products **237b,c** were observed due to the low nucleophilicity of the amide in **236b** and the diminished leaving group ability of the benzoate unit in **236c**.

Similar cyclizations of **234c** bearing substituents at the alkene terminus catalyzed by 10 mol% of  $(\text{CuOTf})_2 \cdot \text{C}_6\text{H}_6$  resulted in contrast in 30–95% yield of 2-alkenylpyrrolidines [327]. Ligand transfer is less favored under these conditions, so that SET oxidation of the cyclized radical by coformed Cu(II) and subsequent deprotonation prevailed. 6-exo Cyclizations were also probed.

A number of formal ATRC of *O*-acylated oximes (review [328]) catalyzed by 5–20 mol%  $\text{CuBr} \cdot \text{SMe}_2$  was disclosed by Narasaka's group (Fig. 62) [329]. *O*-Acyl oxime derivatives of homoallyl ketones **238** provided 5-(bromomethyl)-1-pyrrolines **239** in 53–91% yield when the reactions were carried out in the presence of excess LiBr. The cyclization starts probably by generation of an iminyl radical **238A** by reductive cleavage of the oxime N–O bond. This radical cyclizes generating alkyl radical **238B**. The product forms by ligand transfer from the mixed Cu(II) bromide to the cyclized radical. The reaction capitalizes subsequently on the facile anion exchange of the copper carboxylate by LiBr. A similar cyclization was subsequently applied in a total synthesis of the alkaloid peduncularine [330].

It was found that indole-substituted *O*-pentafluorobenzoyl oximes **240** underwent 6-endo cyclizations to the appended indole unit in the presence of 20 mol% of copper and stoichiometric amounts of PMDETA **214b** giving dihydro- $\alpha$ -carboline **240B**, which were immediately dehydrogenated by chloranil (Fig. 63) [331]. Products **241**

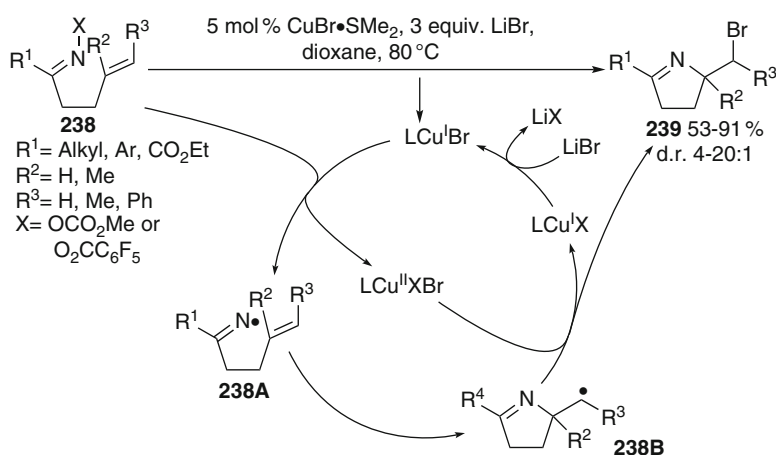
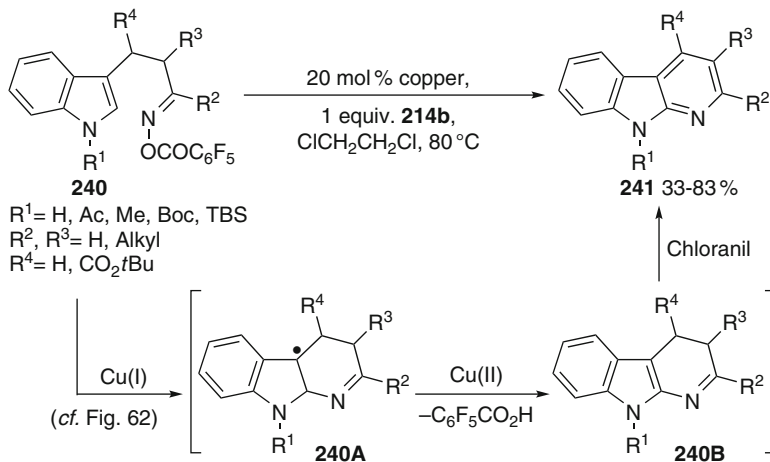


Fig. 62 Cu(I)-catalyzed iminyl radical cyclization reactions



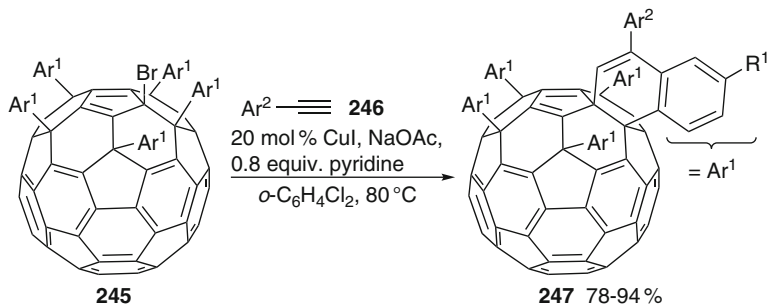
**Fig. 63** Synthesis of  $\alpha$ -carbolines by Cu(I)-catalyzed cyclization reactions

were isolated in 33–83% yield. Although the starting materials **240** are not sensitive to hydrolysis the remainder of the mass balance accounted for the ketone derived from **240**. The reactions are initiated by the generation of a copper(I) species from copper by reaction with the substrate or the solvent 1,2-dichloroethane. Reductive electron transfer from Cu(I) to **240** leads to an iminyl radical (cf. Fig. 62), which cyclizes to the indole 2-position. The resulting benzylic radical **240A** is oxidized by coformed Cu(II) to a benzylic cation, which deprotonates furnishing product **240B**. At the same time the Cu(I) catalyst is regenerated. A part of the iminyl radicals does apparently not cyclize, but stabilizes by hydrogen abstraction from the solvent to an imine, which is subject to hydrolysis to the ketone side product.

#### 5.4 Cu(I)–Cu(II) Catalysis: Other Radical Additions

Since copper(I) compounds are very active in Fenton-type reactions, this methodology can be used to trigger radical additions. Zhang and coworkers developed oxygenative radical additions of tetrahydrofuran or 1,3-dioxolane **243** to styrenes **242a** catalyzed by 10 mol% of CuBr in the presence of *tert*-butyl hydroperoxide in air (Fig. 64) [332]. Ketones **244a** were isolated in 47–67% ( $\text{X}=\text{CH}_2$ ) and 37–55% yield ( $\text{X}=\text{O}$ ), respectively. Dioxane or tetrahydropyran gave only low yields in this addition process. The reaction can be rationalized by initial generation of a *tert*-butoxyl radical from *t*BuOOH and CuBr. Hydrogen abstraction from **243** generates radical **243A**, which adds to styrenes **242a**. Trapping of the benzylic radical **243B** by oxygen is very facile leading to peroxy radical **243C**. This intermediate has several options to stabilize. One consists of hydrogen abstraction from **243** to initiate a typical chain reaction that would not require further involvement of the



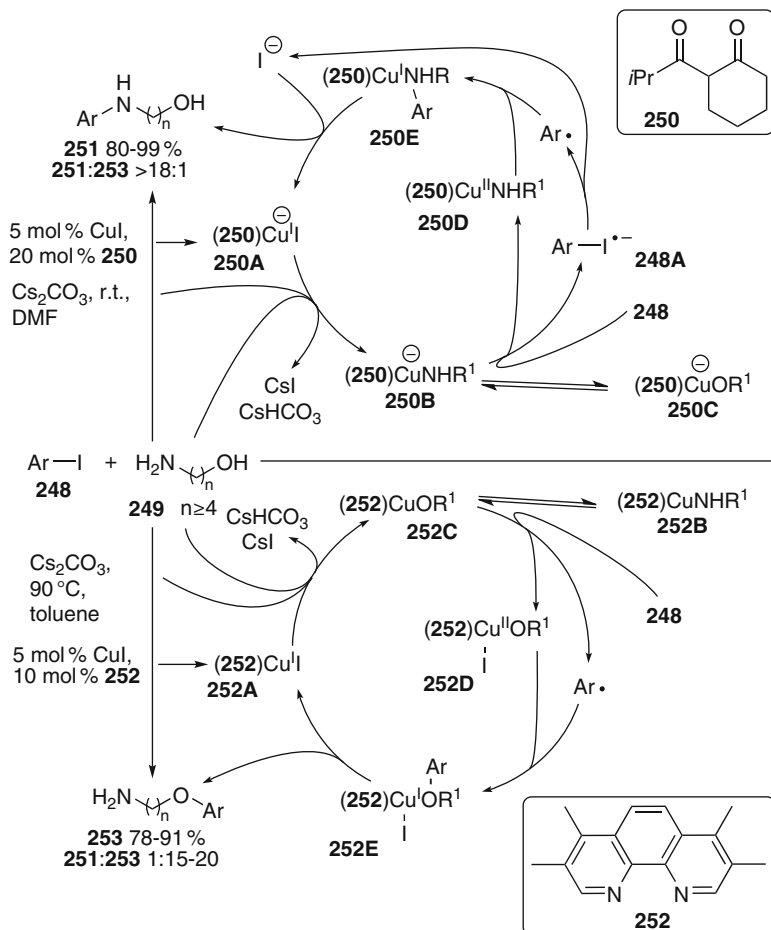


**Fig. 65** Copper-catalyzed radical addition/cyclization sequences with fullerenes **245**

Alkylacetylenes gave only low yields. Deuterated phenylacetylene led to a product in which the vinylic deuterium atom was retained, thus ruling out the involvement of a copper acetylide. Isolated copper acetylides were moreover unreactive under identical conditions. Based on these facts an initial reductive radical generation from the bromofullerene seems to be likely. The resulting fullerene-derived cyclopentadienyl radical adds to **246**. Thus generated vinylic radical cyclizes to the closest adjacent aryl group. The coformed copper(II) species oxidizes the resulting cyclohexadienyl radical to the corresponding cyclohexadienyl cation, which deprotonates to the dihydronaphthalene product **247**.

### 5.5 *Cu(I)–Cu(II) Catalysis: Ullmann Reactions*

The Ullmann and Ullmann–Goldberg reactions have long been known to provide access to functionalized biaryls, diaryl ethers, or arylamines using copper catalysts or mediators. The progress on synthetic and mechanistic aspects of these coupling reactions was reviewed thoroughly and comprehensively up-to-date [339–343]. Over the years different mechanisms were put forward to explain the contrasting experimental results. Radical or radical anion intermediates were invoked early on to play a role in the course of the coupling reactions. Since probe reactions proved not to be unambiguous, two-electron as well as radical (ion) catalytic cycles were proposed. Recently, the Ullmann and related reactions were shown to be facilitated by a number of ligands [339–343]. Since these ligands modify the electronic structure of the copper catalysts strongly, the operating mechanisms of this coupling reaction indeed probably represent a continuum between closed- and open-shell pathways, which is modulated by the electronic properties of the substrates and the involved copper catalysts. A recent example illustrates impressively how the reaction pathways are subtly influenced by ligands and substrates (Fig. 66) [344]. The copper-catalyzed Ullmann reactions of aryl iodides **248** with 1,*n*-amino alcohols **249** provided the aminated product **251** in 80–99% yield and >18:1 selectivity when 2-isobutyrylcyclohexanone **250** was applied as the ligand for



**Fig. 66** Chemoselective Ullmann coupling of aryl iodides with 1,n-amino alcohols

CuI. In contrast, *O*-arylated products **253** were formed in 78–91% yield and 15–20:1 selectivity when phenanthroline **252** was used as the ligand.

Recent computational studies by Buchwald, Houk, and colleagues on the origin of this surprising selectivity revealed that two-electron pathways, such as oxidative addition of Cu(I) complexes to aryl iodides or  $\sigma$ -bond metathesis, proceed through transition states that are very high in energy [345]. Transition states involving reductive SET generating aryl iodide radical anions or iodine atom transfer leading to free or caged aryl radicals are energetically considerably less demanding. The nature of the ligand determines the coordination ability of Cu(I) and the subsequent reaction path significantly. Although *O*-ligation of **249** at copper complex **250A** to ate complex **250C** is favored in equilibrium over *N*-coordination to **250B**, the more electron-rich ( $\beta$ -diketonate)Cu(I) amide complex **250B** is the best single electron

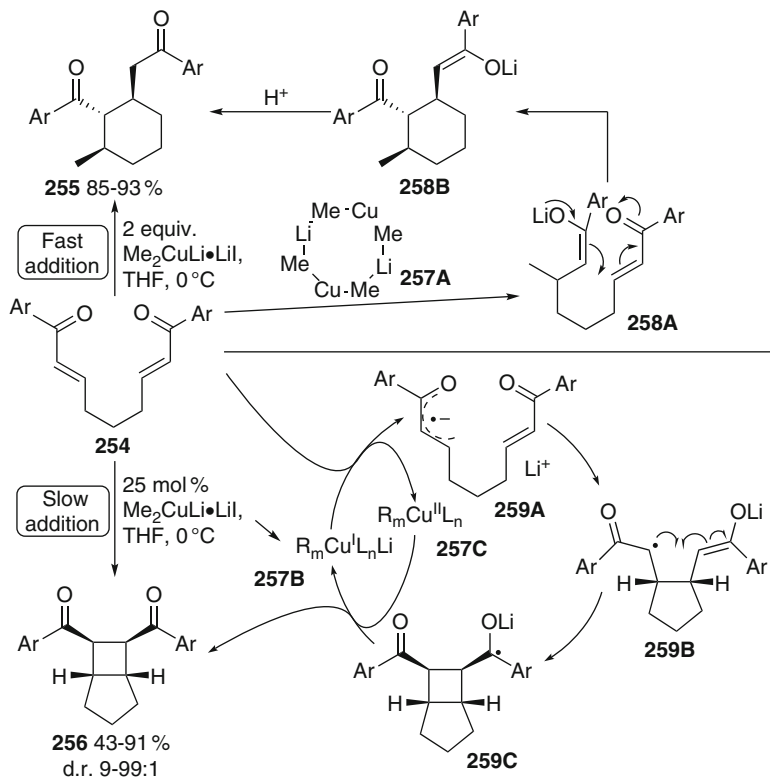
donor and promotes thus SET reduction of aryl iodide **248** as the least energy-demanding pathway. The SET pathway for the corresponding ( $\beta$ -diketonate)copper alkoxide **250C** is higher in energy. The resulting aryl iodide radical anion **248A** fragments to an aryl radical, which couples to the amide ligand of the intermediate copper(II) amide complex **250D**. The resulting (amine)copper(I) complex **250E** liberates the product **251** by ligand exchange.

In the process catalyzed by neutral (phenanthroline)copper complex **252A**, the formation of the alkoxide complex **252C** is also favored in equilibrium. Iodine atom abstraction by **252C** is the energetically most favorable pathway leading to the corresponding copper(II) iodide complex **252D** and an aryl radical. The latter couples subsequently with **252D** forming (aryl ether)copper(I) complex **252E**, from which aryl ether **253** is liberated subsequently. A SET or hydrogen abstraction pathway with the corresponding amide complex **252B** is higher in energy. Coupling of the aryl radical to the copper atom of the intermediate Cu(II) complexes **250D** or **252D** leading to a potential Cu(III) complex was energetically not feasible under any circumstances. Thus, the most favorable pathway is the attack of the aryl radical at the Cu(II) alkoxide or amide ligand. For a discussion of other pathways, see the very recent review by van Koten and colleagues [343]. Another very recent theoretical study on this ligand-dependent Ullmann reaction revealed, however, that two-electron pathways may also account for the observed results. Further experimental and theoretical work will be necessary to explain the selectivity better [346].

## 5.6 *Cu(I)–Cu(II) Catalysis: Electron Transfer in Conjugate Addition Reactions*

Electron transfer pathways were invoked for a long time in copper-mediated conjugate additions, but the evidence was always a matter of debate [347, 348]. Electron transfer can lead to derailing of Cu(I)-catalyzed conjugate addition reactions [253]. Alexakis and colleagues demonstrated recently that styrene corrects this problem. It does not interfere with the desired conjugate addition, but is the more effective acceptor for competitively generated radicals [349]. Thus, non-selective radical conjugate addition cannot interfere with desired polar conjugate addition reactions anymore.

The Krische and Bauld groups investigated the reaction behavior of lithium dialkylcuprates to bis(enones) **254** (Fig. 67) [350]. They found that a fast addition of superstoichiometric amounts of lithium dimethylcuprate triggered tandem conjugate addition/intramolecular Michael addition reactions leading to cyclohexane derivatives **255**. When the cuprate was introduced slowly in catalytic amounts under otherwise identical conditions, bicyclic cyclobutanes **256** were isolated as the sole products with good to excellent diastereoselectivity. Intermediate amounts of Gilman cuprates provided mixtures of **255** and **256**. The amount of cyclobutane **256** increased strongly on dilution of the reaction mixture even when the cuprate



**Fig. 67** Conjugate addition/cyclizations vs. reductive cyclizations induced by cuprates

was present in stoichiometric amounts. These results can be rationalized by the fact that cuprates exist in solution as an equilibrium mixture of dimeric and monomeric species **257A** and **257B**, respectively. At high cuprate concentration dimers **257A** are the principal species. They show a high reactivity in conjugate addition reactions, and thus products **255** form as the sole products via enolates **258A** and **258B**. In contrast, cuprate monomers **257B**, which are much less reactive in conjugate additions compared to **257A**, are preferred at higher dilution. Monomer **257B** thus acts rather as a SET reductant toward **254** forming radical anion **259A** and Cu(II) species **257C**. Radical anion **259A** undergoes a fast 5-exo radical anion cyclization similar to the process using ruthenium or cobalt catalysts (see Part 2, Sects. 3.2 and 5.4). The resulting distonic radical anion **259B** is well arranged to a 4-exo cyclization. So formed ketyl-type radical anion **259C** has several options to stabilize. One is SET oxidation by coformed Cu(II) species **257C** leading to the product and the reduced catalyst. Alternatively, the excess electron may also be transferred directly to substrate **254** initiating a radical anion chain reaction (not shown), in which the cuprate plays a role only as the initiating species.

## 5.7 *Cu(I)-Catalyzed Photochemical [2+2] Photocycloaddition Reactions*

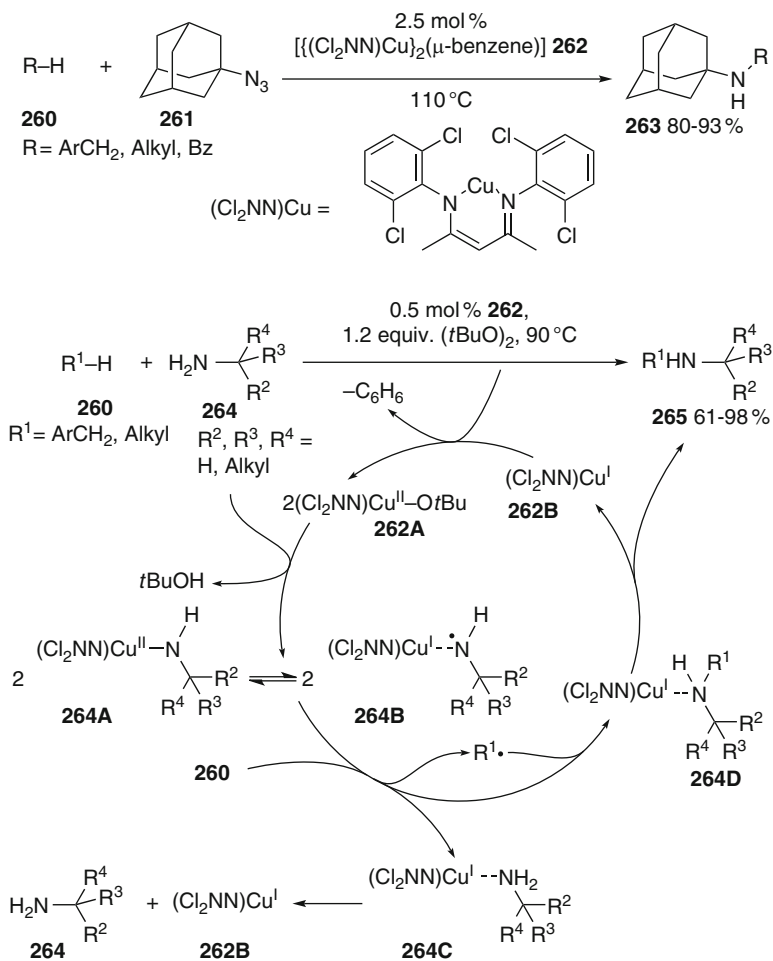
Copper(I) catalysis is very well established to promote intramolecular [2+2] photocycloaddition reactions of 1,n-dienes (review [351]). The methodology recently enjoyed a number of applications [352–354]. It is assumed that CuOTf, which is commonly applied as the catalyst, coordinates the diene and in this way mediates a preorganization. The Ghosh group recently reported a number of CuOTf-catalyzed photochemical [2+2] cycloaddition reactions, in which an organocopper radical complex was proposed as a cyclization intermediate (which should, however, have a formal Cu(II) oxidation state) (selected references [355–357]). A radical complex must, however, not be invoked, since the process may either proceed by a [2+2] photocycloaddition in the coordination sphere of copper(I) without changing the oxidation state or according to a cycloisomerization/reductive elimination process.

## 5.8 *Cu(I)–Cu(II) Catalysis: Amination of Hydrocarbons*

Metal nitrene complexes were used in a number of C–H amination reactions (recent reviews [358, 359]). Copper(I) ketiminate complexes react with azides to nitrene complexes, which were isolated [360]. ( $\beta$ -Ketiminate)copper(I) complex **262** (2.5 mol%) serves therefore as an efficient catalyst for the intermolecular C–H amination of arylarenes, cycloalkanes, or benzaldehydes **260** using adamantyl azide **261** as the nitrogen source (Fig. 68) [361]. The corresponding adamantyl amines or amides **263** were isolated in 80–93% yield. Copper complex **262** forms initially a dinuclear bridged complex with **261**. From this a copper nitrene complex is generated by elimination of nitrogen, which mediates the hydrogen abstraction from **260**.

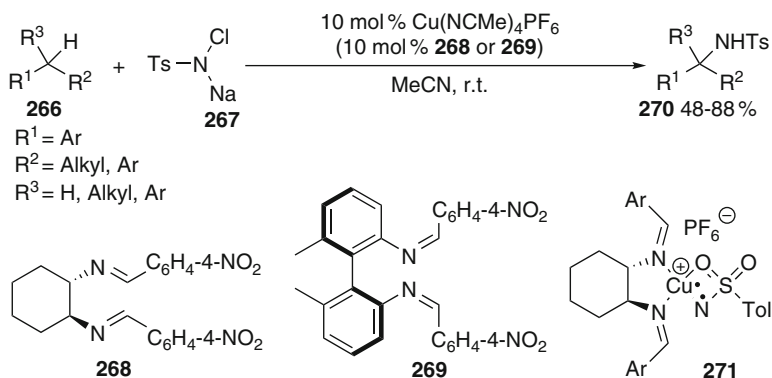
A similar, but significantly more versatile catalytic protocol works on the basis of analogous Cu(II) complexes **262A** [362]. It allows the use of much cheaper primary amines **264** as nitrogen sources in the presence of only 0.5 mol% of the copper(I) precatalyst **262**. Dialkylamines **265** were obtained in 61–98% yield. Morpholine as a secondary amine reacts analogously, but the reaction took much longer to form 53–72% of *N*-benzylic morpholines. No reaction was observed with cyclohexane. Di-*tert*-butyl peroxide serves as the stoichiometric oxidant in this protocol to convert starting complex **262** to copper(II) *tert*-butoxide **262A**, which is subject to ligand exchange by amine **264** forming copper(II) amide complex **264A**. According to ESR investigations, copper(II) amide complexes possess a significant spin density at nitrogen resulting from a significant contribution of a copper(I) aminyl radical valence tautomer **264B** [363]. This facilitates on the one hand hydrogen abstraction from **260** and on the other the coupling of the resulting radical with the ligated amine unit. (Amine)copper(I) complex **264C** formed in the hydrogen abstraction step dissociates to the copper precatalyst **262B** and the free amine **264**. Both can reenter the catalytic cycle. The product complex **264D** is subject to dissociation to product **265** and the precatalyst **262B**.





**Fig. 68** Cu(I)- and Cu(II)-catalyzed C–H amination reactions of hydrocarbons

The Nicholas group reported a Cu(I)-catalyzed C–H amination protocol for alkylarenes **266** using chloramine-T **267** as the nitrogen source (Fig. 69) [364, 365]. *N*-Benzylic toluenesulfonamides **270** were obtained in 48–88% yield. Chiral diimines **268** or **269** proved to be suitable as ligands for the  $\text{Cu}(\text{MeCN})_4\text{PF}_6$  catalyst. The reaction displays a significant primary kinetic H/D isotope effect  $k_{\text{H/D}} = 4.6$ . A benzyl cyclopropane provided a mixture of ring-closed and ring-opened products, suggesting radical intermediates (cf. Part 1, Fig. 8) [366]. Negligible asymmetric induction was observed when ligand **268** was applied, while the axially chiral ligand **269** provided up to 39% ee [365]. According to the experimental results and a theoretical investigation, Cu(I) imido complex **271** formed from the Cu(I) precatalyst, the diimine and chloramine-T being the active amination catalyst. It has a triplet ground state. Although hydrogen abstraction is



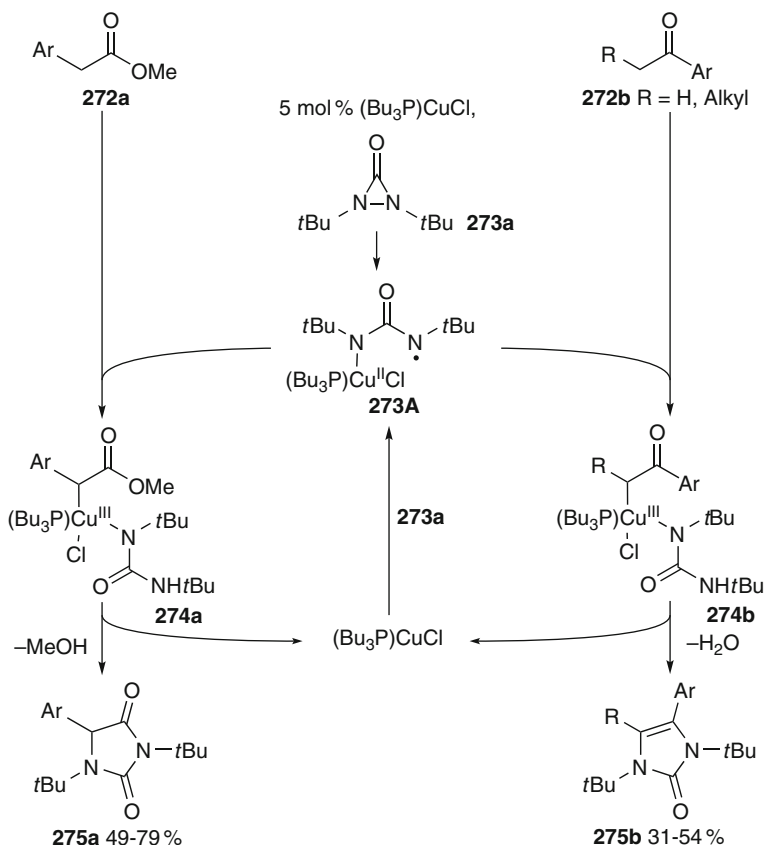
**Fig. 69** Cu(I)-catalyzed C–H amination of alkylarenes using chloramine T

possible via singlet and triplet transition states, the latter proved to be lower in energy under all circumstances. The resulting benzylic radical attacks the copper amide complex after spin inversion with release of the copper(I) catalyst. A concerted singlet pathway can, however, also contribute to a minor extent. Other catalysts, such as (tris(pyrazolyl)borate)Cu(I), were also employed for similar C–H amination reactions of hydrocarbons using  $\text{PhI}=\text{NTs}$  or **267** as the nitrogen sources [367, 368]. The combination of NBS, amides, or amines in conjunction with 20 mol% CuBr induced benzylic C–H amination and amidation reactions [369].

Shi and coworkers recently reported  $\alpha$ -aminations of arylacetates **272a** [370] or arylketones **272b** [371] catalyzed by 5 mol% of a  $\text{CuCl}/\text{PBU}_3$  catalyst using diaziridinone **273a** as the reagent (Fig. 70). 5-Arylimidazolidin-2,4-diones **275a** were isolated in 49–79% yield, while ketone-derived 4-arylimidazolin-2-ones **275b** were obtained in 31–54% yield. The reaction proceeds likely by a similar mechanism as the diamination reaction (see Sect. 5.10). Reductive ring opening of the strained diaziridinone leads to a copper(II) amide-aminyl radical **273A**. This species is able to abstract a hydrogen atom from substrates **272** generating radicals, which couple subsequently to the resulting copper(II) urea complex. Reductive elimination from the amidocopper(III) enolates **274** and subsequent condensation reactions furnish imidazolidinediones **275a** or imidazolinones **275b**.

### 5.9 Cu(I)–Cu(II) Catalysis: Radical Reactions Triggered by Oxaziridine Ring Opening

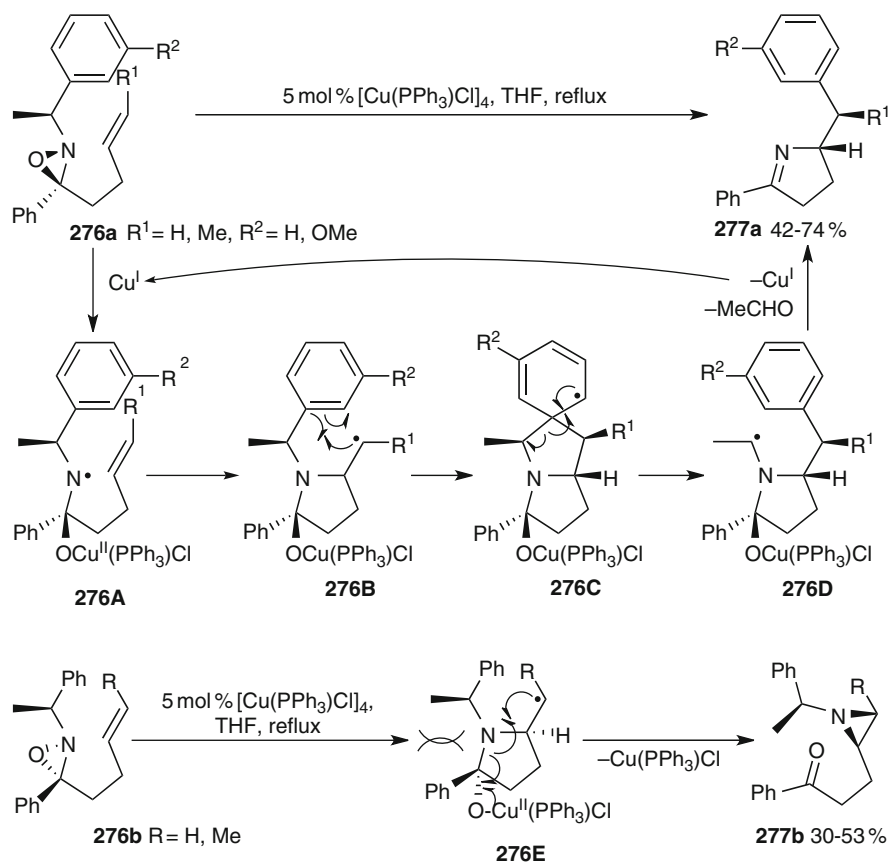
Aube reported Cu(I)-catalyzed radical cyclization reactions triggered by catalytic reductive ring opening of oxaziridines **276** (Fig. 71) [372, 373]. In this process an aminyl radical **276A** is generated first, which cyclizes to the appended alkene unit. The resulting primary radical **276B** undergoes a second cyclization to the aryl ring of the 1-(phenylethyl) unit. Subsequently, alternative ring opening of **276C** leads to the



**Fig. 70** Cu(I)-catalyzed  $\alpha$ -amination of carbonyl compounds

more stable 1-aminoethyl radical **276D**. In a number of elementary steps 1-pyrrolines **277a** are liberated in 42–74% yield and >95% ee together with acetaldehyde and the catalyst. Black and colleagues reported that a proline-derived oxaziridine underwent a similar cyclization to a pyrrolizidine derivative when refluxed with 5 mol% of  $[\text{Cu}(\text{PPh}_3)\text{Cl}]_4$  in THF [374, 375]. The diastereomeric oxaziridine **276b** provided surprisingly the chiral keto aziridines **277b** in 30–53% yield. This can be rationalized by the fact that the second cyclization of radical **276E** to the aryl ring cannot occur due to the steric constraints of the system. The primary radical stabilizes instead by a 1,3- $\text{S}_{\text{H}}\text{I}$  reaction, which affords **277b** and releases the Cu(I) catalyst at the same time.

The outcome of the reaction is also dependent on the substituent in 3-position of the oxaziridines **276c** (Fig. 72) [373]. When the substituent R is an ester, group  $\beta$ -fragmentation of an alkoxy carbonyl radical from aminyl radical **276F** is faster than cyclization, resulting in acyclic amide **277c** in 85% yield. A 1-furyl substituent led to mixtures of cyclized product **277a** and amide **277c** in 27% and 48% yields, respectively. Alkyl groups in 1-position except methyl groups also underwent fragmentation to **277c** instead of cyclization [376]. This process can be used favorably to trigger alkyl

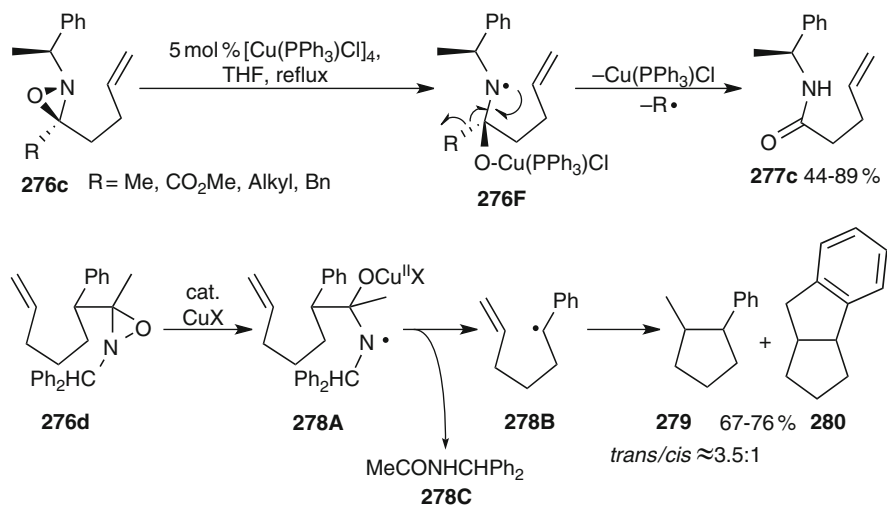


**Fig. 71** Radical reactions triggered by reductive ring opening of oxaziridines

radical cyclizations with oxaziridines **276d** as precursors. Iron(II) or Cu(I) catalysts open **276d** reductively.  $\beta$ -Fragmentation of radical **278A** gives amide **278C** and 5-hexenyl radicals **278B** that cyclize. Hydrogen abstraction from the solvent provides cyclopentanes **279** as a *trans/cis* mixture. A minor part of the cyclized radical is subject to a second cyclization, affording tricycle **280** as a side product.

### 5.10 *Cu(I)–Cu(II) Catalysis: Diamination Reactions Triggered by Diaziridinone Ring Opening*

Recently the diamination reaction of alkenes attracted much attention (reviews [377, 378]). Shi and coworkers disclosed a versatile palladium-catalyzed intermolecular diamination methodology [379]. For dienes, this process is selective for the internal double bond and occurs according to a classical two-electron catalytic



**Fig. 72** Cu(I)-catalyzed  $\beta$ -fragmentations and its application as a trigger for a radical cyclization reaction

cycle. In parallel, a Cu(I)-catalyzed process was developed (Fig. 73) [380]. 1,3-Dienes **281a** reacted with diaziridinone **273a** in the presence of 10 mol% of a CuCl/P(OPh)<sub>3</sub> catalyst for most substrates selectively at the terminal double bond and provided 4-vinyl imidazolidin-2-ones **284a** in 50–89% yield. The reaction occurred with stereochemical scrambling of the vinylic substituent in **284a** if R<sup>1</sup> is phenyl. A terminal (*Z*)-dideuterated olefin gave a 2:1 *cis/trans*-mixture of 4,5-dideuterioimidazolidinone indicating the stepwise nature of the process.

Similar conditions (10 mol% CuCl/20 mol% PPh<sub>3</sub>) served well to produce cyclic *N*-cyanoimidazolidine-2-imines **284b** in 48–86% yield with diaziridine *N*-cyanoimine **273b** as the reagent [381]. Asymmetric diamination variants were also developed. The diamination of dienes **281a** catalyzed by 10 mol% of CuCl and 5.5 mol% of (*R*)-DTBM-SEGPHOS **282** provided 4-alkenylimidazolidin-2-ones **284a** in 55–93% yield and 58–74% ee [382]. 3-Methyl-1-phenylbutadiene gave only 23% ee. A BINOL-derived copper(I) phosphate tri(2-naphthyl)phosphine complex **283** gave **284a** in 45–77% yield and 49–61% ee [383]. This demonstrates that both the diphosphine ligand and the phosphate counterion in the intermediate amidocopper complex are able to induce an asymmetric amination.

While apparently all reactions involving phosphine ligands occur at the terminal double bond of the diene system **281a**, a remarkable switch in selectivity was found in the absence of a ligand. When the reactions of dienes **281b** with diaziridinone **273a** were performed with 5 mol% of CuBr only, diamination products **285** at the internal double bond were obtained regio- and stereoselectively in 81–97% yield [384]. It was, however, still necessary that a terminal double bond was present in the substrates. 1-Phenylbutadienes were an exception, since a mixture of terminal and internal diamination products was isolated in a ratio of 3.5:1.

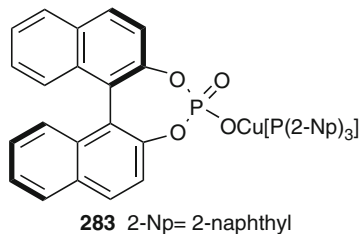
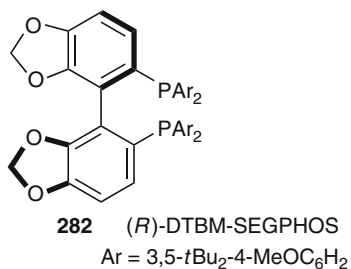
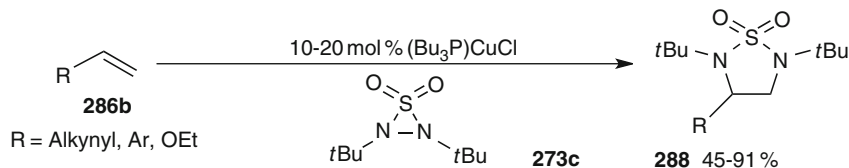
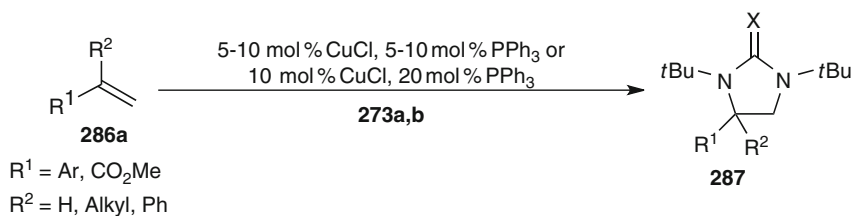
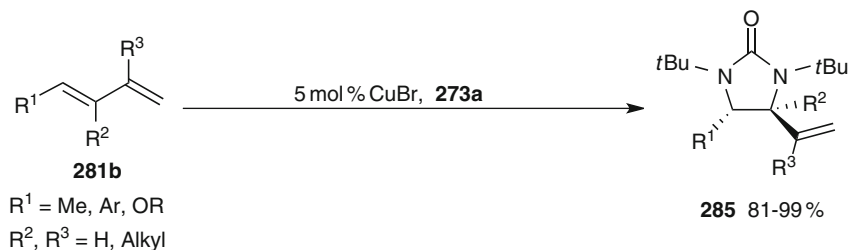
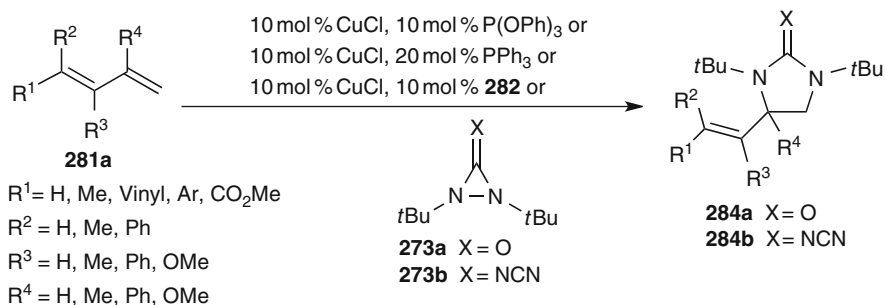


Fig. 73 Cu(I)-catalyzed diamination reactions of dienes or olefins

Diaziridinone **273a** can also be used for the diamination of 1,1-disubstituted arylalkenes **286a** applying 5–10 mol% of a CuCl-PPh<sub>3</sub> catalyst. 4-Alkyl-4-arylimidazolidinones **287** were formed in 47–91% yield [385]. Methyl methacrylate reacted in 54% yield. When thiadiaziridine *S,S*-dioxide **273c** was used as the reagent in the presence of 10 mol% of a CuCl/PBu<sub>3</sub> catalyst system, styrenes, enynes and enol ethers **286b** were transformed to 4-alkynyl-, 4-alkoxy-, or 4-aryl-2,1,3-thiadiazolidine dioxides **288** in 45–91% yield [386]. A 1.7:1 *trans/cis*-diastereomeric mixture was isolated with (*E*)-deuteriostyrene as the substrate. Both diaziridinone **273a** or thiadiaziridine dioxide **273c** serve in the presence of the CuCl-PPh<sub>3</sub> catalyst as suitable dehydrogenation reagents for semi-saturated carbo- and heterocycles, provided they contain easily abstractable hydrogen atoms, but do not add aminyl radicals (not shown) [387].

The divergent course of the reactions can be explained as follows (Fig. 74). The diamination reaction proceeds with electron-rich copper(I)-phosphine complexes by initial SET reduction and ring opening of the diaziridine derivatives **273a,b**. Thus generated copper amide-aminyl radical **273A** adds to the diene **281a**. The resulting allylic radical **281A** can substitute the copper(II) amide in a 1,5-S<sub>H</sub>i reaction step leading to the products **284a,b** and the Cu(I) catalyst. Alternatively, coupling of the allylic radical **281A** with the copper(II) center may occur resulting in organocopper(III) species **281B**, from which reductive elimination would lead to product **284a,b**. Similar catalytic cycles can be formulated for the reactions of olefins **286a,b**.

When the diamination was performed with 5 mol% CuBr in the absence of additional ligands, initial oxidative addition of coordinatively unsaturated CuBr to **273a** is more favorable, resulting in copper(III) diamide **273B**. This species coordinates the terminal double bond of the diene **281b** as an additional ligand forming copper(III) complex **281C**. Migratory insertion of the amide ligand at the internal position provides an (allyl)copper(III) complex **281D**, which gives product **285** by reductive elimination. Thus, by tuning the electronic properties of the copper catalyst, regiodivergent diamination reactions became possible.

### 5.11 Cu(II) Catalysis: [1,2]-Onium Ylide Rearrangements (Stevens Rearrangements)

While [2,3]-onium ylide rearrangements are proceeding most often by concerted pathways (review [388]), [1,2]-onium ylide rearrangements (Stevens rearrangements) often involve radical intermediates (recent reviews [389, 390]). A study aimed at the comparison of Rh(II) and Cu(II)-catalyzed oxonium ylide reactions of oxygenated diazoketones using 3 mol% of the former and 15 mol% of the latter showed that the copper-catalyzed process provided better yields and selectivities for [1,2]-rearrangement products (see Part 2, Sect. 6, Fig. 107) [391, 392].

More recently, West and colleagues demonstrated that rhodium and copper catalysts led to different product ratios when diazo ketones **289** bearing differential

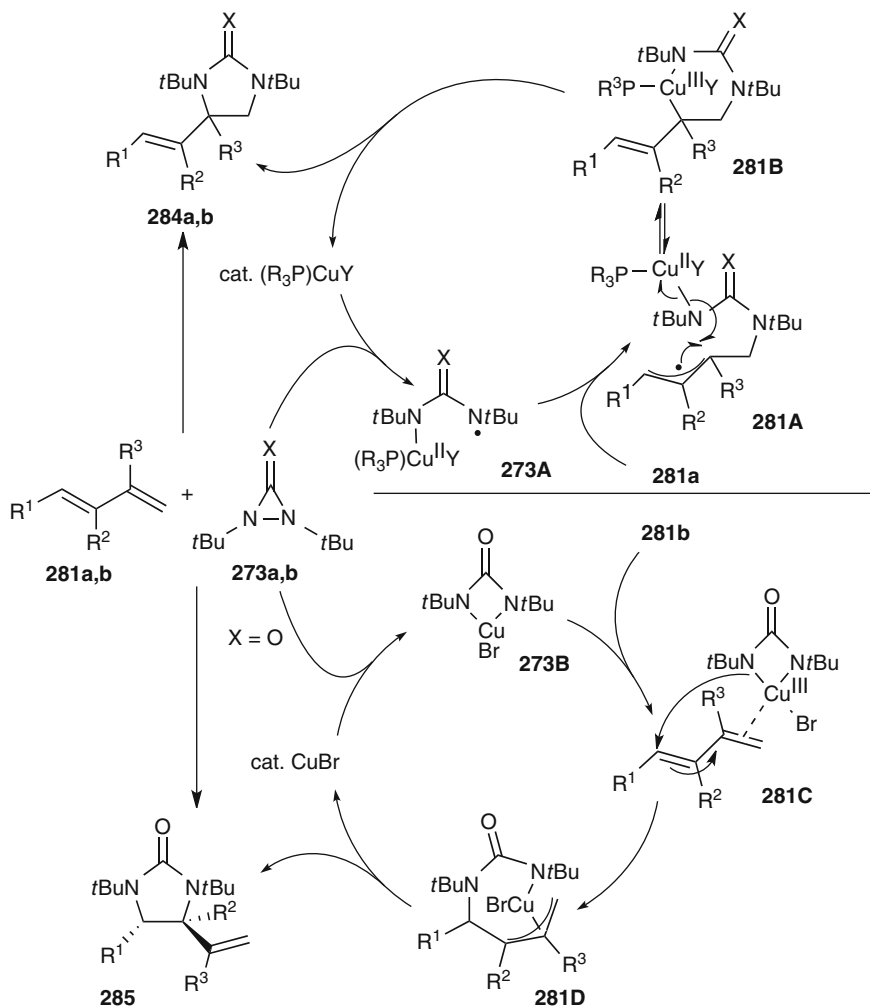


Fig. 74 Mechanistic divergence of copper(I)-catalyzed diamination reactions

ether functions in  $\beta$ - and  $\gamma$ -position were applied as substrates (Fig. 75) [393]. The substituents are amenable to [1,2]- or [2,3]-rearrangements. With benzyloxy substituents in  $\beta$ - and  $\gamma$ -position, the one in  $\beta$ -position reacts as expected, preferentially though not exclusively giving mixtures of five- and six-membered ethers analogous to **291** and **293**, respectively (not shown). With copper catalysts **290a** or **290b** the formation of small amounts of a product analogous to **292** was also observed. With an allyl ether function in  $\beta$ - and a benzyl ether unit in  $\gamma$ -position, a [2,3]-rearrangement to a product analogous to **291** was observed exclusively using  $\text{Rh}_2(\text{OAc})_4$  or copper(II) catalysts **290a,b**. With substrate **289** the selectivity was dependent on the catalyst. Copper catalyst **290a** promoted the predominant



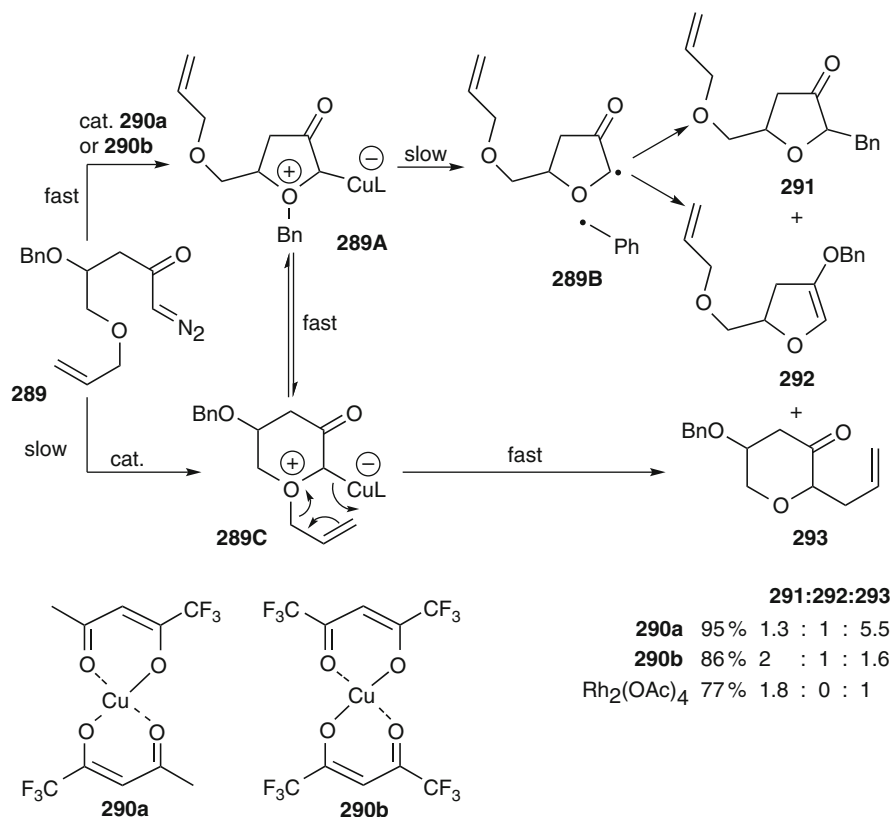
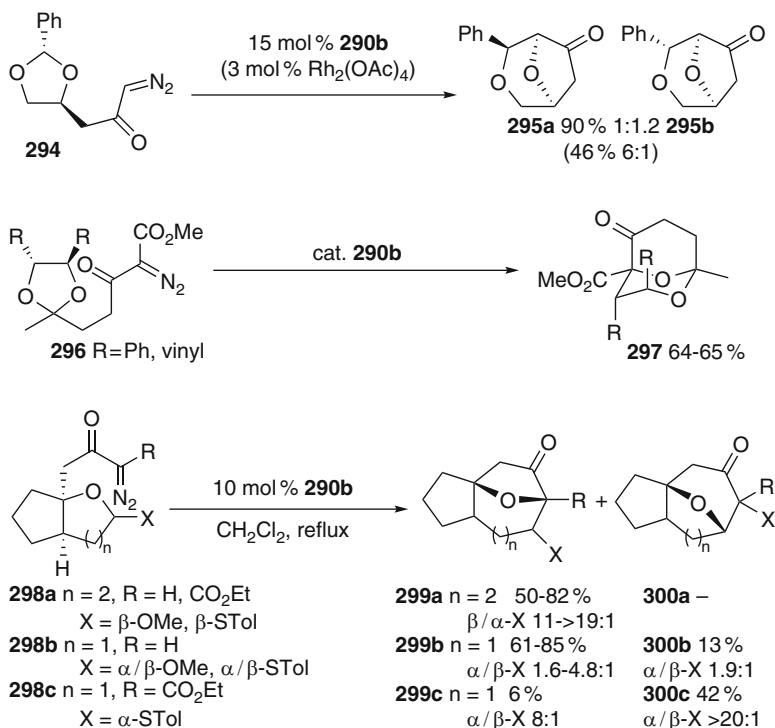


Fig. 75 Copper-catalyzed oxonium ylide [1,2]- vs. [2,3]-rearrangements

formation of tetrahydropyranone **293**, no selectivity was found with **290b**, but the ratio reversed with Rh<sub>2</sub>(OAc)<sub>4</sub> leading preferentially to tetrahydrofuranone **291**. With both catalysts **290a** and **290b**, a significant amount of cyclic enol ether **292** was observed, while it was not detected with Rh<sub>2</sub>(OAc)<sub>4</sub>. This behavior can be explained by invoking that the oxonium ylide formation is reversible and that the copper complex remains attached to the oxonium ylide. For catalyst **290a** the five-membered oxonium ylide **289A** is formed fast. The homolysis of the benzyl substituent leading to **289B**, which triggers the 1,2-rearrangement, is, however, apparently considerably slower than equilibrium with the six-membered oxonium ylide **289C**, from which a fast concerted [2,3]-rearrangement to **293** proceeds. With catalyst **290b** the equilibration of oxonium ylides becomes less favorable, since **291** remains the major product. In the copper catalyzed processes variable amounts of enol ether **292** were formed. This is evidence for a biradical intermediate **289B**, which collapses at both termini of the resonance-stabilized  $\alpha$ -keto radical. In the case of the rhodium catalyst, either oxonium ylide equilibration is slower, or the [1,2]-migration of the benzyl substituent is accelerated.



**Fig. 76** Cu(II)-catalyzed oxonium ylide cyclization/1,2-rearrangement sequences with acetals or ketals

Due to the ease of preparation, work was devoted to the study of the reaction behavior of acetals and ketals in oxonium ylide [1,2]-shifts (Fig. 76). Reactions of diastereomeric acetals **294** with the 1,2- or 1,3-diol unit in the main chain did not proceed with retention of configuration in product **295**, thus supporting a stepwise process [392]. The authors proposed that the involved intermediates are either 1,6-biradicals or the corresponding ion pairs. The diastereoselectivity is in some cases similar, in others the Rh-catalyzed process is more selective.

Brogan and colleagues reported that the [1,2]-rearrangement mode is far preferred over potentially competing [2,3]-rearrangements in substrates **296** (R=vinyl) having the ketal carbon in the main chain. Tricyclic products **297** were obtained in 64–65% yield using 4–15 mol% of **290b** [394]. In an attempt to access the zaragozic acid core by an analogous oxonium ylide [1,2]-rearrangement, the Cu-catalyzed reaction displayed – in contrast to Rh<sub>2</sub>(OAc)<sub>4</sub> – no [1,2]-/[2,3]-rearrangement selectivity [395]. The reaction proceeded diastereodivergent for a *meso*-isomer, thus supporting a stepwise process.

West et al. subsequently studied a number of conformationally restricted carbocyclic acetals **298a–c** with respect to their behavior in copper-catalyzed oxonium ylide cyclization/[1,2]-rearrangement reactions. 5-6-Bicyclic acetals **298a** underwent the

oxonium ylide formation/rearrangement sequence with high regio- and stereoselectivity providing oxabicyclic sulfides **299a** in 50–80% yield and good to exclusive  $\beta$ -selectivity [396, 397].

5-5-Bicyclic acetals **298b,c** underwent the rearrangement much less selectively. This system forms a more strained five-membered metal oxonium ylide in the first step. Therefore, the formation of 1,7-sulfonium ylides competed for hemithioacetals **298b,c** ( $X=STol$ ), but not for acetals ( $X=OMe$ ). Acetals **298b,c** ( $X=OMe$ ) homolyze after oxonium ylide formation apparently more easily to a radical, which also seems to be longer-lived. This allows more significant stereochemical scrambling at the acetal function resulting in less diastereoselectivity for **299b**. The intermediate 1,7-sulfonium ylides rearranged with variable diastereoselectivity to **300b,c** [397, 398]. Either biradical or metal assisted ion pair-based mechanisms may operate for most examples. No systematic studies distinguishing these pathways unambiguously have been conducted so far.

The Stevens rearrangement of ammonium ylides was recently reviewed in detail [389]. More recently, West and colleagues disclosed intermolecular Cu(II)-catalyzed reactions of azetidine-2-carboxylates **301** ( $R^2=CO_2Et$ ) with  $\alpha$ -diazo carbonyl compounds **302** (Fig. 77) [399]. Using 10 mol% of  $Cu(acac)_2$  with microwave irradiation in dichloroethane or heating the mixture in toluene furnished pyrrolidine-2,3-dicarboxylates **303** ( $R^2=CO_2Et$ ) in 24–81% yield as mixtures of diastereomers. The transformation proceeds by initial addition of the copper carbenoid generated from  $Cu(acac)_2$  and **302** to the azetidine **301**. The resulting ammonium ylide **301A** suffers a homolysis under the reaction conditions providing a 1,5-biradical pair **301B**. The unselective collapse of this intermediate leads to the pyrrolidine diastereomers **303**. When *N*-benzylazetidine and diazomalonate **302** ( $R^4=CO_2Et$ ) were applied, preferential migration of the benzyl group was observed. 2-Benzoylpyrrolidines were oxidatively degraded to pyrroline derivatives in a polar process under the reaction conditions. Concerted [2,3]-rearrangements, where possible, did not compete with the observed [1,2]-rearrangement, showing that the relief of ring strain is an important driving force in the reaction.

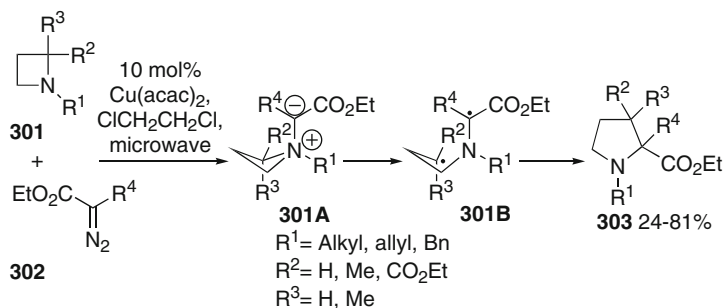


Fig. 77 Ammonium ylide ring expansion reactions

## 5.12 Cu(II)–Cu(I) Oxidative Catalysis: Oxidative Cleavage Reactions and Cyclizations of Amides

After the aerobic oxidative cleavage of enamines catalyzed by CuCl was published by van Rheenen [400], Itoh and colleagues disclosed the first Cu(II)-catalyzed ring opening/oxygenation sequences of bicyclic bridgehead cyclopropylamines **304** leading to cyclic epoxy ketones **305** in 18–28% yield (Fig. 78) [401]. The reactions are thought to proceed by SET oxidation of the tertiary amine function to an aminium radical cation, which undergoes a facile transannular ring opening of the cyclopropane unit. The resulting distonic radical cation **304A** is trapped by oxygen giving peroxy radical **304B**. This can stabilize in a number of steps by reduction, cyclization to the iminium function and epoxide formation, which regenerates the catalyst.

Chemler and colleagues recently published a series of papers dealing with stoichiometric tandem amide cyclization/radical cyclization or amide cyclization/radical functionalization reactions (recent review [402]). More recently catalytic variants were developed. *N*-Arylsulfonyl-4-pentenylamines **306a** provided tricyclic 1,2-thiazine dioxides **307a** in 45–85% yield and 80–94% ee when treated with 20 mol% of Cu(OTf)<sub>2</sub> and BOX ligand **25a** (Fig. 79) [403]. Manganese dioxide served as the stoichiometric oxidizing agent for coformed Cu(I) and K<sub>2</sub>CO<sub>3</sub> to deprotonate the sulfonamide. *N*-(*ortho*-Allylphenyl) arylsulfonamides cyclized similarly, albeit with lower enantioselectivity. The methodology was applied to the total synthesis of the alkaloid (*S*)-(+)-tylophorine [404]. *ortho*-Allyldiarylamines **306b** cyclized similarly in 53–87% yield to dibenzopyrrolizidines **307b** using 20 mol% Cu(OTf)<sub>2</sub> and 25 mol% bipy **26** in the presence of excess MnO<sub>2</sub> [405]. Asymmetric group-selective amidocupration/radical cyclization reactions of *N*-(4,4-dibenzyl-4-pentenyl)sulfonamides **306c** furnishing annulated pyrrolidines **307c** proceeded in 89–99% yield and high diastereo- and enantioselectivity using 20 mol% of Cu(OTf)<sub>2</sub> and 25 mol% of Ph-BOX ligand **25a** [406]. No regioisomers were formed, suggesting a direct radical 6-endo cyclization. *ortho*-Substituted substrates furnished in contrast regioisomers in similar quantities, but both with >95% ee, indicating rearrangement processes in the course of the cyclizations.

Similar conditions were applied in oxygenative cyclizations of **308** applying TEMPO **310** as the oxygenating reagent (Fig. 80) [407]. To obtain good yields and enantioselectivities, 20 mol% of Cu(OTf)<sub>2</sub> and the diphenyl-BOX ligand **309** were

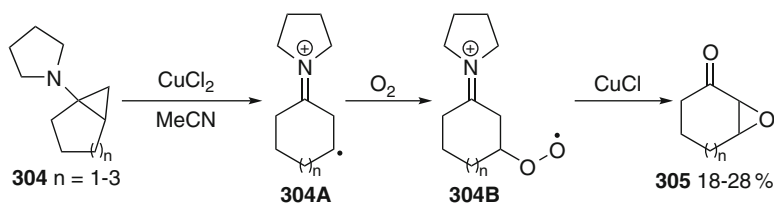
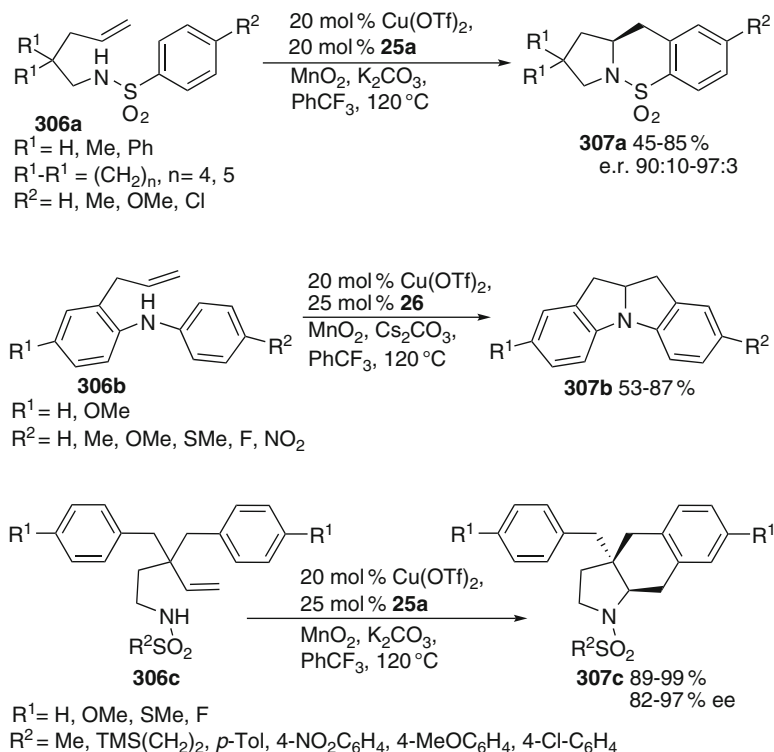


Fig. 78 Oxidative ring opening of cyclopropylamines and subsequent epoxidation

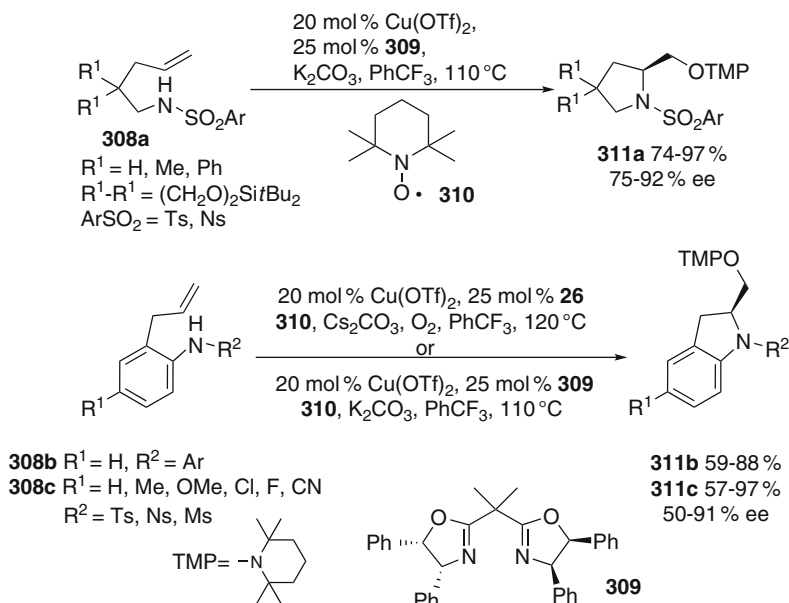


**Fig. 79** Cu(II)-catalyzed tandem amidocupration/radical cyclization reactions

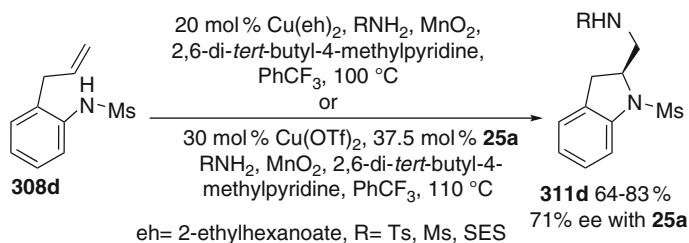
necessary. Using trifluoromethylbenzene as the solvent and  $\text{K}_2\text{CO}_3$  for the initial cupration of the amide, 57–97% of oxygenated pyrrolidines **311a** were obtained. The enantiomeric excess amounted to 75–92%. A catalyst generated from 20 mol%  $\text{Cu}(\text{OTf})_2$  and 25 mol% bipy **26** promoted the cyclization/oxygenation sequence of diarylamines **308b** to indolines **311b** in 59–88% yield with excess  $\text{MnO}_2$  [405]. *N*-Aryltoluenesulfonamides **308c** cyclized in 61–97% yield to *N*-tosylindolines **311c**. Good enantioselectivity was found in the cyclization resulting in 75–92% ee. The corresponding *N*-mesyl or *N*-nosyl amines **308c** gave also good yields of **311c** but lower enantioselectivities of 50–61% ee [407].

Copper(II)-catalyzed aminocyclization/amination sequences of sulfonamides **308d** leading to 2-aminomethylindolines **311d** were also accomplished (Fig. 81). In an asymmetric version a chiral catalyst generated from 30 mol% of  $\text{Cu}(\text{OTf})_2$  and 37.5 mol% of Ph-BOX ligand **25a** induced the formation of 2-(aminomethyl)-indoline **311d** in 64% yield and 71% ee [408].

All these reactions proceed by initial base-promoted formation of copper amide complexes **306A** from diarylamines or sulfonamides **306** or **308**, respectively, which are subject to a concerted *syn*-amidocupration to the adjacent alkene unit via transition state **306B** (Fig. 82). The resulting alkylcopper(II) intermediates **306C** are



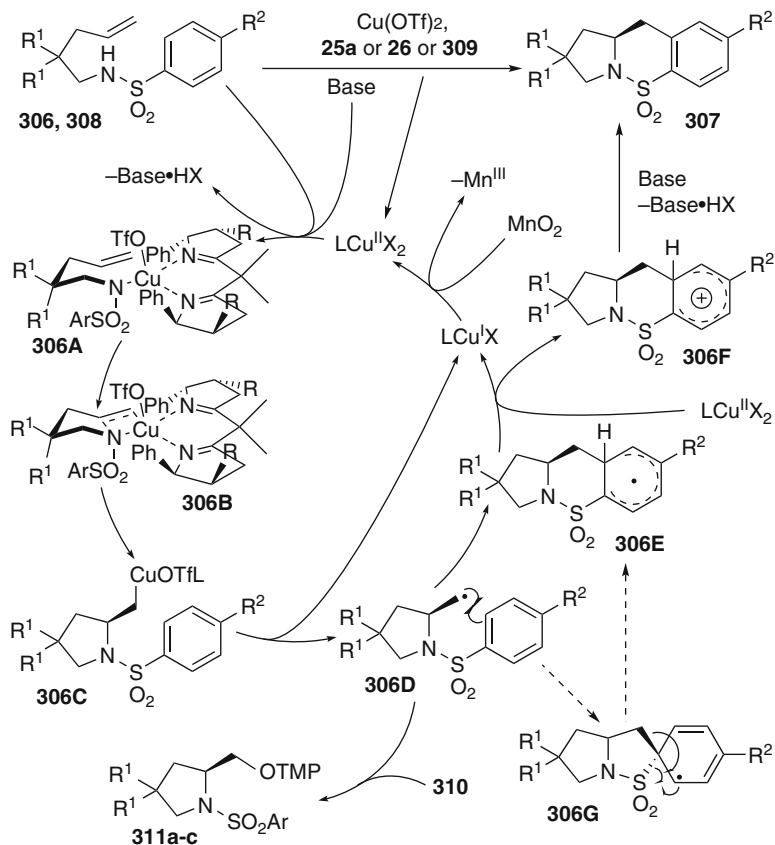
**Fig. 80** Copper-catalyzed amidocupration/radical oxygenation reactions



**Fig. 81** Copper(II)-catalyzed intramolecular diamination reactions

subject to facile homolysis leading to alkyl radicals **306D**. These species can be intercepted in several ways. If efficient traps are not available, a radical cyclization to an adjacent aryl unit prevails, providing cyclohexadienyl radicals **306E**. They are easily oxidizable to cyclohexadienyl cations **306F** under the reaction conditions, from which products **307** form by deprotonation. The proposed amidocupration/radical cyclization sequence is supported by the fact that analogous radical cyclizations of related aminyl radicals proceeded with significantly different diastereoselectivities. Individual classical radical cyclization of pyrrolidinylmethyl radicals gave on the other hand very similar results [409]. With TEMPO **310** interception of radical **306D** leading to products **311a-c** is faster than radical cyclization.

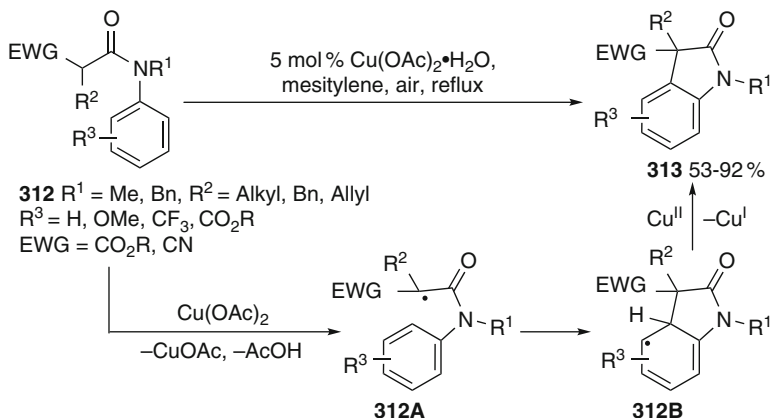
Group-selective cyclizations to aryl units (**306c**→**307c**) indicated that the initial intramolecular amidocupration leads to equatorially oriented radicals, which cyclized to



**Fig. 82** Catalytic cycle of oxidative copper-catalyzed tandem cyclizations

the *cis*-oriented benzylic group. The formation of single regioisomers in most sequences with **306a** and **306c** indicated that the radical cyclization steps proceed preferentially by a direct 6-endo cyclization to the *ortho*-position of the arene (**306E**) and not by an initial 5-exo cyclization to the *ipso*-position via spiro-radicals **306G** followed by a 1,2-rearrangement to the six-membered radical **306E**, a frequently observed reaction channel in radical chemistry (recent reviews [410, 411]). This rearrangement leading to regioisomeric mixtures of products **307c** was observed only with very few substrates. However, both regioisomers were isolated with high ee in these cases, thus substantiating the *syn*-amidocupration pathway in the first cyclization step.

Taylor and colleagues discovered recently that *N*-aryl malonamides or cyanoacetamides **312** cyclized in 53–92% yield to oxindole-3-carboxylates **313** in the presence of 5 mol% of  $\text{Cu}(\text{OAc})_2$  using air as the stoichiometric reoxidant for the catalyst (Fig. 83) [412]. The reactions occur likely by initial formation of a copper enolate of **312**. SET oxidation with elimination of  $\text{CuOAc}$  gives radical **312A**, which undergoes a 5-exo cyclization to the aryl unit. A final oxidative



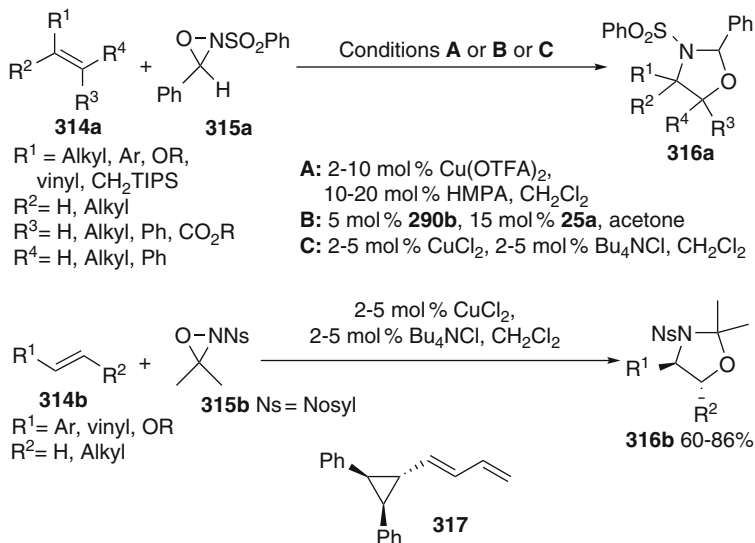
**Fig. 83** Copper(II)-catalyzed oxidative radical cyclizations of malonamides or cyanoacetamides **312**

rearomatization by another SET of the cyclohexadienyl radical **312B** and deprotonation afford the product **313**. This method is especially suited to prepare oxindoles with quaternary centers.

### 5.13 Cu(II)–Cu(III) Catalysis: Ring Opening Reactions of Oxaziridines

Aminohydroxylation reactions (recent highlight [413]) of olefins **314** by *N*-sulfonyloxaziridines **315a** catalyzed by 2–5 mol% of Cu(OTFA)<sub>2</sub> and 10 mol% HMPA as a solubilizing reagent were recently discovered by Yoon and colleagues (Fig. 84, Condition A) [414]. With styrenes **314a** (R<sup>1</sup>=Ar) 4-aryloxazolidines **316a** were formed in 75–87% yield as 2,4-*cis*/2,4-*trans* diastereomeric mixtures (1–10:1). The stepwise nature of the reaction was demonstrated by the stereoconvergent formation of a 2:1 2,4-*cis*-4,5-*trans*/2,4-*trans*-4,5-*trans*-mixture from both *trans*- and *cis*-stilbene. These reactions were initially formulated as Lewis acid-catalyzed trapping of the resulting benzylic carbocation by the cogenerated copper(II) amide. A reductive process analogously to Aube's reactions (see Sect. 5.9) was ruled out based on the opposite regiochemical outcome. An oxidative reaction was also discounted. Electron-poor as well as electron-rich 1,3-dienes **314a** (R<sup>1</sup>=alkenyl) were very good substrates in this aminohydroxylation process giving 4-vinyloxazolidines in 62–89% yield as 1–2.5:1 2,4-*cis*/2,4-*trans* diastereomeric mixtures [415]. Vinyl ethers or allylsilanes also underwent the aminohydroxylation in 66–72% yield. The silyl group in allylsilanes was retained, which speaks for a radical mechanism.





**Fig. 84** Copper(II)-catalyzed aminohydroxylation reactions

An enantioselective aminohydroxylation variant using BOX ligand **25a** was developed on this basis for styrenes **314a** ( $\text{R}^1 = \text{Ar}$ ,  $\text{R}^2 - \text{R}^4 = \text{H}$ ) [416]. Copper bis(hexafluoroacetylacetonate) **290b** (5 mol%) as a catalyst and acetone as the solvent proved to be optimal in these reactions (Condition **B**). The 2,4-diastereoselectivity in products **316a** remained moderate, but good ee-values of 83–89% ee for the *cis*-isomers and 39–79% ee for the *trans*-isomers were obtained. The acceleration by the ligand is apparently not very strong; thus a threefold excess of **25a** is necessary to suppress the background reaction sufficiently.

It was subsequently discovered that an anionic halocuprate(II) complex generated in situ from  $\text{CuCl}_2$  and  $\text{Bu}_4\text{NCl}$  was a much better catalyst for the aminohydroxylation reactions of **314a** with **315a** (Condition **C**) [417]. This catalyst system also allowed the use of achiral 3,3-dimethyloxaziridine **315b** as the reagent, which is not reactive under Conditions **A** or **B**. Styrenes, 1,3-dienes, and enol ethers **314b** gave 60–86% yield of 2,2-dimethyloxazolidines **316b** in 1–4.5 h applying the optimized conditions. The acetonide unit can be easily removed providing an efficient access to 1,2-amino alcohols. The  $\text{CuCl}_2/\text{Bu}_4\text{NCl}$  catalyst was easily applicable to styrenes with strong electron-withdrawing substituents, such as nitro or trifluoromethyl groups, in which carbocationic intermediates become unlikely. Kharasch additions of  $\text{CBr}_4$  to styrene were initiated by **315b** and 5 mol% of the halocuprate reagent providing strong evidence for a catalytic cycle involving radical as well as Cu(II) and Cu(III) intermediates. 1-(*cis*-2,3-Diphenylcyclopropyl)butadiene **317** afforded a 2-(diphenylcyclopropyl)vinyl oxazolidine exclusively; however, the relative configuration of the substituents at the cyclopropane ring was completely scrambled, indicating the intervention of a cyclopropylallyl radical. A corresponding carbocation, if formed, would be expected to react stereospecifically with retention of configuration at the cyclopropane ring.

Another substrate class, for which the outcomes of a radical and a carbocationic process are opposite, are indoles (Fig. 85) [418]. Indeed, when oxaziridines **315a** or **315c** were treated with indoles **314c** in the presence of 2 or 10 mol% of  $\text{CuCl}_2/\text{TBAC}$  oxazolidinoindolines **316c** were obtained as the exclusive products in 53–90% yield. The reaction is applicable to 2-, 3-, and 2,3-disubstituted indoles. Chiral indole derivatives acylated with (*S*)-proline units at nitrogen underwent asymmetric diastereoselective aminohydroxylation reactions with 86–91% de. Tricyclic hemiaminals derived from tryptamine derivatives could be transformed to pyrrolidinoindolines, which are core structures of a number of alkaloids.

The available evidence points to the following reaction course (Fig. 86). Oxaziridines **315** are subject to ring opening by the copper(II) catalyst. This leads to copper(III) amide complexed alkoxy radicals **315A**. These highly reactive radicals add to olefins or dienes **314**. The resulting radicals **315B** stabilize by a 1,5- $\text{S}_{\text{H}}$  reaction at nitrogen, which releases the products **316** and the copper(II) catalyst.

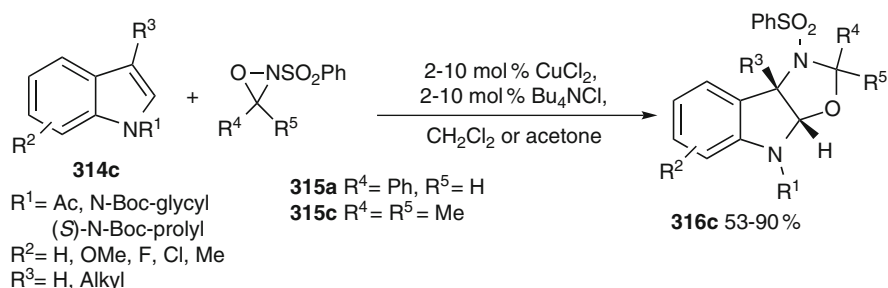


Fig. 85 Aminohydroxylation of indoles

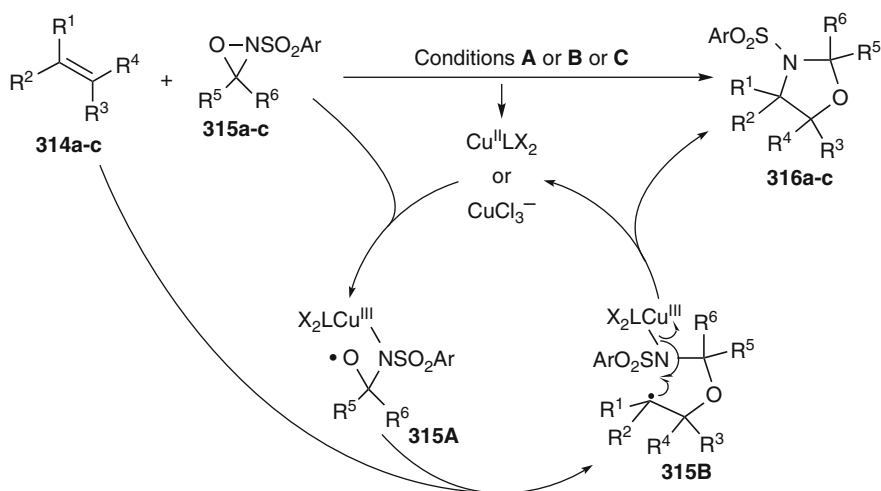


Fig. 86 Catalytic cycle of the copper(II)-catalyzed aminohydroxylation reactions

## 5.14 Miscellaneous

Schoening and colleagues reported a copper-catalyzed method for the preparation of alkoxyamines **320** from aldehydes **318**, hydrogen peroxide, and 4-hydroxy-TEMPO **319** (Fig. 87) [419]. The products **320** were isolated in yields of 24–91%. Common functional groups are tolerated under the oxidative reaction conditions. An initial fast addition of  $\text{H}_2\text{O}_2$  to the carbonyl compound generates a perhydrate **318A**, which is subject to a Fenton-type reaction. The resulting alkoxy radical **318B** releases formic acid and an alkyl radical, which couples with **319** to products **320**. Ketones react similarly, but the yields are generally lower [420]. Other copper(I) and also copper(II) salts in protic media were useful as catalysts. The recycling of the catalyst remained unclear in these reactions.

Kundu and Ball developed a method for remote functionalization of alkyl hydroperoxides **321** via 1,5-hydrogen transfer reactions (Fig. 88) [421]. When treated

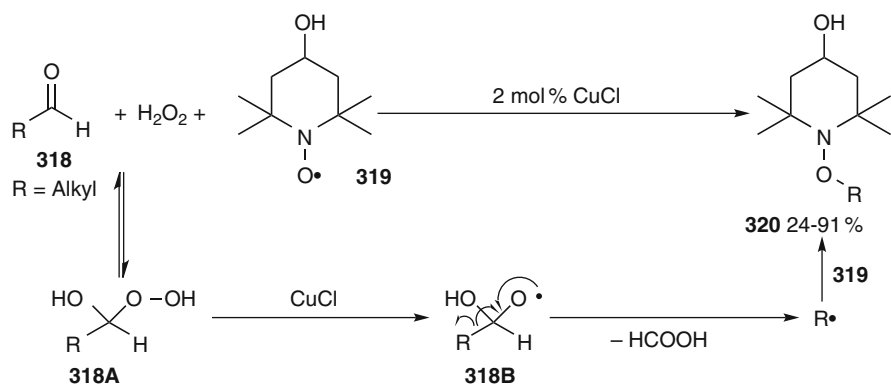


Fig. 87 Copper-catalyzed synthesis of alkoxyamines by a Fenton-type reaction

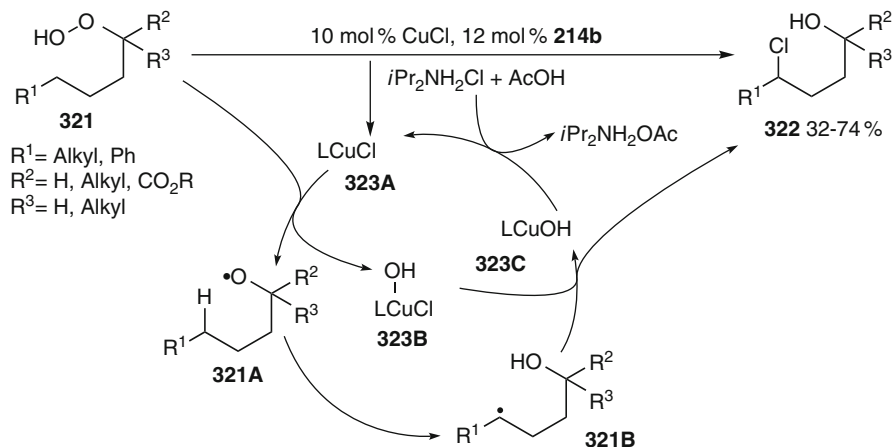


Fig. 88 Copper(I)-catalyzed 1,5-hydrogen transfer/ligand transfer reactions

with 10 mol% of CuCl and 12 mol% of PMDETA **214b** in the presence of  $i\text{Pr}_2\text{NH}_2\text{Cl}$ , acetic acid, and small amounts of water, a selective remote functionalization was observed giving 1,4-chlorohydrins **322** in 32–74% yield. The reaction proceeds probably by an initial Fenton-type reaction of **321** with copper catalyst **323A** leading to alkoxy radical **321A**. A subsequent 1,5-hydrogen transfer reaction is facile for alkoxy radicals, such as **321A**. Chlorine transfer from the oxidized copper(II) chloride catalyst **323B** to alkyl radical **321B** provides the product **322**. The amine hydrochloride additive serves as the stoichiometric chloride source for regeneration of the active catalyst **323A** from coformed copper hydroxide **323C**. A catalytic amount of sodium ascorbate proved to be beneficial to avoid oxidative deactivation of the catalyst.

## 6 Silver-Catalyzed Radical Reactions

Silver salts are common for triggering radical processes by SET between oxidation states Ag(0)–Ag(I) or Ag(I)–Ag(II). They are known to form ate complexes in oxidation states Ag(I) and Ag(II), from which reductive elimination is common to give coupled products. These processes have been used in a number of stoichiometric applications, such as oxidative dimerization reactions of organometallic compounds, enolates, phenols, or alkynes. Catalytic dimerizations of Grignard reagents were reported using  $\text{LiNO}_3$ ,  $\text{N}_2\text{O}_4$ , or dibromoethane as stoichiometric oxidants [422–424]. Whitesides and coworkers showed that individual alkylsilver phosphine complexes generated by transmetalation from Grignard or organolithium reagents are thermally and photochemically very labile. They decompose thermally to give predominantly the alkyl dimer,  $\text{PBu}_3$ , and silver, but only very little disproportionation products [425]. Therefore a concerted process was proposed for the dimerization. A free radical coupling mechanism was considered unlikely, since the extent of disproportionation products in classical radical processes is considerably higher. The presence of TEMPO **310** apparently increased the formation of radical-derived products, while di-*tert*-butyl nitroxyl was inert. Under photochemical conditions radical decomposition of the alkylsilver complex predominated, affording considerable amounts of disproportionation products.  $\beta$ -Hydride elimination did not play a significant role during decomposition of linear alkylsilver complexes, but competed in secondary organosilver complexes with dimerization.

### 6.1 Ag(0)–Ag(I) Catalysis: Cross-Coupling and Addition Reactions

Tamura and Kochi studied the cross-coupling reactions of alkyl halides with alkyl Grignard reagents catalyzed by silver compounds first [422, 426, 427]. The coupling of primary alkyl halides with primary Grignard reagents resulted in a mixture

of the cross-coupling and both homocoupling products, when both were of different chain length. It was noted that during the reaction of Grignard reagents with Ag(I) compounds a soluble form of Ag(0) was formed, which was an active catalyst for the generation of alkyl radicals from alkyl halides. The relative rates of reaction of *tert*-BuBr, *i*-PrBr, and *n*-PrBr amounted to 20:3:1, typical for radical generation. Silver salts catalyzed the addition of ethyl bromide to butadiene, which was followed by coupling of the resulting allyl radical with the Grignard reagent, giving a mixture of ethylated hexenes. A dichotomy of the cross-coupling pathways with respect to the structure of the applied organic halides was demonstrated. In the silver-catalyzed coupling of methyl bromide with *cis*-1-propenylmagnesium bromide, retention of olefin geometry was observed indicating a two-electron catalytic coupling, which is known to occur stereospecific, while the coupling of *cis*-1-propenyl bromide with methylmagnesium bromide led to the formation of a 2:1 *cis/trans*-mixture of coupling products, suggesting SET and equilibration of the intermediate vinyl radicals.

Oshima and colleagues recently reported selective cross-coupling reactions of secondary and tertiary alkyl chlorides, bromides, or iodides **324** with benzylic Grignard reagents **325** catalyzed by 1 mol% of AgNO<sub>3</sub> (Fig. 89) [428]. Branched alkyl arenes **326** (R<sup>4</sup>=Bn) were obtained in 14–88% yield. Allyl Grignard reagents were also applicable providing terminal alkenes in 46–83% yield. Crotyl and prenyl Grignard reagents gave mixtures of α- and γ-allylated products, in which the former

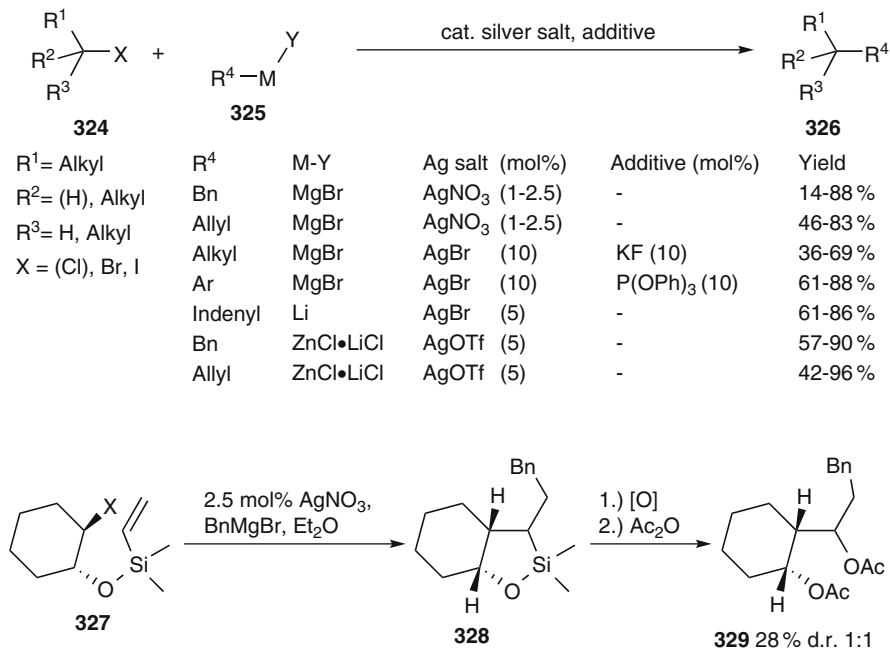


Fig. 89 Silver-catalyzed cross-coupling reactions

prevailed. Primary alkyl bromides reacted only in low yields. The facile cross-coupling of tertiary alkyl halides is especially remarkable. The intermediacy of radicals in the coupling reaction is supported by the stereoconvergent coupling of *endo*- and *exo*-2-bromonorbornanes (cf. Part 1, Fig. 9). *trans*-2-Iodocyclohexyl vinylsilyl ether **327** underwent a clean tandem radical 5-*exo* cyclization/cross-coupling reaction with benzylmagnesium bromide using 2.5 mol% of AgNO<sub>3</sub> providing bicycle **328**. After Tamao–Fleming oxidation and acetylation the protected diol **329** was isolated in 28% yield over the three steps. The cross-coupling selectivity is excellent compared to Tamura's and Kochi's results. This suggests that an anionic ate species is the catalytically active intermediate which leads to the significant improvement of the selectivity of the coupling process [429].

The methodology was extended to the cross-coupling of secondary and tertiary alkyl bromides **324** with alkyl Grignard reagents [430]. The catalytic system consisted of 10 mol% of AgBr and 10 mol% of KF. It was important to perform the reactions at –10°C to avoid decomposition of the alkylsilver intermediates (see above). The use of the AgBr/KF couple proved to be mandatory, since an AgF/LiBr system or AgF alone were less effective. Under these conditions 36–69% of coupling products **326** were isolated. Primary alkyl bromides gave again low yields. Secondary and tertiary Grignard reagents could not be applied. The reaction conditions were compatible with TBS ethers, acetals, or sulfonamides. The use of KF was not beneficial for the coupling with aryl Grignard reagents. Here a catalyst generated in situ from 10 mol% of AgBr and 10 mol% of P(OPh)<sub>3</sub> proved to be optimal. Primary, secondary, and tertiary alkyl bromides as well as *ortho*-substituted aryl Grignard reagents gave good yields of the cross-coupling products **326** (R<sup>4</sup>=Ar). In a competition experiment using 1,10-dibromoundecane it was shown that the reaction at the secondary bromide function is much faster than at the primary in the presence of KF, while the reactivity difference is considerably smaller applying the phosphite ligand.

Oshima's group also demonstrated that selected organolithium reagents, such as indenyl or fluorenyllithium compounds, are suitable nucleophiles in cross-coupling reactions catalyzed by 5 mol% AgBr [431]. Secondary and tertiary alkyl bromides **324** coupled in good to excellent yields (61–86%), while *tert*-butyl iodide or tertiary alkyl chlorides furnished the products only in moderate yield (31–38%). Acetal, sulfonamide, or aryl bromide units are compatible with the reaction conditions. The intermediacy of radicals is supported by a preferred formation of *trans*-(4-*tert*-butylcyclohexyl)indene from a *cis/trans*-mixture of 4-*tert*-butylcyclohexyl bromides (cf. Part 1, Fig. 9). Twofold coupling reactions were explored and furnished 1,3-dialkylindenes in moderate to good yield (not shown). A stoichiometric coupling experiment of indenyllithium with AgBr gave a good yield of 1,1'-biindenyl. On incremental addition of indenyllithium to a mixture of the silver catalyst and alkyl bromide, the cross-coupling set in only after a stoichiometric amount of indenyllithium based on the silver catalyst was consumed, forming biindenyl in almost quantitative yield.

To increase functional group compatibility a silver-catalyzed coupling of tertiary alkyl halides **324** with benzylzinc halides **325** (R<sup>4</sup>=Bn, M=Zn) was

developed [429]. Silver triflate proved to be the catalyst of choice. Knochel-type benzylzinc chloride•LiCl complexes were most effective in suppressing undesired elimination reactions of the sensitive tertiary alkyl bromides. Branched alkylarenes **326** were obtained in 57–90% yield. A secondary alkyl bromide reacted in 57% yield, but required considerably more time to go to completion. Fluoride and ester groups at the alkyl bromide were tolerated under the reaction conditions. *ortho*-Substituted benzylzinc reagents were also applicable. Allylic zinc compounds reacted similarly in 42–96% yield. Regioisomeric mixtures of coupling products were obtained with crotyl and prenylzinc chloride. In control experiments it was shown that the benzylic zinc reagent affords bibenzyl first on reaction with AgOTf.

All the available evidence and control experiments speak for two possible mechanisms for the formation of the coupling products (Fig. 90). Since no silver precipitated from all reactions, it can be assumed that the organometallic compound **325** reacts first with the silver(I) salt to form an organosilver species **330A**. These unstable species (see above) probably form the observed dimer of the organometallic compound and a soluble form of silver(0) by reductive elimination. Based on the large excess of organometallic compound it is likely that a silver(0) ate complex **330B** is generated as the active species. This electron-rich intermediate reduces the alkyl halide **324** to an alkyl radical, which couples to the cogenerated organosilver(I)

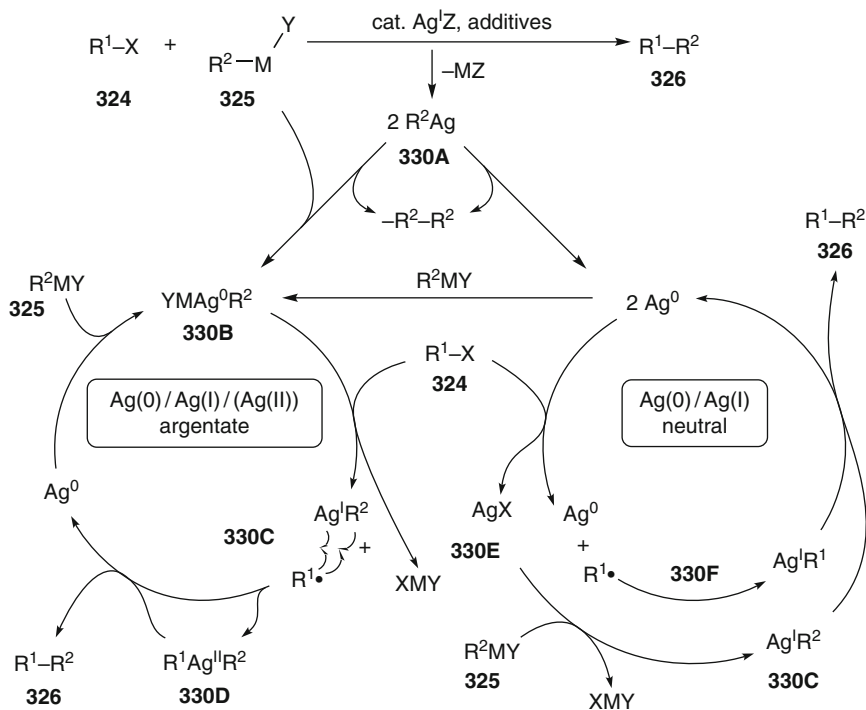
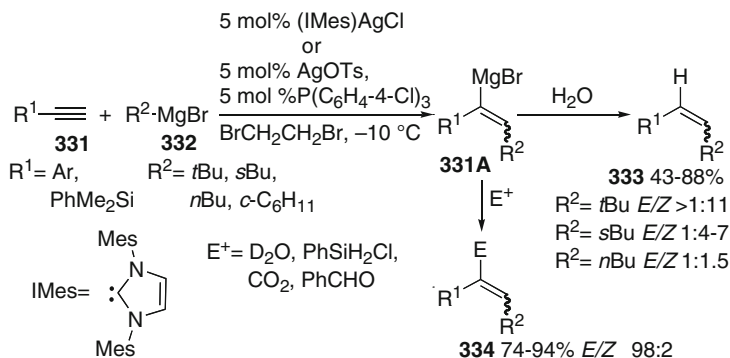


Fig. 90 Possible catalytic cycles of silver-catalyzed cross-coupling reactions



**Fig. 91** Silver(I)-catalyzed carbomagnesation reactions of alkynes

intermediate via **330C**. This can in principle proceed by attack of the radical either to the organic part giving silver(0) and product **326** directly or at the silver atom leading to diorganosilver(II) compound **330D**. This species would be subject to facile reductive elimination providing coupling product **326** and silver(0). The catalytic cycle is closed by regenerating ate complex **330B** with excess **325**. Alternatively, silver(0) itself may act as a SET reducing agent to **324** forming alkyl radicals and silver halide **330E** according to the classical Kochi mechanism. The radical can couple to Ag(0) affording organosilver(I) species **330F**. The coformed silver halide transmetalates **325** to organosilver species **330C**. A group exchange and reductive elimination furnishes product **326** and silver(0). A weak point of the second mechanism compared to the first is that the generation of **330C** and **330E** does not occur at the same species and is also most likely spatially separated.

Kambe and colleagues recently disclosed a silver-catalyzed addition reaction (carbomagnesation) of alkyl Grignard reagents **332** to arylalkynes **331** and enynes (Fig. 91) [432]. (NHC)AgCl or in situ generated Ag(PR<sub>3</sub>)OTs complexes were active and provided 1-aryl-1-alkenes **333** in 43–88% yield after hydrolysis. The bulky *tert*-butyl Grignard reagent provided the product with excellent (*Z*)-selectivity, while other alkyl Grignard reagents afforded (*E/Z*)-mixtures. The application of stoichiometric amounts of 1,2-dibromoethane improved the yields. Although its role as a reoxidant is unclear at present, it may serve to reoxidize Ag(0) formed by unproductive reduction processes. A competition experiment using equimolar amounts of *tert*-butyl-, *sec*-butyl-, and *n*-butylmagnesium chloride gave a ratio of 59:8:<1, which is the typical order for a radical addition process. Apparently, an alkylsilver(I) compound is initially formed, which homolyzes to an alkyl radical. This adds to the alkyne and the resulting vinyl radical couples to the cogenerated silver(0) species. The vinylsilver(I) compound may be transmetalated by the Grignard reagent to a vinylmagnesium halide **331A**. This species can be intercepted by typical electrophiles, such as D<sub>2</sub>O, CO<sub>2</sub>, or aldehydes, giving the corresponding products **334**. However, in light of Whiteside's results (see above) other pathways may also account for product formation.



## 6.2 Ag(I)/Ag(0)-Catalyzed Addition and Cyclization Reactions

Narasaka and coworkers discovered catalytic Booker-Milburn-type cyclopropyloxy radical ring openings catalyzed by 10 mol% of silver nitrate and ammonium peroxydisulfate as the stoichiometric oxidant in the presence of pyridine as a ligand and acid scavenger (Fig. 92) [433]. All components were essential, but only in the presence of silver(I) was the reaction catalyzed. Pyridine accelerated the transformations strongly suggesting its action as a ligand for the catalytically active silver species. The process works as follows. The (pyridine)Ag(I) complex **338** acts as a SET oxidant for a variety of cyclopropanols **335a** generating cyclopropyloxy radicals **335A**, which undergo a fast ring opening to  $\beta$ -keto radicals **335B**. They add to terminal silyl enol ethers **336**. The electron-rich stabilized silyloxyalkyl radicals **335C** are further oxidized to an oxycarbenium ions **335D**, which desilylate to the 1,5-

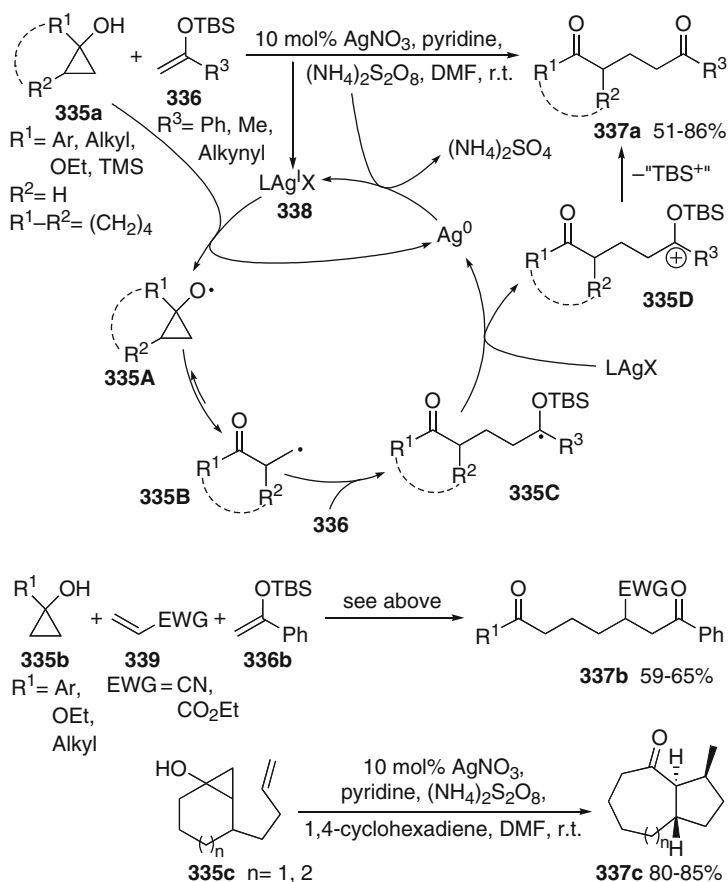


Fig. 92 Oxidative silver(I)-catalyzed cyclopropane ring opening/addition reactions

diketone products **337a**. Reoxidation of coformed Ag(0) occurs by peroxydisulfate. The mechanism is supported by individual experiments, in which the silyl enol ethers **336**, though easily oxidized, proved to be inert towards the present catalytic system in the absence of cyclopropanols **335a**, while **335a** forms homodimers in low yields in the absence of **336**. The method was extended to chemoselective tandem addition reactions controlled by polar effects and the differential ability of the involved radicals to be oxidized. Thus, the reaction of cyclopropanols **335b** with acrylonitrile or ethyl acrylate **339** and acetophenone silyl enol ether **336b** gave the products **337b** in good yields by initial addition of the nucleophilic  $\beta$ -keto radical **335B** to electron-deficient olefins **339**. The resulting electron-poor  $\alpha$ -cyano or  $\alpha$ -ester radicals are not oxidized, but add efficiently to the electron-rich silyl enol ether **336b**. This provides an easily oxidizable radical analogous to **335C**.

The methodology is applicable to cyclopropyloxy radical ring opening/radical cyclization reactions of substrates **337c**. In the presence of cyclohexadiene, the non-oxidizable cyclized primary radical stabilizes by hydrogen abstraction affording bicycles **337c** in good yields. This methodology was applied to the total synthesis of the polycyclic terpene (–)-sordarin [434]. Based on the similarity of the catalytic system to that used in Minisci-type reactions (see Sect. 6.3), it cannot be excluded completely that the reactions occur by an Ag(II)–Ag(I) catalytic cycle using peroxydisulfate as the stoichiometric oxidant.

### 6.3 Ag(II)–Ag(I) Catalysis: Minisci Reactions

Minisci's group developed homolytic substitution reactions of electron-poor arenes or hetarenes providing alkylarenes and -hetarenes extensively (see also Part 2, Sect. 2.5). The state of the art was reviewed thoroughly, so that the methodology is illustrated only by selected examples [435, 436, 437]. A protocol using silver nitrate as the catalyst and sodium peroxydisulfate as the stoichiometric oxidant proved to be very useful for the catalytic oxidative generation of radicals [438].

This allows for instance the radical alkylation of benzoquinones **340a** by alkyl oxalates **341** (Fig. 93) [439]. The silver(I) precatalyst is initially oxidized to Ag(II). Monoalkyl oxalates react with them to unstable alkyl silver(II) oxalates (not shown), which are subject to inner-sphere electron transfer returning the Ag(I) catalyst and carboxyl radicals **341A**. Double  $\beta$ -fragmentation of these species via **341B** is very facile and gives rise to alkyl radicals, which add to **340a**. The resulting resonance-stabilized semiquinones **341C** are reoxidized under the reaction conditions to alkylbenzoquinones **342a**. The double decarboxylation works only if stabilized radicals result. In case of a monoethyl oxalate decarboxylation of **341B** does not proceed anymore and radical alkoxy-carbonylation of **340a** providing benzoquinonecarboxylates prevails (not shown).

Similar alkylations of quinones are also possible with aliphatic carboxylic acids (Fig. 94). 2-Bromonaphthoquinone **340b** was alkylated by a decarboxylation of **343a** catalyzed by  $\text{AgNO}_3/(\text{NH}_4)_2\text{S}_2\text{O}_8$  [440]. The resulting alkylation product

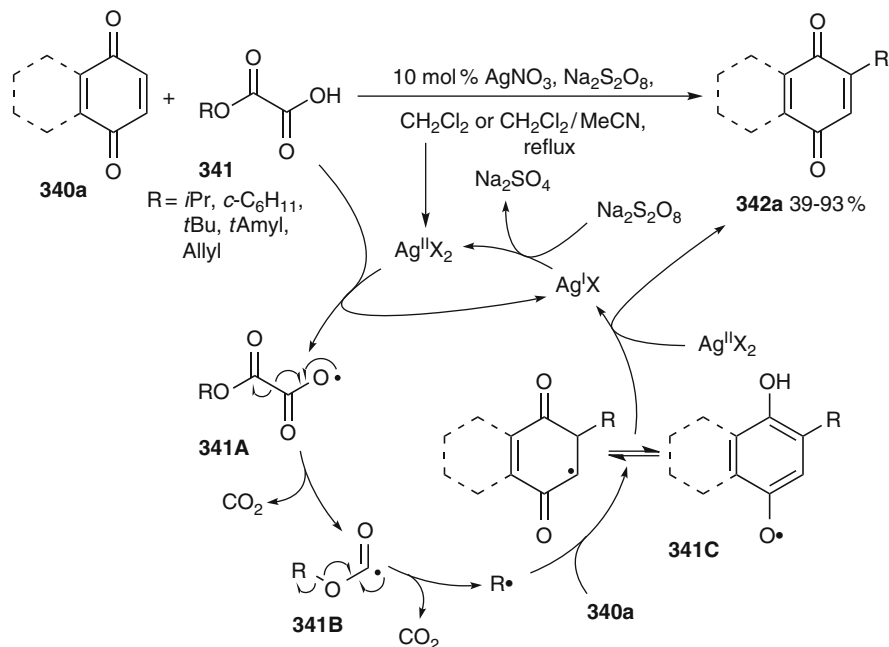


Fig. 93 Silver(II)-catalyzed radical alkylation of benzoquinones by oxalates

**342b** was subsequently applied in a total synthesis of the core structure of marmycin A. When 3-(3-indolyl)propionic acids **343b** were used instead and 30 mol% of silver acetate was applied as the catalyst in the presence of excess  $(NH_4)_2S_2O_8$  a radical addition/cyclization/aromatization sequence proceeded [441]. Naphtho[2,3-a]carbazole-5,13-diones **344** were isolated in 52–72% yield. When non-brominated naphthoquinones were used, the yields were typically lower in the range of 14–65% due to the formation of regioisomeric addition products. Attempted intramolecular Minisci reactions of *N*-alkyl- or *N*-acyl-3-aminopyridines failed due to competing  $\beta$ -fragmentation and 1,5-hydrogen transfer reactions [442].

The silver-catalyzed oxidative decarboxylation methodology can be applied to the synthesis of isocyanates **346** from primary *N*-alkyl oxalic monoamides **345a** (Fig. 95) [443]. From secondary oxalic amides, such as proline-derived **345b**, aminocarbonyl radicals were generated by the catalytic system  $AgNO_3/(NH_4)_2S_2O_8$ , which added to benzoquinone providing benzoquinonecarboxamide **347** in 62% yield [444]. The oxidative decarboxylation method is also suitable for the generation of  $\alpha$ -aminoalkyl radicals from amino acids [445]. The intermediacy of radicals was supported by occurrence of a cyclopropylcarbinyl radical ring opening under the conditions (cf. Part 1, Fig. 8). Silver(II) picolinate reacts in contrast apparently by a concerted pathway without involvement of radicals, since cyclopropanecarbaldehydes were isolated as the exclusive products. The  $AgNO_3/(NH_4)_2S_2O_8$ -catalytic

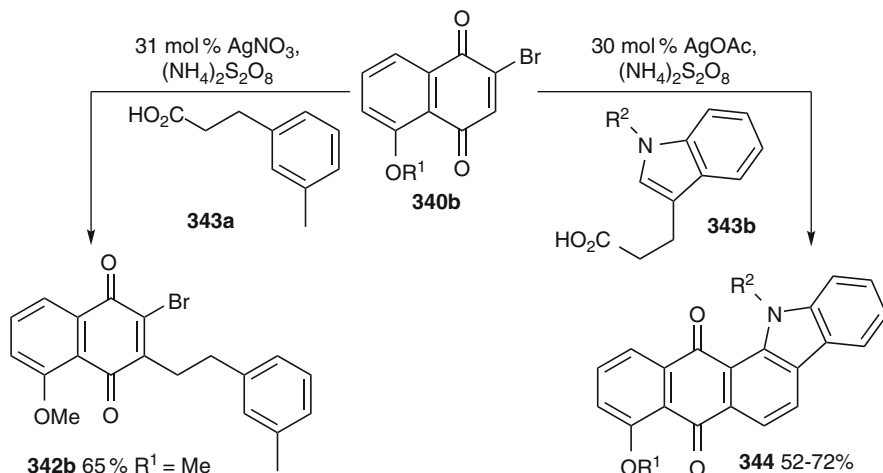


Fig. 94 Silver-catalyzed Minisci alkylation reactions of naphthoquinones

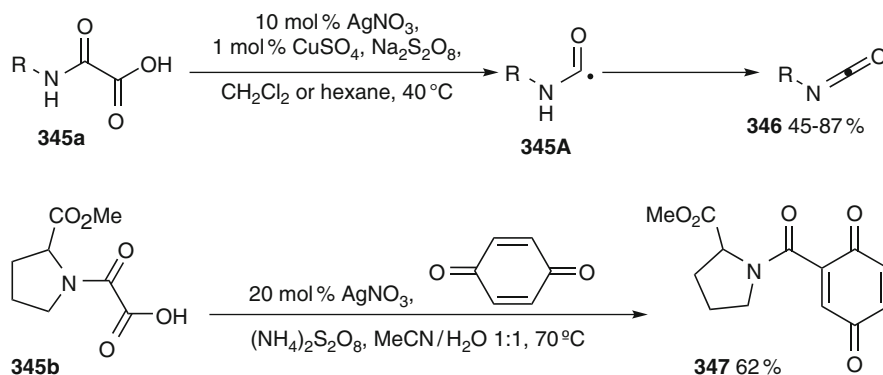
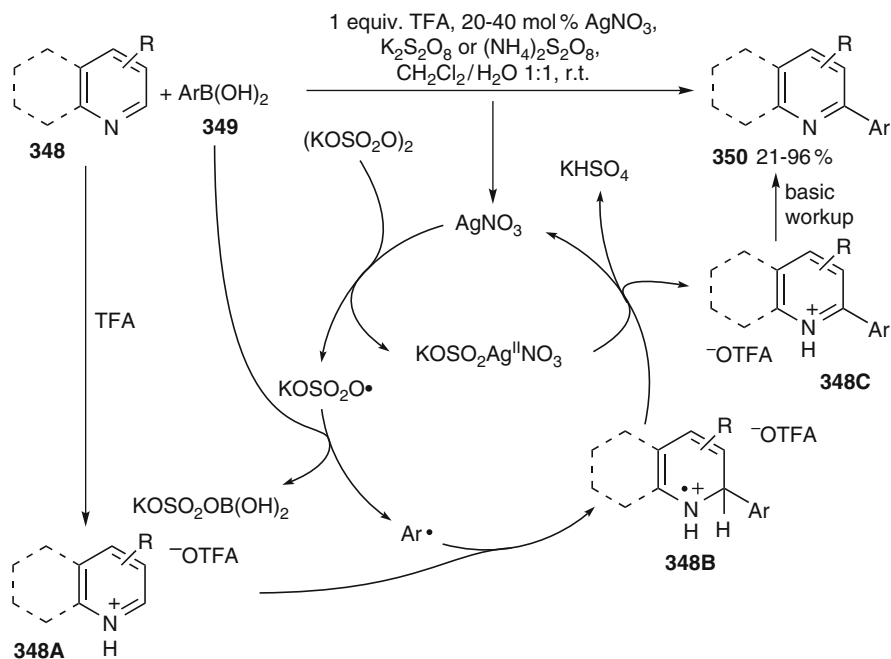


Fig. 95 Oxalic amides in silver-catalyzed Minisci reactions

system can also be used for the decarboxylative aromatization of cyclic amino acids [446] or the formation of imides from *N*-acyl amino acids [447].

Recently Baran and colleagues found that arylboronic acids **349** are suitable precursors to extend the scope of Minisci reactions to arylations (Fig. 96) [448]. Pyridinium salts and related six-membered electron-deficient nitrogen heterocycles **348** gave 2-arylpyridines **350** and related compounds in 21–96% yield using 20–40 mol% of AgNO<sub>3</sub> and K<sub>2</sub>S<sub>2</sub>O<sub>8</sub> as the stoichiometric oxidant. In contrast to benzoic acids, which are inert, arylboronic acids **349** generate aryl radicals under these conditions. The persulfate apparently plays a twofold role in this process. On one hand it serves to oxidize silver(I) to silver (II). On the other, the cogenerated sulfate radical anions may react with boronic acids **349** triggering the release of aryl radicals. They add to electron-deficient protonated heterocycles **348A** leading to radical

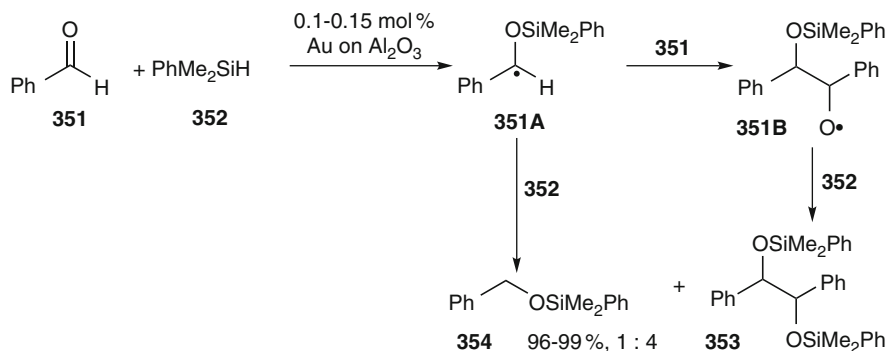


**Fig. 96** Minisci-type arylation reactions catalyzed by silver salts

cations **348B**. These species are subject to oxidative rearomatization by the coformed silver(II) compound, thus regenerating the  $\text{Ag}(\text{I})$  catalyst and forming the protonated products **348C**, from which compounds **350** are liberated during workup.

## 7 Gold-Catalyzed Radical Reactions

The potential of gold complexes in catalytic processes involving radical intermediates is not well developed. Chechik and colleagues demonstrated by a combined EPR and product study using spin traps that gold nanoparticles are highly active in triggering oxidation, hydrogen, and halogen abstraction reactions [449, 450]. It was subsequently found that the hydrosilylation of benzaldehyde **351** with trialkylsilanes, such as  $\text{PhMe}_2\text{SiH}$  **352**, catalyzed by 0.1–0.15 mol% of gold nanoparticles deposited on an  $\text{Al}_2\text{O}_3$  support gave the corresponding pinacol coupling products **353** as the major products as a 1:1 *meso/d,l*-diastereomeric mixture instead of the expected hydrosilylation product **354** (Fig. 97) [451]. The reactions were proposed to proceed by initial SET oxidation of the gold catalyst by the silane to a gold(I) hydride and a silyl radical. This adds to the carbonyl group of benzaldehyde forming radical **351A**. This couples with further **351**. Thus formed



**Fig. 97** Gold(0)-catalyzed pinacol coupling reactions

alkoxy radical **351B** reacts with the silane to furnish the final product **353**. Reductive elimination of dihydrogen regenerates the gold catalyst.

Product **244b** was formed in 56% yield on addition of tetrahydrofuran **243** to phenylacetylene **242b** in the presence of 10 mol% of  $(\text{Ph}_3\text{P})\text{AuCl}$  in the presence of *tert*-butyl hydroperoxide (cf. Fig. 64) [337]. An oxidative cyclization/C–C triple bond cleavage sequence of pent-2-en-4-ynols giving butenolides under aerobic conditions catalyzed by  $\text{Au}(\text{PPh}_3)\text{Cl}$  and cocatalyzed by  $\text{AgOTf}$  was reported by Liu et al. [452]. The reactions were reported to be inhibited by BHT and TEMPO, but further mechanistic evidence concerning the involvement of radical intermediates was not provided.

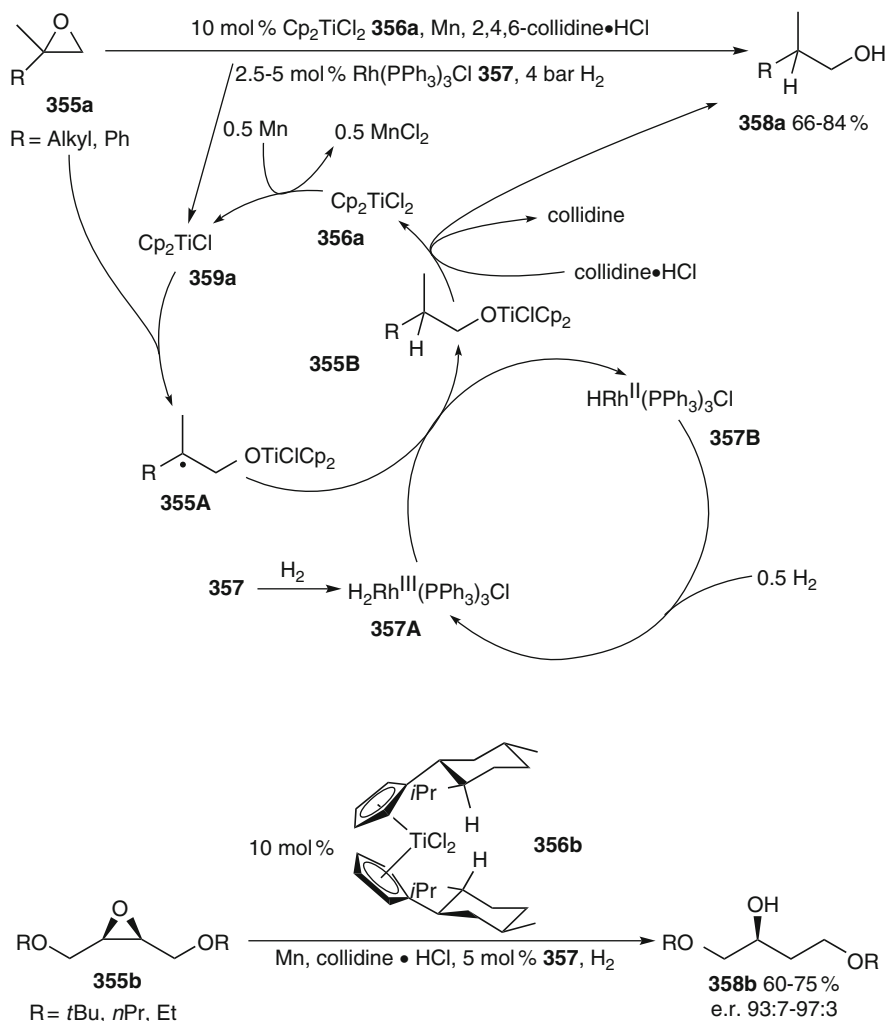
## 8 Bimetallic Catalysis

The use of more than one metal catalyst to mediate organic transformations offers a very interesting potential. Differential catalytic properties of metal complexes can be synergistically coupled to induce processes that are otherwise difficult to catalyze with high regio-, chemo-, and stereoselectivity. This is an emerging field. Its potential has so far not been widely explored in reactions involving radical intermediates.

### 8.1 *Ti(III)–Rh(I) Catalysis*

Gansäuer and coworkers discovered that dihydrogen after activation by rhodium catalysts can be used in hydrogen transfer reactions to radicals [453]. They demonstrated that reductive ring opening of epoxides **355a** cocatalyzed by titanocene dichloride **356a** (see Part 1, Sect. 3.3) and the Wilkinson complex **357** afforded branched primary alcohols **358a** in good yields in the presence of manganese and collidine hydrochloride (Fig. 98). The titanium catalyst **359a** generated in situ from **356a** performs the formation of alkyl radicals **355A** by SET reduction and

ring opening. The titanium-complexed radical **355A** is subsequently reduced by the active rhodium dihydride complex **357A** generated in situ from **357** under an atmosphere of 4 bar dihydrogen. The method capitalizes on the low bond dissociation energy of rhodium(III)-hydride bonds of ca. 58 kcal mol<sup>-1</sup>. Therefore, hydrogen transfer rate constants from **357A** can approach 10<sup>9</sup> M<sup>-1</sup> s<sup>-1</sup>. The coformed rhodium(II) complex **357B** regenerates the active catalyst by reaction with dihydrogen. The use of chiral titanocene catalyst **356b** (see Part 1, Sect. 3.3.2) allows the reductive desymmetrization of *meso*-epoxides with excellent



**Fig. 98** Ti(III)-Rh(I)-catalyzed reductive ring opening reactions of epoxides (for simplicity Cp<sub>2</sub>TiCl<sub>2</sub> **359a** is depicted as a monomer)

enantiomeric ratios. A key to success is that the titanocene complexes are stable to the hydrogenation conditions in both oxidation states, while the hydrogenation system tolerates the reductive titanocene regeneration system. The study was extended to  $\text{Cp}(\text{CO})_3\text{CrH}$  and Vaska's complex  $(\text{Ph}_3\text{P})_3\text{Ir}(\text{CO})\text{Cl}$ , but **357** proved to be optimal for the hydrogen transfer reaction [454].

## 8.2 Cr(II)–Co(II) Catalysis

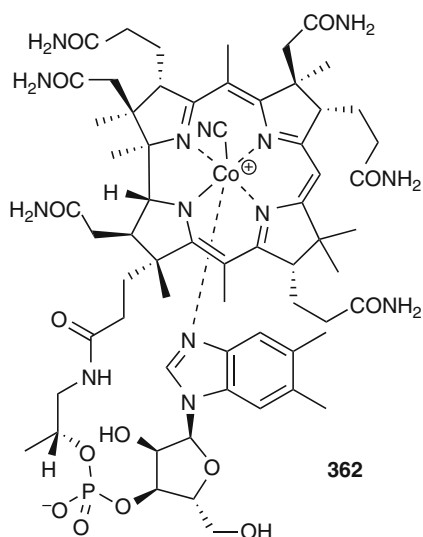
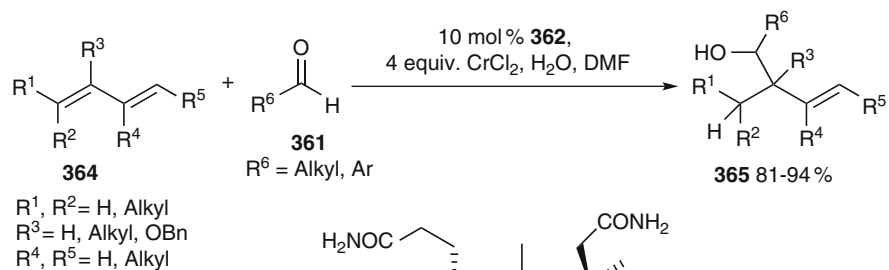
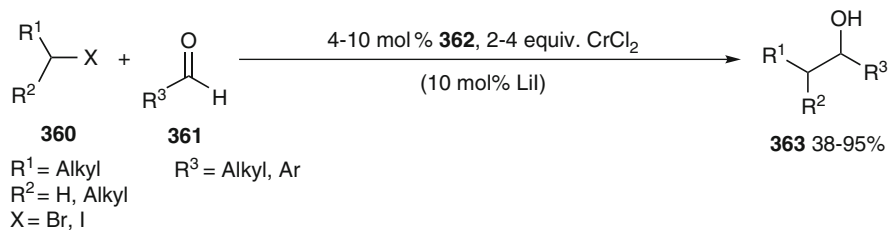
The Takai–Utimoto reaction of alkyl halides **360** with aldehydes **361** is a convenient method for the synthesis of branched alcohols **363** with high functional group tolerance [455]. Vitamin B<sub>12</sub> **362** or cobalt phthalocyanine served as the catalyst and  $\text{CrCl}_2$  as the stoichiometric reducing agent (Fig. 99). The reactions proceeded well with aromatic and aliphatic aldehydes.

The reactivity of secondary alkyl halides in this reaction was also investigated using **362** as the catalyst [456, 457]. This method worked only for aromatic aldehydes and gave branched benzylic alcohols in 39–95% yield. Depending on the electronic and steric factors of the coupling partners Wurtz and pinacol coupling competed. Takai reported a related vitamin B<sub>12</sub>-catalyzed chromium-mediated variant using 1,3-dienes **364** as precursors [458]. In the presence of  $\text{CrCl}_2$  and water, homoallylic alcohols **365** were isolated in 81–94% yield. Moderate to excellent diastereoselectivity was found. Electron-rich alkoxydienes can also be used in the process.

Wessjohann and Schrekker recently developed a methodology on this basis, which is catalytic in chromium as well as in cobalt (Fig. 100). Manganese in combination with TBSCl was the optimal terminal stoichiometric reductant in addition reactions of alkyl bromides **360** to aldehydes **361** giving secondary alcohols **363** in 28–59% yield [459]. The reaction proceeds by initial reduction of cyanocobalamin **362** to the corresponding Co(I) complex **362A**, which substitutes the bromide in **360** leading to alkylcobalt(III) complex **360A**. This intermediate is labile and generates alkyl radicals **360B** easily (see Part 2, Sect. 5.3.1).  $\text{CrCl}_2$  reduces these species to organochromium(III) compounds **360C**, which are subject to nucleophilic addition to aldehydes **361**. The resulting organochromium(III) alkoxides **360D** are transmetalated by TBSCl providing silyl ethers **360E**. They were deprotected to alcohols **363** by TFA.

Usanov and Yamamoto recently found that catalytic amounts of  $\text{Co}(\text{TPP})$  **367** led to a dramatic rate acceleration of Nozaki–Kishi–Hiyama reactions catalyzed by chromium complex **368** (Fig. 101) [460]. The authors attributed the rate enhancement to initial reduction of **367** to a Co(I) complex. The latter is able to undergo an  $\text{S}_{\text{N}}2'$  substitution at propargyl bromide **366** giving an allenylCo(III) species. It was proposed that its homolysis leads to allenyl radical **366A**, which couples to Cr(II) complex **368**. The resulting allenyl Cr(III) complex adds in an  $\text{S}_{\text{N}}2'$  process





**Fig. 99** Original cobalt-catalyzed chromium-mediated Takai–Utimoto reactions

to the aldehyde **361**. The face selection for aromatic aldehydes was good as homopropargylic alcohols **369** were isolated in 40–91% yield and 75–93% ee. Aliphatic aldehydes reacted only in low yields and ees. The cocatalytic system was regenerated by reduction with manganese. However, it seems implausible that a high energy species like **366A** should participate in the reaction course. Aryl or vinylcobalt complexes are usually quite stable. Under the reducing conditions several two-electron transmetalation pathways allowing the generation of an allenylchromium(III) seem to be more favorable than the formation of a destabilized  $\sigma$ -radical.



### 8.3 Mn(II)–Co(II) Catalysis

The  $\text{Mn}(\text{OAc})_2$ – $\text{Co}(\text{OAc})_2$  catalyst system was developed very successfully for oxygenations of hydrocarbons with oxygen using *N*-hydroxyphthalimide as the catalyst [461]. A 1:1  $\text{Mn}(\text{NO}_3)_2$ – $\text{Co}(\text{NO}_3)_2$  couple (2 mol%) was used to catalyze the oxidative fragmentation of aryl ketones **370** to benzoic acids **371** with oxygen. The reaction proceeded for a wide variety of aromatic ketones **370** in 81–98% yield (Fig. 102) [462].  $\text{Co}(\text{NO}_3)_2$  can also be replaced by  $\text{Cu}(\text{NO}_3)_2$  giving almost identical results. The reaction is initiated by catalytic oxidative generation of Mn(III) from the Mn(II) precatalyst. Mn(III) is very well known to oxidize the enol form of ketones to the corresponding  $\alpha$ -carbonyl radicals **370A** [263–267]. This is trapped by oxygen. The resulting peroxy radical **370B** serves to reoxidize Mn(II) to Mn(III). After hydrolysis of manganese peroxide **370C** the  $\alpha$ -hydroperoxy ketone **370D** is cleaved to alkoxy radical **370E** in a Fenton-type reduction catalyzed by Co(II). This fragments to an aroyl radical **370F** and an aldehyde or ketone **370G**. The former is oxidized by coformed Co(III) to an acylium cation **370H**, which is trapped by water to the products **371** and Co(II). This represents a well-defined catalyst system, in which manganese takes the part of the oxidant, while cobalt(II) or copper(I) catalyzes the Fenton-type chemistry triggering the cleavage.

Ishii and colleagues studied radical addition reactions of carbonyl compounds to olefins catalyzed by a Mn–Co catalytic system. Ketones **372a** ( $\text{R}^1 = \text{Alkyl}$ ) added

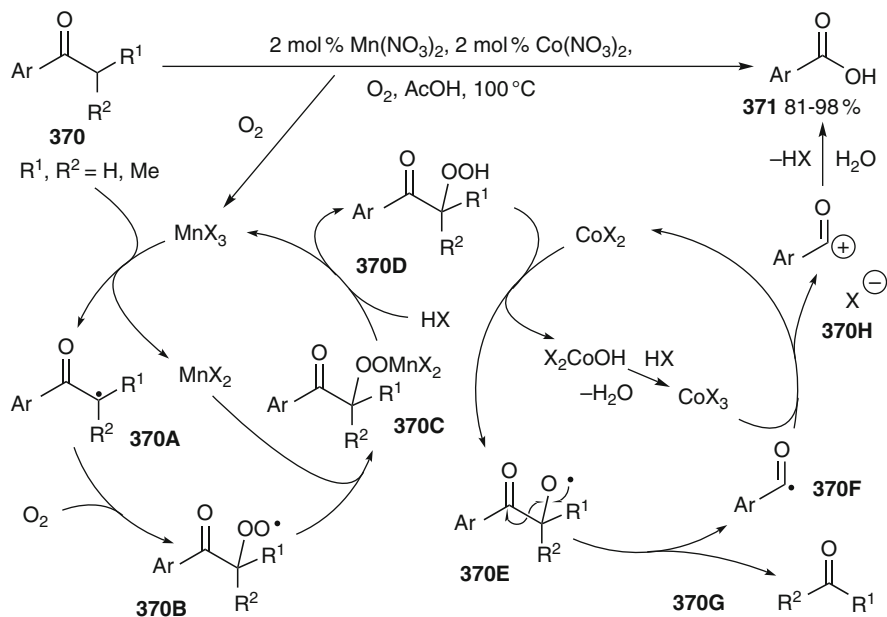
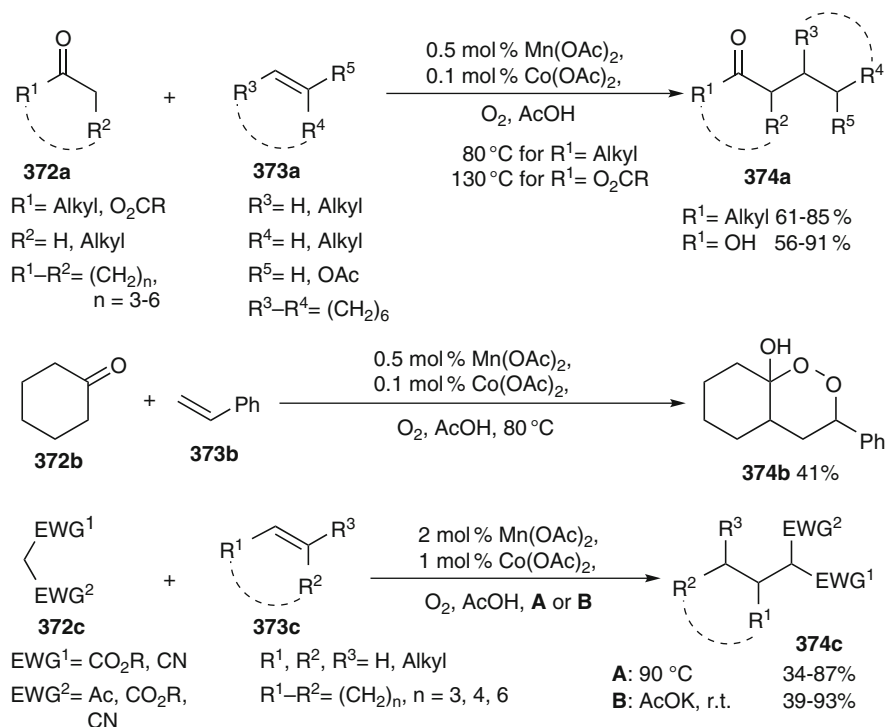


Fig. 102 Mn(II)–Co(II)-catalyzed oxidative cleavage of ketones to benzoic acids



**Fig. 103** Radical addition reactions catalyzed by Mn(II)-Co(II) in the presence of oxygen

to olefins **373a** in the presence of a catalyst system composed of 0.5 mol% Mn(OAc)<sub>2</sub> and 0.1 mol% Co(OAc)<sub>2</sub> in the presence of oxygen as stoichiometric reoxidant (Fig. 103) [463].  $\alpha$ -Alkylated ketones **374a** were obtained with 61–85% selectivity. The reaction was much slower and less selective when the cobalt catalyst was omitted, while it did not proceed at all in the absence of Mn(OAc)<sub>2</sub>. With styrene **373b** as the reagent, oxygenation of the benzylic radical prevailed and endoperoxide **374b** was isolated in 41% yield. Acetic or propionic anhydride **372a** (R<sup>1</sup>=O<sub>2</sub>CR) was also applied [464]. A higher temperature was required to provide carboxylic acids in 56–91% yield. The addition to cyclic internal alkenes proceeded in good yields. A double addition to 1,9-decadiene occurred in 60% yield. With 1,5-cyclooctadiene a tandem radical addition/transannular 5-exo cyclization was observed (cf. Part 1, Fig. 52 **131**→**188**).

A number of  $\beta$ -dicarbonyl compounds **372c** added to alkenes **373c** or alkynes using the Mn(OAc)<sub>2</sub>-Co(OAc)<sub>2</sub>-O<sub>2</sub> catalytic system in 34–87% yield [465]. The transformations require, however, a large excess of **372c** to achieve good yields of addition products **374c**. Moreover, some double addition of olefins **373c** was impossible to avoid. The same catalytic system was much more efficient in the presence of bases such as potassium acetate or triethylamine. The radical additions of ethyl cyanoacetate or malononitrile to alkenes proceeded under these conditions

even at room temperature in yields of 39–93% [466]. No reaction occurred when one of the metal catalysts was omitted from the reaction system and when the oxygen concentration was significantly modified. The effect of the base can probably be traced to the more efficient formation of a manganese enolate, thus facilitating radical generation. With 1,5-cyclooctadiene a tandem radical addition/transannular 5-exo cyclization proceeded in 70% yield (cf. Part 1, Fig. 52 **131**→**188**).

The manganese(II)–cobalt(II)-catalyzed radical addition reactions proceed most likely by an initial facile reaction of the cobalt(II) salt with oxygen giving cobalt(III)-peroxyl species **375** in equilibrium (Fig. 104; see also Part 2, Sects. 5.9 and 5.10). This intermediate is apparently well suited to promote the SET oxidation of manganese(II) acetate to manganese(III) acetate. Manganese(II) is also oxidized to manganese(III) in the absence of the cobalt cocatalyst, but the reactions take much longer. It is known from a multitude of investigations that  $\alpha$ -carbonyl radicals **372A** are reliably generated from **372** by oxidation with  $\text{Mn}(\text{OAc})_3$  [263–267]. Addition of electrophilic radicals **372A** to olefins **373** give alkyl radicals **372B** (see also Part 1, Sect. 9.3.2). The authors suggested that **372B** stabilize to products **374a,c** by hydrogen abstraction from the substrate **372**. According to this proposal the additions would proceed as a free-radical chain reaction, in which the metal catalysts serve just as initiators. Hydrogen abstraction may, however, also occur from the solvent, which is present in much higher concentration. In this case a non-chain reaction with active participation of the catalyst throughout the reaction would operate, since constant metal-catalyzed generation of **372A** would be required. Active participation of the catalyst also seems to be more likely in the reaction of **372b** with **373b**, where the final peroxyl is easily reduced by  $\text{Mn}(\text{II})$  (see above and Part 1, Sect. 9.3.2). The cobalt catalyst is actually not required in this

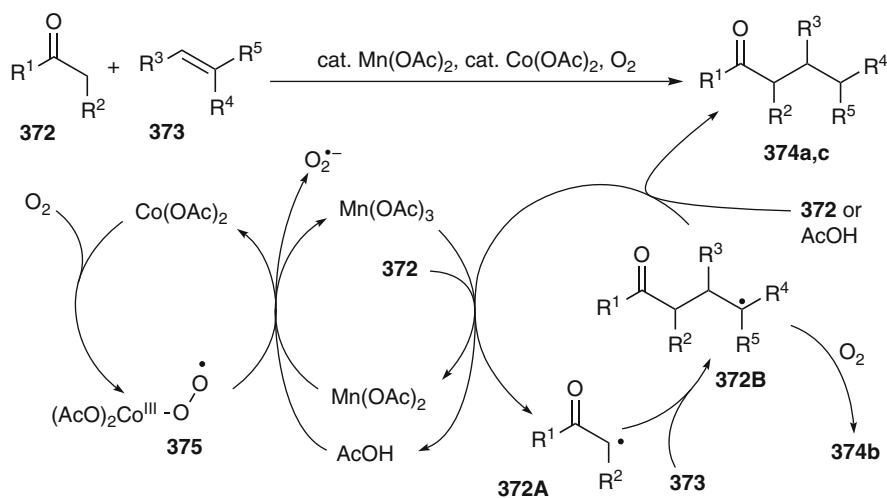
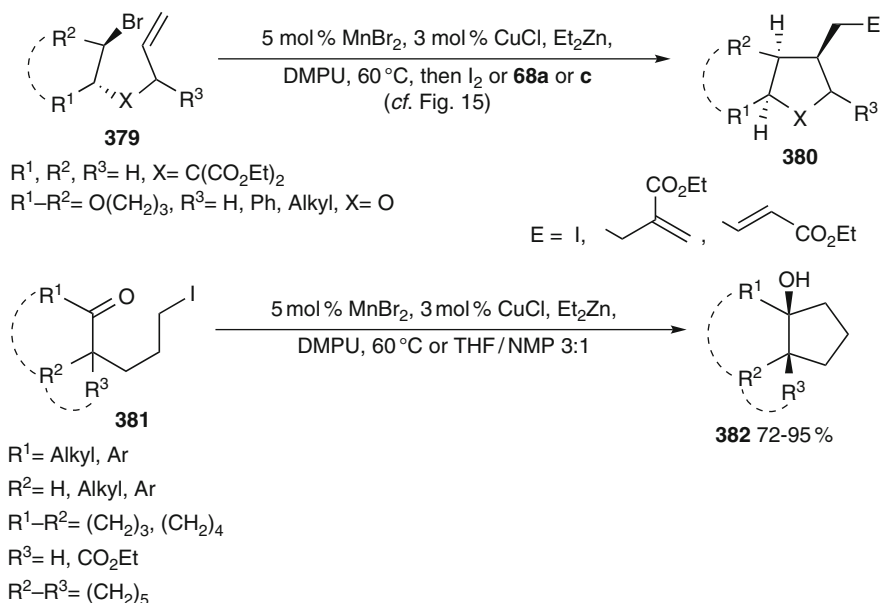


Fig. 104 Catalytic cycle of Mn(II)–Co(II)-catalyzed radical additions





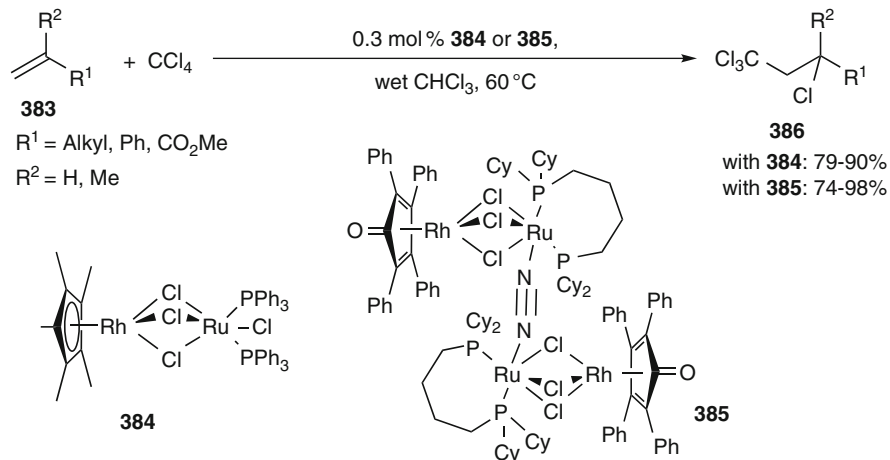
**Fig. 106** Radical-polar cyclization/addition reactions catalyzed by a Mn(II)–Cu(I) catalyst system

organozinc compound by reaction with  $\text{Et}_2\text{Zn}$ . Subsequent transmetalation with the copper catalyst enables allylic substitution or conjugate addition reactions with **68a,c** providing side chain functionalized cycles **380**. In contrast to the corresponding nickel-catalyzed cyclizations, no stoichiometric copper(I) is necessary here.

5-Bromo aldehydes or ketones **381** reacted by cyclization similarly to the carbonyl function to give substituted cyclopentanols **382** [112, 468]. This reaction shows a good functional group tolerance and is especially well suited for the synthesis of cyclopentanols derived from  $\beta$ -keto esters in 72–95% yield with diastereoselectivities of  $>95:5$ . It can also be applied in good yield to annulation and spirocyclization reactions. This method is complementary to samarium diiodide-mediated reactions, but has the advantage of being catalytic and providing the products with better diastereoselectivity.

## 8.5 Ru(II)–Rh(III) Catalysis

Recently, Severin et al. studied Kharasch additions of tetrachloromethane to electronically different olefins **383** using several mixed rhodium(I)–ruthenium(II) and rhodium(III)–ruthenium(II) catalysts (Fig. 107). Best results were achieved with catalysts **384** and **385**, which gave the addition products **386** in 74–98% yield [470]. With catalyst **385** TOF of  $1,200 \text{ h}^{-1}$  and TON of 4,500 were achieved for the



**Fig. 107** Kharasch additions catalyzed by bimetallic Ru(II)–Rh(III) or Ru(II)–Rh(I) complexes

addition of  $\text{CCl}_4$  to styrene. Both parts of the catalysts are essential for the activity, since other bimetallic catalysts using a constant ruthenium fragment are considerably less active. The mode of action is, however, not exactly known. For **385**, dissociation of the labile nitrogen ligand is likely, which generates the necessary coordinative unsaturation for chlorine abstraction from the organic halide.

## 9 Concluding Remarks

Since the middle of the last century the combination of radical intermediates with transition metal catalysis has developed from a laboratory curiosity to a useful methodology. Radicals can be generated oxidatively or reductively by SET from transition metal complexes. This offers an attractive alternative to oxidative addition or transmetalation pathways to activate for a number of C–C and C–heteroatom bond formation reactions. Once generated, radical intermediates can be freely diffusing reacting like in classical free radical coupling, addition, or cyclization reactions. On the other hand, the radical may remain caged with the metal complex. The degree of freedom of the radical intermediate is dependent on the stability of the radical and especially on the electronic structure of the coformed transition metal fragment. Often, the latter is an odd-electron species, which is in fact a metal-centered radical. The lifetime of this metal complex exceeds that of the transient radical species often considerably, so that the persistent radical effect operates and coupling of the radical with the metal species prevails, provided that the complex is coordinatively unsaturated and a stable metal complex results. Thus formed organotransition metal complexes are applicable in further reaction steps that are typical in established two-electron chemistry. The properties of the ligand in



combination with accessible oxidation states of the metal center are also decisive. This is especially true if the coformed oxidized or reduced transition metal center is less reactive toward the radical or coordinatively saturated. Ligand transfer is dominant with halide and related ligands and when only single but not net two-electron transfer is energetically viable at the metal center. Addition of radicals to ligands and radical follow-up chemistry in the coordination sphere is an emerging field that holds much promise, but has not been exploited extensively. Bimetallic radical catalysis is another field that opens many unexplored opportunities.

What challenges lie ahead? The mechanistic understanding of synthetic transition metal catalysis involving radicals is currently not well developed. All new processes, where radical intermediates are possible, should be tested for their involvement. The intermediacy of radicals can often be derived from simple indirect evidence such as radical and stereochemical probes. The sensitivity of these probes should be improved, however, to allow conclusions about the kinetic window, in which the radical may exist. It is important to mention that a single test often does not provide unambiguous evidence. Therefore, several probes that target radical intermediates are useful. Applicable tests are mentioned throughout the review and guidelines of how to detect radical intermediates are derived.

Transition metal-catalyzed radical based processes often occur under mild conditions and are quite fast. The fine-tuning of the electronic properties of the metal complex catalysts to maximize the facility of radical generation and to modulate the lifetime of the radicals for follow-up reactions is still in its infancy and has not been studied systematically. This is, however, important to allow the design of radical processes at the slower end of the reactivity scale, as the current methodology is mostly limited to very fast radical processes in the framework of transition metal catalysis. The kinetics of almost all processes described in this review is not known. Only detailed investigations in this field will allow the rational *design* of radical-based transition metal-catalyzed processes.

To summarize, radicals are very beneficial in transition metal catalysis if their reactivity is coupled intelligently to the properties of the metal catalysts. The methodic arsenal of organic chemistry as well as the understanding of organometallic chemistry will profit strongly from this interplay and a multitude of new useful applications will certainly result.

## 10 Transition Metal-Catalyzed Radical Reactions According to Reaction Type

A table providing an overview of the most common reaction types that were conducted with different metals of different oxidation states can be found in Part 1, Sect. 11. This list summarizes only reaction types that are catalyzed by more than one metal.

**Acknowledgments** This manuscript is dedicated to the memory of Professor Dr. Athelstan L. J. Beckwith, a pioneer of radical chemistry. Generous funding of the work by the Institute of Organic Chemistry and Biochemistry, Academy of Sciences of the Czech Republic (Z4 055 0506), and the Grant Agency of the Czech Republic (203/09/1936) is gratefully acknowledged. I thank my group for critical reading of the manuscript and many helpful comments and discussions. I apologize to all colleagues for the omission of their work that were necessary due to space constraints of the manuscript.

## References

1. Jahn U (2011) Radicals in transition metal catalyzed reactions? Transition metal catalyzed radical reactions? – A fruitful interplay anyway. Part 1. Radical catalysis by Group 4 – Group 7 elements. *Top Curr Chem*. doi:10.1007/128\_2011\_261
2. Jahn U (2011) Radicals in transition metal catalyzed reactions? Transition metal catalyzed radical reactions? – A fruitful interplay anyway. Part 2. Radical catalysis by Group 8 and 9 elements. *Top Curr Chem*. doi:10.1007/128\_2011\_285
3. Tamaru Y (ed) (2005) *Modern organonickel chemistry*. Wiley-VCH, Weinheim, and cited ref
4. Montgomery J, Sormunen GJ (2007) *Top Curr Chem* 279:1
5. Kimura M, Tamaru Y (2007) *Top Curr Chem* 279:173
6. Ng S-S, Ho C-Y, Schleicher KD, Jamison TF (2008) *Pure Appl Chem* 80:929
7. Jeganmohan M, Cheng C-H (2008) *Chem Eur J* 14:10876
8. Anderson TJ, Jones GD, Vivic DA (2004) *J Am Chem Soc* 126:8100
9. Jones GD, McFarland C, Anderson TJ, Vivic DA (2005) *Chem Commun* 4211
10. Miyazaki S, Koga Y, Matsumoto T, Matsubara K (2010) *Chem Commun* 46:1932
11. Lee C-M, Chen C-H, Liao F-X, Hu C-H, Lee G-H (2010) *J Am Chem Soc* 132:9256
12. Kurzion-Zilbermann T, Masarwa A, Maimon E, Cohen H, Meyerstein D (2007) *Dalton Trans* 3959 and cited ref.
13. Hegedus LS, Miller LL (1975) *J Am Chem Soc* 97:459
14. Hegedus LS, Thompson DHP (1985) *J Am Chem Soc* 107:5663
15. Corey EJ, Semmelhack MF (1967) *J Am Chem Soc* 89:2755
16. Kuang C, Yang Q, Senboku H, Tokuda M (2005) *Chem Lett* 34:528
17. Castano AM, Echavarren AM (1994) *Organometallics* 13:2262
18. Knochel P (1995) *Synlett* 393
19. Dunach E, Franco D, Olivero S (2003) *Eur J Org Chem* 1605
20. Dunach E, Medeiros MJ, Olivero S (2006) *New J Chem* 30:1534
21. Amatore C, Jutand A, Perichon J, Rollin Y (2000) *Monatsh Chem* 131:1293
22. Klein A, Budnikova YH, Sinyashin OG (2007) *J Organomet Chem* 692:3156
23. Kochi JK (1978) *Organometallic mechanisms and catalysis*. Academic, New York
24. Kochi JK (1980) *Pure Appl Chem* 52:571
25. Machrouhi F, Hamann B, Namy J-L, Kagan HB (1996) *Synlett* 633
26. Procter DJ, Flowers RA II, Skrydstrup T (2009) *Organic synthesis using samarium diiodide*. RSC, Cambridge
27. Machrouhi F, Namy J-L (1999) *Tetrahedron Lett* 40:1315
28. Phapale VB, Guisan-Ceinos M, Bunuel E, Cardenas DJ (2009) *Chem Eur J* 15:12681
29. Frisch AC, Beller M (2005) *Angew Chem Int Ed* 44:674
30. Rudolph A, Lautens M (2009) *Angew Chem Int Ed* 48:2656
31. Luh T-Y, Leung M-K, Wong K-T (2000) *Chem Rev* 100:3187
32. Netherton MR, Fu GC (2004) *Adv Synth Catal* 346:1525
33. Phapale VB, Cardenas DJ (2009) *Chem Soc Rev* 38:1598
34. Terao J, Watanabe H, Ikumi A, Kuniyasu H, Kambe N (2002) *J Am Chem Soc* 124:4222

35. Terao J, Ikumi A, Kuniyasu H, Kambe N (2003) *J Am Chem Soc* 125:5646
36. Terao J, Naitoh Y, Kuniyasu H, Kambe N (2007) *Chem Commun* 825
37. Terao J, Kambe N (2008) *Acc Chem Res* 41:1545
38. Park K, Yuan K, Scott WJ (1993) *J Org Chem* 58:4866
39. Giovannini R, Stüdemann T, Dussin G, Knochel P (1998) *Angew Chem Int Ed Engl* 37:2387
40. Giovannini R, Stüdemann T, Devasagayaraj A, Dussin G, Knochel P (1999) *J Org Chem* 64:3544
41. Giovannini R, Knochel P (1998) *J Am Chem Soc* 120:11186
42. Jensen AE, Knochel P (2002) *J Org Chem* 67:79
43. Devasagayaraj A, Stüdemann T, Knochel P (1995) *Angew Chem Int Ed Engl* 34:2723
44. Zhou J, Fu GC (2003) *J Am Chem Soc* 125:14726
45. Fischer C, Fu GC (2005) *J Am Chem Soc* 127:4594
46. Arp FO, Fu GC (2005) *J Am Chem Soc* 127:10482
47. Jones GD, Martin JL, McFarland C, Allen OR, Hall RE, Haley AD, Brandon RJ, Konovalova T, Desrochers PJ, Pulay P, Vivic DA (2006) *J Am Chem Soc* 128:13175
48. Phapale VB, Bunuel E, Garcia-Iglesias M, Cardenas DJ (2007) *Angew Chem Int Ed* 46:8790
49. Gong H, Sinisi R, Gagne MR (2007) *J Am Chem Soc* 129:1908
50. Gong H, Gagne MR (2008) *J Am Chem Soc* 130:12177
51. Son S, Fu GC (2008) *J Am Chem Soc* 130:2756
52. Smith SW, Fu GC (2008) *Angew Chem Int Ed* 47:9334
53. Smith SW, Fu GC (2008) *J Am Chem Soc* 130:12645
54. Lundin PM, Esquivias J, Fu GC (2009) *Angew Chem Int Ed* 48:154
55. Zhou J, Fu GC (2004) *J Am Chem Soc* 126:1340
56. Gonzalez-Bobes F, Fu GC (2006) *J Am Chem Soc* 128:5360
57. Liu C, He C, Shi W, Chen M, Lei A (2007) *Org Lett* 9:5601
58. Saito B, Fu GC (2007) *J Am Chem Soc* 129:9602
59. Saito B, Fu GC (2008) *J Am Chem Soc* 130:6694
60. Lu Z, Fu GC (2010) *Angew Chem Int Ed* 49:6676
61. Owston NA, Fu GC (2010) *J Am Chem Soc* 132:11908
62. Lundin PM, Fu GC (2010) *J Am Chem Soc* 132:11027
63. Powell DA, Fu GC (2004) *J Am Chem Soc* 126:7788
64. Strotman NA, Sommer S, Fu GC (2007) *Angew Chem Int Ed* 46:3556
65. Dai X, Strotman NA, Fu GC (2008) *J Am Chem Soc* 130:3302
66. Yuan K, Scott WJ (1991) *Tetrahedron Lett* 32:189
67. Uemura M, Yorimitsu H, Oshima K (2006) *Chem Commun* 4726
68. Csok Z, Vechorkin O, Harkins SB, Scopelliti R, Hu X (2008) *J Am Chem Soc* 130:8156
69. Vechorkin O, Csok Z, Scopelliti R, Hu X (2009) *Chem Eur J* 15:3889
70. Vechorkin O, Hu X (2009) *Angew Chem Int Ed* 48:2937
71. Vechorkin O, Proust V, Hu X (2009) *J Am Chem Soc* 131:9756
72. Lou S, Fu GC (2010) *J Am Chem Soc* 132:1264
73. Vechorkin O, Barmaz D, Proust V, Hu X (2009) *J Am Chem Soc* 131:12078
74. Caeiro J, Sestelo JP, Sarandeses LA (2008) *Chem Eur J* 14:741
75. Powell DA, Maki T, Fu GC (2005) *J Am Chem Soc* 127:510
76. Lou S, Fu GC (2010) *J Am Chem Soc* 132:5010
77. Wunderlich SH, Knochel P (2009) *Angew Chem Int Ed* 48:9717
78. Malpass JR, Handa S, White R (2005) *Org Lett* 7:2759
79. White R, Malpass JR, Handa S, Baker SR, Broad LM, Folly L, Mogg A (2006) *Bioorg Med Chem Lett* 16:5493
80. Armstrong A, Bhonoah Y, Shanahan SE (2007) *J Org Chem* 72:8019
81. Duncton MAJ, Estiarte MA, Tan D, Kaub C, O'Mahony DJR, Johnson RJ, Cox M, Edwards WT, Wan M, Kincaid J, Kelly MG (2008) *Org Lett* 10:3259
82. Glorius F (2008) *Angew Chem Int Ed* 47:8347
83. Adrio J, Carretero JC (2010) *ChemCatChem* 2:1384

84. Breitenfeld J, Vechorkin O, Corminboeuf C, Scopelliti R, Hu X (2010) *Organometallics* 29:3686
85. Echavarren AM (2005) *Angew Chem Int Ed* 44:3962
86. Lin X, Phillips DL (2008) *J Org Chem* 73:3680
87. Yao T, Hirano K, Satoh T, Miura M (2010) *Chem Eur J* 16:12307
88. Vechorkin O, Proust V, Hu X (2010) *Angew Chem Int Ed* 49:3061
89. Lebedev SA, Lopatina VA, Petrov ES, Beletskaya IP (1988) *J Organomet Chem* 344:253
90. Yang Z-Y, Burton DJ (1992) *J Chem Soc Chem Commun* 233
91. Yang Z-Y, Burton DJ (1992) *J Org Chem* 57:5144
92. Huang X-T, Chen Q-Y (2001) *J Org Chem* 66:4651
93. Huang Y-Z, Zhou Q-L (1987) *J Org Chem* 52:3552
94. Zhou Q-L, Huang Y-Z (1988) *J Fluorine Chem* 39:87
95. Zhou Q-L, Huang Y-Z (1989) *J Fluorine Chem* 43:385
96. Mikhaylov DY, Budnikova YH, Gryaznova TV, Krivolapov DV, Litvinov IA, Vivic DA, Sinyashin OG (2009) *J Organomet Chem* 694:3840
97. Sim TB, Choi J, Joung MJ, Yoon NM (1997) *J Org Chem* 62:2357
98. Sim TB, Choi J, Yoon NM (1996) *Tetrahedron Lett* 37:3137
99. Sustmann R, Hopp P, Holl P (1989) *Tetrahedron Lett* 30:689
100. Joung MJ, Ahn JH, Lee DW, Yoon NM (1998) *J Org Chem* 63:2755
101. Gong H, Andrews RS, Zuccarello JL, Lee SJ, Gagne MR (2009) *Org Lett* 11:879
102. Terao J, Kambe N (2006) *Bull Chem Soc Jpn* 79:663
103. Terao J, Nii S, Chowdhury FA, Nakamura A, Kambe N (2004) *Adv Synth Catal* 346:905
104. Terao J, Watabe H, Kambe N (2005) *J Am Chem Soc* 127:3656
105. Terao J, Bando F, Kambe N (2009) *Chem Commun* 7336
106. Vaupel A, Knochel P (1994) *Tetrahedron Lett* 35:8349
107. Vaupel A, Knochel P (1996) *J Org Chem* 61:5743
108. Vaupel A, Knochel P (1995) *Tetrahedron Lett* 36:231
109. Meyer C, Marek I, Courtemanche G, Normant JF (1994) *Tetrahedron* 50:11665
110. Stadtmüller H, Knochel P (1995) *Synlett* 463
111. Stadtmüller H, Vaupel A, Tucker CE, Stüdemann T, Knochel P (1996) *Chem Eur J* 2:1204
112. Stüdemann T, Ibrahim-Quali M, Cahiez G, Knochel P (1998) *Synlett* 143
113. Stüdemann T, Gupta V, Engman L, Knochel P (1997) *Tetrahedron Lett* 38:1005
114. Stüdemann T, Knochel P (1997) *Angew Chem Int Ed Engl* 36:93
115. Durandetti M, Nedelec J-Y, Perichon J (1996) *J Org Chem* 61:1748
116. Durandetti M, Perichon J, Nedelec J-Y (1997) *J Org Chem* 62:7914
117. Cannes C, Condon S, Durandetti M, Perichon J, Nedelec J-Y (2000) *J Org Chem* 65:4575
118. Durandetti M, Perichon J (2004) *Synthesis* 3079
119. Durandetti M, Gosmini C, Perichon J (2007) *Tetrahedron* 63:1146
120. Barhdadi R, Courtinard C, Nedelec JY, Troupel M (2003) *Chem Commun* 1434
121. Everson DA, Shrestha R, Weix DJ (2010) *J Am Chem Soc* 132:920
122. Goldup SM, Leigh DA, McBurney RT, McGonigal PR, Plant A (2010) *Chem Sci* 1:383
123. Healy KP, Pletcher D (1978) *J Organomet Chem* 161:109
124. Gosden C, Pletcher D (1980) *J Organomet Chem* 186:401
125. Ozaki S, Matsushita H, Ohmori H (1993) *J Chem Soc Perkin Trans 1* 649
126. Readman SK, Marsden SP, Hodgson A (2000) *Synlett* 1628
127. Condon S, Dupre D, Lachaise I, Nedelec JY (2002) *Synthesis* 1752
128. Ozaki S, Nakanishi T, Sugiyama M, Miyamoto C, Ohmori M (1991) *Chem Pharm Bull* 39:31
129. Dunach E, Esteves AP, Medeiros MJ, Pletcher D, Olivero S (2004) *J Electroanal Chem* 566:39
130. Olivero S, Perriot R, Dunach E, Baru AR, Bell ED, Mohan RS (2006) *Synlett* 2021
131. Dunach E, Esteves AP, Medeiros MJ, Olivero S (2004) *Tetrahedron Lett* 45:7935
132. Esteves AP, Goken DM, Klein LJ, Leite LFM, Medeiros MJ, Peters DG (2005) *Eur J Org Chem* 4852

133. Esteves AP, Neves CS, Medeiros MJ, Pletcher D (2008) *J Electroanal Chem* 614:131
134. Dunach E, Esteves AP, Medeiros MJ, Olivero S (2005) *New J Chem* 29:633
135. Esteves AP, Ferreira EC, Medeiros MJ (2007) *Tetrahedron* 63:3006
136. Dunach E, Medeiros MJ (2008) *Electrochim Acta* 53:4470
137. Dunach E, Esteves AP, Medeiros MJ, Olivero S (2006) *Green Chem* 8:380
138. Chaminade X, Dunach E, Estevez AP, Medeiros MJ, Neves CS, Olivero S (2009) *Electrochim Acta* 54:5120
139. Katsumata A, Takasu K, Ihara M (1999) *Heterocycles* 51:733
140. Miranda JA, Wade CJ, Little RD (2005) *J Org Chem* 70:8017
141. Ischay MA, Mubarak MS, Peters DG (2006) *J Org Chem* 71:623
142. Mubarak MS, Jennermann TB, Ischay MA, Peters DG (2007) *Eur J Org Chem* 5346
143. Goken DM, Ischay MA, Peters DG, Tomaszewski JW, Karty JA, Reilly JP, Mubarak MS (2006) *J Electrochem Soc* 153:E71
144. Raess PW, Mubarak MS, Ischay MA, Foley MP, Jennermann TB, Raghavachari K, Peters DG (2007) *J Electroanal Chem* 603:124
145. Loots MJ, Schwartz J (1977) *J Am Chem Soc* 99:8045
146. Dayrit FM, Gladkowski DE, Schwartz J (1980) *J Am Chem Soc* 102:3976
147. Dayrit FM, Schwartz J (1981) *J Am Chem Soc* 103:4466
148. Nadal ML, Bosch J, Vila JM, Klein G, Ricart S, Moreto JM (2005) *J Am Chem Soc* 127:10476
149. van de Kuil LA, Grove DM, Gossage RA, Zwikker JW, Jenneskens LW, Drenth W, van Koten G (1997) *Organometallics* 16:4985
150. Gossage RA, van de Kuil LA, van Koten G (1998) *Acc Chem Res* 31:423
151. Knapen JWJ, van der Made AW, de Wilde JC, van Leeuwen PWNM, Wijkens P, Grove DM, van Koten G (1994) *Nature* 372:659
152. Kleij AW, Gossage RA, Jastrzebski JTBH, Boersma J, van Koten G (2000) *Angew Chem Int Ed* 39:176
153. Kleij AW, Gossage RA, Gebbink RJMK, Brinkmann N, Reijerse EJ, Kragl U, Lutz M, Spek AL, van Koten G (2000) *J Am Chem Soc* 122:12112
154. Pandarus V, Zargarian D (2007) *Chem Commun* 978
155. Pandarus V, Zargarian D (2007) *Organometallics* 26:4321
156. Sun X, Zheng W, Wei B-G (2008) *Tetrahedron Lett* 49:6195
157. Lappert MF, Lednor PW (1976) *Adv Organomet Chem* 14:345
158. Kramer AV, Osborn JA (1974) *J Am Chem Soc* 96:7832
159. Simonet J (2005) *Electrochem Commun* 7:74
160. Simonet J (2005) *J Electroanal Chem* 583:34
161. Kobayashi T, Tanaka M (1981) *J Organomet Chem* 205:C27
162. Firmansjah L, Fu GC (2007) *J Am Chem Soc* 129:11340, and cited ref
163. Netherton MR, Fu GC (2005) *Top Organomet Chem* 14:85
164. Cardenas DJ (2003) *Angew Chem Int Ed* 42:384
165. Lopez-Perez A, Adrio J, Carretero JC (2009) *Org Lett* 11:5514
166. Powers DC, Ritter T (2009) *Nat Chem* 1:302, and cited ref
167. Powers DC, Geibel MAL, Klein JEMN, Ritter T (2009) *J Am Chem Soc* 131:17050, and cited ref
168. Khusnutdinova JR, Rath NP, Mirica LM (2010) *J Am Chem Soc* 132:7303, and cited ref
169. Ariaifard A, Hyland CJT, Canty AJ, Sharma M, Brookes NJ, Yates BF (2010) *Inorg Chem* 49:11249, and cited ref
170. Lanci MP, Remy MS, Kaminsky W, Mayer JM, Sanford MS (2009) *J Am Chem Soc* 131:15618
171. Boisvert L, Denney MC, Hanson SK, Goldberg KI (2009) *J Am Chem Soc* 131:15802
172. Tsuji J, Sato K, Nagashima H (1981) *Chem Lett* 1169
173. Tsuji J, Sato K, Nagashima H (1985) *Tetrahedron* 41:393
174. Tsuji J, Sato K, Nagashima H (1982) *Tetrahedron Lett* 23:893

175. Tsuji J, Sato K, Nagashima H (1985) *Tetrahedron* 41:5003
176. Nagashima H, Sato K, Tsuji J (1981) *Chem Lett* 1605
177. Nagashima H, Sato K, Tsuji J (1985) *Tetrahedron* 41:5645
178. Motoda D, Kinoshita H, Shinokubo H, Oshima K (2002) *Adv Synth Catal* 344:261
179. Chen Q-Y, Yang Z-Y, Zhao C-X, Qiu Z-M (1988) *J Chem Soc Perkin Trans 1* 563 and cited ref.
180. Ishihara T, Kuroboshi M, Okada Y (1986) *Chem Lett* 1895
181. Qiu Z-M, Burton DJ (1993) *Tetrahedron Lett* 34:3239
182. Qiu Z-M, Burton DJ (1995) *J Org Chem* 60:5570
183. Yang Z-Y, Burton DJ (1992) *J Org Chem* 57:4676
184. Matsubara S, Mitani M, Utimoto K (1987) *Tetrahedron Lett* 28:5857
185. Shimizu R, Fuchikami T (1996) *Tetrahedron Lett* 37:8405
186. Dneprovskii AS, Ermoshkin AA, Kasatochkin AN, Boyarskii VP (2003) *Russ J Org Chem* 39:933
187. Mori M, Oda I, Ban Y (1982) *Tetrahedron Lett* 23:5315
188. Mori M, Kanda N, Oda I, Ban Y (1985) *Tetrahedron* 41:5465
189. Mori M, Kubo Y, Ban Y (1985) *Tetrahedron Lett* 26:1519
190. Mori M, Kubo Y, Ban Y (1988) *Tetrahedron* 44:4321
191. Mori M, Kanda N, Ban Y, Aoe K (1988) *J Chem Soc Chem Commun* 12
192. Mori M, Kanda N, Ban Y (1986) *J Chem Soc Chem Commun* 1375
193. Curran DP, Chang C-T (1990) *Tetrahedron Lett* 31:933
194. Nagashima H, Isono Y, Iwamatsu S-i (2001) *J Org Chem* 66:315
195. Castle PL, Widdowson DA (1986) *Tetrahedron Lett* 27:6013
196. Yuan K, Scott WJ (1989) *Tetrahedron Lett* 30:4779
197. Ishiyama T, Abe S, Miyaura N, Suzuki A (1992) *Chem Lett* 691
198. Krasovskiy A, Duplais C, Lipshutz BH (2010) *Org Lett* 12:4742
199. Krasovskiy A, Duplais C, Lipshutz BH (2009) *J Am Chem Soc* 131:15592
200. Charette AB, De Freitas-Gil RP (1997) *Tetrahedron Lett* 38:2809
201. Charette AB, Giroux A (1996) *J Org Chem* 61:8718
202. Hadei N, Kantchev EAB, O'Brien CJ, Organ MG (2005) *Org Lett* 7:3805
203. Nasielski J, Hadei N, Achonduh G, Kantchev EAB, O'Brien CJ, Lough A, Organ MG (2010) *Chem Eur J* 16:10844
204. Sustmann R, Lau J, Zipp M (1986) *Tetrahedron Lett* 27:5207
205. Terao J, Naitoh Y, Kuniyasu H, Kambe N (2003) *Chem Lett* 32:890
206. Manolikakes G, Knochel P (2009) *Angew Chem Int Ed* 48:205
207. Kienle M, Knochel P (2010) *Org Lett* 12:2702
208. Urata H, Kosukegawa O, Ishii Y, Yugari H, Fuchikami T (1989) *Tetrahedron Lett* 30:4403
209. Urata H, Ishii Y, Fuchikami T (1989) *Tetrahedron Lett* 30:4407
210. Fukuyama T, Nishitani S, Inouye T, Morimoto K, Ryu I (2006) *Org Lett* 8:1383
211. Hasanayn F, Nsouli NH, Al-Ayoubi A, Goldman AS (2008) *J Am Chem Soc* 130:511
212. Ryu I (2001) *Chem Soc Rev* 30:16
213. Ryu I (2002) *Chem Rec* 2:249
214. Kondo T, Sone Y, Tsuji Y, Watanabe Y (1994) *J Organomet Chem* 473:163
215. Kondo T, Tsuji Y, Watanabe Y (1988) *Tetrahedron Lett* 29:3833
216. Fukuyama T, Inouye T, Ryu I (2007) *J Organomet Chem* 692:685
217. Ishiyama T, Miyaura N, Suzuki A (1991) *Tetrahedron Lett* 32:6923
218. Fusano A, Fukuyama T, Nishitani S, Inouye T, Ryu I (2010) *Org Lett* 12:2410
219. Stadtmüller H, Lentz R, Tucker CE, Stüdemann T, Dörner W, Knochel P (1993) *J Am Chem Soc* 115:7027
220. Stadtmüller H, Tucker CE, Vaupel A, Knochel P (1993) *Tetrahedron Lett* 34:7911
221. Beckwith ALJ, Schiesser CH (1985) *Tetrahedron* 41:3925
222. Spellmeyer DC, Houk KN (1987) *J Org Chem* 52:959
223. Ishiyama T, Murata M, Suzuki A, Miyaura N (1995) *J Chem Soc Chem Commun* 295

224. Ryu I, Kreimerman S, Araki F, Nishitani S, Oderaotoshi Y, Minakata S, Komatsu M (2002) *J Am Chem Soc* 124:3812
225. Bloome KS, Alexanian EJ (2010) *J Am Chem Soc* 132:12823
226. Suzuki M, Oda Y, Noyori R (1981) *Tetrahedron Lett* 22:4413
227. Suzuki M, Oda Y, Hamanaka N, Noyori R (1990) *Heterocycles* 30:517
228. Suzuki M, Noyori R, Hamanaka N (1981) *J Am Chem Soc* 103:5606
229. Muniz K (2009) *Angew Chem Int Ed* 48:9412
230. Yu W-Y, Sit WN, Lai K-M, Zhou Z, Chan ASC (2008) *J Am Chem Soc* 130:3304
231. Yu W-Y, Sit WN, Zhou Z, Chan AS-C (2009) *Org Lett* 11:3174
232. Zhang Y, Feng J, Li C-J (2008) *J Am Chem Soc* 130:2900
233. Chan C-W, Zhou Z, Chan ASC, Yu W-Y (2010) *Org Lett* 12:3926
234. Basle O, Bidange J, Shuai Q, Li C-J (2010) *Adv Synth Catal* 352:1145
235. An G, Zhou W, Zhang G, Sun H, Han J, Pan Y (2010) *Org Lett* 12:4482
236. Yu J-Q, Corey EJ (2002) *Org Lett* 4:2727
237. Lappert MF, Lednor PW (1973) *J Chem Soc Chem Commun* 948
238. Hall TL, Lappert MF, Lednor PW (1980) *J Chem Soc Dalton Trans* 1448
239. Kramer AV, Labinger JA, Bradley JS, Osborn JA (1974) *J Am Chem Soc* 96:7145
240. Nabavizadeh SM, Habibzadeh S, Rashidi M, Puddephatt RJ (2010) *Organometallics* 29:6359
241. Santoro A, Wegryzn M, Whitwood AC, Donnio B, Bruce DW (2010) *J Am Chem Soc* 132:10689
242. Takeuchi R, Tsuji Y, Fujita M, Kondo T, Watanabe Y (1989) *J Org Chem* 54:1831
243. Kondo T, Tsuji Y, Watanabe Y (1988) *J Organomet Chem* 345:397
244. Zazybin AG, Khusnutdinova YR, Solomonov BN (2004) *Russ J Gen Chem* 74:467
245. Zazybin AG, Khusnutdinova YR, Osipova OL, Solomonov BN (2005) *Russ J Gen Chem* 75:734
246. Taduri BP, Ran Y-F, Huang C-W, Liu R-S (2006) *Org Lett* 8:883
247. Odedra A, Wu C-J, Pratap TB, Huang C-W, Ran Y-F, Liu R-S (2005) *J Am Chem Soc* 127:3406
248. Taduri BP, Odedra A, Lung C-Y, Liu R-S (2007) *Synthesis* 2050
249. Stella L (1983) *Angew Chem Int Ed Engl* 22:337
250. Heinrich MR (2009) *Chem Eur J* 15:820
251. Laali KK, Shokouhimehr M (2009) *Curr Org Synth* 6:193
252. Tamagawa H, Takikawa H, Mori K (1999) *Eur J Org Chem* 973
253. Trauner D, Bats JW, Werner A, Mulzer J (1998) *J Org Chem* 63:5908
254. Li C-J, Li Z (2006) *Pure Appl Chem* 78:935
255. Li C-J (2009) *Acc Chem Res* 42:335
256. Scheuermann CJ (2010) *Chem Asian J* 5:436
257. Yoo W-J, Li C-J (2010) *Top Curr Chem* 292:281
258. Eames J, Watkinson M (2001) *Angew Chem Int Ed* 40:3567
259. Andrus MB, Lashley JC (2002) *Tetrahedron* 58:845
260. Punniyamurthy T, Velusamy S, Iqbal J (2005) *Chem Rev* 105:2329
261. Punniyamurthy T, Rout L (2008) *Coord Chem Rev* 252:134
262. Mayoral JA, Rodriguez-Rodriguez S, Salvatella L (2008) *Chem Eur J* 14:9274
263. Melikyan GG (1997) *Organic Reactions* 49:427
264. Snider BB (1996) *Chem Rev* 96:339
265. Nishino H (2006) *Top Heterocycl Chem* 6:39
266. Demir AS, Emrullahoglu M (2007) *Curr Org Synth* 4:323
267. Snider BB (2009) *Tetrahedron* 65:10738
268. Iqbal J, Bhatia B, Nayyar NK (1994) *Chem Rev* 94:519
269. Csaky AG, Plumet J (2001) *Chem Soc Rev* 30:313
270. Tsubaki K (2007) *Org Biomol Chem* 5:2179
271. Kizirian JC (2008) *Chem Rev* 108:140
272. Kozlowski MC, Morgan BJ, Linton EC (2009) *Chem Soc Rev* 38:3193

273. Giri R, Shi B-F, Engle KM, Mangel N, Yu J-Q (2009) *Chem Soc Rev* 38:3242
274. Chen X, Hao X-S, Goodhue CE, Yu J-Q (2006) *J Am Chem Soc* 128:6790
275. Müller P, Fruit C (2003) *Chem Rev* 103:2905
276. Yang Z-Y, Burton DJ (1989) *J Fluorine Chem* 45:435
277. Yang Z-Y, Burton DJ (1991) *J Org Chem* 56:5125
278. Kitagawa O, Miura A, Kobayashi Y, Taguchi T (1990) *Chem Lett* 1011
279. Asscher M, Vofsi D (1963) *J Chem Soc* 1887
280. Murai S, Sonoda N, Tsutsumi S (1964) *J Org Chem* 29:2104
281. Bellus D (1985) *Pure Appl Chem* 57:1827
282. Martin P, Steiner E, Streith J, Winkler T, Bellus D (1985) *Tetrahedron* 41:4057
283. Matyjaszewski K (2002) *Curr Org Chem* 6:67
284. Pintauer T, Matyjaszewski K (2008) *Chem Soc Rev* 37:1087
285. Pintauer T (2010) *Eur J Inorg Chem* 2449
286. Eckenhoff WT, Pintauer T (2010) *Catal Rev* 52:1
287. Zazybin A, Osipova O, Khusnutdinova U, Aristov I, Solomonov B, Sokolov F, Babashkina M, Zabirov N (2006) *J Mol Catal A: Chem* 253:234
288. Sasaki T, Zhong C, Tada M, Iwasawa Y (2005) *Chem Commun* 2506
289. Clark AJ, Geden JV, Thom S (2006) *J Org Chem* 71:1471
290. Motoyama Y, Kamo K, Yuasa A, Nagashima H (2010) *Chem Commun* 46:2256
291. Pintauer T, Matyjaszewski K (2005) *Coord Chem Rev* 249:1155
292. Taylor MJW, Eckenhoff WT, Pintauer T (2010) *Dalton Trans* 39:11475
293. Okano T, Sugiura H, Fumoto M, Matsubara H, Kusukawa T, Fujita M (2002) *J Fluorine Chem* 114:91
294. Nagashima H, Wakamatsu H, Itoh K, Tomo Y, Tsuji J (1983) *Tetrahedron Lett* 24:2395
295. Nagashima H, Wakamatsu H, Itoh K (1984) *J Chem Soc Chem Commun* 652
296. Clark AJ (2002) *Chem Soc Rev* 31:1
297. Nagashima H, Ozaki N, Seki K, Ishii M, Itoh K (1989) *J Org Chem* 54:4497
298. Nagashima H, Ozaki N, Ishii M, Seki K, Washiyama M, Itoh K (1993) *J Org Chem* 58:464
299. Motoyama Y, Gondo M, Masuda S, Iwashita Y, Nagashima H (2004) *Chem Lett* 33:442
300. Motoyama Y, Hanada S, Niibayashi S, Shimamoto K, Takaoka N, Nagashima H (2005) *Tetrahedron* 61:10216
301. Pattarozzi M, Roncaglia F, Giangiordano V, Davoli P, Prati F, Ghelfi F (2010) *Synthesis* 694
302. Pattarozzi M, Roncaglia F, Accorsi L, Parsons AF, Ghelfi F (2010) *Tetrahedron* 66:1357
303. Nagashima H, Ara K-i, Wakamatsu H, Itoh K (1985) *J Chem Soc Chem Commun* 518
304. Hayes TK, Villani R, Weinreb SM (1988) *J Am Chem Soc* 110:5533
305. Ghelfi F, Roncaglia F, Pattarozzi M, Giangiordano V, Petrillo G, Sancassan F, Parsons AF (2009) *Tetrahedron* 65:10323
306. De Buyck L, Cagnoli R, Ghelfi F, Merighi G, Mucci A, Pagnoni UM, Parsons AF (2004) *Synthesis* 1680
307. De Buyck L, Danieli C, Ghelfi F, Pagnoni UM, Parsons AF, Pattarozzi M, Roncaglia F (2005) *Tetrahedron* 61:2871
308. Bellesia F, Danieli C, De Buyck L, Galeazzi R, Ghelfi F, Mucci A, Orena M, Pagnoni UM, Parsons AF, Roncaglia F (2006) *Tetrahedron* 62:746
309. De Buyck L, Forzato C, Ghelfi F, Mucci A, Pagnoni UM, Parsons AF, Pitacco G, Roncaglia F (2006) *Tetrahedron Lett* 47:7759
310. Roncaglia F, Stevens CV, Ghelfi F, Van der Steen M, Pattarozzi M, De Buyck L (2009) *Tetrahedron* 65:1481
311. Felluga F, Forzato C, Ghelfi F, Nitti P, Pitacco G, Pagnoni UM, Roncaglia F (2007) *Tetrahedron: Asymmetry* 18:527
312. Bryans JS, Chessum NEA, Huth N, Parsons AF, Ghelfi F (2003) *Tetrahedron* 59:6221
313. Felluga F, Ghelfi F, Pagnoni UM, Parsons AF, Pattarozzi M, Roncaglia F, Valentin E (2007) *Synthesis* 1882



314. Edlin CD, Faulkner J, Helliwell M, Knight CK, Parker J, Quayle P, Raftery J (2006) *Tetrahedron* 62:3004
315. Helliwell M, Fengas D, Knight CK, Parker J, Quayle P, Raftery J, Richards SN (2005) *Tetrahedron Lett* 46:7129
316. Clark AJ, Geden JV, Thom S, Wilson P (2007) *J Org Chem* 72:5923, and cited ref
317. Pattarozzi M, Ghelfi F, Roncaglia F, Pagnoni UM, Parsons AF (2009) *Synlett* 2172
318. Stevens CV, Van Meenen E, Masschelein KGR, Eeckhout Y, Hooghe W, D'hondt B, Nemykin VN, Zhdankin VV (2007) *Tetrahedron Lett* 48:7108
319. Bull JA, Hutchings MG, Quayle P (2007) *Angew Chem Int Ed* 46:1869
320. Bull JA, Hutchings MG, Lujan C, Quayle P (2008) *Tetrahedron Lett* 49:1352
321. Ram RN, Kumar N (2008) *Tetrahedron Lett* 49:799
322. Göttlich R (2000) *Synthesis* 1561
323. Heuger G, Kalsow S, Göttlich R (2002) *Eur J Org Chem* 1848
324. Hemmerling M, Sjöholm A, Somfai P (1999) *Tetrahedron: Asymmetry* 10:4091
325. Schulte-Wülwer IA, Helaja J, Göttlich R (2003) *Synthesis* 1886
326. Noack M, Göttlich R (2002) *Chem Commun* 536
327. Liu W-M, Liu Z-H, Cheong W-W, Priscilla L-YT, Li Y, Narasaka K (2010) *Bull Kor Chem Soc* 31:563
328. Kitamura M, Narasaka K (2008) *Bull Chem Soc Jpn* 81:539
329. Koganemaru Y, Kitamura M, Narasaka K (2002) *Chem Lett* 784
330. Kitamura M, Ihara Y, Uera K, Narasaka K (2006) *Bull Chem Soc Jpn* 79:1552
331. Tanaka K, Kitamura M, Narasaka K (2005) *Bull Chem Soc Jpn* 78:1659
332. Cheng K, Huang L, Zhang Y (2009) *Org Lett* 11:2908
333. Russell GA (1957) *J Am Chem Soc* 79:3871
334. Miyamoto S, Martinez GR, Medeiros MHG, DiMascio P (2003) *J Am Chem Soc* 125:6172
335. Kunishita A, Ishimaru H, Nakashima S, Ogura T, Itoh S (2008) *J Am Chem Soc* 130:4244, and cited ref
336. Rothenberg G, Feldberg L, Wiener H, Sasson Y (1998) *J Chem Soc Perkin Trans 2* 2429
337. Huang L, Cheng K, Yao B, Zhao J, Zhang Y (2009) *Synthesis* 3504
338. Xiao Z, Matsuo Y, Nakamura E (2010) *J Am Chem Soc* 132:12234
339. Hassan J, Sevignon M, Gozzi C, Schulz E, Lemaire M (2002) *Chem Rev* 102:1359
340. Kunz K, Scholz U, Ganzer D (2003) *Synlett* 2428
341. Beletskaya IP, Cheprakov AV (2004) *Coord Chem Rev* 248:2337
342. Monnier F, Taillefer M (2009) *Angew Chem Int Ed* 48:6954
343. Sperotto E, van Klink GPM, van Koten G, de Vries JG (2010) *Dalton Trans* 39:10338
344. Shafir A, Lichtor PA, Buchwald SL (2007) *J Am Chem Soc* 129:3490
345. Jones GO, Liu P, Houk KN, Buchwald SL (2010) *J Am Chem Soc* 132:6205
346. Yu H-Z, Jiang Y-Y, Fu Y, Liu L (2010) *J Am Chem Soc* 132:18078
347. House HO (1976) *Acc Chem Res* 9:59
348. Nakamura E, Mori S (2000) *Angew Chem Int Ed* 39:3750
349. Li K, Alexakis A (2006) *Angew Chem Int Ed* 45:7600
350. Yang J, Cauble DF, Berro AJ, Bauld NL, Krische MJ (2004) *J Org Chem* 69:7979
351. Salomon RG (1983) *Tetrahedron* 39:485
352. Bach T, Krüger C, Harms K (2000) *Synthesis* 305
353. Braun I, Rudroff F, Mihovilovic MD, Bach T (2006) *Angew Chem Int Ed* 45:5541
354. Chebolu R, Zhang W, Galoppini E, Gilardi R (2000) *Tetrahedron Lett* 41:2831
355. Ghosh S, Banerjee S, Chowdhury K, Mukherjee M, Howard JAK (2001) *Tetrahedron Lett* 42:5997
356. Banerjee S, Ghosh S (2003) *J Org Chem* 68:3981
357. Mondal S, Yadav RN, Ghosh S (2010) *Tetrahedron Lett* 51:4452
358. Collet F, Dodd RH, Dauban P (2009) *Chem Commun* 5061
359. Zalatan DN, Du Bois J (2010) *Topics Curr Chem* 292:347
360. Badiei YM, Krishnaswamy A, Melzer MM, Warren TH (2006) *J Am Chem Soc* 128:15056

361. Badiei YM, Dinescu A, Dai X, Palomino RM, Heinemann FW, Cundari TR, Warren TH (2008) *Angew Chem Int Ed* 47:9961
362. Wiese S, Badiei YM, Gephart RT, Mossin S, Varonka MS, Melzer MM, Meyer K, Cundari TR, Warren TH (2010) *Angew Chem Int Ed* 49:8850
363. Mankad NP, Antholine WE, Szilagyi RK, Peters JC (2009) *J Am Chem Soc* 131:3878
364. Bhuyan R, Nicholas KM (2007) *Org Lett* 9:3957
365. Barman DN, Nicholas KM (2010) *Tetrahedron Lett* 51:1815
366. Barman DN, Liu P, Houk KN, Nicholas KM (2010) *Organometallics* 29:3404
367. Diaz-Requejo MM, Belderrain TR, Nicasio MC, Trofimenko S, Perez PJ (2003) *J Am Chem Soc* 125:12078
368. Fructos MR, Trofimenko S, Diaz-Requejo MM, Perez PJ (2006) *J Am Chem Soc* 128:11784
369. Liu X, Zhang Y, Wang L, Fu H, Jiang Y, Zhao Y (2008) *J Org Chem* 73:6207
370. Zhao B, Du H, Shi Y (2008) *J Am Chem Soc* 130:7220
371. Zhao B, Du H, Shi Y (2009) *J Org Chem* 74:4411
372. Aubé J, Peng X, Wang Y, Takusagawa F (1992) *J Am Chem Soc* 114:5466
373. Aubé J, Gülgeze B, Peng X (1994) *Bioorg Med Chem Lett* 4:2461
374. Black DStC, Edwards GL, Laaman SM (1998) *Tetrahedron Lett* 39:5853
375. Black DStC, Edwards GL, Laaman SM (2006) *Synthesis* 1981
376. Usuki Y, Peng X, Gülgeze B, Manyem S, Aubé J (2006) *ARKIVOC Pt4*:189
377. Cardona F, Goti A (2009) *Nat Chem* 1:269
378. de Figueiredo RM (2009) *Angew Chem Int Ed* 48:1190
379. Du H, Zhao B, Shi Y (2007) *J Am Chem Soc* 129:762
380. Yuan W, Du H, Zhao B, Shi Y (2007) *Org Lett* 9:2589
381. Zhao B, Du H, Shi Y (2008) *Org Lett* 10:1087
382. Du H, Zhao B, Yuan W, Shi Y (2008) *Org Lett* 10:4231
383. Zhao B, Du H, Shi Y (2009) *J Org Chem* 74:8392
384. Zhao B, Peng X, Cui S, Shi Y (2010) *J Am Chem Soc* 132:11009
385. Wen Y, Zhao B, Shi Y (2009) *Org Lett* 11:2365
386. Zhao B, Yuan W, Du H, Shi Y (2007) *Org Lett* 9:4943
387. Ramirez TA, Zhao B, Shi Y (2010) *Tetrahedron Lett* 51:1822
388. Wee AGH (2006) *Curr Org Synth* 3:499
389. Vanecko JA, Wan H, West FG (2006) *Tetrahedron* 62:1043
390. Sweeney JB (2009) *Chem Soc Rev* 38:1027
391. West FG, Naidu BN, Tester RW (1994) *J Org Chem* 59:6892
392. Tester RW, West FG (1998) *Tetrahedron Lett* 39:4631
393. Marmsäter FP, Vanecko JA, West FG (2004) *Org Lett* 6:1657
394. Brogan JB, Zercher CK, Bauer CB, Rogers RD (1997) *J Org Chem* 62:3902
395. Brogan JB, Zercher CK (1998) *Tetrahedron Lett* 39:1691
396. Marmsäter FP, Murphy GK, West FG (2003) *J Am Chem Soc* 125:14724
397. Murphy GK, Marmsäter FP, West FG (2006) *Can J Chem* 84:1470
398. Murphy GK, West FG (2005) *Org Lett* 7:1801
399. Bott TM, Vanecko JA, West FG (2009) *J Org Chem* 74:2832
400. van Rheenen V (1969) *J Chem Soc Chem Commun* 314
401. Itoh T, Kaneda K, Teranishi S (1975) *Tetrahedron Lett* 2801
402. Chemler SR (2009) *Org Biomol Chem* 7:3009
403. Zeng W, Chemler SR (2007) *J Am Chem Soc* 129:12948
404. Zeng W, Chemler SR (2008) *J Org Chem* 73:6045
405. Sherman ES, Chemler SR (2009) *Adv Synth Catal* 351:467
406. Miao L, Haque I, Manzoni MR, Tham WS, Chemler SR (2010) *Org Lett* 12:4739
407. Fuller PH, Kim J-W, Chemler SR (2008) *J Am Chem Soc* 130:17638
408. Sequeira FC, Turmpenny BW, Chemler SR (2010) *Angew Chem Int Ed* 49:6365
409. Sherman ES, Fuller PH, Kasi D, Chemler SR (2007) *J Org Chem* 72:3896
410. Bowman WR, Storey JMD (2007) *Chem Soc Rev* 36:1803

411. Studer A, Bossart M (2001) *Tetrahedron* 57:9649
412. Klein JEMN, Perry A, Pugh DS, Taylor RJK (2010) *Org Lett* 12:3446
413. Knappke CEI, von Wangelin AJ (2010) *ChemCatChem* 2:1381
414. Michaelis DJ, Shaffer CJ, Yoon TP (2007) *J Am Chem Soc* 129:1866
415. Michaelis DJ, Ischay MA, Yoon TP (2008) *J Am Chem Soc* 130:6610
416. Michaelis DJ, Williamson KS, Yoon TP (2009) *Tetrahedron* 65:5118
417. Benkovic T, Du J, Guzei IA, Yoon TP (2009) *J Org Chem* 74:5545
418. Benkovic T, Guzei IA, Yoon TP (2010) *Angew Chem Int Ed* 49:9153
419. Schoening KU, Fischer W, Hauck S, Dichtl A, Kuepfert M (2009) *J Org Chem* 74:1567
420. Dichtl A, Seyfried M, Schoening KU (2008) *Synlett* 1877
421. Kundu R, Ball ZT (2010) *Org Lett* 12:2460
422. Tamura M, Kochi J (1971) *J Am Chem Soc* 93:1483
423. Tamura M, Kochi J (1972) *Bull Chem Soc Jpn* 45:1120
424. Nagano T, Hayashi T (2005) *Chem Lett* 34:1152
425. Whitesides GM, Bergbreiter DE, Kendall PE (1974) *J Am Chem Soc* 96:2806
426. Kochi JK (2002) *J Organomet Chem* 653:11
427. Tamura M, Kochi J (1971) *Synthesis* 303
428. Someya H, Ohmiya H, Yorimitsu H, Oshima K (2008) *Org Lett* 10:969
429. Mitamura Y, Asada Y, Murakami K, Someya H, Yorimitsu H, Oshima K (2010) *Chem Asian J* 5:1487
430. Someya H, Yorimitsu H, Oshima K (2009) *Tetrahedron Lett* 50:3270
431. Someya H, Yorimitsu H, Oshima K (2010) *Tetrahedron* 66:5993
432. Fujii Y, Terao J, Kambe N (2009) *Chem Commun* 1115
433. Chiba S, Cao Z, El Bialy SAA, Narasaka K (2006) *Chem Lett* 35:18
434. Chiba S, Kitamura M, Narasaka K (2006) *J Am Chem Soc* 128:6931
435. Punta C, Minisci F (2008) *Trends Heterocycl Chem* 13:1
436. Minisci F, Vismara E, Fontana F (1989) *Heterocycles* 28:489
437. Minisci F, Vismara E, Fontana F (1989) *J Org Chem* 54:5224
438. Minisci F, Citterio A, Giordano C (1983) *Acc Chem Res* 16:27
439. Coppa F, Fontana F, Lazzarini E, Minisci F (1992) *Chem Lett* 1299
440. Ding C, Tu S, Li F, Wang Y, Yao Q, Hu W, Xie H, Meng L, Zhang A (2009) *J Org Chem* 74:6111
441. Ding C, Tu S, Yao Q, Li F, Wang Y, Hu W, Zhang A (2010) *Adv Synth Catal* 352:847
442. Burgin RN, Jones S, Tarbit B (2009) *Tetrahedron Lett* 50:6772
443. Minisci F, Coppa F, Fontana F (1994) *J Chem Soc Chem Commun* 679
444. Kraus GA, Melekhov A (1998) *Tetrahedron Lett* 39:3957
445. Zelechonok Y, Silverman RB (1992) *J Org Chem* 57:5787
446. Huang W, Li J, Ou L (2007) *Synth Commun* 37:2137
447. Huang W, Wang M, Yue H (2008) *Synthesis* 1342
448. Seiple IB, Su S, Rodriguez RA, Gianatassio R, Fujiwara Y, Sobel AL, Baran PS (2010) *J Am Chem Soc* 132:13194
449. Ionita P, Gilbert BC, Chechik V (2005) *Angew Chem Int Ed* 44:3720
450. Ionita P, Conte M, Gilbert BC, Chechik V (2007) *Org Biomol Chem* 5:3504
451. Raffa P, Evangelisti C, Vitulli G, Salvadori P (2008) *Tetrahedron Lett* 49:3221
452. Liu Y, Song F, Guo S (2006) *J Am Chem Soc* 128:11332
453. Gansäuer A, Fan C-A, Piestert F (2008) *J Am Chem Soc* 130:6916
454. Gansäuer A, Otte M, Piestert F, Fan C-A (2009) *Tetrahedron* 65:4984
455. Takai K, Nitta K, Fujimura O, Utimoto K (1989) *J Org Chem* 54:4732
456. Wessjohann LA, Schmidt G, Schrekker HS (2007) *Synlett* 2139
457. Wessjohann LA, Schmidt G, Schrekker HS (2008) *Tetrahedron* 64:2134
458. Takai K, Toratsu C (1998) *J Org Chem* 63:6450
459. Wessjohann LA, Schrekker HS (2007) *Tetrahedron Lett* 48:4323
460. Usanov DL, Yamamoto H (2010) *Angew Chem Int Ed* 49:8169

461. Recupero F, Punta C (2007) *Chem Rev* 107:3800
462. Minisci F, Recupero F, Fontana F, Bjørsvik HR, Liguori L (2002) *Synlett* 610
463. Iwahama T, Sakaguchi S, Ishii Y (2000) *Chem Commun* 2317
464. Hirase K, Sakaguchi S, Ishii Y (2003) *J Org Chem* 68:5974
465. Hirase K, Iwahama T, Sakaguchi S, Ishii Y (2002) *J Org Chem* 67:970
466. Kagayama T, Fuke T, Sakaguchi S, Ishii Y (2005) *Bull Chem Soc Jpn* 78:1673
467. Kagayama T, Nakano A, Sakaguchi S, Ishii Y (2006) *Org Lett* 8:407
468. Riguet E, Klement I, Reddy CK, Cahiez G, Knochel P (1996) *Tetrahedron Lett* 37:5865
469. Klement I, Knochel P, Chau K, Cahiez G (1994) *Tetrahedron Lett* 35:1177
470. Quebatte L, Scopelliti R, Severin K (2004) *Angew Chem Int Ed* 43:1520

# Index

## A

Acrylamides, cyclizations, chirality transfer, 37  
Acutumine, 40  
*N*-Acyhydrazones, chiral, 61,  
Acyl pyridinium salts, Norton's radical hydrogenation, 103  
Addition, 323  
Alcohols, activation by boron, 116  
Alkaloids, 40  
Alkenes, carbohydroxylation, 45  
    cleaved to aldehydes, 154  
    hydrofunctionalization, 174  
Alkoxy carbonylation, 179  
Alkoxylation, 10  
Alkylarenes, 151  
Alkylations, iron catalyzed, 195  
Alkylcatecholboranes, 116  
Alkyl halides, 61, 126  
    cobalt-catalyzed Heck reactions, 253  
Alkylpolyfluoroarenes, 199  
Alkynes, hydrogenation, 115  
Allylacetophenones, 136  
Amides, vinylogous, cyclization, 36  
Amidocupration/radical cyclization, 412  
Amination (nitrenoid), 179  
Amines, chiral, 61  
    tertiary, cyanation, 14  
Amino acids, synthesis, 74  
Aminohydroxylation, 415  
    iron-catalyzed, 223  
*N*-Aminooxazolidinones, 64,  
Aminosugars, 84  
Anode, 1  
Aphanorphine, 20  
Aporphines, 46  
Arenes, trifluoromethylation, 215

Argemone, 41  
Arylaluminum, 199  
Aryl-aryl coupling reactions intramolecular, tributyltin hydride-mediated, 46  
Arylation, aryl iodides, iron(II)-catalyzed, 216  
5-Arylbutyrolactones, 173  
1-Arylpropan-triol 2-ethers, 153  
Aryl radicals, 33  
    cyclization, manganate-catalyzed, 168  
Aspidospermidine, 39  
Asymmetric synthesis, 61  
Atom transfer radical additions (ATRA), 180  
    copper, 384  
    iron, 206  
    manganese(III) acetate, 169  
    palladium, 363  
    Ru(II)-Ru(III), 232  
Atom transfer radical cyclization (ATRC), 180, 238, 368  
Aziridinium cations, hydrogenation, 104  
Azo sulfides, 53

## B

Barbier reactions, 180  
    titanocene chloride-catalyzed, 143  
Barbiturates, 171  
Barton-McCombie reaction, 116  
Bathophenanthroline, 215  
Benzaldehyde hydrazone, 65  
Benzenes, substituted, cyclizations, 46  
Benzoquinone ketal, 12  
Benzoquinones, 426  
Benzoselenophenes, 38  
Benzotellurophenes, 38  
Benzotriazoles, 52  
Benzoxetane, 37

Bergman cycloaromatization, 105  
 BHT, 130  
 Biaryl coupling, 180  
 Biaryls, 150  
 Biphenols, 16  
 2-Biphenyl alcohols, 53  
 Biphenyls, 48, 51  
 Bis(dipivaloylmethanato)-manganese(II), 174  
 Bis(ortho-phenylenediphosphine)iron(II), 198  
 Bond dissociation energies (BDEs), 93  
 Boronates, radical reduction, 117  
 Boron-doped diamond, 1, 4  
 Bromoacetaldehyde allyl acetals, 157  
 2-Bromobenzyl bromides, 38  
 Bromomagnesium tributylmanganate, 167  
 2-Bromo-2-(4-pentenyl)malonates, 228  
 3-Butenyl radical, 131  
*trans*-4-*tert*-Butylcyclohexylbenzene, 152  
 4-*tert*-Butylcyclohexyl halides, 132  
 4-*tert*-Butyltoluene, anodic methoxylation, 10  
 Butynediol, 15  
 Butyrolactols, 148  
 Butyrolactones, carbon monoxide  
   annulated, 137

## C

C–C bonds, cleavage, 14  
 C–C double bonds, cyclizations, 35  
 C–C triple bonds, cyclizations, 35  
 Carbenes, *N*-heterocyclic (NHCs), 94  
 Carboaminations, 44  
 Carbohalogenations, 43  
 Carbon dioxide, electron acceptor, 7  
 Carbon–heteroatom double bonds,  
   cyclizations, 38  
 Carbonylation, 180  
   manganese-catalyzed, 165  
 Carboxygenations, 45  
 Carbothiolations, 45  
 Carboxylation, reductive, 7  
 Carboxymethylation/lactonization, acetic  
   acid, 172  
 Caryophyllene oxide, cyclization, 111  
 Catalysis, 93  
   bimetallic, 429  
 Catalytic HAT (CHAT), 106  
 Catecholborane, 116  
 Cathode, 1  
 Cavicularin, 50  
 Cephalotaxine, 40  
 Chain reactions, 93, 132  
 5-(1-Chloroalkyl)lactams, 216

Chlorobenzene, arylation with 2-pyridinyl  
   radicals, 55  
 $\alpha$ -Chloro carbonyls, nickel-catalyzed arylation,  
   351  
 Chlorocyclopropanes, 301  
 Chlorodiphenylphosphine, 38  
 2-(2-Chloroisopropyl)cyclopentanol, 144  
 Chromium, 155  
 Cobaloxime, 264  
 Cobalt, 247  
 Co(II) metalloradicals, 102  
 Coniine, hybrid radical-ionic annulation, 72  
 Copper, 384  
 Cr(II)–Co(II), 431  
 Cross-coupling, 19, 121, 191, 323, 350, 369  
   Hiyama-type, 180  
   Kumada-type, 56, 151, 180, 247  
   Negishi-type, 180  
   Stille-type, 180  
   Suzuki-type, 180  
 Cyanation, 13  
 Cyanhydric acid, acidic methanolysis, 11  
 Cyclizations, 121, 191, 323  
   6-*exo* 82  
 Cycloaddition, [2+2], 181, 228  
 Cyclobutanes, 145  
 Cyclobutenes, cyclizations, 40  
 Cyclopropanation, 276  
 Cyclopropanols, 152  
   cleavage, oxidative, 174  
 Cyclopropyl silyl ethers, 152  
 3-Cyclopropylallyl *ortho*-iodophenyl  
   ether, 168  
 Cyclopropylmethyl bromide, 130

## D

Daunosamine, 84  
 Decahydroisoquinoline, 74  
 Diaziridinone ring opening, 403  
 2,4-Dibromoesters, 206  
 Dibutyltitanocene(IV), 138  
 Dibutyltrifluoroethylamine, 14  
 Difluorobenzene, anodic fluorination, 13  
 Dihydrobenzofuran, 35  
 Dihydroindole, 35  
 Dihydroisoquinoline, imidazolyl-annulated, 50  
 $\alpha$ -Diketone tetrathioacetals, 149  
 Dimerization/radical addition/nucleophilic  
   addition, titanium, 142  
 2,5-Dimethoxy-2,5-dihydrofuran, 11  
 2,4-Dimethylphenol, 16  
 1,1-Diphenylethylene, 173

Diphenylphosphanes, 38  
Domino 1,5-hydrogen transfer/Kumada coupling, iron-catalyzed, 204

## E

Electrochemistry, 1  
Electron transfer, 121, 191, 323  
Electrosynthesis, 1  
Enamides, 36, 40  
Endoperoxy propellanes, 173  
Enol ethers, Ru(II)-catalyzed seleno sulfonation, 230  
Epoxides, *anti*-selective reduction, 114  
reduction, 107  
Epoxygeranyl acetate, cyclization, 109  
6,7-Epoxy-2-heptenoate derivatives, 144  
Epoxy ketones, photoredox-catalyzed ring opening, 227  
Epoxyneryl acetate, opening, 110  
Erysotrienes, 40

## F

Fluorenones, cyclization, 48  
Fluorination, 12  
Fluorobenzene, fluorination, 13  
Fragranol, 146  
Fullerenes, copper-catalyzed radical addition/cyclization, 395  
Furan, methoxylation, 11

## G

Galvinoxyl, 130  
Giese additions, photoredox-catalyzed, 230  
Gold, 428  
Gomberg–Bachmann reactions, 33, 48, 51  
Grignard reagents, 200

## H

Haloacetals, radical cyclizations, zirconium, 149  
Heck reaction (redox-neutral radical addition), 181  
Helicenes, 47  
*N*-Heterocyclic carbenes (NHCs), 94  
Hexafluoroisopropanol (HFIP), 5  
5-Hexenyl radical, 131  
Hofmann–Löffler–Freytag reactions, titanium, 148  
Hybrid radical–ionic annulation, 70

Hydrazones, chiral, 61  
Hydroapoerysopinines, 40  
Hydrofunctionalization of olefins, 181  
Hydrogen atom donors, 93  
Hydrogen atom transfer (HAT), 93  
Hydrogermylation, 168  
Hydrohydrazination, manganese(III), 177  
Hydrophosphonylation, 169  
Hydroxycarboxylation, oxidative radical, (phthalocyanine)iron, 218  
Hydroxyhydrazones, 61  
 $\alpha$ -Hydroxy ketones, oxidative cleavage, 152  
*N*-Hydroxyphthalimide (NHPI), 132  
4-Hydroxy-2-quinolone, 173

## I

Imidazoles, cyclizations, 50  
Indolines, 221  
synthesis, 39  
Iridium, 308  
Iron, 192  
3-Isopropenyldihydrobenzofurans, 167  
3-Isopropenylindoline, 167

## J

Jacobsen–Katsuki epoxidation, 124, 164

## K

Ketimines, 38, 78  
Ketones, aromatic, 114  
Kharasch additions, 207  
carbonylation, 159  
cyclizations, 240  
Ru(II)-catalyzed, 232  
Kumada coupling, 56, 151, 180, 247

## L

Lennoxamine, 40  
Lignin model compound, 154  
Lithium tributylmanganate, 168  
Luotonin A, 42  
Lutidine, 15  
Lycorane, 39  
Lycorines, 40

## M

Manganese, 164  
Manganese-mediated radical addition, 70

- Mappicine ketone, 41  
 Meerwein arylations, intermolecular, 43  
 Meerwein cyclizations, 35  
 Meerwein reactions, 33, 35  
 Menthylamine, 9  
 Metal-hydrogen bonds, 93  
 Metal-mediated activation, 123  
 Methanol, activation, 117  
 Methionine hydroxy analog (MHA), 7  
 3-Methyl-1-buten-3-ol, 173  
 4-Methyl guaiacol, 20  
*N*-Methylpyrrole, cyanation, 14  
 Methyltriethylammonium methylsulfate, 5  
 Minisci reactions, 181, 425  
 Mn(II)–Co(II), 434  
 Mn(II)–Cu(I), 437  
 Molybdenum, 158
- N**
- Natural product syntheses, 33  
 Neomenthylamine, 9  
 Neopentyl-type primary radical, 111  
 Nickel, 325  
 Niobium, 150  
 Nitrenoids, hydrogen transfer/ $S_{\text{H}}$   
     cyclizations, 222
- O**
- Octylmesitylene, 201  
 Olefins, Grignard reagents, titanium, 137  
     radical hydrogenation, 117  
 [1,2]-Onium ylide rearrangements, 406  
 Organomanganese, 164  
 Osmium, 246  
 2-Oxabicyclo[3.3.0]octanone dithioketals, 220  
 Oxalic amides, 427  
 Oxaziridines, ring opening, 401, 415  
 Oxazolidinones, 64  
 Oxidative catalysis, Mn(II)–Mn(III), 170  
 Oxidative photoredox catalysis, 231  
 Oxidative radical additions, 208, 217  
     lactonization, Mn(OAc)<sub>3</sub>, 172  
 Oxidative radical generation, 124  
 Oximes, reduction, 8
- P**
- Palladium, 363  
 Paramagnetic metal complexes, 127  
 Pauson–Khand-type reactions, titanium-  
     catalyzed, 137
- Peroxides, reductive cleavage, 182  
 Phase-transfer Gomberg–Bachmann (PTGB)  
     reactions, 51  
 Phenanthrene, 14  
 Phenol–arene cross-coupling, 19  
 Phenolates, radical arylation, 54  
 Phenol coupling reactions, anodic, 16  
 Phenols, radical arylation, 54  
 Phenylacetaldehyde *N*-acylhydrazone, 75  
 Phenylazides, *ipso* cyclization, 49  
 Phenyliodine(III)-bis(trifluoroacetate), 20  
*exo*-Phenylnorbornane, 152  
 Phenylsilyl ethers, *ipso* cyclization, 49  
 Phosphinates, *ipso* cyclization, 48  
 Phosphine oxides, 38  
 Photocarbonylation, ruthenium(0)/  
     phenone-cocatalyzed, 224  
 Photoredox catalysis, 181  
 (Phthalocyanine)iron, 214  
 Pinacol coupling, 150, 181  
 Platinum, 382  
 Propargylic trichloroethyl ethers, 159  
 Pschorr reactions, 33, 46  
 Pyrazolidin-3,5-diones, 171  
 Pyridine-3,5-dicarboxylic acid, 15  
 Pyridines, cyclizations, 50  
 Pyrrole, anodic cyanation, 14  
 Pyrrole-quinazolines, 42
- Q**
- Quinacrine, 74  
 Quinine, radical addition, 73  
 Quinoline-2,4-diones, 171
- R**
- Radical additions, 33, 61, 181, 295, 341, 353  
     /oxidation, manganese(III), 171  
 Radical carbomagnesation, 141  
 Radical cation cyclizations, 220  
 Radical cyclizations, 33, 144, 299, 347, 354  
     addition/dimerization sequence, Zr(II), 150  
     Co(0)-catalyzed, 256  
     reductive, chromium, 156  
 Radical inhibitors, 130  
 Radical–organometallic hybrids, 55  
 Reductive photoredox reactions,  
     Ru(I)–Ru(II), 226  
 Reductive radical generation, 125  
 Rhenium, 178  
 Rhodium, 302  
 Riccardin C, 50



Ru(II)–Rh(III), 438

Ruthenium, 224

## S

Sesamol, 18

Siloxanes, *ipso* cyclization, 49

Silver, 419

Single electron transfer (SET), 123

Snapper designed tandem RCM/ATRC reactions, 241

Spirocyclohexadienone, 50

Stereoconvergence, 78

Stevens rearrangements, 406

Stilbenes, 10

oxidative cyclizations, 221

Styrenes, cobalt-catalyzed Heck reactions, 253

dialkylation, titanium, 138

radical cyclizations/dimerizations, 102

radical-polar carbosilylation, 140

Sulfinamides, 38

$\beta$ -Sulfonyl selenoacetals, 230

Sulfur-directed cyclization, 41

Suzuki–Miyaura coupling, 199

## T

Tandem ATRA/ATRC, 182

Tandem radical cyclization, 182

Tantalum, 150

Tetrafluorocyclohexadiene, 13

Tetrahydroquinolines, 221

Tetrakis(tetrabutylammonium) decatungstate, 161

Tetramethylbiphenol, 16

Tetraphenylbiphosphine, 38

Ti(III)–Rh(I), 429

Tin hydrides, 33

Titanate enolates, 237

Titanium compounds, 136

Titanocene aqua-complex, 113

Transition metals, 121, 191, 323

Trialkylboranes, 115

Trichloroacetates, iron(II)-catalyzed ATRC, 212

Triethylborane, 35

Trimethylorthoformate, 11

Triphenylgermyl radical, 168

Triphenylmethane, 34

Tubuphenylalanine, 76

Tubovaline, 75

Tungsten, 161

## U

Ueno–Stork cyclizations, 98

## V

Vanadium, 150

Vaska's complex, 107

Vindoline, 39

Vitamin B<sub>12</sub>, 102, 268

## W

Water, activation by boron, 115  
activation by Ti(III), 108

Wilkinson's complex, 106

## X

Xanthates, deoxygenation, 95

## Z

Zirconium catalysis, 148